Investigations into the role of Toll-Like Receptors in the modulation of the inflammatory response during Osteoarthritis

Submitted to National University of Ireland Maynooth for the degree of Doctor of Philosophy

NUI MAYNOOTH

Ollscoil na hÉireann Má Nuad

Ashwini Maratha, M.Sc

Institute of Immunology
Department of Biology
National University of Ireland Maynooth

Head of Department	**Supervisor**	**Co. Supervisor**
Prof. Paul Moynagh	Dr. Sinead Miggin	Prof. Paul Moynagh

Publications and Presentations

Journal publications

Published paper

1. The NF-κB subunits RelB and cRel negatively regulate TLR3-mediated IFN-β production via induction of the transcriptional repressor protein YY1. *J. Biol. Chem.* 2011 jbc.M111.250894. doi:10.1074/jbc.M111.250894. *Jakub Siednienko[1,2], **Ashwini Maratha[1]**, Shuo Yang, Magorzata Mitkiewicz[2], Sinéad M. Miggin[1*] and Paul N. Moynagh[1*].* [1]Institute of Immunology, National University of Ireland Maynooth, Co. Kildare, Ireland, and the [2]Institute of Immunology and Experimental Therapy[2], Polish Academy of Sciences, Wroclaw, Poland. * Contributed equally as senior authors.

Submitted paper's

2. TLR3 as a therapeutic target for OA ? ***Ashwini Maratha[1]**, Maheshwar Lakkireddy[2] ,J.V.S Vidyasagar [2] and Sinead Miggin[1].* [1]Institute of Immunology and Department of Biology, National University of Ireland Maynooth, Maynooth, Ireland. [2] Department of Orthopaedics, Orthopaedics Research Unit, Aware Global Hospitals, Hyderabad, India. ***Nature Medicine (Manuscript under preparation).***

3. Osteoarthritis is associated with upregulation and functional activation of Toll-like receptor 3 on synovial fibroblasts and explant tissue. **Ashwini Maratha[1]**, Mary Connolly[2], Douglas J Veale[2], Ursula Fearon[2] and Sinead M. Miggin[1]. From the [1]Immune Signalling Group, Institute of Immunology, Department of Biology, National University of Ireland Maynooth, Maynooth, Co. Kildare, Ireland; [2]Department of Rheumatology, Dublin Academic Medical Centre, St. Vincent's University Hospital, and University College Dublin, Dublin, Ireland. ***Arthritis Research & Therapy***.

4. TRIF-mediated TLR3 and TLR4 signalling is negatively regulated by ADAM15. *Suaad Ahmed, **Ashwini Maratha**, Aisha Qasim Butt, Enda Shevlin, Sinead Miggin.* From

the Immune Signaling Group, Institute of Immunology, Department of Biology, National University of Ireland Maynooth, Co. Kildare, Ireland. ***Journal of Immunology.***

5. Analysis of serum cytokines in patients with Type 2 Diabetes and associated complications. *S Gupta[2*], **A Maratha[1*],** A Natarajan[2,] T Gajanayake[1], J Siednienko[1], S Hoashi[2*] and S Miggin[1*]* ****joint authorship.*** [1]Immune Signalling laboratory, Institute of Immunology, National University of Ireland Maynooth, [2]Midlands Regional Hospital, Mullingar, Co Westmeath, Ireland. ***Diabetes Care.***

6. Acute Serum Amyloid A is an endogenous TLR2 ligand that mediates inflammation and angiogenesis in rheumatoid arthritis. *Mary C Connolly*, **Ashwini Maratha§**, Peter R Rooney*, Sinead M Miggin§, Douglas J Veale* and Ursula M Fearon**. *Dublin Academic Medical Centre and Conway Institute of Biomolecular and Biomedical Research, Dublin 4, Ireland. §Institute of Immunology, National University of Ireland Maynooth, Maynooth, County Kildare, Ireland. ***Journal of Immunology.***

Papers under review for submission

7. Proteomic investigations in to stage-related alterations in Osteoarthritis synovial tissue through 2D-DIGE and Protein Network Analysis. ***A Maratha[1]**, M Lakkireddy[2], E Mullen, J.V.S Vidyasagar [2] and S Miggin[1]*. [1]Institute of Immunology and Department of Biology, National University of Ireland Maynooth, Maynooth, Ireland. [2] Department of Orthopaedics, Orthopaedics Research Unit, Aware Global Hospitals, Hyderabad, India.

8. Proteomic evaluation of the role of necrotic RNA in Osteoarthritis progression. ***Ashwini Maratha*** *and Sinead Miggin**. Institute of Immunology and Department of Biology, National University of Ireland Maynooth, Maynooth, Ireland.

9. Extracellular ATP suppresses poly (I:C)-induced RANTES (CCL5) through inhibition of NF-kB pathway in human rheumatoid fibroblast-like synoviocytes. *Thusitha Gajanayake, **Ashwini Maratha**, Jakub Siednienko, Suaad Ahmed, Sinead Miggin**. Institute of Immunology and Department of Biology, National University of Ireland Maynooth, Maynooth, Co. Kildare, Ireland.

Conference presentations and publications (Abstract)

1. Oral presentation on 'Comparative cytokine profiling of synoviocytes in response to Toll-Like Receptor ligands and sterile inflammatory mediators' at the **8th World Congress on Trauma, Shock, Inflammation and Sepsis-TSIS 2010** in conjunction with the 23rd SIS-Europe Congress on Surgical Infections and 2nd Interdisciplinary Summit on Inflammation, 9-13th March 2010, Munich, Germany**. Abstract published at Inflamm. Res. (2010), 59, (Suppl 1):S1–S8, A427, DOI 10.1007/s00011-010-0169-5.**

2. Oral-poster on 'Cytokine profiling of pre-diabetic patients' at th**e Annual meeting of Irish Endocrine Society,** 5-6th November 2010, Cork, Ireland. S Gupta[2]*, **A Maratha[1]* **joint authorship***. **Abstract published at Irish J Med Scien Volume 179, Supplement 13, S513, 1863-4362 (Online, Tuesday, November 09, 2010).**

3. Equal contribution for the poster presented on 'TLR2 mediates Acute Serum Amyloid A induced pro- inflammatory effects in Rheumatoid Arthritis' at **The 74th Annual Scientific Meeting of the American College of Rheumatology,** 7-11th November 2010, Atlanta, USA. Connolly M[1], **Maratha A[2]. Abstract published at Arthritis Rheum 2010; 62, Suppl 10:1533, DOI: 10.1002/art.29299.**

4. Oral-poster on 'Cytokine profiling of pre-diabetic patients' at the **British Endocrine Society Annual Meeting,** 11-14th April 2011, Birmingham, UK. S Gupta[2]*, **A Maratha[1]* **joint authorship***. **Abstract published at Endocrine Abstracts (2011), 25, P119, Birmingham, UK.**

5. Oral presentation on 'Characterisation of osteoarthritic synoviocytes' at the **Fourth National Immunology Postgraduate Masterclass with Professor Max Cooper**, 18th July 2008, NUIM, Maynooth, Ireland.

6. Poster on 'Subcellular localisation and role of RACK-1 and PKCζ in T-lymphocyte migration' at the **Annual symposium HRB PhD Scholars in Immunology**, 18th July 2008, NUIM, Maynooth, Ireland.

7. Poster on 'Comparative analysis of cytokine production by synoviocytes in response to Toll-Like Receptor ligands and sterile inflammatory mediators' at the **Keystone Symposia for "Innate Immunity: Mechanisms Linking with Adaptive Immunity"** 7-12th June 2010, Trinity College Dublin, Dublin, Ireland.

8. Poster on 'Cytokine storms in Arthritic Synoviocytes' at the **Irish Society Of Immunology Annual meeting,** 15th October 2010, Trinity College Dublin, Dublin, Ireland.

9. Poster on 'Cytokine profiling in Type 2 Diabetes' at the **ENDO 2011 : The 93rd Annual Meeting and Expo in the Endocrine Society**, 4 -7th June 2011, Boston, USA. S Gupta[2]*, **A Maratha[1]* **joint authorship.***

Attended Practical Proteomics Workshop at Waters/Warwick Centre for BioMedical Mass Spectrometry and Proteomics Unit, University of Warwick, Coventry, U.K, 14th to 16th December 2009.

Table of Contents

		Page
Declaration		xvi
Acknowledgement		xvii
Abstract		xix
Abbreviations		xxi
Chapter 1	**Introduction**	
1.1.	The immune response	1
1.2.	Innate Immunity	1
1.3.	DCs	2
1.4.	PRRs	3
1.5.	Toll-Like Receptors	3
	1.5.1. TLR1, TLR2 and TLR6	4
	1.5.2. TLR3	5
	1.5.3. TLR4	7
	1.5.4. TLR5	8
	1.5.5. TLR7, TLR8 and TLR9	8
	1.5.6. TLR10, TLR11, TLR12 and TLR13	9
1.6.	Cytosolic PRRs	10
1.7.	TLR signalling pathways	11
1.8.	TLR adaptors	12
	1.8.1. MyD88	12
	1.8.2. Mal	14
	1.8.3. TRIF	15
	1.8.4. TRAM	16
	1.8.5. SARM	17
1.9.	Activation of transcription factors	17
	1.9.1. NF- κB	18
	1.9.2. IRFs	19

1.10. Osteoarthritis 22
1.11. Epidemiology and pathology of OA 23
1.12. Inflammation and OA 25
1.13. Role of the synovium in OA pathogenesis 27
1.13.1. Physiology of the synovial joint 28
1.13.2. Features of the inflamed synovium 30
1.13.3. Mediators of Inflammation and joint destruction 32
1.13.4. FLSs in the joint 34
1.14. Inflammatory cytokines in OA 35
1.15. Therapeutic treatment in OA – past, present and future 38
1.15.1. Cytokines as potential targets for biological therapy in OA 39
1.16. Innate immune system activation in OA 42
1.17. Specific aims of the study 45

Chapter 2 General Materials and Methods

2.1. General Materials and Suppliers 46
2.2. General Laboratory Procedures 49
2.2.1. Centrifugation 49
2.2.2. Spectrophotometry 49
2.2.3. Measurement of pH 49
2.2.4. PCR 49
2.2.5. ELISA 49
2.2.6. General sterility 49
2.2.7. Cryopreservation 50
2.3. General Experimental Methods 51
2.3.1. Cell culture technique 51
2.3.2. Quantification of FLS cell viability 51
2.3.2.1. Trypan blue exclusion assay 51
2.3.2.2. LDH cytotoxicity assay 52
2.3.3. RNA extraction and quantification 53
2.3.4. Reverse transcription and first strand cDNA synthesis 53
2.3.5. Quantitative real time PCR 54
2.3.6. Enzyme-linked immunosorbent assay (ELISA) 54

2.3.7. Western blot analysis 55
2.3.7.1. Cell lysis and sample preparation 55
2.3.7.2. SDS-PAGE 56
2.3.7.3. Immunoblotting 56
2.3.8. Immunofluorescent Assay 57
2.3.9. Statistical Analysis 57

Chapter 3 In-vitro characterisation of Osteoarthritic synovial fibroblasts through gene and protein expression profiling

3.1. Introduction 60
3.1.1. Specific aims of chapter 3 63
3.2. Experimental Materials and Suppliers 64
3.3. Experimental Methods 65
3.3.1. Culture of immortalised human FLS cells 65
3.3.2. Sub culturing of human primary FLS 65
3.3.3. PBMC isolation, mRNA extraction and quantification 66
3.3.4. Synthesis of first strand cDNA of PBMCs from mRNA 66
3.3.5. Quantitative real time PCR 66
3.3.6. Agarose gel electrophoresis 67
3.3.7. Meso Scale Human MMP 3-Plex Assay 67
3.3.8. Human IFN-β ELISA design and optimization 68
3.3.9. Statistical Analysis 69
3.4. Results 71
3.4.1. Analysis of basal expression profile of TLRs 1-9 in FLS 71
3.4.2. Analysis of TLR agonist induced and time dependent expression profile of TLR 1-9 genes in FLS 72
3.4.3. Agarose gel electrophoresis quantification of RT-PCR products for TLR 1-10 in FLS 76
3.4.4. Analysis of TLR 2, 3, 4 protein expression in FLS using confocal microscopy 76
3.4.5. Analysis of basal expression profile of major proinflammatory cytokine and chemokine genes in FLS 79

3.4.6. Analysis of TLR or RLR (RIG-I) ligand induced expression profile of major pro-inflammatory cytokine or chemokine genes in FLS 81
3.4.7. Analysis of TLR agonists or sterile inflammatory mediators induced cytokine or chemokine production using human immortalised K4 FLS 83
3.4.8. Analysis of spontaneous and TLR or RIG-I ligand induced secretion of cytokines and chemokines in FLS 84
3.4.9. Analysis of TLR/RIG-I agonist induced pro-inflammatory cytokine secretion in FLS 89
3.4.10. Analysis of sterile inflammatory mediators induced cytokine / chemokine secretion in FLS 93
3.4.11. Analysis of differential TLR 1-9 genes induced with major TLR agonists or inflammatory cytokines or chemokines in FLS 96
3.4.12. Expression profile of RLRs and the adaptor molecules TRIF, MyD88 in FLS 99
3.4.13. Analysis of TLR 3, 4, 7 ligand induced and time dependent gene expression profile of major TLR / cytosolic receptors / adaptor molecules in FLS 100
3.4.14. Analysis of time dependent effect of Poly(I:C) on MMP 1, 3, 9, 13 gene expression in N-FLS and OA-FLS 104
3.4.15. Analysis of TLR/RIG-I agonist induced pro-inflammatory MMPs in FLS 105
3.5. Discussion 108

Chapter 4 Ex-vivo characterisation of OA synovial tissue, fibroblasts and fluid- TLR3 as a therapeutic target for OA?

4.1. Introduction 114
4.1.2. Specific aims of chapter 4 117
4.2. Experimental Materials and Suppliers 118
4.3. Experimental Methods 120
4.3.1. Research design and clinical cohorts 120
4.3.2. Arthoscopic synovial biopsy 120
4.3.3. Processing of arthoscopic synovial biopsies and fluid 125

4.3.4. Synovial tissue histology 125
4.3.4.1. Synovial tissue preparation 125
4.3.4.2. Haematoxylin/Eosin Staining 125
4.3.4.3. Histopathological assessment 126
4.3.5. Isolation and culture of primary OA FLS 126
4.3.6. OA synovial tissue explant culture 127
4.3.7. Meso Scale Human Pro-inflammatory 7-Plex Assay 127
4.3.8. Meso Scale Human RANTES and IFNβ Assay 128
4.3.9. Neutralisation Assays 129
4.3.10. Real time PCR and ELISA analysis of N-FLS stimulated with grade-specific OA-SFs 129
4.3.11. Western blot analysis of Poly(I:C)/OA-SF stimulated FLS 130
4.3.12. Luciferase reporter gene assay 130
4.3.13. Cellular nuclear fraction extraction assay 131
4.3.14. Confocal Microscopy 131
4.3.15. Statistical Analysis 132
4.4. Results 133
4.4.1. *Ex-vivo* analysis of pro and anti-inflammatory cytokines, chemokines and MMP levels in OA synovial tissue explant cultures 133
4.4.1.1. Analysis of spontaneous and TLR agonists induced secretion of pro-inflammatory cytokines in OA synovial tissue explant cultures *ex-vivo* 134
4.4.1.2. Analysis of spontaneous and TLR agonists induced IFNβ and RANTES secretion in OA synovial tissue explant cultures 135
4.4.1.3. Analysis of TLR agonists induced secretion of IL-10, IL-12 p70 and IFNγ cytokines in OA synovial tissue explant cultures 138
4.4.1.4. Analysis of spontaneous and TLR agonists induced pro-inflammatory MMP-1, -3 and -9 secretion in OA synovial tissue explant cultures 139
4.4.2. Histopathological evaluation of synovial inflammation in grade-specific OA synovial tissue 140

4.4.3. *Ex-vitro* analysis of basal and TLR/RIG-I induced pro and anti-inflammatory cytokines, chemokines and MMPs in early and late OA-patient derived synovial tissue FLS 145

4.4.3.1. Analysis of TLR/RIG-I agonist induced pro-inflammatory cytokine and chemokine secretion in early and late OA-FLS 145

4.4.3.2. Analysis of TLR/RIG-I agonist induced IFNβ and RANTES secretion in early and late OA-FLS....146

4.4.3.3. Analysis of TLR/RIG-I agonist induced IL-10, IL-12 p70 and IFNγ secretion in early and late OA-FLS 147

4.4.3.4. Analysis of TLR/RIG-I agonist induced pro-inflammatory MMP-1,-3 and -9 secretion in early and late OA-FLS 150

4.4.4. *In-vitro* analysis of pro and anti-inflammatory cytokines, chemokines and MMPs in grade-specific OA-patient derived cell-free synovial fluid 154

4.4.4.1. Analysis of pro-inflammatory cyto-chemokines in grade-specific OA synovial fluid 154

4.4.4.2. Analysis of IFNβ and RANTES levels in grade-specific OA synovial fluid 158

4.4.4.3. Analysis of IL-10, IL-12 p70 and IFNγ levels in grade-specific OA synovial fluid 158

4.4.4.4. Analysis of MMP-1, MMP-3 and MMP-9 levels in grade-specific OA synovial fluid 160

4.4.5. Analysis of TLR agonist/grade-specific OA-SF induced expression of TLR genes in FLS 164

4.4.6. *In-vitro* analysis of major TLR and cytokine neutralisation assays in N and OA FLS 166

4.4.6.1. Analysis of the effect of anti-TLR/anti-cytokine antibodies on IL-1β secretion in N and OA FLS 166

4.4.6.2. Analysis of the effect of anti-TLR/anti-cytokine antibodies on TNFα secretion in N and OA FLS

167

4.4.6.3. Analysis of the effect of anti-TLR/anti-cytokine antibodies on IL-6 secretion in N and OA FLS 168

4.4.6.4. Analysis of the effect of anti-TLR/anti-cytokine antibodies on IFNβ secretion in N and OA FLS 169

4.4.6.5. Analysis of the effect of anti-TLR/anti-cytokine antibodies on RANTES secretion in N and OA FLS 170

4.4.6.6. Analysis of the effect of anti-TLR/anti-cytokine antibodies on IL-15 secretion in N and OA FLS 170

4.4.6.7. Analysis of the effect of anti-TLR/anti-cytokine antibodies on IL-10 secretion in N and OA FLS 171

4.4.7. Analysis of the effect of TLR3 blockade on TLR, cyto-chemokine and MMP gene expression and on the levels of pro-inflammatory cyto-chemokine secretion in N-FLS 180

4.4.7.1. Modulation of TLR3 and TRIF gene expression by TLR3 blockade in FLS 181

4.4.7.2. Modulation of pro-inflammatory cyto-chemokine gene expression by TLR3 blockade in FLS 182

4.4.7.3. Modulation of pro-inflammatory MMP 3, 9, 13 gene expression by TLR3 blockade in FLS 183

4.4.7.4. Effect of TLR3 blockade on the levels of pro-inflammatory cyto-chemokine secretion in N-FLS 184

4.4.8. *Ex-vitro* analysis of the effect of TLR3 blockade on Poly (I:C) induced pro and anti-inflammatory cytokine, chemokine and MMP levels in early and late OA-patient derived synovial tissue FLS 189

4.4.8.1. Modulation of Poly (I:C) induced pro-inflammatory cyto-chemokine secretion by TLR3 blockade in early and late OA-FLS 189

4.4.8.2. Modulation of Poly (I:C) induced IFNβ and RANTES secretion by TLR3 blockade in early and late OA-FLS 190
4.4.8.3. Modulation of Poly (I:C) induced IL-10, IFNγ and IL-12p70 secretion by TLR3 blockade in early and late OA-FLS 193
4.4.8.4. Modulation of Poly (I:C) induced MMP-1, MMP-3 and MMP-9 secretion by TLR3 blockade in early and late OA-FLS 195
4.4.9. Immunoblot and confocal evaluation of signal transduction modulatory effects of TLR3 blockade in FLS 197
4.4.9.1. Immunoblot analysis of Poly (I:C) induced NF-κB and IRF3 activation in N and OA FLS 197
4.4.9.2. Confocal analysis of modulation of Poly (I:C) induced p65 translocation by anti-TLR3 antibody in N and OA FLS 198
4.4.9.3. Confocal analysis of modulation of Poly (I:C) induced IRF3 translocation by anti-TLR3 antibody in N and OA FLS 198
4.4.9.4. Immunoblot analysis of Poly (I:C) or grade-specific OA-SF induced NF-κB and IRF3 activation in N-FLS, early and late OA FLS 199
4.4.9.5. Confocal analysis of modulation of OA-SF induced p65 and IRF3 translocation by anti-TLR3 antibody in N-FLS 199
4.4.10. Luciferease reporter gene assays to evaluate the specific TLRs and IRFs activating ability of OA-SF and immunomodulatory effect of TLR3 blockade 206
4.4.10.1. Analysis of OA-SF induced NF-κB, IFN-β, RANTES reporter gene activity 206
4.4.10.2. Analysis of OA-SF induced IRF-3, -5, -7, -9 and PRD-II, I-III, IV reporter gene activity 207

4.4.10.3. Modulation of OA-SF induced IFN-β, RANTES, PRD-II and PRDI-III reporter gene activity through TLR3 blockade in HEK293-TLR3 cells 211
4.4.10.4. Modulation of OA-SF induced NF-κB, IRF-3, IRF-7 and IRF-9 reporter gene activity through TLR3 blockade in HEK293-TLR3 cells 211
4.4.11. Confirmatory analysis of immuno-modulatory effects of TLR3 blockade in FLS 213
4.5. Discussion 217

Chapter 5 Proteomic analysis of OA synovial tissue and FLS

5.1. Introduction 223
5.1.1. Specific aims of chapter 5 224
5.2. Experimental Materials and Suppliers 225
5.2.1. Buffers for sample preparation 227
5.2.2. Buffers for In-gel trypsin digestion 228
5.3. Experimental Methods 229
5.3.1. FLS stimulations and protein sample preparation 229
5.3.2. Synovial tissue protein extraction for DIGE analysis 229
5.3.3. Acetone precipitation 229
5.3.4. Bradford Assay 230
5.3.5. Passive In-gel rehydration and IEF 230
5.3.6. 2D-PAGE 231
5.3.7. RUBP's gel staining and image acquisition 231
5.3.8. Analysis of 2D SDS-PAGE gels using Progenesis Software 231
5.3.9. DIGE analysis 232
5.3.10. DIGE image acquisition and analysis 233
5.3.11. Colloidal Coomassie Staining 233
5.3.12. In-Gel Trypsin Digestion and LC-MS analysis 233
5.3.12.1. Tryptic Digestion 234
5.3.12.2. Peptide Extraction 234
5.3.12.3. LC-MS analysis 234

5.3.13. Differential protein quantification though western blot and confocal analysis 235
5.4. Results 236
5.4.1. Differential proteomic analysis of N-FLS and OA-FLS 236
5.4.2. Differential proteomic analysis of Poly (I:C) treated N-FLS and OA-FLS 237
5.4.3. Differential proteomic analysis of CLO-97 treated N and OA-FLS 238
5.4.4. Differential proteomic analysis of RIG-I ligand treated N and OA-FLS 239
5.4.5. Differential proteomic analysis of LPS treated N and OA-FLS 240
5.4.6. Differential proteomic analysis of Pam_2CSK_4 treated N and OA-FLS 240
5.4.7. Differential proteomic analysis of OA-SF treated N-FLS versus control N-FLS and OA-FLS 241
5.4.8. DIGE proteomic analysis of grade-specific OA synovial tissue biopsies 241
5.4.9. Differential protein quantification of vimentin though western blot and confocal analysis 251
5.4.10. Differential protein quantification of prohibitin though western blot and confocal analysis 251
5.4.11. Differential protein quantification of caldesmon though western blot and confocal analysis 251
5.5. Discussion 256

Chapter 6 General discussion

6.1. General discussion 262
6.2. Future work 279
6.3. Conclusions 280

Bibliography 282
Appendix 332

Declaration

This thesis has not been submitted in whole or in part to this or any other university for any degree, and is the original work of the author. The work and information of others have been acknowledged and cited in the text.

Signed_____

Date _____

Acknowledgements

I wish to express my indebtedness and deep sense of gratitude to my thesis supervisor and guide Dr. Sinead Miggin for giving me this opportunity to work in her laboratory and for her keen interest and encouragement throughout the course of this work endeavor. Her guidance and constructive criticism enriched the quality of scientific component and led to the successful completion of this study. Sinead, many thanks for all the understanding and patience all through these years and for having faith in me and offering a post doc position in your lab. I would also like to record my deepest sense of gratitude and sincere thanks to Prof. Paul Moynagh for his fervid cooperation and guidance during the course of my rotational projects and this work .

I also wish to express my heartfelt thanks to Dr. Jakub Siednienko, for his encouragement, guidance and critical appreciation, especially when I was down with yet another flop experiment, and for giving me all the needed help and support to start my work in the lab. To Suaad, what can I say about you.....I feel fortunate to work with you for these three years, and wish to have many more years of work together.....please don't forget to buzz me for a late night chat, I will definitely miss you.

I take this opportunity to thank all the past and present members of the Immune Signalling laboratory, Thusitha, Edel, Enda-(radio kushi) and Aisha for all the understanding and pleasant time in the lab. I would also like to thank all the students (Catriona, James, Dean, Ursula and Cait) who worked on the project with me. And Saket....I can't stop smiling at your silly pipetting….I think you made me laugh the most on my hard days in the lab…thanks for that. I would also like to thank all the Biology Department staff at NUIM for their constant help through these years.

I would like to thank Dr. J.V.S Vidyasagar and Dr. L. Maheshwar, Aware Global Hospitals, Hyderabad, India, for understanding and appreciating the bench-side research and for providing all the required samples for my research work in-time. I also would like to thank all the OA patients who donated their tissue for this research and calmly listened to all my long hours of research detailing without a complaint, I really can't just thank you guys for what you have given me…and wish to give back some hope with our findings. I

also would like to thank Dr. Ursula Fearon and Dr. Mary Conolly, St. Vincents University Hospital, Dublin, Ireland, for their constant help with my *ex-vivo* experiments and patient samples.

"This work was funded by the Health Research Board of Ireland under Grant No. PhD/2007/9"

I would also like to thank my family, especially my god-father…..kaka...I can't thank you for all the love and affection you showered on me all these years, and my parents for giving me this wonderful life….thank you.

And my beloved husband-chandu……..I love you, you are my strength, life and I feel useless without you, and this thesis would not have been possible without your support and constant encouragement. **To you I dedicate this work.**

Abstract

Osteoarthritis (OA) is a multifactorial, painful and disabling disease that affects millions of people globally, with a largely unknown aetiology. OA remains undiagnosed until it becomes symptomatic with advanced structural alterations evident, thus joint replacement may be required. OA is now considered a whole-joint inflammatory disease, associated with synovitis of the fibroblast-like synoviocytes (FLS). FLS are sentinel cells that contribute to OA pathogenesis, through secretion of various catabolic and pro-inflammatory mediators, though the downstream stimuli which initiate and propagate the inflammatory pathway remain poorly defined. Activation of the innate immune Toll-Like Receptors (TLRs) leads to the induction of inflammatory mediators and cellular infiltration seen in most of the joint arthropathies, though the role of TLRs in OA is poorly understood.

The aim of this research work was to characterise the role and functionality of TLRs in OA and to identify the key TLRs that modulate OA pathology. Interestingly, we found that TLR3, activated by dsRNA and endogenous alarm signals contained in the OA synovial fluid (SF), plays a key role in OA and this was confirmed by neutralisation of TLR3 expression which shifted the balance from pro-inflammatory to an anti-inflammatory cytokine milieu. Next using a proteomic approach, we found that prohibitin 1 (PHB1), an anti-proliferative molecule, was drastically down-regulated in FLS upon Poly(I:C) stimulation and this was validated through confocal and immunoblot analysis. Thus, PHB1 may be considered as a potential biomarker for tracing RNA borne synovial hyperplasia, indicative of synovitis which directly implies for OA severity and progression. Following proteomic analysis of grade-specific whole synovial tissue, suppression of key complement C3b in grade-2 OA, was evident.

Furthermore, grade-specific OA-SF showed an ability to predominantly induce IFNβ in FLS and in HEK293-TLR3 cells in a TLR3 dependent manner. Neutralisation of TLR3 significantly inhibited IFNβ production, probably through regulation/blockade of downstream signalling cascades of OA-SF-induced persistent TLR3 activation. Further, luciferase reporter gene assays have suggested that, this effect may be mediated through the transcription factors IRF3 and IRF9, leading to sustained activation of IFNβ genes. Therefore, TLR3 blockade in FLS may inhibit OA-SF-induced activation of TLR3 and

concomitant induction of IFNβ. Likewise, TLR3 blockade also inhibited RANTES production, primarily through blocking of NF-κB. Together, these data indicate that TLR3, expressed on the plasma membrane of FLS, may be a critical target for OA disease intervention.

In conclusion, our data suggests, for the first time that, TLR3 hyper-activation plays a key role in perpetuating synovial inflammation in OA and suggests that therapeutic intervention of OA may be achieved through TLR3 blockade. Despite the significant advances in the understanding and management of OA, significant research must still be undertaken before clinicians can guarantee a quality of life for OA patients, which is free of the debilitating pain. We hope that our efforts would, at least in part, contribute to a better understanding of the pathogenic molecular mechanisms that drive this chronic inflammatory disease. The provision of better treatments will thereby improve the quality of life for patients whose lives are marred by OA and related inflammatory diseases.

Abbreviations

ACN	Acetonitrile
AP-1	Activating protein 1
APC	Antigen presenting cell
APS	Ammonium persulfate
ATP	Adenosine-5'-triphosphate
BMDM	Bone marrow derived macrophages
BSA	Bovine serum albumin
cDNA	Complementary DNA
CHAPS	3-[(3-Cholamidopropyl)dimethylammonio]-1 propanesulfonate
CLO-97	2-(ethoxymethyl)-1H-imidazo[4,5-c]quinolin-4-amine
COX	Cyclo-oxygenase
CpG	2‘ deoxyribocytidine-phosphate-guanosine
DAPI	4‘,6-diamidino-2-phenylindole
DC	Dendritic cell
DMEM	Dulbecco‘s Modified Eagle‘s Medium
DMSO	Dimethylsulfoxide
DNA	Deoxyribonucleic acid
dNTP	Deoxyribonucleotide triphosphate
dsRNA	Double-stranded RNA
dToll	Drosophila Toll
DTT	Dithiothreitol
ECM	Extracellular matrix

E. coli	Escherichia coli
EDTA	Ethylenediaminetetraacetic acid
EIF2AK	Eukaryotic translation initiation factor 2-alpha kinase 2
ELISA	Enzyme-Linked Immunosorbent Assay
ERK	Extracellular-signal-regulated kinases
ESI	Electrospray ionisation
ESR1	Estrogen receptor 1
EV	Empty vector
FADD	FAS-associated death domain protein
FBS	Foetal bovine serum
FLS	Human Fibroblast Like Synoviocytes
g	Gram/s
HEK	Human embryonic kidney
h	Hour/s
HRP	Horseradish peroxidase
HSP	Heat shock protein
HSV	Herpes simplex virus
IAD	IRF association domain
ICAM-1	Intercellular adhesion molecule 1
ICE	IL-1-converting enzyme
ID	Intermediate domain
IFN	Interferon
IFNβ	Interferon beta

IFNAR	Interferon-alpha/beta receptor
Ig	Immunoglobulin
IκB	Inhibitor of NFκB
IKK	IκB kinase
IKKi	Inducible IκB kinase
IL-1	Interleukin-1
IL-1R	Interleukin-1 receptor
IL-1Ra	IL-1 receptor antagonist
IL-1RAcP	IL-1R accessory protein
iNOS	Inducible nitric oxide synthase
IP-10	IFN-γ- inducible protein 10
IPAF	ICE-protease activating factor
IPC	IFN-producing cell
$iPLA_2$	Calcium-independent phospholipase A_2
IPS1	IFN-β promoter stimulator 1
IRAK	IL-1 receptor-associated kinase
IRAK4	IL-1R-associated kinase 4
IRF	Interferon regulatory factor
ISGF3	IFN-stimulated gene factor 3
ISRE	Interferon-stimulated response element
JAK	Janus-activated kinase
JC	Jacob–Creutzfeldt
JNK	c-Jun N-terminal kinase

KD	Kinase-dead
kDa	Kilo Daltons
KO	Knockout
LBD	Ligand binding domain
LBP	LPS-binding protein
Leu	Leucine
LPS	Lipopolysaccharide
LRRs	Leucine-rich repeats
LTA	Lipoteichoic acid
MAL	MyD88-adaptor-like
MALP-2	mycoplasma macrophage-activating lipopeptide-2 kD
MAP	Mitogen-activated protein
MAPK	MAP kinase
MAPKAP	MAPK activated protein kinase
MBP	Myelin basic protein
MCMV	Murine cytomegalovirus
MCP-1	Monocyte-chemoattractant protein 1
MD-2	Myeloid differentiation protein 2
MDA5	Melanoma differentiation-associated gene 5
mDC	Myeloid DC
MDP	Muramyl dipeptide
MHC	Major histocompatibility complex
MIP	Macrophage inflammatory protein

MMTV	Mouse mammary tumour virus
MRI	Magnetic resonance imaging
mRNA	Messenger RNA
MyD88	Myeloid differentiation primary response gene 88
mg	Milligram
ml	Millilitre
µg	Microgram
µl	Microlitre
mQ	MilliQ water
min	Minutes
NALPs	NACHT-LRR and pyrin containing proteins
NBD	Nucleotide binding domain
N-FLS	Normal Fibroblast Like Synoviocytes
NF-κB	Nuclear factor-κB
ng	Nano gram
NK	Natural killer
NLR	Nod-like receptor
N terminal	Amino terminal
OA	Osteoarthritis
OA-FLS	Osteoarthritic Fibroblast Like Synoviocytes
O.D	Optical Density
Pam_2CSK_4	S-[2,3-bis(palmitoyloxy)-(2RS)-propyl]-[R]-cysteinyl-[S]-seryl-[S]-lysyl-[S]-lysyl-[S]-lysyl-[S]-lysine x 3 CF3COOH

Pam_3CSK_4	N-Palmitoyl-S-[2,3-bis(palmitoyloxy)-(2RS)-propyl]-[R]-cysteinyl-[S]-seryl-[S]-lysyl-[S]-lysyl-[S]-lysyl-[S]-lysine
PAMPs	Pathogen-associated molecular patterns
PBMC	Peripheral blood mononuclear cells
PBS	Phosphate-buffered saline
PCR	Polymerase chain reaction
pDC	Plasmacytoid DC
PDK1	3-phosphoinositidedependent protein kinase 1
PG	Peptidoglycan
PHB	Prohibitin
PI3K	Phosphatidylinositol-3 kinase
PKC	Protein kinase C
PMSF	Phenylmethylsulfonyl fluoride
Poly:(I:C)	Polyriboinosinic:polyribocytidylic acid
PRD	Positive regulatory domain
proIL-1β	Pro-interleukin-1β
PRR	Pathogen recognition receptor
PTX	Pertussis toxin
PYD	Pyrin domain
P2X7R	P2X7 receptor
5’ ppp dsRNA	5' triphosphate double stranded RNA
RA	Rheumatoidarthritis
RA-FLS	Rheumatoid arthritis Fibroblast Like Synoviocytes

RANTES	Regulated on activation normal T cell expressed and secreted
RD	Regulatory domain
RIG-I	Retinoic acid-inducible protein
RIP	Receptor-interacting protein
RIP-1	Receptor Interacting protein-1
RLR	RIG-I like receptor
RNA	Ribonucleic acid
rpm	Rotations per minute
RSV	Respiratory syncytial virus
RT	Room Temperature
RT-PCR	Reverse transcriptase- polymerase chain reaction
SARM	sterile α- and armadillo-motif-containing protein
SD	Standard deviation
SDS	Sodium dodecyl sulphate
SDS-PAGE	SDS-polyacrylamide gel electrophoresis
Ser	Serine
siRNA	Small interfering RNA
SNP	Single-nucleotide polymorphism
SOCS	Suppressor of cytokine signalling
ssRNA	Single-stranded RNA
sTLR	Soluble TLR
STAT	Signal transducer and activator of transcription
SV	Sendai virus

T	Thymus
TAB	TAK-1 binding protein
TAD	Transcription activation domain
TAE	Tris-acetate-EDTA
TAK-1	TGF-β-activated protein kinase 1
TANK	TRAF family-member-associated NFκB activator
TBK-1	TANK binding kinase 1
TBST	Tris buffered saline containing Tween 20
TCR	T cell receptor
TE	Tris-EDTA
Th	T helper
TICAM	Toll/IL-1 receptor domain-containing adaptor molecule
TIR	Toll/IL-1 receptor
TIRAP	TIR-associated protein
TIRAP/Mal	TIR-containing adaptor protein
TLR	Toll like receptor
Tm	Melting temperature
TNF	Tumour necrosis factor
TNFR	TNF receptor
TRADD	TNFR1-associated death domain protein
TRAF	TNF receptor associated factor
TRAF6	TNFR associated factor 6
TRAM	TRIF-related adaptor molecule

TRIF	TIR domain-containing adaptor inducing IFN-β
Tregs	T regulatory
TTBS	Tris buffered saline containing Tween 20
VCAM-1	Vascular cell adhesion molecule-1
V	Volts
VEGF	Vascular endothelial growth factor
v/v	Volume per volume
WB	Western blot
wt	Wild Type

Chapter 1

General Introduction

1.1. The immune response

Immunity to disease may be defined as the body's ability to mount an effective defence against a pathogen to prevent such an organism from infiltrating, proliferating and resulting in damage to the host. The key role of immune response is to prevent the infiltration of pathogens and aid in their clearance. This response can be divided into two parts owing to their distinctive characteristics, namely the adaptive and the innate immune response and both these responses communicate and modulate with each other to mount an effective immune response. The innate immune response serves as the first line of defence against invading organism and the adaptive or acquired immune response essentially abet a prolonged pathogen specific defence. Further, adaptive response also establishes immunological memory which allows for a quick resurgence of the pathogen specific response in the event of any recurring challenges to the body by the pathogenic organism. The acquired immune response is centred upon T and B lymphocytes whose activation is dependent upon innate immune cells (Medzhitov and Janeway, 1997b). These lymphocytes are specific for antigens from the pathogen. The adaptive immune response is mediated by these effector cells, wherein, few of these cells expand into dormant memory cells that quickly proliferate and mount a rapid effective immune response, once presented with a specific pathogen derived antigen. Such establishment of potent memory response serves key for successful vaccination (Burgio et al., 1975).

1.2. Innate Immunity

The innate immune response is the non-adaptive first line of defence against a pathogen and is also required to initiate and educate an acquired immune response against the pathogen (Hornef et al., 2002). The innate defences primarily consist of physical barriers to pathogens including the skin and mucosa and also the cilia of the trachea that function to maintain a clear respiratory system. The cells of the mucosa form a tight barrier that prevents the entry of large macromolecules, such as large peptides, viruses, parasites and bacteria, into sensitive somatic sites (Cario et al., 2002). Many pathogens, however, do breach the physical barriers of the epithelium, which results in the mobilisation of innate effector cells to the site of infection to assist in the elimination of such invading organism (Cassatella, 1995). The innate response is mediated to a large extent by phagocytic cells, which include macrophages, dendritic cells (DCs) and polymorphonuclear cells that have direct effector functions in the clearance of pathogens and in the initiation of an adaptive immune response and further, these cells constantly sample their environment by

phagocytosis and may themselves engulf and destroy pathogens (Janeway Jr and Medzhitov, 2002). They also play an important role by secreting a large variety of soluble signalling proteins such as cytokines and chemokines that can regulate the function of the innate phagocytic cells and signal for the infiltration of more innate cells to assist in clearance of the infection (Cassatella, 1995, Melchjorsen et al., 2003). These soluble proteins are also important in the regulation and activation of the adaptive immune response against the pathogen (Melchjorsen et al., 2003, Luster, 2002). Mediators of the innate immune system also induce upregulation of co-stimulatory molecules on dendritic cells (DCs), resulting in recruitment of cells of the adaptive immune system (Janeway Jr and Medzhitov, 2002, Medzhitov and Janeway, 1997b, Cooper et al., 2004). The adaptive immunity detects non-self through recognition of peptide antigens using antigen receptors expressed on the surface of B and T cells (Takeda et al., 2003).

1.3. DCs

The innate and adaptive arms of the immune response function to eliminate pathogens and to generate protective and long lasting immunity against infectious diseases. Innate cells, such as macrophages, neutrophils and DCs, not only play an important role as phagocytic effector cells but also function as sentinels, constantly sampling for pathogens and pathogen-derived molecules such as lipopolysaccharide (LPS), CpG motifs in bacterial DNA and double-stranded RNA from viruses, which are recognised by pattern recognition receptors (PRRs) including Toll Like Receptors (TLRs) (Banchereau and Steinman, 1998, Medzhitov and Janeway, 2000), which are discussed in detail in this chapter. Also, recent studies have even showed that the plasma proteins of the complement system are able to directly target and destroy pathogens and facilitate their phagocytosis (Sarma and Ward, 2011). The stimulation of TLRs by pathogen derived molecules result in DCs maturation. DCs are the most potent of the antigen presenting cells and generate an antigen specific immune response by directing the differentiation of naive $CD4^+$ T cells into functionally distinct T helper type Th1, Th2, Th17 or regulatory T (Tr) cell subtypes, which secrete regulatory cytokines and chemokines (Akira et al., 2001, Kaisho and Akira, 2001, Medzhitov and Janeway, 1997a). Subsequently, these cells aid in activation of the adaptive immune system and thus signify the critical role for TLRs in linking innate and adaptive immunity (Kaisho and Akira, 2001). Apart from random sampling of their external milieu, these phagocytic innate cells also possess specific receptors for the recognition of

conserved pathogen associated molecular patterns (PAMPs) (Medzhitov and Janeway, 2000, Banchereau and Steinman, 1998, Kaisho and Akira, 2001).

1.4. PRRs

It was thought that the innate immune system largely functions in a non- specific manner However, Janeway et al in 1989, reported that the innate immune system specifically detect pathogens via germ line-encoded receptors termed pattern recognition receptors (PRRs) (Janeway Jr, 1989). Hence the cellular recognition of pathogens is thus mediated by a conserved set of receptors that are referred to as PRRs and these receptors recognise conserved pathogen-associated molecular patterns (PAMPs), that are shared by a large group of microorganisms and other pathogens and thereby initiate an immune response (Medzhitov and Janeway Jr, 1999, Medzhitov and Janeway, 1997a). These receptors, which include mannose binding protein, TLRs, integrins and complement receptors, each bind a specific motif shared by a variety of pathogens and the resulting intracellular signalling cascades cause the innate cell to initiate a defensive immune response against the invading microorganism (Medzhitov and Janeway, 1997a, Gordon, 2002). The first proof of specificity in innate immunity came with the discovery of the Drosophila protein Toll (dToll), which was critical for effective immune response to fungus Aspergillus fumigatus in the adult fly (Lemaitre et al., 1996). Soon after that, a human homologue of Toll (hToll, later called Toll-like receptor 4 -TLR4) was discovered (Medzhitov and Janeway, 1997a). Consequently the TLRs form an intensely studied group of PRRs.

1.5. Toll-Like Receptors

To date 13 mammalian TLRs have been identified and have been shown to be required for the activation of responses against pathogens (Takeda et al., 2003). Both humans and mice express TLRs 1-9. In addition humans, but not mice, express TLR-10. Mice, but not humans, express TLR-11, -12, and -13 (O'Neill and Dinarello, 2000, Takeda and Akira, 2005). A large group of cells such as, certain subsets of T cells, B cells, hematopoietically derived sentinel cells such as neutrophils, macrophages and DCs and stromal cells such as fibroblasts, nonhematopoietic epithelial and endothelial cells express TLRs (West et al., 2006).

TLRs are type I transmembrane receptors, consisting of N-terminal leucine-rich repeats (LRR) in the extracellular domain, a Toll/interleukin (IL)-1R (TIR) domain in the

conserved C-terminal cytoplasmic domain and a transmembrane domain (Figure 1.1) (O'Neill and Dinarello, 2000, Takeda and Akira, 2005, Bell et al., 2003). The LRR domain with 24 amino acids aids in PAMP recognition (West et al., 2006).. The TIR domain is analogous to the intracellular cytoplasmic domain of the IL-1R and is highly homologous among individual TLRs. Multiple LRRs are present in the extracellular N terminal domain of TLR's while immunoglobulin (Ig)-like domains are to be found in the extracellular domain of the IL-1R (O'Neill and Dinarello, 2000, Takeda and Akira, 2005) (O'Neill and Dinarello, 2000, Takeda and Akira, 2005). The TLR expression in various cell types can be differentiated depending upon their ligand specificity, cellular responses they induce, signalling adaptors they utilise (Iwasaki and Medzhitov, 2004, Chaturvedi and Pierce, 2009). TLRs are activated by a broad array of PAMPs (Takeda et al., 2003). TLRs 1-9 are well categorized and can be generally specified into two groups depending on their PAMP specificity (Medzhitov and Janeway, 2000). The first group consist of the cell surface TLR 1, TLR2, TLR4, TLR5 and TLR6. The second group includes TLR3, TLR7, TLR8 and TLR9 which are localised to intracellular compartments. A brief illustration of TLR signalling is depicted in Figure 1.2. TLRs have been subject to intensive characterisation as they are key recognition receptors of the innate immune system.

1.5.1. TLR1, TLR2 and TLR6

TLR1, TLR2 and TLR6 are expressed on the plasma membrane (West et al., 2006). Cell wall components including peptidoglycan (PG), lipoproteins and lipoteichoic acid (LTA) from Gram-positive and Gram-negative bacteria are recognised by homo- and heterodimers of TLR2 (Akira et al., 2006). For example, a study reported that gram positive bacteria such as *Staphylococcus aureus* rapidly and effectively caused infection in TLR2 deficient mice (Takeuchi et al., 2000). Further, interaction of PG with cluster of differentiation 14 (CD14) activates TLR2 and supports the hypothesis that CD14 aids in transferring PG to TLR2 thereby facilitating subsequent signalling (Sellati et al., 1998, Vasselon et al., 2004).

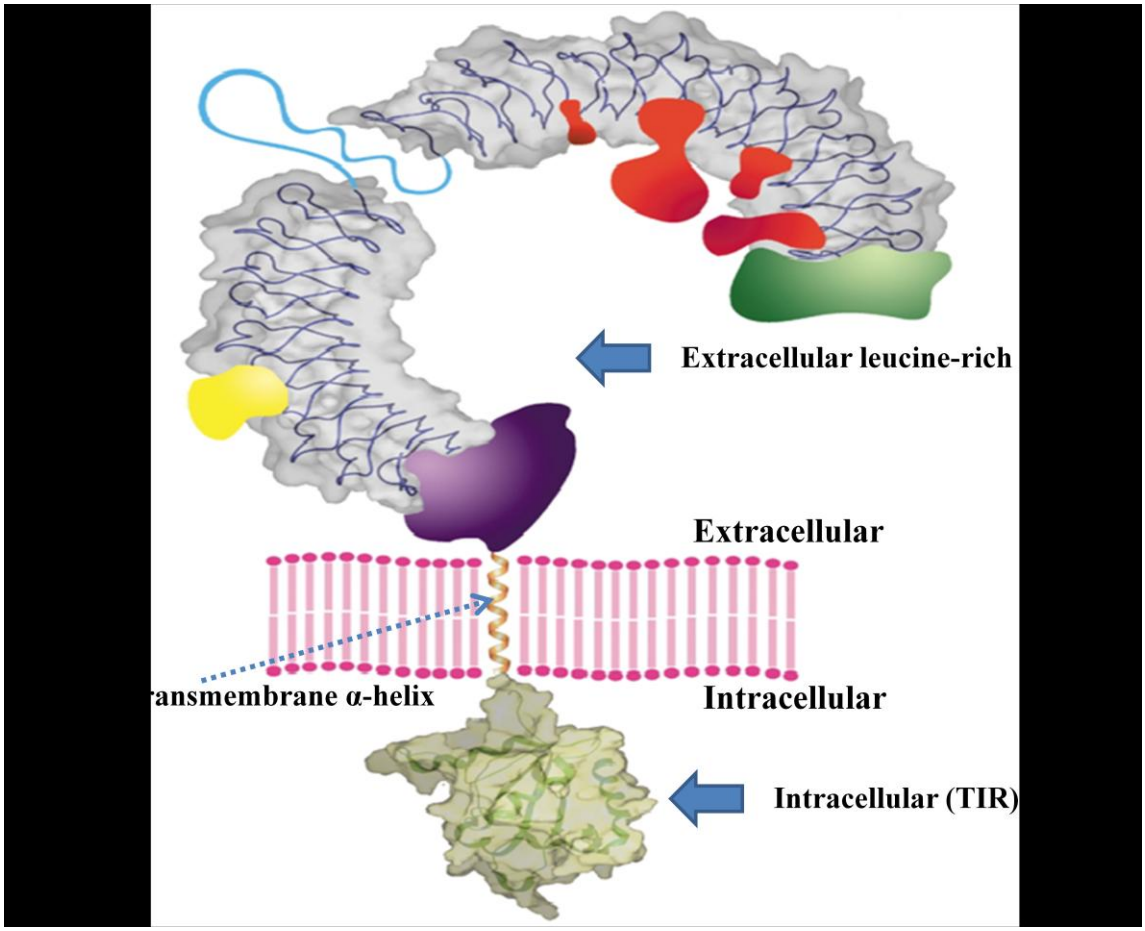

Figure 1.1: General structure of a toll like receptor (Adapted from (Bell et al., 2003)).

Triacyl lipopeptides such as Pam_3CSK_4 (a synthetic bacterial lipopeptide) are sensed by TLR1/2 heterodimers, whereas diacyl lipopeptides such as MALP2 are sensed by TLR2/6 heterodimers (Takeda et al., 2003, Akira et al., 2006, Akira, 2003). This was confirmed by a study which showed that TLR6 deficient mice respond normally to triacylated lipoproteins stimulation, but could not produce tumour necrosis factor alpha (TNF-α) in response to diacylated lipoprotein stimulation (Takeuchi et al., 2000). The sorting adaptor TIRAP and signalling adaptor MyD88 are recruited by TLR2 upon ligand recognition, initiating the MyD88-dependent signalling pathway and inflammatory cytokine production (O'Neill and Bowie, 2007, O'Neill et al., 2003).

1.5.2. TLR3

TLR3 is expressed in DCs, intestinal epithelial cells, uterine, airway, corneal, astrocytes, glioblastoma cells and in as well in stromal cells such as fibroblasts (Akira et al., 2006).

TLR3 is localised both intracellularly on the membranes of intracellular vacuoles as in immature

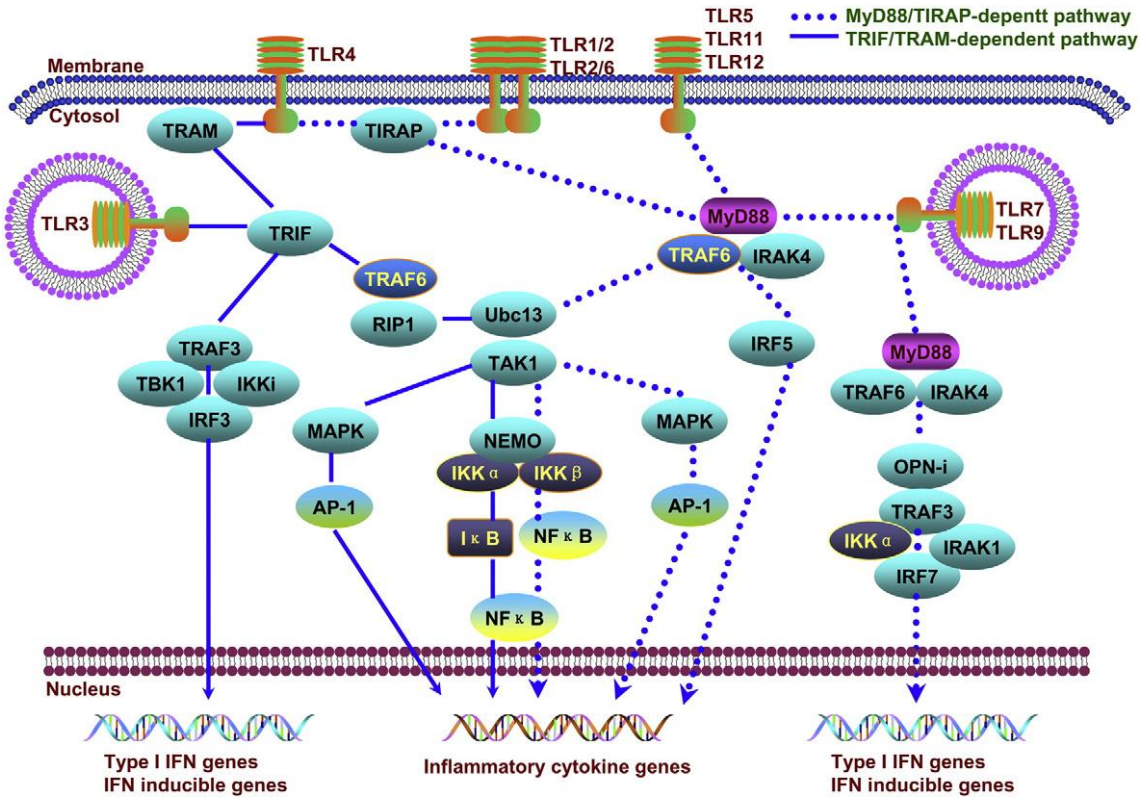

Figure 1.2: Schematic representation of human TLR signalling, showing ligand-induced TLR pathways employing specific adaptor molecules to transduce inflammatory cytokines or type I IFN gene expression (Adopted from (Lin et al., 2011).

DCs, and on the plasma membrane, e.g. fibroblasts (Sun et al., 2006). TLR3 detects dsRNA, a critical intermediary during viral replication (West et al., 2006). Though TLR3 is primarily associated with detection of dsRNA and viruses, it also senses polyriboinosinic: polyribocytidylic acid (Poly (I:C), a synthetic form of dsRNA. TLR3 has also been shown to sense RNA released from necrotic cells (Brentano et al., 2005). The extracellular portion of TLR3 is glycosylated. However, one face is glycosylation free and facilitates its interaction with its ligand whereby the negatively charged dsRNA binds to the positively-charged residues that are present in the form of two distinct patches on this glycosylation-free face (Choe et al., 2005). Ligand binding interaction rapidly increases

TLR expression and recruitment of TRIF which leads to late phase nuclear factor κ B (NF-κB) and early interferon (IFN) regulatory factor- (IRF)-3 activation (Akira et al., 2006). This results in the production of type I IFNs, and inflammatory cytokines, as well leading to the upregulation of co-stimulatory molecules (Akira et al., 2006). Ligation of TLR3 using poly(I:C) and RNA released from necrotic cells resulted in production of inflammatory mediators by synovial fibroblasts in the joint (Brentano et al., 2005). Interestingly, arthritis was induced following intra-articular administration of viral dsRNA in mice, thus supporting the importance of TLR3 in arthritis (Zare et al., 2004). While its expression in epithelial and intestinal epithelial cells was found to act as efficient barrier to infection (Akira et al., 2006), inflammatory diseases such as West Nile virus-driven CNS inflammation are associated with excessive TLR3 activation (Wang et al., 2004). More recent studies have reported that cytoplasmic receptors such as retinoic acid–inducible gene (RIG-I) and melanoma-differentiation-associated gene 5 (MDA5) recognise dsRNA independent of TLR3 (Yoneyama and Fujita, 2009, Yoneyama et al., 2004).

1.5.3. TLR4

TLR4 was the first TLR to be cloned and it has been extensively studied. It recognises endotoxin or lipopolysaccharide (LPS), which is a main component of the outer membrane of gram-negative bacteria (Medzhitov and Janeway, 1997a). It is expressed on monocytes/macrophages, mast cells, myeloid DCs (mDCs) and the intestinal epithelium (Sallusto and Lanzavecchia, 2002). LPS is composed of Lipid A and a polysaccharide joined by a covalent bond and it is the Lipid A that is recognised by TLR4 (Akira et al., 2006). Lipid A, a distinctive phosphoglycolipid, is highly conserved among species (Tsubery et al., 2002). However, the presence of phosphate substituents, phosphorylation status and the number and position of the acyl groups leads to alterations in Lipid A (Tsubery et al., 2002). LPS from Gram-negative bacteria associates with the acute phase protein, LPS-binding protein (LBP) which serves to present LPS to TLR4 and the co-receptor, CD14 (Schumann et al., 1994).. CD14 functions as a receptor for the LPS/LBP complex as LPS/LBP complex is delivered to CD14 following this association. Subsequently, CD14 associates with myeloid differentiation protein 2 (MD-2) and TLR4 since CD14 is deficient of intracellular signalling domain. MD-2 is a small accessory protein belonging to the MD-2 related lipid-recognition family. The extracellular domain of TLR4 is found associated to this MD-2 (Shimazu et al., 1999). The significance of MD-2 in TLR4 ligand recognition has been demonstrated (Schromm et al., 1996). A recent

study reported that, even in the absence of CD14, rough LPS is capable of initiating signals by binding to TLR4-MD2, however these signals can be limited to MyD88- dependent pathway and on the contrary smooth LPS could not initiate signals without co-receptor CD14, yet both rough LPS and smooth LPS can activate MyD88-dependent and independent pathways with CD14 (Akashi-Takamura and Miyake, 2008).

As well as being activated by molecules derived from pathogens several endogenous molecules have been identified which can activate the immune system by signalling along the TLR4 pathways. It has been suggested that these endogenous TLR ligands act as danger signals for the activation of the innate immune system and could be released by dying or stressed cells (Gallucci and Matzinger, 2001). Fibronectin, a molecule that is released from damaged tissue, has been shown to bind TLR4 (Okamura et al., 2001). Heat shock protein (HSP) 60 has also been shown to activate the TLR4 pathway (Vabulas et al., 2001). Cells, including pathogens, produce HSP-60 during stress and may signal the need for an innate response to be directed to the site of stress. Such innate immune system activation by the damage associated molecular patterns (DAMPs) has been demonstrated in OA joint, where binding of Hyaluronan (from tissue damage) to TLR4 initiated the inflammatory signalling cascade (Scanzello et al., 2008). Two important intracellular signalling pathways, the MyD88-dependent and TRIF-dependent (MyD88-independent) pathways are initiated by TLR4 and its vital co-receptor MD2, upon LPS recognition (Miggin and O'Neill, 2006, Fitzgerald et al., 2004). TRIF-dependent pathway primarily induces the expression of type I IFNs along with upregulation of co-stimulatory molecules, while inflammatory cytokines such as IL-6, IL-12, and TNFα, are mostly expressed as a result of MyD88-dependent pathway downstream of TLR4 (Fitzgerald et al., 2004, Takeda, 2005, Miggin and O'Neill, 2006).

1.5.4. TLR5

TLR5 recognizes an evolutionarily conserved site on bacterial flagellin that is required for flagellar filament assembly and motility (Andersen-Nissen et al., 2005). Various immune cells as monocytes, T cells, DCs and NK cells all express TLR5. Expression of TLR5 on epithelial cells provides a sensing mechanism for flagellated bacteria that attempt to cross the epithelium (Akira, 2003). Flagellin-induced TLR5 responses have been detected in various cells types such as DCs, T cells, macrophages, epithelial and endothelial cells (Akira, 2003).

1.5.5. TLR7, TLR8, and TLR9

TLR7 and TLR8 are structurally highly conserved proteins and recognize ssRNA moieties (Wang et al., 2006). Whilst mice express both TLR7 and TLR8, numerous reports suggest that murine TLR8 is non-functional (Zhu et al., 2008). TLR7 recognises resiquimod (R848) which is a synthetic RNA homolog of vesicular stomatitis virus (VSV), an ssRNA virus. R848 is also detected by TLR8 in humans, but not mice (Demaria et al., 2010). Following stimulation with R848 the synthetic antiviral imidazoquinoline compound; TLR7 is overexpressed in TLR8-deficient DCs and enhanced NF-κB activation was observed (Demaria et al., 2010). Nucleosides, uridine or guanosine are extensively found in viral ssRNA and TLR7 cannot differentiate viral RNA or self because these nucleosides are not exclusive to viruses. Also, any ssRNA detected in the endosome triggers a TLR7 triggered inflammatory response (Diebold et al., 2006). Host nucleic acids can still initiate TLR signalling despite the fact that they are not present in endosomal compartments, breaking self-tolerance, and resulting in autoimmunity should the apoptotic debris not be removed efficiently (Midwood et al., 2009). Similarly, autoantibodies produced against self-nuclear antigens such as chromatin, initiates systemic lupus erythematosus (SLE) (Somarelli et al., 2011). TLR9 expression is considered to be restricted to the endoplasmic reticulum and upon recognition of its respective ligand, it is recruited to late endosomes or lysosomes (Leifer et al., 2004). Whilst host DNA does not enter the endosomal compartments, microbial DNA does. Thus, the endosomal localisation of TLR9 is very crucial in discerning self and non-self DNA. Studies have shown that blockade of endosomal acidification by agents completely abate CpG-induced TLR9 activation and signalling (Häcker et al., 1998). Unmethylated CpG motifs and as well synthetic CpG oligonucleotides in bacterial and viral DNA are recognised by TLR9 (Kandimalla et al., 2003). TLR9 along with TLR7 is highly expressed in plasmacytoid DCs (pDCs) (Bekeredjian-Ding et al., 2005). TLR7 and TLR9 undergo stimulation through viral nucleic acids and this induces the production of inflammatory cytokines along with rapid secretion of large amounts of IFNα (Kandimalla et al., 2003) via a MyD88-IRAK4 pathway. A study reported that upon TLR7 and TLR9 interaction, TLR9 antagonises TLR7 signalling (Wang et al., 2006).

1.5.6. TLR10, TLR11, TLR12 and TLR13

Human TLR10 expression was primarily identified in lymphoid tissues e.g. spleen, lymph nodes, tonsil and thymus (Chuang and Ulevitch, 2001) and TLR10 is non-functional in

rodents. Also, the ligand for TLR10 is unknown. Regarding expression, TLR10 expression in human T regulatory (Tregs) was found to be regulated by the transcription factor forkhead box P3 (FOXP3) (Bell et al., 2007). It is believed that TLR10 can both homodimerise and heterodimerise with TLR1 and TLR2 (Hasan et al., 2005). This implies that, TLR10 stimulation can have lipoproteins e.g. as Pam_3CSK_4 as probable target (Govindaraj et al., 2010).

TLR11 is structurally similar to TLR5 and was identified in mice (Zhang et al., 2004). TLR11 was found to be expressed abundantly in bladder and kidneys, recognising uropathogenic bacterial components. Studies have shown that TLR11-deficient mice were susceptible to infections caused by these bacteria (Zhang et al., 2004). However, the exact nature of these ligands has yet to be identified. The presence of a premature stop codon in the gene makes TLR11 dysfunctional in humans and this explicates the cause for human susceptibility to urinary tract infections. Protozoans such as *Toxoplasma gondii* express a class of prolin-like molecules and these can be identified by TLR11 of mouse (Plattner et al., 2008).

Little information exists regarding the expression of TLR12 and TLR13 and their ligand recognition. Macrophages in kidney, bladder epithelial cells and liver were found to express TLR12 and TLR13 (Tabeta et al., 2004), and thus may signify a potential role for TLR12 in preventing urogenital system internal organ infections. Interestingly, in response to murine neurocysticercosis infection, murine TLR12 and TLR13 expression was upregulated in the brain (Mishra et al., 2008). The same group has reported that the endothelial cells of pial blood vessels and astrocytes of the brain expressed TLR13 (Mishra et al., 2008).

1.6. Cytosoilic PRRs

Cytosolic pathogen recognition is mediated by cytosolic PRRs, such as RLRs. They are key players in the recognition of viral nucleic acids (Loo et al., 2008). Viral protein expression and mRNA metabolism along with the cytosolic phase of genome amplification form part of the replication program of all viruses (Wilkins and Gale Jr, 2010) and these molecules are recognised by cytosolic PRRs (Yoneyama and Fujita, 2007). These PRR–PAMP interactions result in PRR-dependent recognition of non-self along with downstream induction of both proinflammatory cytokines and type I IFN (Yoneyama and

Fujita, 2009) which serve to trigger the innate immune signalling programs including inflammation and the maturation of the adaptive immune response (Yoneyama and Fujita, 2007). The RIG-I-like receptors, RIG-I and MDA5, have been identified as vital PRRs for host recognition of a range of RNA viruses (Yoneyama and Fujita, 2009). Although RIG-I and MDA5 are structurally similar, they are activated by distinct viruses (Loo et al., 2008). RIG-I is activated by both positive and negative stranded viruses, including vesicular stomatitis virus, respiratory syncytial virus and related paramyxoviruses, Hepatitis C virus, and influenza A virus (Kato et al., 2006). Conversely, MDA5 recognises picornaviruses and serves as the primary sensor of the dsRNA mimetic poly(I:C) (Kato et al., 2006, Loo et al., 2008). Both RIG-I and MDA5 detect positive stranded RNA viruses, including reoviruses (a segmented dsRNA virus), West Nile virus and Dengue virus (positive stranded RNA viruses) (Loo et al., 2008, Schmidt et al., 2009). Definite RNA structure or nucleotide composition recognized by each of the PRR concludes greatly the virus specificity (Wilkins and Gale Jr, 2010).

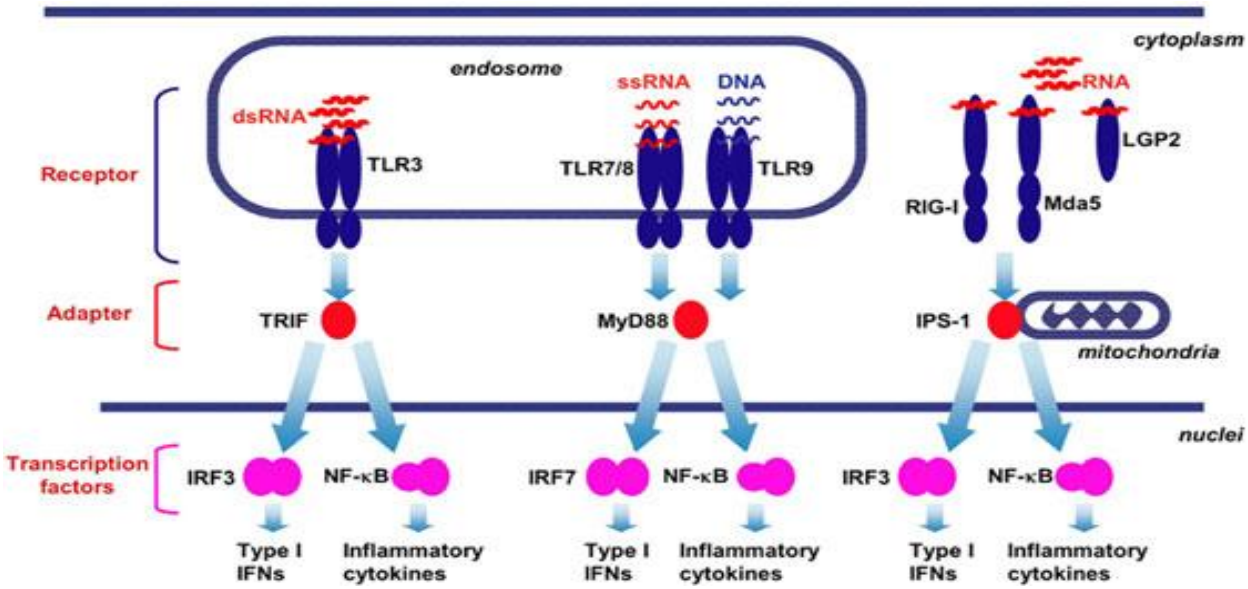

Figure 1.3: TLR and RLR antiviral signalling

TLR3 signals through the TRIF adaptor protein in the presence of dsRNA, whereas, TLR7/8 and TLR9 signals through MyD88 adaptor protein in the presence of ssRNA and DNA respectively. RLRs signals through the receptors RIG-I and MDA5 in the presence cytoplasmic RNA, which as well require mitochondrial localisation and IPS-1 downstream.

In all the events a type I IFN and inflammatory cytokine response is mediated by translocation of IRF and NF-κB transcription factors. Reproduced from (Kawai and Akira, 2008).

1.7. TLR signalling pathways

When highly–conserved PAMPs/ligands are recognised by TLRs, downstream activation of signalling occurs and inflammatory cytokines and chemokines are released. Potent inflammatory responses occur as a result of TLR engagement and the response is characterised by the activation of IFN regulatory factors (IRF), include IRF3, IRF5, and IRF7, and NF-□B thereby inducing the release of pro-inflammatory cytokines (Taniguchi and Takaoka, 2002, Taniguchi et al., 2001) such as TNF-α, IL-1β IL-6, IL-12 and IL-18 and IFNs (Schoenemeyer et al., 2005, Gautier et al., 2005, Taniguchi et al., 2001). NF-κB, is a major transcription factor because of its role in inducing pro-inflammatory molecules such as TNF-α and IL-1β towards the elimination of viral infection (Gautier et al., 2005, Taniguchi and Takaoka, 2002). IRFs induce Type I IFNs such as IFN-α and –β, wherein IFN-α is produced as a result of IRF5 activation (Schoenemeyer et al., 2005, Taniguchi and Takaoka, 2002). IFN-α and IFN-β can be induced by IRF7, however IFN-β is chiefly induced by IRF3 (Sato et al., 2000). When the active IRFs translocate into the nucleus, they bind to promoters which contain the interferon stimulated response element (ISRE), nad induce type I IFNs (Schoenemeyer et al., 2005, Gautier et al., 2005, Sato et al., 2000).

1.8. TLR Adaptors

TLR adaptors play significant role and serve as platforms in organizing downstream signalling events, resulting in specific cellular responses. To date, a total of five adaptor proteins have been discovered, namely MyD88 adaptor-like (Mal, also referred to as TIR-domain containing adaptor protein (TIRAP)), myeloid differentiation protein-88 (MyD88), TIR-domain-containing adaptor inducing interferon (TRIF also known TIR-containing adaptor molecule (Ticam-1)), Trif-related adaptor molecule (TRAM also called TIR-containing adaptor molecule-2 (Ticam-2) and SARM. (Takeda and Akira, 2004).

1.8.1. MyD88

MyD88 was first implicated in TLR signalling in 1998 (Medzhitov et al., 1998), although MyD88 was initially identified in 1990 (Lord et al., 1990). Following IL-1 stimulation, MyD88 recruits IRAK-1 (IL-1R associated protein kinase) to the Interleukin-1 receptor

(IL-1R) complex which results in NF-κB activation (Wesche et al., 1997). MyD88 is 296 amino acids in length and consists of three domains, an N-terminal death domain, an interdomain and a C-terminal Toll/Interleukin-1 receptor (TIR) domain. The C-terminal Toll/Interleukin-1 receptor (TIR) domain enables homotypic interaction with other TIR-containing proteins, while the N-terminal death domain facilitates interactions with the IRAKs (Medzhitov et al., 1998). MyD88 is shared by all the TLRs as it serves as a universal adaptor, except for TLR3 which exclusively recruits TRIF. A study reported that MyD88-deficient mice and macrophages were unable to secrete the pro-inflammatory cytokines TNF-α and IL-6 in response to LPS stimulation (Kawai et al., 1999). Moreover, in LPS-induced cell death events, MyD88 deficient mice were able to survive for longer periods when compared to wild type mice, thus showing that MyD88 plays a fundamental role in TLR signalling (Kawai et al., 1999). It was noted that MAPK and NF-κB activation was still present, albeit delayed in the MyD88 deficient mice in response to LPS but not IL-1or IL-18 signalling and this served as an initial sign for occurrence of MyD88-independent pathways in LPS signalling (Kawai et al., 1999). Other studies conducted using MyD88-deficient macrophages, showed that they were totally unresponsive to TLR2, TLR7 and TLR9 ligands.

Members of the IRAK family are recruited by MyD88 upon stimulation, by means of homotypic interaction via their death domains (Martin and Wesche, 2002, Kollewe et al., 2004), with IRAK1 being of fundamental importance in terms of the ability of LPS to induce NF-κB activation (Li et al., 2002, Swantek et al., 2000). IRAK-4 also plays a significant role in NF-κB activation as it leads to the recruitment and phosphorylation of IRAK-1 (Kollewe et al., 2004, Li et al., 2002, Suzuki et al., 2002). Tumour necrosis factor (TNF)-receptor associated factor 6 (TRAF6) recruitment then occurs a result of the phosphorylation of IRAK-1 (Suzuki et al., 2002). TRAF6, an ubiquitin E3 ligase, works toward the polyubiquitinate of target proteins, including itself (Chen, 2005). Following activation, TRAF6 recruits transforming growth factor activated kinase 1 (TAK1) along with TAK1 binding protein 2 (TAB2). This complex interacts with the upstream kinases for p38 and JNK and with the inhibitor of NF-κB kinase (IKK) complex leading to the activation of NF-κB and subsequent activation of NF-κB dependent genes, including the pro-inflammatory cytokines IL-1, IL-6 and TNFα (Akira and Sato, 2003, Sato et al., 2005, Akira and Takeda, 2004). In pDCs, the activation of TLR7, TLR8 and TLR9 results in IFNα production. This pathway is MyD88 dependent and involves the nuclear translocation of IRF-7 (Honda et al., 2005, Kawai et al., 2004, Honda et al., 2004).

MyD88short (s), IRAK-M and transforming growth factor-b (TGF-□) have been shown to negatively regulate the MyD88 pathway. MyD88s is a splice variant of MyD88 which lacks the interdomain between the DD and TIR (amino acids 110–157). Continuous stimulation with pro-inflammatory cytokines or bacterial products induces MyD88s expression (Burns et al., 2003, Janssens et al., 2003). Studies have shown that TLR2, TLR4 and TLR5 ligand induced NF-κB activation and cytokine production were blocked by TGF- ß and this was mediated through suppression of MyD88 protein without affecting mRNA levels (Naiki et al., 2005). Moreover, IRAK-M downregulates MyD88 signalling by preventing the dissociation of IRAK-1 and IRAK-4, which results in IRAK-1 being unable to interact with TRAF6 and is therefore unable to induce a signalling cascade (Kobayashi et al., 2002). Previous published study in our lab have shown that MyD88 inhibits TLR3 ligand-induced IFN-β production (Siednienko et al., 2011a), thus implying a regulatory role for MyD88 in TLR3 signalling.

1.8.2. Mal

Mal, also termed Toll/interleukin-1 domain-containing adaptor protein (TIRAP was the second TLR adaptor protein to be described (Fitzgerald et al., 2001, Horng et al., 2001). It consist of C-terminal TIR domain and N-terminal PIP2 (phosphatidylinositol 4, 5-bisphosphate) binding domain and is 235 amino acids in size (Horng et al., 2001, Núñez Miguel et al., 2007). Initially, it was identified as a protein that specifically associates with TLR4 (Fitzgerald et al., 2001, Horng et al., 2001)]. Similar to MyD88, over expression of Mal was found to activate NF-κB and JNK (Fitzgerald et al., 2001). Further, Mal was also found to interact with MyD88 in co-immunoprecipitation assays as well as in a yeast two-hybrid screen (Fitzgerald et al., 2001). Whilst Mal-deficient conditions mice responded normally to TLR5, TLR7 and TLR9 ligands (Horng et al., 2002, Yamamoto et al., 2002a), Mal-deficient mice exhibit defects in TLR4 and TLR2 ligand induced cytokine production, activation of NF-κB and MAPK. Like MyD88 deficient mice, Mal-deficient mice showed total resistance to LPS-induced shock. Also, NF-κB and MAPK activation was found to be delayed in response to LPS (Horng et al., 2002). The localization of Mal to the plasma membrane determines its capability to act as a bridging adaptor for MyD88 and this localization is facilitated by its PIP2 binding domain. Distinctively, Mal but not MyD88, contains a putative TRAF6-binding motif (Mansell et al., 2004). Mal is also negatively regulated. For example, polyubiquitination of Mal is mediated by SOCS1 and it occurs on

two N-terminal lysine residues, whereby it mediates the Mal degradation via the 26S proteasome (Mansell et al., 2006). Also, a published study from our lab reported that Mal negatively regulates TLR3-mediated IFNβ gene induction, thus implying a negative regulatory role for Mal in TLR signalling (Siednienko et al., 2010).

1.8.3. TRIF

TRIF was identified during a screen for TIR-containing proteins (Yamamoto et al., 2002b, Oshiumi et al., 2003a). TRIF contains a receptor-interacting protein (RIP) homotypic interaction motif (RHIM) and is 712 amino acids long, large in size compared to other TLR adaptors (Oshiumi et al., 2003b). In contrary to Mal and MyD88, TRIF can activate NF-κB and the IFNβ promoter. Upon examining the interaction of TRIF with various TLRs, it was established that it interacts with TLR3, not TLR2 or TLR4, using a yeast two-hybrid screen and a co-immunoprecipitation assay (Oshiumi et al., 2003b). TRIF was also found to interact with IRF-3. TLR3 activation of NF-κB and IFNβ was inhibited by a dominant negative version of TRIF, but not MyD88 or Mal, and this indicates the distinctive role of TRIF in TLR3 signalling. However, it was also reported that TRIF interacts with both TLR2 and TLR4 in overexpression co-immunoprecipitation assays (Yamamoto et al., 2002b). TRIF-deficient mice failed to produce IFNβ in response to TLR3 and TLR4 ligands and this confirmed the role of TRIF in the MyD88-independent pathway (Yamamoto et al., 2003b). Further, TRIF deficient mice displayed normal LPS-induced MyD88-dependent activation of IRAK-1, NF-κB and MAPK, demonstrating that TRIF is not involved in the TLR4 MyD88-dependent pathway.

Studies have shown that both the MyD88-dependent and MyD88-independent pathways are required for proinflammatory cytokine production (Yamamoto et al., 2003b). It was observed that activation of NF-κB and JNK was entirely suppressed in embryonic fibroblasts from MyD88 and TRIF double knockout mice in response to LPS, substantiating the idea that TRIF is involved in the late activation of NF-κB which was observed in MyD88-deficient mice (Yamamoto et al., 2003a, Kawai et al., 1999). A TRAF6-binding motif was showed to be present in TRIF and it was demonstrated that TLR3-TRIF can activate NF-κB via association with TRAF6 (Sato et al., 2003, Jiang et al., 2004). Various molecules were found to negatively regulate TRIF pathway. SRC homology 2 (SH2) domain containing protein tyrosine phosphatise-2 (SHP2) binds to the kinase domain of TBK1 and was found to restrict the TRIF dependent pathway. SHP2 negatively regulates pro-inflammatory cytokine production in response to TLR3. However,

this was not the case for TLR2, TLR7 or TLR9 ligands. Also, SHP2 was shown to negatively regulate TLR3 and TLR4 ligand induced IFNβ production (An et al., 2006). Consistent with other negative regulators, the knockdown of SHP2 was found to increase TLR3 and TLR4 induced IFNβ production. SARM can also negatively regulate the TRIF, but not the MyD88 pathway (Carty et al., 2006a). A serine protease NS3- 4A expressed by Hepatitis C virus has been shown to lead to proteolysis of TRIF leading to concomitant inhibition of NF-κB and IRF-3, and may possibly attenuate the innate immune response to the virus (Li et al., 2005). Also, a vaccina virus protein called A46R has been shown to interact with all TLR adaptors, excepting SARM (Stack et al., 2005). Interestingly, interaction of A46R with TRIF leads to the inhibition of IRF3 and leads to a suboptimal immune response to the virus (Stack et al., 2005).

1.8.4. TRAM

TRAM, also known as TIR domain-containing adaptor molecule (TICAM-2) and TIR domain-containing protein (TIRP) was identified in 2003 (Oshiumi et al., 2003b, Bin et al., 2003, Fitzgerald et al., 2003). TRAM, a 235 aa protein, is composed of a C-terminal TIR domain (73–232 aa) which functions as a bridging adaptor between TRIF and TLR4 in the MYD88-independent pathway (Yamamoto et al., 2003b). TRAM interacts well with TLR4 and it was also found that TRAM interacts well with TRIF, but not with Mal or MyD88 (Oshiumi et al., 2003b, Fitzgerald et al., 2003). RNAi studies confirmed that both TRAM and TRIF are essential for LPS induced IFN□ production (Oshiumi et al., 2003b). TRAM was reported to be exclusively involved in the TLR4 signalling pathway. Initially it was thought that TRAM was localised to the plasma membrane, and, like Mal, this specific localisation was believed to be necessary for signalling (Rowe et al., 2006). However, recent studies have shown that TRAM is comprised of a bipartite sorting signal which controls its trafficking between the plasma membrane and endosomes and also that TRAM is not involved in inducing TRIF-dependent signalling from the plasma membrane (Kagan et al., 2008). The same group also showed that TRAM along with TLR4 must be delivered to the endosomes to facilitate the activation of IRF-3 signalling events(Kagan et al., 2008). Phosphorylation of the serine 16 by protein kinase C□ (PKC□) was found to be critical for its signalling potential and mutation of this phosphorylation site to Alanine resulted in the loss of TRAM phosphorylation and its ability to mediate TLR4 signalling (McGettrick et al., 2006).

1.8.5. SARM

SARM, 690 amino acids in length, contains two sterile □-motif (SAMs) domains, a C-terminal TIR domain and a N-terminal heat Armadillo repeat motif (ARM) (O'Neill et al., 2003). It was established that human SARM acts as a negative regulator of TRIF-dependent TLR signalling. Also, suppression of endogenous SARM expression enhanced TRIF dependent cytokine production (Carty et al., 2006b).

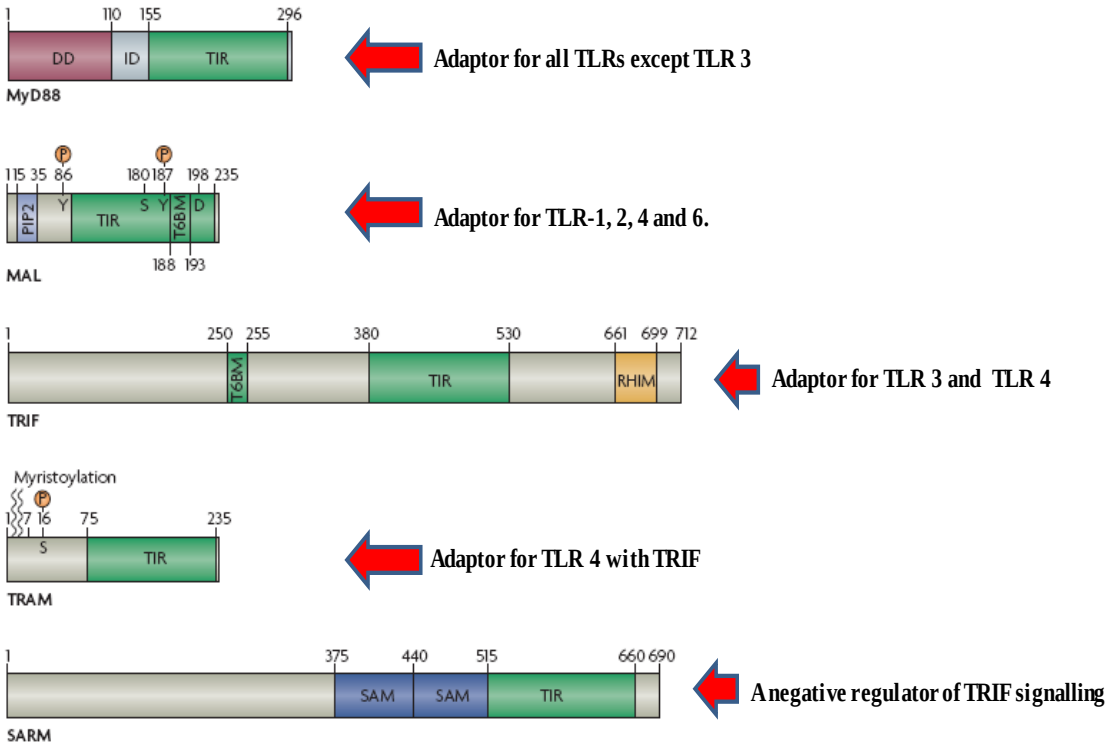

Figure 1.4: Toll-like receptor adaptors family. Toll/interleukin-1 receptor (TIR), Intermediary domain (ID), Death domain (DD), Receptor interacting protein (RIP), Homotypic interaction mMotif (RHIM) (O'Neill and Bowie, 2007).

1.9. Activation of transcription factors

Since the discovery of MyD88, extensive research has been performed towards understanding the dynamics of the TLR signalling pathways. A range of signalling transduction cascades are initiated through individual TLRs and result in the selective recruitment of distinct adaptor molecules. Ultimately, several transcription factors including IRFs and NF-κB are activated and may either act alone or together towards the regulation of gene expression.

1.9.1. NF- κB

Since its discovery, it has become increasingly appreciated that NF-κB is a crucial mediator of the inflammatory signalling pathway and is a central regulator of cell survival (Sen and Baltimore, 1986). Initially, NF-κB was identified in a DNA-binding complex that controlling the Ig light chain gene in mature B cells and nuclear transcription-enhancing factor (Sen and Baltimore, 1986). Since, gene promoters that were not B cell specific were also identified as contained NF-κB binding sites. Thus, ubiquitous NF-κB expression was established, as was the role of NF-κB as a crucial modulator in regulating many inflammatory related gene expressions. Studies have also confirmed that an extrinsic stimulus such as LPS or phorbol ester is required in certain cell types for NF-κB activation (Sen and Baltimore, 1986).

NF-κB is structurally and evolutionarily conserved and consists of five family members namely p100/52, p105/p50, p65 (RelA), c-Rel and RelB. Whilst RelB only forms heterodimers, all the other subunits occur as homo and heterodimers in the cytoplasm of resting cells (Ghosh et al., 1998). A Rel homology domain (RHD) is present in each of the NF-κB subunits at its N terminus and serves to modulate nuclear localisation, dimerisation and cytoplasmic retention by IκB (Ghosh et al., 1998). The DNA-binding domain is located in the N terminal part of the RHD, while the C terminal region of the RHD contains the dimerisation domain. Notably, only the C terminus of p65, c-Rel, and RelB subunits contain the transcription activation domain (TAD) which is essential for target gene expression (Ghosh et al., 1998). The immature precursors, p105 and p100 are cleaved to p50 and p52, respectively, through the action of the ubiquitin/proteasome pathway. As p50 and p52 lack a TAD, they act as transcriptional repressors (Moynagh, 2005). However, p50 and p52 do not act as transcriptional repressors if they heterodimerise with RelB, p65 or c-Rel. Mice lacking RelA, c-Rel or RelB are highly susceptible to Streptococcus pneumoniae and Toxoplasma gondii infections (Ghosh et al., 1998). We have recently showed that the NF-κB subunits RelB and c-Rel negatively regulates TLR3-mediated IFN-β production via induction of the transcriptional repressor protein YY1 (Siednienko et al., 2011b).

IL-1R or TLR ligand stimulation results in downstream activation of the IKK signalosome and this causes further phosphorylation and trafficking of the inhibitory IκBs to the 26S

proteasome for degradation (Hacker and Karin, 2006). The NF-κB complex is then liberated for consequent nuclear translocation and target gene transcription. Two catalytic subunits, IKKα, IKKβ are present in the IKK signalosome complex in conjunction with a regulatory subunit, NFκB essential modulator (NEMO) also known as IKKγ. Previous studies using IKKβ and IKKα-deficient cells established that canonical NF-κB activation is modulated primarily by IKKβ. Also, NEMO-deficient cells failed to activate NF-κB in response to the ligand stimulation by TNFα, IL-1β, and LPS, indicating the significance of NEMO in NF-κB activation (Israël, 2006). I□Bs serve to sequester NF-□B dimers, via the ankyrin repeats sequences contained in I□Bs. By virtue of their ankyrin repeat domains, the IκB proteins mask the nuclear localization signals (NLS) of NF-κB proteins and keep them sequestered in an inactive state in the cytoplasm (Hoffmann and Baltimore, 2006).The IκBs family is comprised of IκBα, -β, -ε and Bcl-3, though the best studied is I□B□. Notably, due to the presence of ankyrin repeats in their C-terminal portion of p105 and p100, they too function as I□B proteins.

Upon stimulation of cells, activation of the NF-κB is initiated by the signal-induced degradation of IκB proteins, through activation of the IKK signalsome. The IKK complex phosphorylates two serine residues located in an IκB regulatory domain. When phosphorylated on these serines (e.g., serines 32 and 36 in human IκBα), the IκB inhibitor molecules are ubiquitinated and degraded. With the degradation of IκB, the NF-κB complex is free to enter the nucleus where it can activate gene transcription through interaction with the NF-□B transcription factor binding sites (Hoffmann and Baltimore, 2006). The canonical NF-κB pathway includes both TLRs and TNF receptor (TNFR) pathways stimulation and finally converges on the IKK complex. In contrast, stimulation of a subset of TNFR superfamily members, including the B cell activating factor (BAFF) receptor, induces NF-κB activation through a non-canonical pathway involving the activation of NFκB-inducing kinase (NIK) and the IKKα subunit. The non-canonical pathway is crucial in the maturation of B cells, regulation and survival (Pomerantz and Baltimore, 2002), as defects of NIK or IKKα in B cells impairs their ability to mature or survive.

1.9.2. IRFs

Interferon inhibition of viral replication was discovered originally in 1954 (Nagano and Kojima, 1954), and the word "interferon" was coined and used for the first time in 1957 by Isaacs and Lindenmann, whose work attained wider recognition (Lindenmann et al., 1957).

Exposure to various infectious agents initiates type I IFN expression and these are multigene family evolutionarily conserved in vertebrates. Considering their capability to interfere with virus replication, type I IFNs are thought as characteristic of an antiviral response (Samuel, 2001). Among cytokine families, type I IFNs are found to be quite variant with multiple subtypes including IFN-α, -β and type II IFNs including IFN–γ are currently identified. Type I IFN secretion is induced in various cell types, primarily pDCs, macrophages and other haemopoietic cells and these cell types are recognised as the main IFN-producing cells (IPCs) (Taniguchi and Takaoka, 2001). Constitutive low level IFN-α/β production by these cells provides cells ready-to-go for the enrichment of cellular responses to external stimuli.

The transcription of multiple types I IFN genes is induced by viral infection and activation of the IRFs mediates this response, at least in part. Recently IRF1 and IRF2 have been included in the family of nine IRFs (Taniguchi et al., 2001). IRF3, IRF5, and IRF7 have been implicated as positive-feedback regulators of type I IFN expression (Tamura et al., 2008). IRFs contain two domains, a C-terminal IRF related domain (IAD) (also termed a regulatory domain (RD)) modulates signal transduction and the N-terminal contains a DNA-binding domain (Mamane et al., 1999, Taniguchi et al., 2001). The DNA-binding domain facilitates binding to 5′-GAAA-3′ and 5′-AANNGAAA-3′ sequences within ISRE, and all promoters of all genes activated by IRFs, respectively (Taniguchi et al., 2001). The C terminal IAD domain also contains a cyclic AMP-response element binding protein (CREB)-binding protein (CBP)/p300 interaction surface, an autoinhibitory domain and various phosphorylation sites. The autoinhibitory domain was found to suppress the transcriptional activity of IRF3, IRF5 and IRF7 (Barnes et al., 2002) and is the mechanism usually used in resting cells to prohibit their activation. Ligand induced phosphorylation activates the IRFs, causing a conformational change, dimerisation and nuclear translocation of the IRFs. Whereas IRF3 contains two autoinhibitory domains, at N and C termini (Lin et al., 1999), the N terminus of IRF5 and IRF7 contain one autoinhibitory domain (Marie, Smith et al. 2000; (Barnes et al., 2002). The N terminus of IRF3, IRF5 and IRF7 contains a NLS to direct their nuclear translocation (Chen and Royer Jr, 2010).

Type I IFN gene expression in response to viral infection is critically regulated by IRF3 and IRF7. The Epstein Bar Virus (EBV) Qp promoter, which regulates expression of the EBV nuclear antigen 1 (EBNA1) was initially described to be bound and repressed by

IRF7 (Zhang and Pagano, 1997 (Zhang and Pagano, 1997). Nuclear accumulation, DNA-binding, dimerization and transcriptional transactivation occur following a conformational change in the transcription factor which is induced by virus-mediated phosphorylation of IRF7 at Ser483 and Ser484 (Yang et al., 2003). Furthermore, phosphorylation of IRF3 induces IFN-β expression, whereas, IRF7 preferentially induces IFN-α (Noppert et al., 2007). Whilst IRF7 expression is very low and cell type dependent, IRF3 expression is pervasive and constitutive in various cell types (Izaguirre et al., 2003). Nevertheless, IRF7 is constitutively expressed by pDCs leading to TLR7 and TLR9 activation, and thus causing rapid induction of type I IFN production through MyD88-dependent pathway (Izaguirre et al., 2003).

Also, IFN-β and IFN-α4 activation mediated via IRF3 can signal through the type I IFN receptor (IFNAR), which activates the Janus activated kinase (JAK)–signal transducer and activator of transcription (JAK–STAT) pathway (Noppert et al., 2007). Such activation of the JAK–STAT pathway leads to activation of IFN-stimulated gene factor 3 (ISGF3) transcriptional regulator, which can induce IRF7 expression. Similar to IRF3, the phosphorylated IRF7 translocates to the nucleus, wherein, binds to positive regulatory domain (PRD) on the IFN-α promoter. Additionally, the biological action of Type I IFNs are also mediated through a well characterised IFNAR signal transduction pathway that elicits the recruitment of a JAK1 and inturn phosphorylation of STAT, STAT1, STAT2 and Interferon regulatory factor (IRF)-9 (Schindler and Brutsaert, 1999, Stark et al., 1998).The phosphorylated STAT1, STAT2 and IRF9 form heterodimers that translocates to the nucleus also leading to the formation of IFN-stimulated gene factor 3 (ISGF3) and culminates in the regulated transcription of many Type I IFN-regulated genes. Therefore, a positive feedback loop ensues due the induction of type I IFN, which aids in production of large amounts of IFN-α/β by cells during viral infection and which if unchecked or dysregulated may as well lead to chronic inflammatory pathologies.

Given that, TLRs and their signalling pathways play a key modulatory role in the innate immune system, their dysregulation can often lead to chronic inflammatory diseases, including Osteoarthritis.

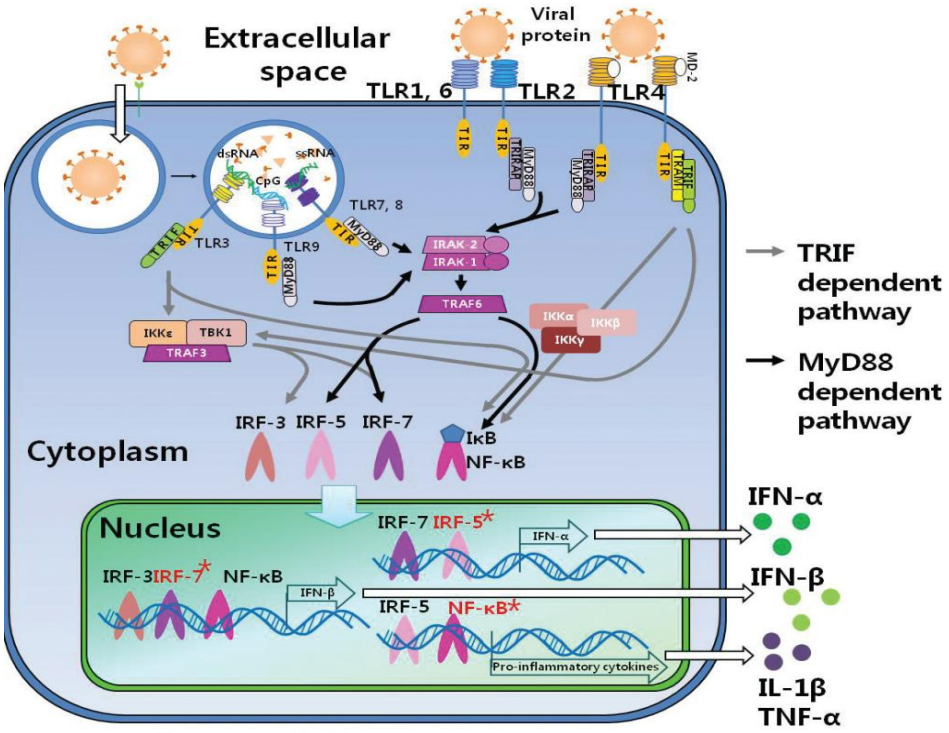

Figure 1.5: Schematic representation of TRIF dependent and MyD88 dependent signalling pathways. Reproduced from (Boo and Yang, 2010).

1.10. Osteoarthritis

Osteoarthritis (OA) is a progressive, debilitating disease of diarthrodial (synovial) joints, previously associated with the aging process and with no known interventions proven to restore cartilage (Harris Jr, 2001, Samuels et al., 2008). At molecular level, OA is characterised by an imbalance between anabolic (i.e. extracellular matrix biosynthesis) and catabolic (i.e. extracellular matrix degradation) pathways, in which articular cartilage and inflammatory synovial processes contribute to OA progression, and OA is now considered as a whole joint disease (Figure 1.6) (David J, 2011, Sellam and Berenbaum, 2010a). It is the most common form of musculo-skeletal disease encountered across all countries of the globe (Table 1.1). In Europe, a joint is replaced due to OA every 1.5 min and the situation is more prevalent in the United States, where a total of nearly 500,000 joint replacements

are performed per annum (Millennium, 2003). According to conservative estimates, the diagnosed symptomatic cases of OA alone represent a huge population (Merx et al., 2003).

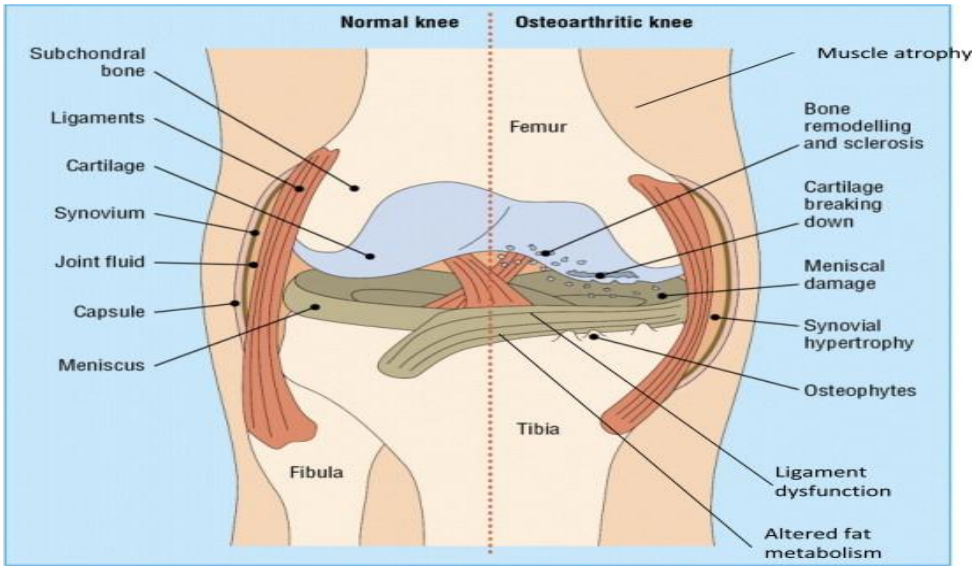

Figure 1.6: Schematic representation of the normal knee joint (to left) and depicting the synovial joint tissues affected in OA (to right). Consistent with the theory that OA is a disease of the whole synovial joint. Reproduced from (David J, 2011).

1.11. Epidemiology and pathology of OA

OA is the most prevalent form of arthritis distressing millions of people globally. OA largely affects joints of the knee, foot, hip and hands, however OA can also affect other joints in the body, but to a lesser extent. Radiological changes such as subchondral bone sclerosis, loss of joint space and presence of osteophytes can be seen in patients suffering with severe OA, which results in joint stiffness, joint pains and loss of function (Samuels et al., 2008, Brandt et al., 1998). However these symptoms may differ with age, time and joint sites and as well individuals, thus the incidence and prevalence of OA is therefore difficult to determine. Age, obesity and joint trauma are considered as important risk factors associated with OA (Wieland et al., 2005). However, a genetic component was also identified (Spector and MacGregor, 2004). Also, OA is common in individuals born with bone and joint disorders e.g. individuals with incorrect joint movement/fitting associated

with congenitally abnormal hip/bowlegs (Carson-DeWitt). OA is expected to increase especially in the developed world due to an aging population. However, the universal feature of ageing cannot be attributed to OA prevalence as many aged people around the world are unaffected by OA (Wieland et al., 2005). Decreased participation in daily activities, limitation of activity coupled with joint or bone pains are the foremost health issues associated with OA. OA in young and middle aged people has become a huge burden due to loss of significant working time and early retirement (Millennium, 2003). Various aetiological risk factors and pathophysiological processes have been attributed to OA (Figure 1.7) (Wieland et al., 2005). Interestingly, RA surprisingly has attracted significantly more scientific and public attention, despite the fact that it is less frequent than OA (Millennium, 2003, Wieland et al., 2005) (Table 1.1).

Table 1.1: Osteoarthritis Epidemiology

Country	2002	2007	2012
United States	13.2	14.4	15.5
Europe	14.5	15.2	15.8
Japan	6.6	6.9	7.2
OA total prevalent cases	34.3	36.5	38.6
RA total prevalent cases	2.8	3.1	3.4

*Number (in millions) of diagnosed total prevalent cases of OA

Reproduced from Decision Resources, Inc., Waltham, Massachusetts, 2004.

Degenerative cartilage breakdown with episodic synovitis observed in OA patients appears to be the primary morphological characteristic of OA (Figure 1.8). Gross knee joint (e.g. Genu varum and genu valgum) deformities are a predisposing factor towards advanced OA and symptoms for this include bone remodelling and attrition, severe cartilage loss and osteophyte formation (Brandt et al., 1998, McDermott et al., 1988).

Increasing evidence suggests that cytokines, growth factors, proteases and other inflammatory mediators which are largely implicated with OA progression are produced

by the synovium, bone and cartilage and OA and all these factors increase the severity of disease by affecting the three constituents of diarthrodial / synovial joints initiating progressive changes in synovium, muscle and bone (Samuels et al., 2008).

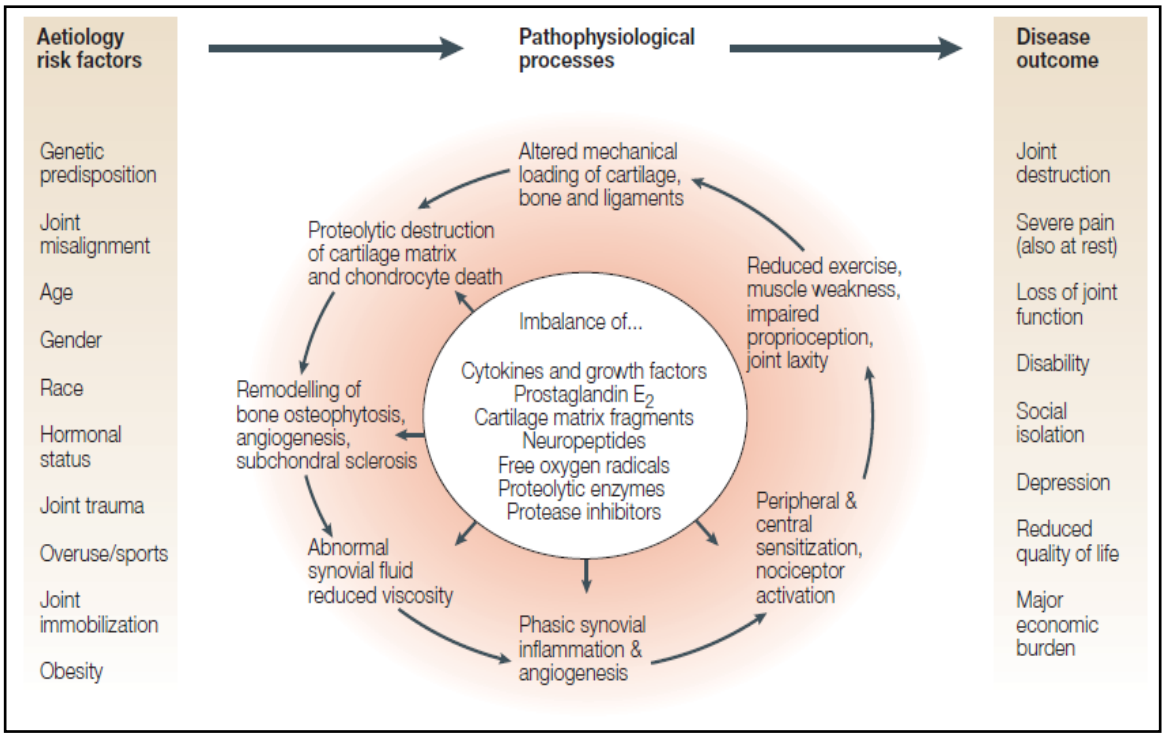

Figure 1.7: Representation of vicious osteoarthritis cycle. A simplified scheme showing the intricate relationship between aetiological factors (left), pathophysiological processes (central) and disease outcome (right). The dysregulation of certain biochemical factors shown in the inner cycle drives the disease process that finally leads to joint destruction. The individual trigger of disease onset is often unknown. Reproduced from (Wieland et al., 2005).

1.12. Inflammation and OA

Although there is an ample evidence supporting the hypothesis that synovial inflammation plays a role in OA disease pathology, OA is still considered as a non-inflammatory disorder owing to the lower than threshold level of leukocytes in the synovial fluid that may be expected in an inflammatory disorder like RA (Dougados, 1996). The synovial membrane plays a protective role in the inflamed joint, by removing unwanted metabolites and products of matrix degradation. Metabolically active synoviocytes are present in the synovial membrane and the serves to nurture the chondrocytes of the joint cartilage (Sutton et al., 2009). Studies within the last 5 years have established that synovial inflammation

and proliferation are key components in OA and play a significant role in disease progression (Sutton et al., 2009, Sellam and Berenbaum, 2010a). Synovial inflammation that develops in OA leads to synovitis and can be identified by arthroscopy, imaging and histology (Figure 1.9) (Samuels et al., 2008).

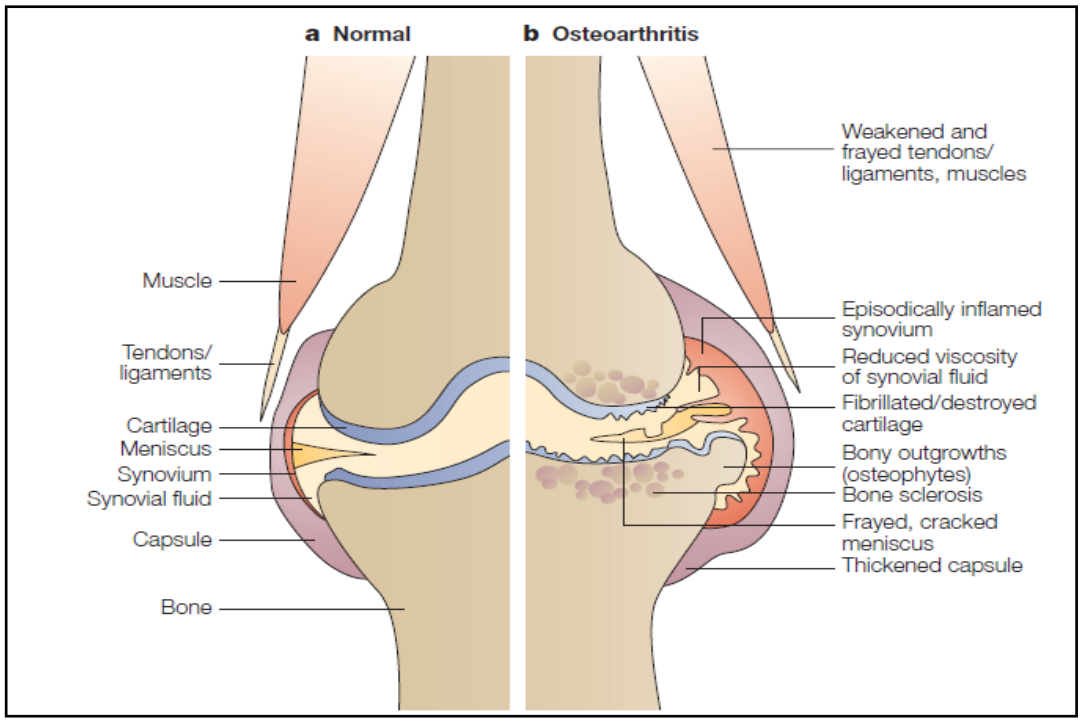

Figure 1.8: Articular structures affected in OA. (a) Healthy tissue showing normal cartilage without synovial inflammation (b) OA tissue showing synovitis and other associated symptoms. Adopted from (Wieland et al., 2005).

Significant variances were found between knee pain and radiographically diagnosed OA of the knee in population-based study (Hannan et al., 2000). Structural variations are asymptomatic in some patients while joint pain in the absence of radiographically detectable alterations were recorded in a few other patients (Attur et al., 2010). Structural variations cannot be made based on joint-space width alone and this could be the central cause for discrepancies observed in the latter case (Attur et al., 2010). More precise measurements such as magnetic resonance tomography (3T-MRI) may be very helpful in the future towards trying to determine the correlation between structural processes and symptoms (Figure 1.10) (Attur et al., 2010). Thus, pathological, arthroscopic and imaging substantiate the hypothesis that synovitis is an integral component of progressive OA (Ayral et al., 2005). It remains to be determined whether synovitis contributes to cartilage

destruction and, therefore, whether drugs targeted at synovial inflammation can slow disease progression (Attur et al., 2010).

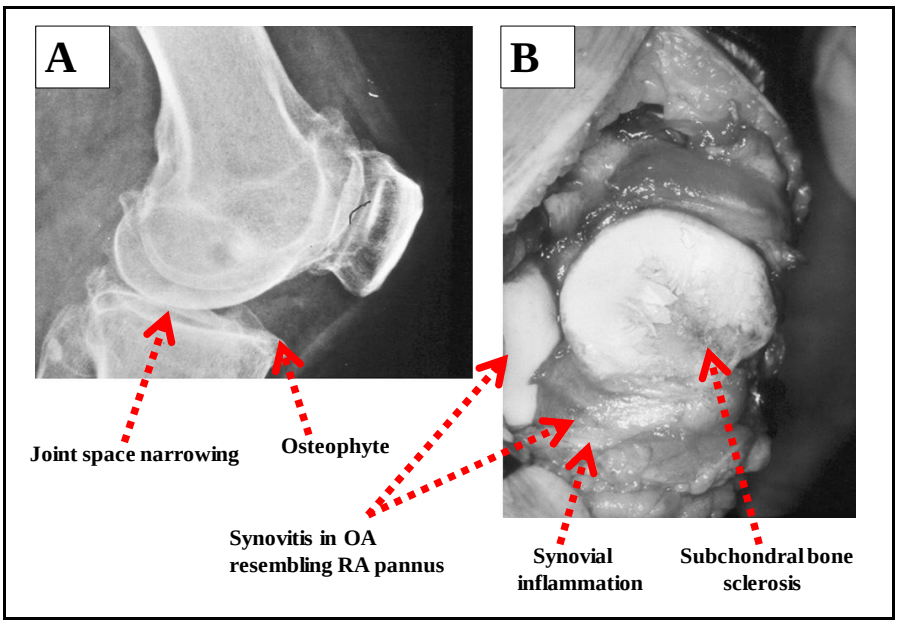

Figure 1.9: Representation of end stage OA knee, showing knee radiograph (A, left) and an intra-operative view of associated synovitis (B, right). Reproduced from (Samuels et al., 2008).

1.13. Role of the synovium in OA pathogenesis

Until recently, OA was believed to be non-inflammatory disease. However, convincing evidence has been provided to support the notion that OA is as inflammatory disease involving synovitis (Sellam and Berenbaum, 2010c). Synovial inflammation produces various catabolic and pro-inflammatory mediators that instigate OA pathogenesis, thus altering the balance between cartilage matrix degradation and repair (Bondeson et al., 2010). The synovium increases matrix metalloproteinase production following pro-inflammatory cytokine stimulation. In the future, anti-inflammatory therapies may facilitate the dampening of pro-inflammatory cytokine induced MMP production.

1.13.1. Physiology of the synovial joint

A minimum of two articulating bones, the joint capsule and the articular cartilage form the synovial joint. The two articular surfaces are held in place by surrounding ligaments and the fibrous joint capsule.

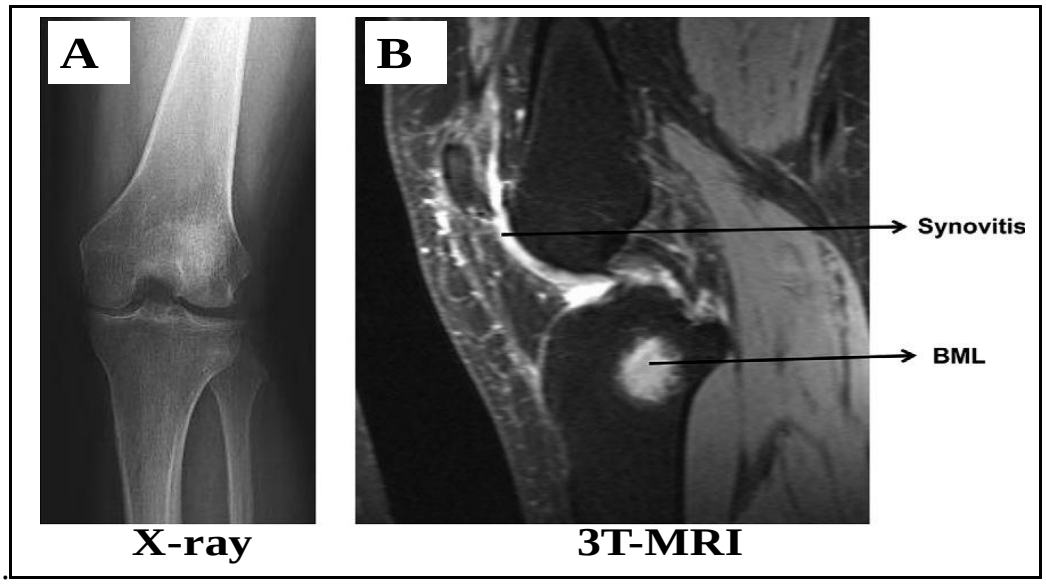

Figure 1.10: Representation of knee OA, showing left panel (A) radiograph of routine semi-flexed AP (anteroposterior) knee and right panel (B) 3 T-MRI of the same patient's knee, showing extensive synovitis and a large bone marrow lesion (BML), demonstrating that the degree of OA is underappreciated on the radiograph. Reproduced from (Attur et al., 2010).

Internally, the capsule is made up of synovial membrane which is a large cellular layer of tissue and externally includes fibrous layer, which is a continuance of the periosteum. The joint capsule is highly innervated and vascularised. The articular surfaces of the joint bones are covered by an avascular supportive connective tissue namely hyaline cartilage tissue. Hyaline cartilage is made up of chondrocytes positioned in extracellular matrix (ECM), and mainly comprise of type II collagen, aggregating proteoglycan and aggrecan, while these components principally provide strength and viscoelasticity (Watanabe et al., 1998). Sulfated glycosaminoglycans (GAGs) such as chondroitin sulfate aid cartilage to stand against compressive forces (Murray et al., 2001). Glycoproteins such as cartilage oligomeric matrix protein (COMP) play a vital role in holding ECM components adhered

(Chen et al., 2007). Furthermore COMP acts as an aggrecan binding protein whereby support cartilage ECM interactions (Smith et al., 2006).

OA leads to fissure development leads to decreased ECM and weakening of the chondrocytes ability to regulate apoptosis and collagen gene transcription (Izumisawa et al., 1996). The joint health and condition are mainly controlled by synovial tissue (ST) as it supplies important nutrient sources and signalling factors to cartilage. Normal synovium, in addition to its role of controlling synovial fluid volume and composition, also contributes to the lubricant characteristics of the synovial fluid by synthesizing and secreting glycosaminoglycans such as hyaluronic acid, into the articular cavity (Firestein et al., 1994, Edwards, 2000). Depending on their cellular composition tissue is arranged such that, it may be segregated into two parts as a sub-lining (subintimal) layer supporting a specialised lining layer or intima. The intima layer of OA hyperplastic synovial tissue mainly consists of type B-synoviocytes or fibroblast-like synoviocytes (OA-FLS), that are usually called as OA synovial fibroblasts and synovial macrophages (type A synoviocytes) (Figure 1.11).

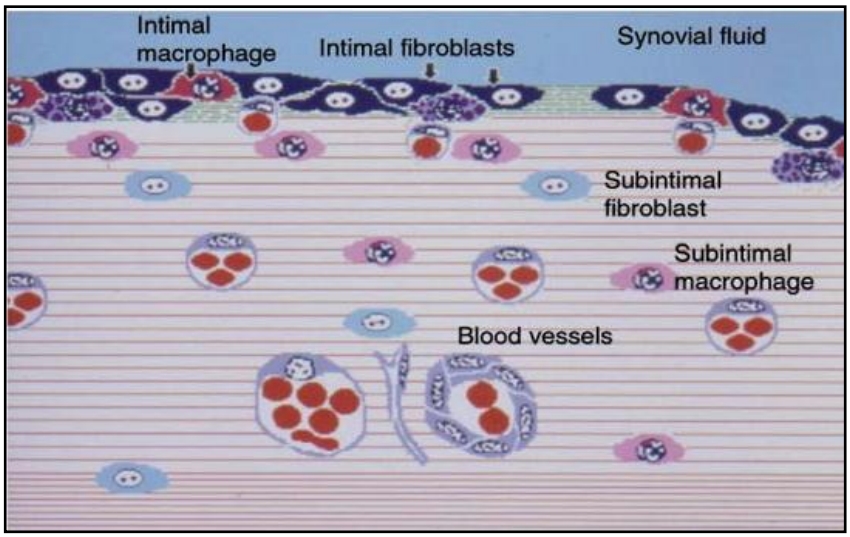

Figure 1.11: Representation of a normal synovium. The intima contains specialised fibroblasts expressing vascular cell adhesion molecule-1 (VCAM-1), decay accelerating factor (DAF) and uridine diphosphoglucose dehydrogenase (UDPGD) (dark blue), and the specialised macrophages expressing FcγRIIIa (dark red). The deeper subintima contains relatively unspecialized counterparts (pale colours). Adopted from (Edwards, 2000).

Areolar or fibrous stromal tissue beneath the surface of the synovium contains a rich microvascular network (Edwards, 2000). Lymphocytes and mast cells are usual, while chondroitin-4-sulphate-containing proteoglycans and collagen are present in distributed state and rather with small amounts of hyaluronic acid. Nutrient diffusion into cartilage of the articulating surfaces of the joint from rich capillary network of the sublining layer enables synovial lining layer nutrition Additionally, the synovial blood provides a channel for influx of inflammatory cells in to the joints in several inflammatory joint diseases.

1.13.2. Features of the inflamed synovium

Hypertrophy (increase in volume) and hyperplasia (abnormal proliferation of cells) are the most significant histological changes occurring in OA and these result in increased number of synovial lining cells. Studies have established a correlation between the histopathological of the inflamed joint and MRI of the synovium, especially in early OA stages (Fernandez-Madrid et al., 1995). The essential features of inflamed synovial tissue in OA have been described and include an increase in the SF volume (Ayral et al., 1996). The typical synovium consists of small amounts of translucent, slender villi with a fine vascular network whilst the reactive synovium consists of thick compact villi and the vascular network becomes undetectable because of loss of transparency. as Also, hypervascularisation of synovial membrane along with propagation of hypertrophic and hyperaemic villi may also be evident (Sutton et al., 2009).

Inflammation in OA generally appears only within a confined area within the joint. However, few biomarkers of inflammation may be traced detected in the circulation. It is believed that inflammatory mediators are released into the circulation from synovium due to the probable release of synovial molecules from inflamed synovial tissue or due to triggering of systemic inflammatory response by damaged cartilage (Sellam and Berenbaum, 2010a). A rise in inflammatory cell infiltration of the synovial tissue is correlated with an increased concentration of C-reactive protein (CRP), and is also associated with increased levels of IL-6 in the SF (Pearle et al., 2007). In OA, the IL-6 concentration is positively correlated with the total leukocyte count (Nishimoto et al., 2008). Rapid disease progression in early knee OA is indicated by large concentrations of high-sensitivity CRP (Spector et al., 1997). In addition, hsCRP is also related to clinical severity, number of involved joints, pain level, and disability. Since hsCRP level correlates with pertinent characters of OA, comprising of structural alterations and clinical inflammatory symptoms, the hsCRP level can be measured as a biomarker of synovial

inflammation in OA patients (Stürmer et al., 2004). Yet, few others studies reported a positive correlation between CRP concentration and body mass index (Pearle et al., 2007). Furthermore, this capability to indicate OA progression is complicated by factors such as BMI, age, and serum concentration of IL-6. Cartilage glycoprotein-39 (CGP-39), secreted by chondrocytes and synoviocytes, has been shown to positively correlate with CRP in OA patients. Thus, it was suggested that CGP-39 could be applied as a surrogate marker of joint inflammation in OA (Conrozier et al., 2000). Typically, aggrecans which are the type II collagen fragments, can act as potential biochemical markers for the synthesis and degradation of these proteins which are highly abundant in OA cartilage matrix (Tabassi and Garnero, 2007). Increased volumes of matrix metalloproteases (MMPs) were detected in synovial cells of patients with rapidly destructive hip OA. It was found that the measure of these enzymes was also elevated in synovial fluid, sera and plasma of these patients (Masuhara et al., 2002).

In contrast to RA, synovial inflammation is not a diffusive process in OA. Synovial inflammation dispersion is patchy and is limited to areas close to cartilage damage sites in OA (Ayral et al., 2005). However, in late primary OA associated with infiltration of macrophages, neovascularisation within the joint becomes indistinguishable from that observed during RA, microscopically. Also, secondary OA is radiographically attributed to deposition of calcium pyrophosphate dehydrate (CDDP) crystals. CDDP itself is an extremely potent proinflammatory agent. Yet, the relationship between CDDP crystals in the joint and the incidence of histological synovitis is yet to be proved (Walsh et al., 2007). Whilst early stage OA present with less extensive cartilage, pathological changes have occurred and this implies that synovium is involved early in the disease process. However, it is yet to be established that, if the morphological changes arising in OA synovial membrane are primary or they occur just because of cartilage degradation, lesions of the subchondral bone and joint inflammation. Degenerative cartilage is not constantly and entirely related to synovitis even though it was noticed purely at the sites adjoining to degenerative cartilage and this implies that cartilage-breakdown products may trigger the inflammation (Sutton et al., 2009). $CD4^+$ are the key T cells that infiltrate the synovium, however they are complemented by $CD8^+$ T cells and B cells (Fernandez-Madrid et al., 1995). CD3 expression is receded on $CD4^+$ T cells and it appears to be an indicator of their activation suggesting involvement of local chronic T-cell stimulation in OA. A study reported on reactivity of T cells towards chondrocyte membranes and it specifies that products of cartilage breakdown serve as source of antigens for these T cells (Alsalameh et

al., 1990). Synovial membranes rarely show B cells, but those present, show an activated state. CXC chemokine ligand (CXCL-a potent chemoattractant of B-cells) can exist in the synovial membrane lymphoid aggregates and its presence could attract activated B-cells (Shi et al., 2001, Luster, 2002). Breakdown products of type II collagen, antibodies against autoantigens were recognised and their presence indicates that synovium-infiltrating B cells produced these antibodies locally (Jasin, 1985).

1.13.3. Mediators of Inflammation and joint destruction

Clinical symptoms, such as joint swelling, inflammatory pain and synovitis are observed in OA due to synovial inflammation. The inflamed synovium produces catabolic and proinflammatory mediators such as cytokines, prostaglandin E2, neuropeptides and nitric oxide. These products then affect cartilage destruction and repair, triggering excessive proteolytic enzyme production that intensifies the cartilage breakdown (Figure 1.12) (Sellam and Berenbaum, 2010a). Synovial inflammation is further amplified by increased cartilage catabolism; as a result a vicious circle is created. Activated synovial T cells, B cells and infiltrating macrophages further exaggerate the inflammatory response. Since synovitis reflects joint deterioration in OA, and is also related with clinical symptoms, synovium-targeted therapy may be helpful in assuaging the disease symptoms and prevent structural progression. Structural progression of the disease can be determined by synovitis as it is identified to be subject for various clinical symptoms. Owing to the action of numerous soluble mediators, it appears to be a significant component in OA pathophysiology. Hence it is believed that, developing synovitis targeted treatment would be very useful for both structural changes that occur in OA and disease symptoms (Sellam and Berenbaum, 2010a).

In addition, MMPs are produced by OA chondrocytes and synovial cells and serve to break down cartilage. Immunohistochemistry has been used to detect MMP-3 and the level of staining of MMP-3 is directly interrelated to the infiltration of inflammatory cells into the synovium (Yuan et al., 2004). Inflammation in OA synovial membrane was thought less pronounced than RA, but studies reported that OA patients both in early and advanced stages have revealed significant amounts of cellular infiltration and neovascularisation (Walsh et al., 2007). It was also noted that activation markers such as CD69 were often expressed by infiltrating lymphocytes.

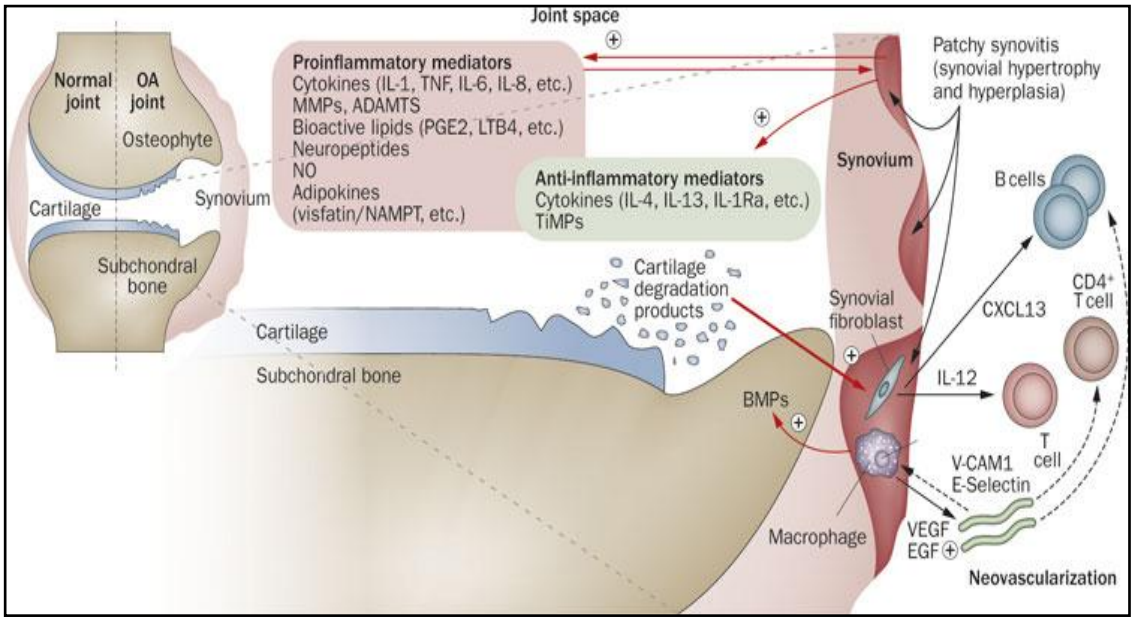

Figure 1.12: Representation of the synovium involvement in OA pathophysiology and progression, showing pro- and anti-inflammatory mediators, cartilage degradation products and adhesion molecules perpetuating the chronic inflammatory milieu prevalent in the OA joint. Reproduced from (Sellam and Berenbaum, 2010a).

The three factors, inflammation, macrophage infiltration and endothelial cell proliferation are found to be closely inter-related as these were noted to be in higher extent in OA patients compared to healthy controls (Walsh et al., 2007). These processes may also influence pain severity and disease progression. Angiogenesis facilitates inflammation, as inflammation actuates angiogenesis. Angiogenesis in the synovium may appear at all stages of OA and is intently associated with chronic synovitis (Haywood et al., 2003). Neovascularisation is specified by increased production of the proangiogenic factor VEGF in the OA synovium. Angiogenesis in the OA synovium can also be brought about by hypoxia through the production of hypoxia inducing factor-1α. Endothelial cell proliferation measures are higher in RA compared to OA. However, vascular densities are same in both diseases (Haywood et al., 2003). In the recent times, it is considered that by potentiating and perpetuating rather than initiating inflammation, angiogenesis contributes to the progression from acute to chronic inflammation (Haywood et al., 2003).

1.13.4. FLSs in the joint

An altered arthritic fibroblast-like synoviocyte (FLS) phenotype was reported in 1983 (Fassbender and Simmling-Annefeld, 1983). Since then, increasing evidences suggest that FLS are significant contributors for joint destruction in various arthriditis (Fassbender and Simmling-Annefeld, 1983). FLS in healthy joints aid in matrix remodelling and supplies lubricating molecules such as hyaluronic acid and nutrients to the joint cavity and nearby cartilage. Various studies have recognised FLS transition from mesenchymel cells to destructive cells (Firestein, 1996, Ritchlin, 2000), whereby the synovial cells proliferate, adhere and consequently invade the joint structures prior to migration of inflammatory cells into the synovium (Gay et al., 1993). Another study reported that in the severe combined immunodeficient (SCID) mouse model of cartilage destruction, in the absence of inflammatory cells, implanted human RA-FLS degraded co-implanted human cartilage, thus confirming inflammation-independent RA-FLS activation (Müller-Ladner et al., 1996). Various studies have reported high invasive phenotypes and low proliferative indices in RA-FLS (Seemayer et al., 2003), whereas, OA-FLS have been shown to possess high proliferative indices (Benito et al., 2005, Fernandez-Madrid et al., 1995, Sutton et al., 2009) and very little or no information exists regarding the invasive phenotype of OA-FLS. It may be speculated that OA-FLS at a similar end stage disease to RA-FLS may also exhibit an invasive phenotypes upon activation by endogenous/exogenous stimuli.

An inflammatory microenvironment within the joint impairs apoptotic pathways and has been proposed to be responsible in part for the survival and invasive phenotype of RA-FLS cells; a similar mechanism may be shown in OA-FLS. Microbial fragments stimulate FLS through TLRs and, as sentinel cells, are considered to contribute significantly to various inflammatory pathways in the joint. FLS behave as effector cells in the synovium, secreting chemokines to mediate the chemoattraction of leukocytes (Müller-Ladner et al., 2007, Buckley et al., 2001). T-cell migration towards fibroblasts is enhanced by stromal cell derived growth factor-1. This growth factor-1 production as well CXCL16 production by FLS rapidly intensifies $CD4^+$ T cells influx into the synovium (Ruth et al., 2006). Furthermore, various chemotactic molecules such as macrophage inflammatory protein (MIP), monocyte chemoattractant protein (MCP), IL-8 and RANTES can be produced by FLS following cell-cell contact with T lymphocytes (Sutton et al., 2009). Direct contact between fibroblast and macrophage leads to the activation of inflammation processes and tissue damage and consequential production of proinflammatory cytokines such as IL-6,

IL-8 and GM-CSF (Sutton et al., 2009, Sellam and Berenbaum, 2010a, Kapoor et al., 2010). Regulatory cytokines such as IL-10, IL-13 and the IL-1 receptor antagonist (IL-1RA) are also induced and serve to downregulate or enhance proinflammatory cytokine production (Sellam and Berenbaum, 2010a). Using an *in vitro* monocyte-synoviocyte interaction model, induction of IL-6 was seen and this was regulated by the monocyte specific cell surface marker, CD14 (Chomarat et al., 1995). Another *in vitro* study on cartilage degradation reported that the degradation is promoted by the synergistic interaction of mouse macrophages and fibroblasts in a co-culture model (Janusz and Hare, 1993). Thus, FLS play a significant role in synovial joint homeostasis through the direct secretion of proinflammatory cytokines and through their synergistic effects on other cells within the joint.

1.14. Inflammatory cytokines in OA

Cytokines, non-structural proteins between 8 to 50 kDa, modulate cell replication, differentiation, survival, cell death, tissue repair and fibrosis (Westacott and Sharif, 1996, Goldring and Goldring, 2004). Cytokine secretion from the inflamed tissue, may act in an autocrine (acting on the same cell), juxtacrine *(via* cell-cell contact) or paracrine (on surrounding cells) dependent manner. Various processes such as articular destruction, inflammation, and the co-morbidities associated with disease are triggered and affected by active cytokines in the arthritis joint (Sellam and Berenbaum, 2010a). However, the exact instigators that bring about the local inflammation in synovium and leads to activation of downstream pathways require further investigation.

Numerous studies have shown that ccytokines modulate OA pathogenesis by impacting on cartilage, synovial membrane and the bone during disease progression (Figure 1.12 and 1.13) (Kapoor et al., 2010, Sutton et al., 2009, Sellam and Berenbaum, 2010a). Further, these cytokines are thought to induce the production of other cytokines and degenerative proteases by stimulating chondrocytes and synoviocytes in the cartilage (Sellam and Berenbaum, 2010a, Kapoor et al., 2010). Since TNFα inhibition was successful in abating RA, cytokines have attained significance as prognostic biomarkers to determine other joint diseases such as OA and a search for probable targets for therapeutic intervention began. IL-1β, TNFα and IL-6 have been linked with OA pathogenesis (Sellam and Berenbaum, 2010a). These cytokines are primarily produced by activated synovial fibroblasts, macrophages, mononuclear cells, and articular cartilage (Kapoor et al., 2010). Significant

quantities of IL-6 and IL-10 along with various chemokines are present in OA synovium (Furuzawa-Carballeda et al., 2008). High levels of IL-1β and TNFα were detected in synovial fluid of patients with early OA compared to late OA patients. These stage specific distinctions in released cytokines and mediator profiles are now considered to be linked to alterations in mononuclear cell infiltration level (Benito et al., 2005). IL-1β and TNFα can stimulate their own products in an autocrine manner because synovial fibroblasts bear high concentration of the IL-1β and the TNF receptors.

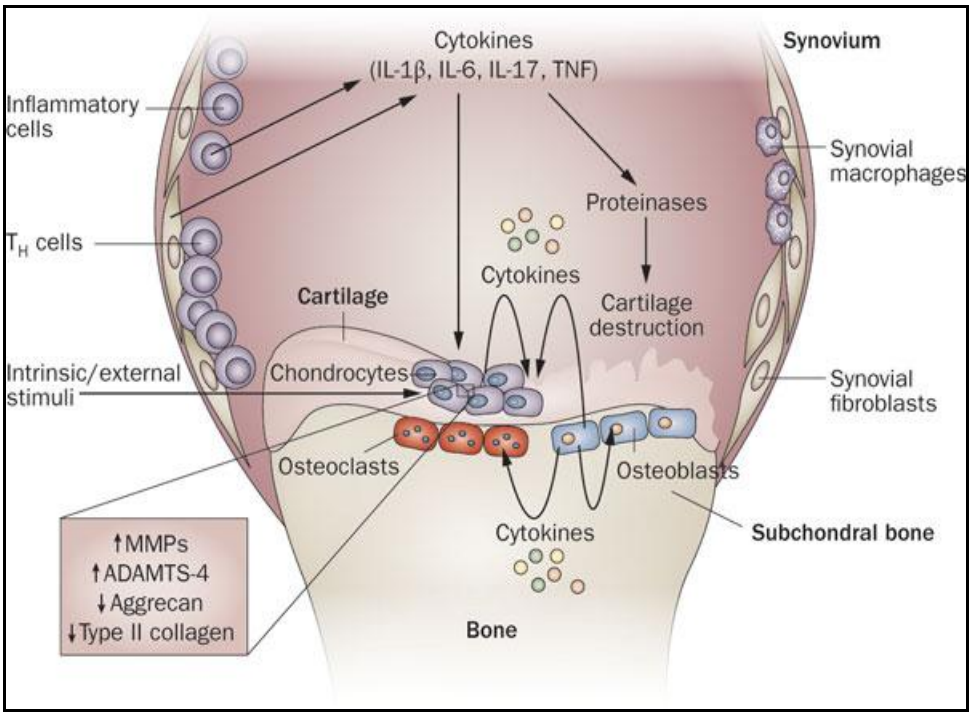

Figure 1.13: Representation of the role of proinflammatory cytokines in the pathophysiology of osteoarthritis, showing secretion of inflammatory cytokines by synovial fibroblasts and their action on cartilage degradation. Adopted from (Kapoor et al., 2010).

These cytokines can also induce other cytokines as IL-6 and IL-8 by stimulating synovial cells and chondrocytes. Further, these proinflammatory cytokines can then diffuse into the synovial fluid and act on the cartilage matrix and chondrocytes (Sadouk et al., 1995). IL-15 is produced by innate immune response and higher concentrations of IL-15 levels were detected in synovial fluid of patients with early OA compared to late-stage OA, for which

IL-15 is linked to early OA. Cells of outer synovial lining and the endothelium hold the IL-15 receptor. This IL-15 may actuate MMP production, as well the recruitment or survival of $CD8^+$ T cells within the OA joint (Scanzello et al., 2009).

Regarding the IL-1 superfamily, most of these cytokines are associated with various arthropathies such as OA and RA. IL-1α and IL-1β are produced as precursors of approximately 35kDa and are encrypted by two distinct genes. In addition to natural IL-1 receptor antagonist (IL-1ra), IL-1α and IL-1β are extensively expressed within the synovial membrane (Dayer, 2003, Fernandes et al., 2002, Firestein et al., 1992). IL-1 is synthesised by various cell types following cytokine stimulation, they include synovial cells, endothelial cells, mononuclear phagocytic cells, neutrophils and keratinocytes and particularly by OA-FLS (Sadouk et al., 1995). This results in IL-1-directed regulation of the inflammatory response, such as stimulation of further cytokines and chemokines, the up-regulation of adhesion molecules, and the synthesis and secretion of MMPs and growth factors (Dinarello, 1998, Abramson and Yazici, 2006, Goldring and Goldring, 2004). For example IL-1β was reported to be the major autocrine cytokine involved in the stimulation of metalloproteases and IL-6 synthesis in OA synovium (Pelletier et al., 1995).

TNFα is synthesised by various cell types such as activated NK cells, neutrophils, monocytes, lymphocytes, macrophages and fibroblasts (Sadouk et al., 1995). Research studies demonstrating the capability of TNFα to degrade both bone (Bertolini et al., 1986, Martel-Pelletier et al., 1999) and cartilage (Dayer et al., 1985, Loeser et al., 2005) confirmed its significant role in arthritis. TNFα acts as autocrine stimulator and also as powerful paracrine inducer of various other pro-inflammatory cytokines as IL-1, IL-6, IL-8 and GM-CSF (Choy and Panayi, 2001, Sutton et al., 2009). Furthermore, TNFα is chemotactic for leukocytes, is a potent inducer of angiogenesis (Frater-Schroder et al., 1987, Leibovich et al., 1987, Fràter-Schröder et al., 1987, Walsh et al., 2007), stimulates adhesion molecule expression in OA and RA FLS *in vitro* (Marlor et al., 1992, Sakurada et al., 1996, Furuzawa-Carballeda et al., 2008) and lymphoid migration into inflamed synovial tissue *in vivo* (Wahid et al., 2000).

IL-6 is produced by B lymphocytes, T lymphocytes, and fibroblast and levels are elevated in the synovial tissue of OA and RA patients (Asquith and McInnes, 2007, Sutton et al., 2009). It is now established that IL-6 facilitates various functions and the maturation and activation of B and T cells, chondrocytes, endothelial cells, osteoclasts, and macrophages, are significantly affected by IL-6 in RA (Brennan and McInnes, 2008). IL-6 receptor (IL-

6R) is a heterodimeric receptor of IL-6α and gp130 subunits and it aids in IL-6 signalling as IL-6 signals *via* this receptor (IL-6R) (Nishimoto and Kishimoto, 2006a).

1.15. Therapeutic treatment in OA – past, present and future

Numerous factors including mechanical, biochemical and genetic factors contribute to OA pathogenesis, thus makes it demanding to determine definitive target for the therapy. As mentioned earlier, the present pharmacological interventions mainly emphasise on enhancing disease symptoms (Schulte et al., 1994). With the exception of anti-inflammatory corticosteroids and nonsteroidal anti-inflammatory drugs (NSAIDs) which inhibit cyclooxygenase-2 (COX2), the enzyme responsible for prostaglandin biosynthesis in inflammation, no specific therapy based on fundamental intracellular pathways of chondrocytes and synoviocytes exists for the medical management of OA (Malemud, 2004). Typically, simple analgesics such as acetaminophen, and the NSAIDs were used in the medical management of OA so far, where primary focus being signs and symptoms for the disease treatment (Flower, 2003, Topol, 2004, Petit-Zeman, 2004, Felson, 2004). Though COX2 agents and NSAIDs are widely used, their usage is limited due to side effects such as gastrointestinal, cardiovascular and renal effects in many patients (Figure 1.14) (Hannan et al., 2000, Flower, 2003).

Articular injections of corticosteroids and hyaluronans have been adopted as secondary therapies and were found to yield symptomatic benefits in a few patients. However, approved disease-modifying OA drugs (DMOADs) that can restore functional integrity to the diarthrodial joint or reverse cartilage destruction are not currently available. Symptomatic treatment is the only existing oral drug therapy for OA, where analgesics or anti-inflammatory agents, such as acetaminophen (also known as paracetamol) or COX2 inhibitors are used. However, in September 2004, the COX2 inhibitor, Rofecoxib (Vioxx; Merck) was withdrawn from the market (Flower, 2003). In some countries, intra-articular hyaluronic acid preparations

are used as drugs for symptomatic relief. Symptom modifying treatment focuses on non-specific relief of pain. However, a therapeutic approach towards curtailing the progressive joint destruction associated with OA must be central for DMOAD therapy (Petit-Zeman, 2004, Topol, 2004, Flower, 2003). Considering the complexity of OA, pharmacological or biological interventions that can target key biochemical and molecular pathways involved in OA are essential towards the development of DMOADs.

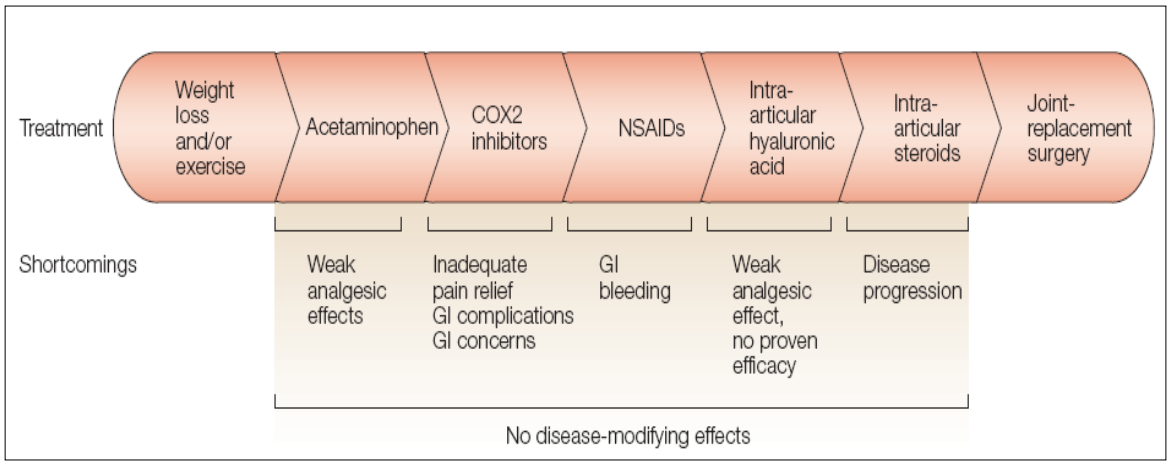

Figure 1.14: Representation of current OA treatment options, as issued in the guidelines from the American College of Rheumatology, which are fairly limited. As no drugs exist that prevent or halt OA joint destruction, the ultimate measure is joint replacement. COX-2, cyclooxygenase 2; GI, gastrointestinal; NSAID, non-steroidal anti-inflammatory drug. Reproduced from (Wieland et al., 2005).

1.15.1. Cytokines as potential targets for biological therapy in OA

Increased cytokine levels in the affected synovial joint regulate cartilage extracellular matrix (ECM) biosynthesis and suppression of chondrocyte ECM degradation. Initially OA was considered as a 'noninflammatory arthropathy', but the latest studies have demonstrated that increased inflammatory cytokines and growth factor production are evident in all the joint components namely cartilage, synovial membrane and subchondral bone (Clegg et al., 1997, Samuels et al., 2008, Sellam and Berenbaum, 2010b, Sutton et al., 2009). The contribution of specific joint components to OA pathology in a patient at a definite disease stage is still not yet fully delineated. Given that synovial inflammation plays a critical role in OA pathogenesis and progression through producing inflammatory mediators leading to series of complex variations such as hypertrophy, proliferation, and catabolic alterations, ultimately resulting in irreversible joint damage, it is essential to target the molecular pathways in synovial tissue, inducing such dysregulation in joint homeostasis. Various in vitro and in vivo studies have shown that advanced articular cartilage destruction is chiefly instigated by pro-inflammatory and catabolic cytokines such

as IL-1β, IL-6 and TNF-α and this provides the basis to consider anti-cytokine therapy for OA treatment (Martel-Pelletier et al., 1999). Considering the fact that increased levels of IL-1□ and TNF-□, serve to elevate levels of prostaglandins, catabolic enzymes, nitric oxide and other markers in OA fluids and tissues, anti-cytokine therapy may prove useful for the molecular intervention of OA (Dudhia, 2005). In fact, the latest research focusing on OA pathology indicates that cytokine inhibitors (especially active IL-1β, TNFα, IL-6 which mostly are the major cytokines involved in articular cartilage destruction) may hold high potential for disease modification therapy in OA (Dudhia, 2005).

A reduction in inflammation and articular damage was reported in rodent models of arthritis following the molecular targeting of IL-1 and the receptor for IL-1 (Joosten et al., 1999, Berg et al., 1994). In contrast, IL-17 produced from activated T cells developed spontaneous arthritis in an IL-1ra deficient mouse (Nakae et al., 2003). Though not as efficacious as anti-TNFα therapy in RA, Anakinra (a recombinant human Il-1ra drug) was found to abate bone erosion and inflammation in RA patients (Furst et al., 2005). However local IL-1 blockade was noted to be not very efficient in OA till now (Sellam and Berenbaum, 2010b). Regarding anti-TNFα therapies, about one quarter of patients fail to obtain a significant clinical response as per ACR20 criteria (20 % improvement in disease activity). Research is underway in determining the impact of systemic TNFα-blocking agents in OA (Sellam and Berenbaum, 2010b)

Regarding IL-6, substantial suppression of inflammation and clinical disease was noted upon blocking IL-6R activity in RA (Choy et al., 2002, Nishimoto and Kishimoto, 2006b). Clinical trials for IL-6 have now reached phase III, where tocilizumab, a human mAb specific for IL-6R, has been shown to suppress disease activity and erosive progression in patients with RA that is resistant to disease modifying anti-rheumatic drugs (DMARDs) (Smolen et al., 2008) and systemic-onset juvenile idiopathic arthritis (Yokota et al., 2008). Given the significance of IL-6 in OA, it may be an exciting approach for OA treatment according to latest research studies. Hence, it may be possible to treat clinical symptoms and impede the structural alterations associated with OA by focusing on the synovial membrane, as it appears to be a novel strategy for future treatments. Anti-TNF□ agents, anti-fibrotic compounds and anti-proteases interfere with specific targets and these may form part of the new OA therapies (Figure 1.15) (Berenbaum, 2010, Malemud, 2010).

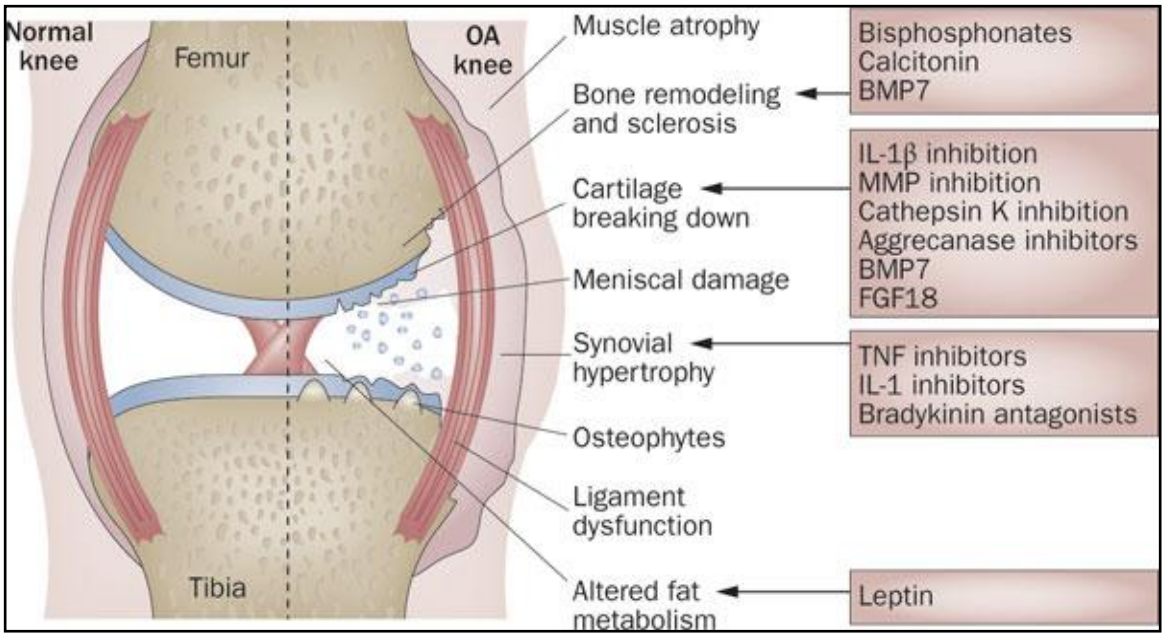

Figure 1.15: Representation of current DMOAD developments, targeting synovial-joint tissue structures including bone, cartilage and synovium. Consistent with the theory that OA is a disease of the whole synovial joint. Some of the agents that target these relevant tissues are listed (left panels). BMP, bone morphogenetic protein; DMOAD, disease-modifying OA drug; FGF, fibroblast growth factor. Reproduced from (Hunter, 2010).

The strategy to retard the progression of a multifactorial and complex disease by targeting a single, dominant cytokine mirrors that adopted for the successful treatment of rheumatoid arthritis, psoriatic arthritis and ankylosing spondylitis. Therapeutic interventions are mainly aimed at blocking or reversing structural damage and are most efficient in the early stages, especially if the possibility of preserving normal homeostasis still remains, hence identifying the methods for early diagnosis is very crucial. In the later stages, anti-cytokine therapy may be necessary following cartilage tissue engineering with or without gene therapy, to prevent further mutilation to newly repaired cartilage (Goldring, 2001) and to understand the molecular pathways that are critical towards decreasing synovial inflammation.

1.16. Innate immune system activation in OA

Synovial inflammation is established to be an important pathophysiologic process in OA (Scanzello et al., 2008). Inflammatory mediators and specific cellular infiltrates linked with OA are induced through activation of the innate immune system in response to

various pathogens and endogenous signals (Scanzello et al., 2008). Given this, understanding the role of TLRs and their signaling pathways in the context of OA is of importance (Scanzello et al., 2008).

The inflammatory response to tissue injury (such as that seen in OA) resembles the early inflammatory response to infection, mediated in response to PAMPs and DAMPs. For example, high mobility group box (HMGB)-1 (Tsung et al., 2005), hyaluronan (Jiang et al., 2007), and various heat-shock proteins (Ohashi et al., 2000) are thought to act as DAMPs. These have all been shown to bind to TLRs or to the receptor for advanced glycation end products (RAGE) which has been associated with cartilage catabolism in OA (Loeser et al., 2005). Hyaluronan is a significant component of the SF and the ECM of many tissues, comprising the joint, and is a large linear carbohydrate polymer. In cartilage injury diseases such as in OA and RA patients, the hyaluronan level was found to be reduced and this suggests that its metabolism has been altered (Belcher et al., 1997). Numerous proteins, including hyaluronidases, the cell surface receptor CD44, and lysosomal enzymes are activated involving hyaluronan breakdown (Knudson et al., 2002, Csoka et al., 2001).

Proangiogenic and immunostimulatory response were also noted to be elicited upon binding to various receptors namely, CD44 and TLR-2 and TLR-4 from certain sized Hyaluronan fragments (Taylor et al., 2007). Hyaluronan upon interaction with TLR-4 is noted to be very effective in activating DCs (Termeer et al., 2002). It was found that murine macrophages and human endothelial cells can also be activated by Hyaluronan through TLR-2 (Scheibner et al., 2006). As TLR-2 and TLR-4 are receptors for bacterial lipopeptides and LPS during innate responses to pathogens it has been questioned whether the in-vitro effects demonstrated by hyaluronan could be mediated by bacterial contaminants. However, it was found that, though overlapping was generated by LPS and hyaluronan, definite patterns of gene expression in macrophages were noted (Taylor et al., 2007). Additionally, CD14 and CD44 are also involved in hyaluronan mediated TLR-4 responses (Takeda and Akira, 2005). The capability of hyaluronan species produced within the OA joint to activate TLR signalling requires further investigation. In addition, fibronectin, another ECM component, may drive TLR signalling. In contrast to normal adult tissue, during aging, inflammation and wound healing, several splice variants of fibronectin are expressed. Particular splice variants showed increased expression in OA when compared to normal cartilage (Chevalier et al., 1996). Further, fibronectin fragments

have been shown to activate chondrocytes causing cartilage damage, wherein, the isoforms of fibronectin are found to activate TLR pathway. A recent study showed that MMP-9 expression was induced by the extra type III domain A (EDA) domain of fibronectin, probably through TLR4 pathway in monocytic cells. Unlike hyaluronan, it is still unclear whether the fibronectin fragments produced in the joint could stimulate TLR pathways in OA (Okamura et al., 2001). Even in the absence of pathogens, both hyaluronan and fibronectin activate the innate immune (TLR signalling) response and serve as endogenous damage/danger signals during normal wound healing process. It is now proposed that both of these ligands might have their involvement during aging and injury by altering the biology of OA joint tissue.

Given the association between TLRs, inflammation and proinflammatory cytokine production, it is highly likely that TLRs may play significant role in OA development and progression (Matsumura et al., 2003). Moreover, molecular signals of tissue damage trigger the innate immune response in OA, and this model represents a framework for future inflammation research in this joint disease (Ojaniemi et al., 2006). A range of immune cells including macrophages and monocytes were found to express TLRs. Regarding the OA and RA synovial joint, expression of TLR2 and TLR4 implies that may play a role in these diseases (Radstake et al., 2004, Ospelt et al., 2008). OA synovial membrane showed TLR2 and TLR4, but comparatively these were more highly expressed in the synovial membrane of RA (Radstake et al., 2004, Ospelt et al., 2008). Remarkably, RA and OA synovial cells showed a similar responsiveness to the TLR4 ligand, LPS and the TLR2 ligand, peptidoglycan (Kyburz et al., 2003). In end stage OA patients, lesional areas of cartilage showed up regulated TLR2 and TLR4. It is now assumed that both TLR2 and TLR4 are involved in synovial activation and inflammation, particularly, given that the DAMPs fibronectin and hyaluronan are prevalent in the OA cartilage matrix (Scanzello et al., 2008).

The activation of TLR2 and TLR4 initiates a signalling cascade which eventually results in the activation of transcription factors such as IRFs, AP-1 and NF-κB which increase the transcription of inflammatory associated genes (Akira and Sato, 2003). The transcription factor NF-κB is found to be central to all TLR pathways except for TLR3 (Akira and Sato, 2003). It has been proposed that unchecked NF-□B may lead to chronic inflammatory conditions (Takeda and Akira, 2005, Abdollahi-Roodsaz et al., 2011). Recent studies have reported that NF-κB plays a significant role in OA and found that NF-κB significantly

affected the production of IL-6, IL-8, MCP-1, and MMP-13 in OA-FLS. Also, it has been shown that NF-κB regulated the baseline and IL-1 stimulated levels of A Disintegrin and Metalloproteinase with Thromospondin Motifs (ADAMTS)-4, a destructive cartilage aggrecans (Scanzello et al., 2008, Bondeson et al., 2007, Amos et al., 2006). Although these two studies implicate NF-□B in mediating OA disease progression, the relative contributions of specific stimuli such as TLR or cytokine activity at different stages of disease is still unclear. The implication of the published data pertaining to TLR activation in OA is still unclear, but points to the complexity of TLR responses in vivo and their possible interaction with other signaling pathways. Although, the innate immune system activation through TLRs is well defined in RA, further research is needed to determine the same in OA pathogenesis.

1.17. Specific aims of the study

1. *In-vitro* characterisation of OA synovial fibroblasts through gene and protein expression profiling.

2. *Ex-vivo* characterisation of synovial tissue, fluid and fibroblasts and investigation of the therapeutic potential of TLRs in OA.

3. Proteomic analysis of OA synovial tissue and fibroblasts.

Chapter 2

General Methods and Materials

2.1. General Materials and Suppliers

Biosera

Foetal Bovine Serum, Cat. # S1810-500

ECACC

Synoviocyte basal growth media and a supplement, Cat. # 06091516

Gibco®

Dulbecco's modified eagle medium + GlutaMAX™, Cat. # 61965026

OPTI-MEM + GlutaMAX™, Cat. # 51985026

RPMI 1640 + GlutaMAX™, Cat. # 61870010

Dulbecco's phosphate buffered saline, Cat. # 14190094

HyClone Europe, Northumberland, UK.

Dulbecco's minimal essential medium, Cat. # B-7501

RPMI 1640, Cat, # B9006-L

Minimal essential medium, Cat. # B-2071-L

Invitrogen

TRIzol, Cat. # 15596-018

InvivoGen™

Normocin, Cat. # ant-nr-1

Life Technologies Inc., Gaithersburg, MD., U.S.A.

Random hexamers, Cat. # 48190-011

2.5 % Trypsin solution, Cat. # 25090-010

New England Bio Labs

Prestained protein marker Broad range, Cat. # 977085

dNTP Nucleotide Solution Mix, Cat. # N04475

Nunc A/S., Roskilde, Denmark.

Cryovials, Cat. # 363401

96 well Nunc-Immuno™ MaxiSorp plates, Cat. # M9410-1CS

PAA laboratories Ltd., Kingston Upon Thames, UK.

Foetal calf serum (FCS), Cat. # A-15042

Foetal bovine serum (FBS), Cat. # A-15045

Promega Corporation, Madison, WI., U.S.A.

Mouse moloney leukaemia virus (MMLV) reverse transcriptase (RT), Cat. # M1701

Recombinant RNasin® ribonuclease inhibitor, Cat. # N2511

DNA polymerase I Large (Klenow) fragment, Cat. # M2201

RQ DNase I, Cat. # M6101

Deoxynucleotode triphosphates, Cat. # U1240

Thermophillic DNA poly 10 × buffers, Cat. # M190A

$MgCl_2$, Cat. # A351B

Random primers, Cat. # C118A

M-MLV RT 5x Buffer, Cat. # M513A

Roche Molecular Biochemicals, Sussex, U.K.

Taq DNA polymerase (1 unit/µl), Cat. # 1647679

Cytotoxicity Detection Kit^{Plus} (LDH), Cat. # 04744926001.

Sigma®

N, N, N', N',-tetramethylethylenediamine (TEMED), Cat. # 036K0694

Ammonium persulphate (APS), Cat. # 105K0700

Albumin bovine, Cat. # A2153-506

Albumin from bovine serum, Cat. # A7030

DMEM high glucose Cat. # D5796

Potassium phosphate, Cat. # P0662

PenStrep 100 x Cat. # P4333

Sodium phosphate, Cat. # S0751

Trypan Blue Solution (0.04 %), Cat. # T8154

Trypsin EDTA solution, Cat. # T4174

Tween®-20, Cat. # P1379

Sarstedt Ltd. Drinagh, Wexford, Ireland

96 well tissue culture plate, Cat. # 83.1835

24 well tissue culture plate, Cat. # 83.1836

175 tissue culture flasks, Cat. # 83.1813

100 mm cell culture dishes, Cat. # 83.1813

60 mm cell culture dishes, Cat. # 83.1801

10 ml blow-out pipettes, Cat. # 83.1802

1 ml blow-out pipettes, Cat. # 86.1251-001

Filtropur S Plus filtration units, 0.2 µM, Cat. # 83.1826. 102

Thermo Fisher Scientific

Nalgene™ Cryo freeze container, Cat. # 5100

Cryogenic vials, Cat. # 5000

2.2. General Laboratory Procedures

2.2.1. Centrifugation

All bench top centrifugations were performed using a Hettich Mikro 120 centrifuge. Ultracentrifugations were performed using an Eppendorf centrifuge 5810R refrigerated ultracentrifuge. Unless stated otherwise, all centrifugations were performed at RT.

2.2.2. Spectrophotometry

All spectrophotometric determinations were performed using a Nanodrop ND-1000 spectrophotometer or Hitachi U2000 UV/VIS spectrophotometer.

2.2.3. Measurement of pH

All pH measurements were performed using a pH meter (Hanna Instruments, Singapore) with a combination electrode (AgCl sealed internal reference). Prior to use, the pH meter was calibrated using standard reference buffers, pH 4.0, pH 7.0, and pH 10.0 (Sigma).

2.2.4. PCR

PCR was performed using an inputted PCR programme on an Eppendorf Mastercycler personnal. Real time PCR (qPCR) was performed using an inputted PCR programme on a DNA Engine OPTICON system; MJ Research.

2.2.5. ELISA

ELISA was performed using BioTek® ELx800 plate reader. Meso Scale multi-plex ELISAs were performed using Meso Scale Discovery (MSD) SECTOR imager with MSD Discovery Workbench analysis software.

2.2.6. General sterility

All plasticware, pipette tips, microfuge tubes and solutions were sterilised by heating at 121 ^{o}C for 15 min. Plasticware was subjected to oven-drying for 5-6 h. Where appropriate, solutions were sterilised using a 0.2 µM Filtropur filtration unit (Sarstedt). Aseptic techniques were employed when handling TLR ligands and sterile inflammatory mediators. All cell culture work was performed in a class II sterile laminar flow cabinet using at-most aseptic measures.

2.2.7. Cryopreservation

All mammalian cells were detached from the flask and subjected to centrifugation at 3000 rpm for 5 min at 4 ^{o}C. The supernatant was removed and the cell pellet was gently resuspended in the appropriate culture medium containing 10 % FCS and 10 % DMSO (Sigma). The cell suspension was transferred into cryovials (NUNC) and incubated at -70 ^{o}C for 4 h in an isopropanol box. Thereafter, the vials were transferred to liquid phase N_2 for long time storage. To confirm cell viability, a cryovial was taken on a subsequent day from liquid phase N_2 and allowed to quick thaw at RT. Next, the cell suspension was immediately transferred into a 15 ml falcon containing 10 ml of appropriate culture medium and was centrifuged at 1200 rpm for 2 min to remove the DMSO used for cryopreservation. Subsequently, the supernatant was discarded and the cell pellet was resuspended in appropriate culture medium supplemented with 10 % FCS, and was then transferred to a sterile tissue culture flask. Next, these flasks bearing cells were incubated at 37 ^{o}C humidified atmosphere with 5 % CO_2 overnight to allow cells to adhere. The following day the medium was aspirated to remove any trace amounts of DMSO, followed by replenishment with new medium. Finally, the cell viability was determined using either trypan blue exclusion assay or lactate dehydrogenase (LDH) cytotoxicity assay.

2.3. General Experimental Methods

2.3.1. Cell culture technique

All mammalian cells were grown at 37 °C in a humid environment with 5 % CO_2 in the appropriate culture medium. FLS were grown in complete synoviocyte medium (ECACC) made up using basal synoviocyte growth medium supplemented with growth supplement (ECACC), 100 U/ml penicillin, 100 µg/ml streptomycin and 0.25 µg/ml fungizone. The FLS were cultured and propagated until passage 6 and utilised for all the experiments between 2 to 6 passages. The FLS were then seeded appropriately either in tissue culture plates or 8-well chamber slides or T125 tissue culture flasks until confluent. Prior to stimulation FLS were rendered quiescent by maintaining the cells in serum free Opti-MEM for 24 h. Further, all the cell stimulations were carried out in Opti-MEM for 24 h using the agonists as described in (table 2.2) or grade-specific osteoarthritic fluid (OA-SF). The cell free supernatants were collected for ELISA analysis and the adherent cells on the culture plates were either utilised for RNA extraction with TRIzol reagent or for protein extraction with lysis buffer for western blot analysis.

Furthermore, the adherent cells in the T125 culture flasks were utilised for protein extraction with lysis buffer for 2D-proteomic analysis and the cells on the 8-well chamber slides were utilised for confocal microscopy analysis. Prior to performing the above experiments, the cell viability of cultured FLS was quantified using trypan blue exclusion assay or LDH cytotoxicity assay. Moreover, all the cell types employed in this study were also routinely tested for Mycoplasma contamination using the MycoAlert kit (MycoAlert®; Lonza), which if unchecked can activate TLR2/6 and thus compromise TLR signalling events. Furthermore, given that endotoxin contamination can acutely affect our TLR signalling studies, we routinely used certified endotoxin-free reagents where possible. Similarly, all other reagents used in this study were tested for endotoxin levels using the HEK-Blue™ LPS detection kit (Invivogen).

2.3.2. Quantification of FLS cell viability

2.3.2.1. Trypan blue exclusion assay

Trypan blue exclusion assay was performed to quantify the number of viable cells (data not shown). Briefly, FLS were seeded at 1×10^5 cells/well in triplicates in a 6-well tissue culture plate and were left till confluent at 37 °C in a humid environment with 5 % CO_2.

Prior to stimulation, FLS were rendered quiescent by maintaining the cells in serum free Opti-MEM for 24 h. Further, all stimulations were carried out in Opti-MEM for 24 h, using the agonists as mentioned in table 2.2. Next, the supernatant was discarded and the cells were washed with 500 µl PBS. Then, 150 µl/well of trypsin was added to the plates and were incubated for 5-10 min at 37 °C until the cells had detached from the plates. Next, 500 µl of complete synoviocyte medium was added to the cells and this solution was collected in micro-centrifuge tubes, which were then centrifuged at 1200 rpm for 5 min at RT. The supernatant was disposed and 50 µl of complete synoviocyte medium was added to re-suspend the pellet. Thereafter, 50 µl of the cell suspension and 50 µl of 0.4 % trypan blue was pipetted into an eppendorf tube and mixed by gentle pipetting (to give a final concentration of 0.2 % trypan blue). A haemocytometer and cover slip were cleaned with 70 % ethanol and 10 µl of this suspension was allowed to flow under the cover slip of the haemocytometer by capillary action, to fill the measuring compartment. The percentage of viable cells was calculated by counting the viable cells which appeared yellow/orange in appearance whilst dead/non-viable cells appeared blue in colour.

2.3.2.2. LDH cytotoxicity assay

To assess cell death in FLS cells following stimulation with TLR/RLR ligands and osteoarthritis synovial fluid (OA-SF), a Cytotoxicity Detection Kit^{Plus} (Roche; Lactate dehydrogenase (LDH)) was used (data not shown). LDH is an enzyme located almost exclusively in the cytoplasm and is used as a measure of cell integrity and has some advantages over trypan blue staining. Thus, FLS were seeded at 1×10^5 cells/ml in a 24-well tissue culture plate and were grown till confluent at 37 °C in a humid environment with 5 % CO_2. Prior to stimulation, FLS were rendered quiescent by maintaining the cells in serum free Opti-MEM for 24 h. Further, all stimulations were carried out in Opti-MEM for 24 h, using the agonists as mentioned in table 2.2 and as well with OA-SF. Next, total LDH release was achieved by adding Triton X-100 (1 % solution) to untreated control cells. Treatment values were then expressed as a percent of the total LDH release. The supernatants were removed and centrifuged at 2200 rpm for 5 min at 4 °C. Then, 50 µl of cell-free supernatant was added to a 96-well plate followed by 100 µl of reaction mixture (provided in the kit). The plate was then incubated at RT for 30 min in dark. Next, 50 µl/well of stop solution (provided in the kit), was added to the plate and was left on a shaker for 10 seconds. The plate was then read using a BioTek® ELx800 plate reader at 490 nm OD. Percentage cytotoxicity was calculated as follows: % Cytotoxicity =

{[(Sample – BC) – (low control - BC)] / [(high control – BC) – (low control – BC)]} 100, where BC = Background control (i.e. assay medium; Opti-MEM), low control = supernatant from untreated cells and high control = supernatant from 1 % Triton treated cells. For ease of comparison with the Trypan blue exclusion method, % cytotoxicity as determined by LDH cytotoxicity assay was converted to cell viability using the formula: % Viability = 100 – % Cytotoxicity.

2.3.3. RNA extraction and quantification

Total RNA was extracted from 1×10^7 cells using 1 ml of Trizol reagent per well (1 ml/well in 6 well plate) was added and the cells were thus lysed passing through the pipettes several times with the reagent. 200 µl of chloroform was added to 1 ml of Trizol and mixed vigorously by hand and incubated at RT for 10 min. The cells were then centrifuged at 14,000 rpm for 15 min at 4 ^{o}C. The upper phase (60 % volume) around 400-500 µl of colourless liquid was then transferred into a sterile eppendorf tube. To this, equal volumes of isopropyl alcohol was added and mixed well. This mixture was left for 10 min at RT to precipitate RNA and was then centrifuged at 14,000 rpm for 15 min at 4 ^{o}C, and the supernatant was discarded. To the RNA pellet, 500 µl of 75 % ethanol was added followed by centrifugation at 14,000 rpm for 15 min at 4 ^{o}C. The supernatant was discarded and the pellets were then air-dried for 5 min at RT. The RNA pellets were re-suspended in 10-50 µl of RNAse free water. The concentration of RNA, thus extracted was measured using a Nanodrop spectrophotometer, pre-blanked using 1 µl of RNAse free water and A260/280 nm was determined. RNA was stored at -80^{o}C until further use.

2.3.4 Reverse transcription and first strand cDNA synthesis

To 1 µg of RNA in a total volume of 11 µl was added 1 µl of random hexamers (100 pM/µl). This solution was mixed well and placed at 70 ^{o}C for 5 min, followed by 5 min incubation on ice. To this solution, the other components/reagents were added in the following order, 4 µl of 5 × RT buffer, 2 µl of dNTP (10 mM), 1 µl of RNasin and 1 µl of MMLV Reverse transcriptase and mixed well. The samples were placed at 37 ^{o}C for 40 min, followed by 42 ^{o}C for 40 min and finally at 80 ^{o}C for 5 min. The first strand cDNA was stored at -20 ^{o}C until further use.

2.3.5. Quantitative real time PCR

Total first strand cDNA was used as a template for real-time PCR quantification using a DyNAmoHS SYBR Green kit (Finnzymes) and a real-time PCR system (DNA Engine OPTICON® system; MJ Research). For the amplification of TLRs, cytokines, MMPs the respective primers were used as described in table 3.1 (chapter 3). For each TLR mRNA quantification, the housekeeping gene hypoxanthine phosphoribosyl transferase *(HPRT)* was used as a reference point using the respective primers.

2.3.6. Enzyme-linked immunosorbent assay (ELISA)

Cells were seeded at 1×10^5 cells/well in triplicate in a 6-well tissue culture plate until confluent. Prior to stimulation, cells were rendered quiescent by maintaining the cells in serum free Opti-MEM for 24 h. Further, all stimulations were carried out in Opti-MEM for 24 h, using the agonists described in table 2.2. The cell free supernatants were then collected and stored at -80 ^{o}C for ELISA analysis. Subsequently, the supernatants were analysed for TNFα, IL-1β, IL-6, IL-15, RANTES, IL-10 and IFNβ levels utilising the ELISA kits as described in table 2.1. Briefly, 96-well NUNC-Maxisorb plates were coated with respective capture antibodies (dilutions as per table 2.1) in PBS, and were incubated overnight at RT. Next, plates were washed three times with wash buffer (PBS with 0.05 % (v/v) Tween-20) and dried. Plates were then blocked for 1 h with 200 µl/well of PBS containing 1% (w/v) bovine serum albumin (BSA). Next, the plates were washed three times with wash buffer and were pat dry. Subsequently, 100 µl/well of samples or standards (dilutions as in table 2.1) were diluted in reagent diluent (0.1 % (w/v) BSA, 0.5 % (v/v) Tween in 10 mM Tris–HCl, pH 7.5 containing 150 mM NaCl in Tris-buffer saline (TBS) were added. Wherein, a 8 point standard curve was prepared with assay range 4000 to 0 pg/ml for IFNβ, 500 to 0 pg/ml for IL-1β, 1200 to 0 pg/ml for IL-6, 3000 to 0 pg/ml for IL-10, 1000 to 0 pg/ml for IL-15, 3000 to 0 pg/ml for RANTES and 3000 to 0 pg/ml for TNFα respectively. Plates were incubated with 100 µl/well of samples or standards for 2 h and then the series of washes with wash buffer was repeated and was pat dry. Next, 100 µl/well of the respective detection antibodies (biotinylated anti-human antibody, dilutions as in table 2.1) diluted in reagent diluent was added and incubated for 2 h at RT, followed by series of wash steps with wash buffer. Next, 100µl/well streptavidin-horseradish peroxidase (HRP) conjugate (dilutions as in table 2.1) was added to each well and incubated in dark for 20 min followed by repeated was steps and was pat dry. Subsequently, 100 µl/well of 3, 3', 5, 5'-TeTRAMethylbenzidine liquid substrate (TMB, 1.25 mM/L) solution was added to all plates and were incubated in dark for 20 min.

Immediately, 50 µl/well of 1N sulphuric acid (H_2SO_4) was used to stop the reaction and the absorbance was read at OD 450 with a BioTek® ELx800 plate reader. The concentrations of cytokine/chemokine in each sample were extrapolated from a standard curve that related the OD of each standard amount to the known concentration. Standard samples were assayed in duplicate to generate the standard curve, while all samples were assayed in triplicate.

2.3.7. Western blot analysis

2.3.7.1. Cell lysis and sample preparation

Cells were seeded at 1×10^6 cells/well in triplicates in a 6-well tissue culture plate until confluent. Prior to stimulation, cells were rendered quiescent by maintaining the cells in serum free Opti-MEM for 24 h. Further, all stimulations were carried out in Opti-MEM for various time points, using the agonists described in table 2.2. The cell free supernatants were collected and stored at -80 ^oC for further ELISA analysis and the adherent cells were then washed with 500 µl of ice cold PBS. Next, 65 µl/well of sample buffer (10 % β-mercaptoethanol, 2 % SDS, 30 % Glycerol, 0.025 % bromophenol blue, 50 mM Tris-HCL pH 6.8, 1 mM dithiothreitol and 0.1mM phenyl methyl sulfonyl fluoride) was added and the cells were thus lysed on ice for 10 min. The lysed cells were then pipetted into a microfuge tube followed by centrifugation at 13,000 rpm for 5 min to pellet the cell debris. The supernatant containing the protein was pipetted into a sterile microfuge tube followed by boiling for 10 min at 100 ^oC and subsequent SDS-polyacrylamide gel electrophoresis (SDS-PAGE).

2.3.7.2 SDS-PAGE

The protein 1D-gel casting apparatus was assembled using glass plates that were cleaned with 70 % ethanol. Next, the 10 % resolving gel solution (5 ml Acrylamide, 3.8 ml 1.5M Tris-HCL pH 8.8, 5.9 ml water, 150 µl 10 % SDS, 15 µl 10 % APS and 6 µl TEMED) was prepared and was poured into the assembled glass plates. The gel was overlaid with 500 µl of water and allowed to polymerise for 40 min. Following polymerisation the overlaid water was decanted and the resolving gel was overlaid with 5 % stacking gel (1 ml Acrylamide, 1.5 ml 0.5 M Tris-HCL pH 6.8, 3.35 ml H_20, 60 µl 10 % SDS, 60 µl 10 % APS and 6 µl TEMED). A 12-well plastic comb was then inserted and the gel was allowed to polymerise before being assembled in the SDS-PAGE apparatus (BioRAD). The upper and lower chambers of this apparatus was filled with running buffer (0.3 % Tris base, 1.44

% glycine and 0.1 % SDS). Appropriate samples (20 µl) and prestained protein marker (5 µl) were loaded into separate wells and electrophoresis was performed at 80 V through the stacking gel and then 100 V through the resolving gel for approximately 3 h, depending on the size of the proteins being electrophoresed.

2.3.7.3. Immunoblotting

Following separation by SDS-PAGE, the proteins were transferred electrophoretically to polyvinyl difluoride (PVDF) membrane in a Bio-Rad wet-blot transfer unit with transfer buffer (25 mM Tris-base, 0.2 M glycine, 20 % (v/v) methanol. Briefly, one piece of PVDF membrane was cut to a similar size as the gel and pre-wet with methanol followed by rinsing with distilled water. The PVDF membrane, four pieces of chromatography paper (cut to similar size as gel) and two pieces of Scotch Brite padding were soaked in transfer buffer prior to use. The transfer apparatus was then assembled as follows: One layer of Scotch Brite padding was overlaid with two pieces of chromatography paper. The gel was placed on top of the chromatography paper followed by the PVDF membrane, two more pieces of chromatography paper and one piece of Scotch Brite padding then followed. The transfer was then clamped together and placed in the wet-blot transfer apparatus (Bio-Rad). Next, the chamber was filled with transfer buffer and the transfer was performed at a constant voltage of 100 V for 1 h, after which the PVDF membrane was retrieved. Following transfer, non-specific binding was blocked by incubating the PVDF membrane at RT for 2 h (or overnight) in TBS (20 mM Tris-HCl pH 7.5, containing 0.05 % (v/v) Tween 20 and 0.5 M NaCl) containing 5 % (w/v) skimmed milk powder. The membranes were then washed 3 times for 10 min each in TBS prior to incubation at 4 °C overnight with the primary antibodies diluted in TBS containing 2.5 % (w/v) skimmed milk powder. The membranes were subsequently subjected to 5 x 10 min washes in TBS prior to incubation with secondary antibody (1:5000 dilution) specific for the primary antibody in question (anti-rabbit or anti-mouse) for 1 h at RT. The membranes were then washed a further 5 times for 10 min each in TBS. Blots were then developed using a 1:1 mixture of enhanced chemiluminescent substrate (Pierce) for detection of horse radish peroxidise and visualised through CCD imaging. Molecular weight marker was used to calculate molecular weights of proteins represented by immunoreactive bands.

2.3.8. Immunofluorescent Assay

Cells were seeded at a density of 0.5 x 10^5 cells/ml in 8-well chamber slides and grown for 24 h till confluent. Prior to stimulation cells were rendered quiescent by maintaining the cells in serum free Opti-MEM for 24 h. Further, all the cell stimulations were carried out in Opti-MEM using the agonists. Following stimulations cells were fixed in 4 % para-formaldehyde, permeabilised with 0.2 % Triton X-100 in PBS for 10 min at RT followed by blocking with 10 % goat serum for 2 h. Next, cells were treated overnight at 4 °C with primary antibody on a rotary shaker with gentle agitation. Cells were then washed and incubated with secondary antibody for 1 h at RT with gentle shaking in dark, followed by incubation with DAPI (1.5 μg/ml) in PBS for 30 min at RT. Slides were washed and mounted using antifade mounting media (Vectashield; Vector Laboratories), and were visualised under confocal microscopy.

2.3.9. Statistical Analysis

All the data presented are representative of at least three independent experiments performed in triplicate and all the data are expressed as mean ± standard error of the mean (S.E.M.) (mean ± S.E.M). Statistical comparisons were performed either using parametric (Student T-test) or non-parametric statistical tests (Mann Whitney U test), unless stated otherwise. Differences with a *p* value less than 0.05 were denoted with (*), values less than 0.01 as (**) and values less than 0.001 as (***), and were considered statistically significant.

Table 2.1: Human cytokine and chemokine ELISA kits

The human cytokine and chemokine ELISA kits employed in this research were purchased from the companies detailed in the table below. The table indicates the working antibody dilutions used for the research, upon optimisation using human monocytic leukaemia cells (THP1) and Immortalised K4 synovial fibroblast (K4 FLS) cell lines as the model cell lines.

ELISA kit	Company	Catalogue Number	Capture antibody dilution factor	Standard antibody: top working standard dilution factor	Detection antibody dilution factor	Streptavidin-HRP conjugate dilution factor
Human IL-1β	R&D system	Dy 201	1:180	1:100	1:180	1:200
Human IL-6	R&D system	Dy 206	1:180	1:30	1:180	1:200
Human IL-15	R&D system	Dy 247	1:180	1:110	1:180	1:200
Human TNF-α	Peprotech	900-K25	1:100	1:333.3	1:200	1:2000
Human IL-10	Peprotech	900-K21	1:100	1:333.3	1:200	1:2000
Human RANTES	Peprotech	900-K33	1:100	1:333.3	1:200	1:2000
Human IFN-β	PBL Interferon Source	41410	1:180	1:50	1:180	1:200

Table 2.2: TLR and RLR agonists utilised during the study

The human primary fibroblast like synoviocytes (FLS) and whole synovial tissue explants were stimulated with the indicated working concentrations of the ligands. The concentrations of these ligands were initially optimised using K4 FLS cells.

TLR/RLR	TLR/RLR Ligand	Stock Ligand Concentration	Optimised Working Ligand Concentration	Company	Catalogue Number
TLR 1/2	Pam_3CSK_4	1 mg/ml	1 µg/ml	EMC microcollection	L2000
TLR 2/2	Pam_2CSK_4	1 mg/ml	1 µg/ml	EMC microcollection	L2020
TLR 3	Poly (I:C)	1 mg/ml	10 µg/ml	Invivogen	tlrl-pic
TLR 4	LPS	1 mg/ml	1 µg/ml	Invivogen	tlrl-pelps
TLR 5	Flagellin	1 mg/ml	1 µg/ml	Invivogen	tlrl-bsfla
TLR 2/6	MALP-2	5 µM/ml	20 nM/ml	Alexis	162-027-C050
TLR 7/8	CLO-97	1 mg/ml	1 µg/ml	Invivogen	tlrl-c97
TLR 9	CpG	3 mg/ml	3 µg/ml	MWG-Biotech AG	ODN2216
RIG-I	5'ppp-dsRNA	1 mg/ml	1 µg/ml	Invivogen	tlrl-3prna

Chapter 3

In-vitro characterisation of Osteoarthritic synovial fibroblasts through gene and protein expression profiling

3.1. Introduction

The complexity of the human immune system, their critical regulators like TLRs, and their adaptor molecules continues to intrigue researchers, despite being studied for over a decade. Ever since the discovery of the first mammalian TLR, TLR4 (Medzhitov and Janeway, 2000), significant research has been carried out towards characterising these receptors and their fundamental role in the innate and adaptive immune response. TLRs are a class of pattern recognition receptors (PRRs) whose recognition of varied microorganisms initiates intricate signalling pathways ultimately leading in to the induction of various transcription factors like NF-κB, IRFs, AP-1 and CREB and pro-inflammatory cytokine production (Takeda et al., 2003, Miggin and O'Neill, 2006). However, improper regulation of the same pathways can result in the onset of various chronic inflammatory and autoimmune diseases like asthma, atherosclerosis, cancer (Li, 2004), sepsis, SLE (Roelofs et al., 2008) and rheumatoid arthritis (McGettrick and O'Neill, 2010, Roelofs et al., 2008). Recently, convincing studies have showed that the activation of TLR pathways in osteoarthritis plays a central role in disease development and progression (Scanzello et al., 2008). Thus, TLRs may play a significant role in modulating Osteoarthritis (McCormack et al., 2009). Despite this, little background information exists regarding the TLR receptors, their ligands, mediators and indeed, the OA pathophysiology itself.

Regarding OA and RA, various inflammatory mediators such as cytokines, chemokines and MMPs are induced upon innate immune system activation (Scanzello et al., 2008, McCormack et al., 2009, Roelofs et al., 2008). Hence, TLRs and their signalling pathways are of particular interest towards understanding arthritis progression. Specific TLRs (e.g.TLR2, TLR3, TLR4 and TLR9) have been associated with diverse inflammatory arthropathies (Abdollahi-Roodsaz et al., 2008). Growing evidence suggest that TLRs may also be activated by endogenous non infectious signals called damage associated molecular patterns such as hyaluronan and fibronectin (Scanzello et al., 2008).This makes the study of TLRs more interesting as they are significant inducers of cytokines in diseases with no palpable infection, such as OA.

Various TLRs are constitutively expressed by a range of immune cells, including monocytes and macrophages but are found to be up-regulated on other cells in response to

both IL-1 and TLR-4 (Ojaniemi et al., 2006). TLR-2 and TLR-4 are found to be present in OA synovial membrane, but are more highly expressed in the RA synovial membrane (Ospelt et al., 2008). Interestingly, synovial cells from both disorders have been shown to have equal responsiveness to the TLR-4 ligand LPS and the TLR-2 ligand peptidoglycan (Kyburz et al., 2003). TLR-2 and TLR-4 have been found to be upregulated in lesional areas of cartilage in patients with advanced OA (Kim et al., 2006). Murine models of auto-immune arthritis showed that TLR-4 deficiency resulted in reduced disease severity, reduced levels of cellular influx, cartilage damage and bone erosion was seen (Abdollahi-Roodsaz et al., 2008). In contrast, TLR-2 deficient mice developed a more severe disease, suggesting a protective role for this receptor in this particular model (Abdollahi-Roodsaz et al., 2008). Together, these data demonstrate the complexity of the TLR signalling pathways *in vivo* in the context of RA and suggest the possible interaction of TLRs with other signalling pathways (Abdollahi-Roodsaz et al., 2008). Both hyaluronan and fibronectin may act as endogenous damage signals in the process of normal wound healing by activating the innate immune (TLR signalling) response even in the absence of pathogens within the joint (Okamura et al., 2001). Both of these ligands are now suspected to be involved in the altered biology of joint tissues that occurs during aging and injury in OA (Scanzello et al., 2008). Taken together, these findings have perpetuated an increasing interest in investigating TLR-mediated activity in OA.

Primary OA is considered as idiopathic with no particular defined aetiology. Conversely, secondary OA is induced as a result of traumatic injury to the joint (Martel-Pelletier et al., 1999). OA is a chronic degenerative disease occurring as a result of an imbalance between extracellular matrix destruction and repair leading to destruction of articular cartilage components, predominantly cartilage specific proteoglycans and type II collagen (Todhunter, 1996). Besides the cartilage, the disease also harms the complete joint structure along with the subchondral bone, joint capsule and, synovium. OA is frequently classed as a non-inflammatory disease and the precise cause for the disease is unknown. However, various studies have identified inflammation of the synovium as playing a crucial role in the OA pathogenesis (Fell and Jubb, 1977, Ghosh and Cheras, 2001, Pearle et al., 2007, Fiorito et al., 2005, Pelletier et al., 2001). Synovial inflammation is typified by an incursion of monocytes, T lymphocytes and neutrophils, along with synovial vascularisation and hyperplasia (De Clerck et al., 1995, Schulte et al., 1994). Synovitis is considered to perpetuate pain, cartilage degradation and joint inflammation in OA (Sutton

et al., 2009). Together with synoviocytes (type A macrophages- 20 % and type B fibroblasts- 80 %), chondrocytes and infiltrating leukocytes are also involved in OA pathogenesis (Fiorito et al., 2005). Acute synovitis may be one of the initial changes to occur, as inflammatory mediators such as cytokines are detected in synovial fluid from early OA patients (Sutton et al., 2009).

During the disease process, pro-inflammatory cytokines like TNF-α and interleukin IL-1β are produced particularly by synoviocytes (Sutton et al., 2009). MMPs and lysosomal enzymes are released by the chondrocytes, synoviocytes and infiltrating leukocytes leading to cartilage proteoglycan, collagen and matrix degradation (Clegg and Carter, 1999). Additionally, other biologically active substances prostaglandin E2 (PGE_2), nitric oxide (NO) and chemokines are induced by these pro-inflammatory cytokines and all of these contribute to the pathogenesis of OA (Von Rechenberg et al., 2000). In addition, a range of anti-inflammatory substances molecules modulate OA including IL-4, IL-10, IL-13 and IL-1β receptor antagonist (IL-1Ra) (Pelletier et al., 2001).

Thus, synovial inflammation or synovitis is commonly observed in the osteoarthritic joints. It promotes OA pathogenesis by the creation of catabolic and pro-inflammatory mediators towards altering the balance between cartilage matrix degradation and repair. However, the stimuli and downstream pathways involved in this process have yet to be clearly identified (Scanzello et al., 2008, Pelletier et al., 2001). In recent years, research focused on chondrocytes and synovial macrophages and their role in OA disease progression. However, the relative contributor of synovial fibroblasts and fibroblast like synoviocytes (FLS) and their contribution to OA pathology has not been studied in detail. During the inflammatory episodes associated with OA and RA, the activated synovial fibroblasts or FLS, secrete a wide variety of proinflammatory cytokines, chemokines, and matrix-degrading enzymes like MMPs-1, 3, 9, 13 (Sutton et al., 2009, Firestein, 1996), which perpetuate the chronic inflammatory state and lead to progressive, irreversible damage of the affected joint (Sutton et al., 2009, Pelletier et al., 2001, Ghosh and Cheras, 2001, Fernandes et al., 2002). Among the proinflammatory cytokines that are present at high levels in the synovial fluid of inflamed joints are TNFα and IL-6 (Sutton et al., 2009, Fernandes et al., 2002). Notably, proinflammatory cytokines such as TNF-α, IL-6 and IL-1 have proven to be excellent therapeutic targets for diseases such as RA (Arend and Dayer, 1990). Moreover, in recent times, mechanisms whereby the cytokines are induced have

become a primary area of interest for researchers. The recognition of TLRs as key drivers of cytokine production in RA was recently demonstrated (Roelofs et al., 2009). Such progress in signalling receptor research has led to a renewed interest in innate immunity particularly TLRs, among immunologists.

To this end, we have assessed TLRs, cytokines, chemokines and MMP functionality in OA, RA and normal N FLS in response to PAMPs and inflammatory mediators like cytokines and chemokines and DAMPs like Hyaluronan using real-time mRNA profiling and ELISA cytokine profiling. We found that differences exist between OA/RA FLS, when compared to N-FLS in terms of their cellular responses to various TLR ligands and to inflammatory mediators and DAMPs. These differences give an insight into the disease mechanisms that perpetuate the pathological processes associated with OA and offer a greater understanding of the molecular mechanisms involved in chronic inflammatory pathology.

3.1.1. Specific aims of chapter 3

1. To evaluate the optimal concentration of TLR agonists, sterile inflammatory mediators and DAMPs using a defined immortalised synoviocyte cell line –K4 FLS.
2. To characterise basal and TLR, RLR and cytokine induced expression of TLRs, RLRs and cytokines in FLS following stimulation with TLR agonists, inflammatory cytokines and chemokines.
3. To analyse the gene expression profile of major proinflammatory cytokines and chemokines in N, OA, RA FLS treated with inflammatory cytokines and DAMPs.
4. To quantify the effect of TLR/RIG-I agonists on proinflammatory MMP 1, 3, 9, 13 protein and gene expression profiles in OAVs N FLS.

3.2. Experimental Materials and Suppliers

Axis-Shield, Norway

Lymphoprep, Prod. no.1114544

Gibco®

Dulbecco's modified eagle medium + GlutaMAX™, Cat. # 61965026

OPTI-MEM + GlutaMAX™, Catalog No. 51985026

Invitrogen

Alexa Fluor 546 Donkey Anti-Rabbit IgG, Cat. # A10040

Peprotech

Recombinant human IFN-β, Cat. # 300-02BC

Biotinylated polyclonal rabbit anti-human IFN-β antibody, Cat. # 500-P32BBt

Pro Sci Inc

Rabbit Polyclonal TLR2 Antibody (NT), Cat. # 3135 (50µg).

Rabbit Polyclonal TLR3 Antibody (CT), Cat. # 3643 (50µg).

Rabbit Polyclonal TLR4 Antibody (NT), Cat. # 3141 (50µg).

Santa Cruz Biotechnology, INC

Mouse monoclonal antibody rose against IFN-β of human origin, Cat. # sc-57203

Sigma-Aldrich

Agarose, Cat. # A5304

Tris Acetate-EDTA buffer, Cat. # T4038

Ethylene diamine tetra acetic acid (EDTA), Cat. # E9884

Trypsin-EDTA Solution 10X, Cat. # 59418C

3.3. Experimental Methods

3.3.1. Culture of immortalised human FLS cells

Immortalised K4 synovial fibroblasts (K4 FLS) (a generous gift from Dr. Evelyn Murphy, UCD, Ireland), were maintained in Dulbecco's Modified Eagle Medium (DMEM), which was supplemented with 10 % (v/v) foetal bovine serum (FBS), 100 U/ml penicillin and 100 µg/ml streptomycin. Cells were maintained in a 37 ºC humidified atmosphere with 5 % CO_2. Cells were passaged every 2 to 3 days using 1 % (w/v) Trypsin/EDTA solution in phosphate-buffered saline (PBS). K4 FLS were subcultured and maintained at 1.0×10^6 cells/ml and seeded at 1×10^5 cells/well in triplicates in a 6 well tissue culture plate at the 23^{rd} passage until confluent. Prior to stimulation K4 FLS were rendered quiescent by maintaining the cells in serum free Opti-MEM (Minimum Essential Media) for 24 h. Further all the cell stimulations were carried out in Opti-MEM using the agonists/ligands as described in table 2.2 (chapter 2). The cell free supernatants were collected for ELISA analysis.

3.3.2. Sub culturing of human primary FLS

Cryopreserved FLS isolated from the synovial tissues obtained from patients with RA, OA or from normal tissue (N) were purchased from ECACC at passage two. The FLS were grown in complete synoviocyte medium (ECACC) made up using the following components-basal synoviocyte growth medium supplemented with growth supplement (ECACC), 100 U/ml penicillin and 100 µg/ml streptomycin. The FLS were cultured and propagated until passage 6. N, OA, RA FLS utilised for this study were passage 2 to 6. Confluent cell monolayers were detached from the tissue culture flasks with the aid of 0.25 % trypsin. Briefly, the complete medium was removed and the cells were washed with phosphate buffered saline (PBS) and 1 mM EDTA pH 8.0. An aliquot (1 ml/T75 flask) of the trypsin solution (0.25 % trypsin in PBS, 1 mM EDTA pH 8.0) was added to the cell monolayer. After 30 seconds, 9 ml of complete medium was added to the detached cells. After gentle mixing, an aliquot (500 µl) of the detached cells were removed for estimation of cell number. The cells were then seeded at 1×10^5 cells/well in triplicates in a 6 well tissue culture plate until confluent. Prior to stimulation FLS were rendered quiescent by maintaining the cells in serum free Opti-MEM (Minimum Essential Media) for 24 h. Further, all the cell stimulations were carried out in Opti-MEM using the agonists/ligands as described previously (table 2.2). The cell free supernatants were collected for ELISA

analysis and the cells adherent on the culture plates were utilized for RNA extraction with TRIzol reagent.

3.3.3. PBMC isolation, mRNA extraction and quantification

Human primary peripheral blood mononuclear cells (PBMCs) were isolated from heparinised peripheral blood from healthy donor by centrifugation in the density gradient (Lymphoprep, Axis-Shield, Norway). Total RNA was extracted from 1×10^7 PBMCs using 1 ml of Trizol reagent per well (1 ml/3.5 cm) was added and the cells were thus lysed passing through the pipettes several times with the reagent. 200 µl of chloroform was added to 1 ml of Trizol and mixed vigorously by hand and incubated at RT for 10 min. The cells were then centrifuged at 14,000 rpm for 15 min at 4 ^{o}C. The upper phase (60 % volume) around 400-500 µl of colourless liquid was then transferred into a sterile eppendorf tube. To this, equal volumes of isopropyl alcohol was added and mixed well. This mixture was left for 10 min at RT to precipitate RNA and was then centrifuged at 14,000 rpm for 15 min at 4 ^{o}C, and the supernatant was discarded. To the RNA pellet, 500 µl of 75 % ethanol was added followed by centrifugation at 14,000 rpm for 15 min at 4 ^{o}C. The supernatant was discarded and the pellets were then air-dried for 5 min at RT. The RNA pellets were re-suspended in 10-50 µl of RNAse free water. The concentration of RNA, thus extracted was measured using a Nanodrop spectrophotometer, pre-blanked using 1 µl of RNAse free water and A260/280 nm was determined. RNA was stored at -80^{o}C until further use.

3.3.4. Synthesis of first strand cDNA of PBMCs from mRNA

To 1 µl of random hexamers (100 pM/µl), was added 1 µg of RNA in a total volume of 16 µl. This solution was mixed well and placed at 70 ^{o}C for 5 min, followed by 5 min incubation on ice. To this solution, the other components/reagents were added in the following order, 4 µl of 5 × RT buffer, 2 µl of dNTP (10mM), 1 µl of RNasin and 1 µl of MMLV Reverse transcriptase and mixed well. The samples were placed at 37 ^{o}C for 40 min, followed by 42 ^{o}C for 40 min and finally at 80 ^{o}C for 5 min. The first strand cDNA was stored at -20 ^{o}C until further use.

3.3.5. Quantitative real time PCR

Total first strand cDNA was used as a template for real-time PCR quantification using a DyNAmoHS SYBR Green kit (Finnzymes) and a real-time PCR system (DNA Engine

OPTICON® system; MJ Research). For the amplification of TLR 1-10, the respective primers were used as described in table 3.1. For each TLR mRNA quantification, the housekeeping gene hypoxanthine phosphoribosyl transferase *(HPRT)* was used as a reference point using the respective primers.

3.3.6. Agarose gel electrophoresis

An agarose gel (0.8 %) was prepared by melting 0.8 g of agarose in 100 ml of 1 × TAE in the microwave for approximately three min until it appeared clear. This solution was allowed to cool until hand hot and then poured in to a casting tray and a plastic comb was inserted to create the wells. The molten agarose was allowed to solidify. The plastic comb was removed and the gel was placed in the gel electrophoresis base unit (Hoefer Scientific Instruments) filled up with 1 × TAE, so that the gel was completely submerged. Next, 7 µl of PCR product in 2 µl of DNA loading buffer (6.25 ml of H_2O, 25 mg of Xylene Cyanol, 25 mg of Bromophenol Blue, 1.25 ml of 10 % SDS and 12.5 ml of glycerol in 1 µl of TE (0.04 Tris-acetate, 1 mM EDTA, pH 8.0) or the 100 bp DNA ladder were loaded on to the gel. After the complete assembly of the gel unit, the electrophoresis was run at constant volts (100 V DC, 250 mA and 20 W) for approximately 30 min. Care was taken to ensure that the samples did not run off the end of the gel. The gel was removed and placed in ethidium Bromide for 10 min. The gel was de-stained in water and visualised using the Eagle Eye camera system/ UVPGDS8000 gel documentation system.

3.3.7. Meso Scale Human MMP 3-Plex Assay

Cell free supernatants were used for measuring MMP 1, MMP 3, and MMP 9 using Meso Scale 96-Well MMP 3-plex ultra sensitive assay kit (Meso Scale Discovery (MSD)). The Human MMP 3-Plex assay detected MMP 1, 3, 9 in a sandwich immunoassay format. The MSD supplied a 96 well ultra sensitive plate pre-coated with MMP 1, 3, 9 capture antibodies on spatially distinct spots on the plate. First, the pre-coated MMP 3-plex plate was incubated with 25 µl/well of Diluent 2 (R51BB-4) supplied with the kit for 30 min at room temperature (RT) with vigorous shaking at 1000 rpm. Next, the samples (cell free supernatants) or appropriate dilution of Calibrator (highest calibrator point was obtained by diluting the stock by 10 fold in Diluent 2 and from this an 8 point standard curve with 4-fold serial dilution was prepared-assay range 500,000 to 0 pg/ml) was added to separate wells of the MSD plate in duplicates. The plate was sealed with an adhesive seal and incubated for 2 h with vigorous shaking (1000 rpm) at RT. Next, the plate was washed

three times with wash buffer (PBS-T) and was pat dry. The SULFO-TAG Detection Antibody Blend provided as 50 × stock solution was diluted to a final working concentration of 1 ×, by mixing 60 µl of stock antibody blend with 2.94 ml of Diluent 3 (R51BA-4) supplied with the kit. Further, 25 µl/well of the 1 × detection antibody solution was added to each well of the MSD plate and the plate was sealed and incubated for 2 h with vigorous shaking (1000 rpm) at RT. Next, the wash step was repeated and 150 µl/well of 2× diluted Read Buffer T (R92TC-3) was added in to each well of the MSD plate. The plate was immediately read on the SECTOR Imager and the data was analysed using the MSD Discovery Workbench analysis software.

3.3.8. Human IFN-β ELISA design and optimization

To detect human IFN-β levels in the cell free supernatants, a sandwich ELISA method was designed and optimized using an anti-human IFN- mouse monoclonal capture antibody (sc-57203-A; Santa Cruz Biotechnology), human recombinant IFN- standard (300-02BC; Peprotech) and an affinity purified polyclonal antibody biotinylated rabbit anti-human IFN-β detection antibody (500-P32BBt; Peprotech). First, the 96-well NUNC Maxisorb ELISA plate was coated with 100 µl/well of mouse anti-human IFN-β capture antibody 1:100 diluted in PBS followed by incubation overnight at RT. The following day, the plate was washed three times with wash buffer (PBS with 0.05 % (v/v) Tween-20) and pat dried. The plate was blocked for at least 2 h with 200 µl/well of PBS containing 3 % (w/v) bovine serum albumin (BSA) and 1 % Tween (v/v). Next, the wash step was repeated for three times and the plate was pat dried. Next, the samples (cell free supernatants) or standard (the recombinant human IFN-β, 100 µl diluted in reagent diluent (0.1 % (w/v) BSA, 0.5 % (v/v) Tween in 10 mM Tris–HCl, pH 7.5 containing 150 mM NaCl in Tris-buffer saline (TBS)) was added at 100 µl/well. The IFN-β standard concentrations were between 0 and 2000 pg/ml. The plate was incubated with samples or standards for 2 h at RT and washing of the plate was repeated. The detection antibody (100 µl per well; biotinylated rabbit anti-human IFN-β antibody diluted 1:200 in reagent diluent) was added to each well and the plate was incubated for 2 h at RT and washed. Next, the streptavidin-horseradish peroxidase (HRP) conjugate (100 µl) was added to each well and the plate was further incubated in the dark for at least 30 min at RT and then the wash step was repeated. Next 100 µl of substrate, Tetra methyl benzidine liquid substrate (TMB, 1.25 mM/L) was added to each well of the plate and incubated in the dark for 20 min. After 20 min, 50 µl of 1N sulphuric acid (H_2SO_4) was used to stop the reaction and the OD was measured for

each well at 450 nm and 590 nm using an ELx800TM microplate reader with Gen5 Data Analysis Software. The concentration of IFN-β in each sample was extrapolated from a standard curve that related the OD of each standard amount to the known concentration. Standard samples were assayed in duplicate to generate the standard curve, while all samples (cell supernatants) were assayed in triplicates.

3.3.9. Statistical Analysis

All the data presented are representative of at least three independent experiments performed in triplicate and all the data are expressed as mean ± standard error of the mean (S.E.M.) (mean ± S.E.M). Statistical comparisons were performed using an unpaired Student's t-test. Differences with a *p* value less than 0.05 were denoted with (*) and the values less than 0.01 as (**) and were considered statistically significant

Table 3.1: Human real time PCR Oligonucleotides used for the amplification of human genes (TLR, cytokine/chemokine, adaptor, RLR, MMP) and HPRT-housekeeping gene.

Human Gene	Gene accession number	Forward primer sequence (5'-3')	Reverse primer sequence (5'-3')	Predicted fragment size (bp)	Annealing Temperature (T_m, ^oC)
HPRT	NM_000194.2	AGCTTGCTGGTGAAAAGGAC	TTATAGTCAAGGGCATATCC	104	60
TLR1	NM_003263.3	TATTCCTCCTGTTGATATTGCTGCT	TAAATGGTGAACTGCGACCCGAAG	135	60
TLR2	NM_003264.3	ACCTGTCCAACAACAGGATCACCT	TGTTCAAGACTGCCCAGGGAAGAA	139	60
TLR3	NM_003265.2	AAGAACTCACAGGCCAGGAATGGA	AAGAGGCTGGAATGGTGAAGGAGA	182	60
TLR4	NM_138554.3	GCCGAAAGGTGATTGTTGTGGTGT	TACCAGCACGACTGCTCAGAAACT	108	60
TLR5	NM_003268	GTTGCAACTTGCCTGGGAAACTGA	AGCCTGTTGGAGTTGAGGCTTAGT	162	60
TLR6	NM_006068.2	TGAGGTTAGCCTGCCAGTTAGAGA	TTTGGGAAAGCAGAGTGGAGAGGA	126	60
TLR7	NM_016562	TATTCCCACGAACACCACGAACCT	GCAGCCTCTTGATGCACATGTTGT	164	60
TLR8	NM_138636	TGTCTCAGAGGCTGCAATGTAGGT	AGGCTCGCATGGCTTACATGAGTA	136	60
TLR9	NM_017442	CCACAACAACATCCACAGCCAAGT	TGGGACAAGTCCAGCCAGATCAAA	162	60
TLR10	NM_030956	CTGGCAACATGTCACACCTGGAAA	AAGATGGGCAGGCTACCTTCTTCA	151	60
IL-6	NM_000600.3	AGCCACTCACCTCTTCAGAACGAA	CAGTGCCTCTTTGCTGCTTTCACA	121	60
TNF-α	NM_000594.2	CACCACTTCGAAACCTGGGA	CACTTCACTGTGCAGGCCAC	115	60
IFN-β	NM_002176.2	AACTGCAACCTTTCGAAGCC	TGTCGCCTACTACCTGTTGTGC	123	60
RANTES/CCL5	NM_002985.2	TGCCTGTTTCTGCTTGCTCTTGTC	TGTGGTAGAATCTGGGCCCTTCAA	92	60
IP-10/CXCL10	NM_001565.3	ATTATTCCTGCAAGCCAATTTTG	TCACCCTTCTTTTTCATTGTAGCA	127	60
TRIF	NM_182919.2	AGCTCCAGAAACCAGCACCAACTA	TGAAAGCTGAGTGGTCTATGGCGT	166	60
MYD-88	NM_001172567.1	TCCACAGTGATGCCTACTGATGCT	ATGCAGATGAGAGGTGGACCCATT	154	60
RIG-I/DDX58	NM_014314.3	ATTGCCACCTCAGTTGCTGAT	ACATACTCATAAAGGATGACAAGATTG	149	60
MDA-5/IFIH1	NM_022168.2	AGGCACCATGGGAAGTGATTCAGA	TGGGCAACTTCCATTTGGTAAGGC	99	60
MMP-1	NM_004530.4	AGAAGGATGGCAAGTACGGCTTCT	AGTGGTGCAGCTGTCATAGGATGT	125	60
MMP-3	NM_002422.3	AGTGGTGCAGCTGTCATAGGATGT	ACAAGGTTCATGCTGGTGTCCTCA	191	60
MMP-9	NM_004994.2	TACCACCTCGAACTTTGACAGCGA	GCCATTCACGTCGTCCTTATGCAA	193	60
MMP13	NM_002427.3	AGTTTGCAGAGCGCTACCTGAGAT	TCGTCAAGTTTGCCAGTCACCTCT	145	60

3.4. Results

In this study, a quantitative Real time RT-PCR based approach was developed and optimised to screen for and determine the relative gene expression profiles of major OA related cytokines and chemokines like IL-6, IFNβ, TNFα, RANTES/CCL5, IP-10 (Sutton et al., 2009, Fernandes et al., 2002). Additionally, the role of key innate immune receptors namely TLRs 1-9 and cytosolic RIG-I and MDA-5 receptors and their respective adaptor proteins, MyD88 and TRIF, in OA pathology was investigated. Furthermore, the modulation of matrix degrading enzymes such as MMP 1, 3, 9, 13, which are attributed to cartilage destruction (Yamanishi et al., 2002) and synovitis in OA were also studied in this chapter. Also, immunofluorescent staining for major TLR proteins was performed and the specific immunoreactivity was visualized using confocal microscopy. Where possible, to compliment our hypothesis that key TLRs may induce OA related inflammatory cytokines/chemokines/MMPs secretion, we employed a relevant cell model namely FLS derived from Normal (N), Osteoarthritis (OA) and Rheumatoid Arthritis (RA) patients, where RA-FLS were primarily used for comparative purposes, as they have a well established role in RA progression (Kim et al., 2007, Firestein, 1996). Screening of N-FLS Vs OA-FLS Vs RA-FLS, for basal TLR gene expression profiles or by measuring the spontaneous cyto-chemokine secretions or by stimulating the above cell types with synthetic TLR specific agonists/ligands (Roelofs et al., 2008) or with inflammatory mediators like IL-6, IL-β, IFNβ, TNFα, RANTES/CCL5 (Martel-Pelletier et al., 1999) or by DAMPs such as hyaluronan (Scanzello et al., 2008) was undertaken. The read outs for the above mentioned screening studies were either in the form of levels of protein (pg/ml of cytokines (IL-6, IFNβ, TNFα, IL-10, IL-1β, IL-15) / chemokines (RANTES/CCL5, IP-10) / MMPs (MMP-1, 3, 9, 13)) measured through ELISA or relative mRNA expression / fold gene induction of basal or induced TLRs 1-9, RLRs (RIG-I, Mda5), TLR adaptor molecules (e.g. TRIF, MyD88) gene expression and as well OA related inflammatory cytokines, chemokines and MMPs as indicated above.

3.4.1. Analysis of basal expression profile of TLRs 1-9 in FLS

Given the increasing evidence that TLR activation may play a crucial role in OA progression (Scanzello et al., 2008) by mediating synovitis, it was essential to investigate the basal expression profiles of TLRs 1-9 in FLS, given that very little is known about the role of FLS in OA progression. This was achieved by employing a real time RT-PCR

approach whereby total RNA isolated from FLS was used as a template for RT-PCR analysis of TLR expression using TLR1-TLR9 specific oligonucleotides. Accordingly basal TLR gene expression profile in these three types of FLS (N, OA, and RA) is presented in the Figure 3.1. No significant differences in TLR 1, 5, 6 and 8 expression among N, OA and RA FLS was observed (Figure 3.1, panels A, E, F, H, n=3). Whereas, a two fold increase in TLR-2 expression in RA-FLS was observed in (Figure 3.1, panel B, n=3), when compared to OA and N FLS, and this correlates with previous studies (Abdollahi-Roodsaz et al., 2008, Seibl et al., 2003). A similar two fold increase in TLR-4 expression was observed in RA-FLS, when compared to N-FLS (Figure 3.1, panel D, n=3), and this correlates with previous findings (Ospelt et al., 2008). OA-FLS showed a trend towards increased TLR-4 expression compared to N-FLS, but was not significant. Furthermore, a similar increase in TLR-9 expression in RA-FLS was detected (Figure 3.1, panel I, n=3). Regarding TLR3, a 2.5 fold induction was detected in OA-FLS when compared to RA and N FLS (Figure 3.1, panel C, n=4). This is in contrast to previous publications (Ospelt et al., 2008). A 0.7 fold induction of TLR-7 was observed in OA-FLS when compared to RA and N-FLS (Figure 3.1, panel E, n=3). Thus N, OA, RA FLS express all the TLRs 1-9, however significant differences were observed in the basal expression magnitude of few TLRs like TLR-3 in OA ($p \leq 0.05$) and TLR-2, 4, 9 in RA ($p \leq 0.05$) relative to N-FLS, which might signify a probable role for TLR activation downstream the arthritis progression.

3.4.2. Analysis of TLR agonist induced and time dependent expression profile of TLR 1-9 genes in FLS

Given the evidence that activation of innate immune system, particularly the TLR pathways may play a central role in OA progression (Scanzello et al., 2008, McCormack et al., 2009) and synovitis, it was critical to further assess the TLR activation and functionality in FLS cells. While it is know that TLRs on various cell types can be selectively activated by specific agonists/PAMPs (Takeda et al., 2003, Miggin and O'Neill, 2006), herein, an attempt was made to characterise ligand-induced TLR gene expression profiles in FLS. Hence, N, OA, RA FLS were stimulated with TLR ligands for different time points, followed by analysis of

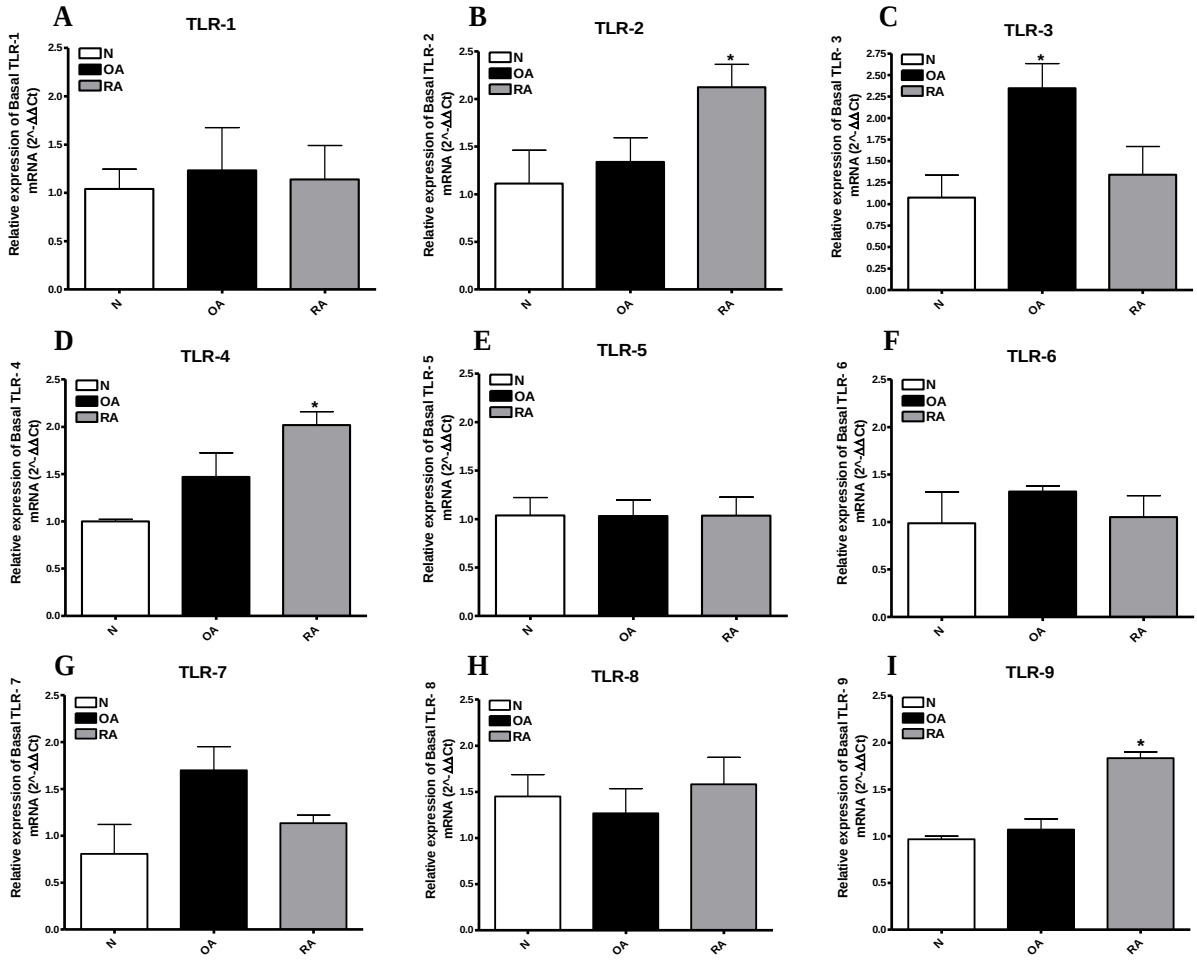

Figure 3.1: Basal expression profile of TLRs 1-9 in FLS. Total RNA was isolated from unstimulated N-FLS, OA-FLS and RA-FLS (n=3 for each cell type) and used as a template for quantitative real-time RT-PCR to assay the basal mRNA expression levels of TLR1 (A), TLR2 (B), TLR3 (C), TLR4 (D), TLR5 (E), TLR6 (F), TLR7 (G), TLR8 (H) and TLR9 (I). The levels of the relevant mRNAs were normalised relative to the housekeeping gene HPRT and are expressed relative to normalised values from unstimulated cells. All the data presented are representative of at least three independent experiments performed in triplicate (mean ± S.E.M). Data was subjected to an unpaired Student's t test. * $p<0.05$ denotes the level of significance relative to N-FLS.

TLR mRNA expression. Stimulation of N, OA, RA FLS with Pam_3CSK_4 (1µg/ml), induced a maximum of 4-fold increase in TLR-1 expression at 16 h in OA-FLS and a 2-fold increase in RA-FLS at 3 h when compared to N-FLS (Figure 3.2, panel A, n=3). Similarly upon stimulation with MALP-2 (20nM), a significant 8-fold increase in TLR6 expression in OA-FLS and a 4-fold increase in RA-FLS at 60 min, was evident when compared to N-FLS (Figure 3.2, panel F, n=3). Alternatively, Flagellin (1µg/ml) induced a 16-fold increase in TLR-5 mRNA expression in RA-FLS when compared to OA and N-FLS at 60 min and a consistent 10-fold increase in RA-FLS at 30 min, 3 h and 16 h respectively (Figure 3.2, panel E, n=3, $p \leq 0.05$). Likewise, stimulation with CLO-97 (10µg/ml) for 60 min, induced a 6-fold increase in TLR-8 mRNA expression in RA-FLS relative to N-FLS (Figure 3.2, panel H, n=3, $p \leq 0.05$). Whereas, upon stimulation with CLO-97 (1µg/ml) for 3 h, a significant 12-fold induction in TLR-7 mRNA expression was observed in OA-FLS relative to RA and N FLS (Figure 3.2, panel G, n=3, $p \leq 0.05$). Moreover, a significant 14-fold increase in TLR-9 mRNA expression was evident in RA-FLS, when treated with CpG (3µg/ml) for 60 min (Figure 3.2, panel I, n=3, $p \leq 0.05$).

Interestingly, the highest and most significant difference in TLR mRNA expression was observed in OA-FLS upon Poly(I:C) stimulation. Stimulation with Poly(I:C) for 60 min induced an 80-fold induction of TLR-3 mRNA in OA-FLS ($p \leq 0.001$), and a 20-fold increase in TLR3 mRNA in RA-FLS ($p \leq 0.05$) when compared to N-FLS (Figure 3.2, panel C, n=3). As expected, a 30-fold increase in TLR-2 mRNA expression was detected upon stimulation with Pam_3CSK_4 for 3 hr (1µg/ml) in RA-FLS ($p \leq 0.01$) and this was sustained even at 16 h relative to N-FLS. In OA-FLS ($p \leq 0.05$), a 12-fold induction of TLR-2 was detected at 3 hr (Figure 3.2, panel B, n=3). Moreover, a 70-fold increase in TLR-4 mRNA expression was detected in RA-FLS ($p \leq 0.001$) and a 50-fold increase in OA-FLS ($p \leq 0.01$), respectively, upon stimulation with LPS (1µg/ml) for 60 min, and a trend towards TLR-4 mRNA at 3 h and 16 h in both RA and OA-FLS relative to N-FLS was detected (Figure 3.2, panel D, n=3), which was in contrary to the TLR-2 mRNA, which showed an increasing trend line at 3 h and 16 h. These data correlate with previous studies demonstrating a time dependent differential induction of TLR-2 and TLR-4 mRNA expression in RA-FLS (Ospelt et al., 2008, Kim et al., 2007). In contrast to a previous study (Ospelt et al., 2008), TLR-3 mRNA induction was higher in OA-FLS compared to N-FLS upon Poly(I:C) stimulation.

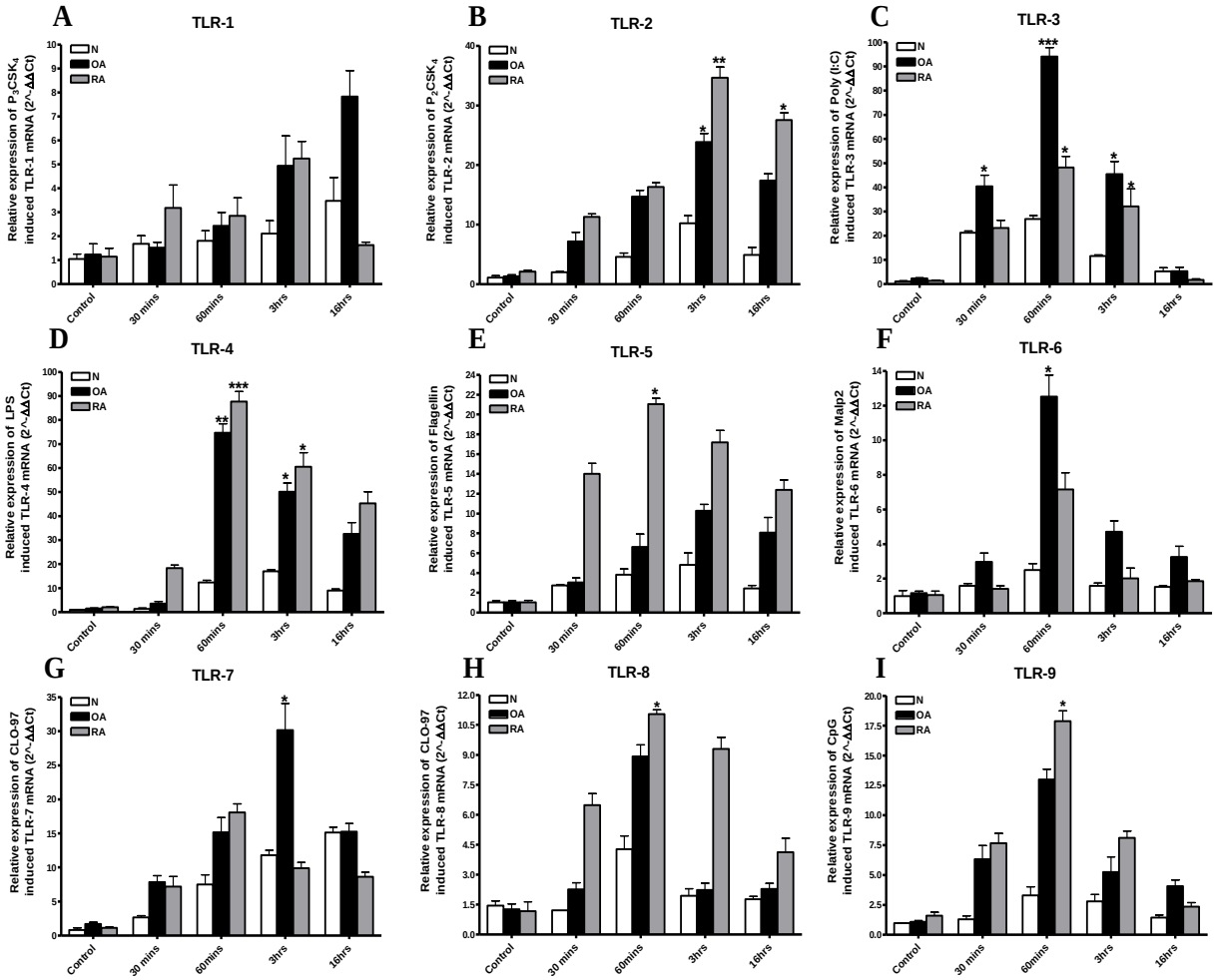

Figure 3.2: Analysis of TLR agonist induced and time dependent expression profile of TLRs 1-9 genes in FLS. (A-I) N-FLS, OA-FLS and RA-FLS (n=3 for each cell type) were treated with Pam_3CSK_4 (1 µg/ml; TLR1/2 ligand), Pam_2CSK_4 (1 µg/ml; TLR2 ligand), Poly(I:C) (10 µg/ml; TLR3 ligand), LPS (1 µg/ml; TLR4 ligand), Flagellin (1 µg/ml; TLR5 ligand), MALP-2 (20nM/ml; TLR2/6 ligand), CLO-97 (1 µg/ml; TLR7/8 ligand) and CpG (3 µg/ml; TLR9 ligand) for 30 min, 60 min, 3 h and 16 h respectively. Total RNA was then isolated from control and stimulated N-FLS, OA-FLS, RA-FLS and used as a template for quantitative real-time RT-PCR to assay the mRNA expression levels of TLR1 (A), TLR2 (B), TLR3 (C), TLR4 (D), TLR5 (E), TLR6 (F), TLR7 (G), TLR8 (H) and TLR9 (I). The levels of the relevant mRNAs were normalised relative to the housekeeping gene HPRT and are expressed relative to normalised values from unstimulated or control cells. All the data presented are representative of at least three independent experiments performed in triplicate (mean ± S.E.M). Data was subjected to an unpaired Student's t test. * $p<0.05$, ** $p<0.01$ denotes the level of significance relative to respective cell type control.

3.4.3. Agarose gel electrophoresis quantification of RT-PCR products for TLR 1-10 in FLS

Routinely, to substantiate the above TLR mRNA expression studies in FLS and to further validate the accuracy and TLR oligonucleotide specificity of the RT-PCR amplified TLR products in FLS, agarose gel electrophoresis was performed using the RT-PCR generated products from N-FLS (Figure 3.3, panel A), OA-FLS (Figure 3.3, panel B) and PBMCs (Figure 3.3, panel C). Wherein, PBMCs served as positive cell controls, as these cells were previously shown to express all TLRs (Siednienko and Miggin, 2009). The relevant PCR products were qualitatively identified for correct TLR amplicon sizes as indicated on the Figure 3.3, using a 100 bp DNA ladder (denoted as M), where HPRT served as a house keeping gene to ascertain whether the RT-PCR procedure itself was successful. The RT-PCR generated TLR mRNA amplicons were of correct size, as the mRNA lacks an intronic region, and should genomic DNA contamination have occurred, an incorrect and much larger amplification product would have been amplified. Moreover, increased levels of TLR2, 3 and 4 RT-PCR products were detected in OA-FLS relative to N-FLS and PBMCs (Figure 3.3, panel B).

3.4.4. Analysis of TLR 2, 3, 4 protein expression in FLS using confocal microscopy

To substantiate the finding that TLR 2, 3, 4 mRNA expression was more predominant in OA-FLS relative to N-FLS, indirect immunofluorescent staining using anti-TLR2, anti-TLR3 and anti-TLR4 antibodies was performed. Appropriate TLR specific immunoreactivity was visualised by confocal microscopy using an Alexa Fluor 546 fluorescent labelled secondary antibody which was observed as red staining in N-FLS (Figure 3.4, panel A) and OA-FLS (Figure 3.4, panel B) and cell nuclei were stained in blue using DAPI.. Firstly, it was clear that TLR 2, 3, 4 protein is expressed in N and OA-FLS and secondly a marked increase in basal TLR 2, 3, 4 immunofluorescence was detected in OA-FLS relative to N-FLS. This is consistent with the TLR2, 3, 4 mRNA expression studies and supports the notion that TLR 2, 3, 4 may play a role in OA development.

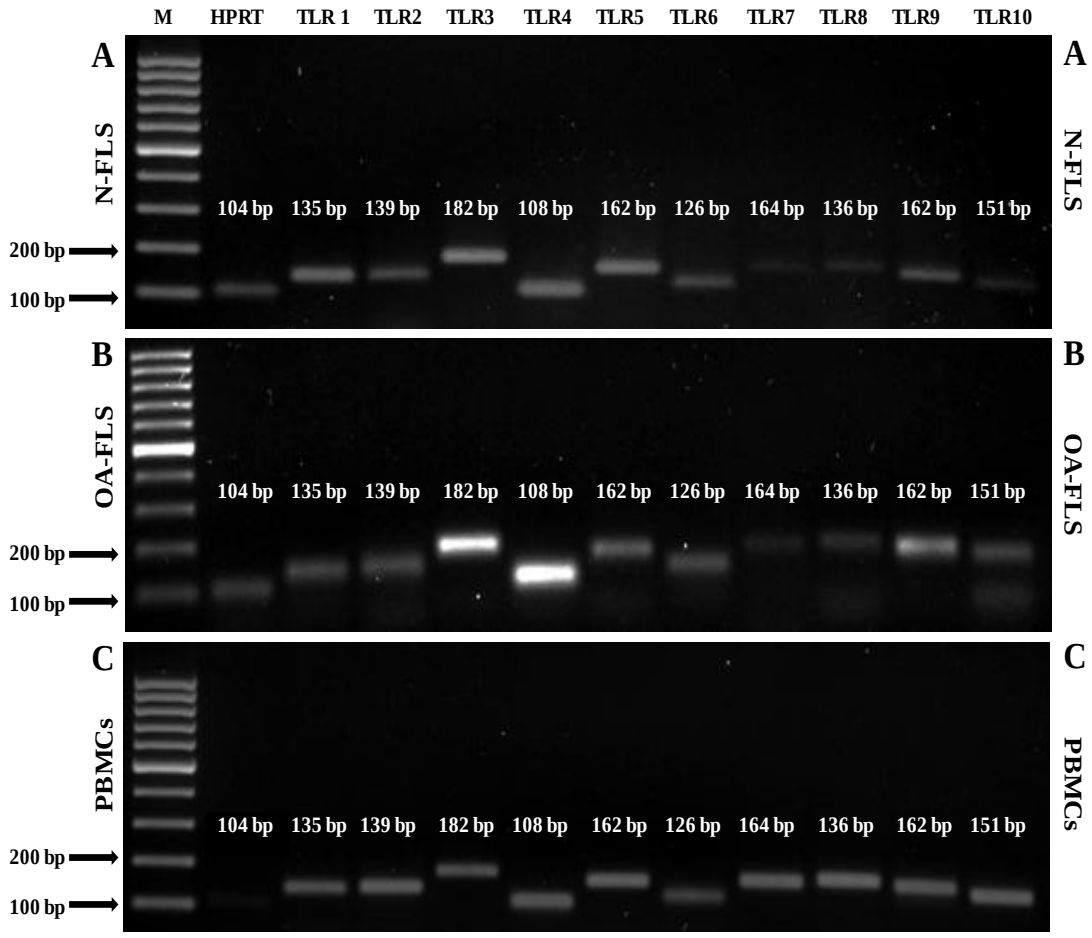

Figure 3.3: Agarose gel electrophoresis quantification of RT-PCR products for TLRs (1-10) in FLS. Total RNA was isolated from N-FLS (panel A) and OA-FLS (panel B). Also, total RNA was isolated from peripheral blood mononuclear cells (PBMCs, panel C) from healthy donors. The RNA was used as a template for RT-PCR to assay the basal mRNA expression levels of TLR1-10. Correct RT-PCR product size was confirmed using the 100 bp DNA molecular weight marker (M; from Promega).

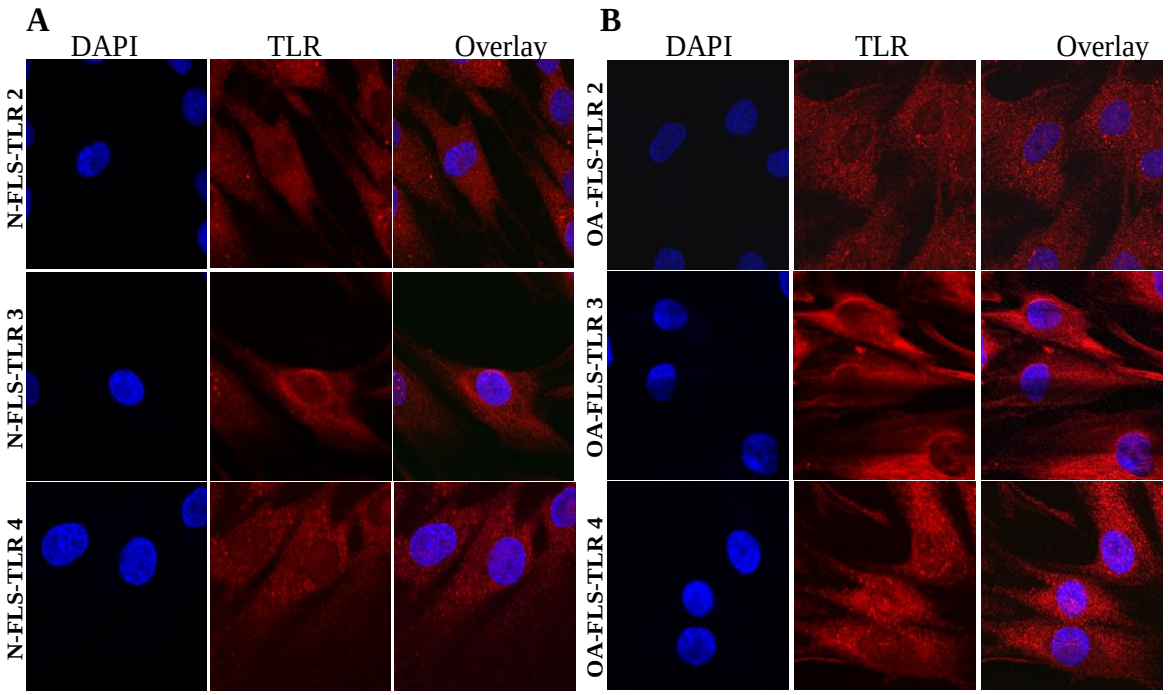

Figure 3.4: Analysis of TLR2, 3, 4 expression in FLS using confocal microscopy. N-FLS (A) and OA-FLS (B) were grown on glass cover slips and were permeabilised, fixed and probed for immunoreactivity with anti-TLR2 (1:100 dilution), anti-TLR3 (1:100 dilution) and anti-TLR4 (1:100 dilution) antibodies. Immunoreactivity was visualized by confocal microscopy using an Alexa Fluor 546 (1:500 dilution) labelled secondary antibody seen as red staining. DAPI staining of nuclei is also included and seen as blue staining, and confirmed no off-target binding by the fluorescent secondary antibody (DAPI panels in A and B are DAPI + Alexa Fluor 546). Confocal images were captured using an Olympus FluoView FV1000 System laser scanning microscope equipped with the appropriate filter sets. Data analysis was performed using the Olympus FV 1.6 b imaging software. All results are representative of at least three independent experiments.

3.4.5. Analysis of basal expression profile of major proinflammatory cytokine and chemokine genes in FLS

During the inflammatory episodes associated with OA and RA, the activated FLS secrete a wide variety of proinflammatory cytokines and chemokines (Sutton et al., 2009, Firestein, 1996), which may perpetuate the chronic inflammatory state and lead to progressive, irreversible damage of the affected joint (Sutton et al., 2009, Pelletier et al., 2001, Ghosh and Cheras, 2001, Fernandes et al., 2002). Also, the proinflammatory cytokines, TNFα and IL-6, are present at high levels in the synovial fluid of inflamed joints (Sutton et al., 2009, Fernandes et al., 2002). Given this, an attempt was made to characterise the actual/basal mRNA expression profiles of key cytokines that may be linked with OA and RA, namely, TNFα, IL-6, IFNβ and chemokines, namely, RANTES/CCL5 and IP-10 in N, OA and RA-FLS. Interestingly, a significant 2-fold increase in basal IFNβ mRNA expression was detected in OA-FLS relative to N-FLS (Figure 3.5, panel E, n=3, $p < 0.05$). A similar increase in basal IL-6 mRNA expression was observed in OA-FLS (Figure 3.5, panel B, n=3) and as well a significant increase in TNFα mRNA expression was detected in OA-FLS relative to N-FLS (Figure 3.5, panel A, n=3, $p \leq 0.05$).

In contrast, a trend towards increased levels of basal IFNβ, IL-6, TNFα mRNA expression was observed in RA-FLS relative to N-FLS respectively, though this was not significant (Figure 3.5, panels E, B, A). Also, a non significant increase in basal RANTES/CCL5 was detected in OA-FLS and RA-FLS relative to N-FLS (Figure 3.5, panel C, n=3). Also, a non-significant decrease in IP-10 mRNA expression was detected in OA-FLS relative to N-FLS (Figure 3.5, panel D, n=3) and this correlates with recent findings (Saetan et al., 2011), but is in contrast to a previous publication (Hanaoka et al., 2003). Hence, the differential basal cytokine and chemokine mRNA expression levels in OA-FLS may signify a critical role for inflammatory mediators in OA pathogenesis. Moreover, the stimuli that serve to modulate such differences in expression are not yet fully known, thus further investigation of the cytokine and chemokine signalling pathways in the contest of OA is indispensable.

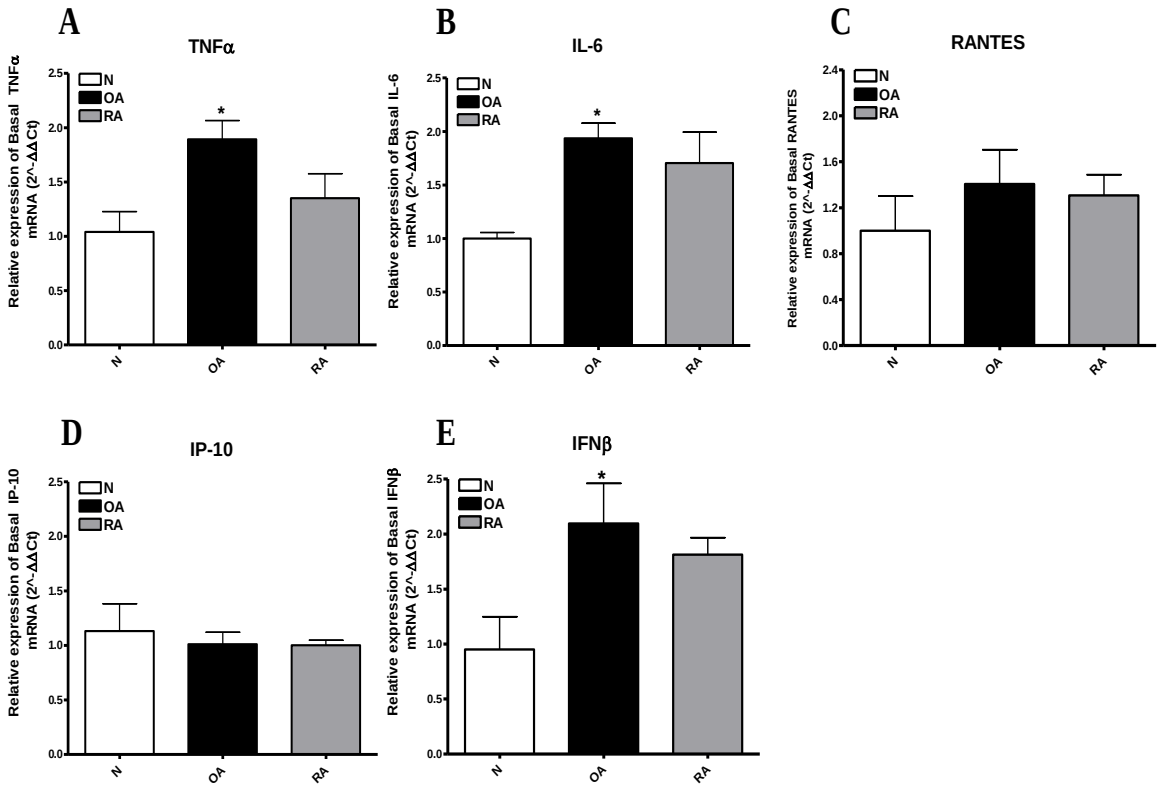

Figure 3.5: Analysis of basal expression profile of cytokine/chemokine genes in FLS. Total RNA was isolated from unstimulated and stimulated N-FLS, OA-FLS and RA-FLS (n=3 for each cell type) and used as a template for quantitative real-time RT-PCR to assess the mRNA expression levels of TNFα (A), IL-6 (B), RANTES/CCL5 (C), IP-10 (D) and IFNβ (E). The levels of the relevant mRNAs were normalised relative to the housekeeping gene HPRT and are expressed relative to normalised values from unstimulated cells. All the data represented are representative of at least three independent experiments performed in triplicate (mean ± S.E.M). Data was subjected to an unpaired Student's t test. * $p < 0.05$ denotes the level of significance relative to N-FLS.

3.4.6. Analysis of TLR or RLR (RIG-I) ligand induced expression profile of major pro-inflammatory cytokine or chemokine genes in FLS

Many research groups have shown that inflammation of the synovium plays a crucial role in OA pathogenesis (Fell and Jubb, 1977, Ghosh and Cheras, 2001, Pearle et al., 2007, Fiorito et al., 2005, Pelletier et al., 2001) and FLSs have been described as the major effector cell type in the synovium (Müller-Ladner et al., 2007). These cells have been attributed with the production of proinflammatory cytokine and chemokines in the OA joint (Sutton et al., 2009). Given that FLS may become activated by exogenous pathogenic stimuli like the synthetic TLR agonists (Ospelt et al., 2008), and our previous observation that TLRs are modulated in OA (Figure 3.2), it was essential to further investigate pro-inflammatory cytokines and chemokines that may be secreted by FLS upon TLR activation. As there is a possibility that the RLRs may also be involved in OA, FLSs were also stimulated with a RIG-I ligand namely, 5' triphosphate double stranded RNA (5' ppp-dsRNA) as described previously (Hornung et al., 2006), in conjunction with the previously described TLR ligands (section 3.4.2). Accordingly, N, OA and RA-FLS were stimulated with the following TLR ligands: Pam_3CSK_4 (1 µg/ml; TLR1/2 ligand), Pam_2CSK_4 (1 µg/ml; TLR2 ligand), Poly(I:C) (10 µg/ml; TLR3 ligand), LPS (1 µg/ml; TLR4 ligand), Flagellin (1 µg/ml; TLR5 ligand), MALP-2 (20nM; TLR2/6 ligand), CLO-97 (1 µg/ml; TLR7/8 ligand), CpG (3 µg/ml; TLR9 ligand) and 5' ppp dsRNA (1 µg/ml; RIG-I ligand) followed by analysis of TNFα, IL-6, RANTES/CCL5, IP-10 and IFNβ mRNA expression (Figure 3.6).

Predominantly Poly(I:C) (10 µg/ml) stimulation significantly increased TNFα mRNA expression by 17-fold in OA-FLS ($p \leq 0.01$) and by 7-fold in RA-FLS relative to N-FLS. In contrast, LPS and Pam_2CSK_4 induced a 6-fold and 2-fold increase in TNFα mRNA expression, respectively, in OA-FLS relative to N-FLS. Other TLR ligands and the RIG-I ligand did not induce TNFα mRNA expression in FLS (Figure 3.6, panel A, n=3). Regarding, IL-6 mRNA expression, a significant 16-fold increase in IL-6 expression was detected in OA-FLS ($p \leq 0.05$) relative to N-FLS upon Poly(I:C) stimulation. Similarly, a significant 15-fold increase in IL-6 expression was detected in RA-FLS ($p \leq 0.05$) upon Pam_2CSK_4 stimulation. Likewise, a significant 13-fold increase in IL-6 expression in RA-FLS ($p \leq 0.05$) was evident with Pam_3CSK_4 stimulation, while other TLR or RIG-I ligands failed to induce IL-6 mRNA expression in FLS (Figure 3.6, panel B, n=3). Furthermore, a

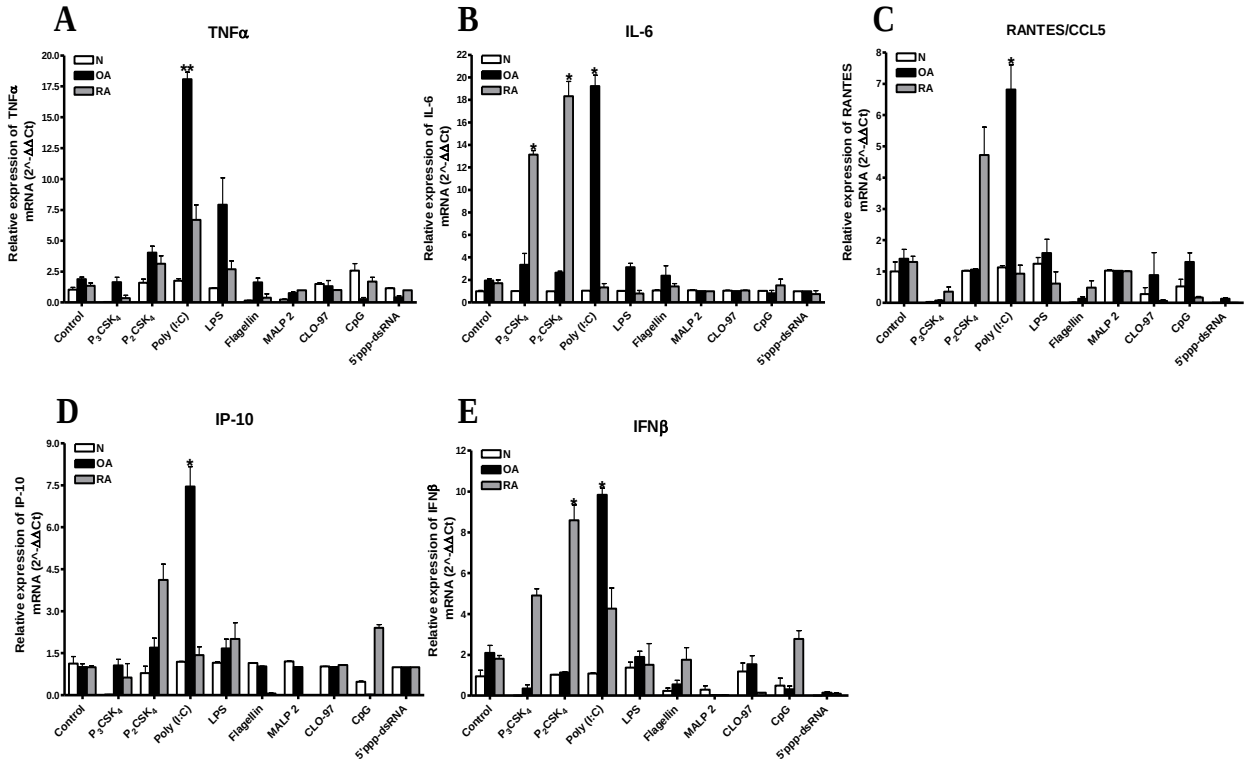

Figure 3.6: Analysis of TLR/RIG-I ligand induced expression profile of major pro-inflammatory cytokines/chemokine genes in FLS. (A-E) N-FLS, OA-FLS and RA-FLS (n=3 for each cell type) were treated with Pam_3CSK_4 (1 µg/ml; TLR1/2 ligand, Pam_2CSK_4 (1 µg/ml; TLR2 ligand), Poly(I:C) (10 µg/ml; TLR3 ligand), LPS (1 µg/ml; TLR4 ligand), Flagellin (1 µg/ml; TLR5 ligand), MALP-2 (20nM; TLR2/6 ligand), CLO-97 (1 µg/ml; TLR7/8 ligand), CpG (3 µg/ml; TLR9 ligand) and 5' ppp dsRNA (1 µg/ml; RIG-I ligand) for 16 h. Total RNA was then isolated from control and stimulated N-FLS, OA-FLS, RA-FLS and used as a template for quantitative real-time RT-PCR to assay the mRNA expression levels of TNFα (A), IL-6 (B), RANTES/CCL5 (C), IP-10 (D) and IFNβ (E). The levels of the relevant mRNAs were normalised relative to the housekeeping gene HPRT and are expressed relative to normalised values from unstimulated or control cells. All the data presented are representative of at least three independent experiments performed in triplicate (mean ± S.E.M). Data was subjected to an unpaired Student's t test. * $p<0.05$, ** $p<0.01$ denotes the level of significance relative to respective cell type control.

significant 6.5-fold increase in RANTES/CCL5 mRNA expression was detected in OA-FLS ($p \leq 0.05$) relative to N-FLS upon Poly(I:C) stimulation. A nonsignificant 4.5-fold increase in RANTES expression in RA-FLS was evident upon Pam_2CSK_4 stimulation. Other TLR or RIG-I ligands were without effect on RANTES mRNA expression in FLS (Figure 3.6, panel C). A significant 7-fold increase in IP-10 mRNA expression was detected upon Poly(I:C) stimulation in OA-FLS ($p \leq 0.05$) relative to N-FLS. A nonsignificant 3.5-fold increase in IP-10 expression was observed in RA-FLS upon stimulation with Pam_2CSK_4 stimulation and other TLR or RIG-I ligands did not affect IP-10 mRNA expression in FLS (Figure 3.6, panel D). Correspondingly, a significant 9-fold increase in IFNβ mRNA expression was detected in OA-FLS ($p \leq 0.05$), and a 4-fold increase in RA-FLS relative to N-FLS upon stimulation with Poly(I:C). Similarly, a significant 8-fold increase in IFNβ expression in RA-FLS ($p \leq 0.05$) relative to N-FLS was evident upon Pam_2CSK_4 stimulation and no significant increase in IFNβ expression in RA-FLS was detected upon Pam_3CSK_4 stimulation (Figure 3.6, panel E). Other TLR or RIG-I ligands had little or no effect on IFNβ mRNA expression in FLS (Figure 3.6, panel E). These data suggest that TLRs rather than RLRs might play a key role in modulating OA by inducing proinflammatory cytokine and chemokine cascades in FLS, as suggested previously (McCormack et al., 2009). The cytokine and chemokine cascades may work both in an autocrine and a paracrine fashion and may serve to perpetuate synovial inflammation, ultimately leading to joint destruction and OA progression (McGettrick and O'Neill, 2010, Roelofs et al., 2008). The findings suggest a probable role for TLR-3 activation in OA disease perpetuation, though further validation at the protein level is required.

3.4.7. Analysis of TLR agonists or sterile inflammatory mediators induced cytokine or chemokine production using human immortalised K4 FLS

K4 FLS represents a valuable and unique tool to study the mechanisms that induce and maintain synoviocyte activation (Aicher et al., 2003, Biniecka et al., 2011). K4 FLS were employed for preliminary investigations towards the optimisation of TLR/DAMP ligand concentrations (data not shown) and to study the cytokine and chemokine profiles in synoviocytes upon stimulation with various TLR agonists, sterile inflammatory mediators and DAMPs, as growing evidence suggest that TLRs may also be activated by endogenous non infectious signals called DAMPs namely hyaluronan (Scanzello et al., 2008), and cytokines namely IL-1β and TNFα (Zhu et al., 2011). Herein, we investigated the effect of

TLR 1-9 ligands and inflammatory mediators namely, hyaluronan, IL-1β and TNFα on the secretion of vital cytokines and chemokines in a joint using K4 FLS by ELISA. K4 FLS were stimulated with various TLR ligands and sterile inflammatory mediators for 16 h. Notably, unstimulated control cells also secreted small amounts of cytokines and chemokines, which showed the spontaneous cytokine secretion ability of synoviocytes, and this correlates with previous findings (Arend and Dayer, 1990). More specifically, K4 FLS secreted notable amounts of pro-inflammatory cytokines namely, IL-6, IFNβ, TNFα, IL-15, IL-1β, chemokine RANTES/CCL5 and an anti-inflammatory cytokine IL-10 (Figure 3.7, panels A, B, D, E, G, C and F). It was clear from Figure 3.7, that Poly(I:C) (10 µg/ml) induced highest amounts of IL-6 secretion in K4 FLS (4401.1 ± 222.2 pg/ml from basal 3479.1 ± 207.1 pg/ml), IFNβ (4736.1 ± 233.5 pg/ml from basal 3968.6 ± 133.2 pg/ml), RANTES (6427.0 ± 311.6 pg/ml from basal 2929.7 ± 204.1 pg/ml). Hyaluronan (20µg/ml) was found to induce the highest TNFα secretion in K4 FLS (1573.8 ± 145.4 from basal 203.3 ± 9.7 pg/ml). Stimulation with IL-1β induced its own secretion (399.1 ± 9.7 from basal 33.3 ± 0.7 pg/ml). Stimulation with MALP-2 (20 nM) induced the highest levels of IL-15 secretion in K4 FLS (88.0 ± 6.8 from basal 25.5 ± 3.5 pg/ml). MALP-2 also induced IL-10 secretion in K4 FLS (2443.0 ± 239.0 from basal 886.3 ± 14.9 pg/ml). Together, these data provide evidence that FLS can be activated specifically by the selected concentrations of TLR ligands and DAMPs *in-vitro*, which in turn, induces the recurrent secretion of inflammatory mediators which may aid in perpetuating synovitis and joint destruction.

3.4.8. Analysis of spontaneous and TLR or RIG-I ligand induced secretion of cytokines and chemokines in FLS

To further corroborate our the cytokine/chemokine mRNA expression studies (Figure 3.5) and to substantiate the observations of Figure 3.6, we aimed to further investigate the protein expression profiles of these cytokines/chemokines using the optimised concentration of the PAMPs or DAMPs as described (Figure 3.7) and N, OA and RA-FLS as models. Initially, to examine whether perturbations in the spontaneous cytokine production as evident in earlier K4 FLS study, occur as a consequence of disease pathology and to define how prevalent these mediators are in the disease, the actual cytokines or chemokines secreted by the FLS without any external stimuli were examined and illustrated in (Figure 3.8, panel A). Accordingly, it was evident that N.OA.RA.FLS, spontaneously secreted IL-6, IFNβ, TNF-α, RANTES, IL-10, IL-1β and IL-15 to varying

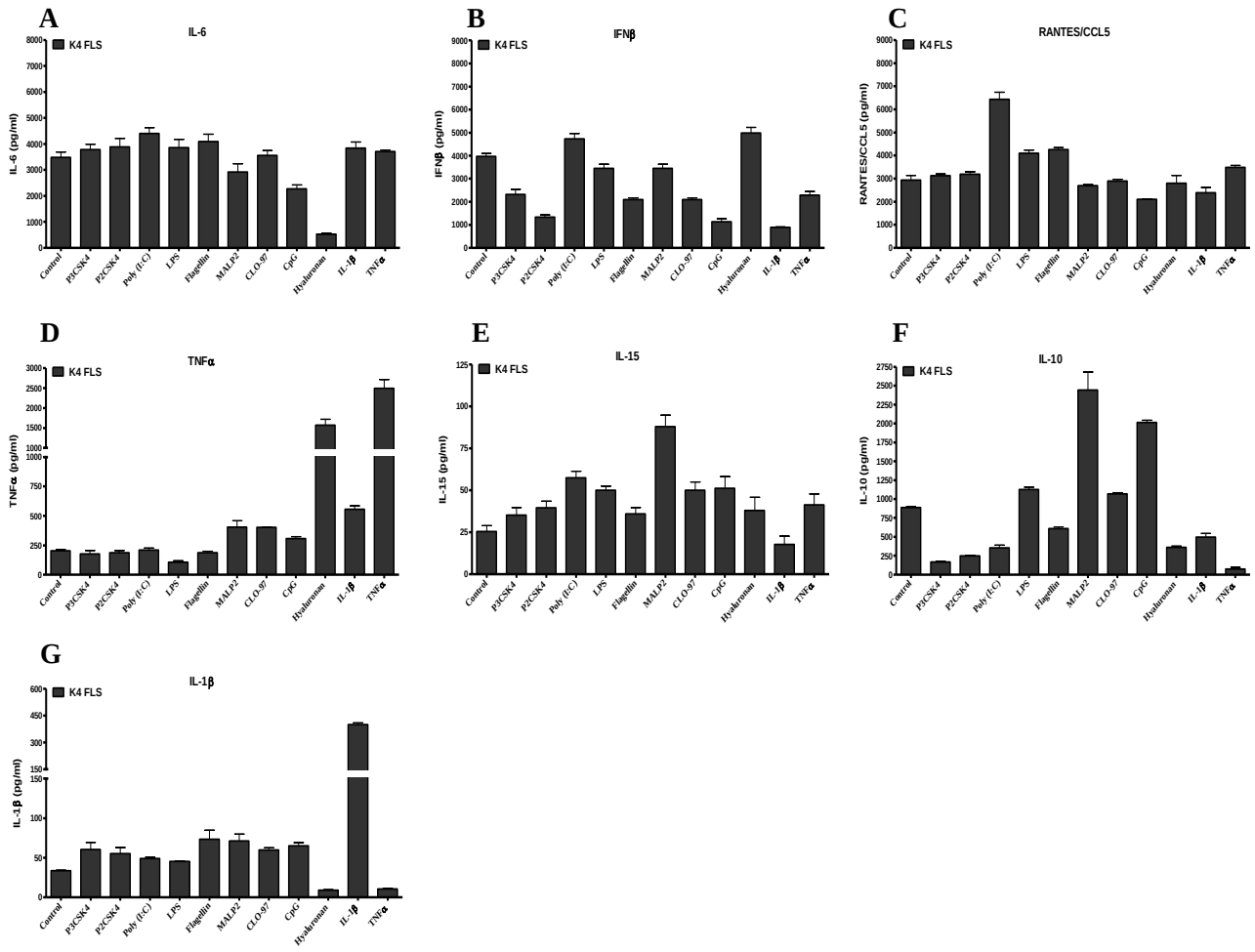

Figure 3.7: Analysis of TLR agonists or sterile inflammatory mediators induced cytokine/chemokine production using immortalised human K4 FLS. The concentrations of TLR ligands or sterile inflammatory mediators were initially optimised using the immortalised synoviocyte cell line K4 FLS. Immortalized synoviocytes were cultured from 23rd passage and were seeded at 1 x 10^6 cells/well density in a 6 well tissue culture plate. These K4 FLS were either treated only with TLR agonists, Pam_3CSK_4 (1 µg/ml; TLR1/2 ligand, Pam_2CSK_4 (1 µg/ml; TLR2 ligand), Poly(I:C) (10 µg/ml; TLR3 ligand), LPS (1 µg/ml; TLR4 ligand), Flagellin (1 µg/ml; TLR5 ligand), MALP-2 (20nM; TLR2/6 ligand), CLO-97 (1 µg/ml; TLR7/8 ligand), CpG (3 µg/ml; TLR9 ligand or with known sterile inflammatory mediators like Hyaluronan (25 µg/ml), IL-1β (100 pg/ml), TNFα (1 ng/ml) for 16 h. Cell free supernatants were analyzed for (A) IL-6, (B) IFN β, (C) RANTES/CCL5, (D) TNFα, (E) IL-15, (F) IL-10, (G) IL-1β by ELISA. All the data presented are representative of at least three independent experiments performed in triplicate (mean ± S.E.M). Data was subjected to an unpaired Student's t test. * $p<0.05$ denotes the level of significance relative to control.

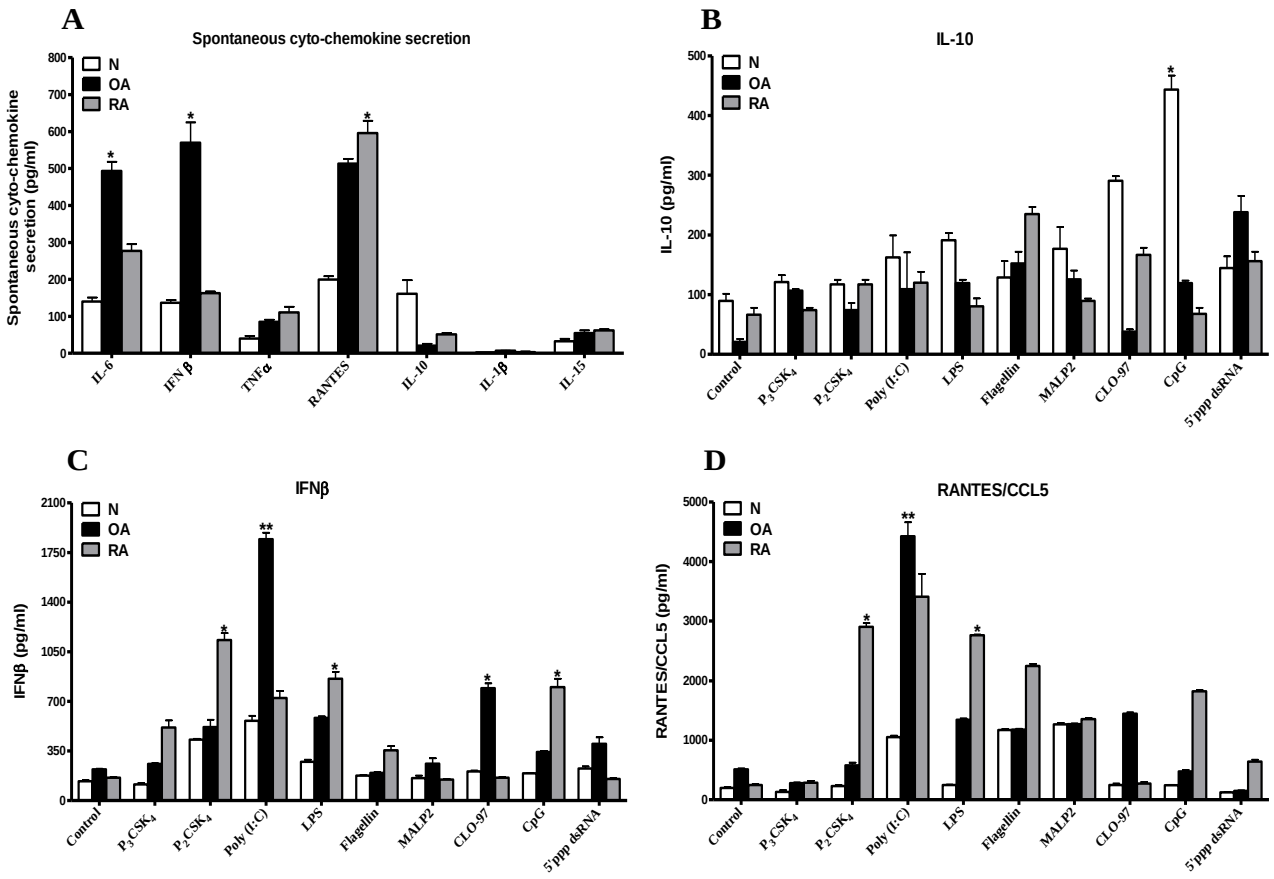

Figure 3.8: Analysis of spontaneous or TLR/RIG-I ligand induced secretion of cytokines/chemokines in FLS. (A-C) N-FLS, OA-FLS and RA-FLS (n=3 for each cell type) were treated with Pam_3CSK_4 (1 µg/ml; TLR1/2 ligand, Pam_2CSK_4 (1 µg/ml; TLR2 ligand), Poly(I:C) (10 µg/ml; TLR3 ligand), LPS (1 µg/ml; TLR4 ligand), Flagellin (1 µg/ml; TLR5 ligand), MALP-2 (20nM; TLR2/6 ligand), CLO-97 (1 µg/ml; TLR7/8 ligand), CpG (3 µg/ml; TLR9 ligand) and 5' ppp dsRNA (1 µg/ml; RIG-I ligand) for 16 h. Cell free supernatants were analyzed for (A) IFNβ, (B) RANTES/CCL5, (C) IL-10 by ELISA. The panel (D) denotes spontaneous cytokine/chemokine (IL-6, IFNβ, TNFα, RANTES/CCL5, IL-10, IL-1β, and IL-15) secretion by FLS in serum free opti-MEM subsequently measured by respective ELISAs. All the data presented are representative of at least three independent experiments performed in triplicate (mean ± S.E.M). Data was subjected to an unpaired Student's t test. * $p<0.05$, ** $p<0.01$ denotes the level of significance relative to respective cell type control.

amounts in the joint, and this correlates with previous publications (Ultaigh et al., 2011, Katsikis et al., 1994). A significant secretion of IL-6 was evident in OA-FLS relative to N-FLS (OA: 493.6 ± 24.6 pg/ml vs. N: 140.1 ± 10.3 pg/ml). Similarly, OA-FLS secreted significantly higher levels of IFNβ secretion relative to N-FLS (OA: 569.8 ± 55.3 pg/ml vs. N: 136.4 ± 7.3 pg/ml, $p \leq 0.05$). OA-FLS also secreted high levels of RANTES relative to N-FLS (OA: 513.0 ± 13.2 pg/ml vs. N: 199.2 ± 9.4 pg/ml). RA-FLS also showed significant secretion of RANTES relative N-FLS (RA: 595.9 ± 33.4 pg/ml vs. N: 199.2 ± 9.4 pg/ml, $p \leq 0.05$). IL-6 secretion by RA-FLS was not significantly different relative to N-FLS (RA: 277.2 ± 17.8 pg/ml vs. N: 140.1 ± 10.3 pg/ml). IL-1β secretion was barely detectable in N, OA and RA-FLS (N: 2.4 ± 0.1, OA: 7.0 ± 0.1, RA: 3.4 ± 1.2 pg/ml respectively). Similarly, modest IL-15 secretion was observed with minor differences detected between N, OA and RA-FLS (N: 32.9 ± 6.7, OA: 54.9 ± 6.9, RA: 62.0 ± 2.7 pg/ml). Thereafter, TLR/RLR ligand induced expression of anti-inflammatory cytokine IL-10 (Figure 3.8, panel B, n=3), anti-viral cytokine IFNβ (Figure 3.8, panel C, n=3) and a pivotal chemokine RANTES/CCL5 (Figure 3.8, panel D, n=3) were examined in N, OA and RA-FLS. It was evident that CpG (3μg/ml) significantly induced IL-10 levels in N-FLS (443.5 ± 23.4 pg/ml from basal 89.9 ± 11.8 pg/ml, $p \leq 0.05$) (Figure 3.8, panel B). In OA-FLS, the highest induction of IL-10 levels was evident upon 5' ppp dsRNA stimulation (238.2 ± 27.3 pg/ml from a basal 20.7 ± 5 pg/ml). Flagellin stimulation induced the highest levels of IL-10 in RA-FLS (235.0 ± 11.8 pg/ml from a basal 66.3 ± 11.8 pg/ml). These data indicate a protective role for these ligands in FLS by inducing IL-10, a previously known anti-inflammatory cytokine, which is thought to have an important immunoregulatory role in the cytokine network of OA and RA probably by regulating monocytes and in some cases T cell cytokine production (Katsikis et al., 1994).

Furthermore, it was evident that Poly(I:C) stimulation significantly induced IFNβ levels in OA-FLS (1843.9 ± 46.7 pg/ml from a basal 219.8 ± 5.2 pg/ml, $p \leq 0.01$) (Figure 3.8, panel C). Similarly, CLO-97 induced IFNβ levels significantly in OA-FLS (793.0 ± 34.7 pg/ml from a basal 219.8 ± 5.2 pg/ml, $p \leq 0.05$). in RA-FLS, Pam_2CSK_4, LPS and CpG significantly induced IFNβ levels (1132.2 ± 219.6 pg/ml, 859.0 ± 25.8 pg/ml, 800.8 ± 6.3 pg/ml respectively from a basal 219.8 ± 5.2 pg/ml, $p \leq 0.05$). However, Poly(I:C) induced notable IFNβ levels in RA-FLS (724.0 ± 50.3 pg/ml from a basal 219.8 ± 5.2 pg/ml) and N-FLS (563.6 219.8 ± 34.51 pg/ml from a basal 136.4 ± 7.3 pg/ml). Thus, these findings corroborate our previous IFNβ mRNA expression study (Figure 3.6, panel E) which

demonstrated a TLR3 dependent trend in inducing this potent anti-viral cytokine, a molecule that is currently considered to be a pro-inflammatory cytokine owing to the studies in rats following pristine induced arthritis (Meng et al., 2010, Zhu et al., 2011). Type I IFNs have also been shown to behave as crucial participants in disease amplification in autoimmunity by a feed-forward mechanism employing IFNAR1 and IFNAR2 receptors (Hall and Rosen, 2010). Further, IFNβ was also shown to play a role in other chronic inflammatory diseases by prolonged T-cell survival (Buckley et al., 2001).

Poly(I:C) also induced significant levels of RANTES secretion in OA-FLS (4425.0 ± 235.1 pg/ml from a basal 513.0 ± 13.2 pg/ml, $p \leq 0.01$) (Figure 3.8, panel D). Similarly, a significant increase in RANTES secretion was observed in RA-FLS upon Poly(I:C) stimulation (3411.9 ± 382.9 pg/ml from a basal 245.9 ± 16.6 pg/ml, $p \leq 0.05$). Furthermore, Pam_2CSK_4 and LPS also induced significant levels of RANTES in RA-FLS (2903.6 ± 61.8 pg/ml and 2762.4 ± 11.0 pg/ml from a basal 245.9 ± 16.6 pg/ml, $p \leq 0.05$). Likewise, a marked increase in RANTES secretion was observed upon Flagellin and CpG was evident in RA-FLS (2248.2 ± 34.3 pg/ml and 1824.0 ± 17.0 pg/ml from a basal 246.0 ± 17.0 pg/ml). LPS, Flagellin, MALP-2 and CLO-97 did not induce significant levels of RANTES in OA-FLS (Figure 3.8 panel D). In N-FLS, only Poly(I:C), Flagellin and MALP-2 induced RANTES secretion. Chemokines such as RANTES and its receptor CCR5 may be involved in the perpetuation of chronic inflammatory joint diseases, like RA and OA, through acting in autocrine or paracrine pathways, in which RANTES increased the expression of its own receptor, CCR5 on FLS (Haringman et al., 2004, Vergunst et al., 2005). Another study demonstrated that RANTES activated chondrocytes dysfunctionality associated with joint inflammation and cartilage degradation in OA (Yuan et al., 2003, Borzì et al., 2004). Given the predominant poly(I:C) driven induction of RANTES secretion in both OA-FLS and RA-FLS, a TLR3 dependent signalling pathway may be critical in the initiation and propagation of OA and RA pathologies.

Thus, TLR3-targeted therapies may prove useful as a therapeutic intervention towards restoring the balance between anabolic and catabolic pathways in such diseases. Thus, FLS may regulate the switch from acute resolution to chronic persistent inflammation (Buckley et al., 2001).

3.4.9. Analysis of TLR/RIG-I agonist induced pro-inflammatory cytokine secretion in FLS

Increasing evidence suggests that synovitis may play a significant role in OA pathogenesis through the pro-inflammatory cytokine networks (Fernandes et al., 2002). The activated synovial fibroblasts maintain and perpetuate such inflammatory status in the joint as marked in OA (Firestein, 1996, Müller-Ladner et al., 2007, Sutton et al., 2009). In OA and RA, the activation of innate immune signalling cascades, like TLR activation might help maintain the vicious inflammatory loop, however, the modulation of cytokines in response to TLR/RLRs has not been well characterised (Scanzello et al., 2008, Kim et al., 2007, McCormack et al., 2009, Ospelt et al., 2008, Abdollahi-Roodsaz et al., 2011). Thus, to further assess the role of TLR activation in FLS and pro-inflammatory cytokine secretion, we have investigated the expression profiles of critical pro-inflammatory cytokines namely, IL-1β, TNFα, IL-6, IL-15 induced upon stimulation with TLR ligands (TLRs 1-9) in N, OA, RA FLS. A RIG-I ligand was employed to investigate cytosolic receptor activation in these cells and to study whether TLRs/RIG-I may differentially contribute to the disease progression. Upon stimulation with Poly(I:C), IL-1β secretion was significantly induced in OA-FLS (35.1 ± 1.0 pg/ml from a basal 7.0 ± 0.1 pg/ml, $p \leq 0.05$; Figure 3.9, panel A). Similarly, CLO-97 induced high IL-1β secretion in OA-FLS (25.3 ± 2.3 pg/ml from basal 7.0 ± 0.1 pg/ml). Alternatively, Pam_2CSK_4 (1µg/ml) or LPS (1µg/ml) were found to significantly induce IL-1β secretion in RA-FLS (27.0 ± 2.3 pg/ml and 24.0 ± 2.1 pg/ml from a basal 3.4 ± 1.2 pg/ml, $p \leq 0.05$).

Likewise, stimulation with Poly(I:C), CLO-97 and CpG increased IL-1β secretion in RA-FLS (16.0 ± 2.3, 18.0 ± 1.5 and 20.0± 1.3 pg/ml respectively from a basal 3.4 ± 1.2 pg/ml). Moreover, Pam_3CSK_4, Poly(I:C) and CLO-97 induced IL-1β secretion in N-FLS (10.7 ± 1.1, 10.6 ± 1.4 and 10.0 ± 0.7 pg/ml respectively from a basal 2.4 ± 0.1 pg/ml). Thus, dsRNA/ssRNA can induce IL-1β secretion in OA-FLS, whereas the similar effect was observed in RA-FLS upon exposure to gram positive and gram negative bacterial products. These molecules may critically mediate an imbalance in IL-1β , its receptor and IL-1RA levels in the joint which may lead to progressive joint damage by maintaining an inflammatory feed-forward loop aided by prolonged TLR activation (Firestein et al., 1992, Firestein et al., 1994, Arend and Dayer, 1990, Abdollahi-Roodsaz et al., 2011). Furthermore, previous studies have shown that IL-1β may be involved in joint destruction, through induction of chemokines and other pro-inflammatory mediators secretion, namely

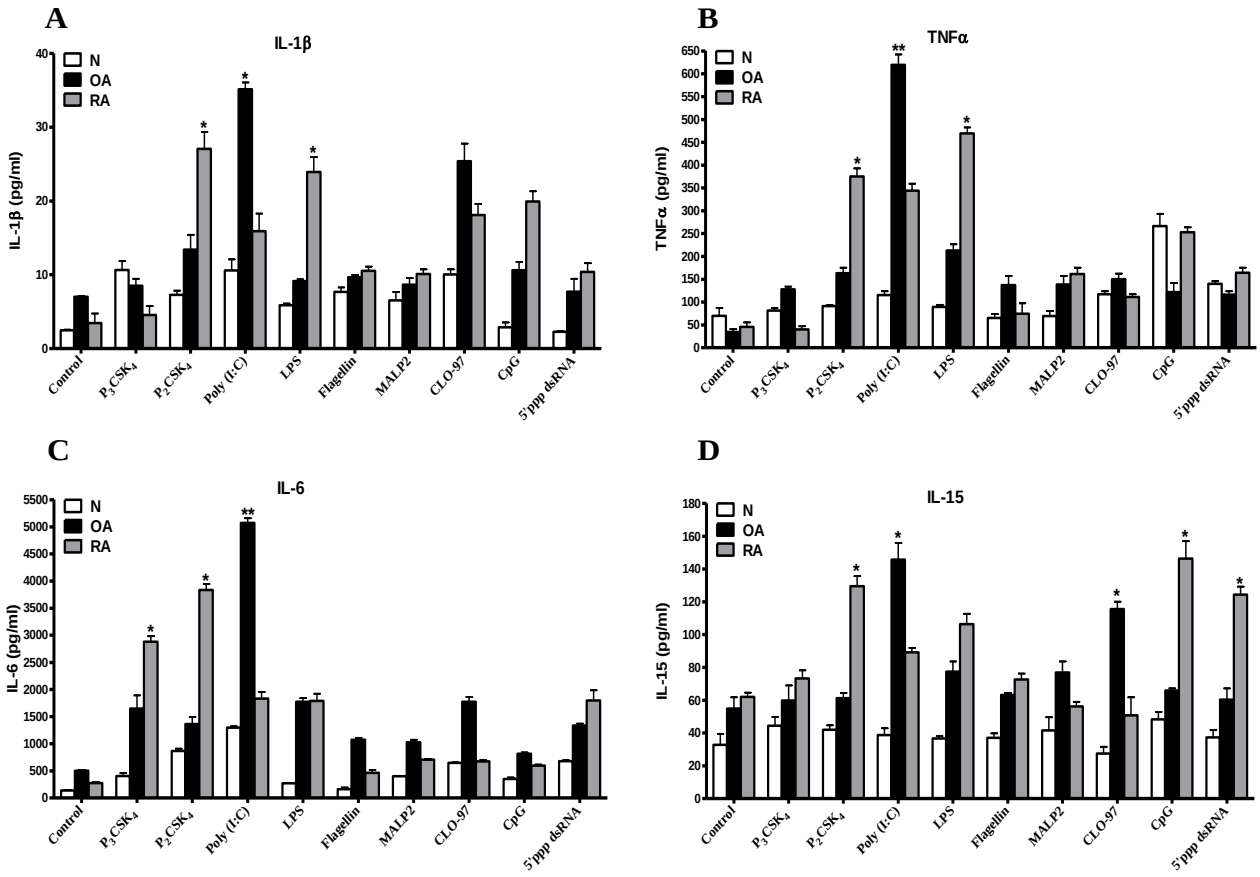

Figure 3.9: Analysis of TLR/RIG-I agonist induced pro-inflammatory cytokine secretion in FLS. (A-D) N-FLS, OA-FLS and RA-FLS (n=3 for each cell type) were treated with Pam_3CSK_4 (1 µg/ml; TLR1/2 ligand, Pam_2CSK_4 (1 µg/ml; TLR2 ligand), Poly(I:C) (10 µg/ml; TLR3 ligand), LPS (1 µg/ml; TLR4 ligand), Flagellin (1 µg/ml; TLR5 ligand), MALP-2 (20nM; TLR2/6 ligand), CLO-97 (1 µg/ml; TLR7/8 ligand), CpG (3 µg/ml; TLR9 ligand) and 5' ppp dsRNA (1 µg/ml; RIG-I ligand) for 16 h. Cell free supernatants were analyzed for (A) IL-1β, (B) TNFα, (C) IL-6, (D) IL-15 by ELISA. All the data presented are representative of at least three independent experiments performed in triplicate (mean ± S.E.M). Data was subjected to an unpaired Student's t test. * $p<0.05$, ** $p<0.01$ denotes the level of significance relative to respective cell type control.

IL-6 and MMPs, which may aid in the maintenance of the vicious cyto-chemokine-MMP cycle leading to prolonged synovitis in chronic inflammatory joint diseases (Pulsatelli et al., 1999, Pelletier et al., 1995, Smith et al., 1997). Thus further understanding of the activated receptors and their stimuli which serve to induce critical cytokines such as IL-1β may identify new venues for therapeutic targets, as, to date, single cytokine or cytokine receptor antagonists have had limited success in the treatment of such diseases (Martel-Pelletier et al., 1998, Pelletier et al., 1997).

Furthermore, TNFα secretion in FLS following treatment with TLR and RIG-I ligands was investigated. It was evident that Poly(I:C) significantly induced TNFα secretion in OA-FLS (619.5 ± 22.5 pg/ml from a basal 35.0 ± 5.9 pg/ml, $p \leq 0.01$; Figure 3.9, panel B). Similarly, a marked increase in TNFα levels was observed in RA-FLS upon Poly(I:C) stimulation (344.2 ± 15.1 pg/ml from a basal 45.8 ± 10.0 pg/ml). Likewise, Pam_2CSK_4 and LPS were found to significantly induce TNFα secretion in RA-FLS (375.4 ± 17.7 and 469.4 ± 13.0 pg/ml from a basal 45.8 ± 10.0 pg/ml, $p \leq 0.05$). A notable increase in TNFα levels in RA-FLS and N-FLS was evident upon CpG stimulation (253.0 ± 10.9 pg/ml, 266.8 ± 26.7 pg/ml from a basal 45.8 ± 10.0 and 70.0 ± 17.4 pg/ml, respectively). Likewise 5'ppp dsRNA was found to induce TNFα levels in N, OA and RA FLS relative to their respective cell type controls. Together, these data show that Poly (I:C), a synthetic ligand mimicking dsRNA from viruses, can significantly induce the most potent pro-inflammatory cytokine, TNFα, a prevalent cytokine in the joint. These data suggest that TLR3 may have a role in OA pathology and correlates with another study showing TLR3 overactivation in such joint pathologies (Ospelt et al., 2008). Given the limited success of anti-TNFα therapy in such joint pathologies, and the increasing evidence that blockade of certain TLRs on key cell types in the synovium, can prevent the upregulation of catabolic mediators in the joint (Ultaigh et al., 2011), it is essential to investigate such TLR dependent cytokine production in FLS, as cytokines play a well established active involvement in such joint diseases (Buckley et al., 2001, Fiorito et al., 2005, Firestein, 1996, Sutton et al., 2009).

Furthermore, IL-6 was measured, as it was previously known to positively correlate with various disease markers in many inflammatory disease pathologies (Houssiau et al., 1988, Pearle et al., 2007). It is evident that Poly(I:C) significantly induced IL-6 secretion in OA-

FLS (5071.7 ± 87.8 pg/ml from a basal 503.6 ± 14.7 pg/ml, $p \leq 0.01$; Figure 3.9, panel C). Similarly, Poly(I:C) stimulation also induced IL-6 secretion in RA-FLS (1834.3 ± 121.1 pg/ml from a basal 277.2 ± 17.8 pg/ml). Pam_3CSK_4 and Pam_2CSK_4 were found to significantly induce IL-6 levels in RA (2881.2 ± 101.6 pg/ml and 3834.1 ± 112.4 pg/ml from a basal 277.2 ± 17.8 pg/ml, $p \leq 0.05$). Also, comparable levels of IL-6 secretion were evident following LPS (1µg/ml) stimulation in OA and RA-FLS (1775.0 ± 67.7 and 1791.7 ± 130.7 pg/ml). Similarly, Pam_2CSK_4, Pam_3CSK_4 and CLO-97 stimulations induced a marked increase in IL-6 levels in N and OA FLS. Also, 5'ppp dsRNA was found to increase IL-6 levels in OA and RA FLS. Thus, it may be hypothesised that dsRNA either from viruses or from necrotic cells in the synovial fluid (Brentano et al., 2005b) may potentially activate OA-FLS in the synovium towards the production of pro-inflammatory cytokine in the joint (Guerne et al., 1989), probably through TLR3 activation.

Moreover, IL-15 was measured as it was previously detected in high levels even in early knee OA synovial fluid and was also found to associate with IL-6 and MMP levels, thus indicating an early innate immune response in the OA synovium (Scanzello et al., 2009). Thus, the ability of FLSs to secrete IL-15 upon activation by various PAMPs was investigated. It was evident that Poly (I:C) and CLO-97 significantly induced IL-15 secretion in OA-FLS (145.3 ± 6.2 pg/ml and 115.7 ± 4.51pg/ml from a basal 32.9 ± 6.7 pg/ml, $p \leq 0.05$; Figure 3.9, panel D). Pam_2CSK_4, LPS, CpG and 5'ppp dsRNA were found to induce significant IL-15 secretion in RA-FLS (129.5269 ± 6.087809 pg/ml, 106.3 ± 6.3 pg/ml, 146.3 ± 10.6 and 124.3 ± 5.3 pg/ml respectively from a basal 54.9 ± 6.9 pg/ml, $p \leq 0.01$).

In summary, owing to the predominant induction of IL-1β, TNFα, IL-6, IL-15, IFNβ and RANTES secretion in OA-FLS following Poly(I:C) stimulation, it may therefore be concluded that a TLR3 dependent initiation of cytokine production may be associated with synovitis observed in OA. Whereas in RA-FLS, a trend towards a TLR2 and TLR4 dependent activation of cytokines was evident. These data signify the importance of TLRs as significant inducers of pro-inflammatory cytokines and chemokines in diseases with no palpable infections such as in OA.

3.4.10. Analysis of sterile inflammatory mediators induced cytokine/chemokine secretion in FLS

TLR activation has been well documented in inducing inflammatory mediators like cytokines and chemokines in OA and RA, as evident from Figure 3.8 and 3.9, and this correlates with previous findings (Ospelt et al., 2008). Given the increasing evidence that DAMPs/endogenous ligands namely, low molecular weight hyaluronan activates TLRs in OA (Shirali and Goldstein, 2008, Scanzello et al., 2008), it was essential to explore, how the FLS react to hyaluronan and secrete the inflammatory mediators in the joint. Additionally, it was critical to understand how the locally prevalent cytokines namely IL-1β, TNFα, IL-6 and IFNβ in the arthritic joint act on FLS and aid in the induction of an inflammatory loop either by synergistically inducing their own secretion or by inducing the secretion of other inflammatory cytokines or chemokines. Hence, to unravel the crosstalk of such interactions, the FLS were either treated with hyaluronan or other inflammatory cytokines to measure pivotal cytokine and chemokine secretions in the joint. Upon stimulation with IFNβ, a notable induction of IFNβ secretion was evident, wherein OA-FLS showed a maximal increase in IFNβ levels compared to N and RA FLS (OA: 3773.5 ± 214.2 pg/ml Vs RA: 2611.3 ± 43.7 pg/ml and N: 2393.6 ± 48.5 pg/ml; Figure 3.10, panel A). Whereas stimulation with IL-6 induced maximal IFNβ in OA-FLS relative to treated N and RA-FLS (1257.379 ± 36.7 pg/ml Vs 573.3 ± 5.4 pg/ml and 434.0 ± 24.0 pg/ml). Likewise, stimulation with hyaluronan induced maximal IFNβ secretion in RA-FLS and comparable levels in OA-FLS relative to N-FLS (777.0 ± 36.9 pg/ml, 676.2 ± 28.3 pg/ml vs. 476.0 ± 57.4 pg/ml respectively).

Further, RANTES secretion was also measured. Hyaluronan induced the highest RANTES secretion in RA-FLS when compared to OA and N FLS (1550.1 ± 33.0 pg/ml Vs 897.1 ± 37.9 pg/ml and 431.4 ± 51.2 pg/ml; Figure 3.10, panel B). A similar trend was observed with TNFα stimulation. Interestingly, stimulation with IFNβ induced maximal RANTES secretion in OA-FLS and comparably in RA-FLS relative to treated N-FLS (1406.5 ± 15.1 pg/ml and 1215.3 ± 6.0 pg/ml Vs 585.7 ± 9.4 pg/ml). Furthermore, stimulations with IL-6 or IL-1β induced a similar trend in RANTES levels in OA-FLS relative to treated RA and N-FLS.

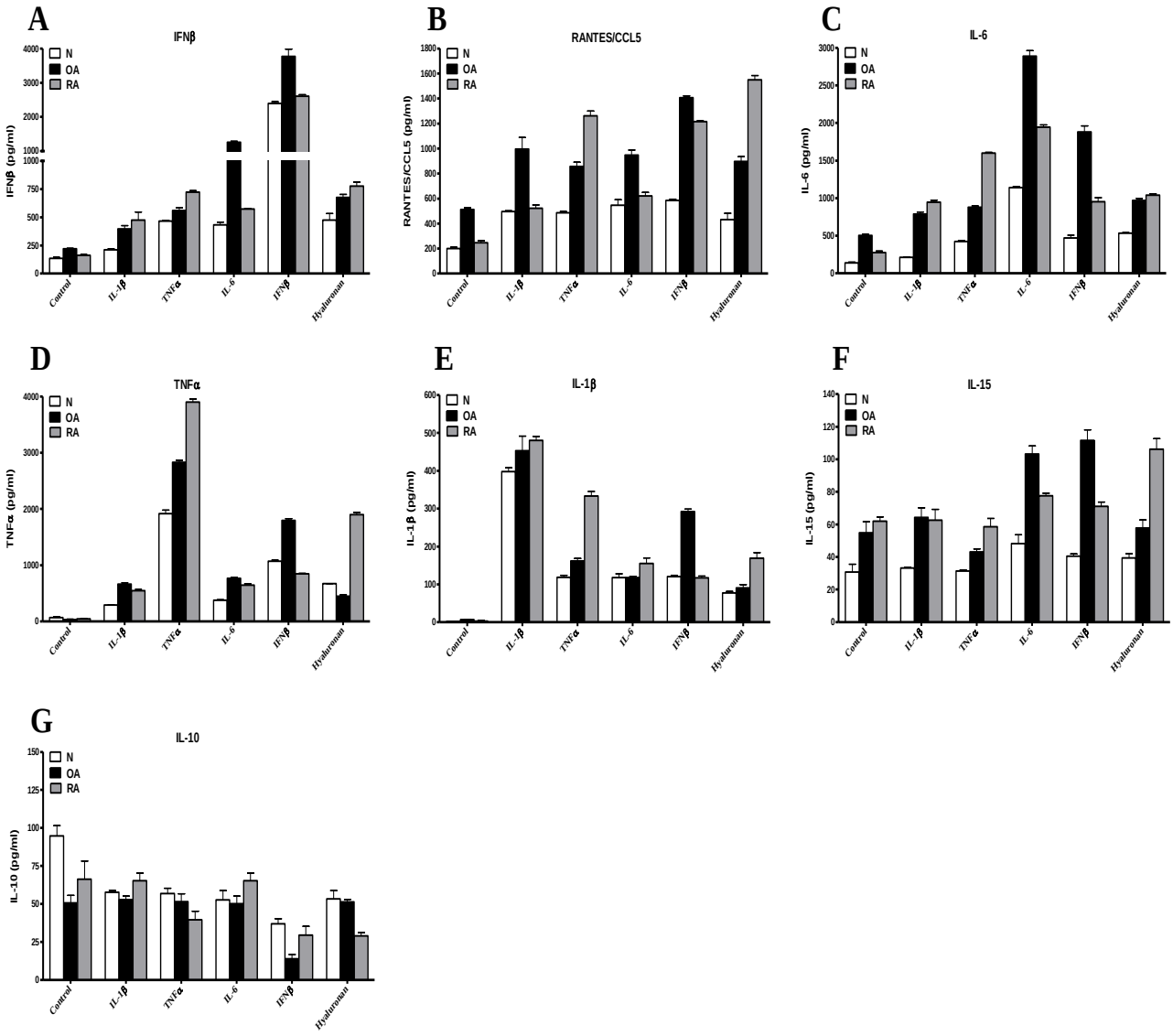

Figure 3.10: Analysis of sterile inflammatory mediators induced cytokine/chemokine secretion in FLS. (A-G) N-FLS, OA-FLS and RA-FLS (n=3 for each cell type) were treated either with one of the known sterile inflammatory mediators like Hyaluronan (25 µg/ml), IL-1β (100 pg/ml), TNFα (1 ng/ml), IFNβ (100 pg/ml), IL-6 (100pg/ml) for 16 h or left unstimulated. Cell free supernatants were analyzed for (A) IFNβ, (B) RANTES/CCL5, (C) IL-6, (D) TNFα, (E) IL-1β, (F) IL-15, (G) IL-10, by ELISA. All the data presented are representative of at least three independent experiments performed in triplicate (mean ± S.E.M). Data was subjected to an unpaired Student's t test. * $p<0.05$ denotes the level of significance relative to respective cell type control.

Next, IL-6 was measured, wherein, stimulation with IL-6 induced maximal IL-6 levels in OA-FLS (OA: 2890.0 ± 74.7 pg/ml, RA: 1600.1 ± 10.0 pg/ml and N: 1140.9 ± 14.7 pg/ml Figure 3.10, panel C). Similarly, stimulation with IFNβ induced maximal IL-6 levels in OA-FLS relative to treated RA and N-FLS (OA: 1880.0 ± 82.4 pg/ml, RA: 953.7 ± 52.4 pg/ml and N: 472.8 ± 36.0 pg/ml). A similar trend in IL-6 levels was observed upon stimulation with hyaluronan, TNFα and IL-1β, showing high IL-6 secretion from RA-FLS than OA and N-FLS. Subsequently, TNFα secretion was measured. Stimulation with TNFα itself induced the highest levels of TNFα secretion in RA, OA and N FLS relative to the respective cell type controls (RA: 3897.9 ± 56.8 pg/ml, OA: 2831.4 ± 34.0 pg/ml, N: 1915.6 ± 63.9 pg/ml; Figure 3.10, panel D). Next, the highest levels of TNFα secretion were evident in OA-FLS (1796.4 ± 30.9 pg/ml) upon stimulation with IFNβ stimulation and in RA-FLS (1897.1 ± 42.3 pg/ml) upon stimulation with hyaluronan. Stimulation with IL-1β or IL-6 lead to a comparable increase in TNFα levels in OA and RA FLS.

Furthermore, ligand-induced IL-1β secretion was also measured. Wherein, stimulation with IL-1β resulted in significant and comparable levels of IL-1β in N, OA and RA-FLS relative to respective cell type control (N: 398.2 ± 10.0 pg/ml, OA: 452.8 ± 38.7 pg/ml, RA: 480.4 ± 10.2 pg/ml Figure 3.10, panel E). Stimulation with TNFα induced maximal IL-1β secretion in RA-FLS (333.1 ± 12.0 pg/ml) and comparable levels in N and OA FLS. Similarly, stimulation with IFNβ induced maximal IL-1β secretion in OA-FLS (292.0 ± 6.5 pg/ml) and comparable levels in N and RA-FLS. Stimulation with hyaluronan or IL-6 yielded high IL-1β levels in RA-FLS (169.4 ± 14.4 pg/ml and 155.4 ± 14.8 pg/ml). Stimulation with hyaluronan or IL-6 resulted in comparable IL-1β levels in OA and N-FLS.

Regarding IL-15, stimulation with IFNβ induced the highest levels of IL-15 in OA-FLS relative to the treated RA and N FLS (OA: 111.6 ± 6.5 pg/ml, RA: 71.5 ± 2.5 pg/ml, N: 40.4 ± 1.5 pg/ml; Figure 3.10, panel F). Similarly, stimulation with IL-6 yielded the highest levels of IL-15 in OA-FLS relative to RA and N FLS (OA: 103.3 ± 4.9 pg/ml, RA: 77.5 ± 1.6 pg/ml, N: 48.2 ± 5.5 pg/ml). In contrast, stimulation with hyaluronan induced the highest levels of IL-15 in RA-FLS relative to the treated OA and N FLS (RA: 106.2 ± 6.5 pg/ml, OA: 57.8 ± 5.1 pg/ml, N: 39.5 ± 2.6 pg/ml). Neither IL-1β nor TNFα induced IL-15 secretion in N, OA and RA FLS relative to the respective cell type controls.

Following measurement of IL-10, a trend towards decreased secretion was observed upon stimulation with all ligands under study. In OA-FLS, a maximal decrease in IL-10 levels was evident upon IFNβ stimulation and comparable decreases in IL-10 levels were observed in RA and N FLS (Figure 3.10, panel G; OA: from 50.6 ± 5.2 pg/ml to 13.9 ± 2.7 pg/ml, RA: from 66.3 ± 11.8 pg/ml to 29.5 ± 5.8 pg/ml, N: from 94.8 ± 6.7 pg/ml to 36.9 ± 3.4 pg/ml). Stimulation with hyluronan induced significant decreases in IL-10 levels in RA-FLS and N-FLS but not in OA-FLS relative to respective cell type controls (N: from 94.8 ± 6.8 pg/ml to 53.3 ± 5.5 pg/ml, RA: from 66.3 ± 11.8 pg/ml to 28.9 ± 2.2 pg/ml, OA: from 50.6 ± 5.1pg/ml to 51.3 ± 1.7 pg/ml).

In summary, IFNβ or IL-6 were the most potent inducers of pro-inflammatory mediators in OA-FLS, wherein, stimulation with IFNβ predominantly increased the inflammatory milieu by inducing RANTES, IL-6, TNFα, IL-1β and IL-15 levels and by suppressing anti-inflammatory cytokine IL-10 secretion in OA-FLS. Whereas stimulation with hyaluronan or TNFα resulted in the induction of RANTES, IL-6, TNFα, IL-1β and IL-15 levels and suppression of IL-10 levels in RA-FLS. Thus, OA and RA FLS are differentially activated by various endogenous ligands, though similar patterns of inflammatory mediators are evident, thereby leading to a comparable end stage process, though the two diseases display distinct patterns of cytokine production upon stimulation with the various ligands.

3.4.11. Analysis of differential TLR 1-9 genes induced with major TLR agonists or inflammatory cytokines or chemokines in FLS

Thus far, the data indicate that PAMPs and DAMPs may drive the inflammatory locale in the joint during synovitis, by critically creating an imbalance between catabolic and anabolic pathways, possibly through specific TLR. Next, it was essential to identify the stimulus and the TLR which distinctively gets activated and initiates or propagates the whole process of synovitis in the OA joint. Thus, a crossectional TLR 1-9 mRNA expression profiling was conducted in N and OA FLS, following stimulation with TLR2, TLR3 and TLR4 ligands as our previous experiments demonstrated that these TLRs are relevant to OA and RA pathology (Figure 3.11). It was evident that stimulation with Pam_2CSK_4 induced a significant 5-fold increase in TLR-2 expression in OA-FLS ($p \leq 0.05$), and a 2-fold increase in N-FLS (Figure 3.11, panel A). Interestingly, stimulation with Pam_2CSK_4 was also found to induce a 2-fold increase in TLR-4 and a 3-fold increase in TLR-6 expression in OA-FLS relative to similarly stimulated N-FLS. Similarly, a 2-fold

increase in TLR-1 and 1-fold increase in TLR-5 expression was evident in OA-FLS following stimulation with Pam_2CSK_4. In contrast, TLR3, TLR7, TLR8 and TLR9 expressions were comparably induced in N and OA-FLS with following stimulation with Pam_2CSK_4. Stimulation with Poly (I:C), as expected, induced a 6-fold significant increase in TLR3 expression in OA-FLS ($p \leq 0.01$) relative to treated N-FLS (Figure 3.11, panel B). OA-FLS treated with Poly (I:C), displayed an insignificant 4-fold increase in TLR-4 expression, a 4-fold increase in TLR-7 expression, a 3-fold increase in TLR-9 expression and a 2-fold increase in TLR-5 expression relative to poly(I:C) treated N-FLS. Stimulation with LPS, as expected, induced a maximal 4-fold significant increase in TLR4 expression in OA-FLS relative to treated N-FLS (Figure 3.11, panel C). Also, LPS induced a 3-fold increase in TLR-3 expression, a 2-fold increase in TLR-2 expression, a 3-fold increase in TLR-5 expression, a 1-fold increase in TLR-6 and TLR-1 expression, a 2-fold increase in TLR-7 expression and a 3-fold fold increase in TLR9 expression relative to the respective treated N-FLS.

Subsequently, the most pro-inflammatory cytokines and chemokine prevalent in the joint during the OA disease process were selected and used to treat N and OA FLS, towards understanding their effects on TLR expression. It was found that stimulation with IL-1β induced a significant 1.5-fold increase in TLR-3 expression in N-FLS relative to treated OA-FLS (Figure 3.11, panel D). Additionally, a 0.5-fold increase in TLR-2, TLR-4 and TLR-7 were evident in N-FLS relative to OA-FLS treated with IL-1β. Interestingly, in N FLS, a trend towards increased TLR expression following IL-1β relative to OA FLS was observed (Figure 3.11, panel D). This may be attributed to the fact that OA-FLS may have already been primed for such stimulus and are thus rendered less sensitive to IL-1β stimulation; N-FLS, being naïve, thus display a tendency towards higher levels of TLR expression. Stimulation with RANTES induced a similar trend towards an increase in TLR expression in N-FLS when compared to OA-FLS, with TLR-1, -2 and -4 expression being the exception, where OA-FLS showed a 0.5-fold increase in these TLR expressions relative to N-FLS (Figure 3.11, panel H). Whereas a 1-fold maximal increase in TLR-3 expression in N-FLS was evident upon RANTES stimulation, relative to OA-FLS, wherein a comparable 0.5-fold induction in TLR 5, 6, 7, 8 and 9 expression was observed in both N and OA-FLS. Stimulation of FLS with TNFα, induced a significant 1.5-fold increase in TLR3 expression in OA-FLS ($p \leq 0.05$) relative to treated N-FLS Figure 3.11, panel E.

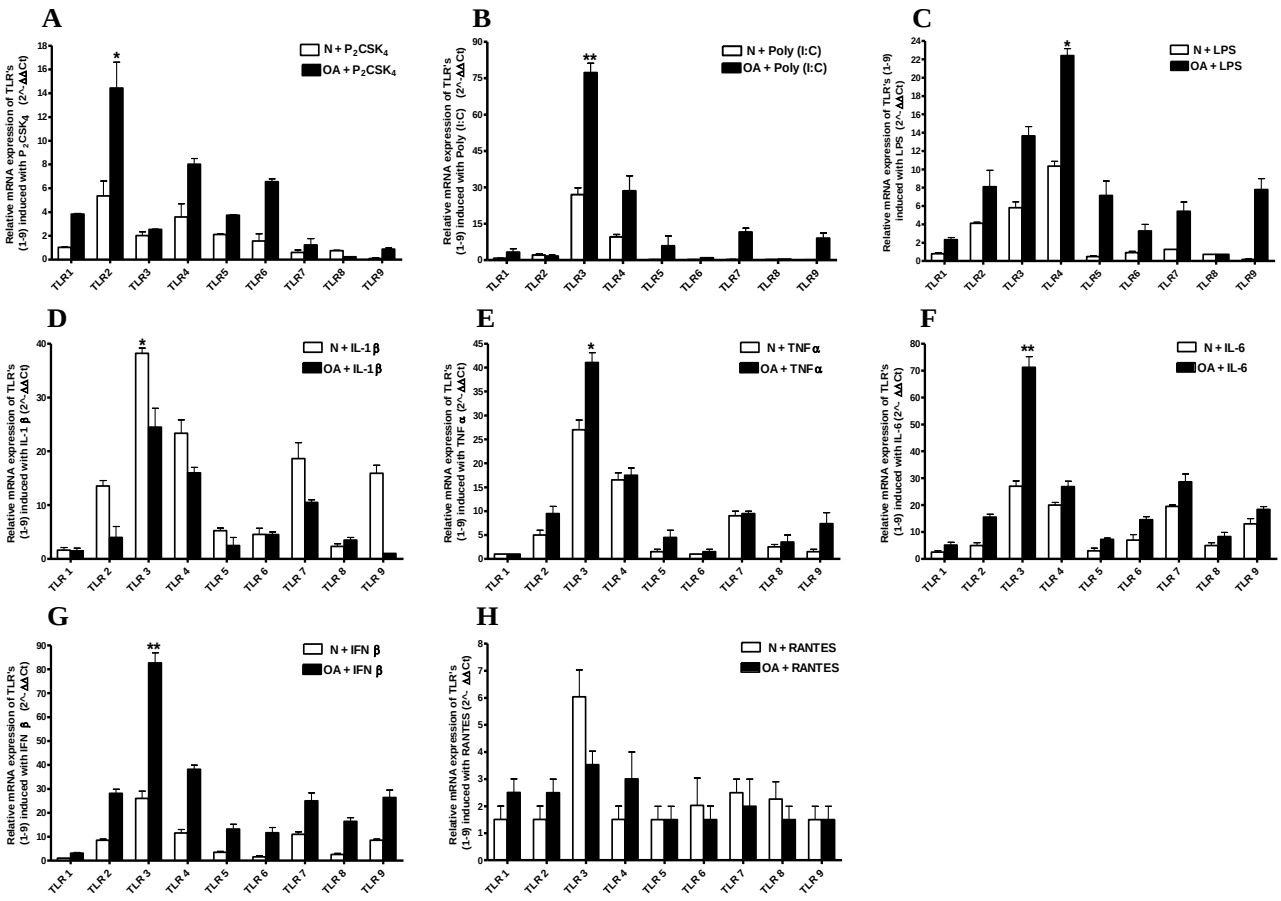

Figure 3.11: Differential TLR 1-9 gene analysis induced with TLR agonists / inflammatory cytokines / chemokines in FLS. (A-C) Induced expression of TLR1 through TLR9 mRNA treated with respective TLR agonists and (D-H) induced expression of TLR1 through TLR9 mRNA, treated with respective inflammatory cytokines/chemokine in FLS (n=3 for each cell type) from human N and OA knee synovium. N-FLS and OA-FLS were treated with Pam_2CSK_4 (1 µg/ml) (A), Poly(I:C) (10 µg/ml) (B), LPS (1 µg/ml) (C), IL-1β (100 pg/ml) (D), TNFα (1 ng/ml) (E), IL-6 (100 pg/ml) (F), IFNβ (100 pg/ml) (G) or RANTES/CCL5 (100 pg/ml) (H) for 16 h or left unstimulated. Total RNA was isolated from control and stimulated N-FLS or OA-FLS and used as a template for quantitative real-time RT-PCR to assay the crossectional mRNA expression levels of TLR1 through TLR9 irrespective of specific ligand based receptor stimulations. The levels of the relevant mRNAs were normalised relative to the housekeeping gene HPRT and are expressed relative to normalised values from unstimulated or control cells. All the data presented are representative of at least three independent experiments performed in triplicate (mean ± S.E.M). Data was subjected to an unpaired Student's t test. * $p<0.05$, ** $p<0.01$ denotes the level of significance relative to respective cell type control.

A similar trend towards increased TLR expression in OA-FLS relative to N-FLS was observed with TNFα stimulation, except for TLR-4 and TLR-7 expression where N and OA FLS showed comparable TLR expression levels upon TNFα treatment.

Stimulation with IL-6 resulted in a 4-fold significant increase in TLR3 expression in OA-FLS ($p \leq 0.01$) relative to treated N-FLS (Figure 3.11, panel F). Regarding the other TLRs, a trend towards comparably increased TLR expression in OA-FLS and N-FLS was observed, wherein notable a 1-fold increase in TLR-4 and TLR-7 expression was evident in OA-FLS when compared to N-FLS following stimulation with IL-6. Stimulation with IFNβ resulted in a highest 5-fold significant increase in TLR3 expression in OA-FLS ($p \leq 0.01$) relative to treated N-FLS (Figure 3.11, panel G). A similar trend towards increased TLR expression was observed in OA-FLS relative to N-FLS following IFNβ stimulation. Stimulation with IFNβ resulted in a notable 2-fold increase in TLR-2 and TLR-4 expression and a 1-fold increase in TLR7 and TLR9 expression in OA-FLS compared to N-FLS.

In summary, it was discernible that TLR3 was the most inducible and prominent TLR among others in FLS, being significantly induced by IFNβ, IL-6 and TNFα in OA-FLS, with induction on a par with its synthetic ligand, Poly (I:C). Therefore, these data strongly suggest that TLR3 activation might play a critical role in perpetuating the chronic inflammatory milieu prevalent in the OA joint, probably through the induced expression of TLR3 on FLS in the synovium.

3.4.12. Expression profile of RLRs and the adaptor molecules TRIF, MyD88 in FLS

Given the role of RLRs as major viral sensors in fibroblasts, in conjunction with the TLR3-TRIF pathways (Yoneyama and Fujita, 2007), and the fact that stimulation of cells with Poly(I:C) differentially induces TLR3, RIG-I and MDA-5 expression in FLS (Carrión et al., 2011), it was essential to investigate the interplay between the RLRs, RIG-I, MDA-5, and TRIF, MyD88 adaptor expression in N, OA and RA FLS. It was evident that OA FLS basally express a 2-fold significant increase in TRIF expression and a notable increase in MDA-5 expression than when compared to N-FLS (Figure 3.12, panel A), whereas, RA-FLS showed a significant increase in basal RIG-I expression and a notable

increase in MDA-5 expression when compared to N-FLS. Basal MyD88 expression levels were comparable in N, OA, RA FLS (Figure 3.12, panel A, $p \leq 0.05$).

Given that RIG-I receptor senses PAMPs on viral RNA and triggers an antiviral immune response by activation of type-I IFNs (Yoneyama and Fujita, 2007), it was vital to characterise the RIG-I receptor expression following stimulation with its ligand, 5' ppp dsRNA, as described previously (Hornung et al., 2006). Previously, we have shown that stimulation with 5' ppp dsRNA induces a significant increase in IL-15 levels in RA-FLS and also induced IL-6, TNFα and IL-1β in RA-FLS (Figure 3.9). In agreement with our previous data, stimulation with 5' ppp dsRNA significantly induced RIG-I expression in RA-FLS by 40-fold at 60 min and by 30-fold at 16 h (Figure 3.12, panel B). Thus, an increase in pro-inflammatory cytokine secretion by RA-FLS may be attributed to the increased RIG-I receptor levels, whereby the viral PAMPs may be equally sensed by RIG-I and TLRs in RA, which correlates with previous findings (Carrión et al., 2011). Whereas, RIG-I was previously known to induce apoptosis in FLS, a vital process in RA pathogenesis (Carrión et al., 2011).

3.4.13. Analysis of TLR 3, 4, 7 ligand induced and time dependent gene expression profile of major TLR / cytosolic receptors / adaptor molecules in FLS

Given the pivotal role for RNA viruses in arthritis progression, and having observed the predominant role of Poly (I:C) induced pro-inflammatory cytokines and chemokine in OA and RA, it was critical to investigate the viral receptors and their subsequent adaptor molecule recruitment which initiate signalling cascades leading to inflammation in OA and RA. Therefore, the mRNA expression levels of TLR3, RIG-I, and MDA5 (which recognizes (dsRNA)/Poly(I:C) and recruits TRIF adaptor), TLR4 (which recognizes LPS and recruits MyD88/TRIF adaptors) and TLR-7 (which recognizes (ssRNA)/CLO-97 and recruits MyD88/TRIF adaptors), were investigated in N, OA and RA FLS at various time points. Though TLR4 does not recognise viral nucleic acids, it senses components of viral pathogens and, similar to TLR3, it utilises TRIF. Herein, the differential interplay between these molecules was investigated. Stimulation with Poly (I:C) induced a significant 20-fold increase in TRIF expression and a notable 10-fold increase in TLR3 expression at 60 min in N-FLS, an 18-fold increase in RIG-I expression and a 9-fold increase in MDA-5 expression at 16 h in N-FLS (Figure 3.13, panel A, $p \leq 0.05$).

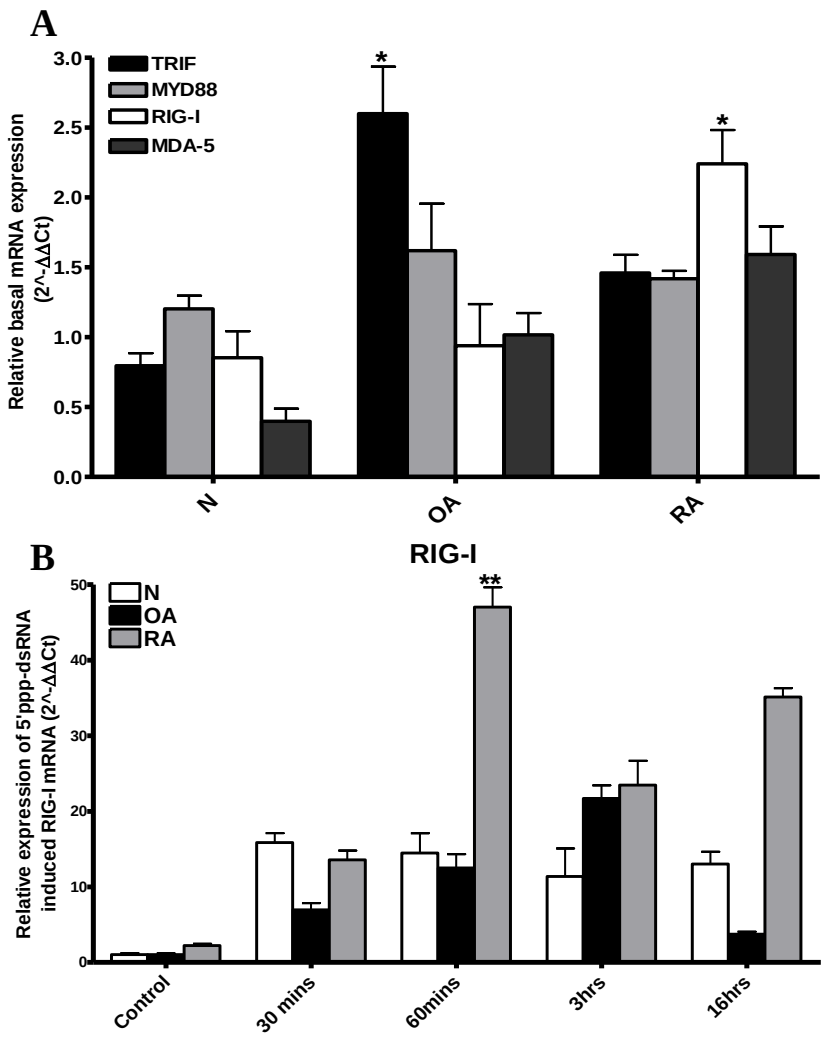

Figure 3.12: Expression profile of cytosolic receptors RIG-I (basal and induced), MDA-5 and the adaptor molecules TRIF, MyD88 in FLS. (A) Basal expression profile of TRIF, MyD88, RIG-I, MDA-5 genes in N-FLS, OA-FLS, RA-FLS. (B) Time dependent 5' ppp dsRNA (1 μg/ml) induced RIG-I mRNA expression in N, OA and RA FLS at 30 min, 60 min, 3 h and 16 h respectively. Total RNA was then isolated from stimulated and unstimulated N-FLS, OA-FLS or RA-FLS and used as a template for quantitative real-time RT-PCR to assay the basal mRNA expression levels of TRIF, MyD88, RIG-I, MDA-5 (A) and 5' ppp dsRNA induced RIG-I mRNA expression in N-FLS, OA-FLS and RA-FLS. The levels of the relevant mRNAs were normalised relative to the housekeeping gene HPRT and are expressed relative to normalised values from unstimulated cells. All the data presented are representative of at least three independent experiments performed in triplicate (mean ± S.E.M). Data was subjected to an unpaired Student's t test. * $p<0.05$ denotes the level of significance relative to respective cell type control.

In OA-FLS, Poly(I:C) stimulation resulted in significant 28-fold induction in TLR3 expression at 30 min ($p \leq 0.05$), a 65-fold increase in TLR3 and 52-fold increase in TRIF expression at 60 min ($p \leq 0.01$) and a 25-fold increase in TLR3 and 36-fold increase in RIG-I expression at 3 h ($p \leq 0.05$) (Figure 3.13, panel B). Stimulation of RA-FLS with Poly(I:C) induced a significant 20-fold induction of TLR3 expression at 30 min ($p \leq 0.05$), a 47-fold increase in TLR3 expression and a 39-fold increase in RIG-I expression at 60 min ($p \leq 0.05$) and a 26-fold increase in TLR3 expression and a 37-fold increase in MDA-5 expression at 3 h ($p \leq 0.05$) (Figure 3.13, panel C). Stimulation of N-FLS with LPS resulted in a significant 12-fold increase in MyD88 expression at 30 min ($p \leq 0.05$), a significant 14-fold increase in TRIF expression at 60 min ($p \leq 0.05$) and a significant 19-fold increase in TLR4 expression at 3 h ($p \leq 0.05$) which was sustained even at 16 h (Figure 3.13, panel D). Furthermore, stimulation of OA-FLS with LPS resulted in a significant 40-fold increase in TLR4 expression and a 32-fold increase in TRIF expression at 60 min ($p \leq 0.01$) and a sustained increase in TLR expression observed at 3 h and 16 h (Figure 3.13, panel E).

Similarly, stimulation of RA-FLS with LPS showed a trend towards increased TLR4 expression until 3 h (Figure 3, panel F). More specifically, a significant 38-fold increase in TLR-4 expression was observed at 60 min ($p \leq 0.05$) and a 54-fold increase in TLR-4 expression was evident at 3 h ($p \leq 0.01$). In RA-FLS, TRIF was significantly induced by LPS at 60 min ($p \leq 0.05$), while MyD88 was significantly induced at 3 h ($p \leq 0.05$) (Figure 3.13, panel F, n=3). Following stimulation of N-FLS with CLO-97 stimulation, a trend towards increased TLR-7 and MyD88 expression up until 60 min was detected and followed by a trend towards decreased TLR-7 and MyD88 expression thereafter (Figure 3, panel G). Furthermore, stimulation of OA-FLS with CLO-97 resulted in a significant 16-fold induction in TRIF expression at 60 min ($p \leq 0.05$), and a significant 20-fold increase in MyD88 expression at 3 h ($p \leq 0.05$) (Figure 3.13, panel H). Wherein, a trend towards increased TLR-7 expression was observed between 30 min and 16 hr inclusive (Figure 3.13, panel H). Likewise, stimulation of RA-FLS with CLO-97 stimulation resulted in a trend towards increased TLR-7 and TRIF expression till 60 min and a trend towards increased MyD88 expression till 16 h (Figure 3.13, panel I). Wherein, the greatest 10-fold increase in TLR7 and 12-fold increase in TRIF expression was observed at 60 min in RA-FLS following stimulation with CLO-97 stimulation ($p \leq 0.05$).

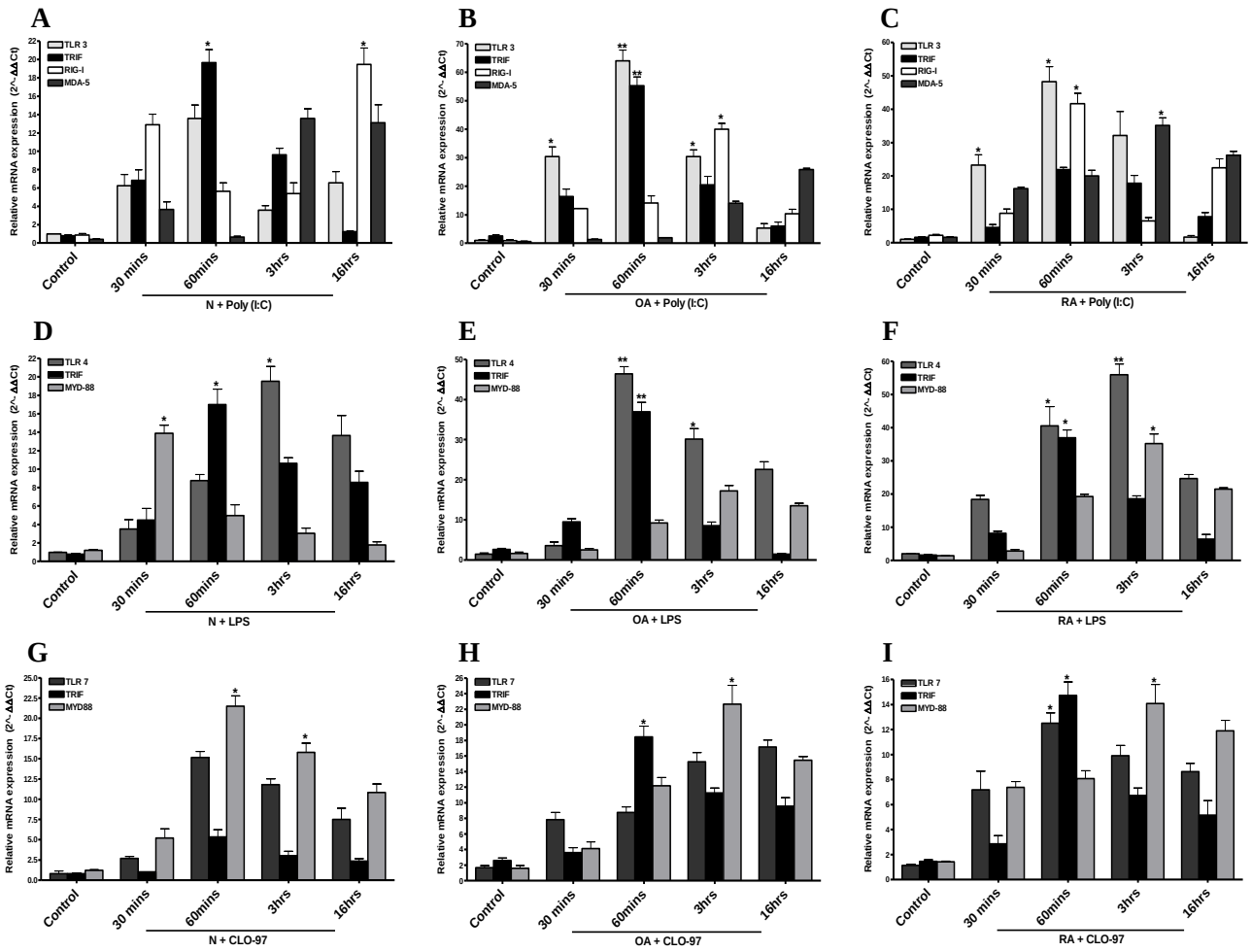

Figure 3.13: Analysis of TLR 3, 4, 7 ligand induced and time dependent gene expression of TLR 3, 4, 7 / cytosolic receptors / adaptor molecules in FLS. (A-C) Expression profile of TLR3, TRIF, RIG-I, MDA-5 genes with Poly(I:C) (10 µg/ml) stimulation for 30 min, 60 min, 3 h, 16 h in N-FLS (A), OA-FLS (B), RA-FLS (C). (D-F) Expression profile of TLR4, TRIF, MyD88 genes with LPS (1 µg/ml) stimulation for 30 min, 60 min, 3 h, 16 h in N-FLS (D), OA-FLS (E), RA-FLS (F). (G-I) Expression profile of TLR7, TRIF, MyD88 genes with CLO-97 (1 µg/ml) stimulation for 30 min, 60 min, 3 h, 16 h in N-FLS (G), OA-FLS (H), RA-FLS (I). Total RNA was isolated from respective stimulated and control N, OA, RA FLS (n=3 for each cell type) and used as a template for quantitative real-time RT-PCR to assay the above mentioned respective mRNA expression levels. The levels of the relevant mRNAs were normalised relative to the housekeeping gene HPRT and are expressed relative to normalised values from unstimulated/control cells. All the data presented are representative of at least three independent experiments performed in triplicate (mean ± S.E.M). Data was subjected to an unpaired Student's t test. * $p<0.05$ denotes the level of significance relative to respective cell type control.

A 12-fold increase in MyD88 expression was evident at 3 h in RA-FLS ($p \leq 0.05$) (Figure 3.13, panel I). In summary, it is clear that a significant induction of TRIF was evident in OA-FLS following stimulation with Poly(I:C), LPS, CLO-97 at 60 min. In contrast, RA-FLS differentially induce RIG-I following Poly(I:C) stimulation at 60 min. Following stimulation of RA FLS with LPS and CLO-97, TRIF is induced at 60 min. These data correlate with previous findings showing that Poly(I:C) induces a more substantial increase in RIG-I expression in RA-FLS when compared to OA-FLS, thus indicating a critical role for RLRs in RA progression (Carrión et al., 2011).

3.4.14. Analysis of time dependent effect of Poly(I:C) on MMP 1, 3, 9, 13 gene expression in N-FLS and OA-FLS

Given our previous observations that Poly (I:C) induces the key inflammatory mediators in OA through TLR3 activation in FLS (Figures 3.2, 3.6, 3.8, 3.9), and having known that MMPs 1, 3, 9 and 13 play a vital role in OA pathogenesis (Sutton et al., 2009, Firestein, 1996), it was critical to investigate whether MMP genes may be induced with Poly(I:C) in FLS. It was found that Poly(I:C) induced a 2-fold increase in MMP-1 expression levels in OA-FLS at 60 min, after which a trend towards decreased MMP-1 expression was evident in OA-FLS (Figure 3.14, panel A). A trend towards increased MMP-3 expression was observed in OA-FLS following stimulation with Poly (I:C), wherein, a significant 5-fold increase at 3 h and 16-fold increase at 16 h in MMP-3 expression was evident in OA-FLS (Figure 3.14, panel B, $p \leq 0.05$). Similarly, a trend towards increased MMP-9 expression in OA-FLS was evident with Poly (I:C) stimulation. A significant 4-fold induction in MMP-9 expression was observed in OA-FLS at 16 h with Poly (I:C) stimulation (Figure 3.14, panel C, $p \leq 0.05$). Likewise, a similar trend towards increased MMP-13 expression in OA-FLS was observed following Poly (I:C) stimulation. Wherein, a significant 5-fold induction in MMP-13 at 3 h and a similar 7-fold increase in MMP-13 at 16 h was detected in OA-FLS with Poly (I:C) stimulation (Figure 3.14, panel D, $p \leq 0.05$). Thus, it was clear that Poly(I:C) induces the catabolic MMP 1, 3, 9 and 13 gene expression in OA-FLS. Given that these MMPs are involved in extracellular matrix turnover in pathological conditions such as in OA, and given that Poly(I:C) predominantly mediates its effects through TLR3 in OA-FLS, it proposed that TLR3 may be a potential target for therapeutic intervention towards the ablation of OA progression.

3.4.15. Analysis of TLR/RIG-I agonist induced pro-inflammatory MMPs in FLS

Given that the activated FLS secrete a wide variety of catabolic MMPs, which perpetuate the chronic inflammatory state and lead to progressive irreversible damage of the affected joint (Sutton et al., 2009, Pelletier et al., 2001, Ghosh and Cheras, 2001, Fernandes et al., 2002), and having observed the role of TLR-2, 3, 4, 7, 9 and RIG-I PAMPs in OA, it was essential to investigate the inflammatory MMPs that could be secreted in the joint by these PAMPs in OA-FLS. It was found that stimulation of OA-FLS with Poly (I:C) induced a significant increase in MMP-1 levels in OA-FLS when compared to the other PAMPs under investigation (20314.1 ± 105 pg/ml from a basal 1694.43 ± 55 pg/ml; Figure 3.15, panel A, $p < 0.01$). Similarly, the most significant increase in MMP-3 levels was observed following stimulation of OA-FLS with Poly(I:C) (10756.2 ± 100.125 pg/ml form a basal 3091.14 ± 53.68 pg/ml; Figure 3.15, panel B, $p < 0.05$). Likewise, a significant increase in MMP-9 levels was observed following Poly (I:C) stimulation in OA-FLS (677.44 ± 40 pg/ml from a basal 81.31 ± 15 pg/ml). Thus, it is clear that Poly(I:C) predominantly induces secretion of the catabolic MMP 1, 3, 9 in OA-FLS. This substantiates our previous observations that these MMPs can be induced, particularly by Poly (I:C), which exclusively employs TLR3 in OA-FLS, thus making it a critical target for OA disease intervention.

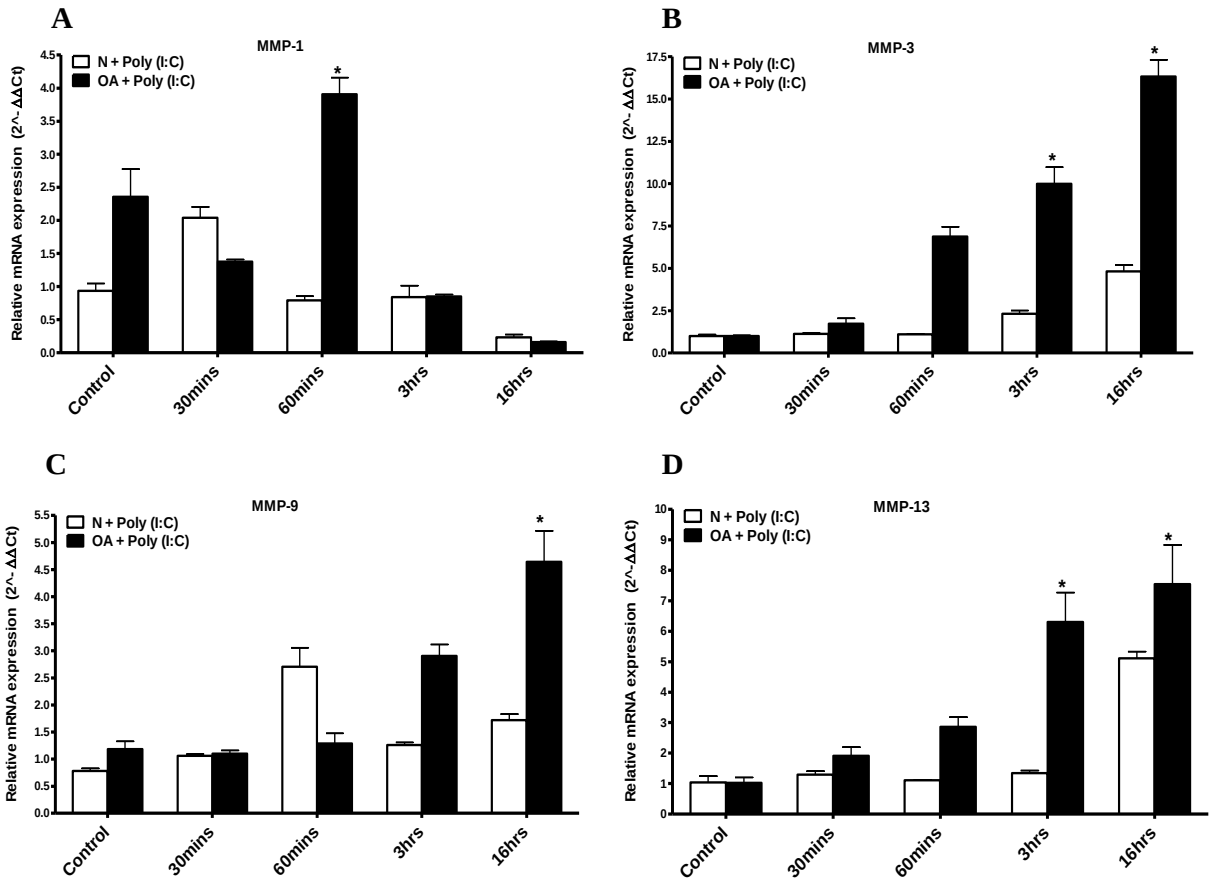

Figure 3.14: Time dependent effect of Poly(I:C) on MMP 1, 3, 9, 13 gene expression in N-FLS and OA-FLS. (A-D) Expression profile of MMP 1, 3, 9, 13 genes with Poly(I:C) (10 µg/ml) stimulation for 30 min, 60 min, 3 h, 16 h in N-FLS and OA-FLS. Total RNA was isolated from respective stimulated and control N/OA FLS (n=3 for each cell type) and used as a template for quantitative real-time RT-PCR to assay MMP-1 (A), MMP-3 (B), MMP-9 (C) and MMP-13 (D) mRNA expression levels. The levels of the relevant mRNAs were normalised relative to the housekeeping gene HPRT and are expressed relative to normalised values from unstimulated/control cells. All the data presented are representative of at least three independent experiments performed in triplicate (mean ± S.E.M). Data was subjected to an unpaired Student's t test. * $p<0.05$ denotes the level of significance relative to respective cell type control.

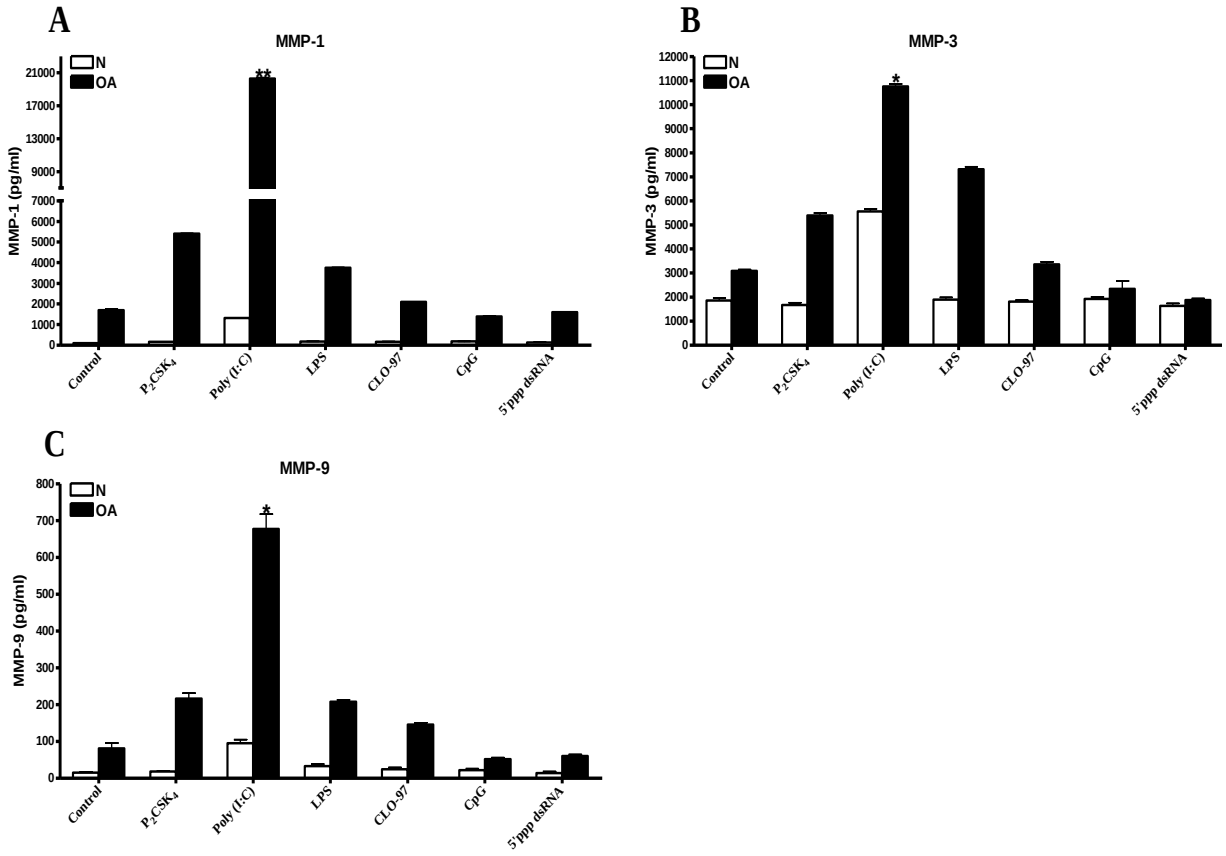

Figure 3.15: Analysis of TLR/RIG-I agonists induced pro-inflammatory MMPs in FLS. (A-C) N-FLS and OA-FLS (n=3 for each cell type) were treated with Pam_2CSK_4 (1 µg/ml; TLR2 ligand), Poly(I:C) (10 µg/ml; TLR3 ligand), LPS (1 µg/ml; TLR4 ligand), CLO-97 (1 µg/ml; TLR7/8 ligand), CpG (3 µg/ml; TLR9 ligand) and 5' ppp dsRNA (1 µg/ml; RIG-I ligand) for 16 h or left unstimulated. Cell free supernatants were analyzed for (A) MMP-1, (B) MMP-3, (C) MMP-9, by Meso Scale MMP multi-plex ELISA kit. All the data presented are representative of at least three independent experiments performed in triplicate (mean ± S.E.M). Data was subjected to an unpaired Student's t test. * $p<0.05$, ** $p<0.01$ denotes the level of significance relative to respective cell type control.

3.5. Discussion

Given that inflammatory episodes are associated with OA progression, it is now considered as a chronic inflammatory disease, which is characterised by progressive destruction of the joint architecture particularly through synovial inflammation (Pelletier et al., 2001, Ospelt et al., 2004, Vergunst et al., 2005). Albeit inflammatory cells are detected at the site of inflammation, OA and RA FLS are the key players in disease progression and tissue destruction (Müller-Ladner et al., 2007, Buckley et al., 2001). FLS are the resident cells of the synovial lining and are the main cell type in the normal synovial tissue. The activation of FLS in OA and RA are mediated by a variety of inflammatory cytokines (Ospelt et al., 2004, Vergunst et al., 2005). The role of FLS in joint destruction has been extensively studied given that they produce inflammatory cytokines, chemokines and metalloproteinases that contribute to synovitis/synovial inflammation and cartilage degradation, ultimately leading to irreversible OA progression (Firestein et al., 1992, Firestein et al., 1994, Buckley et al., 2001). Although proinflammatory cytokines are known to induce the proliferation, collagenase and aggrecanase production in FLS (Alvaro-Gracia et al., 1993, Yamanishi et al., 2002), the downstream stimuli are poorly established and less understood. The activation of FLS is also driven in a cytokine independent manner, particularly through the activation of TLRs (Kim et al., 2009, Brentano et al., 2005a). Ongoing arthritis research has shown that FLS express the innate immune receptors such as TLRs, which upon activation by exogenous or endogenous stimuli can secrete a plethora of inflammatory mediators like cytokines, chemokines and MMPs critically involved in chronic joint arthropathies like OA and RA (Scanzello et al., 2008, Ospelt et al., 2004, Scanzello et al., 2009, Vergunst et al., 2005). Recently, convincing studies have showed that the activation of particular TLR pathways in OA may play a central role in the disease development and progression (Scanzello et al., 2008).

Hence, in this chapter to better understand the synovial inflammation in OA molecular pathogenesis and to explore the key trigger signals in the chronic inflammatory milieu prevalent in OA synovium, we employed N, OA and RA FLS, which served as useful cell type models for studying the differences in expression and regulation of TLRs, inflammatory cytokines, chemokines, and MMPs ubiquitous in the synovial joint. In an attempt to define whether activation of TLR signalling in FLS may be an early event in the pathogenesis of OA, we comparatively analysed the expression and function of TLRs 1-9

in FLS, wherein N-FLS served as experimental control and RA-FLS served as positive inflammatory control in comparison to OA-FLS. We have shown that N, OA and RA FLS express both basal and ligand induced upregulation of mRNA encoding TLR 1-9, and this is, at least in part, contradictory to a previous publication (Ospelt et al., 2008).

Although previous studies state that FLS express TLR 1-6 and poorly express TLR-5, -7, -8 and -9 (Ospelt et al., 2004), our observations clearly show that FLS express TLR1-9. Interestingly, we have demonstrated in the present study that the most abundant modulatory TLR at the end stages of OA is TLR3, which showed both early basal and ligand-induced expression in OA-FLS when compared to N and RA-FLS, and this partly correlates with previous findings (Carrión et al., 2011). In OA-FLS, activation of TLRs with their appropriate PAMP lead to increases in TLR4, TLR2, TLR6 and TLR7 mRNA expression, which partly correlates with previous studies (Scanzello et al., 2008). Whereas in RA FLS, the most prominently expressed TLRs were found to be TLR2 and TLR4, which showed both basal and ligand-induced expression and this is in contrast to OA and N-FLS, and correlates with previous studies (Kim et al., 2007). Following TLR ligand-induced activation of RA-FLS, TLR5, TLR3 and TLR9 mRNA expression was detected and this correlates with previous studies (Ospelt et al., 2008, Hornung et al., 2002, Lund et al., 2003, Lebre et al., 2006). Thus, our findings are also consistent with several studies using various tissues, and confirm that TLR3 is the main nucleic acid-specific TLR in non-immune cells like FLS (Brentano et al., 2005b, Tissari et al., 2005, Tsuboi et al., 2002, Zarember and Godowski, 2002).

Accordingly, arthritis was induced by intra-articular administration of viral dsRNA as a TLR3 ligand in mice supporting the importance of TLR3 in arthritis (Zare et al., 2004). Also, ligation of TLR3 using poly(I:C) and RNA released from necrotic cells resulted in production of inflammatory mediators by FLS (Brentano et al., 2005b). Although TLR3 induced activation of inflammation has been demonstrated in immunological cells, its regulation role in FLS has been poorly studied. Here in this study we have shown that Poly (I:C) induces a significant fold increase in TLR3 mRNA expression in OA-FLS and, to a lesser extent, in RA-FLS. Consistent with the basal TLR expression pattern in OA and RA FLS, the most abundant of the measured TLRs in the FLS were TLR2, TLR3 and TLR4. Of particular interest is the finding that the basal and ligand-induced expression of TLR-3 in OA-FLS is elevated when compared with levels in RA-FLS. This result suggests that the

overexpression of TLR3 is an early event and that its levels do not change over the course of the disease. Since TLRs can be induced within hours, as demonstrated in the *in vitro* experiments, we cannot rule out the possibility that up-regulation of TLRs is a secondary event in the course of the development of a destructive joint disease like OA. However, the fact that specific TLRs were expressed early at elevated levels in OA-FLS demonstrates that activation of TLR pathways is not a late event that is restricted only to the severe destructive stages of such inflammatory and degenerative joint disorders. Given the predominant basal and poly(I:C)-induced TLR3 expression in OA-FLS, we can speculate that viral component may be involved in synovial inflammation leading to OA progression. Although, it must be noted that induction of TLRs may also be due to the presence of endogenous ligands.

It was previously demonstrated that double-stranded RNA released from necrotic cells stimulates FLS in a TLR3–dependent manner (Brentano et al., 2005b) and bacterial or viral products deposited in the joints can activate RA-FLS via TLRs (Van Der Heijden et al., 2000). Additionally, TLR activation by hyaluronan, fibrin, and heat-shock proteins has also been shown to activate TLR-4 in FLS and other synovial cell types (Brentano et al., 2005b, Sanchez-Pernaute et al., 2007, Scanzello et al., 2008). Since these endogenous ligands are present in elevated amounts in inflamed joints, the TLR expression levels and responsiveness of FLS to TLR ligands are critical factors. Based on previously published data, it might also be hypothesised that the availability of endogenous ligands might determine which TLRs are up-regulated in FLS (Roelofs et al., 2006, Brentano et al., 2005b). Here, we have demonstrated that TLR3 in OA-FLS and TLR4 and TLR2 in RA-FLS are expressed basally at high levels when compared to N FLS and stimulation of these TLRs with their respective exogenous and endogenous ligands produced a wide range of proinflammatory cytokines, chemokines, and MMPs. Wherein, Poly (I:C) induced maximal amounts of IFNβ, TNFα, IL-6 and RANTES in OA-FLS at both gene and protein levels. Additionally, Poly (I:C) induced maximal amounts of IL-1β and IL-15 when compared to that induced by other TLR ligands and poly(I:C) suppressed IL-10 secretion in OA-FLS; these findings correlate with previous findings (Scanzello et al., 2009, Fernandes et al., 2002, Scanzello et al., 2008). Given that the activation of RLR, namely RIG-I and MDA-5, with Poly (I:C) stimulation has been previously observed in various other tissues (Yoneyama and Fujita, 2009), it was essential to investigate the role of these receptors in activated FLS. We have shown that Poly (I:C) predominantly employed TLR3

and TRIF to mount an early immune response in OA-FLS, whereas in RA-FLS, Poly(I:C) concomitantly engaged TLR3 and RIG-I receptors, thus demonstrating a preference for the TLR3 signalling pathway in OA-FLS. However, even though the constitutive expression of TLR mRNA did not differ significantly between OA-FLS and RA-FLS, activation of these cells with PAMPs or DAMPs resulted in differential patterns of proinflammatory cytokines, chemokines and matrix-degrading enzymes expression. In particular, OA-FLS with Poly (I:C) or IFNβ stimulation produced significantly higher amounts of pro-inflammatory IL-6, IFNβ, TNFα, IL-15, RANTES, MMP-1, 3, 9, 13 and suppressed anti-inflammatory IL-10 levels, whereas the similar effect was observed in RA-FLS with Hyaluronan. These data indicate that PAMP/DAMP-induced activation of OA and RA FLS favour a skew towards a Th1 response, mediating synovial inflammation rather than a reparative Th2 response. Therefore, our data suggest that stimulation of TLR3 pathway occurs early in OA and TLR2 and TLR4 pathways occurs early in RA, resulting in the activation of FLS which secrete a plethora of pro-inflammatory mediators which further contribute to the development of synovial inflammation and joint destruction.

The imbalance between anabolic and catabolic pathways which are under the control of cytokines play a critical role in articular cartilage degradation and synovitis in OA (Scanzello et al., 2009). Moreover, a novel class of small cytokines, namely chemokines, have a broad array of effects in numerous different cell types, equally inside and outside of the immune system. There is accumulating evidence that the interaction of chemokines with their receptors play a role in the processes underlying synovitis in RA. More recently, a possible role for chemokines, in addition to biomechanical stress, has been suggested in cartilage and bone damage in OA (Vergunst et al., 2005). Chemokines secreted from FLS play an important role in disease progression in patients with OA and RA (Borzì et al., 2004, García-Vicuña et al., 2004). Activated FLS express several chemokines, including CCL2, CCL5/RANTES and CXCL8 (Alaaeddine et al., 2001, Borzì et al., 2004, García-Vicuña et al., 2004). Here, we have demonstrated that RANTES induces TLR3 expression in both N and OA FLS and also showed that stimulation of OA-FLS with Poly (I:C) induced significant levels of RANTES both at gene and protein levels, thus forming a feed forward loop aiding in OA progression. Interestingly, RANTES targeted therapeutic approaches have been used towards the amelioration of experimental RA by using the RANTES antagonistic met-RANTES (Shahrara et al., 2005). In OA, the exact role and

regulation of RANTES in the disease process is less established and requires more research.

The MMP regulation in joint tissues is long known for both tissue degradation and repair. Emerging evidence has shown that TLR pathway activation may be involved in MMP production in joint. Most recently, TLR-2 ligands were shown to induce MMP-1 and MMP-13 in OA chondrocytes (Zhang et al., 2008). Similarly, in RA synoviocytes a baseline MMP-1, MMP-2, MMP-3, and MMP-13 production was observed, which was found to be dependent on the TLR pathway adaptor proteins MyD88 and Mal/TIRAP (Sacre et al., 2007). In yet another study, the TLR-2 ligand peptidoglycan was shown to augment MMP-1 and MMP-3 expression on synoviocytes (Kyburz et al., 2003). Although numerous *in vitro* reports have purported a link between RA synovial or chondrocyte production of MMPs and TLR activation, very little is known about MMPs in the context of OA. In this study, we have shown that the most prominent MMPs in OA synovium, namely MMP-1, 3, 9 and 13 (Sutton et al., 2009, Pelletier et al., 1995), can be induced by stimulation of FLSs with PAMPs and this promotes disease progression. In particular, we demonstrate that stimulation of OA-FLS with Poly(I:C) induced the highest levels of these MMPs at both the gene and protein level. Furthermore, it was previously shown that IL-1β signalling up regulates the activity of ADAMTS-4 and MMP-13 and suppresses aggrecan and collagen synthesis in chondrocytes.

However, targeted therapy to block IL-1β in OA was tested but could not reach the efficacy as expected (Chevalier et al., 2005). Regarding TNFα, which like IL-1 can activate chondrocyte mediated catabolic protease production (Fernandes et al., 2002), a study showed that TNFα-blockade for the treatment of pain and inflammation in 12 patients with erosive hand OA, did not demonstrate significant efficacy on the whole, but improvement in pain and physical function scores was reported for some individuals (Magnano et al., 2007). In another study, elevated levels of synovial IL-15 was evident in patients with early cartilage damage that underwent arthroscopic procedures, compared with end-stage knee OA patients (Scanzello et al., 2009). However, the events that stimulate IL-15 and other pro-inflammatory cytokines production in OA are as yet unknown, though TLR-2/4 activation has been implicated in RA patients (Jung et al., 2007). In this study, we have shown that stimulation of OA-FLS with Poly (I:C) induced both the gene and protein levels of these prevalent pro-inflammatory cytokines namely IL-

1β, TNFα, IL-6 and IL-15 in a TLR3 dependent manner. Wherein, OA-FLS stimulated with pro-inflammatory cytokines or chemokines prevalent in the synovium predominantly induced TLR3 gene expression, thus indicating a possible role for enhanced TLR3 expression in OA pathogenesis. Thus, TLR3 targeted therapies may be of significant benefit towards the amelioration of synovial inflammation observed in OA, when compared to blocking a single dominant cytokine / chemokine / their receptors in OA.

These significant differences obtained through the mRNA and protein profiling of OA-FLS have shed light on the initial OA progression processes and ultimately may lead to the better understanding of many chronic inflammatory disease pathologies. Taken together, these data illustrate the importance of OA-FLS as sentinel cells of the innate immune response, considering their ability to react to various PAMPs and DAMPs towards induction of different effecter molecules according to the needs of the tissues of which they are part.

Although RA and OA are considered to be different diseases, they sometimes show similarities; for example, secondary OA may be seen in RA, and in OA secondary inflammation is often observed (Vergunst et al., 2005). Unravelling pathogenic processes underlying both cartilage degradation and synovial inflammation may provide new insights into both diseases, leading to the identification of novel therapeutic targets. This study shows that synovitis in OA and RA can show great similarities with regard to the early effecter mechanisms including the cytokine, chemokine, MMP and TLR expression in OA and RA FLS, thus dismissing earlier hypotheses that OA is purely degenerative and the synovial inflammation observed in OA is secondary.

In conclusion, given our observations in this chapter, it can be hypothesised that the innate immune response such as TLR3 expression in OA-FLS, is one potentially modifiable process augmenting various pathological changes observed in OA. Thus, the future research in this area is essential to identify the specific TLR pathways that predominate in vivo/ex vivo, and how they relate to patient subsets, stage of disease, and OA prognosis. Further integrated research approaches, employing patient-derived materials, isolated cells and animal models, will enable us to develop efficient anti-inflammatory treatments to optimise comprehensive joint care approaches for the diversity of patients with OA.

Chapter 4

Ex-vivo characterisation of OA synovial tissue, fibroblasts and fluid- TLR3 as a therapeutic target for OA?

4.1. Introduction

OA is a very common rheumatic pathology characterised by inflammation of the synovial membrane, cartilage breakdown and alteration of the joint capsule (Sellam and Berenbaum, 2010). It causes pain, swelling and stiffness leading to loss of joint function in various phases of the disease particularly in the late phase (Sutton et al., 2009). The traditional view of OA as a cartilage-only disease has been strongly disproven by recent research and OA is now regarded as a whole-joint disease which primarily includes the synovial tissue (Sellam and Berenbaum, 2010). Although, the cause of the disease hasn't been identified yet, it has been shown that inflammation of the synovial membrane plays a key role in OA pathogenesis and disease progression (Sutton et al., 2009, Sellam and Berenbaum, 2010, Benito et al., 2005). The main cell types involved in OA are synoviocytes, chondrocytes and infiltrating leukocytes. Synoviocytes are the building blocks of the synovial membrane, which consist of the three to four cells thick layer surrounding the joint, chiefly consisting of FLS which produce the synovial fluid and the matrix components like hyaluronic acid (Sutton *et al*., 2009). As we have shown in chapter 3, activated FLS release proinflammatory cytokines and catabolic mediators such as MMPs. These perpetuate local synovitis and ultimately lead to cartilage breakdown. The products of the cartilage damage can in turn activate the FLS and this process forms a positive loop of inflammation (Sellam & Berenbaum, 2010). The FLS also release the chemokines attracting the macrophages and adaptive immune system cells, which cause amplification of inflammation (Sellam & Berenbaum, 2010).

Given that the immune system is constantly challenged by an enormous variety of pathogens, necessitating a complex and multifaceted response, a key element of which are the TLRs, an increased interest in the role of TLRs in OA research has arisen. TLRs, as described earlier, are membrane bound receptors which though several activation pathways generate gene expression in rheumatic diseases *via* NF-κB or the IRF family (Scanzello et al., 2008, McCormack et al., 2009). The expressed genes result in the classic inflammatory response of localised heat, redness, inflammation and pain. This innate immune response is very effective and often sufficient to clear pathogens from the body and also provides the impetus to activate and prepare the adaptive immunity though cytokine and chemokine production and dendritic maturation (Kim et al., 2009). Nevertheless, dysregulation of such an immune response often leads to chronic inflammatory pathologies, chiefly though

inducing inflammatory cytokines, chemokines and matrix degrading enzymes in the joint. It has been previously shown that the TLRs and induction of their concomitant cytokines, chemokines and MMPs play an important role in the pathogenesis of OA, as well in other chronic inflammatory diseases (Drexler and Foxwell, 2010). A similar finding was demonstrated in our previous chapter wherein we demonstrated that activated OA-FLS secreted a plethora of pro-inflammatory cytokines, chemokines and MMPs that may serve to perpetuate the chronic inflammatory milieu prevalent in the joint in a TLR dependent manner. Thus, the cytokines which are ephemerally produced by most cell types, particularly FLS in OA synovium, can act though binding to their specific cytokine receptors, thereby inducing signal transduction pathways like activation of NF-kB or IRFs, which lead to activation of effector mechanisms like secretion of proinflammatory cytokines, chemokines and MMPs within the responding cells (Sutton et al., 2009, Fernandes et al., 2002). Thus, tight regulation of cytokine and TLR signalling is very crucial for chronic inflammatory disease states, like OA. Therefore, to establish activation of such signal transduction pathways in OA, we have employed OA-FLS isolated from early and late OA synovium to elucidate the underlying pathological mechanisms aiding in OA progression. Notably, it is probable to speculate that these cells may have been activated by PAMPs/DAMPs in the synovium.

The therapeutic potential and importance of TLRs, cytokines and their blocking agents (e.g. soluble cytokine receptors, natural antagonists and antibodies) in treating various clinical conditions such as OA and RA has been greatly recognised and this lead to extensive research in the field of TLRs and cytokines in the last decade (Arend and Dayer, 1990, Fernandes et al., 2002, Abramson et al., 2006, Martel-Pelletier et al., 1999, Tsuboi et al., 2002, Ultaigh et al., 2011). The most common pro-inflammatory cytokines involved in joint arthopathies are IL-6 and TNFα (Fiorito et al., 2005), and IFNβ (Akbar et al., 2000). Given our observations in the previous chapter that increased levels of IL-6, TNFα and IFNβ secretion by OA-FLS following stimulation with Poly(I:C), and, to a lesser extent, with Pam_2CSK_4, LPS and CpG stimulations, it was compelled to employ cytokine and TLR inhibitory molecules towards understanding the regulatory effects of such cytokines/TLRs in OA pathology. As synovial tissue mediated synovitis is associated with clinical symptoms and also reflects joint degradation in OA, synovium-targeted therapy may help alleviate the symptoms of the disease and may also prevent structural degradation of the joint (Sellam and Berenbaum, 2010). Synovitis is recognised to be

directly responsible for several clinical symptoms and reflects the structural progression of the OA pathology. It is an important factor in OA pathophysiology due to the action of several soluble mediators and thought that developing treatment which specifically target synovial tissue mediated synovitis could be beneficial for both the symptoms and structural changes that occur in OA (Sellam and Berenbaum, 2010, Sutton et al., 2009, Fiorito et al., 2005). Furthermore, the synovial tissue primarily aids in synovitis development even in early OA, by releasing inflammatory mediators in to the synovial fluid though synoviocytes (Sellam and Berenbaum, 2010, Sutton et al., 2009, Fiorito et al., 2005, Benito et al., 2005). Increasing evidence show that the activated FLS, an effecter cell type synoviocyte in the synovium, predominantly alleviates the synovial inflammation in a TLR dependent mode (Scanzello et al., 2008, Sellam and Berenbaum, 2010).

To better understand the molecular mechanisms and to identify pathologic mediators involved in synovial inflammation associated with OA, we performed an *ex-vivo* assay, wherein, OA whole synovial tissue explants were treated with selected PAMPs to mimic the pathological conditions in the joint. Additionally, to better understand the inflammatory milieu prevalent in different phases of the OA progression, OA synovial fluid (OA-SF) taken from patients with various grades of OA were characterised in terms of cytokine/chemokine/MMP profiles. To identify and explore the key inflammatory signals propagated in the crosstalk between FLS and the synovial fluid in the joint, we have performed an in-vitro assay, wherein, normal FLS were treated with grade specific OA-SF, to mimic the intricate cell-fluid contact in the joint, which otherwise maintains the joint homeostasis, and if unchecked may lead to chronic inflammatory disease conditions like OA.

Given that over expression of TLR3 in FLS aids in arthritis progression (Ospelt et al., 2008) , and given that pristane induced arthritis in rats was curtailed with TLR3 pathway intervention using anti-TLR3 neutralising antibody (Zhu et al., 2011), we therefore examined the ability of a TLR3 blocking antibody to modulate the OA-SF mediated inflammatory milieu using early and late OA FLS, to better understand the underlying molecular mechanisms in such a complex disease condition. Likewise, to further differentiate the role of TLRs and RLRs in OA progression, we assessed the functional ability of OA-SF to activate specific TLRs using a reporter gene assay and employing

Human Embryonic Kidney cells (HEKs), which over express particular TLRs and MAVS-deficient Mouse Embryonic Fibroblast cells (MEFs)**.**

4.1.2. Specific aims of chapter 4

1. To analyse the differential cytokine, chemokine and MMP levels in OA synovial tissue explant cultures and early/late OA-FLS following stimulation with a panel of TLR agonists.

2. To evaluate grade-specific OA pathology in terms of histology, cytokine, chemokine and MMP expression patterns.

3. To examine the temporal effects of cytokine and TLR neutralising antibodies on cytokine and chemokine levels in N and OA-FLS following stimulation with respective TLRs, cytokines and end stage OA-SF.

4. To characterise the effect of TLR3 neutralisation on gene, cyto/chemokine and protein expression patterns in N-FLS following stimulation with grade-specific OA-SF or early/late OA-FLS stimulated with Poly (I:C).

5. To evaluate the ability of OA-SF to activate specific TLRs using HEK293 cells over-expressing specific TLRs and using MAVS-deficient MEFs.

4.2. Experimental Materials and Suppliers

Bio-Rad

Precision plus protein dual core marker, Cat. # 161-0374

Biosynth®

Luciferin, Cat. # L8200

Biotium

Coelenterazine, Cat. # 10110-1

Cell Signalling

Mouse monoclonal IκBα antibody, Cat. # 4814

Rabbit monoclonal NF-κB p65, Cat. # 4764

Rabbit monoclonal Phospho-NF-κB p65, Cat. # 3033

Rabbit monoclonal Phospho-IRF3, Cat. # 4947

Rabbit monoclonal β-actin, Cat. # 4970

Anti-rabbit IgG, HP-linked antibody, Cat. # 7074

Anti-mouse IgG, HP-linked antibody, Cat. # 7076

eBioscience

Anti-Human IFN-β Functional Grade Purified, Cat. # 16-9978-81

Mouse IgG1 K Isotype Control Functional Grade Purified, Cat. # 16-4714

Mouse IgG2a K Isotype Control Functional Grade Purified, Cat. # 16-4724

Invitrogen

Lipofectamine 2000™, Cat. # 11668-019

DH5α competent cells, Cat. # 18265-017

Invivogen

Neutralising IgA monoclonal antibody to human TLR2, Cat. # maba2-htlr2

Purified monoclonal antibody to human TLR3, Cat. # mab-htlr3

Neutralising IgA monoclonal antibody to human TLR4, Cat. # maba2-htlr4

Purified monoclonal antibody to TLR9, Cat. # mab-mtlr9

Neutralising IgA monoclonal antibody to human interleukin 6, Cat. # maba-hil6
Neutralising IgA monoclonal antibody to human TNF-α, Cat. # maba-htnfa
Human IgA2 Isotype Control, Cat. # maba2-ctrl

Meso Scale Discovery (MSD), Gaithersburg, USA

Human Pro-inflammatory 7-Plex Assay Ultra Sensitive Kit, Cat. # K15008C-1
Human RANTES Ultra Sensitive Kit, Cat. # K151BFC-1
Human IFN-β Tissue Culture Kit, Cat. # K151ADB-1
Human MMP 3-Plex Ultra Sensitive Kit, Cat. # K15034C-1

Pro Sci Inc

Rabbit Polyclonal TLR3 Antibody (CT), Cat. # 3643

Sigma-Aldrich

Xylene, ACS Reagent, Cat. # 33817
10 % Formalin, Cat. # HT5011
Harris Haematoxylin, Cat. # HHS32
Eosin Y, Cat. # E4382
Potassium dichromate, Cat. # P2588
Acetyl CoEnzyme A, Cat. # A2181
4′, 6-Diamidino-2-phenylindole dihydrochloride (DAPI), Cat. # 9542
Magnesium carbonate hydroxide, Cat. # 105H00101

Santa Cruz Biotechnology, INC

Rabbit polyclonal IRF-3 antibody, Cat. # sc-9082
Mouse monoclonal IRF-7 antibody, Cat. # sc-74471
Rabbit polyclonal IRF-9 antibody, Cat. # sc-10793
Anti-nucleolin antibody, C23 (H-6), Cat. # sc-55486)
Mouse monoclonal antibody rose against IFN-β of human origin, Cat. # sc-57203

4.3. Experimental Methods

4.3.1. Research design and clinical cohorts

A total of 40 patients were recruited from the orthopaedic outpatient clinic at Aware Global Hospital, Hyderabad, India and were followed up prospectively for 3 months. All the subjects fulfilled the 1986 American College of Rheumatology criteria for a diagnosis of OA (Altman et al., 1986). All participants had not previously received any biologic therapy. Synovial tissue and fluid samples were obtained from the patients during needle arthroscopy of the knee as part of their treatment regime (Youssef et al., 1998) and OA patients undergoing needle arthroscopy had active synovitis or joint effusion of the knee. Patients were not prescribed DMOADs at the time of synovial tissue/fluid sampling. However, some patients received DMOADs in the past but were not treated with DMOADs at the time of or up to three months prior to tissue sampling. Reasons for discontinuation of previous DMOAD were intolerance and non-compliance. Disease duration at the moment of tissue sampling varied from 20 days to more than 10 years. Regarding trauma participants, patients with a history of trauma for various problems like meniscal tears, Acl tears etc were recruited to the study. The clinical characteristics of the patient cohorts are summarized in table 4.1 and the OA classification system employed for grading the disease stage in these patients is depicted in table 4.2. Approval for the study was given by the institutional ethics committee and all patients gave written informed consent. All treatment was fully compliant with the Helsinki Declaration. The synovial fluid and synovial tissue biopsies thus obtained from a total of 40 patients were stored at -80 °C until further analysis.

4.3.2 Arthroscopic synovial biopsy

The entire arthroscopic procedure was performed in a standard operating theatre under sterile conditions using a lateral infra- and supra patellar approach (Baeten et al., 1999). Briefly, following povodine-iodine antiseptic solution wash, the knee joint was bent to 90 degrees and 10 ml of 2 % lignocaine was administered into the subcutaneous deep tissues and capsule at the lateral infra-patellar arthroscope portal site (Figure 4.1, A). Similarly, a further 10 ml of 2 % lignocaine was administered to the subcutaneous and deep tissues at the lateral suprapatellar biopsy forceps portal site (Figure 4.1, B). Next, the synovial membrane was punctured at the lateral suprapatellar biopsy portal site using a sterile syringe and needle. Synovial fluid was aspirated for future analysis. Subsequently, 20 ml

of 2 % Marcaine was administered intra-articularly, followed by up to 50 ml 0.9 % normal saline. The arthroscopy was performed using a 2.7mm Hopkins rodlens telescope/ needle arthroscope (Storz, Tuttlingen, Germany) (Baeten et al., 1999). Further, with the knee flexed at 90 degrees, a small incision was made at the lateral infrapatellar portal site down to the synovial membrane (Figure 4.1, C). A blunt obdurator and arthroscope sheath were then inserted into the knee joint. Following penetration of the capsule, the knee joint was slowly extended to allow the obdurator and sheath to pass cranially within the knee joint between the patella and the femur. Subsequently, the blunt obdurator was removed and the arthroscope was inserted though the sheath into the knee joint (Figure 4.1, D). A 1L bag of irrigation fluid containing 0.9 % saline, 1 % lignocaine was then connected to the arthroscope irrigation port. The arthroscope was then connected to the recording unit to enable direct visualisation of the synovial membrane on a video screen. A small incision to puncture the synovial membrane at the lateral supra-patellar biopsy portal was then made. The biopsy portal and blunt obdurator were then inserted into the knee and a drain was attached at the biopsy portal site (Figure 4.1, E). Once sufficient irrigation has been performed to achieve a clear view of the synovial cavity, a survey of the synovial membrane was performed to record the degree of vascularity and synovitis within the joint. Synovial biopsies of representative areas of inflamed synovial membrane were obtained through direct visualisation using grasping forceps (Figure 4.1, F). Biopsy samples were placed on gauze soaked with 0.9 % normal saline and placed in a 30 ml sterilin container for immediate processing or were immediately stored in a sterile cryovial at -80 °C until further analysis.

After the procedure, the arthroscopy equipment was removed from the joint, and both portals were closed using steri-strips and covered with a self-adhesive absorbent dressing. The knee was then dressed with cotton wool and gentle compression bandages. The patient was instructed to remove the bandages after 24 h but to keep the knee dry and keep the steri-strip and self-adhesive absorbent dressing over the wound sites for 7 days. This method was adapted, in part, from the procedure performed by Professor Douglas Veale, Consultant Rheumatologist, St. Vincent's University Hospital and all the pictures depicted in this method were captured by Dr. Mary Connolly and Dr Ursula Fearon, Rheumatology Department, St. Vincent's University Hospital, UCD, Ireland (Youssef et al., 1998). A similar procedure was performed by Dr. Maheshwar and Dr. Vidyasagar at Aware Global

Hospital, Orthopaedics Department, Hyderabad, India, to procure the synovial biopsies and fluid for this study.

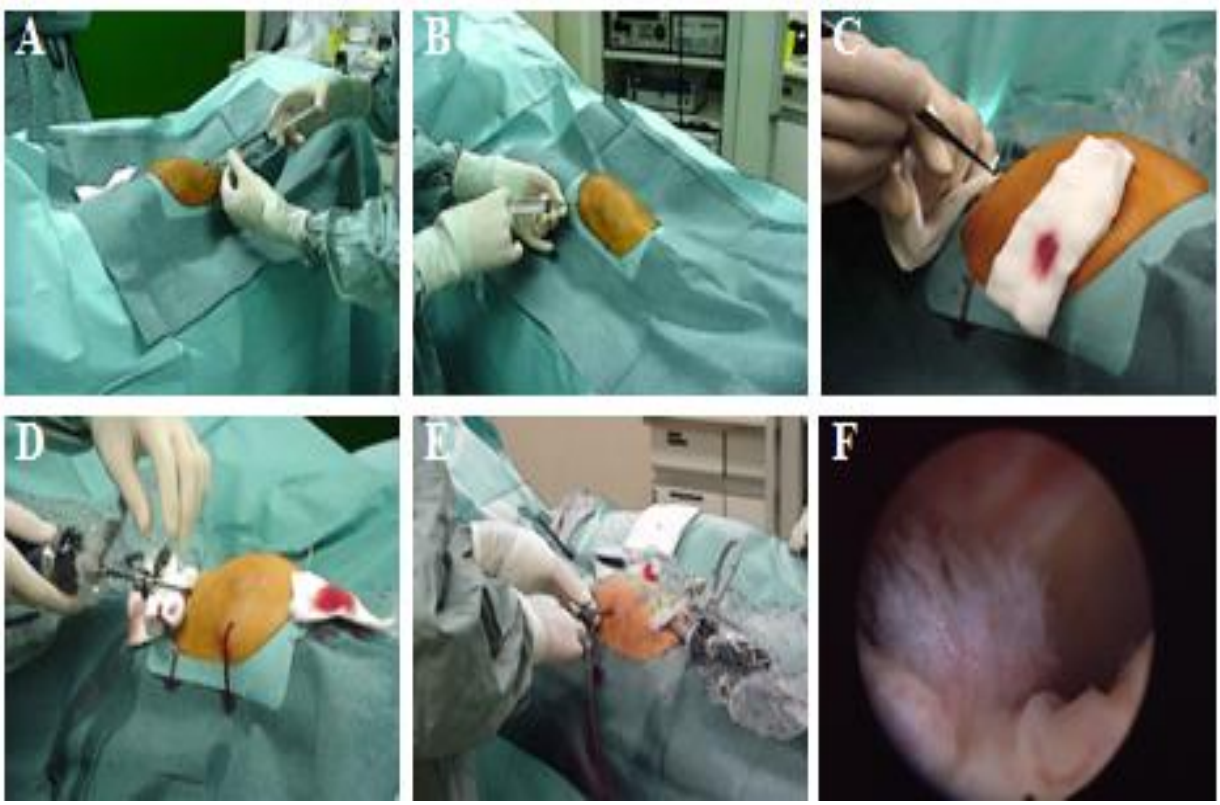

Figure 4.0: Representation of Arthroscopic Knee Surgery. (A) Lateral infra-patellar anaesthetic administration, (B) Lateral supra-patellar anaesthetic administration, (C) Incision of Arthroscopy Portal, (D) Arthroscope insertion into the knee joint, (E) Insertion of Biopsy Forceps and Drain, (F) Direct visualization of inflamed synovial membrane. **(Courtesy Dr Mary Connolly and Dr Ursula Fearon, St. Vincent's University Hospital, Dublin 4, Ireland).**

Table 4.1: Classification System followed for OA synovial tissue biopsy and fluid procurement

Classification System (Lysholm et al., 1987)	**Grade 0**	**Grade 1**	**Grade 2**	**Grade 3**	**Grade 4**
Radiographic System (Kellgren and Lawrence, 1957)	Normal Knee X-ray	Joint space narrowing and/or osteophytes seen on X-ray	Grade 1 + Subchondral sclerosis and/or cysts	Grade2 + Some deformation of the edge of bone/deformity and increased joint space narrowing	Grade 3 + Complete loss of joint space, deformity (varus/valgus)
Arthroscopic System (Ayral et al., 2005)	Normal Cartilage	Softening and swelling of the cartilage	Fibrillation/fragmentation/ fissuring/superficial ulceration less than 0.5 inches/1.25 cm in diameter or less than 50% depth of the cartilage	Fibrillation/fragmentation /fissuring/deep ulceration more than 0.5 inches/1.25 cm in diameter or more than 50% depth of the cartilage not exposing the subchondral bone	Full thickness wear of cartilage with exposure of subchondral bone

Table 4.2: Baseline subject characteristics

Baseline characteristics by diagnostic category	**Trauma controls**	**OA**	**OA**	**OA**	**OA**
Characteristics	**Grade 0 (n=7)**	**Grade 1 (n=8)**	**Grade 2 (n=9)**	**Grade 3 (n=6)**	**Grade 4 (n=10)**
Age in years	26.5 ± 4.44	39.12 ± 9.89	48.14 ± 12.26	52 ± 8.17	56.3 ± 7.86
Sex (M/F)	7/0	5/3	3/6	3/3	5/5
Duration in years	0.43 ± 0.37	1.071 ± 0.18	3.12 ± 2.1	4 ± 0.70	5.9 ± 2.30
OA Grading (RG/AS)	0/0	I/I	II/II	III/III	IV/IV
OA Classification (P/S)	NA	P	P	P	P
BMI (Kg/m^2)	23.1 ± 2.61	23.67 ± 4.95	23.99 ± 2.74	26 ± 4.56	27.83 ± 5.30
ESR (mm/h)	14.66 ± 4.16	17.37 ± 6.86	21.5 ± 9.71	21.8 ± 10.05	26.7 ± 10.55
CRP (mg/L)	2.04 ± 1.32	2.5 ± 1.23	2.87 ± 1.91	3.35 ± 2.40	4.53 ± 3.10
Baseline Analgesics-A/ Hyaluronan Injections-I	A	A	A	A	A
Diabetes (Y/N)	N	N	N	N	N
Hypertension (Y/N)	N	N	N	N	N
Hypo/Hyper Thyriodism (Y/N)	N	N	N	N	N

Data are expressed as mean ± S.D., RG/AS: Radiographic/Arthroscopic grading, P/S: Primary/Secondary OA, BMI: Body Mass Index, ESR: Erythocyte sedimentation rate, CRP= C-reactive protein, Y/N: Yes/No, NA: Not applicable.

4.3.3. Processing of arthroscopic synovial biopsies and fluid

A set of grade-specific OA synovial tissues were placed in formalin for histological analysis as discussed in section 4.3.4, and for immediate isolation of primary synovial fibroblast cells as discussed in section 4.3.5. The synovial fluid samples were centrifuged at 4000 rpm for 15 min at 4°C to sediment particles and cells. The cell-free supernatants were collected and used either for direct cyo/chemokine-MMP analysis using the MSD Mesoscale platform as discussed in section 4.3.7, or used for N-FLS stimulation assays as discussed in section 4.3.10. An aliquot of the synovial tissue and fluid samples were also snap frozen in liquid nitrogen for future protein or mRNA analysis.

4.3.4. Synovial tissue histology

Grade-specific synovial tissues were marked and fixed in 10 % formalin (Sigma- Aldrich), embedded in paraffin, sectioned and stained with haematoxylin and eosin (H&E) for examination by light microscopy. Histopathological changes were graded according to a semi-quantitative scoring system (Cook et al., 2010, Tsubaki et al., 2005, Kraan et al., 2000).

4.3.4.1. Synovial tissue preparation

Grade-specific synovial tissue (n=3 per grade) was processed for histology using an automated processor (Shandon Path centre, Runcorn, UK). Specifically, the tissue was immersed in fixative and dehydrating solutions, namely formalin (x 1), ethanol (x 6), xylene (x 3) (BDH AnalaR® Laboratory supplies, Poole, UK). Next, the samples were embedded in paraffin wax using a Shandon Histocentre 2 (Shandon) and allowed to harden overnight. Then, 4 μm sections were cut using a microtome (Shandon Finesse 325, Thermo-Shandon, Waltham, MA, USA). Next, to remove any creases, the tissue sections were placed in cold water containing ethanol followed by transfer to a hot water bath set at 42 °C. To facilitate the clearance of wax, the tissue sections were heated to 56 °C for a minimum of 1 h prior to staining.

4.3.4.2. Haematoxylin/Eosin Staining

Synovial tissue slide sections were immersed in 2 changes of xylene, 10 min each, followed by rehydration in 3 concentrations of ethanol ranging from 100 % to 80 %. The sections were then placed in 2 changes of water, followed by Harris Haematoxylin (Sigma) solution for 3 min. Slides were washed in water for 2 min, and then immersed in 1 % acid

alcohol for 20 seconds, followed by another washing step. Slide sections were counterstained in Eosin Y (Sigma) for 3 min and washed again. Finally, the slides were put though a series of dehydration steps in ethanol concentrations ranging from 80 % to 100 % for 5 min each. Slides were mounted with DPX mountant (BDH) and examined under a light microscope.

4.3.4.3. Histopathological assessment

A validated semi-quantitative scoring system for synovial tissue was used (Cook et al., 2010, Tsubaki et al., 2005, Kraan et al., 2000). The analysis included all areas of the biopsy samples and a global semi-quantitative score was given for each parameter (0-3 scale where 0=lowest expression and 3=highest). In cases of discordant scores, which differed by a maximum of 1 point, the mean of the 2 scores was used. Histological evaluation of the paraffin embedded H & E stained sections included the mean synovial lining layer thickness (0 = 1-2 cell layers, 1 = 3-4 cell layers, 2 = 5-6 cell layers, and 3 = ≥ 7 cell layers), degree of vascularity of the sublining layer, degree of infiltration of the sublining layer, number of plasma cells and neutrophils, and number of lymphoid aggregates. Comparison of histological semi-quantitative scores was performed using the Non-parametric Mann-Whitney U test. P values less than 0.05 were considered to be statistically significant.

4.3.5. Isolation and culture of primary OA FLS

Early (Grade 1-2) and Late (Grade 3-4) stage OA synovial biopsies were obtained from patients attending the Rheumatology Clinic at St Vincent's University Hospital, Dublin 4, Ireland, in collaboration with Professor Douglas Veale and Dr. Ursula Fearon. Briefly, the synovial biopsies were digested using 1 mg/ml collagenase type 1 (Worthington Biochemical, Freehold, NJ, USA) in RPMI 1640 (Gibco-BRL) for 4 hs at 37 °C humidified atmosphere with 5 % CO_2. The dissociated cells were grown to confluence in RPMI 1640 supplemented with 10 % FCS, 10 ml of 1mM HEPES (Gibco-BRL), 100 U/ml penicillin, 100 µg/ml streptomycin and 0.25 µg/ml fungi zone, before passaging. This aspect of the project was performed in collaboration with Dr. Mary Connolly and Dr Ursula Fearon, St. Vincent's University Hospital, UCD, Ireland. The cells were maintained in a 37 ºC humidified atmosphere with 5 % CO_2 and were passaged every 2 to 3 days using 1 % (w/v) Trypsin/EDTA solution in PBS. Early and Late OA-FLS utilised for this study

were passage 2 to 6. Similarly N and OA-FLS utilised for this study were subcultured as described in section 3.3.2 (chapter 3).

4.3.6. OA synovial tissue explant culture

An *ex vivo* OA synovial tissue explant model was established to investigate the effect of TLR agonists in early and late OA synovial joint, which maintains the synovial architecture and cell-cell contact, and therefore more closely reflects the *in vivo* environment. Briefly, synovial tissue was sectioned into 3mm cubes and cultured in 96 well plates in serum free RPMI 1640 supplemented with 100 U/ml penicillin and 100 µg/ml streptomycin for 24 h at 37 °C humidified atmosphere with 5 % CO_2. To minimize heterogeneity between biopsy specimens, individual biopsies were sectioned into smaller pieces for each experimental condition therefore allowing cellular consistency. OA synovial explants were either stimulated with Pam_2CSK_4 (1 µg/ml), Poly (I:C) (10 µg/ml), LPS (1 µg/ml) or CpG (3 µg/ml) in serum free RPMI 1640 for 24 h or left unstimulated to measure basal protein profiles. This aspect of the project was performed in collaboration with Dr Mary Connolly and Dr Ursula Fearon, St. Vincent's University Hospital, UCD, Ireland. The supernatants were harvested and levels of IL-1β, TNFα, IL-6, IL-8, IFNγ, IL-12p70, IL-10, RANTES, IFNβ and MMP-1, 3, 9 were assessed using Meso Scale Ultrasensitive ELISA System (MSD, USA). Similarly, spontaneous release of such cyto-chemokine-MMPs was also measured using MSD system, following 24 h culture of synovial biopsies from OA (n=4) patients in RPMI 1640 supplemented with 10 % FCS, 10 ml of 1mM HEPES, 100 U/ml penicillin, 100 µg/ml streptomycin and 0.25 µg/ml fungizone.

4.3.7. Meso Scale Human Pro-inflammatory 7-Plex Assay

Cell free supernatants were used for measuring IL-1β, TNFα, IL-6, IL-8, IFNγ, IL-12p70, and IL-10 levels, using Meso Scale 96-Well Human Pro-inflammatory 7-plex ultra sensitive assay kit (Meso Scale Discovery (MSD)). The Human 7-Plex assay detected IL-1β, TNFα, IL-6, IL-8, IFNγ, IL-12p70, and IL-10 in a sandwich immunoassay format. The 7-plex assay was supplied as a 96 well ultra sensitive plate pre-coated with IL-1β, TNFα, IL-6, IL-8, IFNγ, IL-12p70, and IL-10 capture antibodies on spatially distinct spots on the plate. First, the pre-coated plate was incubated with 25 µl/well of Diluent 2 (R51BB-4) supplied with the kit for 30 min at room temperature (RT) with vigorous shaking at 1000

rpm. Next, the samples (cell free supernatants) or appropriate dilution of stock calibrator blend (highest calibrator point was obtained by diluting the stock by 100 fold in Diluent 2 and from this an 8 point standard curve with 4-fold serial dilution was prepared-assay range 2500 to 0 pg/ml) was added to separate wells of the MSD plate in duplicates. The plate was sealed with an adhesive seal and incubated for 2 h with vigorous shaking (1000 rpm) at RT. Next, the plate was washed three times with wash buffer (PBS-T) and was pat dry. The SULFO-TAG Detection Antibody Blend (D2008-2) provided as 50 × stock solution was diluted to a final working concentration of 1 ×, by mixing 60 µl of stock antibody blend with 2.94 ml of Diluent 3 (R51BA-4) supplied with the kit. Further, 25 µl/well of the 1 × detection antibody solution was added to each well of the MSD plate and the plate was sealed and incubated for 2 h with vigorous shaking (1000 rpm) at RT. Next, the wash step was repeated and 150 µl/well of 2× diluted Read Buffer T (R92TC-3) was added in to each well of the MSD plate. The plate was immediately read on the SECTOR Imager and the data was analysed using the MSD Discovery Workbench analysis software.

4.3.8. Meso Scale Human RANTES and IFNβ Assay

Cell free supernatants were used for measuring RANTES and IFNβ levels using a meso scale 96-Well Human RANTES assay kit and Human IFNβ assay kit respectively (MSD). The Human RANTES assay plate (L451BFA-1) detected RANTES and Human IFNβ assay avidin plate (L15AA-1) detected IFNβ in a sandwich immunoassay format. The 96 well ultra sensitive plate was pre-coated with human RANTES capture antibody on the RANTES plate. Regarding the IFNβ plate, a 50× anti-hIFNβ biotinylated capture antibody was diluted to 1x working concentration in Diluent 100 (R50AA-4), and 20 µl/well of this 1 × capture antibody was manually pipetted onto the MSD plate and incubated at RT with gentle shaking for 1 h. Subsequently, the RANTES and IFNβ plates were incubated with 25 µl/well of Diluent 2 (R51BB-4) supplied with the kit for 30 min at RT with vigorous shaking at 1000 rpm. Next, the samples (cell free supernatants) or appropriate dilution of stock calibrators (highest calibrator point for RANTES was obtained by diluting the stock (C01BF-2) by 100 fold in Diluent 2 and from this, an 8 point standard curve with 4-fold serial dilution was prepared-assay range 2500 to 0 pg/ml, and highest calibrator point for IFNβ was obtained by diluting the stock (C01AD-2) by 25 fold in Diluent 1 (R50CK-4) and from this, an 8 point standard curve with 4-fold serial dilution was prepared-assay range 25,000 to 1.5 pg/ml) were added to separate wells of the respective MSD plates in duplicates. The plates were sealed with an adhesive seal and incubated for 2 h with

vigorous shaking (1000 rpm) at RT. Next, the plates were washed three times with wash buffer (PBS-T) and were pat dry. The SULFO-TAG Detection Antibody Blend (D21BF-2) for RANTES and (D21AD-2) for IFNβ detection, provided as 50 × stock solution were diluted to a final working concentration of 1 ×, by mixing 60 µl of stock antibody blend with 2.94 ml of Diluent 3 (R51BA-4). Next, 25 µl/well of the 1 × detection antibody solution was added to each well of the respective MSD plates and the plates were sealed and incubated for 2 h with vigorous shaking (1000 rpm) at RT. Next, the plates were washed three times with wash buffer (PBS-T) and were pat dry. Then, 150 µl/well of 2× diluted Read Buffer T (R92TC-3) was added to each well of the MSD plates. The plates were immediately read on the SECTOR Imager and the data was analysed using the MSD Discovery Workbench analysis software.

4.3.9. Neutralisation Assays

N and OA-FLS were seeded at 1 × 10^5 cells/well in triplicate in a 6-well tissue culture plate until confluent. Prior to stimulation, FLS were rendered quiescent by maintaining the cells in serum free Opti-MEM for 24 h. Further, all stimulations were carried out in Opti-MEM using the agonists/end stage OA-SF and/or blocking antibodies/isotype antibody controls. FLS were pre-treated with the following optimised concentrations of blocking/isotype control antibodies for 90 min prior to the respective ligand stimulation for 24 h. The cell free supernatants were then collected for ELISA analysis. Briefly, N and OA FLS were pre-treated with an anti-TLR2 antibody (5 µg/ml) or Isotype IgA2 antibody (5 µg/ml) for 90 min prior to Pam_2CSK_4 (1 µg/ml) stimulation, an anti-TLR3 antibody (20 µg/ml)/Isotype IgG1 antibody (20 µg/ml) prior to Poly (I:C) (10 µg/ml) stimulation, an anti-TLR4 antibody (5 µg/ml)/Isotype IgA2 antibody (5 µg/ml) prior to LPS (1 µg/ml) stimulation, an anti-TLR9 antibody (15 µg/ml)/Isotype IgG2a antibody (15 µg/ml) prior to CpG (3 µg/ml) stimulation, an anti-IL-6 antibody (5 µg/ml)/Isotype IgA2 antibody (5 µg/ml) prior to IL-6 (100 pg/ml) stimulation, an anti-IFNβ antibody (10 µg/ml)/Isotype IgG1 antibody (10 µg/ml) prior to IFNβ (100 pg/ml) stimulation and an anti-TNFα antibody (5 µg/ml)/Isotype IgA2 antibody (5 µg/ml) prior to TNFα (1 ng/ml) stimulation for 16 hs.

4.3.10. Real time PCR and ELISA analysis of N-FLS stimulated with grade-specific OA-SFs

N-FLS were treated with grade specific (Grade 0, 1, 2, 3, 4) OA-SF for 16 h and Poly(I:C) acted as positive control. Briefly, N-FLS were seeded at 1×10^5 cells/well in triplicates in a 6 well tissue culture plate until confluent. Prior to stimulation N-FLS were rendered quiescent by maintaining the cells in serum free Opti-MEM for 24 h. Cells were pre-treated with an anti-TLR3 (20 µg/ml) antibody or Isotype IgG1 (20 µg/ml) antibody for 90 min in Opti-MEM. Next, stimulations were performed in Opti-MEM using the grade-specific OA-SF (1:5 dilution in Opti-MEM) or Poly(I:C) (10µg/ml) for 16 h. Cell free supernatants were collected followed by ELISA analysis. The cell pellet was utilised for mRNA extraction to study differential TLR and TRIF expression profiles that may be induced by the grade-specific OA-SF and Poly(I:C).

4.3.11. Western blot analysis of Poly(I:C)/OA-SF stimulated FLS

N and OA-FLS were seeded at 1×10^5 cells/well in triplicate in a 6 well tissue culture plate until confluent. Cells were rendered quiescent by maintaining the cells in serum free Opti-MEM for 24 h. Initially, N and OA-FLS were stimulated with Poly(I:C) (10µg/ml) for 30, 60 and 90 min respectively. Alternatively, N and OA-FLS from both early and late stages were seeded at 1×10^5 cells/well in triplicates in a 6 well tissue culture plate until confluent. Cells were pre-treated with an anti-TLR3 antibody (20 µg/ml)/ Isotype IgG1 antibody (20 µg/ml) for 90 min as indicated, followed by stimulation with Poly(I:C) (10µg/ml) or grade-specific OA-SF (1:5 dilution in Opti-MEM/grade) for 3 h (as earlier time points did not show any transcription factor activation in N-FLS (data not shown). The cell pellets were harvested and assayed for IκBα degradation, phosphorylation of p65 and IRF3 activation by immunoblot analysis as described in detail in chapter 2. The antibody dilutions employed for immunoblotting in this method are as follows: β-actin (mouse) 1:1000, phospho-IRF3 (rabbit) 1:1000, IκBα (mouse) 1:200, phospho-p65 (rabbit) 1:1000, anti-mouse and anti-rabbit IgG secondary antibodies are used at 1:5000 dilution.

4.3.12. Luciferase reporter gene assay

HEK293-TLR2, HEK293-TLR3, HEK293-TLR4, HEK293-TLR7, HEK293-TLR9, MAVS Wild type$^{+/+}$ and MAVS-deficient$^{-/-}$ MEFs were grown in DMEM with GlutaMAX (Gibco-BRL) supplemented with 10 % FCS, penicillin-streptomycin, noromycin and 200 µg/ml of G418, except HEK293-TLR3 where the culture medium was supplemented with blasticidin (100 mg/ml), and maintained at 37 °C in a humidified atmosphere of 5 % CO_2. Next, cells (2 x 10^4 cells/well; 96 well plate) were transfected with 80 ng/well luciferase

reporter gene plasmid for NF-κB / IFNβ (p125) / PRD-II / PRD-I-III / PRD-IV / IRF3 / IRF7 and IRF9 using Lipofectamine 2000 as described by the manufacturer (Invitrogen). In all cases, 40 ng/well of phL-TK reporter gene was co-transfected to normalise data for transfection efficiency. After 24 h, cells were either stimulated with their respective ligands namely, Pam_2CSK_4 (1 µg/ml; HEK293-TLR2), Poly(I:C) (10 µg/ml; HEK293-TLR3), LPS (1 µg/ml; HEK293-TLR4), CLO-97 (1 µg/ml; HEK293-TLR7), CpG (3 µg/ml; HEK293-TLR9), 5' ppp ds-RNA (1 µg/ml; $MAVS^{+/+}$ and $MAVS^{-/-}$ MEFs), or with early OA-SF (grade-1), late OA-SF (grade-4) or grade-specific OA-SF (1:5 dilution in Opti-MEM) for 24 h as indicated. Thereafter, cell lysates were prepared and reporter gene activity was measured using the Dual Luciferase Assay system (Promega) as described (Bowie et al., 2000). Data was expressed as the mean fold induction ± S.D. relative to control levels, for a representative experiment from a minimum of three separate experiments, each performed in triplicate.

4.3.13. Cellular nuclear fraction extraction assay

N-FLS, OA-FLS from early (grade 1-2) and late (grade 3-4) stage OA-FLS were seeded at 1×10^5 cells/well in triplicate in a 6 well tissue culture plate until confluent. Cells were rendered quiescent by maintaining the cells in serum free Opti-MEM for 24 h. Cells were pre-treated with an anti-TLR3 antibody (20 µg/ml)/ Isotype IgG1 antibody (20 µg/ml) for 90 min as indicated, followed by stimulation with Poly(I:C) (10µg/ml) for 60 min or early OA-SF (grade 1)/late stage OA-SF (grade 4) (1:5 dilution in Opti-MEM/grade) for 3 h (as earlier time points did not show any transcription factor activation in N-FLS (data not shown). The cell pellets were harvested and nuclear proteins were isolated using the ProteoJET cytoplasmic and nuclear protein extraction kit (Fermentas) as described by the manufacturer. Thereafter, the nuclear fraction was subjected to immunoblot analysis using anti-IRF3 (1:100 dilution), anti-IRF7 (1:100 dilution), anti-IRF9 (1:100 dilution) and anti-nucleolin (1:100 dilution). All the data presented are representative of at least three independent experiments performed in triplicate.

4.3.14. Confocal Microscopy

Primary N and OA FLS were seeded at a density of 0.5×10^5 cells/ml in 8-well chamber slides and grown for 24 h till confluent. Next, cells were pre-treated with anti-TLR3 antibody for 2 h prior to stimulation with Poly(I:C) for 1 h or OA-SF for 3h. Cells were fixed in 4 % para-formaldehyde, permeabilised with 0.2 % Triton X-100 in PBS for 10 min

at RT followed by blocking with 10 % goat serum for 2 h. Next, cells were treated overnight at 4 °C with primary antibody on a rotary shaker with gentle agitation. Further, cells were washed and incubated with secondary antibody for 1 h at RT with gentle shaking in the dark, followed by incubation with DAPI (1.5 μg/ml) in PBS for 30 min at RT. Slides were washed and mounted using antifade mounting media (Vectashield; Vector Laboratories).

4.3.15. Statistical Analysis

All the data presented are representative of at least three independent experiments performed in triplicate and all the data are expressed as mean ± standard error of the mean (S.E.M.) (mean ± S.E.M). Statistical comparisons were performed using a one-way analysis of variance using a post hoc Student‘s Newman-Keuls test. Differences with a *p* value less than 0.05 were denoted with (*) and the values less than 0.01 as (**) and were considered statistically significant.

4.4. Results

In this study, for the first time an *ex-vivo* OA whole synovial tissue explant culture model was utilised to screen for and determine the role of TLRs in inducing differential secretion of major synovial inflammation related cytokines, chemokines and MMPs (Sutton et al., 2009, Fernandes et al., 2002, Scanzello et al., 2009). Additionally, assessment of grade-specific synovial tissue biopsies through histological evaluation was carried out. Furthermore, the effect of TLR and RLR agonist-induced cytokine and chemokines in early and late OA patient derived primary synovial fibroblasts was assayed. Likewise, differential cytokine, chemokine and MMP analysis of grade-specific synovial fluid was performed employing Meso Scale (MSD) multiplex ultra-sensitive ELISA assays. Similarly, a quantitative real time PCR analysis was performed to evaluate the ability of grade-specific OA-SF to induce specific TLR genes in N-FLS. Moreover, optimisation and evaluation of anti-TLR and anti-cytokine neutralising antibodies was performed in N and OA-FLS to assess the ability of these antibodies to modulate TLR/cytokine/OA-SF mediated pro- and anti-inflammatory cyto-chemokine secretions. Subsequently, the ability of anti-TLR3 antibody in modulating Poly(I:C) and grade-specific OA-SF induced TLR3, TRIF, inflammatory cytokine, chemokine and MMP gene and protein expression in N-FLS was evaluated by employing real time RT-PCR and ELISA. Essentially, the immunomodulatory effects of TLR3 blockade using an anti-TLR3 antibody in early and late OA patient derived FLS was evaluated through ELISA and validated by immunoblot and confocal analysis in FLS. Furthermore, the ability of OA-SF to activate specific TLRs was evaluated by luciferase reporter gene assay using HEK293 cells over-expressing specific TLRs and using MAVS-deficient MEFs.

4.4.1. *Ex-vivo* analysis of pro and anti-inflammatory cytokines, chemokines and MMP levels in OA synovial tissue explant cultures

Given the increasing evidence that TLR activation may play a crucial role in OA progression by mediating synovitis, through production of pro-inflammatory cytokines in the OA joint (Scanzello et al., 2008, Sutton et al., 2009), and given our previous observations that upon TLR activation of OA-FLS, a plethora of pro-inflammatory cytokines and chemokines are secreted which help facilitate the progression of synovial inflammation (chapter 3), it was essential to investigate TLR agonist-induced inflammatory mediator secretion in whole synovial tissue explant cultures as the

maintenance of the synovial architecture and cell-cell contact is facilitated, and therefore more closely reflects the *in-vivo* OA synovial joint environment.

4.4.1.1. Analysis of spontaneous and TLR agonists induced secretion of pro-inflammatory cytokines in OA synovial tissue explant cultures *ex-vivo*

Initially, to examine whether perturbations in the spontaneous cytokine production, as evident in earlier studies (chapter 3), occur as a consequence of disease pathology and to define how prevalent these mediators are in the disease, the actual cytokines or chemokines secreted by the OA synovial tissue explants without any external stimuli was examined as previous findings demonstrated the spontaneous cyto-chemokine secretion ability of synoviocytes (Arend and Dayer, 1990) (chapter 3, Figure 3.8 panel A). Furthermore, OA synovial tissue explants were stimulated with TLR 2, 3, 4 and 9 ligands for 24 h or left unstimulated to measure basal and TLR induced IL-6, IL-8, IL-1β and TNF-α levels (Figure 4.1, panel A, B, C and D, n=4). Accordingly, it was evident that OA synovial tissue explants spontaneously secreted IL-6 (4557 ± 839.5 pg/ml), IL-8 (3646 ± 511.8 pg/ml), IL-1β (2.57 ± 1.11 pg/ml) and TNF-α (13.21 ± 1.59 pg/ml) to varying amounts in the joint (mean ± standard error), and this correlates with previous publications (Ultaigh et al., 2011, Sutton et al., 2009). Significantly, stimulation with Poly(I:C) (10 µg/ml) induced the highest levels of IL-6 in OA synovial tissue explants (7689 ± 388.3 pg/ml from basal 636.3 ± 175.2 pg/ml, $p \leq 0.001$) and similarly stimulation with LPS (1 µg/ml) induced IL-6 secretion but the levels were lower when compared with spontaneous IL-6 secretion by OA explants and with Poly(I:C) stimulation (2269 ± 335.1 pg/ml from basal 636.3 ± 175.2 pg/ml, $p \leq 0.05$). Also, stimulation with Pam_2CSK_4 (1 µg/ml) induced IL-6 levels to minimal extent, while in contrast suppression of IL-6 levels was observed with CpG (3 µg/ml) stimulation (Figure 4.1, panel A).

Correspondingly, stimulation with Poly(I:C) induced highest and significant amounts of IL-8 secretion in OA synovial tissue explants (4982 ± 410.5 pg/ml from basal 548.8 ± 7.17 pg/ml, $p \leq 0.01$) and stimulation with LPS induced significantly higher levels of IL-8, but the levels were low when compared with spontaneous IL-8 secretion by OA explants and following Poly(I:C) stimulation (1689 ± 225.3 pg/ml from basal 548.8 ± 7.17 pg/ml, $p \leq 0.05$). Minimal or no IL-8 induction was evident following Pam_2CSK_4 or CpG stimulation (Figure 4.1, panel B). Stimulation with Poly(I:C) induced the highest most significant amounts of IL-1β (7.42 ± 1.02 pg/ml from basal 1.49 ± 0.76 pg/ml, $p \leq 0.05$) secretion in

OA synovial tissue explants. However, insignificant levels of IL-1β induction was observed following Pam_2CSK_4 or LPS stimulations, while in contrast, suppression of IL-1β levels was evident with CpG stimulation (Figure 4.1, panel C). Furthermore, whilst stimulation with Poly(I:C) also induced highest and significant amounts of TNFα (39.94 ± 4.42 pg/ml from basal 7.94 ± 2.51 pg/ml, $p \leq 0.05$) secretion in OA synovial tissue explants, insignificant levels of TNFα induction was observed following Pam_2CSK_4 or LPS stimulations. Suppression of IL-1β levels was evident following CpG stimulation (Figure 4.1, panel D). Interestingly, the highest and most significant induction of pro-inflammatory IL-6, IL-8, IL-1β and TNFα secretions by OA synovial tissue explants cultures was observed upon Poly(I:C) stimulation, and this correlates with our previous data (Chapter 3, Figure 3.6 and 3.9). Together, these data suggest a probable role for the sustained activation of TLR3 in the synovial FLS in the synovium.

4.4.1.2. Analysis of spontaneous and TLR agonists induced IFNβ and RANTES secretion in OA synovial tissue explant cultures

Given the pivotal role for chemokines, RANTES, in cartilage degradation (Alaaeddine et al., 2001, Borzì et al., 2004) and having observed the predominant secretion of the anti-viral cytokine IFNβ in FLS following various inflammatory stimuli (chapter 3), it was critical to identify the stimulus which distinctively induces these inflammatory mediators in the OA synovial tissue explants., thus propagating synovitis in the OA joint. Accordingly, it was evident that OA synovial tissue explants spontaneously secreted varying amounts of IFNβ (36.48 ± 2.97 pg/ml) and RANTES/CCL5 (351.6 ± 9.489 pg/ml) into the joint (Figure 4.2, panel A and B, n=4). Stimulation with Poly(I:C) (10 µg/ml) induced the highest and most significant amounts of IFNβ in OA synovial tissue explants (2011 ± 129.5 pg/ml from basal 8.89 ± 0.45 pg/ml, $p \leq 0.001$) and stimulation with LPS (1 µg/ml) also induced significant levels of IFNβ (137.2 ± 8.53 pg/ml from basal 8.89 ± 0.45 pg/ml, $p \leq 0.05$). In contrast, stimulation with Pam_2CSK_4 (1 µg/ml) or CpG (3 µg/ml) showed no induction of IFNβ levels relative to basal (Figure 4.2, panel A).

Stimulation with Poly(I:C) induced significant levels of RANTES/CCL5 secretion in OA synovial tissue explants (1713 ± 188.7 pg/ml from basal 3.73 ± 1.46 pg/ml, $p \leq 0.001$) and stimulation with LPS also induced significant levels of RANTES (259.4 ± 29.03 pg/ml from basal 3.73 ± 1.46 pg/ml, $p \leq 0.05$). Negligible levels of RANTES induction was evident following Pam_2CSK_4 or CpG stimulations (Figure 4.2, panel B). Interestingly, the highest and most significant induction of inflammatory IFNβ and RANTES/CCL5 secretions by OA synovial tissue explants cultures was observed upon Poly(I:C)

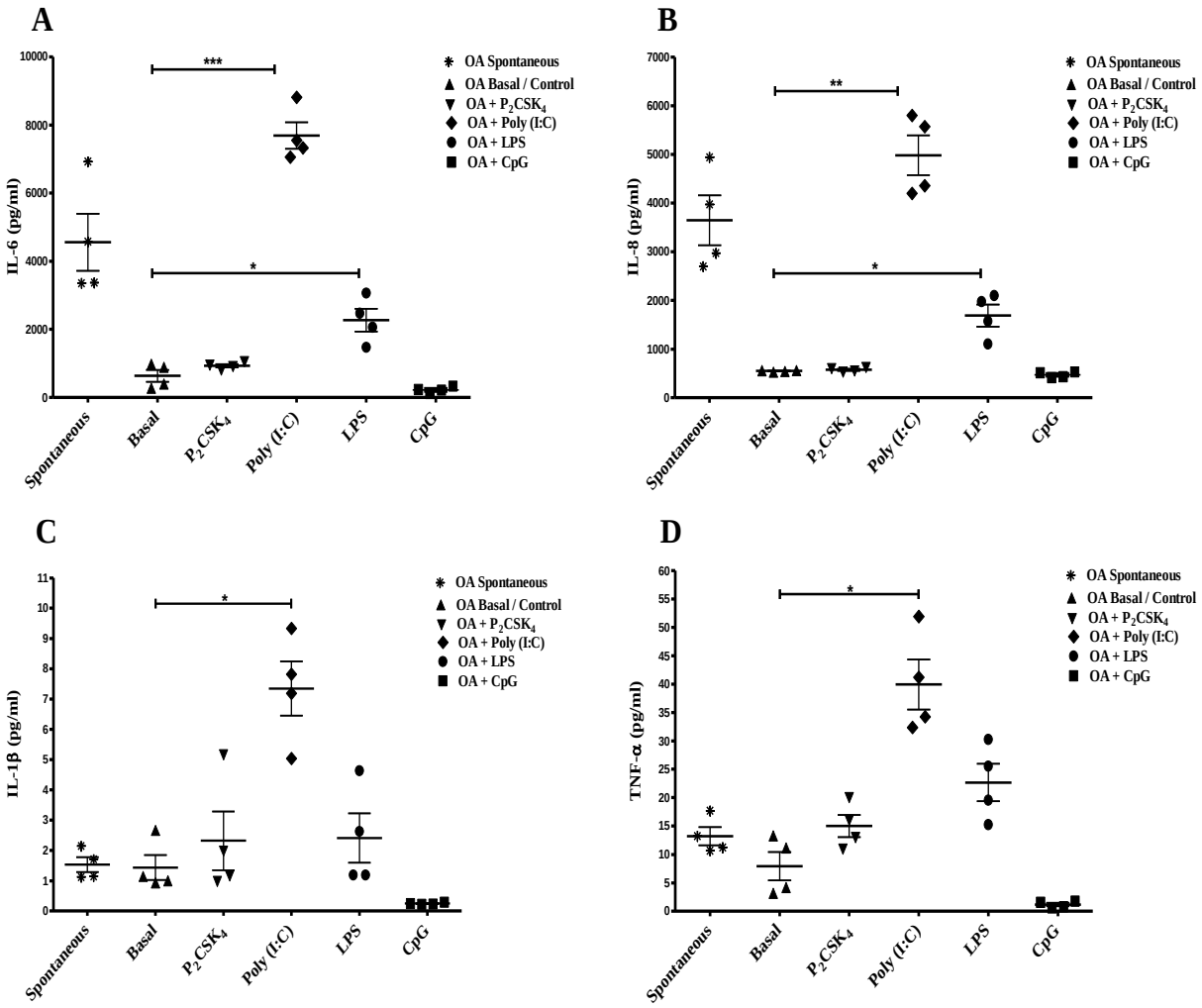

Figure 4.1: Analysis of spontaneous and TLR agonists induced secretion of pro-inflammatory cyto-chemokines in OA synovial tissue explant cultures. (A-D) Whole OA synovial tissue explants (n=4) were either cultured in complete RPMI 1640 medium for 24 h to measure spontaneous cytokine release or treated with Pam_2CSK_4 (1 µg/ml; TLR2 ligand), Poly (I:C) (10 µg/ml; TLR3 ligand), LPS (1 µg/ml; TLR4 ligand), CpG (3 µg/ml; TLR9 ligand) or left unstimulated in serum free RPMI 1640 for 24 h to measure TLR induced and basal protein profiles. The cell-free supernatants were harvested and analyzed for levels of (A) IL-6, (B) IL-8, (C) IL-1β, (D) TNFα using MSD ultrasensitive multiplex ELISA System. All the data presented are representative of at least four independent experiments performed in duplicate (mean ± S.E.M). Data was subjected to an unpaired Student's t test. * $p<0.05$, ** $p<0.01$, *** $p<0.001$ denotes the level of significance relative to basal control.

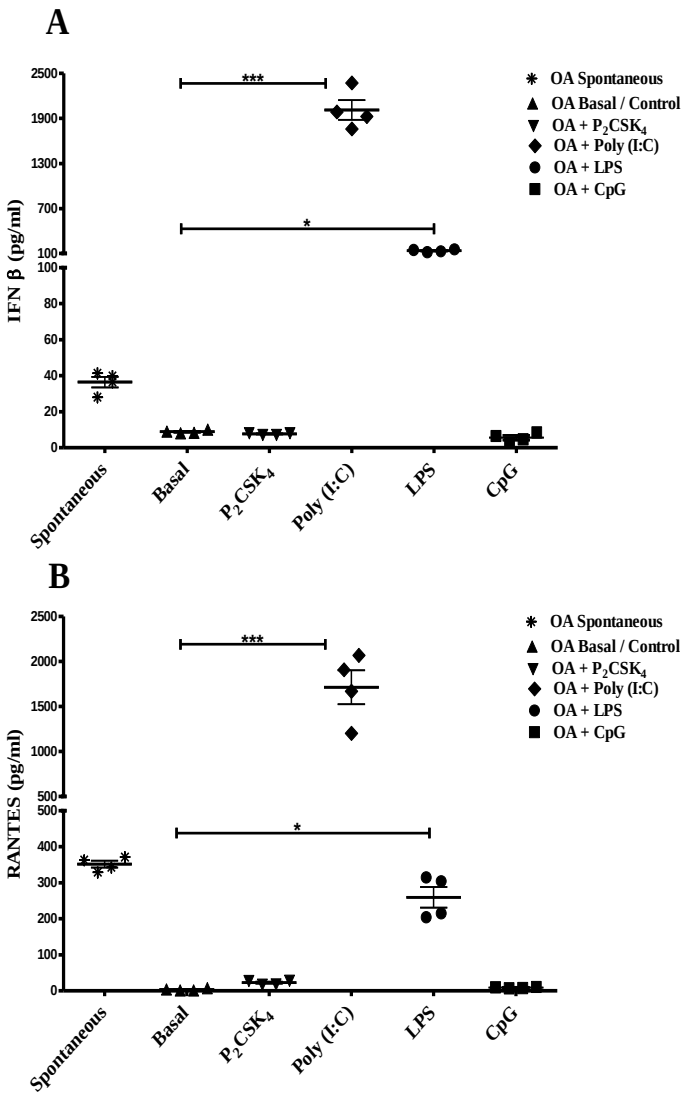

Figure 4.2: Analysis of spontaneous and TLR agonists induced IFNβ and RANTES secretion in OA synovial tissue explant cultures. (A and B) Whole OA synovial tissue explants (n=4), were either cultured in complete RPMI 1640 medium for 24 h, to measure spontaneous cytokine release or treated with Pam_2CSK_4 (1 µg/ml; TLR2 ligand), Poly (I:C) (10 µg/ml; TLR3 ligand), LPS (1 µg/ml; TLR4 ligand), CpG (3 µg/ml; TLR9 ligand) or left unstimulated in serum free RPMI 1640 for 24 h to measure TLR induced and basal protein profiles. The cell-free supernatants were harvested and analyzed for levels of (A) IFNβ and (B) RANTES using MSD ultrasensitive multiplex ELISA System. All the data presented are representative of at least one independent experiment performed in duplicate (mean ± S.E.M). Data was subjected to an unpaired Student's t test. * $p<0.05$, ** $p<0.01$, *** $p<0.001$ denotes the level of significance relative to basal control.

stimulation, and this correlates with previous data (Chapter 3, Figure 3.6 and 3.8). These data suggest a probable role for RNA borne synovial tissue inflammation through recurrent secretion of inflammatory mediators namely RANTES and IFNβ, which may aid in perpetuating synovitis and joint destruction.

4.4.1.3. Analysis of TLR agonists induced secretion of IL-10, IL-12 p70 and IFNγ cytokines in OA synovial tissue explant cultures

Given the increasing evidence that synovial membrane/tissue inflammation mediating synovitis in OA is primarily through an imbalance in the levels of pro versus anti-inflammatory cytokines/chemokines in the joint (Benito et al., 2005, Brigitte, 2002, Martel-Pelletier et al., 1999, Kapoor et al., 2011, Sutton et al., 2009, Scanzello et al., 2011), and having observed TLR ligand induced inflammatory cyto-chemokine induction in OA synovial tissue explants (Figure 4.1 and 4.2), it was essential to investigate the ability of TLR ligands to modulate key cytokines namely IL-12 p70 and IFNγ and anti-inflammatory IL-10 levels in OA synovial tissue explants. Accordingly, it was evident that OA synovial tissue explants spontaneously secreted minimal amounts of IL-10, IFNγ and IL-12p70 relative to basal (Figure 4.3, panel A, B and C, n=4). Interestingly, upon stimulation with Poly(I:C) (10 µg/ml), a non-significant decrease in IL-10, IFNγ and IL-12p70 relative to basal was evident in OA synovial tissue explants and a similar trend towards decreased IL-10, IFNγ and IL-12p70 relative to basal was evident upon CpG stimulation. Stimulation with Pam_2CSK_4 (1 µg/ml) or LPS (1 µg/ml) induced a non-significant increase in IL-10, IFNγ and IL-12p70 relative to basal levels in OA synovial tissue explants (Figure 4.3, panel A, B and C). These data indicate that Pam_2CSK_4 and LPS may play a protective role in the synovium by inducing IL-10, a known anti-inflammatory cytokine, which is thought to have an important immunoregulatory role in the cytokine network of OA and RA probably by regulating monocytes and in some cases T cell cytokine production (Katsikis et al., 1994).

Moreover, we found that levels of the Th1 cytokines, IL-12p70 and IFNγ were suppressed upon Poly(I:C) stimulation of OA synovial tissue explants and this may be attributed to the increased levels of IFNβ in the joint during disease process or with an encounter with the RNA from necrotic cells in the joint or Poly (I:C) stimulation (Figure 4.2, panel A), thus constantly activating TLR3 thereby inducing excess IFNβ, which has also been shown to immunomodulate the Th1/Th2 cytokine profile by attenuating the secretion of IFNγ and IL-12p70 and IL-10 secretion (Sellner et al., 2008). Regarding IL-10, a key Th2 cytokine

with anti-inflammatory properties, a trend towards decreased levels was observed in OA synovial tissue explants upon Poly (I:C) stimulation, suggesting an RNA borne impairment of anti-inflammatory mechanisms in the joint. Also, studies have shown a mutual antagonism between IFNγ and TNFα levels in FLS, wherein, paradoxical induction of IFNγ and TNFα expression was observed in FLS (Alvaro-Gracia et al., 1993, Alvaro-Gracia et al., 1990). This might further explain decreased levels of IFNγ with Poly (I:C) stimulation, as an increased amount of TNFα levels was evident in OA synovial tissue explants with Poly (I:C) stimulation (Figure 4.1, panel D).

4.4.1.4. Analysis of spontaneous and TLR agonists induced pro-inflammatory MMP-1, -3 and -9 secretion in OA synovial tissue explant cultures

Given the differential expression of pro-inflammatory cytokines and MMPs in the synovial membranes of OA patients (Wassilew et al., 2010), and having known that MMPs 1, 3 and 9 play a vital role in OA pathogenesis (Sutton et al., 2009, Firestein, 1996, Scanzello et al., 2011), it was critical to investigate whether these MMPs may be induced with TLR ligands in the whole OA synovial tissue explants, which more closely reflects the *in-vivo* OA synovial joint environment. It was also evident that OA synovial tissue explants spontaneously secreted MMP-1 (9.72 ± 0.11 ng/ml), MMP-3 (21.04 ± 2.23 ng/ml) and MMP-9 (673.3 ± 102.4 pg/ml) to varying amounts (Figure 4.4, panel A, B and C, n=4). Also, it was found that stimulation of OA synovial tissue explants with Poly (I:C) induced the highest and most significant levels of MMP-1 when compared to the other PAMPs under investigation and to spontaneous secretion levels (24.51 ± 0.74 ng/ml from a basal 2.62 ± 0.18 ng/ml, $p < 0.001$, Figure 4.4, panel A, n=4).

Similarly, the most significant increase in MMP-3 levels was observed following stimulation of OA synovial tissue explants with Poly (I:C) (30.42 ± 1.95 ng/ml from a basal 3.20 ± 0.90 ng/ml, $p < 0.001$, Figure 4.4, panel B, n=4). Likewise, a significant increase in MMP-9 levels was observed following Poly (I:C) stimulation of OA synovial tissue explants (1672 ± 157.1 pg/ml from a basal 177.4 ± 35.48 pg/ml, $p < 0.01$, Figure 4.4, panel C, n=4). In contrast, LPS, Pam_2CSK_4 or CpG induced minimal or non-significant amounts of MMP-1, 3 and 9 when compared to their respective spontaneous MMP secretions (Figure 4.4, panel A, B and C, n=4). Thus, it is clear that Poly(I:C) predominantly induces secretion of the catabolic MMP 1, 3 and 9 in whole OA synovial tissue explants. This substantiates our previous observations that these MMPs can be

induced, particularly by Poly (I:C), which exclusively employs TLR3 in OA-FLS (Chapter 3, Figure 3.2, 3.14 and 3.15), thus making TLR3 a critical target for OA disease intervention.

Together, these data provide evidence that OA synovial tissue explants can be activated specifically by the selected concentrations of TLR ligands or DAMPs *ex-vivo*, which in turn, induces the recurrent secretion of inflammatory mediators and suppression of immune-modulatory and anti-inflammatory molecules, which may aid in perpetuating synovitis and joint destruction in OA. Interestingly, the present data indicates that Poly (I:C) / dsRNA / RNA from necrotic cells may drive the inflammatory locale in the joint during synovitis by inducing inflammatory IL-6, IL-8, IL-1β and TNFα (Figure 4.1), IFNβ and RANTES (Figure 4.2), MMP-1, 3 and 9 (Figure 4.4) and by suppressing anti-inflammatory IL-10 and immuno-modulatory IFNγ and IL-12p70 secretions (Figure 4.3), thus critically creating an imbalance between catabolic and anabolic pathways, possibly through sustained TLR3 activation of FLS in the joint synovium, and these data correlate with previous publications (Brentano et al., 2005, Attur et al., 2010).

4.4.2. Histopathological evaluation of synovial inflammation in grade-specific OA synovial tissue

Given the increasing evidence supporting the potential role of synovial tissue inflammation or synovitis in OA progression (Scanzello et al., 2011, Myers et al., 1990, Benito et al., 2005) and given that inflammatory mediators associated with synovitis, namely, cytokines, chemokines and MMPs aid in OA progression (Smith et al., 1997, Sutton et al., 2009, Wassilew et al., 2010), and given that synovitis is considered a potential predictive factor for structural progression of OA (Ayral et al., 2005), it was critical to evaluate stage/grade-specific OA synovial tissue biopsies to further understand the contribution of synovial tissue inflammation in OA progression. To examine this, a histological assessment with hematoxylin-eosin (H & E) staining of OA grade-specific (grade-0 - grade-4) synovial tissues (n=3/grade) was performed. Patient cohorts, encompassing strict inclusion and exclusion criteria, were recruited as described (Section 4.3.1: Experimental methods) and the baseline subject clinical characteristics are summarised in table 4.1 whereby the OA radiographic (Kellgren and Lawrence, 1957) and arthroscopic classification systems (Ayral et al., 2005)) were employed for grading the disease stage in these patients and are described in detail in table 4.2. A validated semi-quantitative scoring system for synovial

tissue was used wherein the analysis included all areas of the biopsy samples (n=3/grade) (Figure 4.5, panels A, B, C, D, E, F, G, H, I and J), and a global semi-quantitative score was given for each parameter (0-3 scale where 0=lowest expression and 3=highest).

Histological evaluation of the paraffin embedded H & E stained sections included the mean synovial lining layer thickness/hyperplasia (0 = 1-2 cell layers, 1 = 3-4 cell layers, 2 = 5-6 cell layers, and 3 = $\geq$ 7 cell layers), degree of vascularity of the sublining layer, degree of infiltration of the sublining layer with mono-nuclear cells (Figure 4.5, panel K). In cases of discordant scores, which differed by a maximum of 1 point, the mean of the 2 scores was used. Interestingly, the histological assessment revealed that, even at the early stages namely grade-1 and grade-2 OA synovial tissues, a significant trend towards increased thickness of the synovial lining layer and infiltration of inflammatory cells relative to grade-0/trauma controls (grade-1: $p \leq 0.05$, (panels C, D, K); grade-2: $p \leq 0.01$ (panels E, F, K) relative to grade-0 (panels A, B, K)) and this correlates with a previous publication (Benito et al., 2005). Similarly, a significant trend towards increased thickness of the synovial lining layer, degree of vascularity and infiltration of inflammatory cells relative to grade-0 was evident with grade-3 and grade-4 OA synovial tissue sections (grade-3: $p \leq 0.01$, (panels G, H, K); grade-4: $p \leq 0.01$ (panels I, J, K) relative to grade-0 (panels A, B, K)).

Thus, these results indicate that synovitis (typically measured employing these three parameters under study for tissues, and cyto-chemoiknes and MMP levels in the synovial fluid) plays a critical part in progressive joint damage, and if targeted, inhibition of synovitis in early generalised OA may limit the rates of progressive cartilage degradation and functional impairment and may as well aid in early disease diagnosis and there by aid in potential OA treatment (Benito et al., 2005). Synovial tissue analysis is also used in clinical trials (Bresnihan et al., 2005), and is currently being targeted for treating OA (Attur et al., 2010). Thus, it is very critical to understand the stimulus which perpetuates the inflammatory mediators in the synovium ultimately aiding in OA progression.

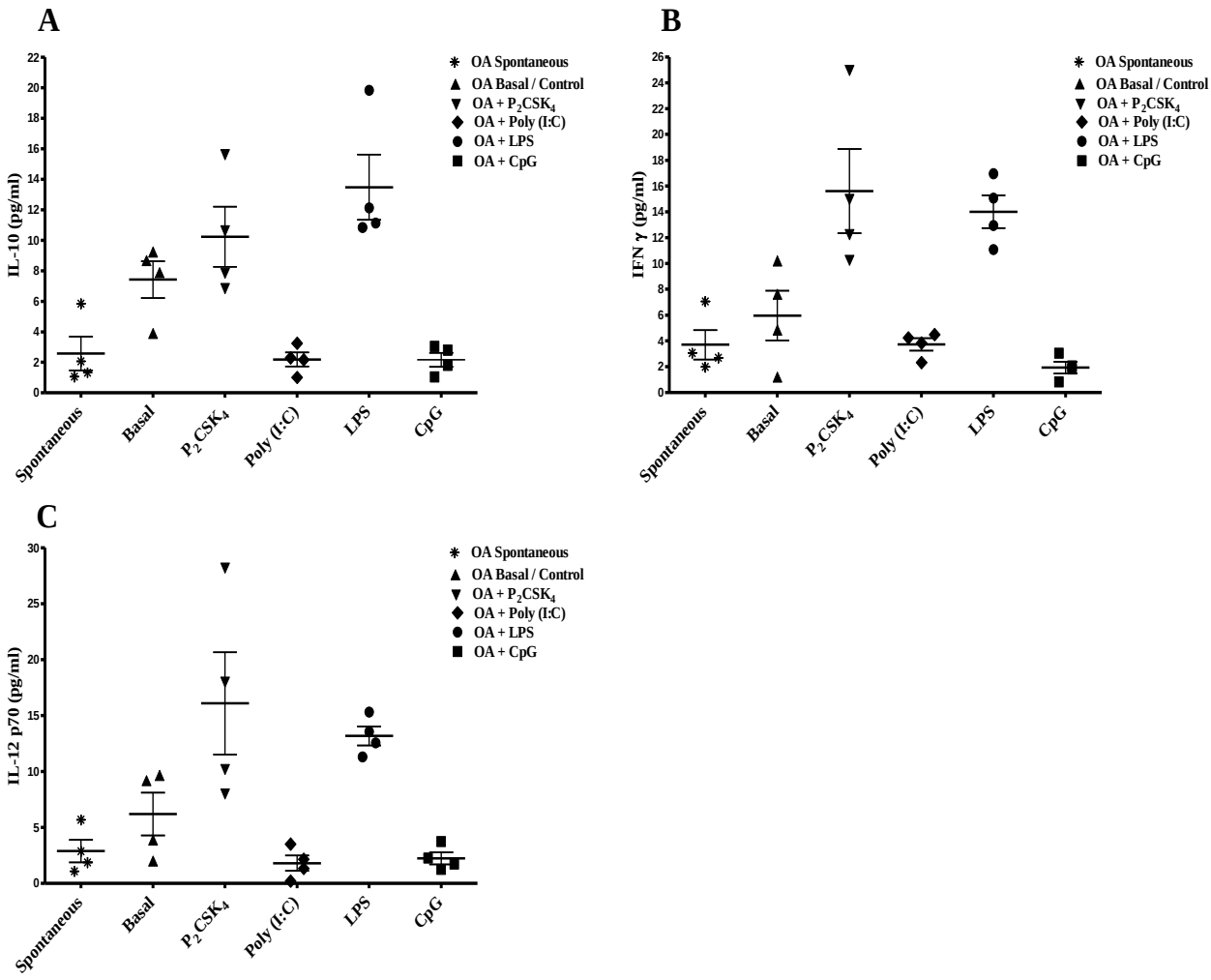

Figure 4.3: Analysis of TLR agonists induced secretion of IL-10, IL-12 p70 and IFNγ cytokines in OA synovial tissue explant cultures. (A-C) Whole OA synovial tissue explants (n=4) were cultured in complete RPMI 1640 medium for 24 h to measure spontaneous cytokine release or treated with Pam_2CSK_4 (1 µg/ml; TLR2 ligand), Poly (I:C) (10 µg/ml; TLR3 ligand), LPS (1 µg/ml; TLR4 ligand), CpG (3 µg/ml; TLR9 ligand) or left unstimulated in serum free RPMI 1640 for 24 h to measure TLR induced and basal protein profiles. The cell-free supernatants were harvested and analyzed for levels of (A) IL-10, (B) IFNγ and (C) IL-12 p70 using MSD ultrasensitive multiplex ELISA System. All the data presented are representative of at least one independent experiment performed in duplicate (mean ± S.E.M). Data was subjected to an unpaired Student's t test. * $p<0.05$, ** $p<0.01$, *** $p<0.001$ denotes the level of significance relative to basal control.

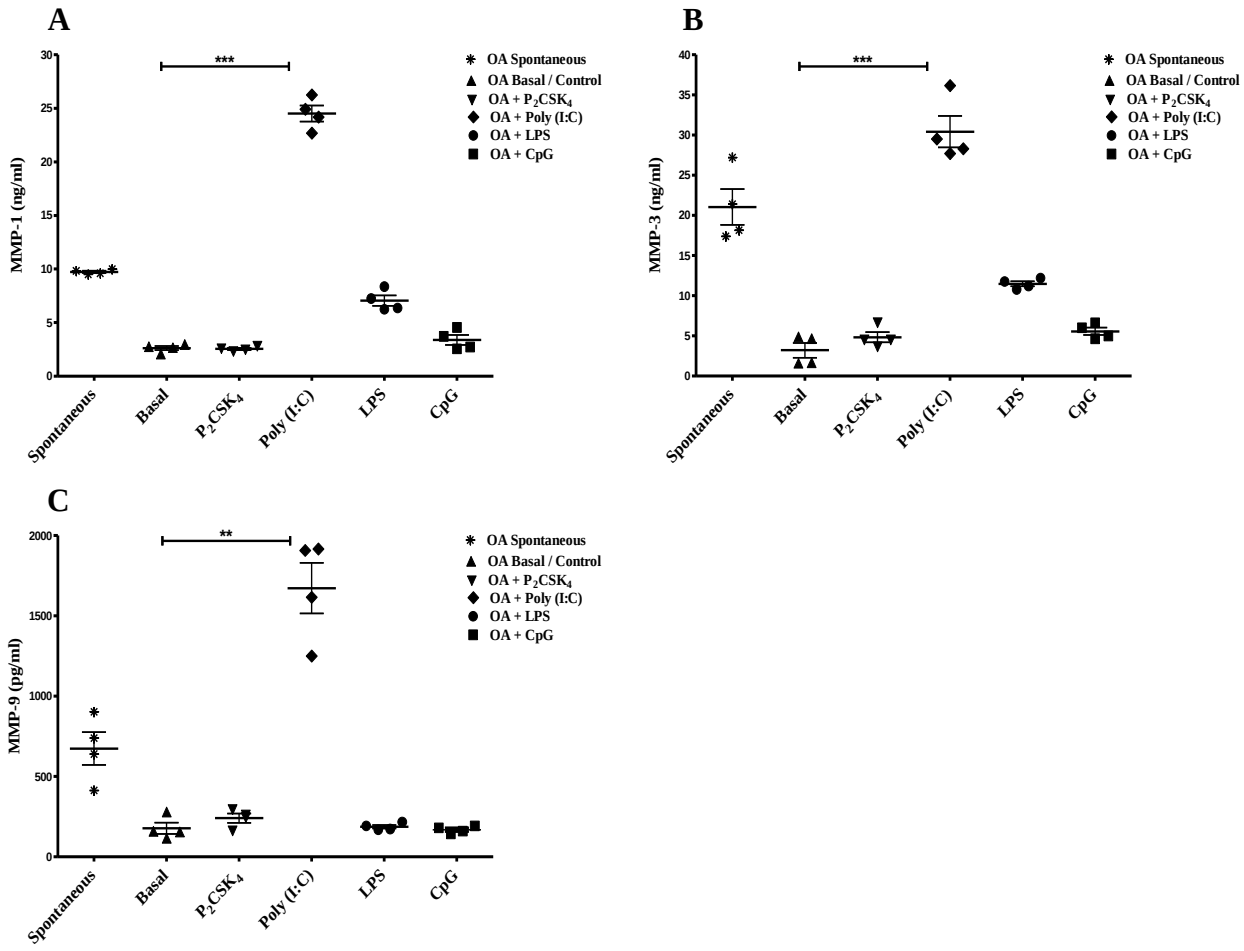

Figure 4.4: Analysis of spontaneous and TLR agonists induced pro-inflammatory MMP-1, -3 and -9 secretion in OA synovial tissue explant cultures. (A-C) Whole OA synovial tissue explants (n=4) were either cultured in complete RPMI 1640 medium for 24 h to measure spontaneous cytokine release or were treated with Pam_2CSK_4 (1 µg/ml; TLR2 ligand), Poly (I:C) (10 µg/ml; TLR3 ligand), LPS (1 µg/ml; TLR4 ligand), CpG (3 µg/ml; TLR9 ligand) or left unstimulated in serum free RPMI 1640 for 24 h to measure TLR induced and basal protein profiles. The cell-free supernatants were harvested and analyzed for levels of (A) MMP-1, (B) MMP-3 and (C) MMP-9 using MSD ultrasensitive multiplex ELISA System. All the data presented are representative of at least one independent experiment performed in duplicate (mean ± S.E.M). Data was subjected to an unpaired Student's t test. * $p<0.05$, ** $p<0.01$, *** $p<0.001$ denotes the level of significance relative to basal control.

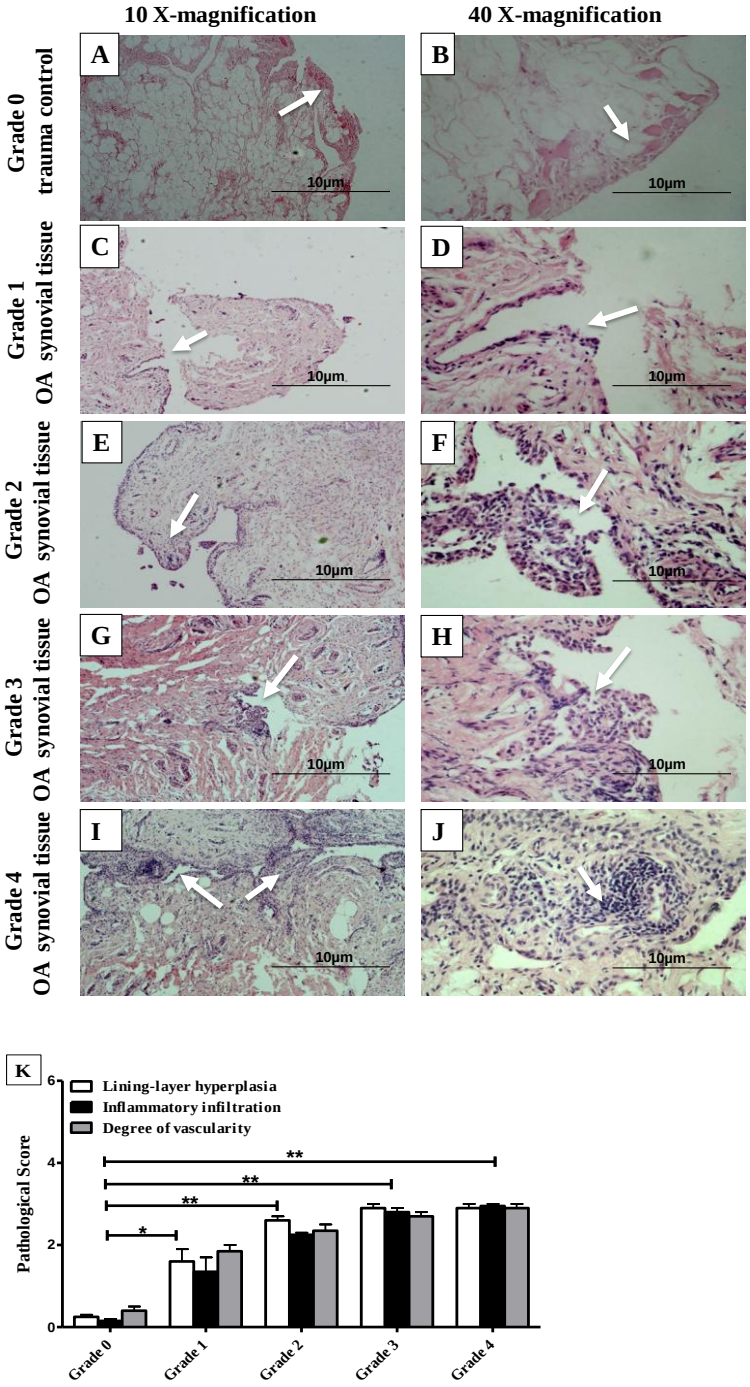

Figure 4.5: Histopathological evaluation of synovial inflammation in grade-specific OA synovial tissue. (A-J) Representative hematoxylin and eosin (H&E)-stained photomicrographs of grade-specific OA synovial tissues (n=3) at 10x and 40x magnification, and arrows indicate lining layer hyperplasia. Shown are H&E stained Grade-0 (A, B), Grade-1 (C,D), Grade-2 (E,F), Grade-3 (G,H) and Grade-4 (I,J) synovial tissues and (K) represents corresponding semi-quantitative score for each of the three characteristic parameters of synovitis as indicated in the figure, in the grade-specific OA synovial tissues (n=3). Data was subjected to an independent Student's t test with Bonferonni correction. * $p<0.05$, ** $p<0.01$ denotes the level of significance relative to Grade-0 or control.

4.4.3. *Ex-vitro* analysis of basal and TLR/RIG-I induced pro and anti-inflammatory cytokines, chemokines and MMPs in early and late OA-patient derived synovial tissue FLS

Given that FLSs are the major effector cell type in the synovium responsible for the production of inflammatory cytokines, chemokines and MMPs in the OA joint (Sutton et al., 2009, Müller-Ladner et al., 2007, Alsaleh et al., 2011) and owing to our previous observations that FLS are activated by exogenous pathogenic stimuli, such as synthetic TLR agonists (Ospelt et al., 2008) and (chapter 3), and to further corroborate our previous observations (chapter 4, section: 4.4.1 and 4.4.2), it was essential to identify the stimulus which distinctively induces the secretion of such pro and anti-inflammatory mediators in stage-specific FLS, thus propagating synovitis in the OA joint.

4.4.3.1. Analysis of TLR/RIG-I agonist induced pro-inflammatory cytokine and chemokine secretion in early and late OA-FLS

Initially, early (Grade 1-2) and late (Grade 3-4) stage OA synovial biopsy derived FLS (n=3/grade), were stimulated with Pam_2CSK_4 (1 µg/ml; TLR2 ligand), Poly(I:C) (10 µg/ml; TLR3 ligand), LPS (1 µg/ml; TLR4 ligand), CLO-97 (1 µg/ml; TLR7/8 ligand), CpG (3 µg/ml; TLR9 ligand) and 5'ppp dsRNA (1 µg/ml; RIG-I ligand) for 24 h or left unstimulated to measure TLR/RIG-I ligand induced IL-6, IL-8, IL-1β and TNF-α levels (Figure 4.6, panel A, B, C and D, n=3). Interestingly, of the TLR ligands utilised in the study, stimulation with Poly(I:C) induced the most significant amounts of IL-6 in both early and late OA-FLSs relative to their respective controls (Poly(I:C) Vs control) (Early: 3287.27 ± 70.01 Vs 228.91 ± 20.10 pg/ml and Late: 4125.72 ± 75.02 Vs 524.71 ± 25 pg/ml, $p \leq 0.01$). Whereas stimulation with LPS induced significant levels of IL-6, though to a lesser extent when compared with Poly (I:C) stimulations (LPS Vs control) (Early: 1125.17 ± 32.5 Vs 228.91 ± 20.10 pg/ml and Late: 2118.28 ± 42.5 Vs 524.71 ± 25 pg/ml, $p \leq 0.05$), other ligands under investigation showed little or no IL-6 induction relative to control (Figure 4.6, panel A). Correspondingly, of the TLR ligands utilised in the study, stimulation with Poly(I:C) induced the highest and most significant levels of IL-8 secretion in both early and late OA-FLSs relative to the respective control (Poly(I:C) Vs control) (Early: 2912.92 ± 40.03 Vs 156.12 ± 30.01 pg/ml and Late: 3994.18 ± 125.02 Vs 477.95 ± 10.01 pg/ml, $p \leq 0.01$). Similarly, stimulation with LPS induced significantly levels of IL-8, but to a lesser extent when compared with Poly (I:C) (LPS Vs control) (Early: 923.05 ± 47.5 Vs 156.12 ± 30.01 pg/ml and Late: 1575.03 ± 37.5 Vs 477.95 ± 10.01 pg/ml pg/ml, p

≤ 0.05). Other ligands under investigation showed little or no IL-8 induction relative to control (Figure 4.6, panel B). Moreover, of the TLR ligands utilised in the study, stimulation with Poly(I:C) also induced the highest and most significant amounts of IL-1β in both early and late OA-FLSs to varying amounts relative to respective controls (Poly(I:C) Vs control) (Early: 22.89 ± 2.01 Vs 1.86 ± 0.50 pg/ml and Late: 31.35 ± 1.02 Vs 4.27 ± 1.50 pg/ml, $p \leq 0.05$). Whereas insignificant levels of IL-1β induction was observed following Pam_2CSK_4 or LPS stimulations, the other ligands under investigation showed little or no IL-1β induction relative to control (Figure 4.6, panel C). Furthermore, stimulation with Poly(I:C) also induced the highest and most significant amounts of TNFα in both early and late OA-FLSs relative to respective controls (Poly(I:C) Vs control) ((Early: 33.48 ± 3.03 Vs 4.74 ± 1.01 pg/ml, $p \leq 0.05$) and (Late: 60.81 ± 2.5 Vs 11.13 ± 0.49 pg/ml, $p \leq 0.01$)). Similarly, stimulation with LPS induced significantly higher levels of TNFα in late, but not early, OA-FLS and the levels were less when compared with Poly (I:C) stimulations (LPS Vs control) (Late: 31.56 ± 1.99 Vs 11.13 ± 0.49 pg/ml pg/ml, $p \leq 0.05$). Other ligands under investigation showed an insignificant level of TNFα induction in late OA-FLS relative to control (Figure 4.6, panel D). Interestingly, the highest and most significant induction of pro-inflammatory IL-6, IL-8, IL-1β and TNFα secretions by early and late OA-FLS was observed upon Poly(I:C) stimulation, and this correlates with our previous findings (Chapter 3, Figure 3.6 and 3.9). Thus, these data suggests a probable role for dsRNA borne activation of synovial FLS in mediating these inflammatory mediators in the synovium, aiding in OA progression.

4.4.3.2. Analysis of TLR/RIG-I agonist induced IFNβ and RANTES secretion in early and late OA-FLS

Given the predominant secretion of IFNβ and RANTES in FLS following stimulation with various stimuli (chapter 3), given the pivotal role of these cyto-chemokines in cartilage degradation (Alaaeddine et al., 2001, Borzì et al., 2004), it was critical to identify the stimulus which distinctively induces such inflammatory mediators in FLS, which further propagates synovitis at different stages of OA progression. Interestingly, of the ligands utilised in the study, stimulation with Poly(I:C) induced the highest and most significant amount of IFNβ in both early and late OA-FLSs relative to respective controls (Poly(I:C) Vs control) (Early: 1389.65 ± 25.01 Vs 152.18 ± 20.0 pg/ml and Late: 1700.66 ± 29.0 Vs 255.95 ± 33.50 pg/ml, $p \leq 0.01$) and similarly stimulation with LPS induced significantly higher levels of IFNβ in both early and late OA-FLSs, but the levels were less when

compared with Poly (I:C) stimulations (LPS Vs control) (Early: 839.85 ± 42.5 Vs 152.18 ± 20.0 pg/ml and Late: 1115.7 ± 62.5 Vs 255.95 ± 33.50 pg/ml, $p \leq 0.05$). Other ligands under investigation showed little or no IFNβ induction relative to control (Figure 4.6, panel A). Correspondingly, of the ligands utilised in the study, stimulation with Poly(I:C) induced highest and most significant amounts of RANTES secretion in both early and late OA-FLSs relative to respective controls (Poly(I:C) Vs control) (Early: 1409.78 ± 25 Vs 123.11 ± 20.01 pg/ml and Late: 2074.18 ± 50.01 Vs 267.09 ± 25.01 pg/ml, $p \leq 0.01$). Similarly, stimulation with LPS induced significantly higher levels of RANTES in late OA-FLS and an insignificant increase in early OA-FLS was evident, however, the levels were less when compared with Poly(I:C) (LPS Vs control) (Early: 467.04 ± 22.5 Vs 123.11 ± 20.01 pg/ml and Late: 956.67 ± 32.5 Vs 267.09 ± 25.01 pg/ml pg/ml, $p \leq 0.05$). Stimulation with CLO-97 also induced significant amounts of RANTES secretion in early, but not late, OA-FLS relative to control (CLO-97 Vs control) (Early: 690.92 ± 22.5 Vs 123.11 ± 20.01 pg/ml ($p \leq 0.05$), and Late: 568.66 ± 32.5 Vs 267.09 ± 25.01 pg/ml pg/ml). Other ligands under investigation showed little or no RANTES induction relative to control (Figure 4.6, panel B). Interestingly, the highest and most significant induction of pro-inflammatory IFNβ and RANTES secretions by early and late OA-FLS was observed upon Poly(I:C) stimulation, and this correlates with our previous findings (Chapter 3, Figure 3.6 and 3.8). These data suggest that RNA borne activation of synovial FLS mediates the induction of these potent mediators, even at the very early stages of OA disease onset in the synovium, which ultimately leads to arthritis progression.

4.4.3.3. Analysis of TLR/RIG-I agonist induced IL-10, IL-12 p70 and IFNγ secretion in early and late OA-FLS

Given the previous observation that TLR ligands induce an imbalance in the levels of pro vs anti-inflammatory mediators in the whole OA synovial tissue explants *ex-vivo* (Figures 4.1, 4.2 and 4.3), it was essential to investigate the effect of TLR ligands in inducing/suppressing the key immunomodulatory cytokines namely IL-12 p70 and IFNγ and anti-inflammatory IL-10 in stage/grade-specific OA-FLS, towards further understanding the stimulus and the role of activated FLS at the various stages of OA progression (Figure 4.8, panels A, B and C, n=3). Interestingly, upon stimulation with Poly (I:C), a significant decrease in IL-10, IFNγ and IL-12p70 levels relative to basal was evident in early OA-FLS ($p \leq 0.05$). In late OA-FLS, a similar significant decrease in IL-10 levels was evident ($p \leq 0.05$), and a non-significant decrease in IFNγ and IL-12p70

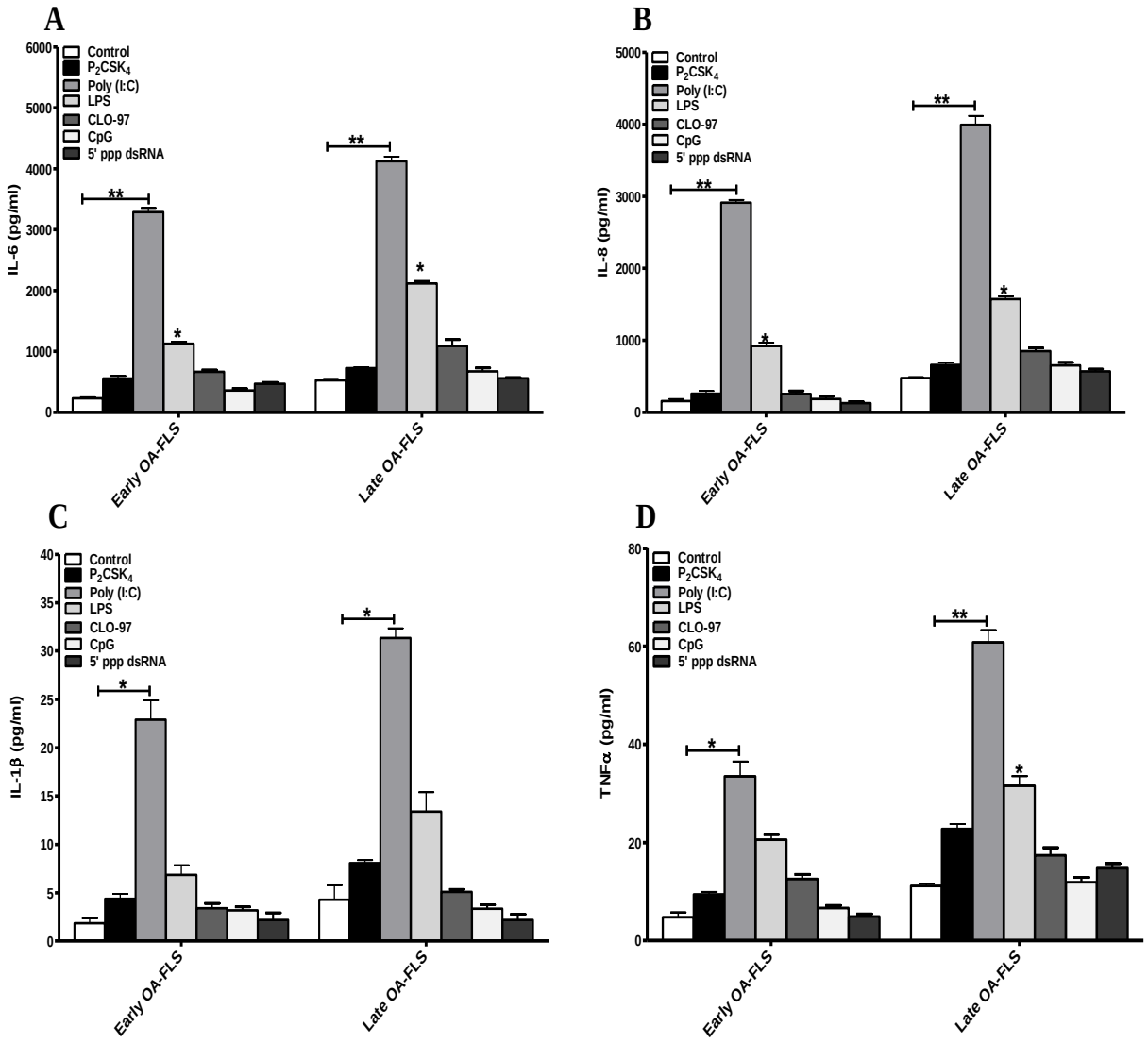

Figure 4.6: Analysis of TLR/RIG-I agonist induced pro-inflammatory cytokine and chemokine secretion in early and late OA-FLS. (A-D) Early (Grade 1-2) and Late (Grade 3-4) stage OA synovial biopsy derived FLS (n=3), were treated with Pam_2CSK_4 (1 µg/ml; TLR2 ligand), Poly(I:C) (10 µg/ml; TLR3 ligand), LPS (1 µg/ml; TLR4 ligand), CLO-97 (1 µg/ml; TLR7/8 ligand), CpG (3 µg/ml; TLR9 ligand) and 5'ppp dsRNA (1 µg/ml; RIG-I ligand) for 24 h. Cell free supernatants were analyzed for (A) IL-6, (B) IL-8, (C) IL-1β, (D) TNFα by ELISA. All the data presented are representative of at least two independent experiments performed in duplicate (mean ± S.E.M). Data was subjected to an unpaired Student's t test. * $p<0.05$, ** $p<0.01$ denotes the level of significance relative to respective cell type control.

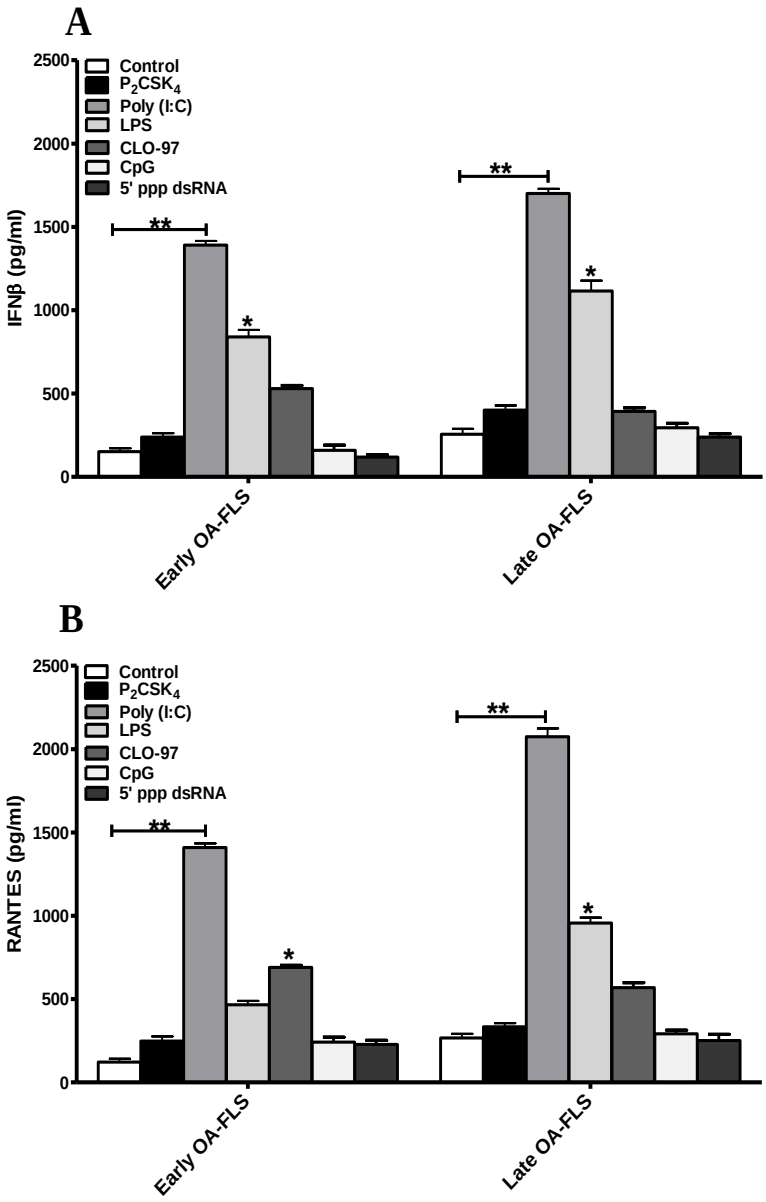

Figure 4.7: Analysis of TLR/RIG-I agonist induced IFNβ and RANTES secretion in early and late OA-FLS. (A-B) Early (Grade 1-2) and Late (Grade 3-4) stage OA synovial biopsy derived FLS (n=3), were treated with Pam_2CSK_4 (1 µg/ml; TLR2 ligand), Poly(I:C) (10 µg/ml; TLR3 ligand), LPS (1 µg/ml; TLR4 ligand), CLO-97 (1 µg/ml; TLR7/8 ligand), CpG (3 µg/ml; TLR9 ligand) and 5' ppp dsRNA (1 µg/ml; RIG-I ligand) for 24 h. Cell free supernatants were analyzed for (A) IFNβ and (B) RANTES by ELISA. All the data presented are representative of at least two independent experiments performed in duplicate (mean ± S.E.M). Data was subjected to an unpaired Student's t test. * $p<0.05$, ** $p<0.01$ denotes the level of significance relative to respective cell type control.

levels relative to basal was observed upon Poly(I:C) stimulation in late OA-FLS (Figure 4.8, panels A, B and C). Moreover, a similar trend towards decreased IL-10, IFNγ and IL-12p70 levels relative to basal was evident following CpG and 5'ppp dsRNA stimulation. Stimulation with Pam_2CSK_4, LPS or CLO-97 induced a notable increase in IL-10, IFNγ and IL-12p70 levels relative to basal in both early and late OA-FLS (Figure 4.3, panel A, B and C). Thus, we found that levels of the Th1 cytokines, IL-12p70 and IFNγ and Th2 cytokine, IL-10 are distinctively suppressed in Poly (I:C) stimulated early and late OA-FLS, and this correlates with our previous observation in OA synovial tissue explants (Figure 4.3). This finding may be attributed to the increased levels of IFNβ in the joint (Figure 4.7, panel A), whereby we propose that FLS encounter RNA from necrotic cells in the joint or viral dsRNA which leads to persistent activation of TLR3 in the synovial FLS, thereby inducing excess IFNβ. The secreted IFNβ immunomodulates the Th1/Th2 cytokine profile by attenuating the secretion of IFNγ and IL-12p70 secretion as previously reported (Sellner et al., 2008). Regarding IL-10, a key Th2 cytokine with anti-inflammatory properties, a significant decrease in IL-10 levels was evident in both early and late OA-FLS upon Poly (I:C) stimulation, suggesting an RNA borne early and sustained impairment of anti-inflammatory mechanism in the joint synovium. Also, studies have shown a mutual antagonism between IFNγ and TNFα levels in FLS, wherein, paradoxical induction of IFNγ and TNFα expression was observed in FLS (Alvaro-Gracia et al., 1993, Alvaro-Gracia et al., 1990). This might further explain the decreased levels of IFNγ upon Poly (I:C) stimulation, as an increased amount of TNFα levels was evident in both early and late OA-FLS (Figure 4.6, panel D) and as well in OA synovial tissue explants (Figure 4.1, panel D), upon Poly (I:C) stimulation.

4.4.3.4. Analysis of TLR/RIG-I agonist induced pro-inflammatory MMP-1, -3 and -9 secretion in early and late OA-FLS

Given the differential induction of MMPs by TLR ligands in the whole synovial tissue explant cultures (Figure 4.4), and previous studies showing that MMPs 1, 3 and 9 play a vital role in OA pathogenesis (Sutton et al., 2009, Firestein, 1996, Scanzello et al., 2011, Wassilew et al., 2010), it was critical to investigate whether these MMPs may be induced in a TLR ligand dependent manner by the stage-specific FLS in the synovium. Interestingly, of the ligands utilised in the study, stimulation with Poly(I:C) induced the highest and most significant amounts of MMP-1 secretion in both early and late OA-FLSs

relative to respective controls (Poly(I:C) Vs control) (Early: 13.21 ± 0.90 Vs 1.71 ± 0.56 ng/ml ($p \leq 0.05$) and Late: 20.47 ± 0.57 Vs 2.91 ± 0.42 ng/ml ($p \leq 0.01$)). Similarly, stimulation with LPS induced significantly higher levels of IFNβ in late OA-FLSs, but the lower when compared with Poly (I:C) stimulations. Other ligands under investigation showed little or no MMP-1 induction relative to control (Figure 4.9, panel A). Correspondingly, of the ligands utilised in the study, stimulation with Poly(I:C) induced the highest and most significant amounts of MMP-3 secretion in both early and late OA-FLSs relative to respective controls (Poly(I:C) Vs control) (Early: 16.91 ± 0.25 Vs 2.4 ± 0.44 ng/ml and Late: 21.88 ± 0.32 Vs 3.84 ± 0.42 ng/ml, $p \leq 0.01$). Similarly, stimulation with LPS induced significantly higher levels of MMP-3 in both early and late OA-FLS, but the levels were less when compared with Poly(I:C) stimulations (LPS Vs control) (Early: 9.44 ± 0.45 Vs 2.4 ± 0.44 ng/ml and Late: 10.57 ± 0.47 Vs 3.84 ± 0.42 ng/ml pg/ml, $p \leq 0.05$). Other ligands under investigation showed little or no MMP-3 induction relative to control (Figure 4.9, panel B). Similarly, stimulation with Poly(I:C) also induced significant amounts of MMP-9 secretion in both early and late OA-FLS relative to control (Poly(I:C) Vs control) (Early: 762.43 ± 25 Vs 88.81 ± 7.5 pg/ml and Late: 919.82 ± 65 Vs 141.96 ± 20 pg/ml $p \leq 0.05$). Other ligands under investigation showed little or no MMP-9 induction relative to control (Figure 4.9, panel C). Thus, it is clear that Poly(I:C) predominantly induces secretion of the catabolic MMP 1, 3 and 9 in early and late OA-FLS (Figure 4.9) and in whole OA synovial tissue explants (Figure 4.4). This substantiates our previous observations that these MMPs can be induced, particularly by Poly (I:C), which exclusively employs TLR3 in OA-FLS (Chapter 3, Figure 3.2, 3.14 and 3.15), thus making TLR3 a critical target for OA disease intervention. These data suggest that RNA borne activation of synovial FLS mediates the induction of these catabolic mediators, even at the very early stages of OA disease onset in the synovium, which ultimately leads to arthritis progression.

Together, these data provide evidence that even at early stages of OA on-set, the FLS may be activated specifically by TLR ligands, chiefly through viral RNA or bacterial LPS, or even DAMPs such as necrotic cell RNA, which in turn, induces the recurrent secretion of inflammatory mediators and suppression of immune-modulatory and anti-inflammatory molecules, which may aid in perpetuating synovitis, joint destruction and end-stage OA. Interestingly, the present data indicates that Poly (I:C) / dsRNA / RNA from necrotic cells may drive the inflammatory locale in the joint during synovitis by inducing inflammatory

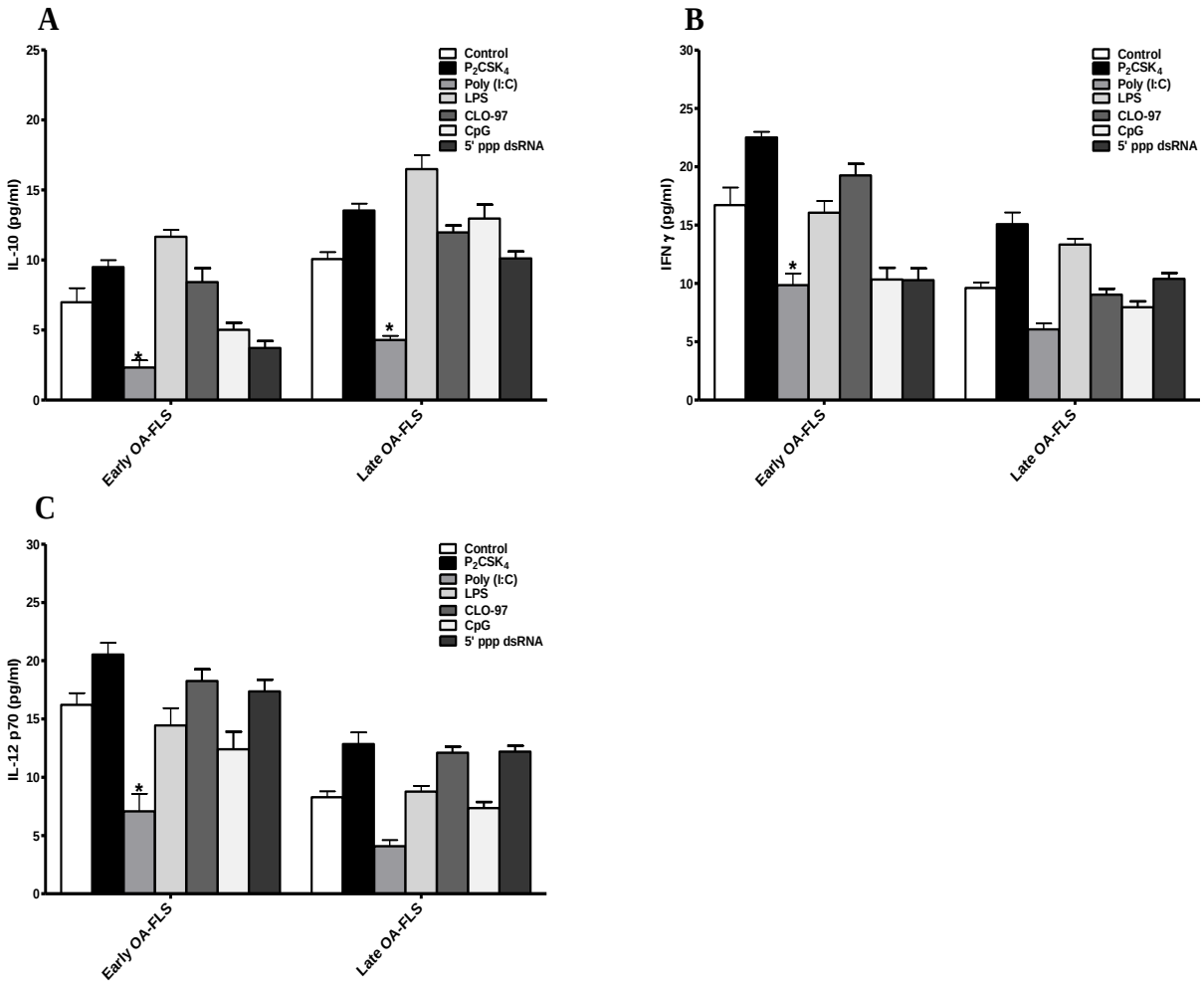

Figure 4.8: Analysis of TLR/RIG-I agonist induced IL-10, IL-12 p70 and IFNγ secretion in early and late OA-FLS. (A-C) Early (Grade 1-2) and Late (Grade 3-4) stage OA synovial biopsy derived FLS (n=3), were treated with Pam_2CSK_4 (1 µg/ml; TLR2 ligand), Poly(I:C) (10 µg/ml; TLR3 ligand), LPS (1 µg/ml; TLR4 ligand), CLO-97 (1 µg/ml; TLR7/8 ligand), CpG (3 µg/ml; TLR9 ligand) and 5'ppp dsRNA (1 µg/ml; RIG-I ligand) for 24 h. Cell free supernatants were analyzed for (A) IL-10, (B) IFNγ and (C) IL-12 p70 by ELISA. All the data presented are representative of at least two independent experiments performed in duplicate (mean ± S.E.M). Data was subjected to an unpaired Student's t test. * $p<0.05$ denotes the level of significance relative to respective cell type control.

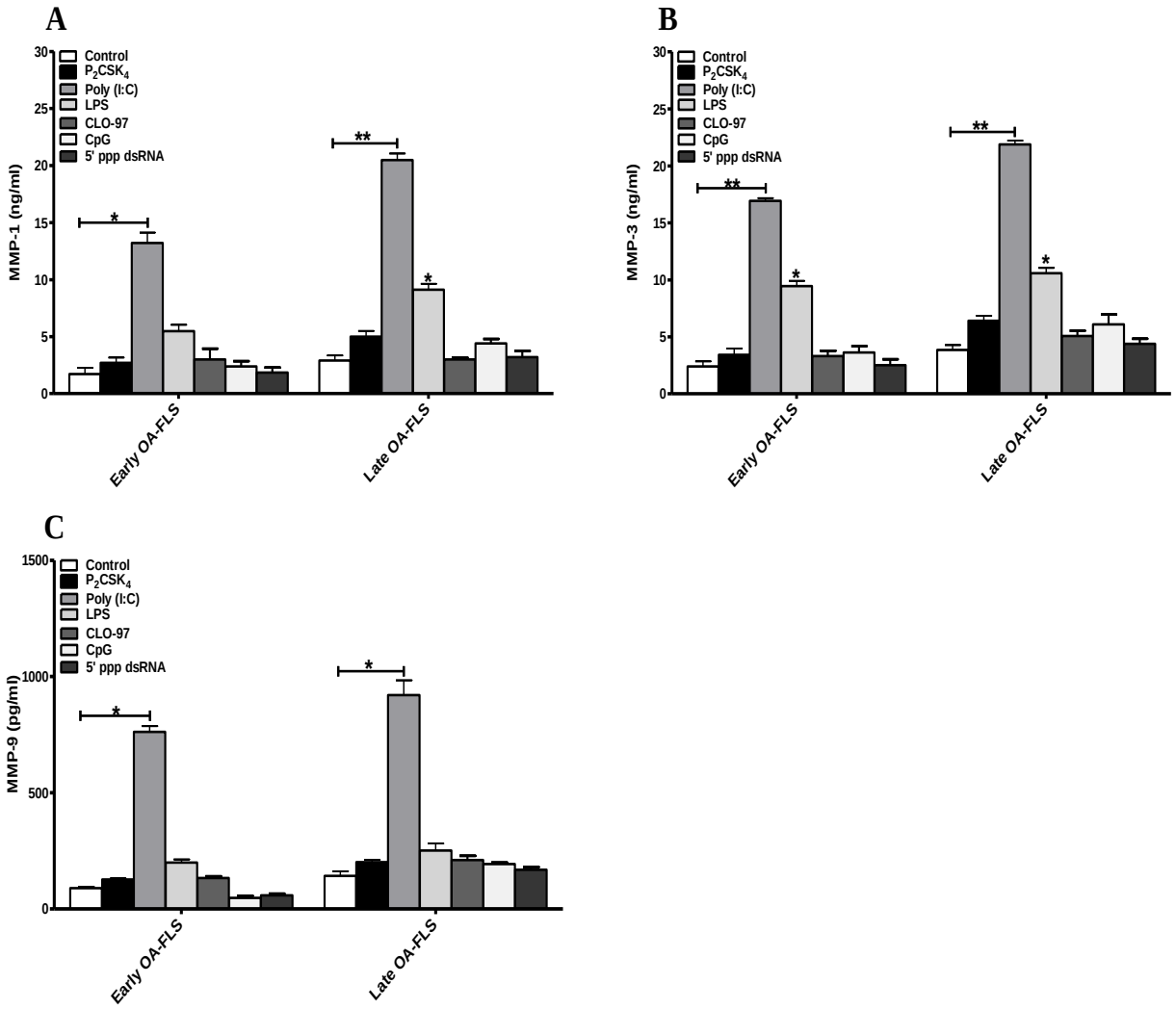

Figure 4.9: Analysis of TLR/RIG-I agonist induced pro-inflammatory MMP-1, -3 and -9 secretion in early and late OA-FLS. (A-C) Early (Grade 1-2) and Late (Grade 3-4) stage OA synovial biopsy derived FLS (n=3), were treated with Pam_2CSK_4 (1 µg/ml; TLR2 ligand), Poly(I:C) (10 µg/ml; TLR3 ligand), LPS (1 µg/ml; TLR4 ligand), CLO-97 (1 µg/ml; TLR7/8 ligand), CpG (3 µg/ml; TLR9 ligand) and 5' ppp dsRNA (1 µg/ml; RIG-I ligand) for 24 h. Cell free supernatants were analyzed for (A) MMP-1, (B) MMP-3 and (C) MMP-9 by ELISA. All the data presented are representative of at least two independent experiments performed in duplicate (mean ± S.E.M). Data was subjected to an unpaired Student's t test. * $p<0.05$, ** $p<0.01$ denotes the level of significance relative to respective cell type control.

IL-6, IL-8, IL-1β and TNFα (Figure 4.6), IFNβ and RANTES (Figure 4.7), MMP-1, 3 and 9 (Figure 4.9) and by suppression of anti-inflammatory IL-10 and immuno-modulatory IFNγ and IL-12p70 secretions (Figure 4.8). These data also suggest that primarily TLR3, rather than TLR7 or TLR9 or RLRs, might play a key role in modulating OA by inducing pro-inflammatory cytokine, chemokine and MMP cascades in FLSs even at the very early stages of the disease on-set, as suggested previously (McCormack et al., 2009, Zhu et al., 2011b, Zhu et al., 2011a). The cytokine, chemokine and MMP cascades may work both in an autocrine and a paracrine fashion and may serve to perpetuate synovial inflammation, ultimately leading to joint destruction and OA progression (McGettrick and O'Neill, 2010, Roelofs et al., 2008). Thus, critically creating an imbalance between catabolic and anabolic pathways, possibly through sustained TLR3 activation of FLS in the joint synovium may facilitate OA disease progression, and this correlates with previous publications (Brentano et al., 2005, Attur et al., 2010).

4.4.4. *In-vitro* analysis of pro and anti-inflammatory cytokines, chemokines and MMPs in grade-specific OA-patient derived cell-free synovial fluid

To better understand how inflammatory cell populations at various stages of OA progression as observed in (Figure 4.4.2) relate to the pattern of cyto-chemokine and MMP production in the joint, a comparative analysis of the levels of these mediators in cell-free grade-specific OA synovial fluid (OA-SF) was investigated. This study is the first of its kind, as much of what is known about the inflammatory response in the synovial membrane and synovial fluid of OA patients comes from studies of end-stage OA (Benito et al., 2005, Ayral et al., 2005, Sutton et al., 2009, Wassilew et al., 2010, Kapoor et al., 2011). In this study, we sought to characterise and quantify the pro- and anti-inflammatory mediators in grade-specific OA-SFs using well characterised SF from early and progressive stages of knee OA and appropriate control SF.

4.4.4.1. Analysis of pro-inflammatory cyto-chemokines in grade-specific OA synovial fluid

Given the increasing evidence that synovitis plays a critical role in OA pathogenesis through the induction of pro-inflammatory cyto-chemokine networks (Fernandes et al., 2002, Kapoor et al., 2011), it was essential to quantify the levels of key pro-inflammatory cyto-chemokines namely IL-1β, TNFα, IL-6, and IL-8 previously attributed with the pathophysiology of OA (Kapoor et al., 2011, Scanzello et al., 2009, Sutton et al., 2009), in

various cell-free grade-specific OA-SFs. Interestingly, a trend towards increased IL-1β, TNFα, IL-6, and IL-8 was evident in the OA-SF, as the pathology progressed from grade-0 to grade-4 (Figure 4.10, panels A, B, C and D). It was found that the highest and most significant levels of IL-1β relative to grade-0/healthy controls were present in grade-4 OA-SF followed by that present in grade-3 OA-SF (grade-3: 2.5 ± 0.31 pg/ml ($p \leq 0.05$) and grade-4: 3.33 ± 0.29 pg/ml ($p \leq 0.01$), from basal/grade-0: 0.3 ± 0.15 pg/ml). A notable, but non-significant, increase in IL-1β levels relative to grade-0/healthy controls was evident in grade-1 and grade-2 OA-SFs (Figure 4.10, panel A). Similarly, the most significant levels of TNFα relative to grade-0/healthy controls was evident primarily in grade-4 and grade-3 OA-SFs (grade-3: 3.04 ± 0.70 pg/ml ($p \leq 0.05$) and grade-4: 7.55 ± 0.76 pg/ml ($p \leq 0.01$), from basal/grade-0: 0.92 ± 0.16 pg/ml). A notable, though non-significant, increase in TNFα levels relative to grade-0/healthy controls was evident primarily in grade-2 and then in grade-1 OA-SFs (Figure 4.10, panel B). Moreover, the most significant levels of IL-6 relative to grade-0/healthy controls was evident primarily in grade-4, followed by grade-3, then grade-2 OA-SFs (grade-2: 278.2 ± 36.76 pg/ml ($p \leq 0.05$), grade-3: 1706 ± 367.7 pg/ml ($p \leq 0.01$), and grade-4: 2779 ± 485.3 pg/ml ($p \leq 0.001$), from basal/grade-0: 48.32 ± 8.35 pg/ml).

A notable, though non-significant, increase in IL-6 levels relative to grade-0/healthy controls was evident in grade-1 OA-SF (Figure 4.10, panel C). Likewise, the most significant levels of IL-8 relative to grade-0/healthy controls was evident primarily in grade-4, then in grade-3 and later in grade-2 OA-SFs (grade-2: 30.74 ± 3.26 pg/ml ($p \leq 0.05$), grade-3: 107.8 ± 15.49 pg/ml ($p \leq 0.01$), and grade-4: 188.4 ± 25.32 pg/ml ($p \leq 0.001$), from basal/grade-0: 9.20 ± 2.66 pg/ml). A notable, though non-significant, increase in IL-8 levels relative to grade-0/healthy controls was evident in grade-1 OA-SF (Figure 4.10, panel D). Thus, significant levels of pro-inflammatory IL-6, IL-8, IL-1β and TNFα in grade-2, -3 and -4 OA-SFs might correlate with the inflammatory cell infiltrates and synovial hyperplasia previously observed (see Figure 4.4.2) and these data correlate with previous publications (Scanzello et al., 2009, Sakkas et al., 1998).

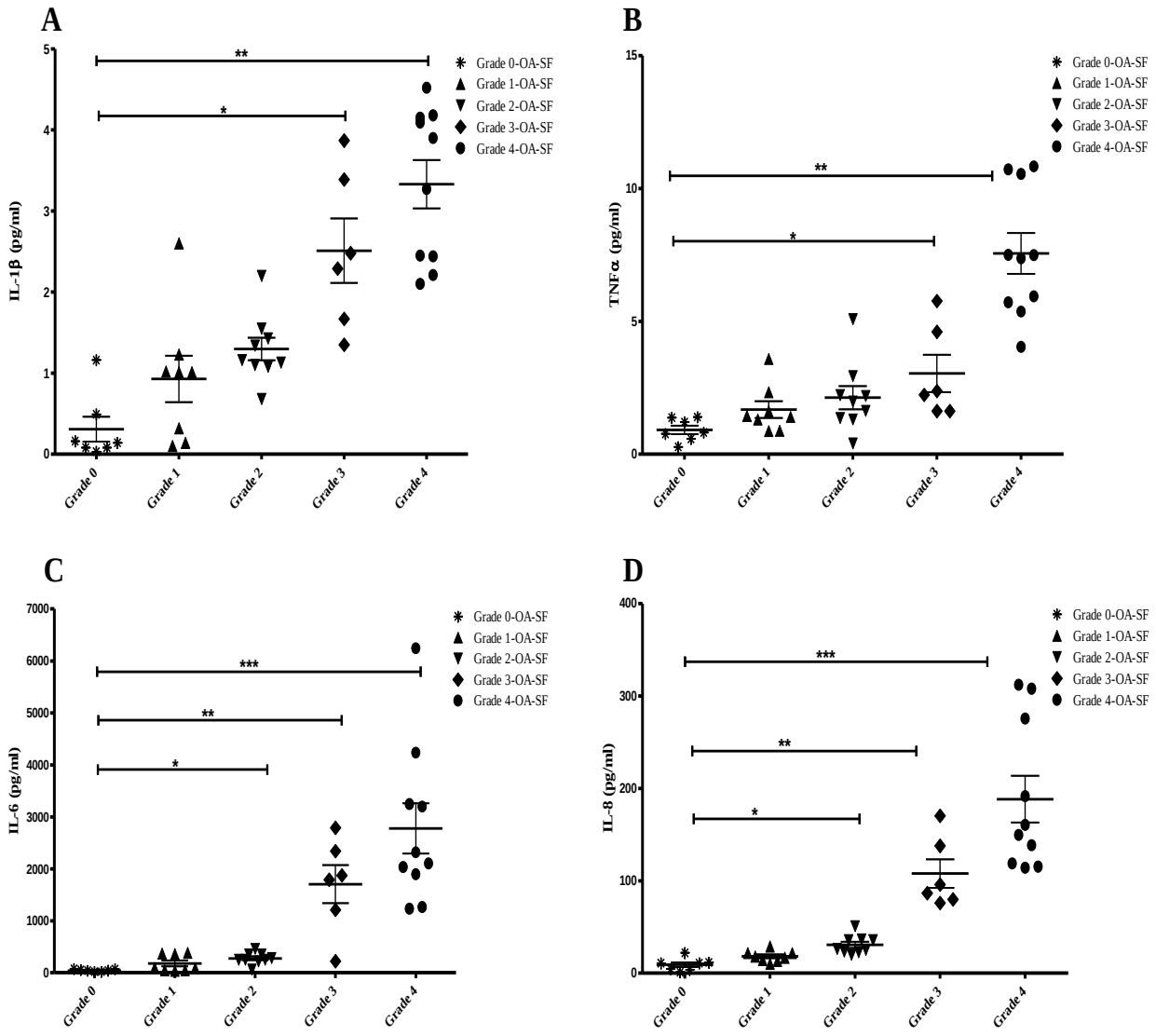

Figure 4.10: Analysis of pro-inflammatory cyto-chemokines in grade-specific OA synovial fluid. (A-D) Cell-free grade-specific OA-SFs: grade-0 (healthy controls, n=7), grade-1 (n=8), grade-2 (n=9), grade-3 (n=6), and grade-4 (end stage OA, n=10), were analyzed for (A) IL-1β, (B) TNFα, (C) IL-6, (D) IL-8, using ultrasensitive MSD multiplex ELISA system. All the data presented are representative of at least one independent experiment performed in duplicate (mean ± S.E.M). Data was subjected to a one-way analysis of variance using a post hoc Student's Newman-Keuls test. * $p<0.05$, ** $p<0.01$, *** $p<0.001$ denotes the level of significance relative to grade-0 or healthy controls.

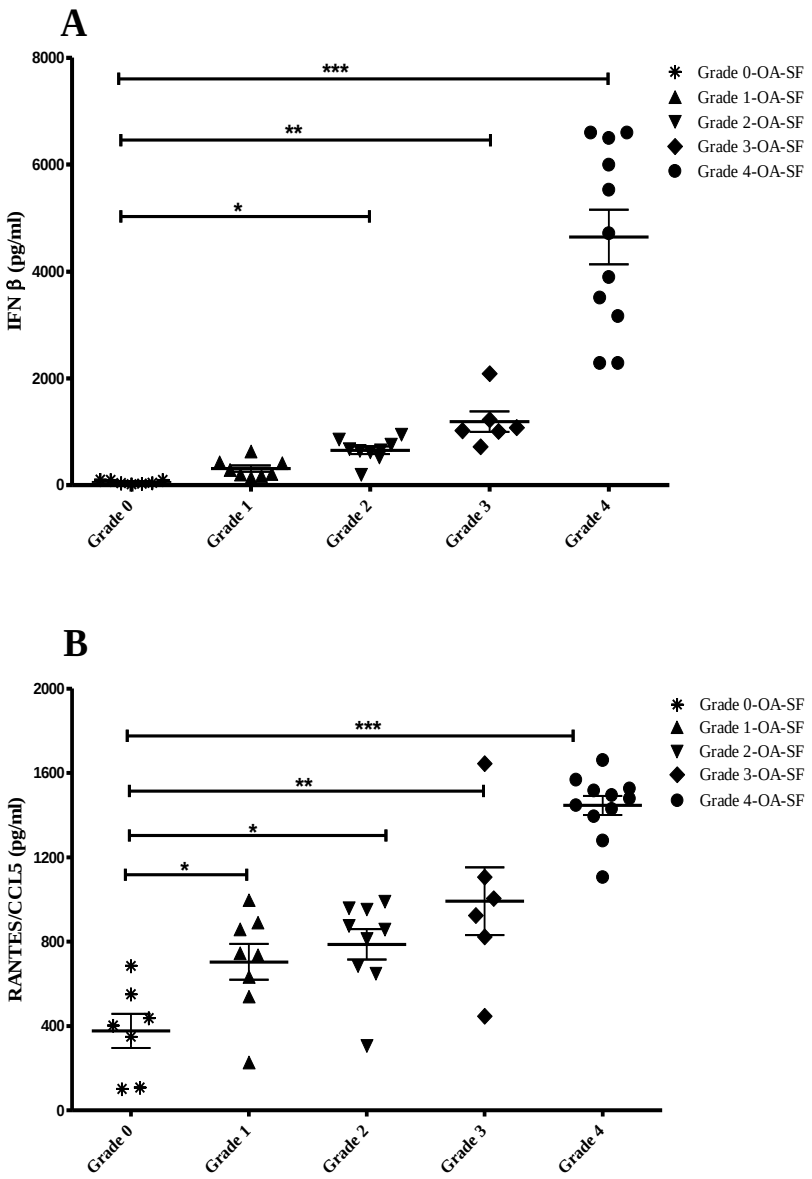

Figure 4.11: Analysis of IFNβ and RANTES levels in grade-specific OA synovial fluid. (A-B) Cell-free grade-specific OA-SFs: grade-0 (healthy controls, n=7), grade-1 (n=8), grade-2 (n=9), grade-3 (n=6), and grade-4 (end stage OA, n=10), were analyzed for (A) IFNβ and (B) RANTES by ultrasensitive MSD ELISA system. All the data presented are representative of at least one independent experiment performed in duplicate (mean ± S.E.M). Data was subjected to a one-way analysis of variance using a post hoc Student's Newman-Keuls test. * $p<0.05$, ** $p<0.01$, *** $p<0.001$ denotes the level of significance relative to grade-0 or healthy controls.

4.4.4.2. Analysis of IFNβ and RANTES levels in grade-specific OA synovial fluid

Given that secretion of IFNβ and RANTES predominates in both early and late OA-FLS and in whole synovial tissue explants following exposure to various stimuli (Figure 4.2 and 4.7), and given the pivotal role of these cyto-chemokines in cartilage degradation (Alaaeddine et al., 2001, Borzì et al., 2004), it was critical to quantify such inflammatory mediators in OA-SFs at different stages of OA progression, as a measure of synovitis and joint destruction. Interestingly, a trend towards increased IFNβ and RANTES levels was evident with the progressive OA-grades (Figure 4.11, panels A and B). It was found that the highest most significant IFNβ levels relative to grade-0/healthy controls was evident primarily in grade-4, then in grade-3 and later in grade-2 OA-SFs (grade-2: 655 ±71.31 pg/ml ($p \leq 0.05$), grade-3: 1193 ± 191.7 pg/ml ($p \leq 0.01$) and grade-4: 4646 ± 511.9 pg/ml ($p \leq 0.001$), from basal/grade-0: 64.65 ± 13.81 pg/ml), whereas a notable but non-significant increase in IFNβ levels relative to grade-0/healthy controls was evident in grade-1 OA-SFs (Figure 4.11, panel A). Similarly, the highest levels of RANTES relative to grade-0/healthy controls was evident primarily in grade-4, followed on by grade-3, grade-2 and grade-1 OA-SFs (grade-1: 703.8 ± 85.07 pg/ml ($p \leq 0.05$), grade-2: 787.5 ± 71.90 pg/ml ($p \leq 0.05$), grade-3: 991.6 ± 160.1 pg/ml ($p \leq 0.01$) and grade-4: 1446 ± 44.95 pg/ml ($p \leq 0.001$), from basal/grade-0: 0.92 ± 0.16 pg/ml). Herein, all the grades of OA-SFs under investigation exhibited a significant increase in RANTES levels relative to grade-0/healthy controls (Figure 4.11, panel B). As the highest and most significant induction of pro-inflammatory IFNβ and RANTES secretions by early and late OA-FLS was observed upon Poly(I:C) stimulation (Figure 4.7), the increased levels of IFNβ and RANTES in grade-specific OA-SFs might signify a probable role for RNA borne activation of synovial FLS in inducing these potent mediators even at the very early stages of OA disease on-set in the synovium downstream OA progression.

4.4.4.3. Analysis of IL-10, IL-12 p70 and IFNγ levels in grade-specific OA synovial fluid

Given that imbalances in the levels of pro vs anti-inflammatory mediators in the joint may aid in synovitis and OA progression (Benito et al., 2005, Brigitte, 2002, Martel-Pelletier et al., 1999, Kapoor et al., 2011, Sutton et al., 2009, Scanzello et al., 2011), and having observed the effect of TLR ligands in suppressing the key immuno-modulatory cytokines namely IL-12 p70 and IFNγ and the anti-inflammatory cytokine, IL-10, in OA synovial

tissue explants (Figure 4.3 and 4.8), it was essential to quantify the levels of such regulatory molecules in grade-specific OA-SFs, to better understand their role in OA progression. Interestingly, a trend towards decreased IL-10, IL-12p70 and IFNγ levels was evident with the progressive OA-grades (Figure 4.12, panels A, B and C). It was found that significantly less IL-10 relative to grade-0/healthy controls was evident even at early stages of OA progression namely grade-1 and grade-2 OA-SFs and, similarly, significantly less IL-10 was evident in grade-3 and grade-4 OA-SFs (grade-1: 2.12 ± 0.39 pg/ml, grade-2: 2.02 ± 0.29 pg/ml, grade-3: 2.00 ± 0.41 pg/ml and grade-4: 2.78 ± 0.36 pg/ml from basal/grade-0: 6.31 ± 0.9 pg/ml, $p \leq 0.05$) (Figure 4.12, panel A). Similarly, significantly less IL-12p70 relative to grade-0/healthy controls was evident even at early stages of OA progression namely grade-1 and grade-2 OA-SFs and, similarly, decreased levels of IL-12p70 was evident in grade-3 and grade-4 OA-SFs (grade-1: 0.10 ± 0.009 pg/ml, grade-2: 0.11 ± 0.03 pg/ml, grade-3: 0.04 ± 0.01 pg/ml and grade-4: 0.05 ± 0.01 pg/ml from basal/grade-0: 4.01 ± 0.14 pg/ml, $p \leq 0.05$) (Figure 4.12, panel B). Moreover, the highest and significantly less IFNγ relative to grade-0/healthy controls was evident primarily in grade-4 and then in grade-3 OA-SFs (grade-3: 1.12 ± 0.35 pg/ml ($p \leq 0.05$) and grade-4: 0.55 ± 0.09 pg/ml ($p \leq 0.01$) from basal/grade-0: 4.97 ± 0.33 pg/ml), though notable, but non-significant less levels of IFNγ relative to grade-0/healthy controls was evident primarily in grade-2 and then in grade-1 OA-SFs (Figure 4.12, panel C).

Thus, the significant suppression of immuno-regulatory molecules in progressive OA grades might signify an early and sustained impairment of anti-inflammatory mechanisms in the joint. This may also be attributed to the increased levels of IFNβ in the joint during disease process or with an encounter with the RNA from necrotic cells in the joint or Poly (I:C) stimulation as previously observed (Figure 4.2 and 4.7, panel A), thus constantly activating TLR3 of FLS in the synovium, thereby inducing excess IFNβ secretions into adjacent synovial fluid, wherein, IFNβ has been shown to immunomodulate the Th1/Th2 cytokine profile by attenuating the secretion of IFNγ, IL-12p70 and IL-10 (Sellner et al., 2008). Further, the trend towards decreased levels of IFNγ, IL-12p70 and IL-10 measured in progressive OA-grades might correlate with the inflammatory cell infiltrates and synovial hyperplasia previously observed (Figure 4.4.2); these data correlate, at least in part, with previous publications (Scanzello et al., 2009, Sakkas et al., 1998). Moreover, studies have shown a mutual antagonism between IFNγ and TNFα levels in FLS, wherein, paradoxical induction of IFNγ and TNFα expression was observed in FLS (Alvaro-Gracia

et al., 1993, Alvaro-Gracia et al., 1990). This correlates with the increased levels of TNFα observed in progressive grades of OA-SFs as observed in (Figure 4.10, panel B).

4.4.4.4. Analysis of MMP-1, MMP-3 and MMP-9 levels in grade-specific OA synovial fluid

Given the pivotal role of MMPs 1, 3 and 9 in OA pathogenesis (Sutton et al., 2009, Firestein, 1996, Scanzello et al., 2011, Wassilew et al., 2010), and having observed the differential induction of these MMPs by TLR ligands in the whole OA synovial tissue explant cultures (Figure 4.4) and in both early and late OA-FLS (Figure 4.9), it was critical to investigate the levels of such key MMPs in the grade-specific OA-SFs to further understand their contribution to various stages of OA progression. Interestingly, a trend towards increased MMP-1, 3 and 9 levels in varying amounts was evident with progressive OA-grades (Figure 4.13, panels A, B and C). It was found that the highest levels of MMP-1 relative to grade-0/healthy controls was present in grade-4, followed by grade-3, grade-2 and grade-1 OA-SFs (grade-1: 539.8 ±75.93 ng/ml ($p \leq 0.05$), grade-2: 578.5 ± 64.17 ng/ml ($p \leq 0.05$), grade-3: 668.4 ± 76.54 ng/ml ($p \leq 0.01$) and grade-4: 673.4 ± 64.38 ng/ml ($p \leq 0.01$), from basal/grade-0: 380.7 ± 94.43 ng/ml) (Figure 4.13, panel A). Similarly, the highest levels of MMP-3 relative to grade-0/healthy controls was present in grade-4, followed on by grade-3, grade-2 and grade-1 OA-SFs (grade-1: 438.7 ± 90.01 ng/ml ($p \leq 0.05$), grade-2: 490.9 ± 95.80 ng/ml ($p \leq 0.05$), grade-3: 759.7 ± 69.80 ng/ml ($p \leq 0.01$) and grade-4: 743.0 ± 50.43 ng/ml ($p \leq 0.01$), from basal/grade-0: 217.0 ± 41.04 ng/ml) (Figure 4.13, panel B). Moreover, the highest and significant levels of MMP-9 relative to grade-0/healthy controls was evident in grade-4, followed on by grade-3 and grade-2 OA-SFs (grade-2: 3.49 ± 0.28 ng/ml ($p \leq 0.05$), grade-3: 4.04 ± 0.39 ng/ml ($p \leq 0.05$) and grade-4: 4.5 ± 0.2 ng/ml ($p \leq 0.01$), from basal/grade-0: 1.41 ± 0.20 ng/ml) and a notable, though non-significant, level of MMP-9 relative to grade-0/healthy controls was evident in grade-1 OA-SFs (Figure 4.13, panel C).

Thus, owing to the previous observation that Poly(I:C) predominantly induced secretion of the catabolic MMP 1, 3 and 9 in early and late OA-FLS (Figure 4.9) and whole OA synovial tissue explants (Figure 4.4) and, given that Poly (I:C) exclusively employed TLR3 in OA-FLS (Chapter 3, Figure 3.2, 3.14 and 3.15), it may be proposed that a RNA borne sustained activation of TLR3 on synovial FLS may be inducing these catabolic mediators in to the synovial fluid, even at the very early stages of OA disease on-set thus ultimately leading in OA progression.

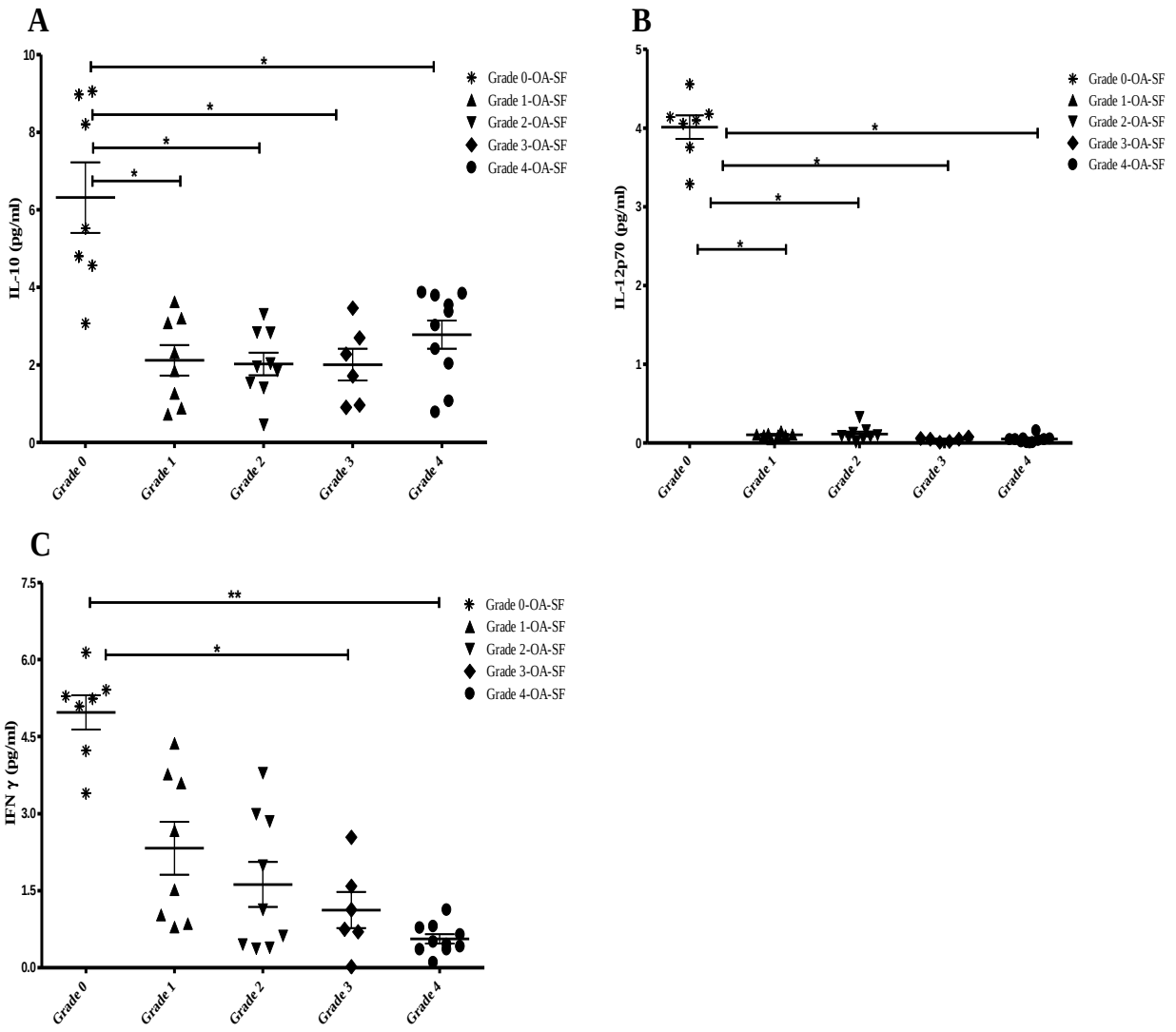

Figure 4.12: Analysis of IL-10, IL-12 p70 and IFNγ levels in grade-specific OA synovial fluid. (A-C) Cell-free grade-specific OA-SFs: grade-0 (healthy controls, n=7), grade-1 (n=8), grade-2 (n=9), grade-3 (n=6), and grade-4 (end stage OA, n=10), were analyzed for (A) IL-10, (B) IL-12 p70 and (C) IFNγ by ultrasensitive MSD multiplex ELISA system. All the data presented are representative of at least one independent experiment performed in duplicate (mean ± S.E.M). Data was subjected to a one-way analysis of variance using a post hoc Student's Newman-Keuls test. * $p<0.05$, ** $p<0.01$ denotes the level of significance relative to grade-0 or healthy controls.

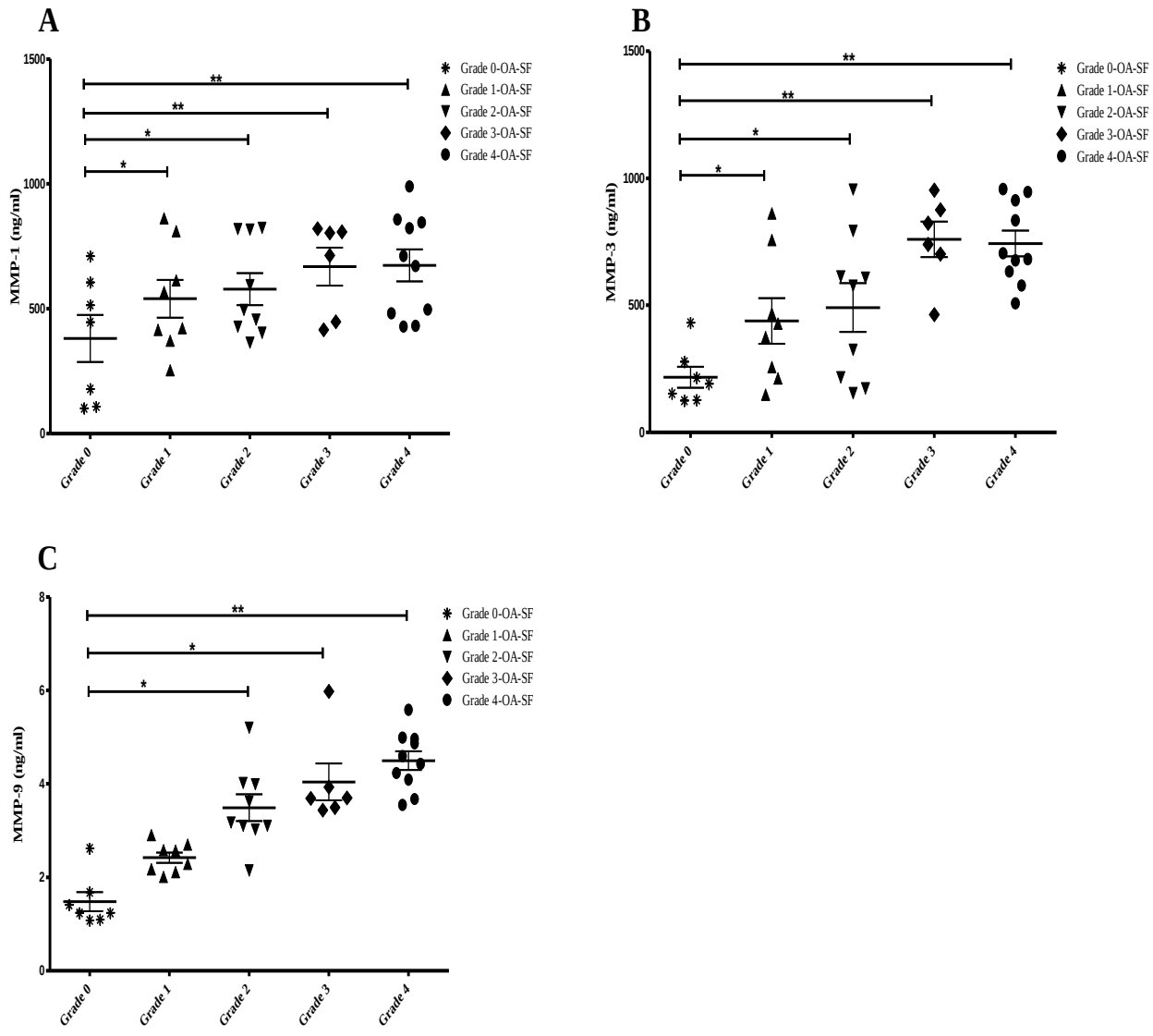

Figure 4.13: Analysis of MMP-1, MMP-3 and MMP-9 levels in grade-specific OA synovial fluid. (A-C) Cell-free grade-specific OA-SFs: grade-0 (healthy controls, n=7), grade-1 (n=8), grade-2 (n=9), grade-3 (n=6), and grade-4 (end stage OA, n=10), were analyzed for (A) MMP-1, (B) MMP-3 and (C) MMP-9 by ultrasensitive MSD multiplex ELISA system. All the data presented are representative of at least one independent experiment performed in duplicate (mean ± S.E.M). Data was subjected to a one-way analysis of variance using a post hoc Student's Newman-Keuls test. * $p<0.05$, ** $p<0.01$ denotes the level of significance relative to grade-0 or healthy controls.

Together, these data provide evidence that a trend towards increased secretion of inflammatory mediators and suppression of immune-modulatory and anti-inflammatory molecules, might aid in perpetuating synovitis, joint destruction and OA progression. Interestingly, the trend towards significant increase in pro-inflammatory IL-6, IL-8, IL-1β and TNFα levels (Figure 4.10), IFNβ and RANTES levels (Figure 4.11), MMP-1, 3 and 9 levels (Figure 4.13) and a significant suppression of anti-inflammatory IL-10 and immuno-modulatory IFNγ and IL-12p70 levels (Figure 4.12) in progressive OA-grades, might create a critical imbalance between catabolic and anabolic pathways. Hence, the levels of pro- vs anti-inflammatory mediators measured in grade-specific OA-SFs may correlate with the inflammatory cell infiltrates and synovial hyperplasia previously observed (Figure 4.4.2), and it may be proposed that the increased number of FLSs may participate in the sustained activation of FLS in the hyperplastic synovium by secreting these inflammatory cyto- chemokines into the synovial fluid. Moreover, given our previous observation (Figure 4.4.1 and 4.4.6) that, the synovial tissue explants and early, late OA-FLS are activated by Poly (I:C)/RNA from necrotic cells and significantly induce IL-6, IL-8, IL-1β TNFα, IFNβ, RANTES and MMPs 1, 3 and 9 levels and suppress IL-10, IFNγ and IL-12p70 levels in the synovial fluid, it may be hypothesised that sustained TLR3-induced activation of synovial FLS in the synovium may be a contributing factor for such an imbalance in pro vs anti-inflammatory mediators in grade-specific OA-SFs. Together, these data provide TLR3 as a critical target for OA disease intervention.

4.4.5. Analysis of TLR agonist/grade-specific OA-SF induced expression of TLR genes in FLS

Given our previous observation that sustained TLR activation of FLS in the synovium may act as a contributing factor towards generating an imbalance in the pro vs anti-inflammatory mediators measured in grade-specific OA-SFs (Section 4.4.4), it was essential to investigate the ability of grade-specific OA-SFs to activate specific TLRs in FLS. To do so, an in-vitro assay was performed, wherein, N-FLS were treated with grade specific OA-SF to mimic the intricate cell-fluid contact in the joint synovium, which otherwise maintains the joint homeostasis, and if unchecked may lead to chronic inflammatory disease conditions like OA, probably through TLR hyper-activation. Hence, an attempt was made to characterise OA-SF-induced TLR gene expression profiles in N-FLS (Figure 4.14, panels A to F, n=3). A trend towards decreased TLR-1 mRNA expression was observed in N-FLS upon stimulation with progressive grades of OA-SFs (grades 1-4) relative to grade-0 stimulation (Figure 4.14, panel A). Whereas, minimal induction of TLR-2 (panel C), TLR-5 (panel E) and TLR-6 (panel F) mRNA expression, no detectable induction of TLR-7, 8 and 9 mRNA expression (data not shown) was evident in N-FLS upon stimulation with progressive grades of OA-SFs (grades 1-4) relative to grade-0 stimulation (Figure 4.14). Interestingly, all the grade-specific OA-SFs (n=3/grade) utilised in the study induced a significant expression of TLR3 mRNA in N-FLS upon stimulation with progressive grades of OA-SFs (grades 1-4) relative to grade-0 stimulation. Wherein, stimulation with grade-1 OA-SF induced a significant 8.5-fold increase, grade-2 OA-SF induced a significant 12.5-fold increase ($p \leq 0.05$), grade-3 OA-SF induced significant 9-fold increase ($p \leq 0.05$), and grade-4 OA-SF induced maximal and significant 15-fold increase ($p \leq 0.01$), in TLR-3 mRNA expression in N-FLS relative to grade-0 stimulation (Figure 4.14, panel C). Moreover, though non-significant, a notable increase in TLR-4 mRNA expression was evident in N-FLS upon stimulation with grade-1, 2 and 3 OA-SFs relative to grade-0 stimulation, while a significant 6.6-fold increase in TLR-4 mRNA expression was observed in N-FLS upon grade-4 OA-SF stimulation (Figure 4.14, panel D). These data, at least in-part, correlate with a recent publication (Nair et al., 2012), and also provide evidence of the ability of grade-specific OA-SFs to distinctively and predominantly activate TLR3 in FLS. Sustained TLR3 activation of FLS in the joint synovium may facilitate OA disease progression (Brentano et al., 2005, Attur et al., 2010, Zhu et al., 2011) possibly through creating an imbalance between catabolic and anabolic

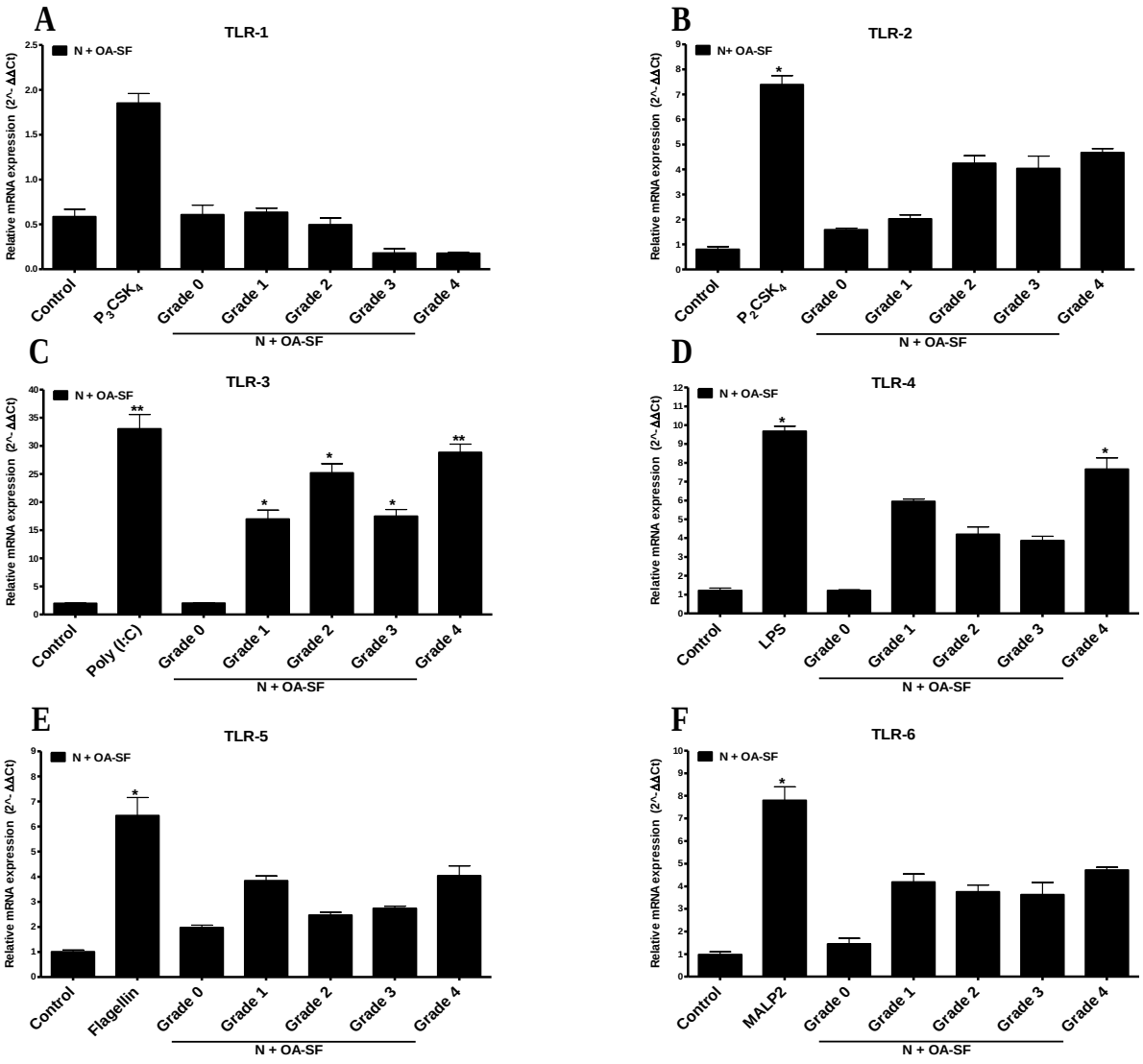

Figure 4.14: Analysis of TLR agonist/grade-specific OA-SF induced expression of TLR genes in FLS. (A-F) N-FLS (n=3), were treated with Pam_3CSK_4 (1 µg/ml; TLR1/2 ligand), Pam_2CSK_4 (1 µg/ml; TLR2 ligand), Poly(I:C) (10 µg/ml; TLR3 ligand), LPS (1 µg/ml; TLR4 ligand), Flagellin (1 µg/ml; TLR5 ligand), MALP-2 (20 nM; TLR2/6 ligand), or with grade specific (Grade 0, 1, 2, 3, 4) OA-SF, respectively, for 16 h. Total RNA was then isolated from control and stimulated N-FLS, and used as a template for quantitative real-time RT-PCR to assay the mRNA expression levels of TLR1 (A), TLR2 (B), TLR3 (C), TLR4 (D), TLR5 (E), TLR6 (F). The levels of the relevant mRNAs were normalised relative to the housekeeping gene HPRT and are expressed relative to normalised values from unstimulated or control cells. All the data presented are representative of at least three independent experiments performed in triplicate (mean ± S.E.M). Data was subjected to an unpaired Student's t test. * $p<0.05$, ** $p<0.01$ denotes the level of significance relative to control or grade-0.

pathways, mediators and inflammatory cell infiltrates (Section 4.4.1, 4.4.2, 4.4.3 and 4.4.4).

4.4.6. *In-vitro* analysis of major TLR and cytokine neutralisation assays in N and OA FLS

Given our previous observations that levels of basal and induced IL-6, TNFα and IFNβ secretions by N -FLS, OA-FLS and whole synovial tissue explant cultures predominate following stimulation with Poly(I:C) (chapter 3 and chapter 4 : Section 4.4.1, 4.4.3), and to a lesser extent, with Pam_2CSK_4, LPS and CpG stimulations, it was essential to explore whether blockade of such cytokines/TLRs using cytokine and TLR inhibitory/neutralising molecules may mediate regulatory effects on OA pathology. Moreover, to evaluate and optimise the concentration and time points for effective outcome of such anti-TLR and anti-cytokine neutralising antibodies, a screen was performed in N and OA-FLS (data not shown). Thus, optimised neutralising antibodies were utilised to assess the ability of these antibodies in modulating TLR/cytokine/OA-SF mediated pro- and anti-inflammatory cyto-chemokine secretions in N and OA FLS.

4.4.6.1. Analysis of the effect of anti-TLR/anti-cytokine antibodies on IL-1β secretion in N and OA FLS

IL-1β plays a pivotal role in joint destruction, primarily through induction of inflammatory mediators, namely IL-6 and MMPs, thus aiding in the vicious cyto-chemokine-MMP cycle leading to prolonged synovitis in chronic inflammatory joint diseases like OA (Pulsatelli et al., 1999, Pelletier et al., 1995, Smith et al., 1997, Pelletier et al., 2001, Scanzello et al., 2009). Herein, it was critical to understand the effects of anti-TLR/anti-cytokine antibodies on IL-1β secretion towards exploring the possibility of identifying an IL-1β regulatory target as, to-date, single cytokine or cytokine receptor antagonists have had limited success in the treatment of such diseases and targeted therapy to block IL-1β in OA was tested, but could reach only some success as expected (Chevalier et al., 2005). Interestingly, of the TLR and cytokine neutralising antibodies utilised in the study, pre-treatment with anti-TLR3 antibody induced the highest and most significant suppression in IL-1β levels in N and OA FLS upon Poly (I:C) or end/late stage OA-SF stimulations, relative to the respective cell type agonist treatment controls. A significant ($p \leq 0.05$) decrease in IL-1β levels was evident in N-FLS pre-incubated with anti-TLR3 antibody, followed by Poly (I:C) or end/late stage OA-SF stimulations. Moreover, the highest and most significant

suppression in IL-1β levels was evident in OA-FLS pre-incubated with anti-TLR3 antibody, followed by Poly (I:C) ($p \leq 0.01$) or late stage OA-SF ($p \leq 0.05$) stimulations (Figure 4.15, panel D, n=3). Similarly, a significant decrease in IL-1β levels was evident in N and OA-FLS pre-incubated with anti-IFNβ antibody, followed by IFNβ or end/late stage OA-SF stimulations (Figure 4.15, panel G, $p \leq 0.05$). Likewise, a significant decrease in IL-1β levels was evident in OA-FLS pre-incubated with anti-TLR4 antibody, followed by LPS stimulation (Figure 4.15, panel B, $p \leq 0.05$). In contrast, pre-incubation with anti-TLR2, anti-TLR9, anti-IL-6 or anti-TNFα antibodies did not show any significant regulation of IL-1β levels in N and OA-FLS upon respective ligand or OA-SF stimulations (Figure 4.15, panels A, C, E and F). Interestingly, the highest and most significant suppression of pro-inflammatory IL-1β secretion by N and OA-FLS was observed upon pre-treatment with anti-TLR3 antibody followed by poly(I:C) stimulation and this corroborates our previous findings showing that activation of TLR3 in synovial FLS may induce IL-1β secretions in the joint synovium and fluid (Figure 4.1 and 4.6; panel C, Figure 4.10; panel A).

4.4.6.2. Analysis of the effect of anti-TLR/anti-cytokine antibodies on TNFα secretion in N and OA FLS

Given the key role of TNFα in mediating catabolic protease production in the joint (Fernandes et al., 2002), and given the limited success of anti-TNFα therapy towards the treatment of erosive hand OA (Magnano et al., 2007), and the increasing evidence that blockade of certain TLRs on RA-FLS in the synovium can prevent the upregulation of catabolic mediators in the joint (Ultaigh et al., 2011), it was essential to investigate the effects of anti-TLR/anti-cytokine antibodies on TNFα secretion by N and OA FLS. Of the TLR and cytokine neutralising antibodies utilised in the study, the most significant decrease in TNFα levels was evident in N ($p \leq 0.05$), and OA-FLS ($p \leq 0.01$) pre-incubated with anti-TNFα antibody, followed by TNFα stimulation, but not with late-stage OA-SF stimulation (Figure 4.16, panel F, n=3). Interestingly, pre-treatment with anti-TLR3 antibody induced the highest and most significant suppression in TNFα levels in N and OA FLS, followed by Poly (I:C) or late stage OA-SF stimulations. A significant ($p \leq 0.05$) decrease in TNFα levels was evident in N-FLS pre-incubated with anti-TLR3 antibody, followed by Poly (I:C) or late stage OA-SF stimulations. Moreover, the highest and most significant suppression in TNFα levels was evident in OA-FLS pre-incubated with anti-TLR3 antibody, followed by Poly (I:C) ($p \leq 0.01$) or late stage OA-SF ($p \leq 0.05$)

stimulations (Figure 4.16, panel D, n=3). Likewise, a significant decrease in TNFα levels was evident in N and OA-FLS pre-incubated with anti-IFNβ antibody, followed by IFNβ or end/late stage OA-SF stimulations (Figure 4.16, panel G, $p \leq 0.05$). Whereas, pre-incubation with anti-TLR2, anti-TLR4, anti-TLR9 or anti-IL-6 antibodies did not show any significant regulation of TNFα levels in N and OA-FLS upon respective ligand or OA-SF stimulations (Figure 4.16, panels A, B, C and E). Thus, the data suggests that TNFα in OA-FLS is predominantly induced by TLR3 and IFNβ and this correlate with (chapter 3). Correspondingly, apart from anti-TNFα antibody, the most significant suppression of pro-inflammatory TNFα secretion by N and OA-FLS was evident with anti-TLR3 antibody pre-treatment. This further substantiates our previous findings that activation of TLR3 in synovial FLS may induce TNFα secretion in the joint synovium and fluid (Figure 4.1 and 4.6; panel D, Figure 4.10; panel B). These findings open a new avenue for a possible combinatorial application of anti-TNFα and anti-TLR3 antibodies towards the effective treatment of OA.

4.4.6.3. Analysis of the effect of anti-TLR/anti-cytokine antibodies on IL-6 secretion in N and OA FLS

Given that IL-6 positively correlates with various disease markers in many inflammatory disease pathologies and OA (Houssiau et al., 1988, Pearle et al., 2007, Scanzello et al., 2009, Kapoor et al., 2011), and given the predominant secretion of IL-6 by OA-FLS upon Poly (I:C) stimulation (chapter 3; Figure 3.9, chapter 4; Figure 4.6), it was critical to investigate the effects of anti-TLR/anti-cytokine antibodies on IL-6 secretion by N and OA FLS. Of the TLR and cytokine neutralising antibodies utilised in the study, the most significant decrease in IL-6 levels was evident in N and OA-FLS pre-incubated with anti-IL-6 antibody followed by IL-6 stimulation ($p \leq 0.01$), or with late-stage OA-SF stimulation in N-FLS ($p \leq 0.05$) (Figure 4.17, panel E, n=3). Interestingly, pre-treatment with anti-TLR3 antibody induced the highest and most significant suppression in IL-6 levels in N and OA FLS, followed by Poly (I:C) or late stage OA-SF stimulations. A significant decrease in IL-6 levels was evident in N and OA-FLS pre-incubated with anti-TLR3 antibody, followed by Poly (I:C) ($p \leq 0.01$) stimulation. Moreover, stimulation with late stage OA-SF also induced significant suppression in IL-6 levels in N and OA-FLS upon pre-incubation with anti-TLR3 antibody ($p \leq 0.05$) (Figure 4.17, panel D, n=3). Likewise, a significant decrease in IL-6 levels was evident in N and OA-FLS pre-incubated with anti-IFNβ antibody, followed by IFNβ stimulation or end/late stage OA-SF

stimulation in N-FLS (Figure 4.17, panel G, $p \leq 0.05$). Similarly, a significant decrease in IL-6 levels was evident in N and OA-FLS pre-incubated with anti-TNFα antibody, followed by TNFα stimulation (Figure 4.17, panel F, $p \leq 0.05$). In contrast, pre-incubation with anti-TLR2, anti-TLR4 or anti-TLR9 antibodies did not show any significant regulation of IL-6 levels in N and OA-FLS upon respective ligand or OA-SF stimulations (Figure 4.17, panels A, B and C). Thus, the data suggests that IL-6 induction in N and OA-FLS can be induced by TLR3, TNFα and IFNβ and this correlates with our previous findings (chapter 3). In addition to the anti-IL-6 antibody, the most significant suppression of pro-inflammatory IL-6 secretion by N and OA-FLS was evident upon anti-TLR3 antibody pre-treatment, and this further substantiates our previous findings that activation of TLR3 in synovial FLS may induce IL-6 secretion in the joint synovium and fluid (Figure 4.1 and 4.6; panel A, Figure 4.10; panel C); this correlates with previous publications (Zhu et al., 2011).

4.4.6.4. Analysis of the effect of anti-TLR/anti-cytokine antibodies on IFNβ secretion in N and OA FLS

Given the key role of IFNβ in chronic inflammatory joint arthropathies and its possible modulation following TLR3 blockade in pristine induced arthritis (Zhu et al., 2011, Meng et al., 2010), it was), it was critical to investigate the effects of anti-TLR/anti-cytokine antibodies on IFNβ secretion by N and OA FLS. Of the TLR and cytokine neutralising antibodies utilised in the study, the most significant decrease in IFNβ levels was evident in N, and OA-FLS pre-incubated with an anti-IFNβ antibody followed by IFNβ stimulation ($p \leq 0.01$), or with late-stage OA-SF stimulation in N-FLS ($p \leq 0.05$) (Figure 4.18, panel G, n=3). Interestingly, pre-treatment with an anti-TLR3 antibody induced the most significant suppression of poly(I:C) mediated IFNβ in OA-FLS ($p \leq 0.01$) and N-FLS ($p \leq 0.05$) stimulation. Moreover, an anti-TLR3 antibody induced significant suppression of late stage OA-SF induced IFNβ levels in N and OA-FLS ($p \leq 0.05$) (Figure 4.18, panel D, n=3). Likewise, a significant decrease late stage OA-SF mediated IFNβ levels was evident in N and OA-FLS following pre-incubation with an anti-IL-6 antibody (Figure 4.18, panel E, $p \leq 0.05$). Similarly, a significant decrease in TNFα mediated IFNβ levels was evident in OA-FLS following pre-incubatation with anti-TNFα antibody (Figure 4.18, panel F, $p \leq 0.05$). In contrast, pre-incubation with anti-TLR2, anti-TLR4 or anti-TLR9 antibodies did not show any significant regulation of IFNβ levels in N and OA-FLS upon respective ligand or OA-SF stimulations (Figure 4.18, panels A, B and C). Thus, the data suggests

that IFNβ in N and OA-FLS can be induced by TLR3, TNFα and IL-6 and this correlates with our previous findings (chapter 3). In addition to the anti-IFNβ antibody, the most significant suppression of pro-inflammatory IFNβ secretion by N and OA-FLS was evident upon anti-TLR3 antibody pre-treatment; this further substantiates our previous findings that activation of TLR3 in synovial FLS may induce IFNβ secretion in the joint synovium and fluid (Figure 4.2 and 4.7; panel A, Figure 4.11; panel A), and also correlates with previous publications (Zhu et al., 2011, Meng et al., 2010).

4.4.6.5. Analysis of the effect of anti-TLR/anti-cytokine antibodies on RANTES secretion in N and OA FLS

Given the vital role for RANTES and its receptor CCR5 in chronic inflammatory joint diseases, like RA and OA, through sustained induction of CCR5 in FLS (Haringman et al., 2004, Vergunst et al., 2005) and given that RANTES induces chondrocyte dysfunctionality associated with joint inflammation and cartilage degradation in OA (Yuan et al., 2003, Borzì et al., 2004), it was critical to understand the effects of anti-TLR/anti-cytokine antibodies on RANTES secretion towards exploring the exact role of RANTES in OA. Interestingly, of the TLR and cytokine neutralising antibodies utilised in the study, pre-treatment with anti-TLR3 antibody followed by Poly (I:C) or late stage OA-SF stimulation induced the most significant suppression of RANTES levels in N and OA FLS relative to the respective cell type agonist treatment controls. A significant decrease in RANTES levels was evident in N-FLS pre-incubated with anti-TLR3 antibody, followed by stimulation with either Poly (I:C) ($p \leq 0.01$) or end/late stage OA-SF ($p \leq 0.05$). Moreover, significant suppression of RANTES was evident in OA-FLS pre-incubated with anti-TLR3 antibody, followed by Poly (I:C) or late stage OA-SF stimulations ($p \leq 0.05$) (Figure 4.19, panel D, n=3). Similarly, a significant decrease in RANTES levels was evident in N and OA-FLS pre-incubated with anti-IFNβ antibody, followed by IFNβ stimulation (Figure 4.19, panel G, $p \leq 0.05$). In contrast, pre-incubation with anti-TLR2, anti-TLR-4, anti-TLR9, anti-IL-6 or anti-TNFα antibodies did not show any significant regulation of RANTES levels in N and OA-FLS upon stimulation with respective ligands or OA-SF (Figure 4.19, panels A, B, C, E and F). Interestingly, the most significant suppression of RANTES secretion by N and OA-FLS was observed upon pre-treatment with an anti-TLR3 antibody, and this corroborates our previous findings that activation of TLR3 in synovial FLS may induce RANTES secretions in the joint synovium and fluid (Figure 4.2 and 4.7; panel B, Figure 4.11; panel B).

4.4.6.6. Analysis of the effect of anti-TLR/anti-cytokine antibodies on IL-15 secretion in N and OA FLS

IL-15 levels were measured as it was previously detected in high levels even in early knee OA synovial fluid and has been linked with IL-6 and MMP levels, thus indicating an early innate immune response in the OA synovium (Scanzello et al., 2009). Thus, it was critical to understand the effects of anti-TLR/anti-cytokine antibodies on IL-15 secretion towards further explore the possibility that IL-15 may be a regulatory target. Interestingly, of the TLR and cytokine neutralising antibodies utilised in the study, pre-treatment with anti-TLR3 antibody caused the most significant suppression of IL-15 levels in N and OA FLS upon Poly (I:C) or end/late stage OA-SF stimulation relative to the respective cell type agonist treatment controls. A significant decrease in IL-15 levels was evident in N-FLS pre-incubated with an anti-TLR3 antibody followed by Poly (I:C) or end/late stage OA-SF stimulation ($p \leq 0.05$). Moreover, the most significant suppression of IL-15 was evident in OA-FLS pre-incubated with an anti-TLR3 antibody, followed by Poly (I:C) stimulation ($p \leq 0.05$), and a non-significant decrease in IL-15 levels was observed with late stage OA-SF stimulation (Figure 4.20, panel D, n=3). Similarly, a significant decrease in IL-15 levels was evident in N-FLS ($p \leq 0.05$) and OA-FLS ($p \leq 0.01$) pre-incubated with an anti-IFNβ antibody, followed by IFNβ stimulation (Figure 4.20, panel G, n=3). In contrast, pre-incubation with anti-TLR2, anti-TLR-4, anti-TLR9, anti-IL-6 or anti-TNFα antibodies did not show any significant regulation of IL-15 levels in N and OA-FLS upon respective ligand or OA-SF stimulation (Figure 4.20, panels A, B, C, E and F). Interestingly, the most significant suppression of pro-inflammatory IL-15 secretion by N and OA-FLS was observed upon treatment with an anti-TLR3 antibody, and this corroborates our previous findings that activation of TLR3 in synovial FLS may induce IL-15 secretions in the joint synovium (chapter 3).

4.4.6.7. Analysis of the effect of anti-TLR/anti-cytokine antibodies on IL-10 secretion in N and OA FLS

Given the pivotal role for suppressed IL-10 levels in OA (Sutton et al., 2009, Scanzello et al., 2009, Kapoor et al., 2011), and given the key immunoregulatory role of IL-10 in OA and RA towards the regulation of monocyte and, in some cases, T cell cytokine production (Katsikis et al., 1994), it was critical to understand the effects of anti-TLR/anti-cytokine antibodies on IL-10 secretion in FLS. Interestingly, of the TLR and cytokine neutralising

antibodies utilised in the study, pre-treatment with anti-TLR3 antibody induced the most significant increase of IL-10 levels in N and OA FLS upon Poly (I:C) or end/late stage OA-SF stimulations, relative to the respective cell type agonist treatment controls. A significant increase in IL-10 levels was evident in N-FLS and OA-FLS pre-incubated with anti-TLR3 antibody, followed by Poly (I:C) or late stage OA-SF stimulations (Figure 4.21, panel D, $p \leq 0.05$). Similarly, a significant increase in IL-10 levels was evident in N-FLS and OA-FLS pre-incubated with anti-IFNβ antibody, followed by IFNβ stimulation (Figure 4.21, panel G, $p \leq 0.05$). Likewise a significant increase in IL-10 levels was also observed in N-FLS with anti-IL-6 antibody pre-incubation followed by IL-6 stimulation (Figure 4.21, panel E, $p \leq 0.05$). In contrast, pre-incubation with anti-TLR2, anti-TLR-4, anti-TLR9 or anti-TNFα antibodies did not show any significant regulation of IL-10 levels in N and OA-FLS upon respective ligand or OA-SF stimulations (Figure 4.21, panels A, B, C and F). Interestingly, the most significant upregulation of anti-inflammatory IL-10 secretion by N and OA-FLS was observed upon treatment with an anti-TLR3 antibody, and this corroborates our previous findings that activation of TLR3 in synovial FLS may suppress IL-10 secretions in the joint synovium, thus we propose that TLR3 blockade may revert this and halt OA progression (Figure 4.3, 4.8 and Figure 4.12; panel A).

Together, these data provide evidence for the immunomodulatory effects of TLR3 blockade in OA. Also, our previous findings suggest that sustained activation of TLR3 is evident in synovial FLS via the TLR ligand Poly(I:C) or via dsRNA/RNA from necrotic cells in OA synovial fluid. Thus, TLR3 may play a key role in OA progression through induction of inflammatory and suppression of anti-inflammatory mediators, thus perpetuating synovitis and joint destruction (Sections 4.4.1, 4.4.3, 4.4.4 and 4.4.5). Accordingly, our current data indicated that, of all the TLR and cytokine neutralising antibodies utilised in this study, neutralisation of TLR3 expression utilising an anti-TLR3 antibody served to shift the balance from a pro-inflammatory to an anti-inflammatory cytokine milieu. Thus, our data suggests that hyper-activation of TLR3 may play a key role in perpetuating synovial inflammation in OA and suggests that therapeutic intervention of OA may be achieved through TLR3 blockade, although further research is warranted to validate the immuno-modulatory effects of TLR3 blockade in OA disease management.

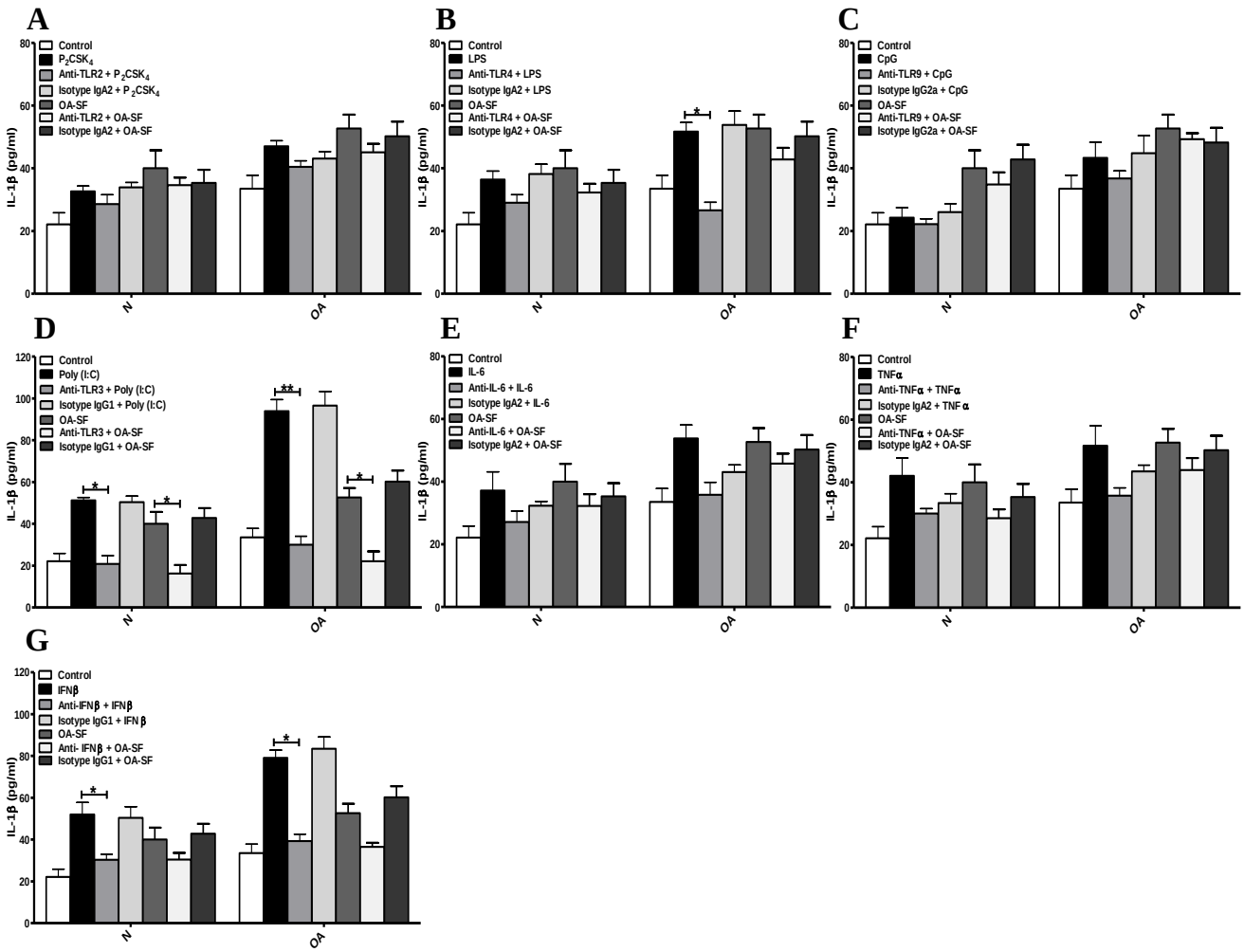

Figure 4.15: Analysis of the effect of anti-TLR/anti-cytokine antibodies on IL-1β secretion in N and OA FLS. (A-G) N-FLS and OA-FLS (n=3 for each cell type), were either pre-incubated with the respective TLR or cytokine-blocking/isotype control antibodies for 90 min prior to stimulation with the respective TLR ligand, cytokine or end-stage OA-SF (1:5 dilution in Opti-MEM, n=3), or stimulated with the respective ligand or left unstimulated for 16 h. (A) Cells were either pre-treated with anti-TLR2 antibody (5 µg/ml) or Isotype IgA2 antibody (5 µg/ml) prior to Pam_2CSK_4 (1 µg/ml) or OA-SF stimulation. (B) Cells were either pre-treated with anti-TLR4 antibody (5 µg/ml) or Isotype IgA2 antibody (5 µg/ml) prior to LPS (1 µg/ml) or OA-SF stimulation. (C) Cells were either pre-treated with anti-TLR9 antibody (15 µg/ml) or Isotype IgG2a antibody (15 µg/ml) prior to CpG (3 µg/ml) or OA-SF stimulation. (D) Cells were either pre-treated with anti-TLR3 antibody (20 µg/ml) or Isotype IgG1 antibody (20 µg/ml) prior to Poly (I:C) (10 µg/ml) or OA-SF stimulation. (E) Cells were either pre-treated with anti-IL-6 antibody (5 µg/ml) or Isotype IgA2 antibody (5 µg/ml) prior to IL-6 (100 pg/ml) or OA-SF stimulation. (F) Cells were either pre-treated with anti-TNFα antibody (5 µg/ml) or Isotype IgA2 antibody (5 µg/ml) prior to TNFα (1 ng/ml) or OA-SF stimulation. (G) Cells were either pre-treated with anti-IFNβ antibody (10 µg/ml) or Isotype IgG1 antibody (10 µg/ml) prior to IFNβ (100 pg/ml) or OA-SF stimulation. Cell free supernatants were analysed for levels of IL-1β by ELISA. All the data presented are representative of at least three independent experiments performed in triplicate (mean ± S.E.M). Data was subjected to an unpaired Student's t test. * $p<0.05$, ** $p<0.01$ denotes the level of significance relative to respective ligand stimulation.

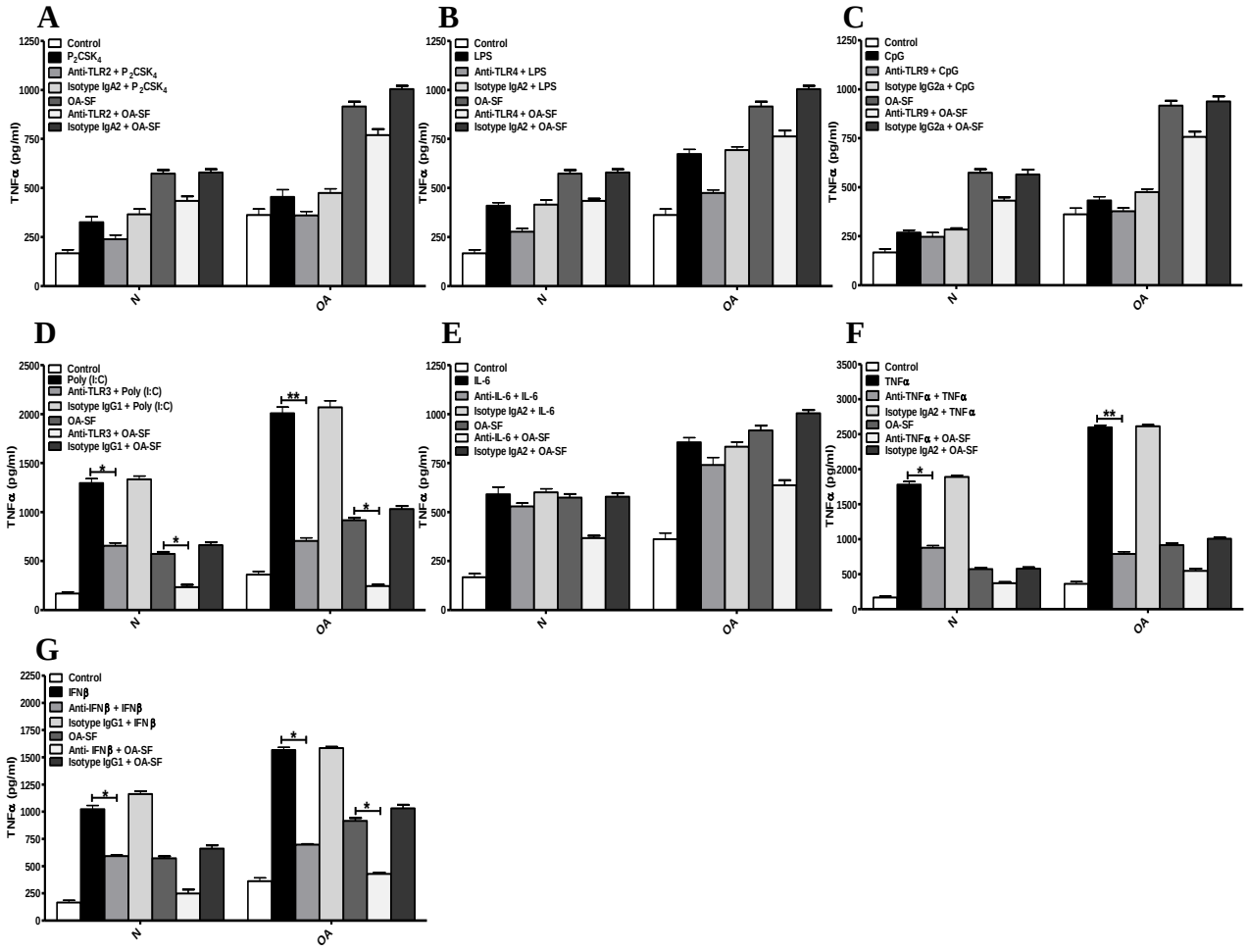

Figure 4.16: Analysis of the effect of anti-TLR/anti-cytokine antibodies on TNFα secretion in N and OA FLS. (A-G) N-FLS and OA-FLS (n=3 for each cell type) were either pre-incubated with the respective TLR or cytokine-blocking/isotype control antibodies for 90 min prior to stimulation with the respective TLR ligand, cytokine or end-stage OA-SF (1:5 dilution in Opti-MEM, n=3) or stimulated with the respective ligand or left unstimulated for 16 h. (A) Cells were either pre-treated with anti-TLR2 antibody (5 µg/ml) or Isotype IgA2 antibody (5 µg/ml) prior to Pam_2CSK_4 (1 µg/ml) or OA-SF stimulation. (B) Cells were either pre-treated with anti-TLR4 antibody (5 µg/ml) or Isotype IgA2 antibody (5 µg/ml) prior to LPS (1 µg/ml) or OA-SF stimulation. (C) Cells were either pre-treated with anti-TLR9 antibody (15 µg/ml) or Isotype IgG2a antibody (15 µg/ml) prior to CpG (3 µg/ml) or OA-SF stimulation. (D) Cells were either pre-treated with anti-TLR3 antibody (20 µg/ml) or Isotype IgG1 antibody (20 µg/ml) prior to Poly (I:C) (10 µg/ml) or OA-SF stimulation. (E) Cells were either pre-treated with anti-IL-6 antibody (5 µg/ml) or Isotype IgA2 antibody (5 µg/ml) prior to IL-6 (100 pg/ml) or OA-SF stimulation. (F) Cells were either pre-treated with anti-TNFα antibody (5 µg/ml) or Isotype IgA2 antibody (5 µg/ml) prior to TNFα (1 ng/ml) or OA-SF stimulation. (G) Cells were either pre-treated with anti-IFNβ antibody (10 µg/ml) or Isotype IgG1 antibody (10 µg/ml) prior to IFNβ (100 pg/ml) or OA-SF stimulation. Cell free supernatants were analysed for levels of TNFα by ELISA. All the data presented are representative of at least three independent experiments performed in triplicate (mean ± S.E.M). Data was subjected to an unpaired Student's t test. * $p<0.05$, ** $p<0.01$ denotes the level of significance relative to respective ligand stimulation.

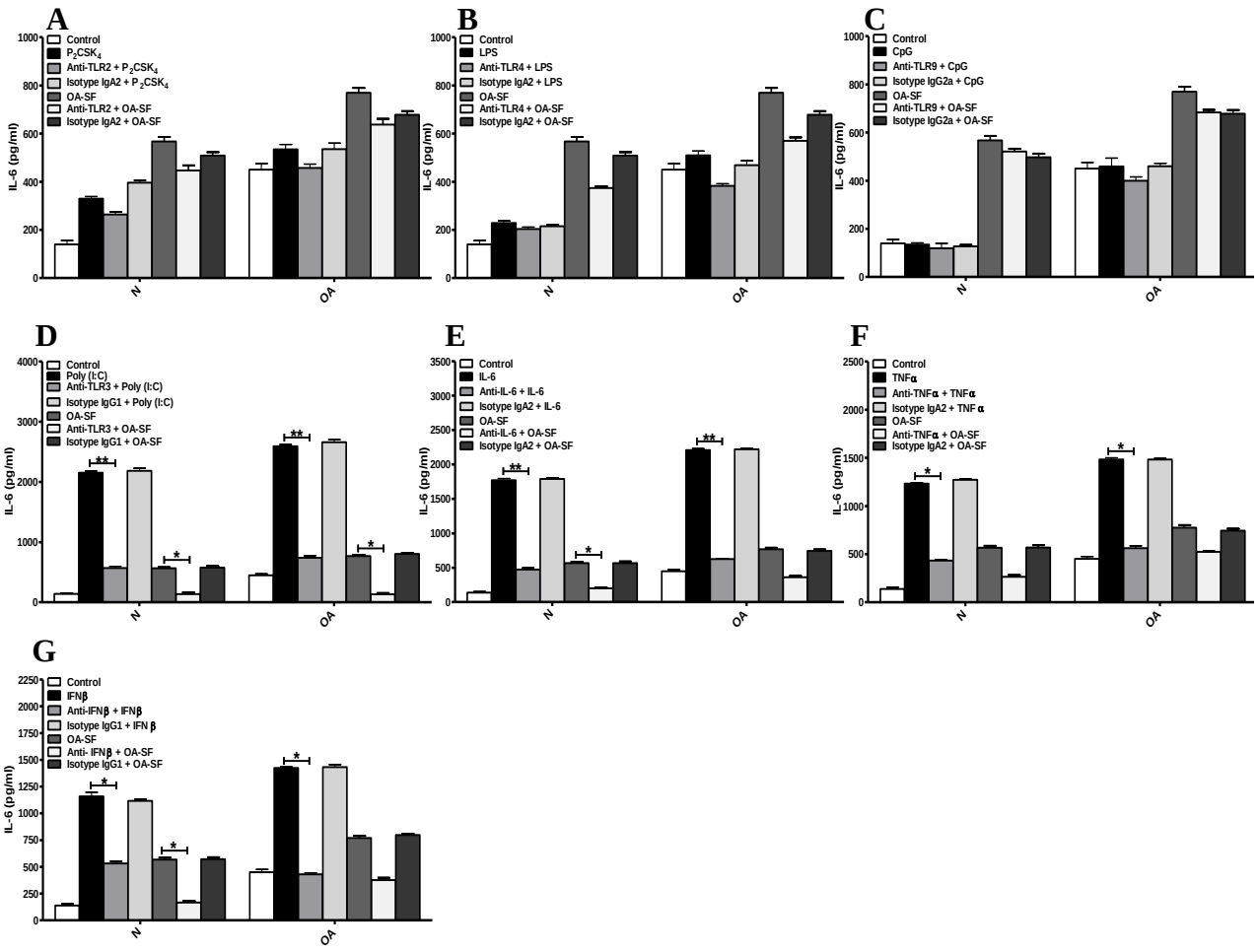

Figure 4.17: Analysis of the effect of anti-TLR/anti-cytokine antibodies on IL-6 secretion in N and OA FLS. (A-G) N-FLS and OA-FLS (n=3 for each cell type) were either pre-incubated with the respective TLR or cytokine-blocking/isotype control antibodies for 90 min prior to stimulation with the respective TLR ligand, cytokine or end-stage OA-SF (1:5 dilution in Opti-MEM, n=3) or stimulated with the respective ligand or left unstimulated for 16 h. (A) Cells were either pre-treated with anti-TLR2 antibody (5 µg/ml) or Isotype IgA2 antibody (5 µg/ml) prior to Pam_2CSK_4 (1 µg/ml) or OA-SF stimulation. (B) Cells were either pre-treated with anti-TLR4 antibody (5 µg/ml) or Isotype IgA2 antibody (5 µg/ml) prior to LPS (1 µg/ml) or OA-SF stimulation. (C) Cells were either pre-treated with anti-TLR9 antibody (15 µg/ml) or Isotype IgG2a antibody (15 µg/ml) prior to CpG (3 µg/ml) or OA-SF stimulation. (D) Cells were either pre-treated with anti-TLR3 antibody (20 µg/ml) or Isotype IgG1 antibody (20 µg/ml) prior to Poly (I:C) (10 µg/ml) or OA-SF stimulation. (E) Cells were either pre-treated with anti-IL-6 antibody (5 µg/ml) or Isotype IgA2 antibody (5 µg/ml) prior to IL-6 (100 pg/ml) or OA-SF stimulation. (F) Cells were either pre-treated with anti-TNFα antibody (5 µg/ml) or Isotype IgA2 antibody (5 µg/ml) prior to TNFα (1 ng/ml) or OA-SF stimulation. (G) Cells were either pre-treated with anti-IFNβ antibody (10 µg/ml) or Isotype IgG1 antibody (10 µg/ml) prior to IFNβ (100 pg/ml) or OA-SF stimulation. Cell free supernatants were analysed for levels of IL-6 by ELISA. All the data presented are representative of at least three independent experiments performed in triplicate (mean ± S.E.M). Data was subjected to an unpaired Student's t test. * $p<0.05$, ** $p<0.01$ denotes the level of significance relative to respective ligand stimulation.

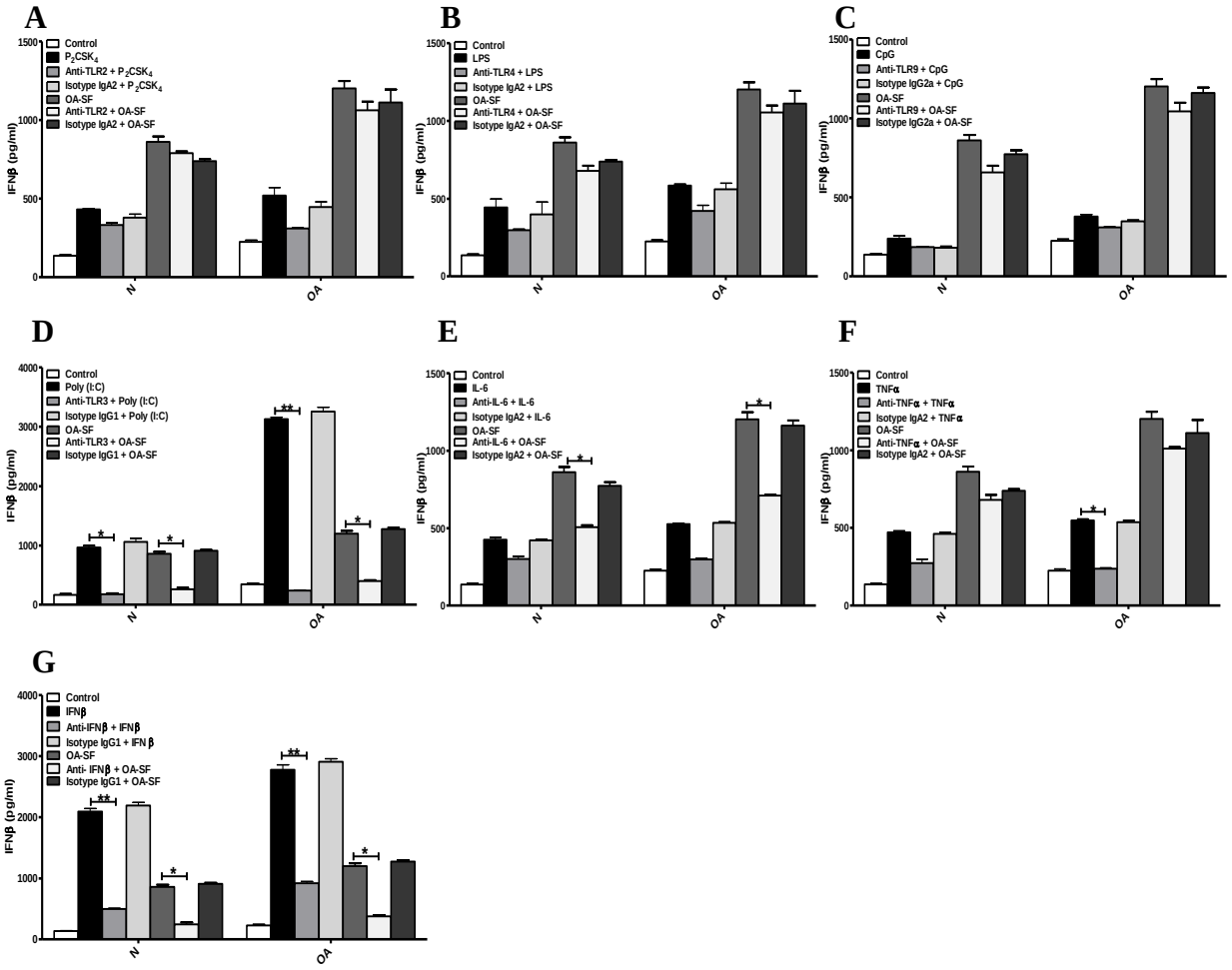

Figure 4.18: Analysis of the effect of anti-TLR/anti-cytokine antibodies on IFNβ secretion in N and OA FLS. (A-G) N-FLS and OA-FLS (n=3 for each cell type) were either pre-incubated with the respective TLR or cytokine-blocking/isotype control antibodies for 90 min prior to stimulation with the respective TLR ligand, cytokine or end-stage OA-SF (1:5 dilution in Opti-MEM, n=3) or stimulated with the respective ligand or left unstimulated for 16 h. (A) Cells were either pre-treated with anti-TLR2 antibody (5 µg/ml) or Isotype IgA2 antibody (5 µg/ml) prior to Pam_2CSK_4 (1 µg/ml) or OA-SF stimulation. (B) Cells were either pre-treated with anti-TLR4 antibody (5 µg/ml) or Isotype IgA2 antibody (5 µg/ml) prior to LPS (1 µg/ml) or OA-SF stimulation. (C) Cells were either pre-treated with anti-TLR9 antibody (15 µg/ml) or Isotype IgG2a antibody (15 µg/ml) prior to CpG (3 µg/ml) or OA-SF stimulation. (D) Cells were either pre-treated with anti-TLR3 antibody (20 µg/ml) or Isotype IgG1 antibody (20 µg/ml) prior to Poly (I:C) (10 µg/ml) or OA-SF stimulation. (E) Cells were either pre-treated with anti-IL-6 antibody (5 µg/ml) or Isotype IgA2 antibody (5 µg/ml) prior to IL-6 (100 pg/ml) or OA-SF stimulation. (F) Cells were either pre-treated with anti-TNFα antibody (5 µg/ml) or Isotype IgA2 antibody (5 µg/ml) prior to TNFα (1 ng/ml) or OA-SF stimulation. (G) Cells were either pre-treated with anti-IFNβ antibody (10 µg/ml) or Isotype IgG1 antibody (10 µg/ml) prior to IFNβ (100 pg/ml) or OA-SF stimulation. Cell free supernatants were analysed for levels of IFNβ by ELISA. All the data presented are representative of at least three independent experiments performed in triplicate (mean ± S.E.M). Data was subjected to an unpaired Student's t test. * $p<0.05$, ** $p<0.01$ denotes the level of significance relative to respective ligand stimulation.

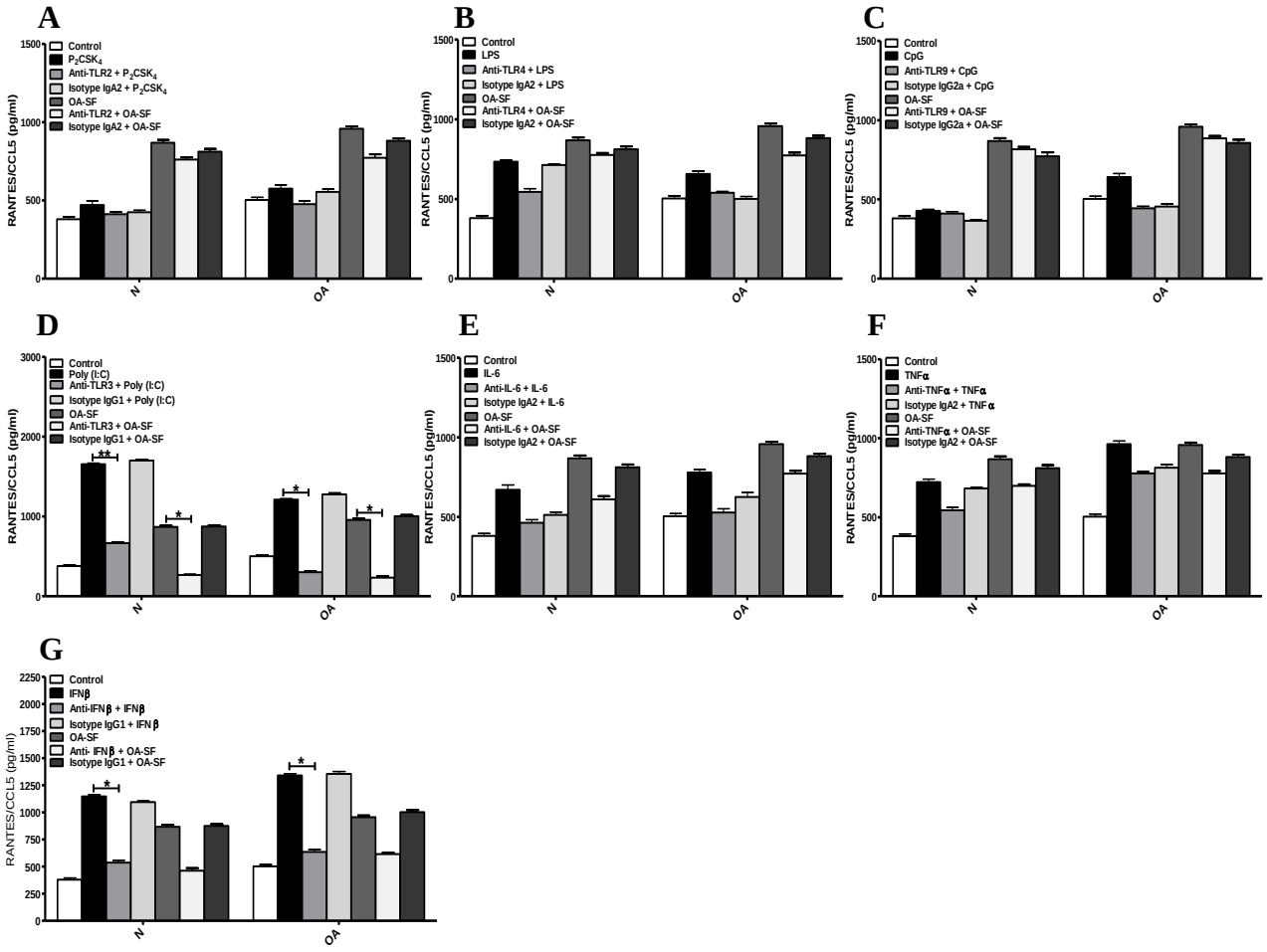

Figure 4.19: Analysis of the effect of anti-TLR/anti-cytokine antibodies on RANTES secretion in N and OA FLS. (A-G) N-FLS and OA-FLS (n=3 for each cell type) were either pre-incubated with the respective TLR or cytokine-blocking/isotype control antibodies for 90 min prior to stimulation with the respective TLR ligand, cytokine or end-stage OA-SF (1:5 dilution in Opti-MEM, n=3) or stimulated with the respective ligand or left unstimulated for 16 h. (A) Cells were either pre-treated with anti-TLR2 antibody (5 µg/ml) or Isotype IgA2 antibody (5 µg/ml) prior to Pam_2CSK_4 (1 µg/ml) or OA-SF stimulation. (B) Cells were either pre-treated with anti-TLR4 antibody (5 µg/ml) or Isotype IgA2 antibody (5 µg/ml) prior to LPS (1 µg/ml) or OA-SF stimulation. (C) Cells were either pre-treated with anti-TLR9 antibody (15 µg/ml) or Isotype IgG2a antibody (15 µg/ml) prior to CpG (3 µg/ml) or OA-SF stimulation. (D) Cells were either pre-treated with anti-TLR3 antibody (20 µg/ml) or Isotype IgG1 antibody (20 µg/ml) prior to Poly (I:C) (10 µg/ml) or OA-SF stimulation. (E) Cells were either pre-treated with anti-IL-6 antibody (5 µg/ml) or Isotype IgA2 antibody (5 µg/ml) prior to IL-6 (100 pg/ml) or OA-SF stimulation. (F) Cells were either pre-treated with anti-TNFα antibody (5 µg/ml) or Isotype IgA2 antibody (5 µg/ml) prior to TNFα (1 ng/ml) or OA-SF stimulation. (G) Cells were either pre-treated with anti-IFNβ antibody (10 µg/ml) or Isotype IgG1 antibody (10 µg/ml) prior to IFNβ (100 pg/ml) or OA-SF stimulation. Cell free supernatants were analysed for levels of RANTES by ELISA. All the data presented are representative of at least three independent experiments performed in triplicate (mean ± S.E.M). Data was subjected to an unpaired Student's t test. * $p<0.05$, ** $p<0.01$ denotes the level of significance relative to respective ligand stimulation.

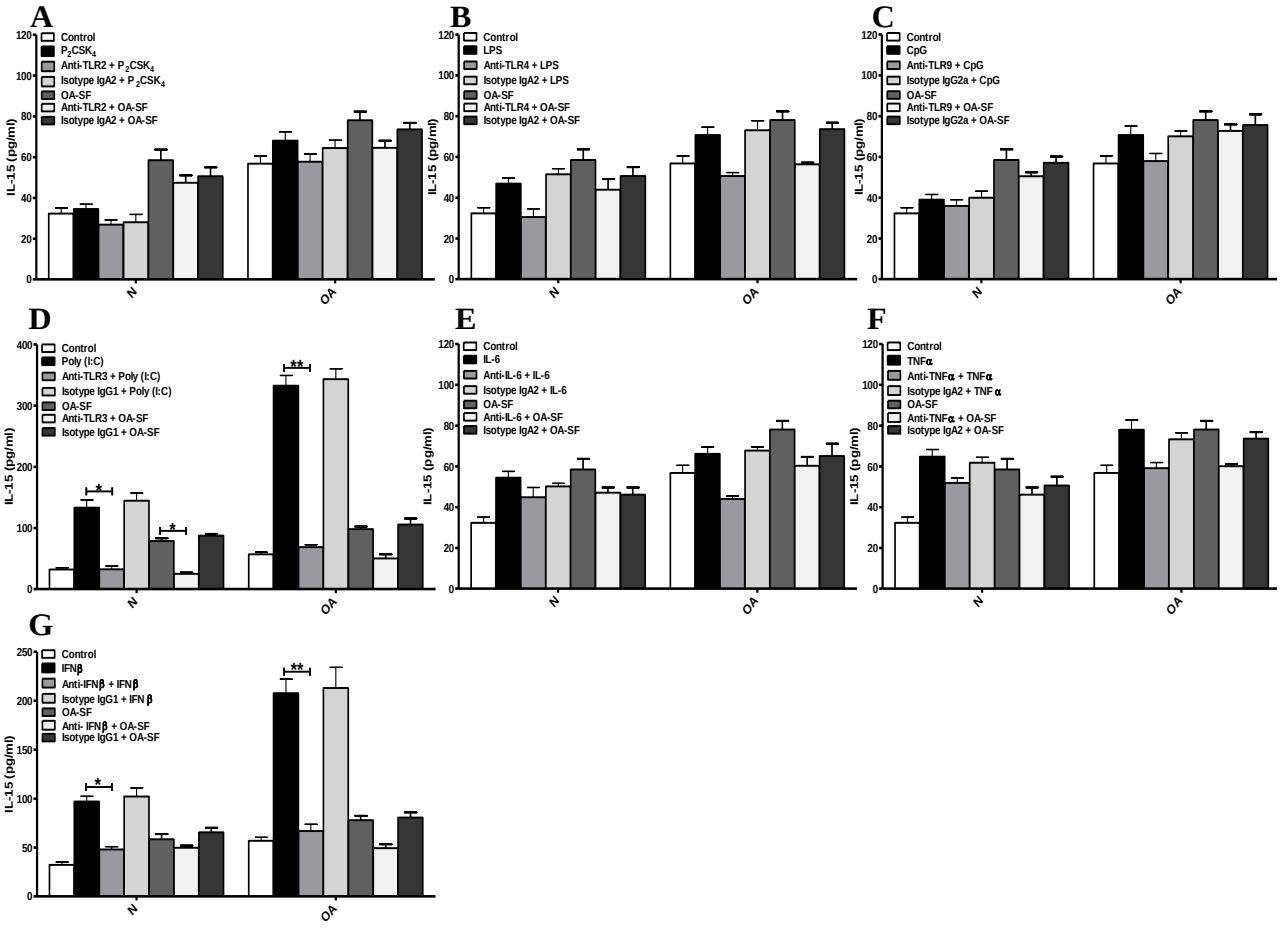

Figure 4.20: Analysis of the effect of anti-TLR/anti-cytokine antibodies on IL-15 secretion in N and OA FLS. (A-G) N-FLS and OA-FLS (n=3 for each cell type) were either pre-incubated with the respective TLR or cytokine-blocking/isotype control antibodies for 90 min prior to stimulation with the respective TLR ligand, cytokine or end-stage OA-SF (1:5 dilution in Opti-MEM, n=3) or stimulated with the respective ligand or left unstimulated for 16 h. (A) Cells were either pre-treated with anti-TLR2 antibody (5 µg/ml) or Isotype IgA2 antibody (5 µg/ml) prior to Pam_2CSK_4 (1 µg/ml) or OA-SF stimulation. (B) Cells were either pre-treated with anti-TLR4 antibody (5 µg/ml) or Isotype IgA2 antibody (5 µg/ml) prior to LPS (1 µg/ml) or OA-SF stimulation. (C) Cells were either pre-treated with anti-TLR9 antibody (15 µg/ml) or Isotype IgG2a antibody (15 µg/ml) prior to CpG (3 µg/ml) or OA-SF stimulation. (D) Cells were either pre-treated with anti-TLR3 antibody (20 µg/ml) or Isotype IgG1 antibody (20 µg/ml) prior to Poly (I:C) (10 µg/ml) or OA-SF stimulation. (E) Cells were either pre-treated with anti-IL-6 antibody (5 µg/ml) or Isotype IgA2 antibody (5 µg/ml) prior to IL-6 (100 pg/ml) or OA-SF stimulation. (F) Cells were either pre-treated with anti-TNFα antibody (5 µg/ml) or Isotype IgA2 antibody (5 µg/ml) prior to TNFα (1 ng/ml) or OA-SF stimulation. (G) Cells were either pre-treated with anti-IFNβ antibody (10 µg/ml) or Isotype IgG1 antibody (10 µg/ml) prior to IFNβ (100 pg/ml) or OA-SF stimulation. Cell free supernatants were analysed for levels of IL-15 by ELISA. All the data presented are representative of at least three independent experiments performed in triplicate (mean ± S.E.M). Data was subjected to an unpaired Student's t test. * $p<0.05$, ** $p<0.01$ denotes the level of significance relative to respective ligand stimulation.

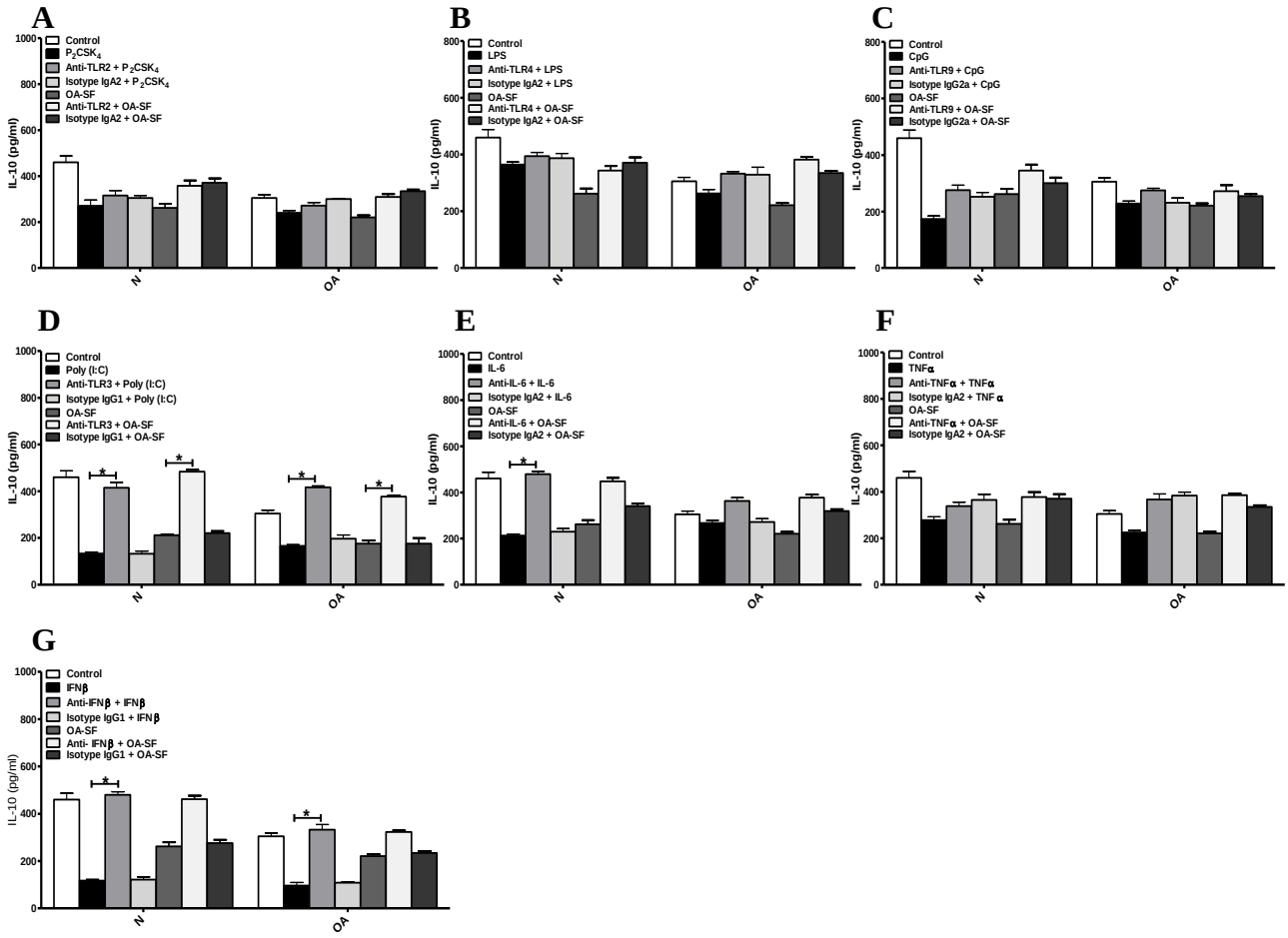

Figure 4.21: Analysis of the effect of anti-TLR/anti-cytokine antibodies on IL-10 secretion in N and OA FLS. (A-G) N-FLS and OA-FLS (n=3 for each cell type) were either pre-incubated with the respective TLR or cytokine-blocking/isotype control antibodies for 90 min prior to stimulation with the respective TLR ligand, cytokine or end-stage OA-SF (1:5 dilution in Opti-MEM, n=3) or stimulated with the respective ligand or left unstimulated for 16 h. (A) Cells were either pre-treated with anti-TLR2 antibody (5 µg/ml) or Isotype IgA2 antibody (5 µg/ml) prior to Pam_2CSK_4 (1 µg/ml) or OA-SF stimulation. (B) Cells were either pre-treated with anti-TLR4 antibody (5 µg/ml) or Isotype IgA2 antibody (5 µg/ml) prior to LPS (1 µg/ml) or OA-SF stimulation. (C) Cells were either pre-treated with anti-TLR9 antibody (15 µg/ml) or Isotype IgG2a antibody (15 µg/ml) prior to CpG (3 µg/ml) or OA-SF stimulation. (D) Cells were either pre-treated with anti-TLR3 antibody (20 µg/ml) or Isotype IgG1 antibody (20 µg/ml) prior to Poly (I:C) (10 µg/ml) or OA-SF stimulation. (E) Cells were either pre-treated with anti-IL-6 antibody (5 µg/ml) or Isotype IgA2 antibody (5 µg/ml) prior to IL-6 (100 pg/ml) or OA-SF stimulation. (F) Cells were either pre-treated with anti-TNFα antibody (5 µg/ml) or Isotype IgA2 antibody (5 µg/ml) prior to TNFα (1 ng/ml) or OA-SF stimulation. (G) Cells were either pre-treated with anti-IFNβ antibody (10 µg/ml) or Isotype IgG1 antibody (10 µg/ml) prior to IFNβ (100 pg/ml) or OA-SF stimulation. Cell free supernatants were analysed for levels of IL-10 by ELISA. All the data presented are representative of at least three independent experiments performed in triplicate (mean ± S.E.M). Data was subjected to an unpaired Student's t test. * $p<0.05$, ** $p<0.01$ denotes the level of significance relative to respective ligand stimulation.

4.4.7. Analysis of the effect of TLR3 blockade on TLR, cyto-chemokine and MMP gene expression and on the levels of pro-inflammatory cyto-chemokine secretion in N-FLS

Given our previous observations of the probable immunomodulatory role of TLR3 blockade on inflammatory mediators secretion in FLS (section 4.4.6), and to further corroborate our observation that grade-specific OA-SF predominantly induces TLR3 expression (section 4.4.5), it was critical to further investigate the mRNA and protein expression profiles of critical inflammatory mediators in FLS upon grade-specific OA-SF stimulations with/without anti-TLR3 antibody pre-treatment. Hence, the ability of an anti-TLR3 antibody to modulate Poly(I:C) and grade-specific OA-SF induced TLR3, TRIF, inflammatory cytokine, chemokine and MMP gene and protein expression in N-FLS was evaluated by employing Real time RT-PCR and ELISA.

4.4.7.1. Modulation of TLR3 and TRIF gene expression by TLR3 blockade in FLS

Given the pivotal role for RNA viruses in arthritis progression, and having observed the ability of Poly (I:C)/late stage OA-SF to induce the key inflammatory cyto-chemokines (section 4.4.6) and differential TLR3 mRNA expression in FLS (section 4.4.5), it was essential to further investigate the effects of TLR3 blockade on the expression of viral receptors and adaptor molecules, which facilitate the initiation of signalling cascades which may lead to synovitis and OA. Therefore, the mRNA expression levels of TLR3, RIG-I, MDA5, TRIF (which recognizes (dsRNA)/Poly(I:C)/OA-SF) and recruits TRIF adaptor, was investigated in N-FLS upon grade-specific OA-SF stimulation with/without prior anti-TLR3 antibody pre-treatment. It was found that stimulation with grade-specific OA-SF did not induce any noticeable levels of RIG-I or MDA-5 mRNA expression, so they were not studied further (data not shown). Interestingly, a trend towards increased TLR3 and TRIF mRNA expression was evident in N-FLS upon stimulation with progressive grades of OA-SFs (grades 1-4) relative to grade-0 stimulation and also upon Poly(I:C) stimulation relative to control(Figure 4.22, panels A and B, n=3). A trend towards suppressed TLR3 and TRIF mRNA expression was observed in N-FLS pre-treated with anti-TLR3 antibody, prior to Poly (I:C) or grade-specific OA-SF stimulation. A significant 3-fold suppression in TLR3 mRNA expression was observed in N-FLS pre-treated with anti-TLR3 antibody, prior to Poly (I:C) stimulation ($p \leq 0.05$). Similarly, in N-FLS pre-treated with anti-TLR3 antibody, a significant 3.7-fold suppression in TLR3

mRNA expression was evident with grade-2 OA-SF stimulation and a 2.9-fold suppression with grade-4 OA-SF stimulation ($p \leq 0.05$). A non-significant decrease in TLR3 mRNA expression was also evident in N-FLS pre-treated with anti-TLR3 antibody following stimulations with grade-1 and grade-3 OA-SF (Figure 4.22, panel A). Likewise, a significant 3.8-fold suppression in TRIF mRNA expression was observed in N-FLS pre-treated with anti-TLR3 antibody, prior to Poly (I:C) stimulation ($p \leq 0.05$). Similarly, in N-FLS pre-treated with anti-TLR3 antibody, a significant 3-fold suppression in TRIF mRNA expression was evident with grade-2 OA-SF stimulation and a 3.4-fold suppression with grade-4 OA-SF stimulation ($p \leq 0.05$), and a non-significant decrease in TRIF mRNA expression was also evident in N-FLS pre-treated with anti-TLR3 antibody following stimulations with grade-1 and grade-3 OA-SF (Figure 4.22, panel B). Thus, these data provide an evidence for sustained activation of TLR3 and TRIF in FLS through dsRNA/ RNA from the necrotic cells in the OA synovial fluid and their modulation by utilising anti-TLR3 antibody, possibly through neutralising/blocking surface bound TLR3 in FLS and this correlates with previous findings (Zhu et al., 2011).

4.4.7.2. Modulation of pro-inflammatory cyto-chemokine gene expression by TLR3 blockade in FLS

Given the evidence that grade-specific OA-SFs has the ability to distinctively and predominantly activate TLR3 and TRIF in FLS and that this process is inhibited by an anti-TLR3 antibody (Figure 4.22), it was essential to investigate the ability of grade-specific OA-SFs to induce key TLR3 dependent inflammatory cyto-chemokines namely, IFNβ, TNFα, IP-10, RANTES (chapter 3, Figure 3.6) mRNA expression and to investigate their modulation by TLR3 blockade in N-FLS. Interestingly, a trend towards increased IFNβ, TNFα, IP-10 and RANTES mRNA expression was observed in N-FLS upon stimulation with progressive grades of OA-SFs (grades 1-4) relative to grade-0 stimulation and also upon Poly(I:C) stimulation relative to control (Figure 4.23, panels A, B, C and D, n=3). An increased trend towards suppressed IFNβ, TNFα, IP-10 and RANTES mRNA expression was observed in N-FLS pre-treated with anti-TLR3 antibody followed by progressive OA grades (grades 1-4) OA-SF stimulation or Poly(I:C) stimulation. N-FLS pre-treated with an anti-TLR3 antibody showed a significant 11.6-fold suppression in IFNβ mRNA expression upon grade-1 OA-SF stimulation, a significant 11.5-fold suppression upon grade-2 OA-SF stimulation, a significant 10-fold suppression upon grade-3 OA-SF stimulation, and the most significant 12.4-fold suppression upon grade-4 OA-SF stimulation relative to

respective grade-specific OA-SF stimulations, and also a 2.7-fold suppression in IFNβ mRNA expression was evident in N-FLS upon anti-TLR3 antibody pre-treatment followed by Poly (I:C) stimulation (Figure 4.23, panel A, $p \leq 0.05$). Similarly, N-FLS pre-treated with an anti-TLR3 antibody showed a significant 5.4-fold suppression in TNFα mRNA expression upon grade-1 OA-SF stimulation, a significant 7-fold suppression upon grade-2 OA-SF stimulation, a significant 7.2-fold suppression upon grade-3 OA-SF stimulation, and the most significant 17.8-fold suppression in TNF mRNA expression upon grade-4 OA-SF stimulation ($p \leq 0.01$), relative to respective grade-specific OA-SF stimulations and also a 4-fold suppression in TNFα mRNA expression was evident in N-FLS upon anti-TLR3 antibody pre-treatment followed by Poly (I:C) stimulation (Figure 4.23, panel B, $p \leq 0.05$). Likewise, N-FLS pre-treated with an anti-TLR3 antibody showed a significant 10-fold suppression in IP-10 mRNA expression upon grade-1 OA-SF stimulation, a significant 6-fold suppression upon grade-2 OA-SF stimulation, a highest and most significant 12-fold suppression upon grade-3 OA-SF stimulation, and a significant 7-fold suppression upon grade-4 OA-SF stimulation, relative to respective grade-specific OA-SF stimulations. Also, a 3.4-fold suppression in IP-10 mRNA expression was evident in N-FLS upon anti-TLR3 antibody pre-treatment followed by Poly (I:C) stimulation (Figure 4.23, panel C, $p \leq 0.05$). N-FLS pre-treated with an anti-TLR3 antibody showed a significant 5.9-fold suppression in RANTES mRNA expression upon grade-1 OA-SF stimulation, a significant 6.1-fold suppression upon grade-2 OA-SF stimulation, a significant 6.7-fold suppression upon grade-3 OA-SF stimulation, and the most significant 7-fold suppression of RANTES mRNA expression was evident upon grade-4 OA-SF stimulation, relative to respective grade-specific OA-SF stimulations. Also, a 4.3-fold suppression in RANTES mRNA expression was evident in N-FLS upon anti-TLR3 antibody pre-treatment followed by Poly (I:C) stimulation (Figure 4.23, panel D, $p \leq 0.05$). These data suggest that TLR3 blockade in OA facilitates the suppression of key inflammatory cyto-chemokine mRNA expression in FLS that may be induced upon contact of the FLS with OA-SF and so mimicks the physiological cell-fluid contact that may occur within the OA joint. These data in-part correlates with a previous finding (Zhu et al., 2011).

4.4.7.3. Modulation of pro-inflammatory MMP 3, 9, 13 gene expression by TLR3 blockade in FLS

The ability of an anti-TLR3 antibody to modulate matrix degrading enzymes such as MMP 3, 9, 13, associated with cartilage destruction (Yamanishi et al., 2002) was investigated. Previously, we have shown a TLR3 dependent induction of these MMPs in FLS (chapter 3, Figure 3.14 and 3.15; chapter 4, Figure 4.4 and 4.9). Herein, the ability of grade-specific OA-SFs to induce MMPs 3, 9 and 13 mRNA expression and their modulation by TLR3 blockade in N-FLS was investigated. Interestingly, a trend towards increased MMPs 3 , 9 and 13 mRNA expression was observed in N-FLS upon stimulation with progressive grades of OA-SFs (grades 1-4) relative to grade-0 stimulation and also upon Poly(I:C) stimulation relative to control (Figure 4.24, panels A, B, and C, n=3). A trend towards suppressed MMPs 3 , 9 and 13 mRNA expression was observed in N-FLS pre-treated with an anti-TLR3 antibody followed by stimulation with progressive grades (grades 1-4) of OA-SF or with Poly(I:C). Herein, N-FLS pre-treated with anti-TLR3 antibody showed a significant 9.8-fold suppression in MMP-3 mRNA expression upon grade-1 OA-SF stimulation, a significant 11.1-fold suppression upon grade-2 OA-SF stimulation, a significant 10.1-fold suppression upon grade-3 OA-SF stimulation, and a significant 9-fold suppression upon grade-4 OA-SF stimulation relative to respective grade-specific OA-SF stimulations, and also a 5.6-fold suppression in MMP-3 mRNA expression was evident in N-FLS upon anti-TLR3 antibody pre-treatment followed by Poly (I:C) stimulation (Figure 4.24, panel A, $p \leq 0.05$). Similarly, N-FLS pre-treated with anti-TLR3 antibody showed a 4-fold suppression in MMP-9 mRNA expression upon grade-1 OA-SF stimulation, a significant 7-fold suppression upon grade-2 OA-SF stimulation, a 5.8-fold suppression upon grade-3 OA-SF stimulation, and the most significant 7.5-fold suppression upon grade-4 OA-SF stimulation, relative to respective grade-specific OA-SF stimulations. Also, an 8.4-fold suppression in MMP-9 mRNA expression was evident in N-FLS upon anti-TLR3 antibody pre-treatment followed by Poly (I:C) stimulation (Figure 4.24, panel B, $p \leq 0.05$). Also, N-FLS pre-treated with an anti-TLR3 antibody showed a significant 6-fold suppression in MMP-13 mRNA expression upon grade-1 OA-SF stimulation, a significant 4-fold suppression upon grade-2 OA-SF stimulation, a significant 4-fold suppression upon grade-3 OA-SF stimulation, and the most significant 7-fold suppression upon grade-4 OA-SF stimulation, relative to respective grade-specific OA-SF stimulations and a 7.2-fold suppression in MMP-13 mRNA expression was evident in N-FLS upon anti-TLR3 antibody pre-treatment followed by Poly (I:C) stimulation (Figure 4.24, panel C, $p \leq 0.05$).

Thus, we propose that either Poly(I:C) or RNA from necrotic cells which may be present in OA-SF predominantly induces secretion of the catabolic MMP3, 9,13 in FLS. These data substantiate our previous observations that these MMPs can be induced, particularly by Poly (I:C)/RNA in OA-SF (Figure 4.4, 4.9) through a mechanism that involves TLR3 in FLS. Thus, TLR3 may be a critical target for OA disease intervention. These data in-part correlates with a previous finding (Zhu et al., 2011).

4.4.7.4. Effect of TLR3 blockade on the levels of pro-inflammatory cyto-chemokine secretion in N-FLS

Given the ability of grade-specific OA-SFs to induce key inflammatory mediator genes in N-FLS and given the immuno-modulatory effects of TLR3 blockade on the gene expression of TLR3 and key inflammatory mediators (Figure 4.22, 4.23 and 4.24), it was essential to investigate the levels of pro-inflammatory cyto-chemokine secretion in N-FLS. To this end, the ability of an anti-TLR3 antibody to modulate Poly(I:C) and grade-specific OA-SF induced IFNβ, RANTES, TNFα, IL-6, IL-10, IL-1β and IL-15 protein expression profiles in N-FLS was evaluated using ELISA (Figure 4.25; panels A, B, C, D, E, F and G; n=3). It was found that stimulation with grade-specific OA-SF induced notable levels of IFNβ, RANTES, TNFα, IL-6, IL-1β, IL-15 and suppressed IL-10 levels in a TLR3 dependent manner as the anti-TLR3 antibody utilised in this study did revert this effect of OA-SF, thus substantiating our previous observation (section 4.4.6) that, neutralisation of TLR3 expression utilising anti-TLR3 antibody, predominantly shifts the balance from pro-inflammatory to an anti-inflammatory cytokine milieu. Wherein, a highest and most significant decrease in IFNβ, RANTES, TNFα, IL-6, IL-1β, IL-15 levels and increase in IL-10 levels was evident in N-FLS upon anti-TLR3 antibody pre-treatment followed by Poly (I:C) stimulation ($p \leq 0.01$). Interestingly, N-FLS pre-treated with anti-TLR3 antibody showed a significant suppression in IFNβ, RANTES, TNFα, IL-6, IL-1β, IL-15 levels and an increase in IL-10 levels respectively, primarily upon grade-1 and grade-4 OA-SF stimulations, although a similar, but non-significant level of modulation of these inflammatory mediators was also evident following pre-treatment of N-FLS with an anti-TLR3 antibody followed by grade-2 and grade-3 OA-SF stimulations (Figure 4.25, panels A, B, C, D, E, F and G, $p \leq 0.05$). These data provide evidence to support the hypothesis that early modulation of inflammatory milieu through TLR3 blockade may be therapeutically beneficial and corroborates with our previous observations (section 4.4.6).

Together, these data further provide evidence for the immune-modulatory effects of TLR3 blockade in OA possibly through regulating the balance between catabolic and anabolic pathways and mediators, through suppression of key inflammatory cyto-chemokine- MMP mRNA and protein expression in FLS, which are otherwise induced upon contact with the

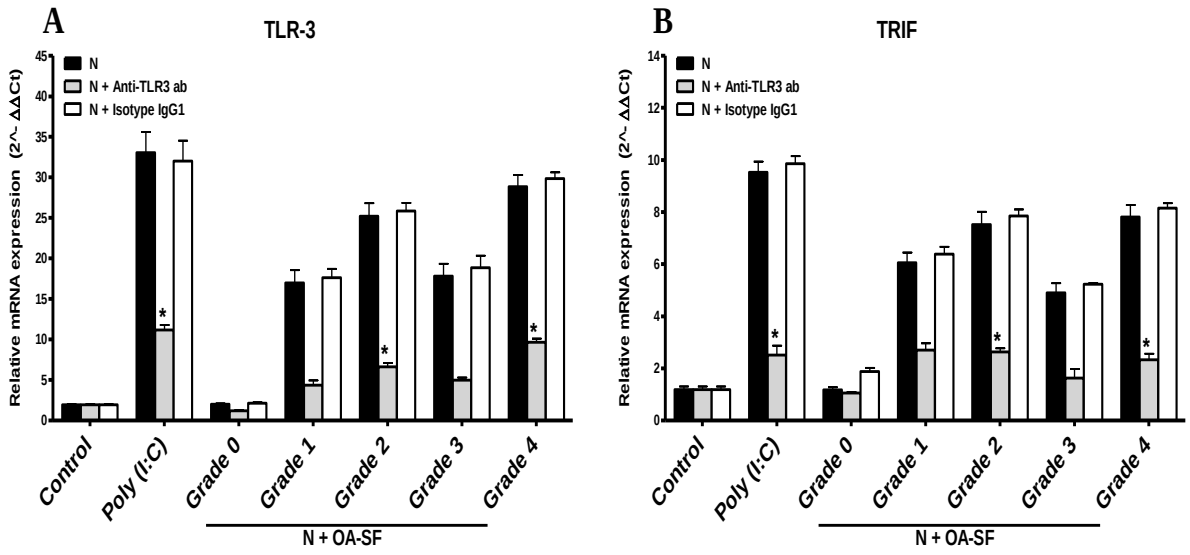

Figure 4.22: Modulation of TLR3 and TRIF gene expression by TLR3 blockade in FLS. N-FLS (n=3), were pre-treated with anti-TLR3 antibody (20 µg/ml) or Isotype IgG1 antibody (20 µg/ml) for 90 min prior to Poly (I:C) (10 µg/ml) or grade-specific (grade-0, 1, 2, 3, 4) OA-SF (1:5 dilution in Opti-MEM, n=3) stimulation for 16 h. (A-B) Total RNA was isolated from control and stimulated N-FLS and used as a template for quantitative real-time RT-PCR to assay the mRNA expression levels of TLR3 (A) and TRIF (B) relative to the housekeeping gene HPRT and are expressed relative to normalised values from unstimulated or control cells. All the data presented are representative of at least three independent experiments performed in triplicate (mean ± S.E.M). Data was subjected to an unpaired Student's t test. * $p<0.05$ denotes the level of significance relative to respective ligand stimulation.

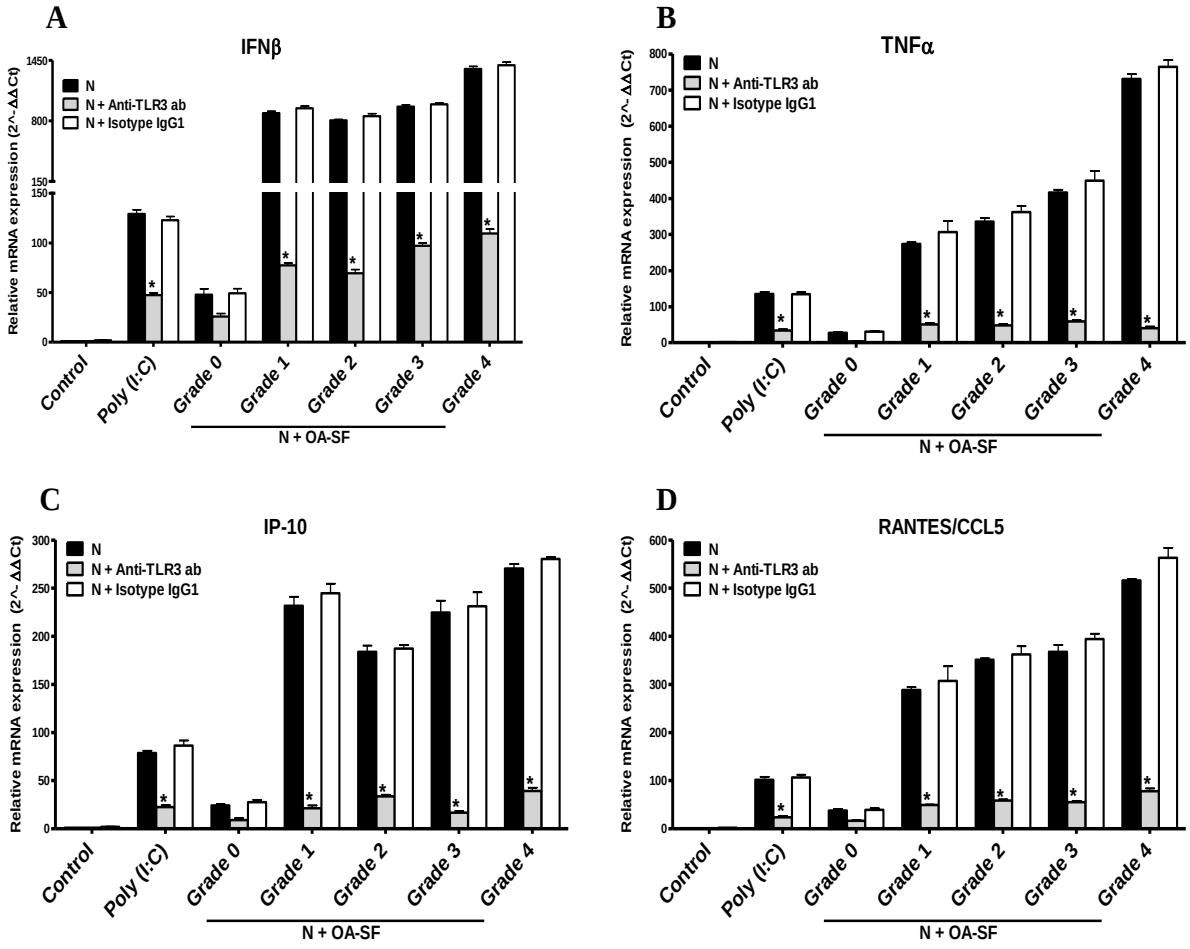

Figure 4.23: Modulation of pro-inflammatory cyto-chemokine gene expression by TLR3 blockade in FLS. (A-D) N-FLS (n=3), were pre-treated with anti-TLR3 antibody (20 µg/ml) or Isotype IgG1 antibody (20 µg/ml) for 90 min prior to Poly (I:C) (10 µg/ml) or grade-specific (grade-0, 1, 2, 3, 4) OA-SF (1:5 dilution in Opti-MEM, n=3) stimulation for 16 h. Total RNA was then isolated from control and stimulated N-FLS, and used as a template for quantitative real-time RT-PCR to assay the mRNA expression levels of IFNβ (A), TNFα (B), IP-10 (C), RANTES (D). The levels of the relevant mRNAs were normalised relative to the housekeeping gene HPRT and are expressed relative to normalised values from unstimulated or control cells. All the data presented are representative of at least three independent experiments performed in triplicate (mean ± S.E.M). Data was subjected to an unpaired Student's t test. * $p<0.05$ denotes the level of significance relative to respective ligand stimulation.

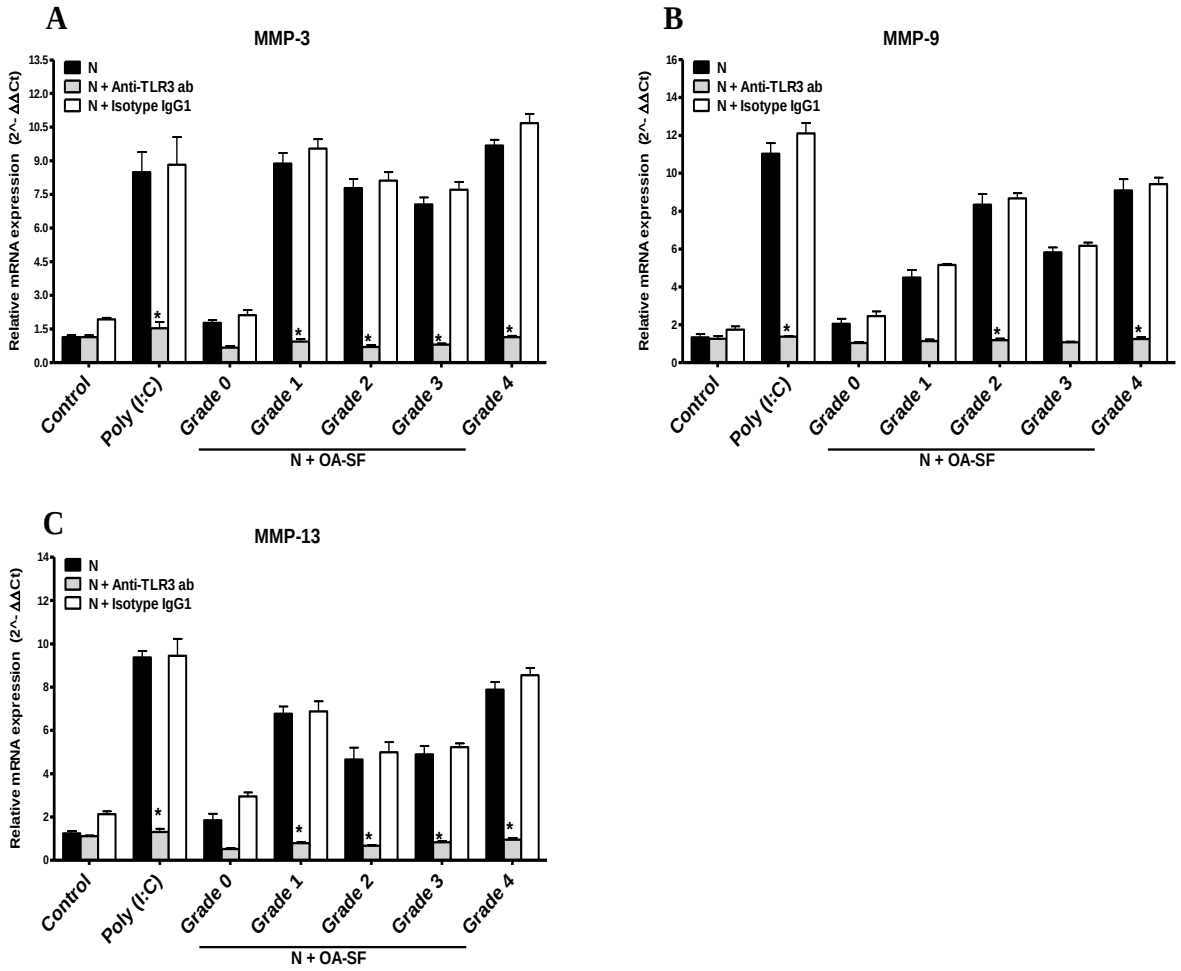

Figure 4.24: Modulation of pro-inflammatory MMP 3, 9, 13 gene expression by TLR3 blockade in FLS. (A-C) N-FLS (n=3), were pre-treated with an anti-TLR3 antibody (20 µg/ml) or Isotype IgG1 antibody (20 µg/ml) for 90 min prior to Poly (I:C) (10 µg/ml) or grade-specific (grade-0, 1, 2, 3, 4) OA-SF (1:5 dilution in Opti-MEM, n=3) for 16 h. Total RNA was then isolated from control and stimulated N-FLS, and used as a template for quantitative real-time RT-PCR to assay the mRNA expression levels of MMP-3 (A), MMP-9 (B) and MMP-13 (C). The levels of the relevant mRNAs were normalised relative to the housekeeping gene HPRT and are expressed relative to normalised values from unstimulated or control cells. All the data presented are representative of at least three independent experiments performed in triplicate (mean ± S.E.M). Data was subjected to an unpaired Student's t test. * $p<0.05$ denotes the level of significance relative to respective ligand stimulation.

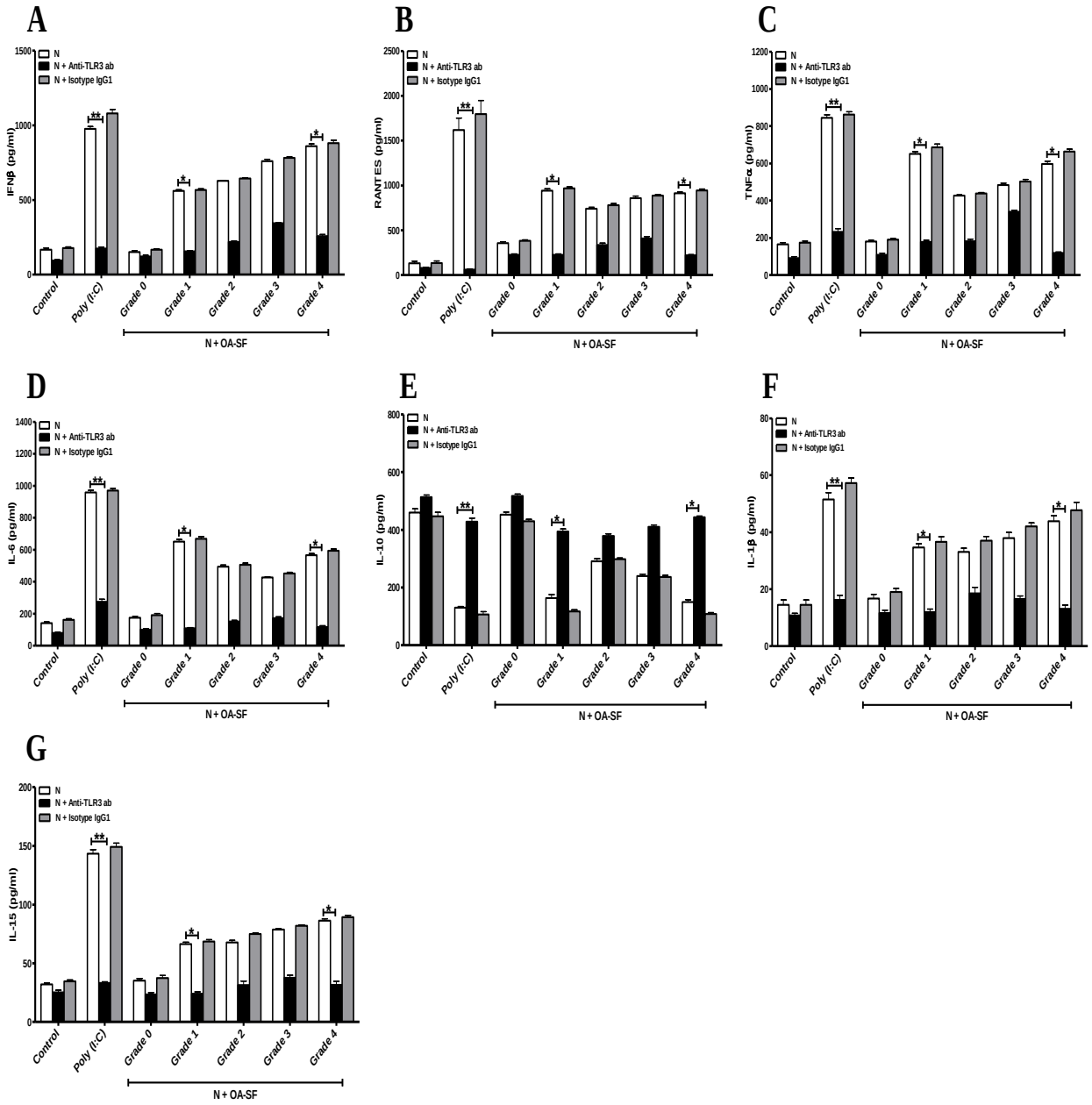

Figure 4.25: Analysis of the effect of TLR3 blockade on the levels of pro-inflammatory cyto-chemokine secretion in N-FLS. (A-G) N-FLS (n=3) were pre-incubated with an anti-TLR3 antibody (20 µg/ml) or Isotype IgG1 antibody (20 µg/ml) for 90 min prior to Poly (I:C) (10 µg/ml) or grade-specific (grade-0, 1, 2, 3, 4) OA-SF (1:5 dilution in Opti-MEM, n=3) stimulation for 16 h. Cell free supernatants were analysed for levels of IFNβ (A), RANTES (B), TNFα (C), IL-6 (D), IL-10 (E), IL-1β (F), IL-15 (G) by ELISA. All the data presented are representative of at least three independent experiments performed in triplicate (mean ± S.E.M). Data was subjected to an unpaired Student's t test. * $p<0.05$, ** $p<0.01$ denotes the level of significance relative to respective ligand stimulation.

inflammatory OA-SF, thus mimicking the physiological cell-fluid contact in the joint. These data in-part correlates with a previous finding (Zhu et al., 2011, Nair et al., 2012), and thus provide TLR3 as a critical target for OA disease intervention.

4.4.8. *Ex-vitro* analysis of the effect of TLR3 blockade on Poly (I:C) induced pro and anti-inflammatory cytokine, chemokine and MMP levels in early and late OA-patient derived synovial tissue FLS

Given the previous observation that TLR3 blockade modulates TLR3-induced inflammatory cyto-chemokine-MMP, mRNA and protein expression profiles in N-FLS following Poly(I:C) and grade-specific OA-SF stimulations (section 4.4.7), it was essential to evaluate the immunomodulatory effects of TLR3 blockade on Poly (I:C) induced secretion of pro and anti-inflammatory mediators in stage-specific FLS. This aspect of the study would aid in the assessment of TLR3 as a therapeutic target for the management of early OA disease.

4.4.8.1. Modulation of Poly (I:C) induced pro-inflammatory cyto-chemokine secretion by TLR3 blockade in early and late OA-FLS

Initially, early (Grade 1-2) and late (Grade 3-4) stage OA synovial biopsy derived FLS (n=3/grade), were pre-incubated with anti-TLR3 antibody (20 µg/ml) or Isotype IgG1 antibody (20 µg/ml) for 90 min prior to Poly (I:C) (10 µg/ml) stimulation for 24 h or non unstimulated followed by measurement of Poly (I:C) induced IL-6, IL-8, IL-1β and TNF-α levels (Figure 4.26, panel A, B, C and D, n=3). Interestingly, in both early and late OA-FLS, a significant decrease in IL-6, IL-8, IL-1β and TNF-α levels were evident upon pre-treatment of cells with an anti-TLR3 antibody followed by Poly (I:C) stimulation when compared to non-pre-treated cells. Of the cytokines measured in this study, the most significant anti-TLR3 antibody mediated suppressive effects were evident with IL-6 in both early and late OA-FLS relative to Poly (I:C) stimulation (anti-TLR3 ab + Poly(I:C) Vs Poly(I:C)) (Early: 797.43 ± 102.5 Vs 3437.27 ± 220 pg/ml and Late: 1126.17 ± 187.5 Vs 4275.72 ± 225 pg/ml, $p \leq 0.01$, Figure 4.26, panel A). Likewise, a significant suppression in IL-8 levels was observed in both early and late OA-FLS upon anti-TLR3 antibody pre-treatment of Poly (I:C) stimulated cells (anti-TLR3 ab + Poly(I:C) Vs Poly(I:C)) (Early: 524.69 ± 67.5 Vs 3212.92 ± 260 pg/ml; ($p \leq 0.01$) and Late: 1860.71 ± 67.5 Vs 3944.18 ± 175 pg/ml; ($p \leq 0.05$), Figure 4.26, panel B). Similarly, a significant suppression in IL-1β levels was evident in both early and late OA-FLS upon anti-TLR3

antibody pre-treatment of cells with Poly (I:C) (anti-TLR3 ab + Poly(I:C) Vs Poly(I:C)) (Early: 6.87 ± 1.01 Vs 22.89 ± 2.0 pg/ml and Late: 15.07 ± 1.3 Vs 31.35 ± 1.0 pg/ml, $p \leq 0.05$, Figure 4.26, panel C). Also, a significant decrease in TNFα levels was evident in both early and late OA-FLS following anti-TLR3 antibody pre-treatment of cells prior to Poly (I:C) stimulation (anti-TLR3 ab + Poly(I:C) Vs Poly(I:C)) (Early: 8.91 ± 1.01 Vs 33.48 ± 3.0 pg/ml; ($p \leq 0.05$) and Late: 14.75 ± 3 Vs 60.81 ± 2.5 pg/ml; ($p \leq 0.01$), Figure 4.26, panel D). Interestingly, a significant induction of pro-inflammatory IL-6, IL-8, IL-1β and TNFα secretions in early and late OA-FLS was observed upon Poly(I:C) stimulation and correlates with our previous findings (section 4.4.2); this effect was modulated by TLR3 blockade utilising an anti-TLR3 antibody and further substantiates our previous observations (section 4.4.7). Together, these data suggests a probable immunomodulatory role for TLR3 blockade, even at the early stages of OA.

4.4.8.2. Modulation of Poly (I:C) induced IFNβ and RANTES secretion by TLR3 blockade in early and late OA-FLS

Given the previous modulatory effects of TLR3 blockade on IFNβ and RANTES mRNA and protein levels in N-FLS upon Poly(I:C) and grade-specific OA-SF stimulations (Figure 4.23 and 4.25), it was essential to evaluate the effect of TLR3 blockade on TLR3 dependent inflammatory mediator secretion using stage-specific OA patient-derived synovial FLS, towards a better understand of the association between TLR3 and OA progression. It was found that, in both early and late OA-FLS, a significant suppression in IFNβ and RANTES levels was evident upon anti-TLR3 antibody pre-treatment of Poly (I:C) stimulated FLS compared to non-pretreated cells (Figure 4.27, panels A and B, n=3). A significant decrease in IFNβ levels was evident in both early and late OA-FLS upon anti-TLR3 antibody pre-treatment of Poly (I:C) stimulated FLS when compared to non-pre-treated cells (anti-TLR3 ab + Poly(I:C) Vs Poly(I:C)) (Early: 265.21 ± 48.5 Vs 1439.65 ± 75 pg/ml and Late: 482.13 ± 64.99 Vs 1700.66 ± 29 pg/ml, $p \leq 0.01$, Figure 4.27, panel A). Likewise, a significant suppression of RANTES levels was evident in both early and late OA-FLS upon anti-TLR3 antibody pre-treatment of Poly (I:C) stimulated cells when compared to non-pre-treated cells (anti-TLR3 ab + Poly(I:C) Vs Poly(I:C)) (Early: 266.09 ± 45.0 Vs 1459.78 ± 75 pg/ml; ($p \leq 0.05$) and Late: 423.65 ± 67.5 Vs 2124.18 ± 100 pg/ml; ($p \leq 0.01$), Figure 4.27, panel B). Interestingly, a significant induction of pro-inflammatory IL-6, IL-8, IL-1β and TNFα secretions by early and late OA-FLS observed upon Poly(I:C) stimulation which correlates with our previous findings

(section 4.4.2) and this effect was modulated by TLR3 blockade utilising an anti-TLR3 antibody; this further substantiates our previous observations (section 4.4.7). Thus, these data suggest a probable immunomodulatory role for TLR3 blockade, even at the early stages of OA. These data suggests a TLR3 dependent induction of these potent inflammatory mediators even at the early stages of OA-onset and these cytokine levels can be modulated by TLR3 blockade in FLS.

.

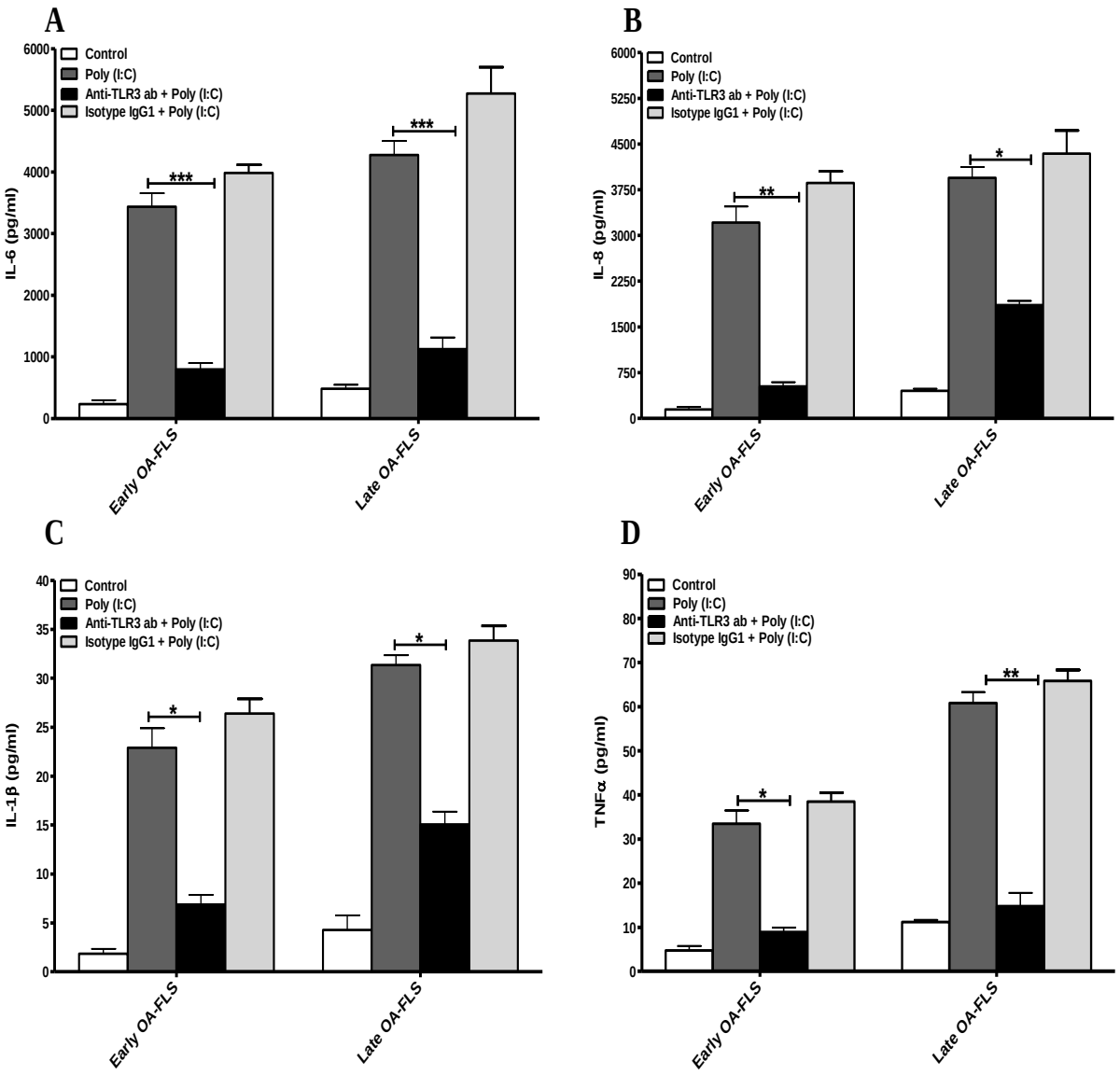

Figure 4.26: Modulation of Poly (I:C) induced pro-inflammatory cyto-chemokine secretion by TLR3 blockade in early and late OA-FLS. (A-D) Early (Grade 1-2) and Late (Grade 3-4) stage OA synovial biopsy derived FLS (n=3), were pre-incubated with anti-TLR3 antibody (20 µg/ml) or Isotype IgG1 antibody (20 µg/ml) for 90 min prior to Poly (I:C) (10 µg/ml) stimulation for 24 h. Cell free supernatants were analyzed for (A) IL-6, (B) IL-8, (C) IL-1β and (D) TNFα by MSD ultrasensitive multiplex ELISA system. All the data presented are representative of at least one independent experiment performed in duplicate (mean ± S.E.M). Data was subjected to an unpaired Student's t test. * $p<0.05$, ** $p<0.01$, *** $p<0.001$ denotes the level of significance relative to respective cell type Poly (I:C) stimulation.

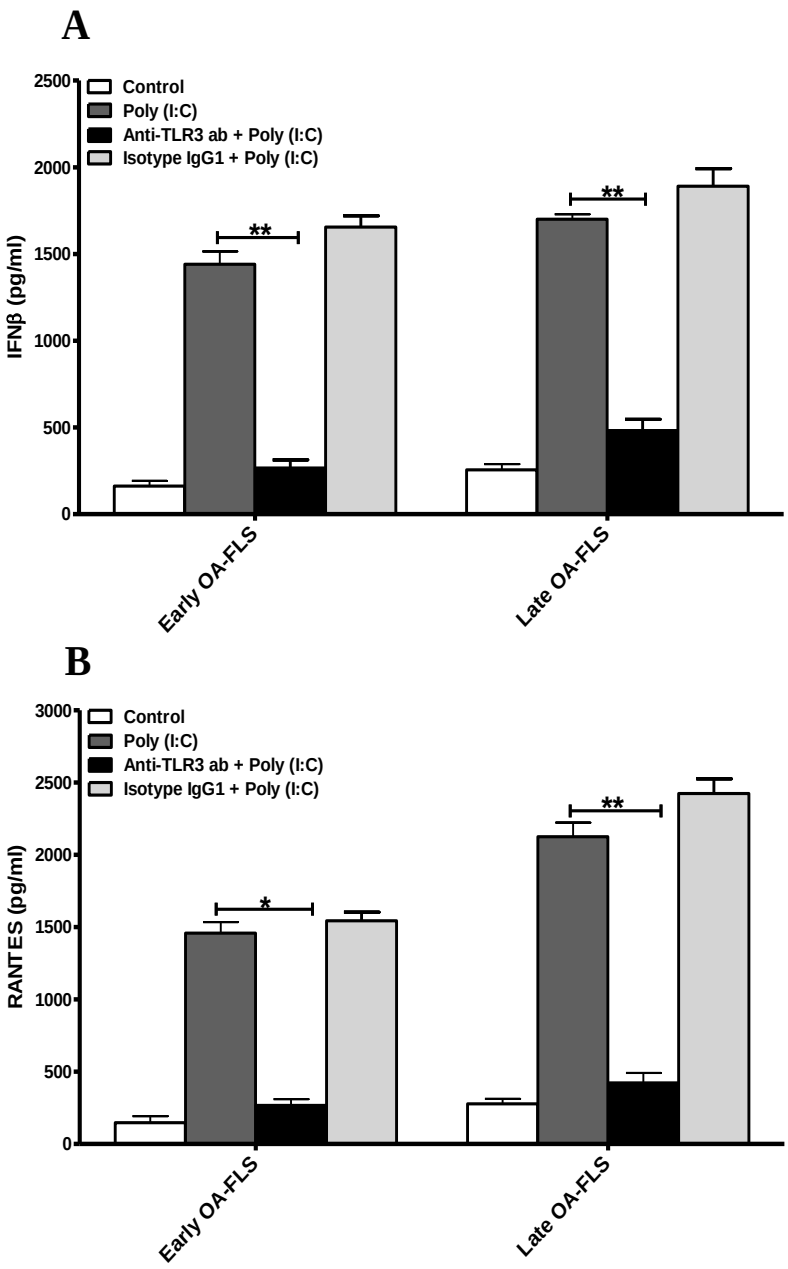

Figure 4.27: Modulation of Poly (I:C) induced IFNβ and RANTES secretion by TLR3 blockade in early and late OA-FLS. (A-B) Early (Grade 1-2) and Late (Grade 3-4) stage OA synovial biopsy derived FLS (n=3), were pre-incubated with anti-TLR3 antibody (20 µg/ml) or Isotype IgG1 antibody (20 µg/ml) for 90 min prior to Poly (I:C) (10 µg/ml) stimulation for 24 h. Cell free supernatants were analyzed for (A) IFNβ and (B) RANTES by MSD ELISA system. All the data presented are representative of at least three independent experiments performed in duplicate (mean ± S.E.M). Data was subjected to an unpaired Student's t test. * $p<0.05$, ** $p<0.01$ denotes the level of significance relative to respective cell type Poly (I:C) stimulation.

4.4.8.3. Modulation of Poly (I:C) induced IL-10, IFNγ and IL-12p70 secretion by TLR3 blockade in early and late OA-FLS

Given the previous observation that TLR3 ligand Poly(I:C) predominantly induces an imbalance in the levels of pro vs anti-inflammatory mediators in early and late stage FLS (Figure 4.8) and given the immuno-modulatory effects of TLR3 blockade in inducing IL-10 levels in N-FLS (Figure 4.25), it was essential to investigate the effect of TLR3 blockade in inducing/suppressing the key immune-regulatory cytokines, namely IL-12 p70 and IFNγ and anti-inflammatory IL-10 in stage/grade-specific OA-FLS, towards further understanding the role of TLR3 at the various stages of OA progression. Interestingly, both early and late OA-FLS showed a significant increase in IL-10, IFNγ and IL-12p70 levels upon pre-incubation with an anti-TLR3 antibody followed by Poly (I:C) stimulation when compared to non-pre-treated FLS cells (Figure 4.28, panels A, B and C, n=3). A significant increase in IL-10 levels was observed in both early and late OA-FLS upon anti-TLR3 antibody pre-treatment prior to Poly (I:C) stimulation when compared to non-pre-treated cells (anti-TLR3 ab + Poly(I:C) Vs Poly(I:C)) (Early: 17.13 ± 1.8 Vs 2.33 ± 0.5 pg/ml; ($p \leq 0.01$) and Late: 14.06 ± 1.49 Vs 4.28 ± 0.30 pg/ml; ($p \leq 0.05$), Figure 4.28, panel A).

Likewise, a significant upregulation in IFNγ levels was observed in early OA-FLS and a notable increase in late OA-FLS was evident, upon anti-TLR3 antibody pre-treatment prior to Poly (I:C) stimulation (anti-TLR3 ab + Poly(I:C) Vs Poly(I:C)) (Early: 20.73 ± 2 Vs 6.86 ± 1pg/ml; ($p \leq 0.05$) and Late: 12.12 ± 1 Vs 5.57 ± 1.02 pg/ml, Figure 4.28, panel B). Also, a significant increase in IL-12p70 levels was evident in both early and late OA-FLS upon pre-treatment with an anti-TLR3 antibody prior to Poly (I:C) stimulation (anti-TLR3 ab + Poly(I:C) Vs Poly(I:C)) (Early: 20.54 ± 0.99 Vs 7.08 ± 1.5 pg/ml and Late: 15.34 ± 1.5 Vs 4.09 ± 0.5 pg/ml, $p \leq 0.05$, Figure 4.28, panel C). Interestingly, a significant induction of such immuno-regulatory and anti-inflammatory cytokine secretions by early and late OA-FLS upon TLR3 blockade further substantiates our hypothesis that IL-10, IFNγ and IL-12p70 levels in OA synovium or fluid or FLS are critically modulated by TLR3 (Figures 4.3, 4.8 and 4.12).

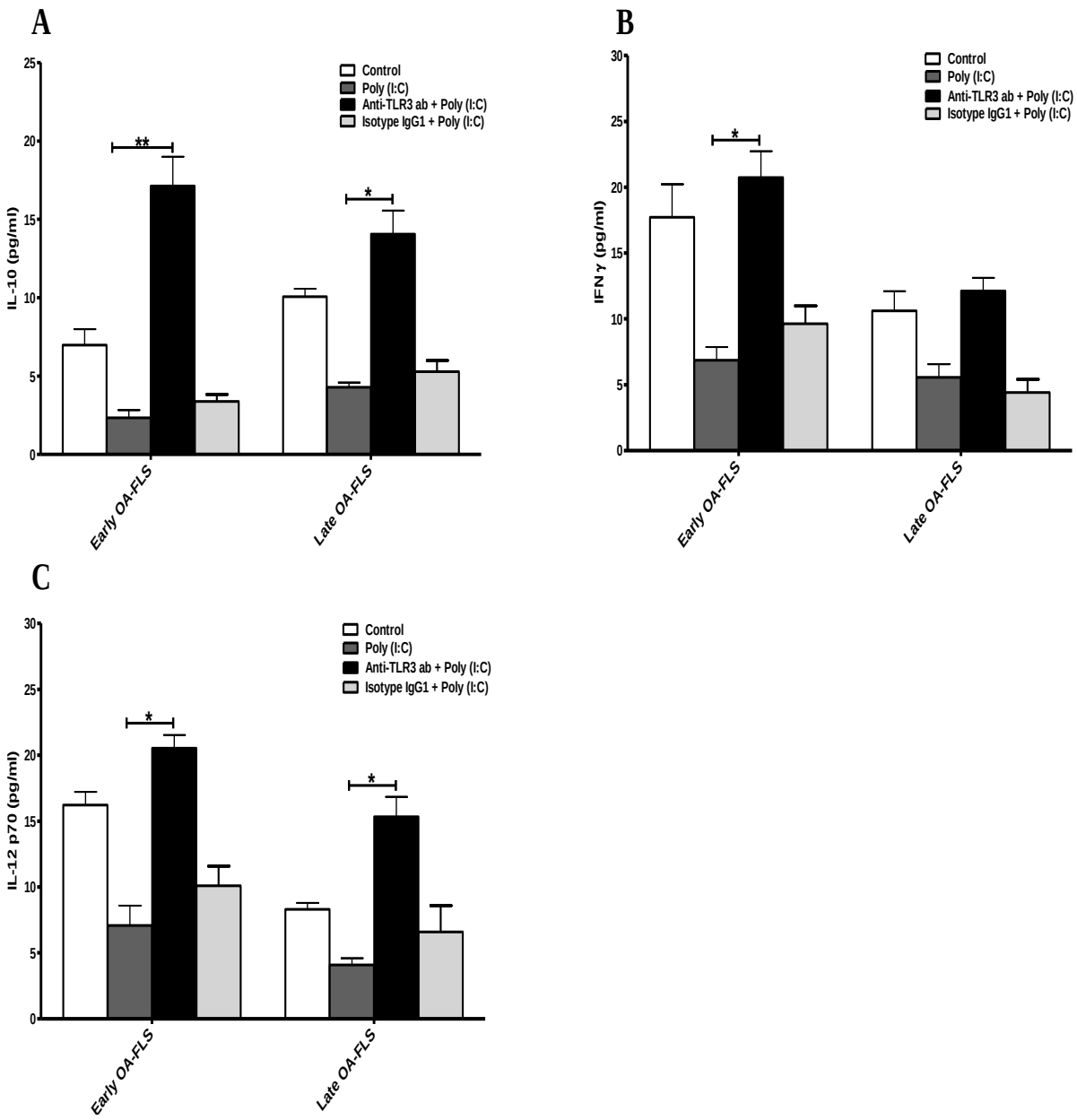

Figure 4.28: Modulation of Poly (I:C) induced IL-10, IFNγ and IL-12p70 secretion by TLR3 blockade in early and late OA-FLS. (A-C) Early (Grade 1-2) and Late (Grade 3-4) stage OA synovial biopsy derived FLS (n=3), were pre-incubated with anti-TLR3 antibody (20 µg/ml) or Isotype IgG1 antibody (20 µg/ml) for 90 min prior to Poly (I:C) (10 µg/ml) stimulation for 24 h. Cell free supernatants were analyzed for (A) IL-10, (B) IFNγ and (C) IL-12p70 by MSD ultrasensitive multiplex ELISA system. All the data presented are representative of at least one independent experiment performed in duplicate (mean ± S.E.M). Data was subjected to an unpaired Student's t test. * $p<0.05$, ** $p<0.01$ denotes the level of significance relative to respective cell type Poly (I:C) stimulation.

4.4.8.4. Modulation of Poly (I:C) induced MMP-1, MMP-3 and MMP-9 secretion by TLR3 blockade in early and late OA-FLS

Given the differential induction of MMPs 1, 3 and 9, predominantly by Poly (I:C) in whole synovial tissue explant cultures and in early and late FLS (Figure 4.4 and 4.9), and given the ability of an anti-TLR3 antibody to modulate these MMP gene induction in N-FLS (Figure 4.24), it was critical to investigate the effects of TLR3 blockade in modulating MMP levels in stage-specific OA FLS. Interestingly, it was found that, both early and late OA-FLS exhibited a significant suppression in MMP 1, 3 and 9 levels, upon anti-TLR3 antibody pre-treatment followed by Poly (I:C) stimulation when compared to non-pre-treated cells (Figure 4.29, panels A, B and C, n=3). A significant decrease in MMP- 1 levels was evident in both early and late OA-FLS upon anti-TLR3 antibody pre-treatment prior to Poly (I:C) stimulation (anti-TLR3 ab + Poly(I:C) Vs Poly(I:C)) (Early: 5.47 ± 0.56 Vs 13.21 ± 0.9 ng/ml and Late: 10.60 ± 0.97 Vs 20.47 ± 0.57 ng/ml, $p \leq 0.05$, Figure 4.29, panel A). Likewise, a significant suppression in MMP-3 levels was evident in both early and late OA-FLS upon anti-TLR3 antibody pre-treatment prior to Poly (I:C) stimulation when compared to non-pre-treated cells (anti-TLR3 ab + Poly(I:C) Vs Poly(I:C)) (Early: 3.47 ± 1.44 Vs 16.91 ± 0.25 ng/ml and Late: 7.90 ± 1.06 Vs 21.88 ± 0.32 ng/ml, $p \leq 0.01$, Figure 4.29, panel B). Also, a significant suppression in MMP-9 levels was evident in both early and late OA-FLS upon anti-TLR3 antibody pre-treatment prior to Poly (I:C) stimulation (anti-TLR3 ab + Poly(I:C) Vs Poly(I:C)) (Early: 149.06 ± 36 Vs 762.43 ± 25 pg/ml and Late: 329.82 ± 48.5 Vs 919.82 ± 65 ng/ml, $p \leq 0.05$, Figure 4.29, panel C). Thus, it is clear that TLR3-dependent induction of catabolic MMP 1, 3 and 9 in early and late OA-FLS, as previously observed in (Figure 4.9) and in whole OA synovial tissue explants (Figure 4.4) can be modulated by TLR3 blockade even at the early stages of OA, thus making TLR3 a critical target for OA disease intervention.

Together these data provide evidence that TLR3-dependent activation of FLS occurs predominantly through Poly(I:C) or RNA from necrotic cells in OA-SF, leading to induction of pro-inflammatory mediators and suppression of immune-regulatory and anti-inflammatory mediators secretion in both early and late OA-FLS. Thus, it can be proposed that the TLR3 dependent signalling pathway may be critical in the initiation and propagation of OA even at initial stages of disease on-set; this may be modulated and primarily managed by TLR3 blockade (section 4.4.8). Thus, TLR3-targeted therapies may prove useful as an intervention towards restoring the balance between anabolic and

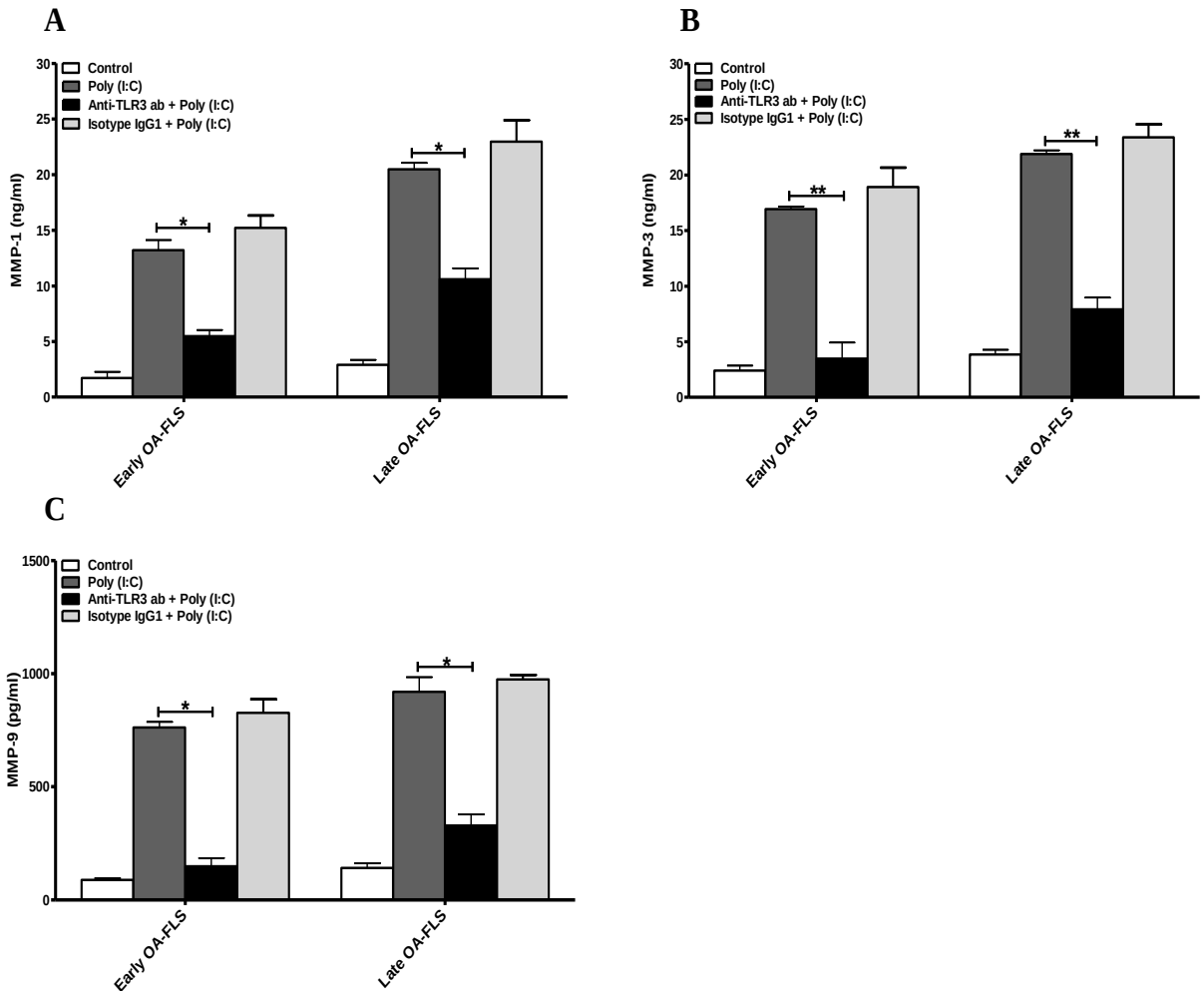

Figure 4.29: Modulation of Poly (I:C) induced MMP-1, MMP-3 and MMP-9 secretion by TLR3 blockade in early and late OA-FLS. (A-C) Early (Grade 1-2) and Late (Grade 3-4) stage OA synovial biopsy derived FLS (n=3), were pre-incubated with an anti-TLR3 antibody (20 µg/ml) or Isotype IgG1 antibody (20 µg/ml) for 90 min prior to Poly (I:C) (10 µg/ml) stimulation for 24 h. Cell free supernatants were analyzed for (A) IL-10, (B) IFNγ and (C) IL-12p70 by MSD ultrasensitive multiplex ELISA system. All the data presented are representative of at least one independent experiment performed in duplicate (mean ± S.E.M). Data was subjected to an unpaired Student's t test. * $p<0.05$, ** $p<0.01$ denotes the level of significance relative to respective cell type Poly (I:C) stimulation.

catabolic pathways in OA (Zhu et al., 2011). Thus, FLS may regulate the switch from acute resolution to chronic persistent inflammation (Buckley et al., 2001).

4.4.9. Immunoblot and confocal evaluation of signal transduction modulatory effects of TLR3 blockade in FLS

In FLS, given that TLR3 may be activated by Poly(I:C) or dsRNA from necrotic cells in the OA SF, and our observation that neutralisation of TLR3 expression in FLS may alter the balance from a pro-inflammatory to an anti-inflammatory cytokine milieu (section 4.4.7 and 4.4.8), we opted to investigate the transcription factors that critically regulate inflammatory cytokine induction through the TLRs, namely NF-κB and IRF. Interestingly, these transcription factors were considered as potential therapeutic targets in chronic inflammatory diseases such as OA and RA (Rosenbach et al., 1984, Matsumoto and Seya, 2008, Sweeney et al., 2010). Therefore, the effects of TLR3 blockade towards the modulation of NF-κB and IRF3 activity in N and OA FLS following Poly(I:C) and grade-specific OA-SF stimulation were investigated.

4.4.9.1. Immunoblot analysis of Poly (I:C) induced NF-κB and IRF3 activation in N and OA FLS

The ability of Poly(I:C) to induce the activation of the transcription factors, IRF3 and NF-κB, as evidenced by their increased phosphorylation and concomitant degradation of IκBα, which is a necessary prelude to NF-κB activation, was evaluated by western blot analysis in N and OA FLS upon stimulation with Poly(I:C) (10μg/ml) for the indicated time points using anti-IκBα, anti-phospho-p65 and anti-phospho-IRF3 antibodies respectively. In OA-FLS, it was found that stimulation of cells with Poly (I:C), even at 30 min, induced the early degradation of IκBα, when compared to treated N-FLS, which showed a delayed degradation of IκBα at 60 min Poly (I:C) stimulation. Moreover, a strong and persistent phosphorylation of p65 and IRF3 was detected in OA-FLS relative to N-FLS upon Poly (I:C) stimulation (Figure 4.30, panel A). Thereafter, the ability of anti-TLR3 antibody to modulate the transcription factor activation effect of Poly (I:C) stimulation in N and OA FLS was examined. To do so, N and OA FLS were pre-incubated with anti-TLR3 antibody (10 and 20 μg/ml) for 90 min prior to Poly (I:C) (10 μg/ml) stimulation for 60 min. It was found that neutralisation of TLR3 suppressed the phosphorylation of p65 and IRF3 transcription factors in both N and OA FLS upon pre-incubation with anti-TLR3 antibody prior to Poly (I:C) stimulation. In N and OA FLS, upon preincubation with an anti-TLR3

antibody (20 μg/ml), prior to Poly(I:C) stimulation, a strong delay in IκBα degradation was evident when compared with a decreased suppressive effect when cells were preincubated with 10 μg/ml of anti-TLR3 antibody. In contrast, anti-TLR3 antibody dose dependent differences were not observed when the ability of the anti-TLR3 antibody to suppress poly(I:C) mediated p65 and IRF3 phosphorylation in both N and OA FLS was examined (Figure 4.30, panel B). Therefore, 20 μg/ml of anti-TLR3 antibody was utilised for the rest of the studies.

4.4.9.2. Confocal analysis of modulation of Poly (I:C) induced p65 translocation by anti-TLR3 antibody in N and OA FLS

To complement our data showing that TLR3 blockade modulates p65 phosphorylation (Figure 4.30, panel B), confocal microscopy was utilised to assess the ability of Poly(I:C) to induce the nuclear translocation of NF-κB p65 and the effects of TLR3 blockade therein was investigated using FLS cells. It was found that the basal p65 expression was localised to the cytoplasmic in N and OA FLS. Following Poly (I:C) stimulation, p65 was found to translocate to the nucleus in both N and OA FLS. Interestingly, pre-treatment of the FLS with an anti-TLR3 antibody inhibited Poly (I:C) mediated nuclear translocation of p65, probably through blocking Poly (I:C) mediated TLR3 activation in FLS. As a control, Poly (I:C) mediated nuclear localisation of p65 was evident following pre-treatment with the Isotype control (Figure 4.31, panels A and B). Therefore, we propose that TLR3 blockade inhibits the nuclear translocation of p65 following Poly(I:C) stimulation in FLS and this finding correlates with our immunoblot analysis of p65 activation status and suggests a pivotal role for TLR3-dependent NF-κB activation in OA progression (Figure 4.30).

4.4.9.3. Confocal analysis of modulation of Poly (I:C) induced IRF3 translocation by anti-TLR3 antibody in N and OA FLS

To investigate the ability of TLR3 blockade to affect Poly (I:C) mediated IRF3 phosphorylation (Figure 4.30, panel B), confocal microscopy was utilised to assess the ability of Poly(I:C) to modulate the expression and nuclear translocation of IRF3 in FLS and to assess the effect of TLR3 blockade therein. In unstimulated/control N and OA FLS, IRF3 was localised predominantly to the cytoplasmic. Stimulation with Poly(I:C) induced an increase in the expression of IRF3 with a predominant nuclear localisation in both N and OA FLS. In N and OA FLS, pre-treatment with an anti-TLR3 antibody prior to Poly (I:C) stimulation inhibited the nuclear translocation of IRF3 and a predominant

cytoplasmic localisation of IRF3 was seen. Also, sustained nuclear localisation of IRF3 was seen upon preincubation of cells with Isotype control followed by stimulation with Poly (I:C) (Figure 4.32, panels A and B). Therefore, it can be proposed that TLR3 blockade, primarily blocks the IRF3 nuclear translocation ability of Poly(I:C) in FLS, and this also corroborates with our previous IRF3 immunoblot analysis, thus suggests a pivotal role for TLR3-dependent IRF3 activation in OA progression (Figure 4.30).

4.4.9.4. Immunoblot analysis of Poly (I:C) or grade-specific OA-SF induced NF-κB and IRF3 activation in N-FLS, early and late OA FLS

Given the ability of stage-specific OA-SF to activate TLR3 in N-FLS (section 4.4.6 and 4.4.7) and the distinctive ability of Poly(I:C) to induce TLR3-dependent key inflammatory mediators in both early and late stage OA patient derived FLS, and given the immuno-modulatory effects of TLR3 blockade in FLS (section 4.4.8), we opted to investigate the ability of Poly(I:C) and OA-SF to activate the transcription factors, NF-κB and IRF3, and to investigate the ability of TLR3 blockade to modulate this effect. It was found that grade-specific (grades 1-4) OA-SFs induced activation of IRF3 *via* its phosphorylation and NF-κB, as evidenced by increased phosphorylation of p65 subunit and the concomitant degradation of IκBα. Pre-treatment of N-FLS with an anti-TLR3 antibody suppressed grade-specific OA-SF mediated phosphorylation of p65 and IRF3 and I□B degradation (Figure 4.33, panel A). Also, the ability of an anti-TLR3 antibody to modulate Poly (I:C) mediated activation of transcription factors in early and late OA FLS was examined. To this end, early and late OA patient derived FLS were pre-incubated with an anti-TLR3 antibody (20 µg/ml) for 90 min prior to Poly (I:C) (10 µg/ml) stimulation for 60 min. It was found that neutralisation of TLR3 prominently suppressed Poly (I:C) mediated phosphorylation of p65 and IRF3 transcription factors and also reduced IκBα degradation in both early and late OA-FLS (Figure 33, panel B). These data suggest an early and persistent TLR3-mediated activation of transcription factors which may be modulated through TLR3 blockade in FLS.

4.4.9.5. Confocal analysis of modulation of OA-SF induced p65 and IRF3 translocation by anti-TLR3 antibody in N-FLS

To compliment the immunoblot analysis data showing that TLR3 blockade inhibits p65 and IRF3 phosphorylation (Figure 4.33, panel A), confocal microscopy was utilised to assess the ability of grade-4 OA-SF to induce, and TLR3 blockade to regulate, the

expression and nuclear translocation of p65 and IRF3 in N-FLS. In unstimulated/control N-FLS, p65 and IRF3 were localised predominantly to the cytoplasm. Upon stimulation with grade-4 OA-SF, nuclear translocation of p65 and IRF3 was observed in N-FLS and this effect was blocked by pre-treatment of FLS with an anti-TLR3 antibody, but not with the Isotype control (Figure 4.34, panels A and B). Therefore, it may be proposed that OA-SF induces the activation of NF-κB and IRF3 in FLS and this effect is inhibited by pre-incubation of cells with an anti-TLR3 antibody; these findings support our previous immunoblot analysis (Figure 4.33, panel A) and suggests a probable role for TLR3-dependent signal transduction activity in OA. Also, further studies are required to explore the ability of OA-SF to activate signal transduction pathways in FLSs.

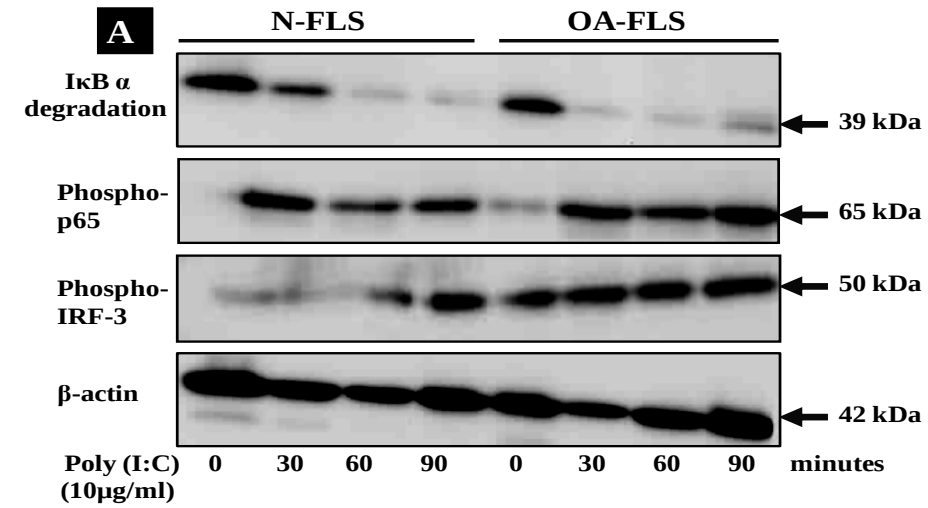

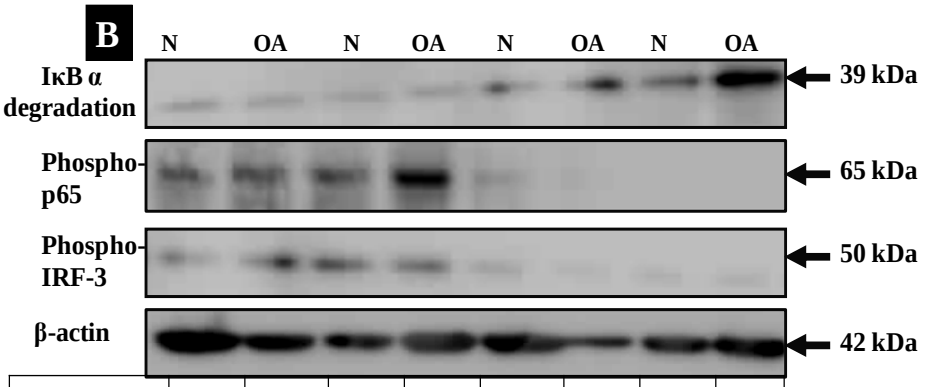

Isotype IgG1	+	+	-	-	-	-	-	-
Poly (I:C)	+	+	+	+	+	+	+	+
Anti-TLR-3 (10 µg/ml)	-	-	-	-	+	+	-	-
Anti-TLR-3 (20 µg/ml)	-	-	-	-	-	-	+	+

Figure 4.30: Immunoblot analysis of Poly (I:C) induced NF-κB and IRF3 activation in N and OA FLS. (A) N and OA FLS were stimulated with Poly(I:C) (10µg/ml) for 30, 60 and 90 min respectively, (B) N and OA FLS were pre-incubated with anti-TLR3 antibody (10 and 20 µg/ml) or Isotype IgG1 antibody (20 µg/ml) for 90 min prior to Poly (I:C) (10 µg/ml) stimulation for 60 min. Immunoblot analysis was performed to assess levels of IκBα degradation, phosphorylation of p65 and IRF3 activation using their respective antibodies; anti–IκBα (1:200 dilution), anti-phospho p65 (1:1000 dilution), anti-phosphoIRF3 (1:1000 dilution) and loading control β-actin antibody (1:1000 dilution). All the data presented are representative of at least two independent experiments performed in duplicate.

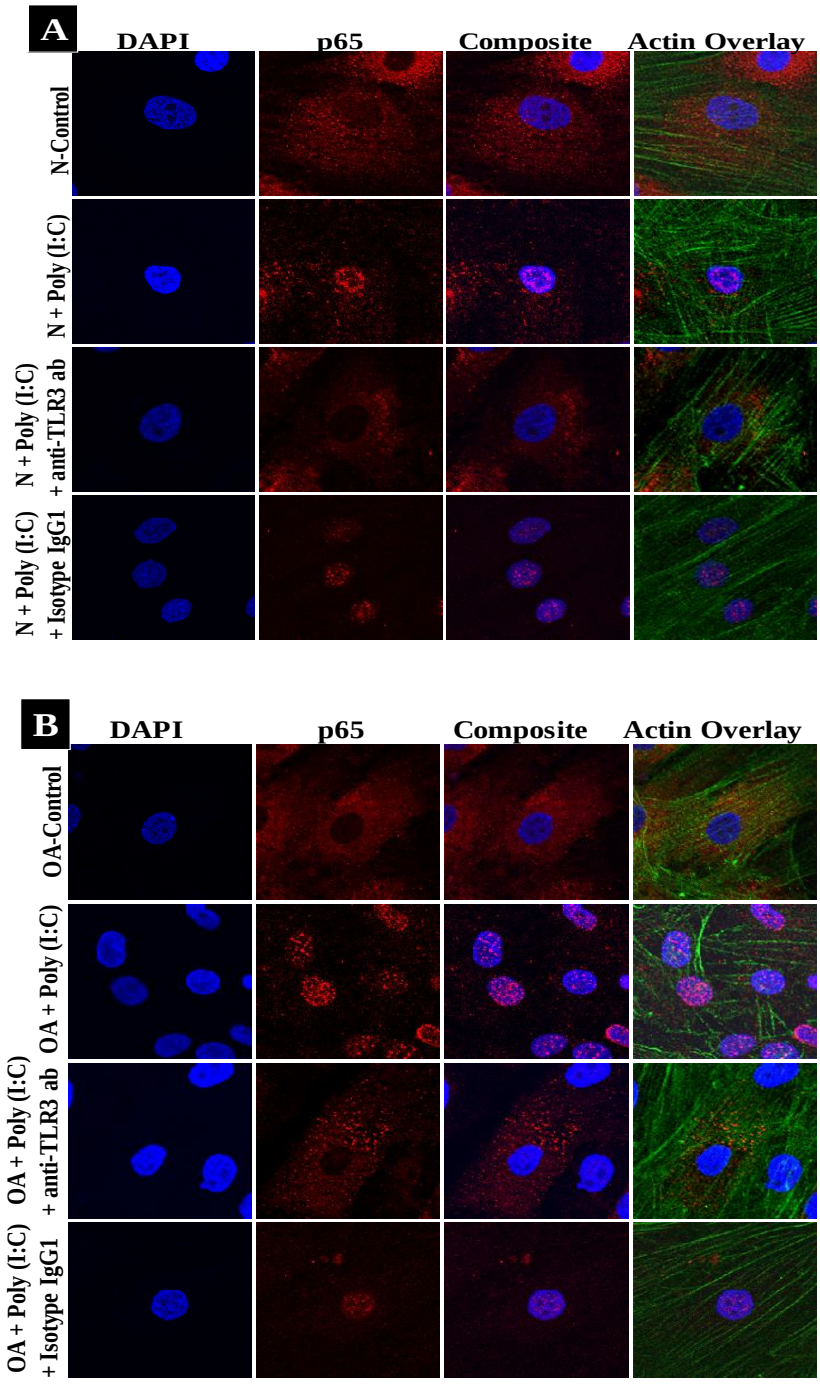

Figure 4.31: Confocal analysis of modulation of Poly (I:C) induced p65 translocation by anti-TLR3 antibody in N and OA FLS. N-FLS (A) and OA FLS (B) were either pre-incubated with anti-TLR3 antibody (20 µg/ml) or Isotype IgG1 antibody (20 µg/ml) for 2 h, prior to Poly (I:C) (10 µg/ml) stimulation for 60 min or left unstimulated. Confocal analysis was performed using an anti-p65 antibody (1:50 dilution; red staining) followed by incubation with an Alexa Fluor 546 (1:500 dilution) labelled secondary antibody. Actin-phalloidin (1:25 dilution) was also employed (green staining) as a cyto-skeletal control marker for FLS. DAPI staining of nuclei is also included and seen as blue staining.

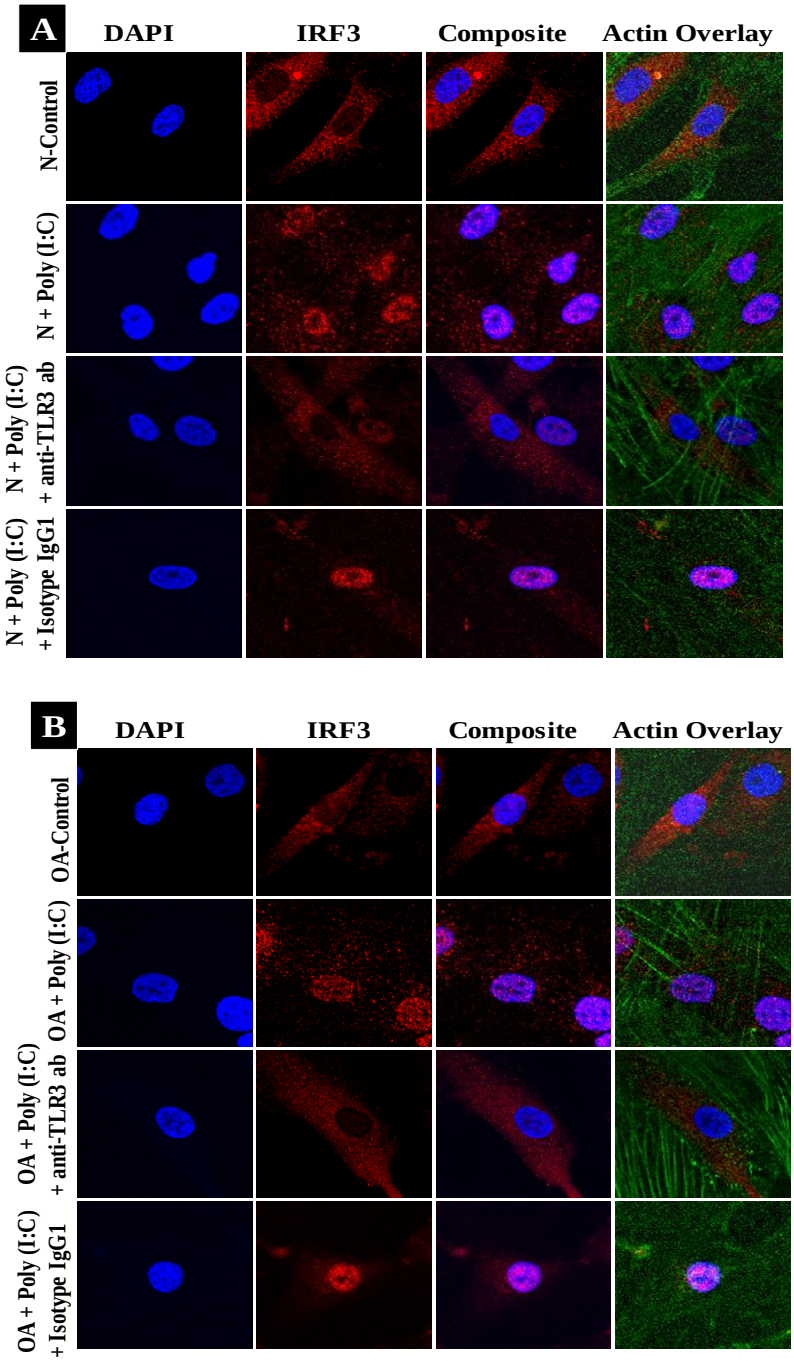

Figure 4.32: Confocal analysis of modulation of Poly (I:C) induced IRF3 translocation by anti-TLR3 antibody in N and OA FLS. N-FLS (A) and OA FLS (B) were either pre-incubated with anti-TLR3 antibody (20 µg/ml) or Isotype IgG1 antibody (20 µg/ml) for 2h, prior to Poly (I:C) (10 µg/ml) stimulation for 60 min or left unstimulated. Confocal analysis was performed using an anti-IRF3 antibody (1:50 dilution; red staining) followed by incubation with an Alexa Fluor 546 (1:500 dilution) labelled secondary antibody. Actin-phalloidin (1:25 dilution) was also employed (green staining) as a cyto-skeletal control marker for FLS. DAPI staining of nuclei is also included and seen as blue staining.

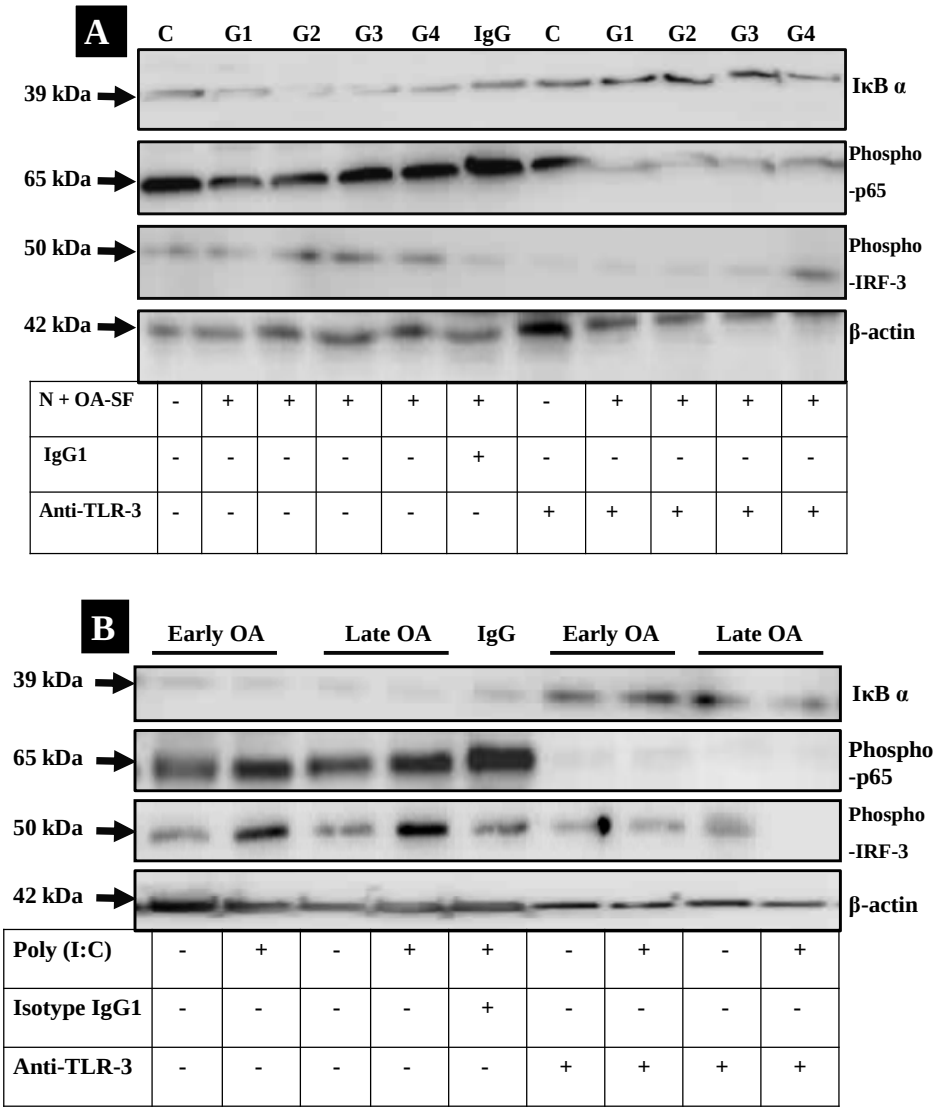

Figure 4.33: Immunoblot analysis of Poly (I:C) or grade-specific OA-SF induced NF-κB and IRF3 activation in N-FLS, early and late OA FLS. (A) N-FLS were either pre-treated with anti-TLR3 antibody (20 µg/ml) or Isotype IgG1 (IgG) antibody (20 µg/ml) for 90 min prior to grade-specific OA-SF: grade 1 (G1), grade 2 (G2), grade 3 (G3), grade 4 (G4) (1:5 dilution in Opti-MEM/grade, n=3) stimulation for 3 h or left unstimulated (C). (B) Early (Grade 1-2) and Late (Grade 3-4) stage OA synovial biopsy derived FLS (n=3), were pre-incubated with anti-TLR3 antibody (20 µg/ml) or Isotype IgG1 antibody (20 µg/ml) for 90 min prior to Poly (I:C) (10 µg/ml) stimulation for 60 min. Cell pellets were harvested and assayed for IκBα degradation, phosphorylation of p65 and IRF3 activation using respective antibodies; anti–IκBα (1:200 dilution), anti-phospho p65 (1:1000 dilution), anti-phospho IRF3 (1:1000 dilution) and loading control β-actin antibody (1:1000 dilution). All the data presented are representative of at least two independent experiments performed in duplicate.

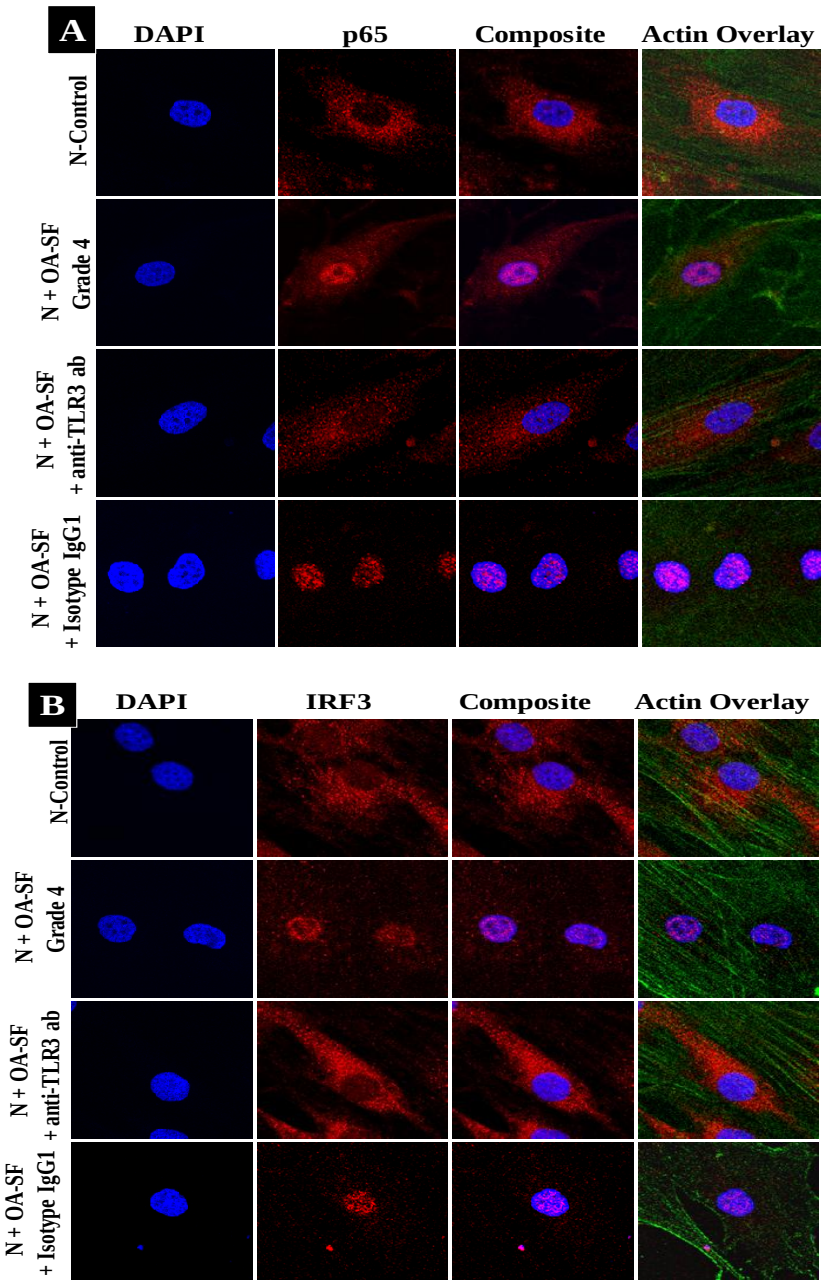

Figure 4.34: Confocal analysis of modulation of OA-SF induced p65 and IRF3 translocation by anti-TLR3 antibody in N-FLS. N-FLS were either pre-incubated with anti-TLR3 antibody (20 µg/ml) or Isotype IgG1 antibody (20 µg/ml) for 2h prior to grade-4 OA-SF (1:5 dilution in Opti-MEM) stimulation for 3h or left unstimulated. Confocal analysis was performed using an (A) anti-p65 antibody (1:50 dilution; red staining), (B) anti-IRF3 antibody (1:50 dilution; red staining) followed by incubation with an Alexa Fluor 546 (1:500 dilution) labelled secondary antibody. Actin-phalloidin (1:25 dilution) was also employed green staining) as a cyto-skeletal control marker for FLS. DAPI staining of nuclei is also included and seen as blue staining.

4.4.10. Luciferease reporter gene assays to evaluate the specific TLRs and IRFs activating ability of OA-SF and immunomodulatory effect of TLR3 blockade

To further investigate the ability of OA-SF to activate specific TLRs and TLR signalling cascades (NF-κB, pro-inflammatory cyto-chemokine expression and IRFs activation) and to further clarify the immunomodulatory effects of TLR3 blockade in OA, luciferase reporter gene assays were performed utilising OA-SF obtained from patients with early (grade-1) and late (grade-4) stage OA as a ligand. Thus, HEK293 cells over-expressing specific TLRs and MAVS wild type and MAVS$^{-/-}$ MEFs were used as models. To delineate the molecular mechanisms involved in the induction of pro-inflammatory cytokines, chemokines and downstream transcription factor activation during OA, the ability of OA-SF (early and late OA stages) and key PAMPs to induce such inflammatory cascades was evaluated by employing luciferase reporter gene assays.

4.4.10.1. Analysis of OA-SF induced NF-κB, IFN-β, RANTES reporter gene activity

Given our previous observations that TLRs, namely TLR2, 3, 4, 7 and 9 and RLRs, namely RIG-I and MDA-5 (which recruit an adaptor protein called mitochondrial antiviral-signaling protein (MAVS)) are involved in OA (chapter 3 and chapter 4), herein, we sought to understand the relative contribution of the RLRs and TLRs during the early and late stages of OA. Thus, the ability of early and late OA-SF to activate specific TLRs was investigated using HEK293 cells over-expressing specific TLRs and. Also, towards understanding the role of RLRs in OA, MAVS-wildtype and deficient MEFs were used. Thus, HEK 293-TLR2, 3, 4, 7, 9 cells and MAVS Wild type$^{+/+}$ MEFs and MAVS-deficient$^{-/-}$ MEFs were transiently transfected with the NF-κB, IFN-β (p125-luc) and Rantes reporter gene constructs, followed by stimulation with respective TLR or RLR ligands and early (grade-1) or late (grade-4) OA-SF (n=3/grade), followed by harvesting of cell lysates and assessment of luciferase reporter gene activity (Figure 4.35, panels A, B, C, D, E, F and G). Interestingly, of all the receptors studied in this section, stimulation with early and late OA-SF induced the highest and most significant activation of IFNβ (p125-luc) and Rantes reporter genes and a notable activation of the NF-κB reporter gene in HEK293-TLR3 cells relative to their respective controls (Figure 4.35, panel B, $p \leq 0.05$). Likewise, stimulation with early and late OA-SF also induced a significant activation of IFNβ (p125-luc) and Rantes reporter genes and a notable activation of NF-κB reporter gene in MAVS-deficient$^{-/-}$ MEFs relative to their respective controls (Figure 4.35, panel G,

$p \leq 0.05$). Moreover, minimal activation of IFNβ (p125-luc), Rantes and NF-κB reporter genes was evident in HEK293-TLR7 cells upon stimulation with early and late OA-SFs, relative to their respective controls (Figure 4.35, panel D). In contrast, activation of IFNβ (p125-luc) or Rantes or NF-κB reporter genes was not detected following stimulation of HEK293-TLR2, HEK293-TLR4, HEK293-TLR9 cells and MAVS Wild type$^{+/+}$ MEFs with early and late OA-SFs, when compared to their respective controls (Figure 4.35, panels A, C, E and F respectively). These data suggest that both early and late OA-SF may contain factors which can directly induce significant levels of inflammatory cyto-chemokine genes, especially IFNβ and RANTES and to lesser extent NF-κB activation in a TLR-3 dependent manner. These data substantiates our previous observation that TLR3 activation predominates in OA, through a mechanism involving DAMPs/PAMPs contained in the grade-specific OA-SF (sections 4.4.5, 4.4.6, 4.4.7,4.4.8 and 4.4.9) and this also correlates with previous publications suggesting that RNA from the necrotic cells in the OA-SF can predominantly induce TLR3 activation in FLS (Yaron et al., 1979, Brentano et al., 2005, Karikó et al., 2004, Scanzello et al., 2011, Nair et al., 2012).

4.4.10.2. Analysis of OA-SF induced IRF-3, -5, -7, -9 and PRD-II, I-III, IV reporter gene activity

Given our previous observations that OA-SF induces the activation of IRF3 in FLS (Figure 4.33 and 4.34), and given the predominant TLR3-dependent induction of IFNβ by OA-SF (Figure 4.35), and also given the pivotal role of IRFsin TLR signalling and concomitant induction of the IFNβ, it was essential to investigate the ability of OA-SF to induce the activation of specific IRFs. To this end, the ability of inflammatory OA-SF (early and late OA stages) to induce IRF activation was evaluated by employing luciferase reporter gene assays, wherein, IRF3, 5 and 7 were studied as recent findings reported these IRFs as therapeutic targets to inhibit activation of the type I IFN response in RA-FLS, and as well are implicated for the treatment of TLR signalling associated chronic inflammatory and autoimmune disorders (Sweeney et al., 2010, Sweeney, 2011). Moreover, IRF9 was studied as it is widely associated with IFNβ signalling-which induced experimental synovitis in humans, and thus may also have potential implications in OA synovitis, wherein, in this study, vast and persistent amounts of IFNβ was detected in the progressive grades of OA-SFs and also predominant and most significant levels of IFNβ gene and protein expression was detected in FLS upon TLR3 ligand-Poly (I:C) stimulation and as well with the current hypothesised endogenous RNA from necrotic OA-SF cells, and we

also showed IFNβ as the potent inducer of inflammatory milieu prevalent in the joint (chapter 3), so an attempt was made to understand the role of TLR3 induced IFNβ and concomitant IRF9 induction-although may be a secondary event to the JAK-STAT IFNAR signalling which might have already been initiated in OA-FLS owing to the excess levels of IFNβ prevalent in the joint (Rosenbach et al., 1984, Akbar et al., 2000, Schindler and Brutsaert, 1999, Hall and Rosen, 2010, Buckley et al., 2001). HEK293-TLR3 and HEK293-TLR7 (these were used as a minimal IFNβ induction was evident with OA-SF in the previous section, Figure 4.35, panel D), cells were transiently transfected with IRF3, IRF5, IRF7 and IRF9, followed by stimulation with early (grade-1) or late (grade-4) OA-SF (n=3/grade), harvesting of cell lysates and assessment of luciferase reporter gene activity (Figure 4.36, panels A and B). Interestingly, of all the IRFs studied in this section, stimulation with early and late OA-SF induced the highest and most significant activation of IRF3 and IRF9 in HEK293-TLR3 cells relative to their respective controls (Figure 4.36, panel A, $p \leq 0.05$). A minimal TLR3 dependent induction of IRF7 activation and no IRF5 activation was evident in HEK293-TLR3 cells upon stimulation with both early and late OA-SFs. Also, a similar minimal TLR7 dependent IRF3, IRF7 and IRF9 activation was evident in HEK293-TLR7 cells upon both early and late OA-SFs stimulation (Figure 4.36, panel B).

Therefore, it was clearly evident that both early and late OA-SF can induce the predominant activation of IRF3 and IRF9 in a TLR3 dependent manner and may induce IFNβ secretion. In order, to further probe the mechanistic basis to the differential effects of OA-SF on the IFN-β promoter, the sensitivity of each of the PRD regions of the IFN-β promoter was then investigated in HEK293-TLR3 cells. Whilst both early and late OA-SFs induced a significant activation of the IRF-regulated PRD I-III domain ($p \leq 0.05$), a non-significant activation of the NF-κB-regulated PRD-II domain was evident and OA-SF failed to regulate the PRD-IV domain (Figure 4.36, panel C). Taken together, these data suggest that OA-SF–mediated activation of TLR3 through IRF3 and IRF9 positively regulates the PRD I-III domain of the IFN-β promoter and the NF-κB-regulated PRD-II domain of the IFN-β promoter towards the persistent expression of IFN□, RANTES and other inflammatory mediators in OA.

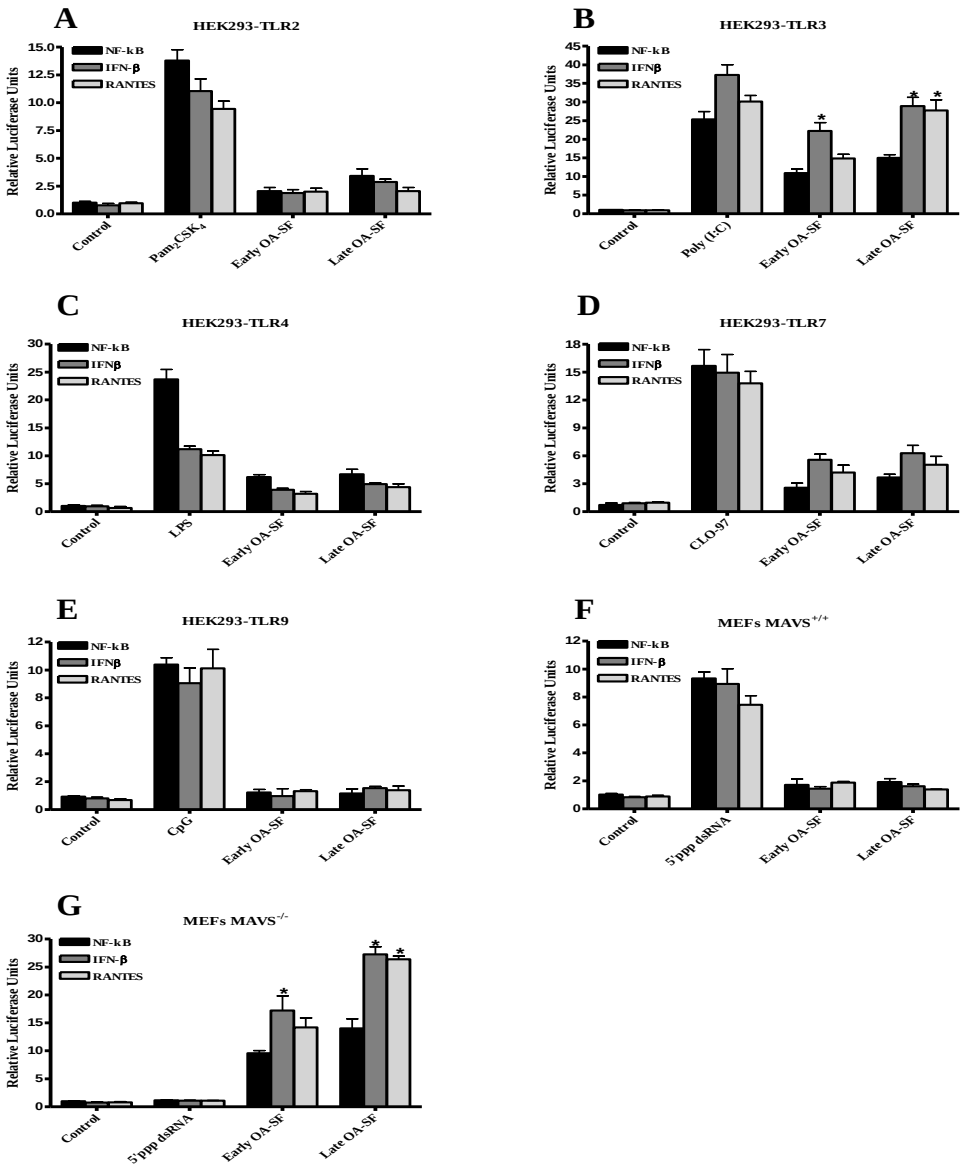

Figure 4.35: Analysis of OA-SF induced NF-κB, IFN-β, RANTES reporter gene activity. (A-G) HEK293-TLR2 (A), HEK293-TLR3 (B), HEK293-TLR4 (C), HEK293-TLR7 (D), HEK293-TLR9 (E), MAVS Wild type$^{+/+}$ MEFs (F) and MAVS-deficient$^{-/-}$ MEFs (G) cells were transfected with 80 ng/well of expression vectors encoding either the reporter genes for NF-κB or full-length IFNβ promoter (p125) or RANTES along with 40 ng/well empty vector. In all cases, 40 ng/well of phRL-TK reporter gene was co-transfected to normalize data for transfection efficiency. After 24 h, cells were stimulated either with Pam_2CSK_4 (A; 1 µg/ml), Poly(I:C) (B ;10 µg/ml), LPS (C ; 1 µg/ml), CLO-97 (D ; 1 µg/ml), CpG (E ; 3 µg/ml), 5' ppp ds-RNA (F-G ; 1 µg/ml), or with Early OA-SF (grade-1), Late OA-SF (grade-4) (1:5 dilution in Opti-MEM/grade, n=3) for 24 h followed by harvesting of cell lysates and assessment of luciferase reporter gene activity. All the data presented are representative of at least three independent experiments performed in triplicates (mean fold induction ± S.D). Data was subjected to an unpaired Student's t test. * $p<0.05$ denotes the level of significance relative to respective cell type control.

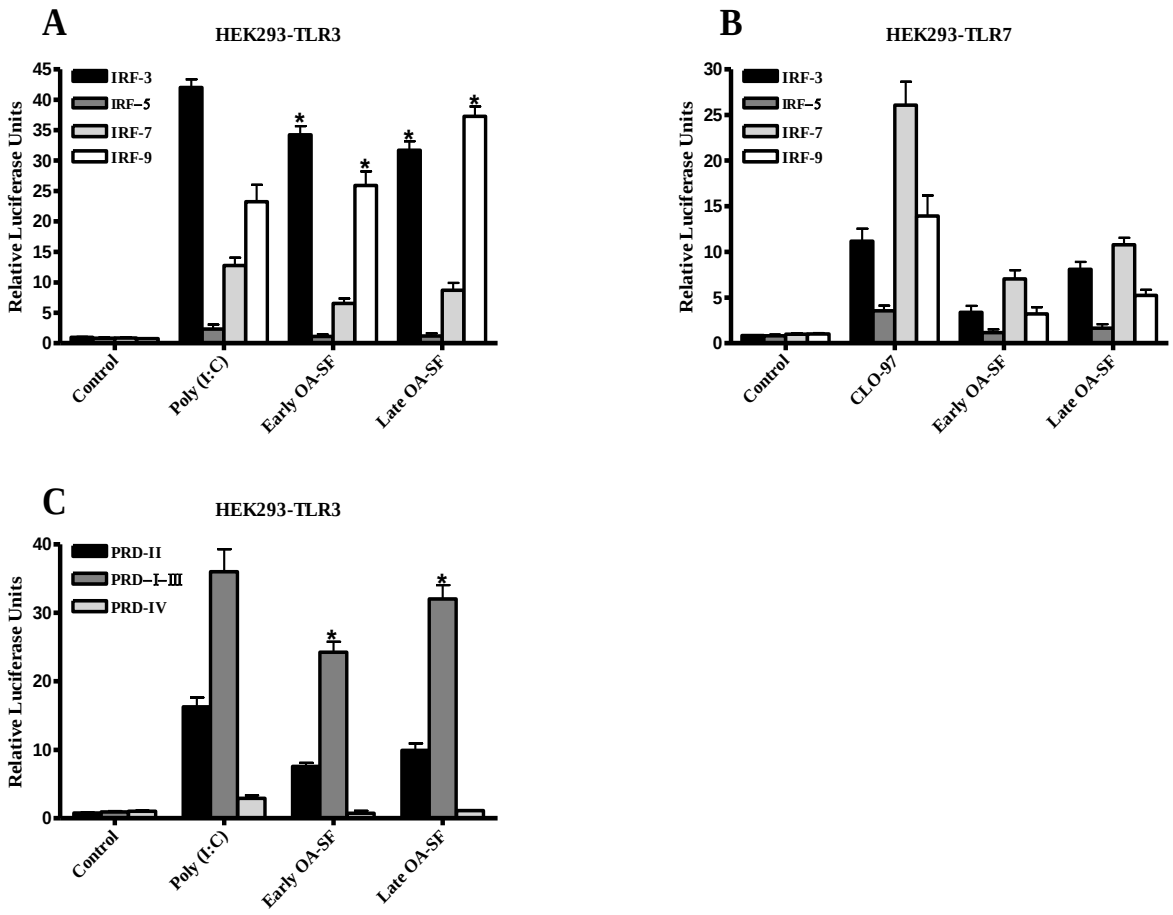

Figure 4.36: Analysis of OA-SF induced IRF-3, -5, -7, -9 and PRD-II, I-III, IV reporter gene activity. (A-B) HEK293-TLR3 (A) and HEK293-TLR7 (B) cells were transfected with 80 ng/well of expression vectors encoding either the luciferase reporter genes for IRF-3, IRF-5, IRF-7 or IRF-9 and HEK293-TLR3 (C) was transfected with 80 ng/well luciferase reporter genes for IFN-β PRD-II, IFN-β PRD-I-III or IFN-β PRD-IV along with 40ng/well empty vector. In all cases, 40 ng/well of phRL-TK reporter gene was co-transfected to normalize data for transfection efficiency. After 24 h, cells were stimulated either with Poly(I:C) (A and C ;10 µg/ml), CLO-97 (B ; 1 µg/ml) or with Early OA-SF (grade-1), Late OA-SF (grade-4) (1:5 dilution in Opti-MEM/grade, n=3) for 24 h followed by harvesting of cell lysates and assessment of luciferase reporter gene activity. All the data presented are representative of at least three independent experiments performed in triplicate (mean fold induction ± S.D). Data was subjected to an unpaired Student's t test. * $p<0.05$ denotes the level of significance relative to respective cell type control.

4.4.10.3. Modulation of OA-SF induced IFN-β, RANTES, PRD-II and PRDI-III reporter gene activity through TLR3 blockade in HEK293-TLR3 cells

Given the potent ability of OA-SF to predominantly induce IFN-β through the PRDI-III domain and RANTES through the PRD-II domain of the IFN-β promoter in a TLR3 dependent manner (Figure 4.35 and 4.36), it was critical to investigate the ability of TLR3 blockade to modulate OA-SF mediated IFN-β, RANTES, PRD-II and PRDI-III luciferase reporter gene activity in HEK293-TLR3 cells. Thus, HEK293-TLR3 cells were transiently transfected with the IFN-β (p125-luc), RANTES, PRD-II and PRDI-III reporter gene constructs, followed by pre-treatment with an anti-TLR3 antibody prior followed by stimulation with OA-SF from patients with early or late OA. Interestingly, TLR3 neutralisation significantly inhibited TLR3-dependent and OA-SF (both early and late OA-SF) induced activation of the IFN-β (p125-luc), RANTES and PRDI-III reporter genes and also showed a non-significant decrease in the activation of the PRD-II reporter gene in HEK293-TLR3 cells relative to the respective OA-SF stimulations (Figure 4.37, panels A, B, C and D, $p \leq 0.05$). In contrast, pre-treatment with the Isotype control did not affect OA-SF mediated activation of the IFN-β, RANTES, PRD-II and PRDI-III luciferase reporter genes in HEK293-TLR3 cells. Therefore, it can be proposed that OA-SF primarily activates TLR3 towards inducing the key inflammatory mediators in OA namely IFN-β and RANTES functioning through PRDI-III and PRD-II domains of the IFN-β promoter.

4.4.10.4. Modulation of OA-SF induced NF-κB, IRF-3, IRF-7 and IRF-9 reporter gene activity through TLR3 blockade in HEK293-TLR3 cells

Given the ability of OA-SF to induce activation of NF-κB, IRF-3, IRF-7 and IRF-9 in a TLR3 dependent manner (Figure 4.35 and 4.36), it was essential to investigate the ability of TLR3 blockade to modulate the OA-SF mediated NF-κB, IRF-3, IRF-7 and IRF-9 luciferase reporter gene activity in HEK293-TLR3 cells. Thus, HEK 293-TLR3 cells were transiently transfected with the NF-κB, IRF-3, IRF-7 and IRF-9 reporter gene contracts, followed by pre-treatment with anti-TLR3 antibody prior to early or late OA-SF stimulations. Interestingly, TLR3 neutralisation significantly inhibited TLR3-dependent and OA-SF (both early and late OA-SF) induced activation of IRF3 reporter genes, and also showed a significant decrease in late OA-SF mediated activation of the NF-κB and IRF-9 reporter gene in HEK293-TLR3 cells relative to the respective OA-SF stimulations (Figure 4.38, panels A, B and D, $p \leq 0.05$). Also, TLR3 neutralisation did not affect

activation of the NF-κB and IRF-9 reporter genes in HEK293-TLR3 cells upon early OA-SF stimulation (Figure 4.38, panels A and D).

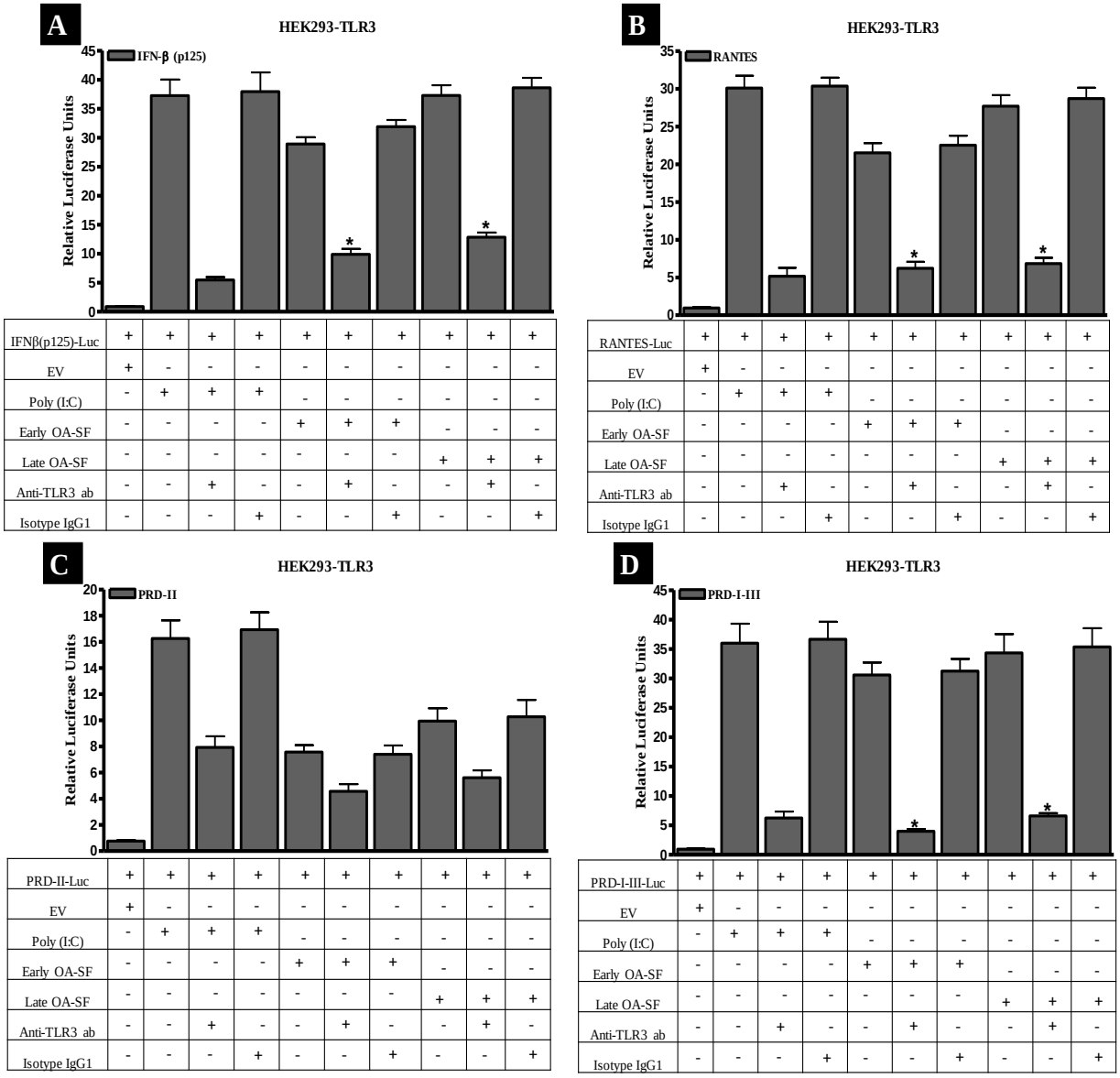

Figure 4.37: Modulation of OA-SF induced IFN-β, RANTES, PRD-II and PRDI-III reporter gene activity through TLR3 blockade in HEK293-TLR3 cells. (A-D) HEK293-TLR3 cells were transfected with 80 ng/well of expression vectors encoding either the luciferase reporter genes for full-length IFNβ promoter (p125) (A), RANTES (B), IFN-β PRD-II (C) or IFN-β PRDI-III (D) along with 40 ng/well empty vector as indicated. In all cases, 40 ng/well of phRL-TK reporter gene was co-transfected to normalize data for transfection efficiency. After 24 h, cells were either pre-treated with anti-TLR3 antibody (20 µg/ml) or Isotype IgG1 (IgG) antibody (20 µg/ml) for 90 min prior to Poly(I:C) (10 µg/ml), or Early OA-SF (grade-1), Late OA-SF (grade-4) (1:5 dilution in Opti-MEM/grade, n=3) stimulation for 24 h followed by harvesting of cell lysates and assessment of luciferase reporter gene activity. All the data presented are representative of at least three independent experiments

performed in triplicates (mean fold induction ± S.D). Data was subjected to an unpaired Student's t test. * $p<0.05$ denotes the level of significance relative to respective ligand stimulation.

Regarding IRF7, TLR3 neutralisation minimally affected late OA-SF mediated activation of IRF7 reporter gene and failed to modulate early OA-SF mediated activation of IRF7 reporter gene in HEK293-TLR3 cells (Figure 4.38, panel C). Isotype control treatment did not affect OA-SF mediated NF-κB, IRF-3, IRF-7 and IRF-9 luciferase reporter gene activity in HEK293-TLR3 cells. Therefore, it can be proposed that OA-SF primarily employs TLR3 in inducing such key transcription factors in OA, given the neutralisation of TLR3 attained through utilising anti-TLR3 antibody significantly inhibited the OA-SF induced activation of the NF-κB, IRF-3 and IRF-9 reporter genes in HEK293-TLR3 cells. Given the ability of TLR3 blockade to inhibit OA-SF mediated activation of key inflammatory mediators, namely IFNβ and RANTES, thus these data suggest a key modulatory role for TLR3 in OA. Therefore, further studies are required to understand the immunomodulatory role of OA-SF in FLSs.

4.4.11. Confirmatory analysis of immuno-modulatory effects of TLR3 blockade in FLS

Given the modulatory role of TLR3 blockade towards blockade of OA-SF and Poly (I:C) induced-TLR3-mediated activation of key inflammatory mediators and the downstream transcription factor activation in HEK293-TLR3 cells (section 4.4.10), and given the predominant TLR3 gene inducing ability of stage-specific OA-SF in N-FLS (section 4.4.6 and 4.4.7), it was essential to evaluate the ability of TLR3 blockade to regulate such OA-SF (early and late OA stages) and Poly(I:C) induced inflammatory cascades in FLS. In all cases Poly (I:C) was used as a positive control. Initially, the ability of TLR3 blockade to modulate OA-SF (early and late stages) induced expression of TLR3 and IFNβ protein in N-FLS and Poly (I:C) induced expression of TLR3 and IFNβ protein in early and late OA patient derived FLS was evaluated by western blot analysis using anti–TLR3 and anti-IFNβ antibodies (Figure 4.39). Primarily, a trend towards increased TLR3 and IFNβ protein expression was

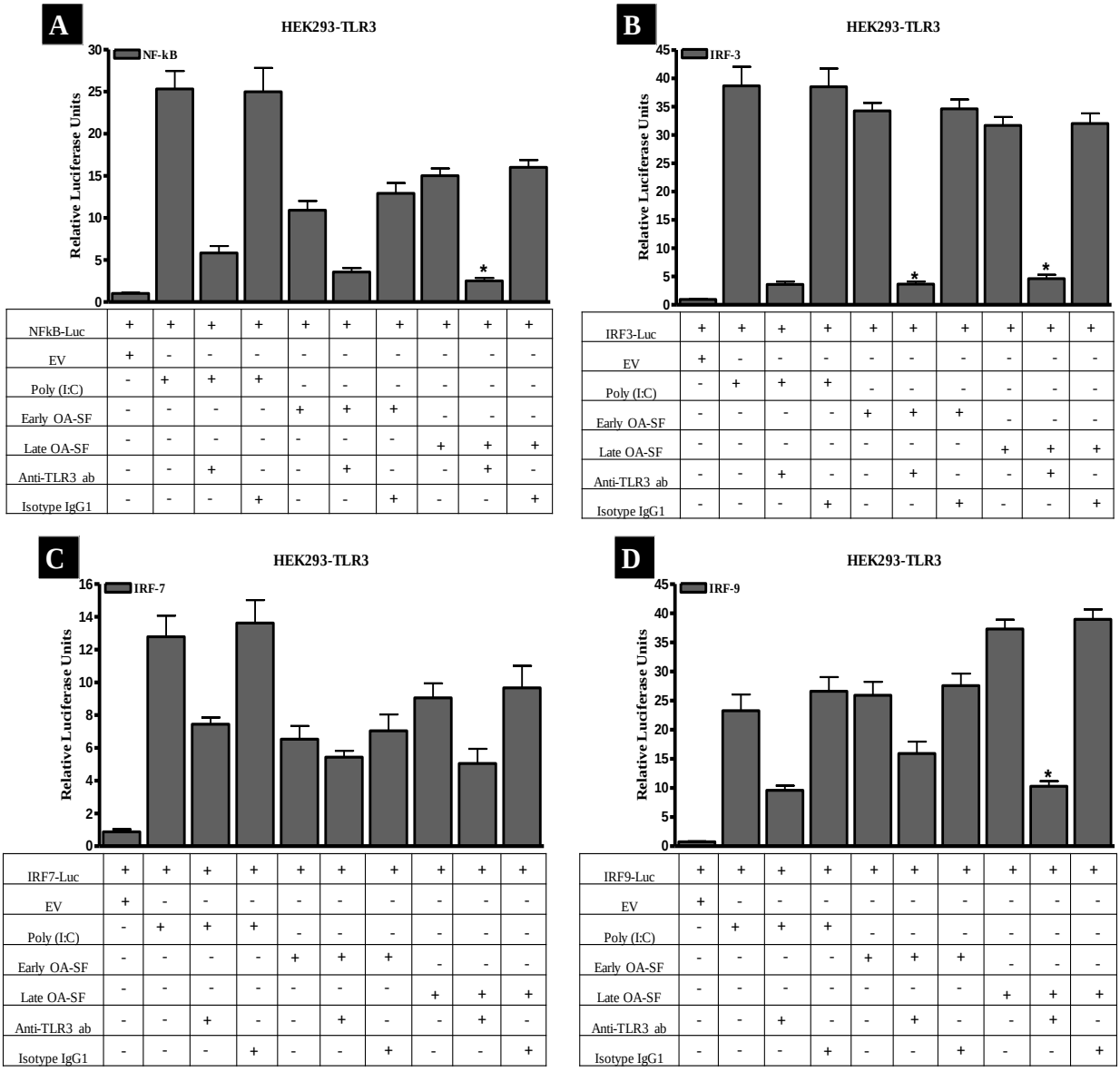

Figure 4.38: Modulation of OA-SF induced NF-κB, IRF-3, IRF-7 and IRF-9 reporter gene activity through TLR3 blockade in HEK293-TLR3 cells. (A-D) HEK293-TLR3 cells were transfected with 80 ng/well of expression vectors encoding either the luciferase reporter genes for NF-κB (A), IRF-3 (B), IRF-7 (C) or IRF-9 (D) along with 40 ng/well empty vector as indicated. In all cases, 40 ng/well of phRL-TK reporter gene was co-transfected to normalize data for transfection efficiency. After 24 h, cells were either pre-treated with anti-TLR3 antibody (20 µg/ml) or Isotype IgG1 (IgG) antibody (20 µg/ml) for 90 min prior to Poly(I:C) (10 µg/ml), or Early OA-SF (grade-1), Late OA-SF (grade-4) (1:5 dilution in Opti-MEM/grade, n=3) stimulation for 24 h followed by harvesting of cell lysates and assessment of luciferase reporter gene activity. All the data presented are representative of at least three independent experiments performed in triplicates (mean fold induction ± S.D). Data was

subjected to an unpaired Student's t test. * $p<0.05$ denotes the level of significance relative to respective ligand stimulation.

evident in N-FLS upon stimulation with early and late OA-SFs, whilst neutralisation of TLR3 prominently suppressed this effect (Figure 4.39, panel A). Likewise, Poly(I:C) induced the expression of TLR3 and IFNβ protein expression in early and late OA-FLS, whereby late OA-FLS showed maximal TLR3 and IFNβ protein expression relative to early OA-FLS and this effect were curtailed following neutralisation with an anti-TLR3 antibody (Figure 4.39, panel B). Furthermore, the ability of TLR3 blockade to modulate OA-SF mediated nuclear localisation of IRF-3, IRF-7 and IRF-9 was evaluated by western blot analysis, utilising nuclear extracts as indicated (Figure 4.39). Interestingly, a trend towards increased nuclear translocation of IRF-3, IRF-7 and IRF-9 protein was detected in N-FLS upon stimulation with early and late OA-SFs and this effect was suppressed following pre-treatment with an anti-TLR3 antibody (Figure 4.39, panel A). Also, Poly(I:C) induced the nuclear translocation of IRF-3, IRF-7 and IRF-9 in both early and late OA-FLS and neutralisation of TLR3 prominently suppressed the Poly(I:C) induced IRF-3 nuclear translocation and showed minimal inhibition of IRF-9 and did not affect the nuclear translocation of IRF-7 in both early and late OA-FLS (Figure 4.39, panel B).

Taken together, these data suggest early and persistent TLR3-associated transcription factor activation namely IRF-3, IRF-9 and NF-κB leading to a persistent induction of inflammatory IFNβ and RANTES in the joint and so makes TLR3 a critical target for OA disease intervention through regulation of key inflammatory mediators and cascades that perpetuate OA progression.

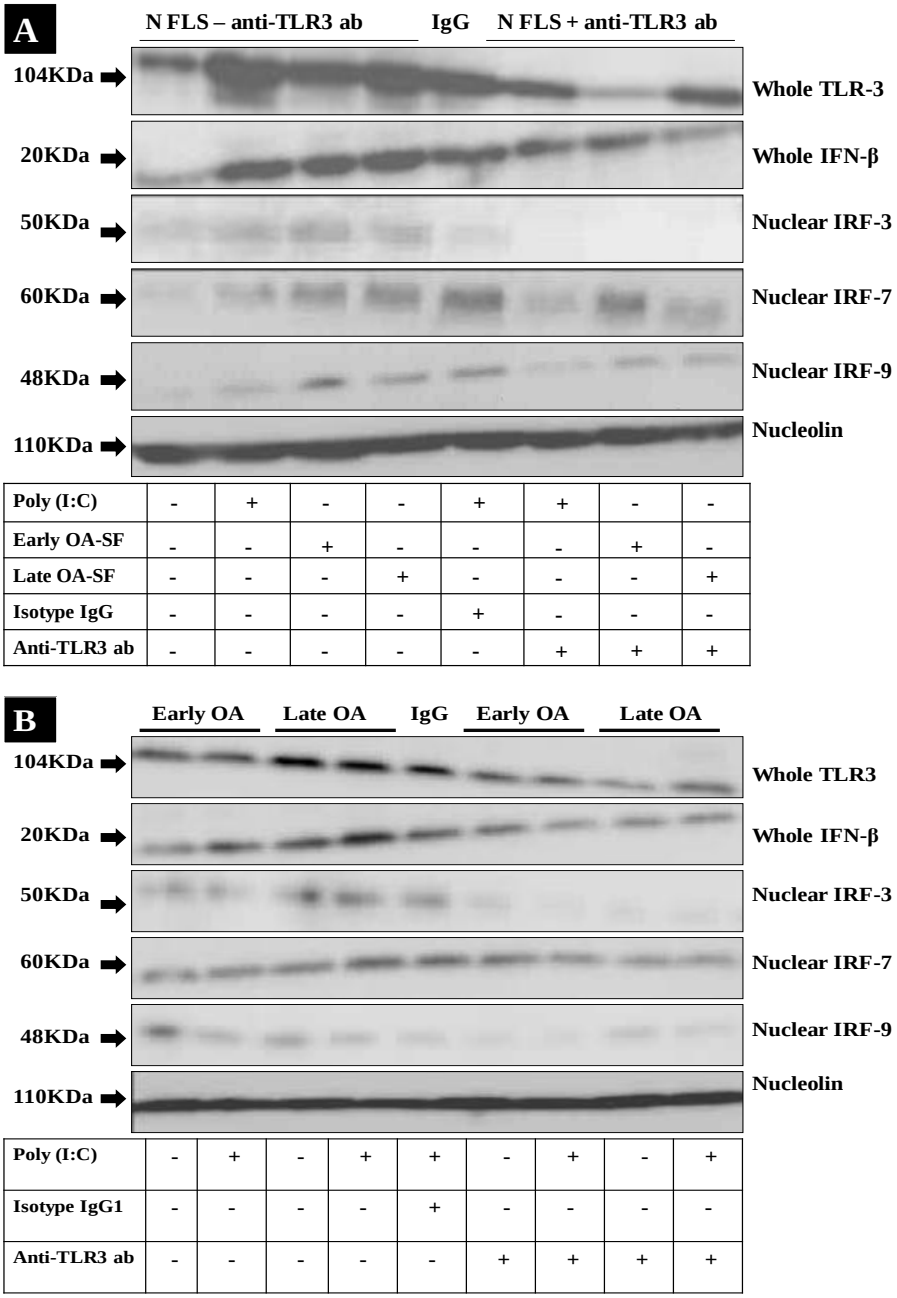

Figure 4.39: Immunoblot analysis of Poly (I:C) or Early or Late OA-SF induced TLR3, IFNβ expression and translocation of IRF3, IRF7 and IRF9 in N-FLS, early and late OA FLS. (A) N-FLS were either pre-treated with anti-TLR3 antibody (20 µg/ml) or Isotype IgG1 (IgG) antibody (20 µg/ml) for 90 min prior to Poly (I:C) (10 µg/ml) stimulation for 60 min, or Early OA-SF: grade 1, or Late OA-SF: grade 4 (1:5 dilution in Opti-MEM/grade, n=3) stimulation for 3 h or left unstimulated. (B) Early (Grade 0-1) and Late (Grade 3-4) stage OA synovial biopsy derived FLS (n=3), were pre-incubated with anti-TLR3 antibody (20 µg/ml) or Isotype IgG1 antibody (20 µg/ml) for 90 min prior to Poly (I:C) (10 µg/ml) stimulation for 60 min. Whole cell pellets were harvested and assayed for TLR3 and IFNβ expression using respective antibodies; anti–TLR3 (1:50 dilution), anti-IFNβ (1:30 dilution). Also, nuclear fractions were extracted as described in materials and methods (chapter 4) and assayed for translocation of IRF3, IRF7 and IRF9 using the respective antibodies; anti-IRF3 (1:100 dilution), anti-IRF7 (1:100 dilution), anti-IRF9 (1:100 dilution) and anti-nucleolin (1:100 dilution). All the data presented are representative of at least three independent experiments performed in triplicate.

4.5. Discussion

The traditional view of OA as a cartilage-only disease has been strongly disproven by recent research and OA is now regarded as a whole-joint disease, encompassing the synovial tissue. The presence of histological inflammation in the OA synovial tissue and early cartilage lesions at the border of the inflamed synovium are strong indicators that synovitis is critical to the pathogenesis of OA (Sellam and Berenbaum, 2010). Accordingly, our data in this chapter showed histological evidence of persistent inflammation in progressive grades of OA synovial tissue. Moreover, given the increasing evidence that TLR activation may play a crucial role in OA progression by mediating synovitis in FLS, through production of pro-inflammatory cytokines in the OA joint (Scanzello et al., 2008, Sutton et al., 2009), and given our previous observations that OA-FLS upon TLR activation secrete a plethora of pro-inflammatory cytokines and chemokines which help facilitate the progression of synovial inflammation (chapter 3), it was essential to investigate TLR agonist-induced inflammatory mediator secretion in whole synovial tissue explant cultures as the maintenance of the synovial architecture and cell-cell contact is facilitated, and therefore more closely reflects the *in-vivo* OA synovial joint environment. Therefore, in this study, for the first time an *ex-vivo* OA whole synovial tissue explant culture model was utilised to screen for and determine the role of TLRs in inducing differential secretion of key synovial inflammation associated cytokines, chemokines and MMPs (Sutton et al., 2009, Fernandes et al., 2002, Scanzello et al., 2009).

Interestingly, we found that, of the TLR ligands utilised in this study, stimulation with Poly(I:C) (synthetic TLR3 ligand) induced the most significant amounts of pro-inflammatory mediators namely, IL-6, IL-8, IL-1β, TNFα, IFNβ, RANTES MMP-1, 3 and 9, and also showed suppression of anti-inflammatory IL-10 and immuno-modulatory IFNγ and IL-12p70 secretions by OA synovial tissue explants cultures. Thus, considering our previous observations in chapter 3 showing that of the TLR ligands, the TLR3 ligand, Poly (I:C) predominantly induces the key inflammatory mediators and MMPs which are involved in extracellular matrix turnover in pathological conditions such as in OA, and given that Poly(I:C) predominantly mediates its effects through TLR3 in OA-FLS, the present data indicates that dsRNA, or perhaps RNA from necrotic cells, may drive the inflammatory locale in the joint during synovitis, by critically creating an imbalance between catabolic and anabolic pathways, possibly through sustained TLR3 activation of

FLS in the joint synovium, and this correlates with previous studies (Cavassani et al., 2008, Brentano et al., 2005, Karikó et al., 2004).

Moreover, to better understand disease progression, attention should focus towards understanding the factors that modulate disease onset and towards understanding the factors that modulate the developmental phases of the disease. Herein, to better understand OA pathology, we utilised early (grade-1) and late (grade-4) OA patient derived synovial FLS to investigate the role of TLRs in mediating the synovitis in OA and also the grade-specific OA synovial fluid. Surprisingly, we have demonstrated in the present study that TLR3 is intimately linked with OA pathology as its expression is seen in early stage OA and TLR3 is stably over-expressed in FLS exclusively at initiation and development stages of OA and serves to mediate the inflammatory milieu in the synovium upon activation with dsRNA/endogenous necrotic cell RNA in the synovial fluid and this correlates with previous studies (Zhu et al., 2011, Brentano et al., 2005, Cavassani et al., 2008). Also, we showed that, stimulation with grade-specific OA-SF predominantly induced TLR3 and TRIF gene and protein expression in FLS at both early and late stages of OA. These data suggests a probable role for sustained TLR3 activation of synovial FLS aiding in arthritis progression, upon constant encounter with the necrotic cell RNA in the synovial fluid of the joint, and this correlates with previous findings (Brentano et al., 2005, Attur et al., 2010, Cavassani et al., 2008, Karikó et al., 2004). Thus, it may be hypothesised that TLR3 may be a potential target for the therapeutic intervention of OA towards the ablation of OA progression.

TLR3 has been reported to be expressed mainly on dendritic cells and fibroblasts, as well as on murine macrophages (Heinz et al., 2003). In the synovium of arthritis patients, it has been found that TLR3 is expressed primarily by the Type B synovial fibroblasts (FLS), rather than the Type A synovial macrophages (Brentano et al., 2005, Ospelt et al., 2008). Consistent with previous observations in humans, in this chapter we show that, TLR3 protein expression was detected by immunoblot analysis in early and late OA-FLS treated with Poly (I:C) and also in N-FLS treated with grade-specific OA-SFs, suggesting that FLSs constitute a major cellular source of TLR3 production in inflamed synovial tissue. In other words, the hyperplasia detected at the various stages of OA (as shown in this chapter) and activation of FLSs in the synovium may be mediated by TLR3 signalling. One possibility is that upregulated TLR3 could recognize the RNA released from necrotic

synovial fluid cells and then activate OA-FLS to promote inflammatory cytokine, chemokine and MMP secretions, which is as well evident in grade-specific OA-SFs and may thereby expedite osteoclastogenesis and also correlates in-part with previous publications (Kim et al., 2009, Brentano et al., 2005, Sutton et al., 2009, Cavassani et al., 2008). According to the above findings, we suggest that TLR3 in FLSs may play an important role in the local synovial inflammation of OA.

In a previous study, intra-articular treatment with poly (I:C) was found to cause a rapid and significant synovitis in rats (Yaron et al., 1979), which suggests the involvement of TLR3 signalling in inflammation mediation. To confirm that hyper-activation of TLR3 in FLS is functional in joint inflammation induced by necrotic cell RNA of the OA-SF, we stimulated N-FLS with grade-specific OA-SF and evaluated its ability to induce the TLR3 TRIF, and inflammatory cyto-chemokine and MMP expression. The results showed that grade-specific OA-SF treated N-FLS exclusively showed a predominant trend towards increased induction in TLR3, TRIF, IFNβ, TNFα, IL-6, IP-10, RANTES and MMP1,3 and 9 mRNA expression and TLR3 and IFNβ protein expression similar to that with Poly(I:C) stimulation and failed to activate MAVS and also failed to respond to RIG-I ligand, thus making TLR3 a critical target for OA intervention which was further confirmed by TLR3 neutralisation studies. TLR3 neutralisation studies in this chapter provide significant support for both an immune and a signal transduction modulatory role of TLR3 blockade in N-FLS and early and late OA-FLS upon grade-specific OA-SF and Poly (I:C) stimulations. Moreover, IFNβ neutralisation also showed a prominent immune-modulatory effects in regulating the inflammatory mediators in FLS, thus further study was conducted to explore the role of IFNβ in the initiation and perpetuation of OA.

Studies have shown that IFNs are capable of stimulating prostaglandin E and hyaluronic acid production by human FLS *in vitro* and of initiating an inflammatory reaction in animal joints, and in chronic arthritis its production may result from persisting viral or other antigenic stimulation. Thus, IFNs may enhance the immune response and mediate the inflammatory process in the joint (Rosenbach et al., 1984). In another study, it was shown that the majority of expanded T cells generated during an immune response are cleared by apoptosis. Prevention of death in some activated T cells enabled the persistence of a memory T-cell pool and both IFNα and IFNβ inhibited the activation of T-cell apoptosis, thus enabling the memory T cells to persist without antigen, and thus excessive IFNα or

IFNβ secretion might lead to chronic inflammation (Akbar et al., 2000). In the current study, we analysed IFNα and IFNβ secretions by FLS and in grade-specific OA-SFs. We found persistent and excessive amounts of IFNβ in particular in progressive grades of OA-SF and found minimal levels of IFNα, so have studied the mechanism of IFNβ induction in detail in OA. Studies have shown that IFNβ triggers experimental synovitis and may potentiate chronic inflammatory and auto-immune diseases in humans (Rosenbach et al., 1984, Akbar et al., 2000, Stark et al., 1998) and increasing evidence shows a role for targeting signal transduction involving IRF3 and IRF7 transcription in inflammatory joint pathologies towards the regulation of Type I IFN production (Berenbaum, 2004, Honda et al., 2006, Sweeney, 2011). Moreover, the regulatory role of various members of the IRF family such as IRF3, IRF5 and IRF7 have already been well characterised and elucidated in TLR signal transduction pathways and numerous studies have now shown the potential role of IRF3 and IRF7 as valuable molecular targets for therapeutic interventions to prevent inflammatory diseases. In the current study, we propose that necrotic cell derived RNA from the grade-specific OA-SF could potentially induce IRF3, 7 and 9, but not IRF5 in FLS. IRF9 is a cellular transcription factor with a molecular mass of 48kDa, and belongs to the IRF family of transcription factors.

Whilst, IRF9 is known to play a crucial regulatory role in JAK-STAT IFNAR signalling pathways for the stimulation of IFN-responsive genes (Schindler and Brutsaert, 1999), in this study we have shown that IRF9 plays a very significant and vital role in the TLR signalling pathway towards the production of Type I IFNs itself. To the best of our knowledge, till date, no studies have shown the role of IRF9 in the TLR signalling pathway in inducing Type I Interferons production and the exact mechanism and functional characterisation of IRF9 in TLR signalling is currently being investigated in our lab. Whilst, in this chapter, for the first time we show that IRF9 possibly gets induced equally like IRF3 and IRF7 transcription factors in a TLR3 dependent manner upon stimulation with the endogenous necrotic cell RNA from the grade-specific OA-SF and also with Poly(I:C) in early and late OA patient derived FLS. Also, for the first time, in this study, we show that IRF9 works possibly through binding to the PRDI-III domain of the IFNβ promoter and potently induces IFNβ expression equally like the IRF3 and IRF7 transcription factors. Herein, we also show that, TLR3 blockade in FLS could partially regulate grade-specific OA-SF and Poly(I:C) induced IRF9 protein levels. Thus, modification of IRF9 may provide a novel regulatory mechanism to prevent unwanted

inflammation and prevent OA progression. A schematic representation of the effects of an anti-TLR3 antibody on TLR3 signalling is depicted in Figure 4.5.1.

We propose that upon sensing of endogenous cell free RNA from the necrotic cells in the synovial fluid or joint, TLR3 recruits the adaptors TRIF, TRAF6 as well as the kinases RIP1, TBK1 and the IKKε. RIP1 and possibly TRAF6 mediated the TLR3-dependent transcriptional activation of NF-kB probably through TAK1/TAB1, leading to the binding of NF-κB to the PRDII domain of the IFNβ promoter. Whereas, TBK1 and IKKε necessitated the transcriptional activation of IRF3, 7 and IRF9 (by an unknown mechanism (dotted line-currently under investigation), IRF9 may be induced probably through the binding of excess IFNβ already available in the synovial fluid to the IFNARs in the FLS), leading to the binding of IRF3, 7 and 9 to the PRDI-III domain of the IFNβ promoter. Together, these resulted in increased expression and release of key inflammatory mediators namely IFNβ, RANTES, TNFα, IL-1β, IL-6, IL-15, IL-8, MMPs-1,3, 9 and 13 in OA-FLS. These mediators may then constitute a second pathway in FLS (not shown), independent of the TLR3 signalling, possibly through the respective cytokine/chemokine receptor activation in an autocrine and a paracrine fashion which leads to excess induction of inflammatory mediators in a feed back/feed forward mechanism in the joint and thus might aid maintain a chronic inflammatory loop ultimately leading in OA progression.

Interestingly, in OA-FLS, neutralisation of surface bound TLR3 utilising anti-TLR3 antibody potently inhibited the translocation of IRF3 and 9 through PRDI-III domain and NF-κB through PRDII domain of the IFNβ promoter, thereby blocking the excess expression and release of key OA associated inflammatory mediators in the joint. Thus, TLR3 may be a critical target for OA disease intervention. Given this, future work holds promise to validate and functionally characterise the role of this novel IRF9 transcription factor in TLR3 signalling in OA upon physiologically relevant endogenous stimuli. More investigations are also needed to define the role of TLR3 in various cell types present in synovial tissue and the communication pathways that occur between cartilage, subchondral bone and synovial tissue have yet to be fully elucidated in the pathogenesis of OA.

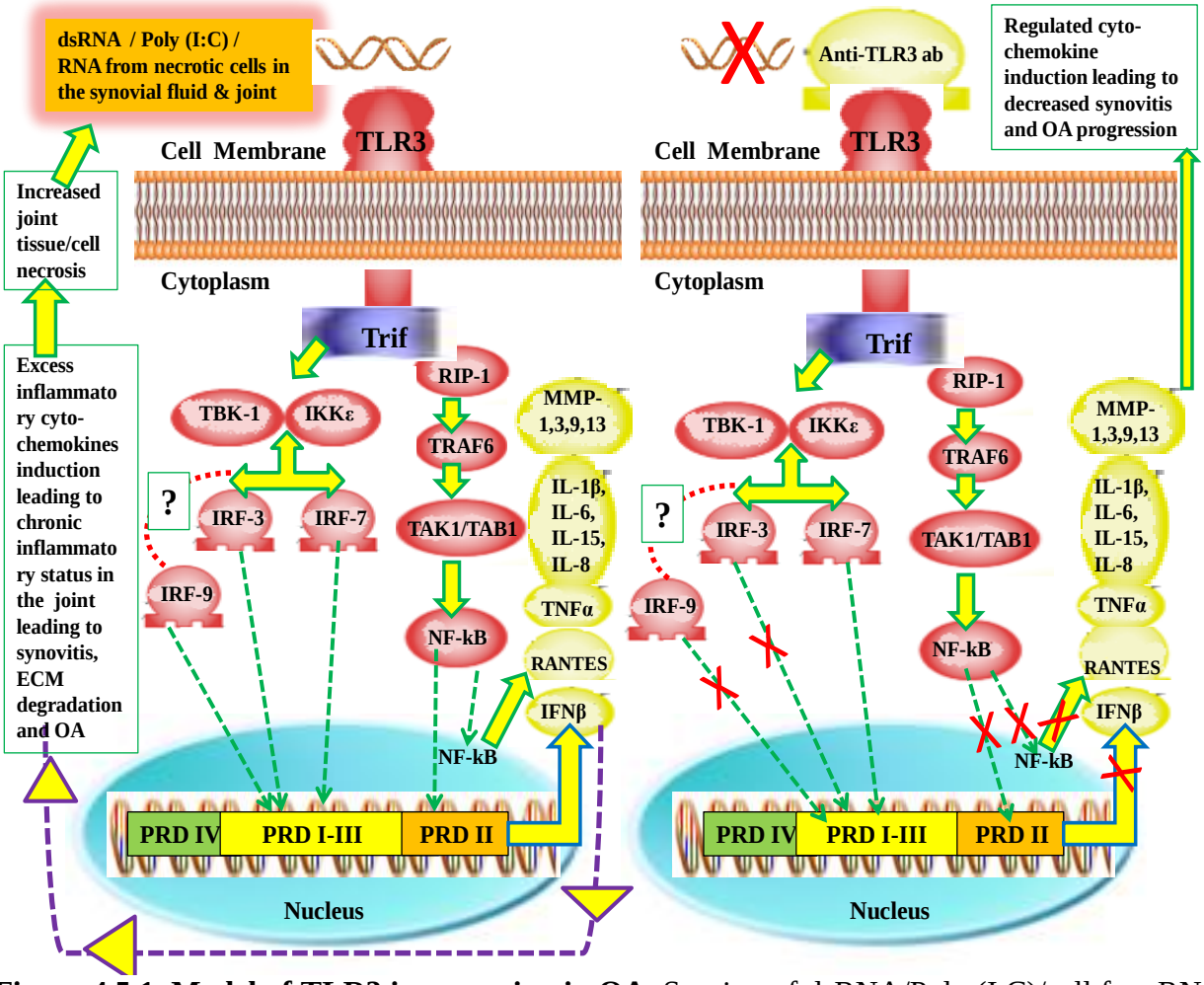

Figure 4.5.1. Model of TLR3 intervention in OA. Sensing of dsRNA/Poly (I:C)/cell free RNA from necrotic cells in the synovial fluid or joint by TLR3 results in the assembly of a receptor complex at least comprising the adaptors TRIF, TRAF6 as well as the kinases RIP1, TBK1 and the IKKε. RIP1 and possibly TRAF6 mediate TLR3-dependent transcriptional activation of NF-κB possibly through TAK1/TAB1, leading to the binding of NF-κB to the PRDII domain of the IFNβ promoter. Whereas, TBK1 and IKKε seems to be essential for the transcriptional activation of IRF3, 7 and IRF9 (by an unknown mechanism (dotted line), leading to the binding of IRF3, 7 and 9 to the PRDI-III domain of the IFNβ promoter. Together, these resulted in increased expression and release of key inflammatory mediators namely IFNβ, RANTES, TNFα, IL-1β, IL-6, IL-15, IL-8, MMPs-1,3, 9 and 13 in OA-FLS. Neutralisation of surface bound TLR3 utilising an anti-TLR3 antibody potently inhibited the translocation of IRF3 and 9 through PRDI-III domain and NF-κB through PRDII domain of the IFNβ promoter, thereby blocking the excess expression and release of key OA associated inflammatory mediators in the joint. Thus, TLR3 is a critical target for OA disease intervention. Also, further work is on-going to place IRF9 in the first or second wave (IFNAR) following TLR3 stimulation.

dsRNA, double-stranded RNA; IRF, interferon-regulatory factor; NF-κB, nuclear factor kappa B; IkB, inhibitor of NF-κB; IKK, IkB kinase; IKKε, IkB kinase epsilon; TRAF6, tumour necrosis factor receptor-associated factor 6; TANK, TRAF family member-associated NF-κB activator; TBK1, TANK-binding kinase-1; TAK1, transforming growth factor beta-activated kinase-1; TAB1, TAK1 binding protein 1; RIP1, receptor interacting protein; PRD, positive regulatory domain; TLR3, Toll-like receptor 3; TRIF/TICAM, TIR domain-containing molecule; TNF-α, tumour necrosis factor-α; IFNβ, nterferon beta; RANTES, Regulated upon Activation, Normal T-cell Expressed, and Secreted; IL, interleukin; MMP, matrix metalloproteinase.

Chapter 5

Proteomic analysis of OA synovial tissue and FLS

5.1. Introduction

Proteins are long considered as attractive biomarker candidates as they can be quantified to a reasonable accuracy with various assays and play an active role in the pathogenesis of arthritis. Furthermore, proteomics is also being used to identify the key proteins involved in modulating the pro-inflammatory response in arthritis. Proteomics is a relatively new research tool in the field of arthritis. Several studies have used proteomics to identify proteins in serum and synovial fluid (Drynda et al., 2004, Gibson and Rooney, 2007, Gibson et al., 2009). In addition, proteomics studies have examined the proteins that are up/down regulated in cartilage or synovial tissue, such as chondrocytes and synovial fibroblasts (Hermansson et al., 2004, Dasuri et al., 2004, Bo et al., 2009). However, these studies can only give a certain amount of information. When analysing synovial tissue the heterogeneity and complex interactions of the several cell types (T cells, NK cells, fibroblasts, macrophages, B cells) suggest that protein markers need to be identified in tissue which mimics the joint environment, and then verified in isolated cell cultures and serum. To date, a limited number of studies have used synovial tissue samples to identify potential diagnostic biomarkers in OA**.**

Therefore, to establish whether differences in relative protein expression occurs during different stages of synovial inflammation in OA, we have performed differential in-gel electrophoresis (DIGE) (De Ceuninck and Berenbaum, 2009) analysis using stage-specific OA synovial explants, wherein fluorescent dyes were used to differentially label up to 3 protein samples prior to 2-dimensional gel electrophoresis (2D-GE). Next, software analysis using 'progenesis' was performed to identify the differentially expressed proteins, followed by mass spectrometry. This aspect of the project was performed in collaboration with Dr. Edel, former Post Doctoral Fellow, Immune Signalling Lab, NUIM. The DIGE allowed multiple samples to be co-separated and visualised on a single 2D gel and offered fentogram sensitivity that is compatible with mass spectrometric analysis. A linear response to variation in protein concentration over 5 orders of magnitude was permitted, thus, low-abundant proteins were detected using small amounts of patient samples.

To better understand the molecular mechanisms and to identify pathologic mediators involved in synovial inflammation associated with OA, we performed a preliminary differential proteomic study to identify proteins in whole tissue synovial explants from 4

patients with stage-specific grades of OA, critically diagnosed and graded using both the arthroscopic and radiological grading systems. Further, to identify and understand the inflammatory mediators involved in OA pathology, N and OA FLS were stimulated with TLR/RLR ligands, namely Pam_2CSK_4, Poly (I:C), LPS, CLO-97 and 5'ppp-dsRNA. Additionally, FLS were stimulated with inflammatory OA synovial fluid (OA-SF). Notably, the sample preparation protocol was designed to extract both extracellular and intracellular proteins from the synovial explants and FLS.

A panel of distinct proteins were identified as being differentially expressed in an OA grade-specific manner and is a TLR/RLR ligand dependent manner. Several of the identified proteins have been implicated in OA pathophysiology previously. Additionally, several proteins that had not been previously reported to be associated with OA pathology were identified.

5.1.1. Specific aims of chapter 5

1. To assess the differential protein expression patterns of grade-specific OA synovial tissue explants using DIGE.
2. To analyse the differential protein expression patterns of N and OA FLS following stimulation with TLR/RLR ligands and OA-SF.
3. To perform confirmatory expression analysis of the selected proteins in N and OA FLS by immunoblot analysis and confocal microscopy.

5.2. Experimental Materials and Suppliers

Affymetrix, Anatrace products

CHAPS, Cat. # 13361

Bio-Rad

Bradford Reagent, Cat. # 500-0006

Cell Signalling

Prohibitin Antibody, Cat. # 2426

Vimentin Antibody, Cat. # 3932

Caldesmon-1 Antibody, Cat. # 2980

Fisher Scientific

Glycine, Cat. # G/0800/60

Sodium Chloride (NaCl) GPR, Cat. # S/3120/60

GE Healthcare

IPG strips (3-10 pH), Cat. # 17-6002-44

Ampholytes (3-10 pH), Cat. # 17-6000-87

Destreak, Cat. # 17-6003-18

CyDye DIGE Fluor, minimal labeling kit, Cat. # 25-8010-65

National Diagnostics

Protogel, Cat. # EC-890

Protogel Buffer, Cat. # EC-892

Promega

Trypsin, Cat. # V511-27619702

Roche

Protease Inhibitor Cocktail Tablets (PICs) (Complete mini), Cat. # 11-836-153-001

Sigma

Brilliant Blue R concentrate, Cat. # B 8647-1EA

Trizma Base, Cat. # 93352

Sigma-Fluka

Methanol, Cat. # 242298

Acetic acid, Cat. # 33209

Formic acid, Cat. # 06440

Acetonitrile (ACN), Cat. # 34967

LC-MS chomasolv water/HPLC grade water, Cat. # 39253

Sigma-Aldrich

Urea, Cat. # 0631

Thiourea, Cat. # T8656

D-Lysine, Cat. # L5876

Glycine, Cat. # G7126

DL-Dithiotheitol, Cat. # D9163

Idoacetamide (IAA), Cat. # I1149

Ammonium bicarbonate, Cat. # 6141

Brilliant Blue R concentrate, Cat. # B 8647-1EA

Siliconised polypropylene tubes, Cat. # T3406250EA

Thermo scientific

Coomassie Brilliant Blue G-250 Dye, Cat. # 20279

5.2.1. Buffers for sample preparation

Lysis buffer: For 50 ml

7 M Urea- 21.021g + 20ml milliQ water (mQ)

2 M Thiourea-7.612g+ 20ml mQ

4 % CHAPS-2g / 50ml

PICs: 1tablet / 10ml, so 5tablets / 50ml.

2X Dilution Buffer: For 50ml

7 M Urea-21.021g + 20ml mQ

2 M Thiourea-7.612g + 20ml mQ

4 % CHAPS-2g / 50ml

2 % Ampholytes-1ml / 50ml

2 % DTT-1g / 50ml

Rehydration Buffer: For 50ml

8 M Urea-24.24g + 20ml mQ

0.5 % CHAPS-250mg

0.2 % DTT (100mg) / Destreak (12µl/ ml)

0.2 % Ampholytes (100µl)

5.2.2. Buffers for In-gel trypsin digestion

100 mM Ammonium bicarbonate (AB): 395 mg of AB was weighed and the volume was made up to 50 ml with HPLC grade water.

50 mM Ammonium bicarbonate (AB): 40 mg of AB was weighed and the volume was made up to 10 ml with HPLC grade water.

1 M DTT:0.154g of DTT was weighed and the volume was made up to 1 ml with HPLC grade water.

10 mM DTT: 23mg of DTT was weighed and the volume was made up to 15 ml with 100mM AB.

55 mM Iodoacetamide: 153 mg of IAA was weighed and the volume was made up to 15 ml with 100 mM AB.

1:1 AB/ACN: 7 ml of 100 mM AB was mixed with 7 ml of pure Acetonitrile (ACN).

Reconstitution Buffer: 1 ml of 100 mM AB and 1 ml of ACN was thoroughly mixed with 8 ml of HPLC grade water.

Extraction Buffer: 1 ml of 5 % Formic acid was mixed with 2 ml of pure ACN

Trypsin working solution: The reconstitution buffer (100µl) was added to the trypsin vial (20 µg/ vial) and then aliquotted into 10 x 10 µl aliquots and was stored at -20 ^{o}C for up to 2 weeks. When ready to use, an aliquot was removed from the -20 ^{o}C freezer and 500 µl of mM AB was added to make the working solution of trypsin.

5.3. Experimental Methods

5.3.1. FLS stimulations and protein sample preparation

N-FLS and end stage OA-FLS were seeded at 5×10^5 cells/flask in pyrogen free T175 tissue culture flasks with 20 ml of complete synoviocyte growth medium (ECACC), and cultured until confluent. Next, the old culture medium in the flasks was decanted and the adherent FLS were then rinsed twice with 2-3 ml of Opti-MEM.(low/no salt present). Prior to stimulation, FLS were rendered quiescent by maintaining the cells in serum free Opti-MEM for 24 h. Further, cells were stimulated with Pam_2CSK_4 (1µg/ml), Poly (I:C) (10µg/ml), LPS (1µg/ml), CLO-97 (1µg/ml), 5' pppdsRNA (1µg/ml) and end stage OA-SF (1:10 dilution in Opti-MEM), for 24 h or were left unstimulated prior to extraction of protein in a final volume of 10 ml Opti-MEM. The FLS were then solubilised with 1ml of lysis buffer as described in section 5.2.1, and were left overnight at -20 ^oC on a shaker to facilitate the slow lysis of the cells. Next, the cells were scraped off the flask with a sterile cell scraper and placed into a 50ml falcon tube. The protein sample thus obtained was desalted and purified using the acetone precipitation method as described in section 5.3.3 and stored at -20 ^oC. Protein quantification was performed using a modified Bradford Assay, as described in section 5.3.4.

5.3.2. Synovial tissue protein extraction for DIGE analysis

Whole synovial tissue biopsies were obtained from grade-specific OA patients and healthy trauma subjects as described in section 4.3.2 (chapter 4). For differential protein analysis of grade-specific synovial tissues, three independent synovial biopsies obtained from OA patients (n=3 per grade) and healthy trauma subjects (n=3), were weighed and snap frozen in liquid nitrogen prior to homogenization using a sterile motor and pestle. The extract samples were then resuspended in DIGE lysis buffer (9.5M urea, 2 % CHAPS, 20mM Tris), for further protein quantification using Bradford Assay and stored at -80°C until further use.

5.3.3. Acetone precipitation

The protein samples were precipitated by adding four volumes of 100 % ice cold acetone to the sample followed by brief vortexing. The mixture was then incubated for 1 h at -20 ^oC. Next, the samples were centrifuged at 4600 rpm for 20 min in a table top centrifuge (Du Pont, U.S.A.), and the supernatant was discarded. Subsequently, the pellet was

resuspended in four volumes of 80 % ice cold acetone and left for 1 h at -20 ^{o}C. Samples were then centrifuged at 4600 rpm for 20 min in a table top centrifuge (Du Pont, U.S.A.), and the supernatant was discarded. This step was repeated for a further three times. The precipitated protein sample was then solubilised in 100 µl of lysis buffer.

5.3.4. Bradford Assay

A standard protein curve was prepared by diluting a stock solution of 5 mg/ml BSA with lysis buffer ranging from 0-100 mg of BSA. Standard dilutions were generated using 10 µl of lysis buffer, 80 µl of mQ, and 10 µl of 0.1 M HCl. Similarly, protein samples for the assay were prepared using 10 µl of protein sample solubilised in 10 µl lysis buffer, 80 µl of mQ, and 10 µl of 0.1 M HCL. Next, 3.5 ml of working Bradford reagent (1 part Bradford reagent dye: 3 parts distilled water) was added to the samples and standards followed by mixing and incubation at RT for 5 min. Absorbance reading for the standards and samples was performed at 595 nm followed by determination of protein concentration from the standard graph (Bradford, 1976). Appropriate amounts of protein sample to be utilised for 2D-PAGE LC-MS and 2D-DIGE LC-MS were thus quantified and 200 µg/24cm strip was used for IEF and 50 mg/24 cm IEF strip, respectively.

5.3.5. Passive In-gel rehydration and IEF

Briefly, 200 µg of protein sample was diluted with an equal volume of 2× dilution buffer (section 5.2.1), and was made-up to a final volume of 450 µl with rehydration buffer (section 5.2.1), and 0.05 % (w/v) bromophenol blue was added as a tracking dye. This solution was mixed well and then was applied to a 24cm linear IPG strip-pH 3-10, for overnight passive rehydration, in a re-swelling tray (Amersham Bioscience/GE Healthcare, Little Chalfont, Bucks, UK). Following overnight passive rehydration, the IPG strips were loaded gel side up on an Amersham Ettan IPG-phor manifold. Cover fluid (108 ml) was added to submerge the strips for better conduction and to avoid drying out of the strips. IEF was performed using an Amersham IPG-phor IEF system and the following conditions: 30 V for 1 h, 100 V for 1 h, 1000V for 1 h, 6000 V for 1 h, 8000 V for 3 h, 500 V for 4 h and finally 8000 V for 3 h as previously described (Donoghue et al., 2005). Following IEF, the IPG strips were equilibrated in 6 M urea, 30 % (w/v) glycerol, 2 % (w/v) SDS, 100 mM DTT for 20 min followed by equilibration in 6 M urea, 30 % (w/v) glycerol, 2 % (w/v) SDS, 100 mM DTT, 0.25 M iodoacetamide for 20 min. The strips were

then briefly washed in SDS running buffer (0. 0125 M Tris, 0.96 M glycine,0.1 % (w/v) SDS) and were applied on 12 % (w/v) resolving gels for 2D-gel electrophoresis.

5.3.6. 2D-PAGE

Briefly, 1.5 mm glass plates were cleaned using 70 % ethanol, dried, and assembled in the Dalt 6 gel caster (GE Healthcare). The 12 % gel mixture was prepared using the following mixture: 120 ml of protogel, 78 ml of protogel buffer, 1.2 ml of 10 % APS (Sigma), 120 µl of TEMED (Sigma) and 98.7 ml of distilled water. The mixture was mixed and immediately poured evenly into the caster until the level of solution was approximately 0.5 cm below the top of the glass plate. A layer of water-saturated was then poured above the gel mixture nad was removed after an h and replaced with de-ionised water. The gels were allowed to polymerise overnight at RT. The equilibrated IPG strip were applied to the top of the 12 % resolving gel and set in place using 1 % (w/v) agarose sealing gel. The gel electrophoretic separation of the stimulated and control FLS proteome in the second dimension was performed by SDS-PAGE using an Amersham Ettan DALT-Twelve system as previously described (Doran et al., 2006). Electrophoresis was performed at 80 V for 2 h, followed by a 500 V step, until the bromophenol dye front had just ran off the gel.

5.3.7. RUBP's gel staining and image acquisition

Following electrophoresis, the 2D-SDS-PAGE gels were fixed overnight with a solution containing 10 % (v/v) acetic acid and 30 % ethanol. The gels were then washed for 30 min with 20 % ethanol and the wash step was repeated a further three times. The gels are then incubated with 1 µM RuBP's (Ruthenium II Bathophenatholine Disulfonate Chelate) solution for 6 h at RT in the dark with gentle agitation. Following saturation with the dye, gels were either equilibrated with mQ or destained overnight using 10 % acetic acid and 40 % ethanol. These gels were briefly washed with mQ for visualisation. Fluorescently labelled proteins were visualised using the Typhoon Trio variable mode imager (Amersham Bioscience/GE Healthcare, Little Chalfont, Bucks, and UK), at a scanning wavelength of 528 nm. The photometric tube (PMT) values for gels analysed were between 500 V and 580 V and scanning was performed at a resolution of 100 mm and a maximum pixel volume of 80,000 and 90,000. The 2-D images were then cropped using Image Quant TL software. The gel images, thus obtained were analysed using Progensis Samespots analysis software.

5.3.8. Analysis of 2D SDS-PAGE gels using Progenesis Software

All gel images were loaded onto the Progenesis (Non-linear dynamics) samespots analysis software, which allowed semi-automated alignment of the gel images. All the gels were aligned to a selected reference gel. Next, the analysis proceeded via automated spot-detection, filtration, normalisation and spot volume calculation. The gel images were then separated into the following groups, Control and PAMPs-stimulated, and the differences in protein expression levels between each group was detected by analysis of normalised spot volumes and a list was then generated of those spots that had changed in abundance. An ANOVA score and fold change parameters were utilised for each spot and any spot with an ANOVA value above 0.5, and fold change below 2 was excluded, and the spots with a change in abundance that met all criteria were subsequently identified by Liquid chomatography –Mass spectrometry (LC-MS).

5.3.9. DIGE analysis

The protein samples extracted from grade-specific OA whole synovial tissue biopsies were labelled with CyDye DIGE Fluor minimal dyes according to the manufacturer's instructions (GE Healthcare). Initially, Cy2, Cy3 and Cy5 DIGE dyes were reconstituted as a stock solution of 1mM in fresh Dimethylformamide and prior to labelling; the stock solution was diluted to a working concentration of 0.2mM. Briefly, 50 mg of grade-specific OA protein samples were solubilised in DIGE lysis buffer (9.5M urea, 2 % CHAPS, 20mM Tris). Each grade-specific OA sample and trauma control sample with biological replicates were separately and minimally labelled with 200 pmol of Cy3 and Cy5 working solutions respectively. A pooled sample was generated utilising equal quantities of protein from all replicates in the experiment and was labelled at 200 pmol of Cy2 working solution to 50 mg of protein and this was used as an internal standard. All samples at pH 8.5 were labelled with the appropriate amount of dye and after brief vortex; these labelled samples were incubated on ice in the dark for 30 min. This labelling reaction was quenched by adding 1 ml of a 10 mM L-lysine solution (Sigma) and left on ice in dark for 10 min. Following, quenching and labelling, grade-specific OA samples, control trauma samples and pooled internal standard protein samples were mixed sufficiently (one of each condition per gel) and was run in a single gel. A volume of the rehydration solution (7 M urea, 2 M thiourea, 4 % CHAPS and 0.8 % IPG Buffer pH 3-10) containing 50 mM DTT/100 mM DeStreak was added to the mixed samples. Proteins (150 mg total protein per gel) were then applied onto 3-10 pH IPG strips with an equal volume of 2× sample

buffer (7M urea, 2M thiourea, 65mM CHAPS, 2 % ampholytes and 2 % DTT) for overnight passive rehydration. Next, the proteins were separated in the first dimension at 0.05 mA/IPG strip in the IPGphor IEF II System (GE Healthcare) until steady state (42 kVh). Thereafter, the strips were either equilibrated and separated by SDS-PAGE on a 12 % polyacrylamide gels (26 x 20 cm) precast into low fluorescence-glass plates using an Ettan Dalt Six device (GE Healthcare) at 2 W/gel for 1 h and 20 W/gel at 25 ºC until the tracking dye had migrated off the bottom of the gel or were alternatively frozen at -80 ^{o}C for future use.

5.3.10. DIGE image acquisition and analysis

The DIGE gels were scanned on a Typhoon Trio variable mode Imager (GE Healthcare) using appropriate wavelengths and filters for Cy2, Cy3 and Cy5 dyes according to the manufacturer's protocol. Scans were acquired at 50 mm resolution. After cropping, images were subjected to automated Differential In-gel Analysis (DIA) and Biological Variation Analysis (BVA) using the DeCyder Differential Analysis Software, Release 6.0 (GE Healthcare). After manual inspection of the automatic matching, the differential protein spots thus identified for ID were taken by parallel pick-up from a single sample colloidal coomassie stained gel that was run simultaneously with the DIGE gel.

5.3.11. Colloidal Coomassie Staining

To visualise and pick the differential gel spots identified by Progenesis and DeCyder, colloidal coomassie staining was performed. This procedure was performed as previously described (Neuhoff et al., 1988). Following electrophoresis, the gels were washed twice with mQ and placed into either Brilliant Blue R concentrate-neat staining solution or in to Colloidal Coomassie staining solution, (1 Part Stock Solution A (5 % (w/v) coomaasie brilliant blue (G250); 40 Parts Stock Solution B (10 % (w/v) ammonium sulphate, 2 % (v/v) phosphoric acid); 10 parts methanol) and left for overnight incubation at RT with gentle agitation on a see-saw rocker. The gels were then rinsed for 1-3 min with neutralisation buffer (0.1 M Tris-PO_4, pH 6.5). Further, a 25 % methanol wash for 1 min was performed to reduce the gel background and the coomaasie dye in the gel was then fixed by a wash in fixation solution (20 % (w/v) ammonium sulphate) overnight. Once adequate protein visualisation was achieved, the gels were then scanned using Umax Image scanner (Amersham Bioscience/GE Healthcare, Little Chalfont, Bucks, and UK). The protein spots were then excised for LC-MS.

5.3.12. In-Gel Trypsin Digestion and LC-MS analysis

The in-gel trypsin digestion of gel plugs was performed according as previously described (Shevchenko et al., 2007) with minor modifications. Briefly, the prototype coomassie stained gel slab previously identified with Progenesis and DeCyder for the differential protein spots to be picked was rinsed in water for few h in laminar flow hood. The protein spots were then excised using a sterile tip, and transferred to a siliconised micro-centrifuge tube and centrifuged at high speed for 1 min. Then, destaining for coomassie gel plugs was carried out by adding 100 µl of 100 mM AB/ACN (1:1) solution (section 5.2.2.) to each gel plug for 30 min with occasional vortexing at RT, until stain was removed. Further, 500 µl of neat Acetonitrile (ACN) was added to the gel plugs for 10 min at RT with occasional shaking, until the gel plugs look opaque.

5.3.12.1. Tryptic Digestion

Approximately, 30-50 µl of trypsin working solution (section 5.2.2), was added to the gel plugs, so that the buffer covers the gel piece, to avoid drying out of the gel plug. These plugs were then incubated at 4 ^{o}C for 30 min, followed by addition of 20 µl of 50 mM AB buffer (section 5.2.2) to the gel plugs and incubation for 90 min at 4 ^{o}C to facilitate the activation of the enzyme and to allow for the slow diffusion of trypsin into the gel pieces. Following incubation, if required, an additional 10-20 µl of 50 mM AB buffer was added to the gel plugs to avoid drying out of the plugs. Next, the gel plugs were incubated with 30 µl of working concentration of trypsin for 24 h at 37 ^{o}C to allow slow and complete tryptic digestion.

5.3.12.2. Peptide Extraction

Extraction buffer 100µl (1:2 ratio of 5 % Formic acid: ACN) was added to the gel plugs followed by incubation at 37 ^{o}C for 15 min on a rotary shaker. The resultant supernatants containing the peptides were pipetted into sterile microcentrifuge tubes using gel loading tips. The samples were then subjected to vacuum centrifugation overnight at RT to dehydrate and concentrate the peptide fractions prior to LC-MS analysis.

5.3.12.3. LC-MS analysis

The concentrated peptide fractions were then resuspended in 10-20 µl of 0.1 % formic acid, vortexed, and then sonicated for 2 min to ensure complete resuspension of the

samples. Next, the samples were centrifuged at 10,000 rpm for 15 min at 4 ^{o}C to sediment remnants of the gel plugs. The supernatants with the peptide fractions were collected and transferred on 0.22 µM cellulose acetate filter columns and centrifuged at 10,000 rpm for 2-5 min at 4 ^{o}C. The required volume of the sample was aliquoted into the LC-MS vial whilst ensuring that air bubbles were avoided. The vials was then subjected to LC-MS as follows: Electrospray ionization (ESI) was employed coupled with Reverse Phase Liquid Chomatography (RPLC) on a HPLC chip in the Agilent 6340 Ion Trap LC-MS machine. The results were collected for 15 min per spot of protein and peptide mass fingerprinting was employed to process the raw data and further proteins were identified with Mascott search engine (http://www.matrixscience.com), using both NCBInr and swiss-prot human databases. The following search parameters were used: precursor-ion mass tolerance of ± 1.5 Da, fragment ion tolerance of ± 1.0 Da with methionine oxidation as variable modification and cysteine carbamidomethylation as fixed modification, and a maximum of 2 missed cleavage sites were allowed.

5.3.13. Differential protein quantification though western blot and confocal analysis

N and OA-FLS were seeded at 1 × 10^5 cells/well in triplicates in a 6-well tissue culture plate for western blot analysis and a density of 0.5 x 10^5 cells/ml in 8-well chamber slide for confocal analysis and were grown until confluent. Prior to stimulation, FLS were rendered quiescent by incubation in serum free Opti-MEM for 24 h. Cells were stimulated with Poly(I:C) (10 µg/ml) for 2 h in OptiMEM. Subsequently, cells in the 6-well culture plates were lysed and utilised for immunoblot analysis and the cells on the 8-well chamber slides were subjected to confocal microscopy. The antibody dilutions employed for immunoblot analysis were as follows: β-actin (mouse; 1:1000), Vimentin (rabbit; 1:1000), Prohibitin (rabbit; 1:1000), Caldesmon-1 (rabbit; 1:1000) and the secondary anti-mouse and anti-rabbit IgG-HP antibodies (1:5000 dilution). The antibody dilutions employed for confocal microscopy were as follows: Vimentin (rabbit; 1:50), Prohibitin (mouse; 1:100) and Caldesmon-1 (rabbit; 1:100).

5.4. Results

Separation of whole synovial tissue explants and FLS intracellular proteins by 2D-GE allow their visualisation and analysis and this strategy facilitates comparative studies between diseased, treated and control cells. Investigating the characteristics and behaviour of synovial cells appears to be a good strategy to gain a better understanding of the phenotypic changes that they undergo in arthitic diseases. To better understand the proteomic changes that FLS undergo in response to TLR/RLR ligands, namely Pam_2CSK_4, Poly (I:C), LPS, CLO-97 and 5'ppp-dsRNA, comparative proteomic analysis was performed. Additionally, to understand the intricate crosstalk of FLS and the synovial fluid in the OA joint, we have stimulated N-FLS with inflammatory OA synovial fluid (OA-SF), to mimic the cell-fluid contact in the joint. Given that, the OA synovial tissue primarily mimics the joint environment, and to establish protein expression patterns during different stages of synovial inflammation in OA, we performed DIGE analysis using stage-specific OA synovial explants. Notably, the sample preparation and protocol was optimised and designed to extract both extracellular and intracellular proteins from the synovial explants and FLS.

5.4.1. Differential proteomic analysis of N-FLS and OA-FLS

The 2D-GE resulted in the identification of 30 protein spots with a changed abundance in N and OA FLS. A representative 2D-gel with electrophoretically separated N-FLS and OA-FLS proteins is shown in Figure 5.1. An increased expression level was shown for 8 proteins and 22 proteins were found to be decreased in OA-FLS when compared to N-FLS. Table 5.1 (Appendix), summarises the results of the mass spectrometric identification of these 30 protein species from N and OA-FLS. The proteins with extremely altered abundance in OA-FLS compared to N-FLS are as follows, the protein spot with the highest 6-fold decrease in protein expression was found to be phosphoglycerate kinase 1 (spot 30), a cytoplasm localised protein with glycolytic enzyme activity (Michelson et al., 1983). Whereas, the spots with maximal 2.8-fold increase in protein expression were found to be vimentin (spot 45), a cytoplasm intermediate filament with cellular component disassembly activity and host-virus interaction ability (Kang et al., 2005) and manganese superoxide dismutase (spot 53), a mitochondrion matrix protein, which removes or destroys superoxide radicals (MacMillan-Crow and Thompson, 1999). The majority of identified proteins were previously shown to be constituents of key metabolic reactions,

cytoskeletal machinery, cellular stress response and cell signalling pathways (Ruiz-Romero and Blanco, 2009). Notably, a novel mitochondrial protein with 2.5-fold decrease in protein expression in OA-FLS than N-FLS was identified for the first time and was found to be prohibitin (spot 79), which has known regulatory role in proliferation, mitochondrial respiration and aging (Coates et al., 2001).

5.4.2. Differential proteomic analysis of Poly (I:C) treated N-FLS and OA-FLS

N and OA FLS were treated with Poly (I:C) (10 µg/ml) for 24 h and the soluble protein extract was resolved using 2D-GE (Figure 5.2), and the differential protein spots were then identified utilising progenesis software and were then subjected to LC-MS analysis. A total of 60 protein spots for N-FLS and a total of 54 protein spots for OA-FLS, with a changed abundance in response to Poly (I:C) stimulations were identified though LC-MS. Among the 60 altered protein species in N-FLS, 31 proteins showed an increased expression level (Figure 5.2, panel B), and 29 proteins were found to be decreased (Figure 5.2, panel A), with Poly (I:C) stimulation in N-FLS when compared to unstimulated or control N-FLS. Table 5.2 (Appendix) summarizes these proteins. Among the 54 altered protein species in OA-FLS, 36 proteins showed an increased expression level (Figure 5.2, panel D), and 18 proteins were found to be decreased (Figure 5.2, panel C), with Poly (I:C) stimulation in OA-FLS when compared to unstimulated or control OA-FLS. Table 5.3 (Appendix) summarizes these proteins. The proteins with extremely altered abundance in response to Poly (I:C) stimulation in N-FLS compared to control N-FLS are as follows, the protein spot with the highest 2.1-fold decrease in protein expression was found to be prohibitin (spot 441), which is localised at various sites namely mitochondrial inner membrane, cell membrane, cytoplasm and nucleus, has been attributed for several regulatory roles such as in apoptosis, cell proliferation angiogenesis and ageing (Misha et al., 2006, Misha et al., 2005). The protein spots with the maximal increase in protein expression in response to Poly (I:C) stimulation in N-FLS, were found to be vimentin (spot 179) and caldesmon (spot 209) with 4.9 and 4.1 fold increase, respectively. Wherein, vimentin, as previously described is a cytoplasm intermediate filament which maintains the chondrocyte phenotype and with an increase in cellular component disassembly activity can disturb the integrity of the articular cartilage, and may ultimately lead to OA (Blain et al., 2006), as well was attributed with host-virus interaction ability (Kang et al., 2005). Caldesmon, a cytoplasm localised, calmodulin and actin binding protein with numerous functions in cell motility, such as migration, invasion and proliferation, exerted via the reorganization of the actin

cytoskeleton (Huber et al., 1993, Mayanagi and Sobue, 2011, Morita et al., 2012). Interestingly, stimulation of OA-FLS with Poly (I:C) stimulation resulted in an elevated expression of both caldesmon (spot 525, with 4.5-fold increase) and vimentin (spot 549, with 5.5-fold increase), thus implying a ligand specific induction of these proteins in FLS. Furthermore, a 55.6-fold increase in the expression of Ubiquitin-like protein ISG15 (spot 1688) was found following stimulation of OA-FLS with Poly (I:C) stimulation; ISG15 is a secreted cytoplasmic protein that plays a role in anti-viral defence, host-virus interaction and the ubiquitin conjugation pathway (Loeb and Haas, 1992, Knight and Cordova, 1991, Narasimhan et al., 1996). Similar to N-FLS, stimulation of OA-FLS with Poly (I:C) resulted in a dramatic 7.4-fold decrease in prohibitin (spot 920) expression. Thus implying a ligand-specific down regulation of this mitochondrial chaperon.

5.4.3. Differential proteomic analysis of CLO-97 treated N and OA-FLS

N and OA FLS were treated with CLO-97 (1 µg/ml) for 24 h, and the soluble protein extract was resolved though 2D-GE (Figure 5.3), and the differential protein spots were identified utilising progenesis software and were then subjected to LC-MS analysis. A total of 43 protein spots for N-FLS and a total of 51 protein spots for OA-FLS, with a changed abundance in response to CLO-97 stimulation when compared to their respective cell type controls, were identified though LC-MS (Appendix, Table 5.5). Among the 43 altered protein species in N-FLS, 17 proteins showed an increased expression level (Figure 5.3, panel B), and 26 proteins were found to be decreased (Figure 5.3, panel A). The data are summarised in Table 5.4 (Appendix). Among the 51 altered protein species in OA-FLS, 30 proteins showed an increased expression level (Figure 5.3, panel D), and 21 proteins were found to be decreased (Figure 5.3, panel C). The proteins with extremely altered abundance in response to CLO-97 stimulation in N-FLS compared to control N-FLS are as follows, the protein spot with drastically high 98.3-fold increase in protein expression was found to be cystatin-B (spot 1177), and protein species with maximal 2.2-fold decrease in expression level was found to be gelsolin (spot 412). Wherein, cystatin-B, localised to the cytoplasm and nucleus, is an intracellular thiol proteinase inhibitor, and also known for reversible inhibitor of cathepsins L, H and B activity (Joensuu et al., 2006). Gelsolin, localised to the cytoplasm, is a calcium regulated, actin-modulating protein, with a role in ciliogenesis (Kim et al., 2010). Regarding OA-FLS, the proteins with altered abundance in response to CLO-97 stimulation compared to control OA-FLS were found to be pyruvate kinase isozymes M1/M2 (PKM2) (spot 365) with 9.8-fold increase in expression and nucleoside diphosphate kinase B (NDK B) (spot 924) with 2.2-fold decrease in expression.

Wherein, PKM2 is localised to the cytoplasm nad is involved in glycolysis and nuclear translocation of PKM2 induces programmed cell death (Steták et al., 2007). While, NDK B, is localised to the cytoplasm and plays a role in nucleotide metabolism and the negative regulation of Rho activity (Postel et al., 1993).

5.4.4. Differential proteomic analysis of RIG-I ligand treated N and OA-FLS

N and OA FLS were treated with 5' ppp-dsRNA (1 µg/ml) for 24 h, and the soluble protein extract was resolved though 2D-GE (Figure 5.4), and the differential protein spots were identified utilising progenesis software and were then subjected to LC-MS analysis. A total of 22 protein spots for N-FLS and a total of 31 protein spots for OA-FLS, with a changed abundance in response to CLO-97 stimulation when compared to their respective cell type controls, were identified though LC-MS. Among the 22 altered protein species in N-FLS, 9 proteins showed an increased expression level (Figure 5.4, panel B), and 13 proteins were found to be decreased (Figure 5.4, panel A). These data are summarised in Table 5.6 (Appendix). Among the 31 altered protein species in OA-FLS, 17 proteins showed an increased expression level and 14 proteins were found to be decreased (Figure 5.4, panel C). These data are summarised in Table 5.7 (Appendix). The proteins with extremely altered abundance in response to RIG-I ligand stimulation in N-FLS compared to control N-FLS are as follows, the protein spot with 18.4-fold increase in expression was found to be Alpha-β Crystalline (spot 604), and the protein species with maximal 2.9-fold decrease in expression was found to be Brain acid soluble protein 1 (spot 570). While, the proteins with particularly altered abundance in response to RIG-I ligand stimulation in OA-FLS compared to control OA-FLS are as follows, the protein spot with 9.5-fold increase in expression was found to be LIM and cysteine-rich domains protein 1 (spot 527), and the protein species with maximal 11.4-fold decrease in expression was found to be superoxide dismutase [Mn] (spot 1081).

5.4.5. Differential proteomic analysis of LPS treated N and OA-FLS

N and OA FLS were treated with LPS (1 µg/ml) for 24 h, and the soluble protein extract was resolved though 2D-GE (Figure 5.5), and the differential protein spots were identified utilising progenesis software and were then subjected to LC-MS analysis. A total of 47 protein spots for N-FLS and a total of 72 protein spots for OA-FLS, with a changed abundance in response to LPS stimulation when compared to their respective cell type controls, were identified though LC-MS. Among the 47 altered protein species in N-FLS, 28 proteins showed an increased expression level (Figure 5.5, panel B), and 19 proteins

were found to be decreased (Figure 5.5, panel A). These data are summarised in Table 5.8 (Appendix). Among the 72 altered protein species in OA-FLS, 46 proteins showed an increased expression level (Figure 5.5, panel D), and 26 proteins were found to be decreased (Figure 5.5, panel C). These data are summarised in Table 5.9 (Appendix). The proteins with extremely altered abundance in response to LPS stimulation in N-FLS compared to control N-FLS are as follows, the protein spot with 16.8-fold increase in expression was found to be Tapasin (spot 63), and the protein species with maximal 8.1-fold decrease in expression was found to be Manganese superoxide dismutase (spot 534). Regarding OA-FLS, the proteins with drastically altered abundance in response to LPS stimulation compared to control OA-FLS are as follows, the protein spot with 80.1-fold increase in expression was found to be Eukaryotic translational initiation factor 4H (KIAA0038) (spot 902), and the protein species with maximal 3.4-fold decrease in expression was found to be vimentin (spot 350).

5.4.6. Differential proteomic analysis of Pam_2CSK_4 treated N and OA-FLS

N and OA FLS were treated with Pam_2CSK_4 (1 μg/ml) for 24 h, and the soluble protein extract was resolved though 2D-GE (Figure 5.6), and the differential protein spots were identified utilising progenesis software and were then subjected to LC-MS analysis. A total of 44 protein spots for N-FLS and a total of 62 protein spots for OA-FLS, with a changed abundance in response to LPS stimulation when compared to their respective cell type controls, were identified though LC-MS. Among the 44 altered protein species in N-FLS, 19 proteins showed an increased expression level (Figure 5.6, panel B), and 25 proteins were found to be decreased (Figure 5.6, panel A). These data are summarised in Table 5.10 (Appendix). Among the 62 altered protein species in OA-FLS, 33 proteins showed an increased expression level (Figure 5.6, panel D), and 29 proteins were found to be decreased (Figure 5.6, panel C). These data are summarised in Table 5.11 (Appendix). The proteins with extremely altered abundance in response to LPS stimulation in N-FLS compared to control N-FLS are as follows, the protein spot with 4.4-fold increase in expression was found to be Manganese superoxide dismutase (spot 909), and the protein species with maximal 12.8-fold decrease in expression was found to be peroxiredoxin-1 (spot 894). Regarding OA-FLS, the proteins with drastically altered abundance in response to LPS stimulation compared to control OA-FLS are as follows, the protein spot with 18.9-fold increase in expression was found to be adenylate kinase 2 (spot 779), and the protein

species with maximal 3.9-fold decrease in expression was found to be tropomyosin alpha-4 (spot 628).

5.4.7. Differential proteomic analysis of OA-SF treated N-FLS versus control N-FLS and OA-FLS

N-FLS were treated with end stage OA-SF (1:10 dilution in opti-MEM) for 24 h, and the soluble protein extract was resolved though 2D-GE (Figure 5.7), and the differential protein spots were identified utilising progenesis software and were then subjected to LC-MS analysis. A total of 21 protein spots were found to be up-regulated in response to OA-SF treatment in N-FLS (Figure 5.7, panel B), when compared to control N-FLS (Figure 5.7, panel A), and a total of 11 protein spots were found to be up-regulated in response to OA-SF treatment in N-FLS (Figure 5.6, panel D), when compared to control OA-FLS (Figure 5.7, panel C).). These data are summarised in Table 5.12 and 5.13 (Appendix). The proteins with drastically altered abundance in response to OA-SF treatment when compared to control N-FLS are as follows, a trend towards increased protein expression pattern was found with alpha-enolase isoform (77.1-fold), 2-phosphopyruvate-hydratase alpha-enolase (23.3-fold), Rab GDP dissociation inhibition beta (16.3-fold), vimentin (16.4-fold), tropomyosin beta (21.1-fold), tubulin beta-5 chain (19.3-fold), annexin V (15.3-fold). The proteins with drastically altered abundance in response to OA-SF treatment when compared to control OA-FLS are as follows, peroxiredoxin-1 (7.1-fold), cyclophilin A (4.5-fold), manganese superoxide dismutase (3.7-fold), glyceraldehyde-3-phosphate dehydrogenase (13.9-fold).

5.4.8. DIGE proteomic analysis of grade-specific OA synovial tissue biopsies

The whole synovial tissue protein samples (50 mg/grade) from grade-specific OA biopsies were subjected to DIGE-LCMS (Figure 5.8). LC-MS identified synovial proteins, with OA grade-specific alterations in protein expression are listed in Tables 5.14, 5.15, 5.16, 5.17, Appendix. A total of 8 differentially altered proteins were identified in grade-1 OA synovial tissue when compared to grade-0, of which only one protein species was identified to be down-regulated with 1.6-fold decrease in expression, and was found to be protein S100-A11 (Table 5.14, Appendix), where this cytoplasmic protein is known to negatively regulate cell proliferation and DNA replication, and as well known to modulate cartilage matrix catabolism in OA (Sakaguchi and Huh, 2011, Cecil, 2008). Also, cyclophilin A (Table 5.14), was found to be up-regulated with a 1.9-fold increase in

expression in grade-1 synovial tissue compared to grade-0, where this cytoplasmic protein is known to accelerate the folding of proteins and also known to interact with HIV-1 Capsid protein (Luban et al., 1993). Previous studies reported that cyclophilin A may contribute to inflammatory processes in arthitis though MMP and inflammatory cytokine secretion (Kim et al., 2005) and may also contribute to cartilage degradation OA (Cloos and Chistgau, 2002). A total of 42 differentially altered proteins were identified in grade-2 OA synovial tissue when compared to grade-0 (Table 5.15), of which 8 protein species were identified to be up-regulated and 34 were down-regulated. Among these proteins were heat shock 60kDa protein 1 was found to be highly altered with 3.9-fold increase in expression, whereas, ATP synthase (mitochondrial precursor) was found as the drastically altered protein with 41.8-fold decrease in expression along with 18-fold decrease in galectin-1 expression was found. Wherein, galectin-1 is known to regulate apoptosis, cell proliferation and cell differentiation (He and Baum, 2004). Several members of the galectin family have been shown to have profound effects on cell survival and they have been implicated as major regulators of inflammatory responses (Rabinovich et al., 2002). Similarly, the genetic delivery of recombinant galectin-1 inhibited a number of experimental autoimmune diseases, including collagen-induced arthitis (Rabinovich et al., 1999). Regarding grade 2 OA synovial tissue, a decrease in complement C3b, was found when compared to grade 0, 3 and 4. Interestingly, activation of the complement cascade in acute arthitides was reported to be associated with a decreased protection of synovial cells against cellular effects and lysis mediated by membrane attack complex, such as in RA (Konttinen et al., 1996) and in OA (Wang et al., 2011).

A total of 23 differentially altered proteins were identified in grade-3 OA synovial tissue when compared to grade-0 (Table 5.16; Appendix), of which 8 protein species were identified to be down-regulated and 15 were up-regulated. Whilst ATP synthase was found to be highly altered with a 4.9-fold decrease in expression, heat shock cognate 71kDa protein was found to be altered protein with 4.7-fold increase in expression. The decrease in ATP synthase was similar to that observed with grade-2, implying an essential dysregulation of ATP synthesis with mitochondrial malfunctioning may be involved in OA progression. Interestingly, heat shock cognate 71kDa protein is a chaperone known to act as repressor of transcriptional activation (Yahata et al., 2000). Furthermore, a total of 17 differentially altered proteins were identified in grade-4 OA synovial tissue when compared to grade-0 (Table 5.17; appendix), of which 8 protein species were identified to be down-regulated and 9 were up-regulated. Among which alpha-enolase, was found to be

highly altered with 2.1-fold decrease in expression, whereas, SH3 domain-binding glutamic acid-ric-like protein, was found to be altered protein with 3.6-fold increase in expression. Wherein, alpha enolase has been previously shown to play a role in the glycolysis pathway in the context of OA pathogenesis (Ruiz-Romero and Blanco, 2009).

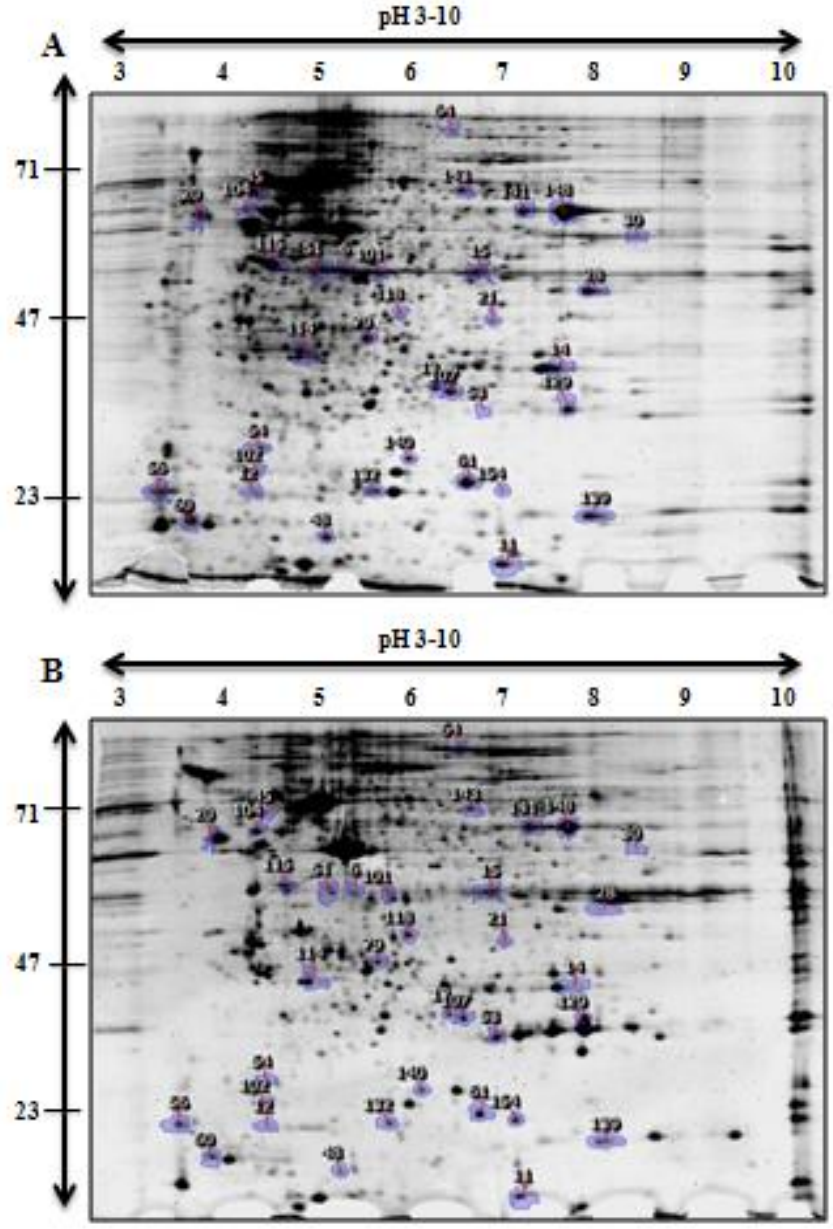

Figure 5.1: Proteomic analysis of N-FLS versus OA-FLS. The 2D-GE resolved total soluble protein extract of N-FLS (A) and OA-FLS (B, n=3, 200 µg/gel), in 3-10 pH range is shown. The 2D gels were primarily stained with RuBPs stain and counterstained with coomassie stain to visualise differentially expressed proteins. The differential protein spots identified though progenesis and analysed with LC-MS are indicated by their corresponding spot number and listed in Table 5.1 (Appendix). The pH values of the first dimension IEF and molecular mass standards (in kDa) of the second dimension gel system are indicated on the top and on the left of the panels respectively. The gels presented are representative of three biological and three technical replicates.

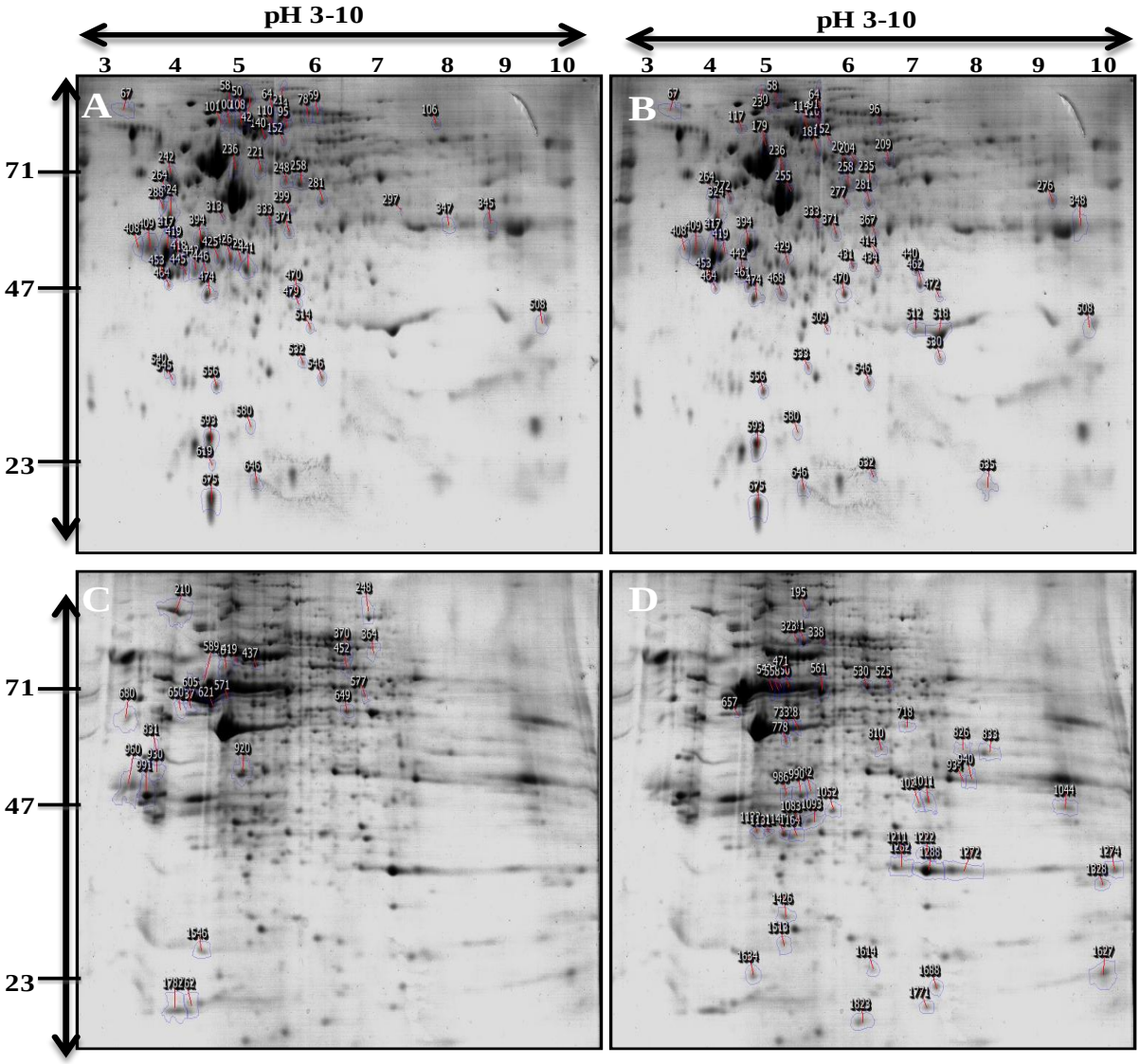

Figure 5.2: Comparative proteomic analysis of Poly (I:C) treated N and OA-FLS. The 2D-GE resolved soluble protein extract of N-FLS (A and B, n=3, 200 µg/gel) and OA-FLS (C and D, n=3, 200 µg/gel) treated with Poly (I:C) (10µg/ml) for 24 h are shown. The differential protein spots identified though progenesis and analysed with LC-MS are indicated by their corresponding spot number and summarized in Tables 5.2 and 5.3 (Appendix). Spots represent down-regulated (A), and up-regulated (B) protein expression in N-FLS with Poly (I:C) stimulation. Spots represent down-regulated (C), and up-regulated (D) protein expression in OA-FLS with Poly (I:C) stimulation. The 2D gels were primarily stained with RuBPs stain and counterstained with coomassie stain to visualise differentially expressed proteins. The pH values of the first dimension IEF and molecular mass standards (in kDa) of the second dimension gel system are indicated on the top and on the left of the panels respectively. The gels presented are representative of three biological and three technical replicates.

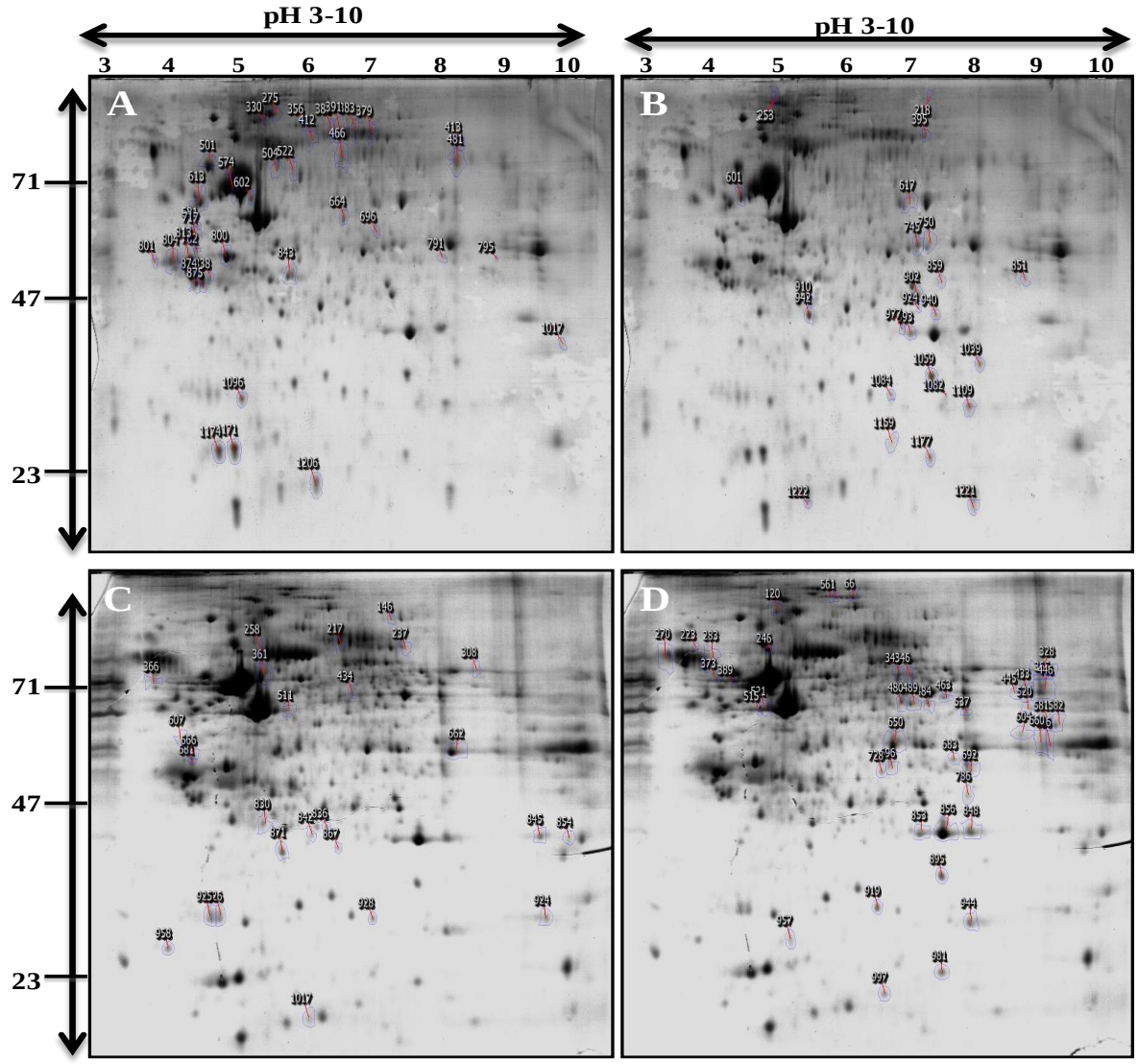

Figure 5.3: Comparative proteomic analysis of CLO-97 treated N and OA-FLS. The 2D-GE resolved soluble protein extract of N-FLS (A and B, n=3, 200 µg/gel) and OA-FLS (C and D, n=3, 200 µg/gel) treated with CLO-97 (1µg/ml) for 24 h are shown. The differential protein spots identified though progenesis and analysed with LC-MS are indicated by their corresponding spot number and summarized in Tables 5.4 and 5.5 (Appendix). Spots represent down-regulated (A), and up-regulated (B) protein expression in N-FLS with CLO-97 stimulation. Spots represent down-regulated (C), and up-regulated (D) protein expression in OA-FLS with CLO-97 stimulation. The 2D gels were primarily stained with RuBPs stain and counterstained with coomassie stain to visualise differentially expressed proteins. The pH values of the first dimension IEF and molecular mass standards (in kDa) of the second dimension gel system are indicated on the top and on the left of the panels respectively. The gels presented are representative of three biological and three technical replicates.

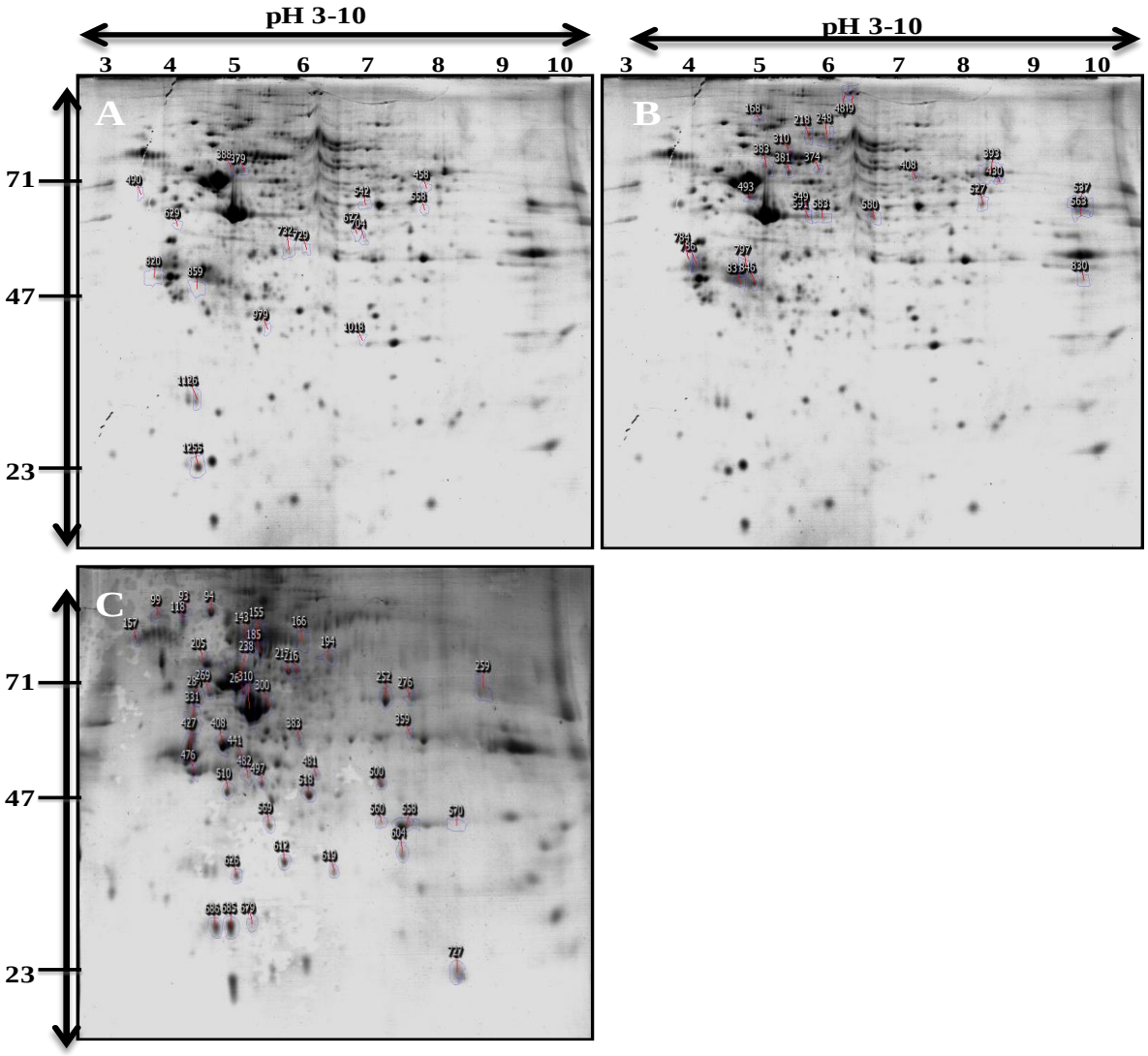

Figure 5.4: Comparative proteomic analysis of RIG-I ligand treated N and OA-FLS. The 2D-GE resolved soluble protein extract of OA-FLS (A and B, n=3, 200 µg/gel) and N-FLS (C, n=3, 200 µg/gel) treated with 5' ppp-dsRNA (1µg/ml) for 24 h are shown. The differential protein spots identified though progenesis and analysed with LC-MS are indicated by their corresponding spot number and summarised in Tables 5.6 and 5.7 (Appendix). Spots represent down-regulated (A), and up-regulated (B) protein expression in OA-FLS with 5' ppp-dsRNA stimulation. Spots represent both up and down-regulated (C) protein expression in N-FLS with 5' ppp-dsRNA stimulation. The 2D gels were primarily stained with RuBPs stain and counterstained with coomassie stain to visualise differentially expressed proteins. The pH values of the first dimension IEF and molecular mass standards (in kDa) of the second dimension gel system are indicated on the top and on the left of the panels respectively. The gels presented are representative of three biological and three technical replicates.

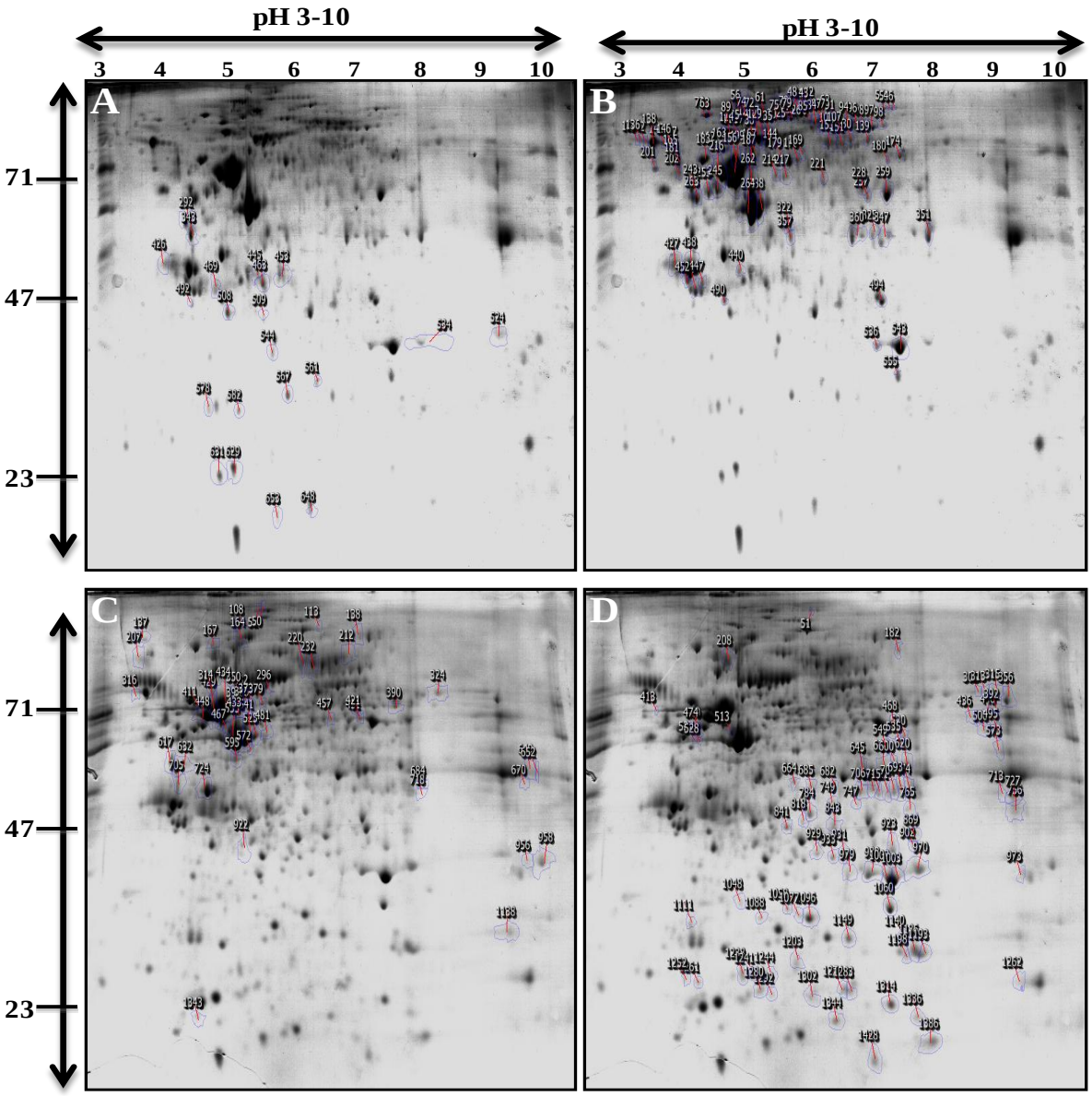

Figure 5.5: Comparative proteomic analysis of LPS treated N and OA-FLS. The 2D-GE resolved soluble protein extract of N-FLS (A and B, n=3, 200 µg/gel) and OA-FLS (C and D, n=3, 200 µg/gel) treated with LPS (1µg/ml) for 24 h is shown. The differential protein spots identified though progenesis and analysed with LC-MS are indicated by their corresponding spot number and summarized in Tables 5.8 and 5.9 (Appendix). Spots represent down-regulated (A), and up-regulated (B) protein expression in N-FLS with LPS stimulation. Spots represent down-regulated (C), and up-regulated (D) protein expression in OA-FLS with LPS stimulation. The 2D gels were primarily stained with RuBPs stain and counterstained with coomassie stain to visualise differentially expressed proteins. The pH values of the first dimension IEF and molecular mass standards (in kDa) of the second dimension gel system are indicated on the top and on the left of the panels respectively. The gels presented are representative of three biological and three technical replicates.

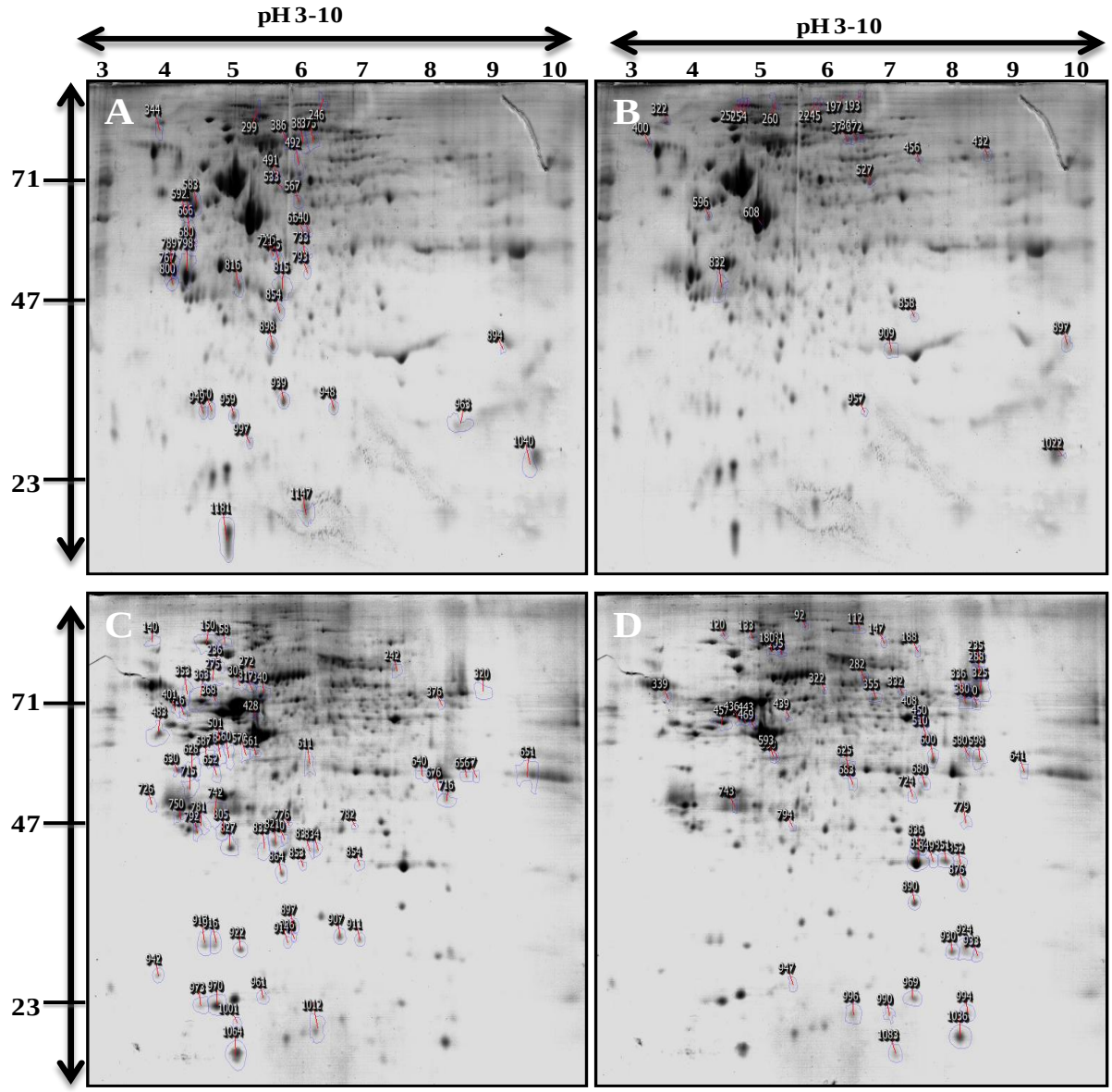

Figure 5.6: Comparative proteomic analysis of Pam_2CSK_4 treated N and OA-FLS. The 2D-GE resolved soluble protein extract of N-FLS (A and B, n=3, 200 µg/gel) and OA-FLS (C and D, n=3, 200 µg/gel) treated with Pam_2CSK_4 (1µg/ml) for 24 h is shown. The differential protein spots identified though progenesis and analysed with LC-MS are indicated by their corresponding spot number and summarized in Tables 5.10 and 5.11 (Appendix). Spots represent down-regulated (A), and up-regulated (B) protein expression in N-FLS with Pam_2CSK_4 stimulation. Spots represent down-regulated (C), and up-regulated (D) protein expression in OA-FLS with Pam_2CSK_4 stimulation. The 2D gels were primarily stained with RuBPs stain and counterstained with coomassie stain to visualise differentially expressed proteins. The pH values of the first dimension IEF and molecular mass standards (in KDa) of the second dimension gel system are indicated on the top and on the left of the panels respectively.

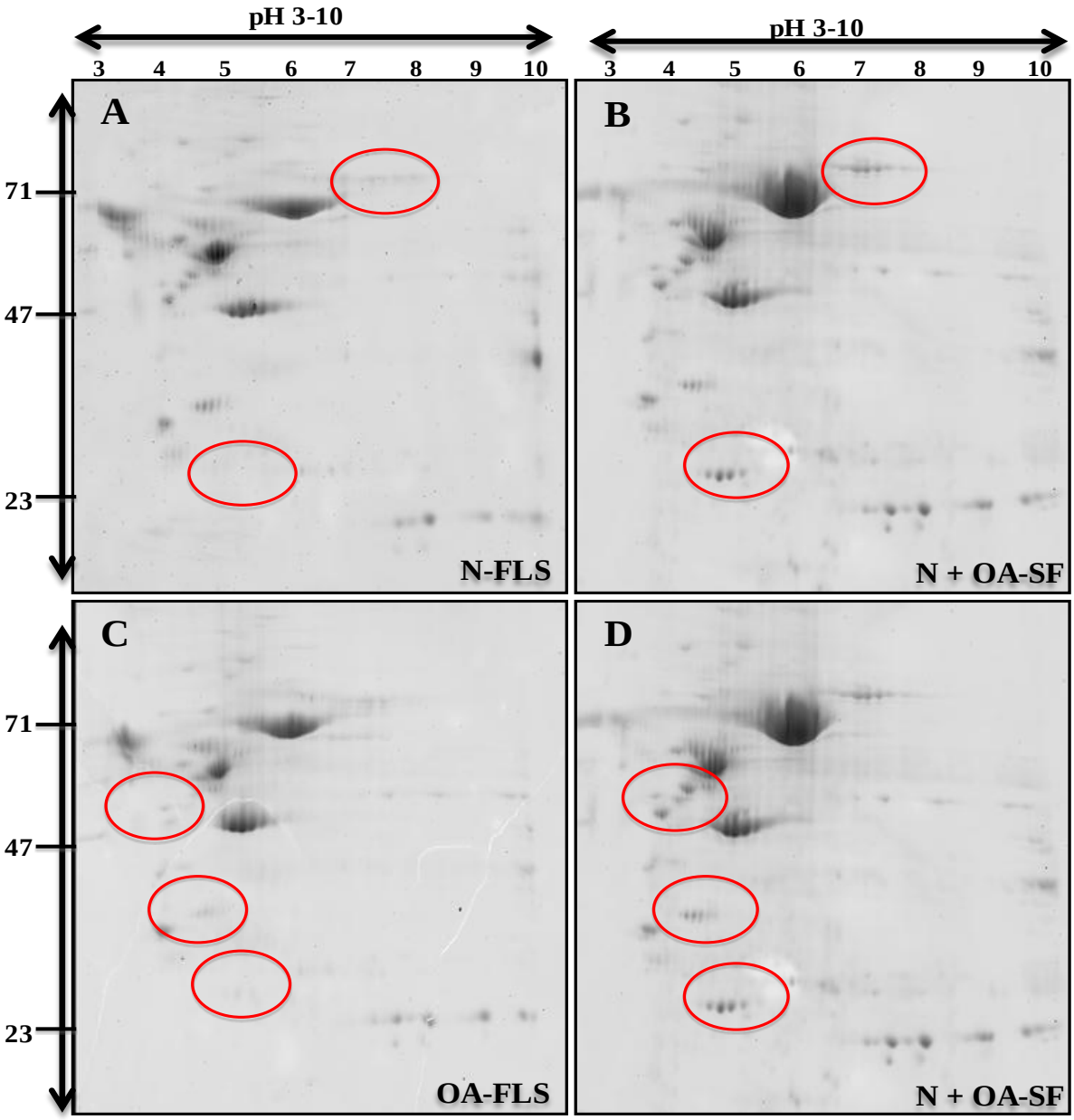

Figure 5.7: Differential proteomic analysis of N-FLS treated with OA-SF versus control N-FLS and OA-FLS. The 2D-GE resolved 200 µg/gel of soluble protein extract from N-FLS treated with end stage OA-SF (1:10 dilution in Opti-MEM) for 24 h (B and D, n=3), control N-FLS (A, n=3) and control OA-FLS (C, n=3) is shown. The differential protein spots identified though progenesis and analysed with LC-MS are circled in red and summarized in Tables 5.12 and 5.13 (Appendix). The pH values of the first dimension IEF and molecular mass standards (in KDa) of the second dimension gel system are indicated on the top and on the left of the panels respectively. The gels presented are representative of three biological and three technical replicates.

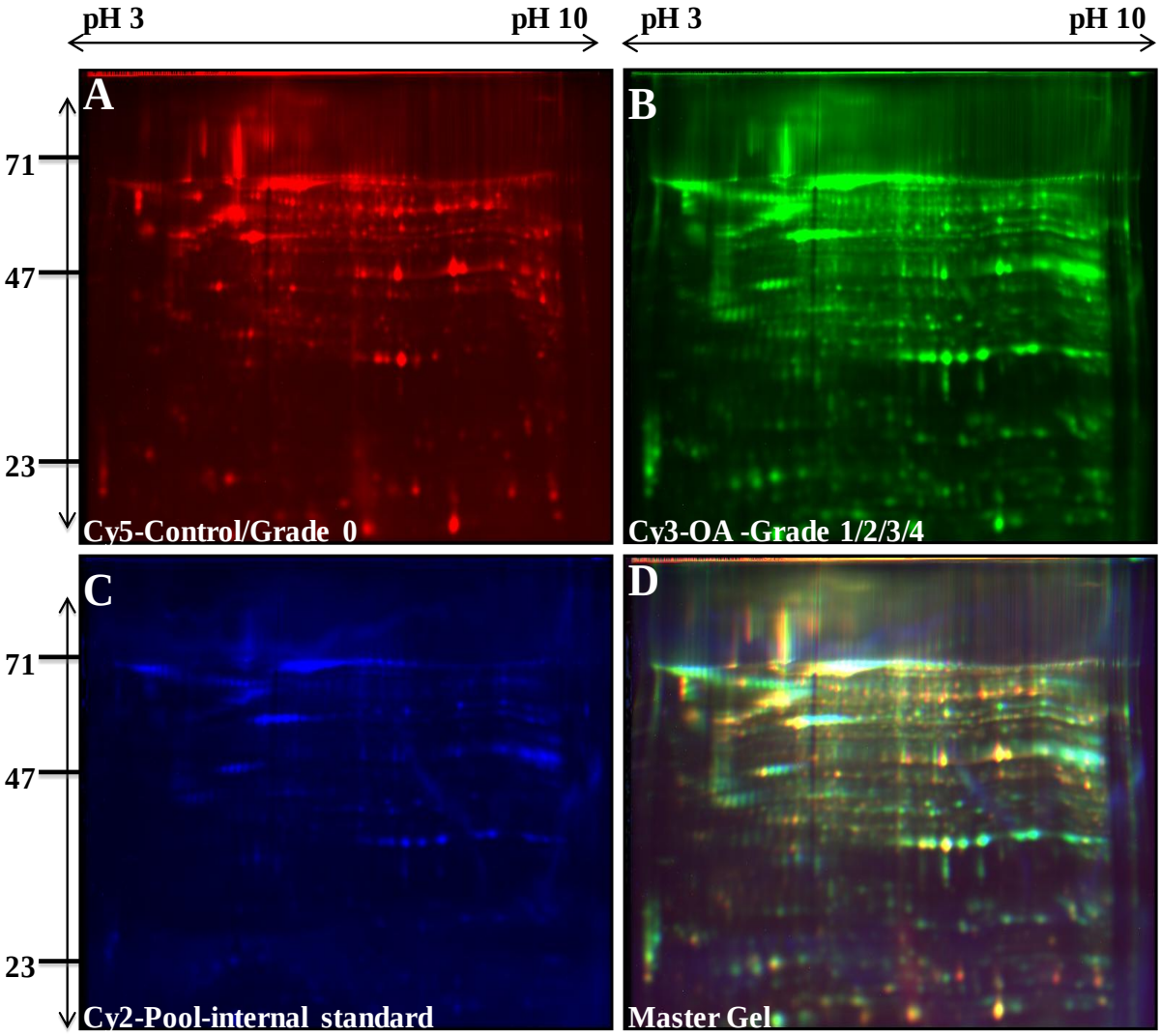

Figure 5.8: DIGE proteomic profiling of grade-specific OA synovial tissue biopsies. Protein extracts (50 mg/grade), of whole synovial tissue samples from grade-specific OA biopsies were separated in the first dimension by IEF and in the second dimension by SDS-PAGE. Shown are Cy5-labeled control or grade-0 samples (A), Cy3-labeled grade-specific (1, 2, 3, 4) samples (B) and Cy2-labeled pooled internal standard (C) and a DIGE master gel is shown in panel (D). LC-MS identified synovial proteins with OA grade-specific alterations in protein expression are listed in Tables 5.14, 5.15, 5.16, 5.17, Appendix. The pH values of the first dimension IEF and molecular mass standards (in kDa) of the second dimension gel system are indicated on the top and on the left of the panels respectively.

5.4.9. Differential protein quantification of vimentin though western blot and confocal analysis

Given that a trend towards elevated vimentin levels was observed in all the grades of synovial tissues (table 5.15, 5.16, 5.17) and a that a similar trend was evident following stimulation with Poly (I:C) stimulation in N and OA FLS (table 5.2, 5.3 and section 5.4.2), and elevated levels of vimentin was evident following stimulation of N-FLS with OA-SF (section 5.4.7 and table 5.12), it was essential to quantify this prominently altered protein in FLS and synovial tissue. A trend towards increased vimentin expression was detected in N and OA FLS following stimulation with Poly (I:C) and OA-SF as detected by confocal and immunoblot analysis (Figure 5.9A, B). A similar trend towards increased vimentin levels was evident in grade-specific OA synovial tissue samples, where grade-4 showed maximum vimentin expression (Figure 5.9C). The data presented here clearly demonstrate that alterations in the relative expression of vimentin are associated with OA.

5.4.10. Differential protein quantification of prohibitin though western blot and confocal analysis

Given that a trend towards decreased prohibitin levels was observed following stimulation of N and OA FLS with poly(I:C) (table 5.1, 5.2, 5.3 and section 5.4.1, 5.4.2), it was critical to confirm and quantify this finding. Differential quantification of prohibitin though 3D progenesis spot analysis (Figure 5.9, panel A), confocal analysis (Figure 5.10, panel B) and immunoblot analysis was performed. A trend towards decreased prohibitin expression was detected in N and OA FLS upon stimulation with Poly (I:C) using confocal analysis, 3D image analysis and immunoblot analysis. More specifically, stimulation of OA-FLS with Poly(I:C) showed the maximal decrease in prohibitin levels when compared to control FLS. The data presented here clearly substantiates the hypothesis that alterations in the relative abundance of prohibitin occur in OA and following stimulation with poly (I:C).

5.4.11. Differential protein quantification of caldesmon though western blot and confocal analysis

Given that a trend towards elevated caldesmon levels was observed upon stimulation of N and OA FLS with poly(I:C) (table 5.1, 5.2, 5.3 and section 5.4.1, 5.4.2), it was critical to confirm these data using an alternative approach. Thus, immunoblot analysis and confocal microscopy was applied towards the detection of caldesmon in OA and N FLS (Figure 5.11). Using confocal analysis and immunoblot analysis, a trend towards increased

caldesmon expression was detected in N and OA FLS following stimulation with Poly(I:C) (Figure 5.11A, B). Wherein, stimulation of OA-FLS with Poly (I:C) showed the maximal increase in caldesmon levels when compared to control FLS. The data presented here clearly substantiates the proteomics data shown that alterationsI in the abundance of caldesmon are evident upon stimulation of FLS with Poly (I:C).

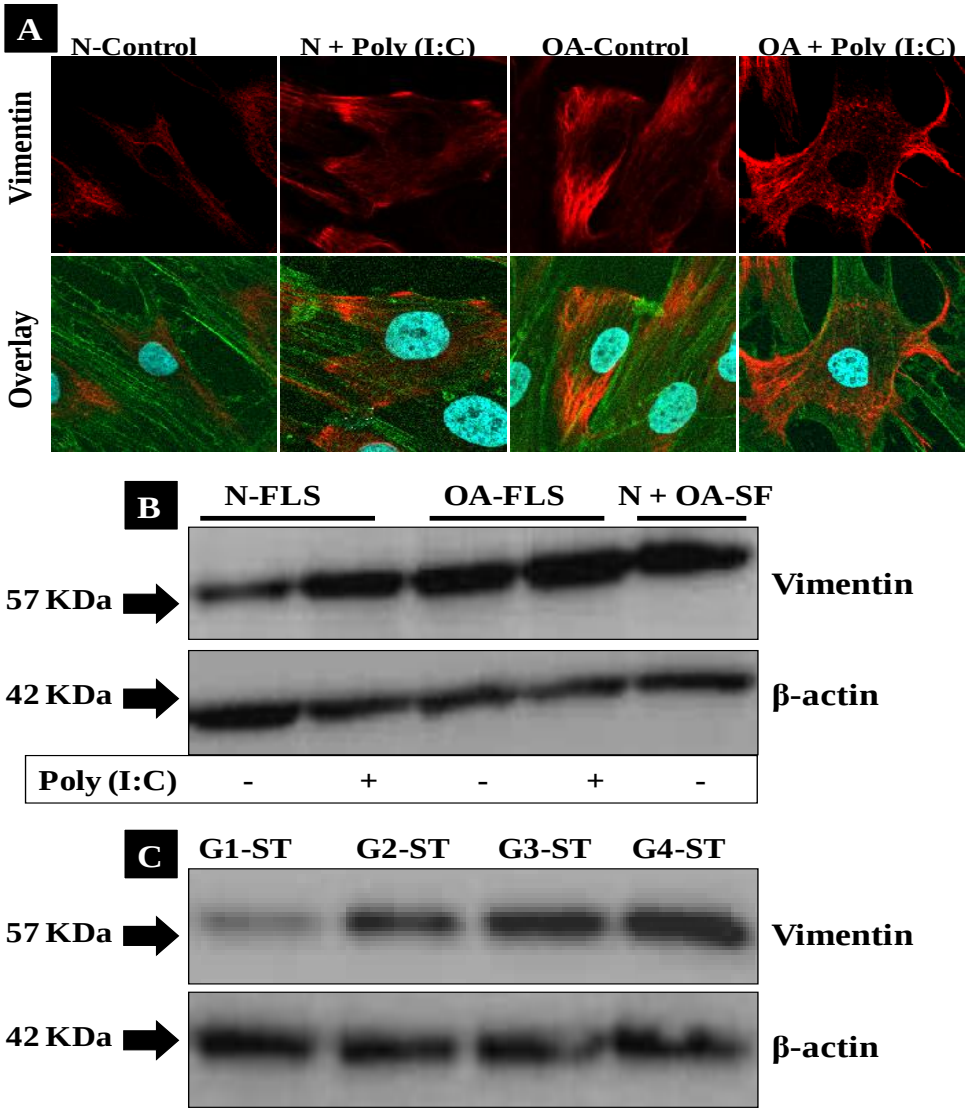

Figure 5.9: Differential quantitative analysis of vimentin in grade-specific OA synovial tissue, N and OA FLS. (A) confocal analysis of N and OA FLS treated with Poly (I:C) (10µg/ml) for 2 h or left unstimulated using an antibody to vimentin (1:100 dilution; red staining) followed by incubation with an Alexa Fluor 546 (1:500 dilution) labelled secondary antibody. Actin-phalloidin (1:25 dilution) was also employed (green staining) as a cyto-skeletal control marker for FLS. DAPI staining of nuclei is also included and seen as cyan staining (B) immunoblot analysis of basal and Poly (I:C) induced vimentin levels in N and OA FLS and as well end stage OA-SF (1:10 dilution) induced vimentin expression in N-FLS was determined, using an anti–vimentin antibody (1:1000 dilution) and β-actin (1:1000 dilution) as a loading control. (C) Immunoblot analysis of crude synovial tissue protein extracts for vimentin and β actin expression in grade-1 (G1-ST), grade-2 (G2-ST), grade-3 (G3-ST) and grade-4 (G4-ST) biopsy tissue.

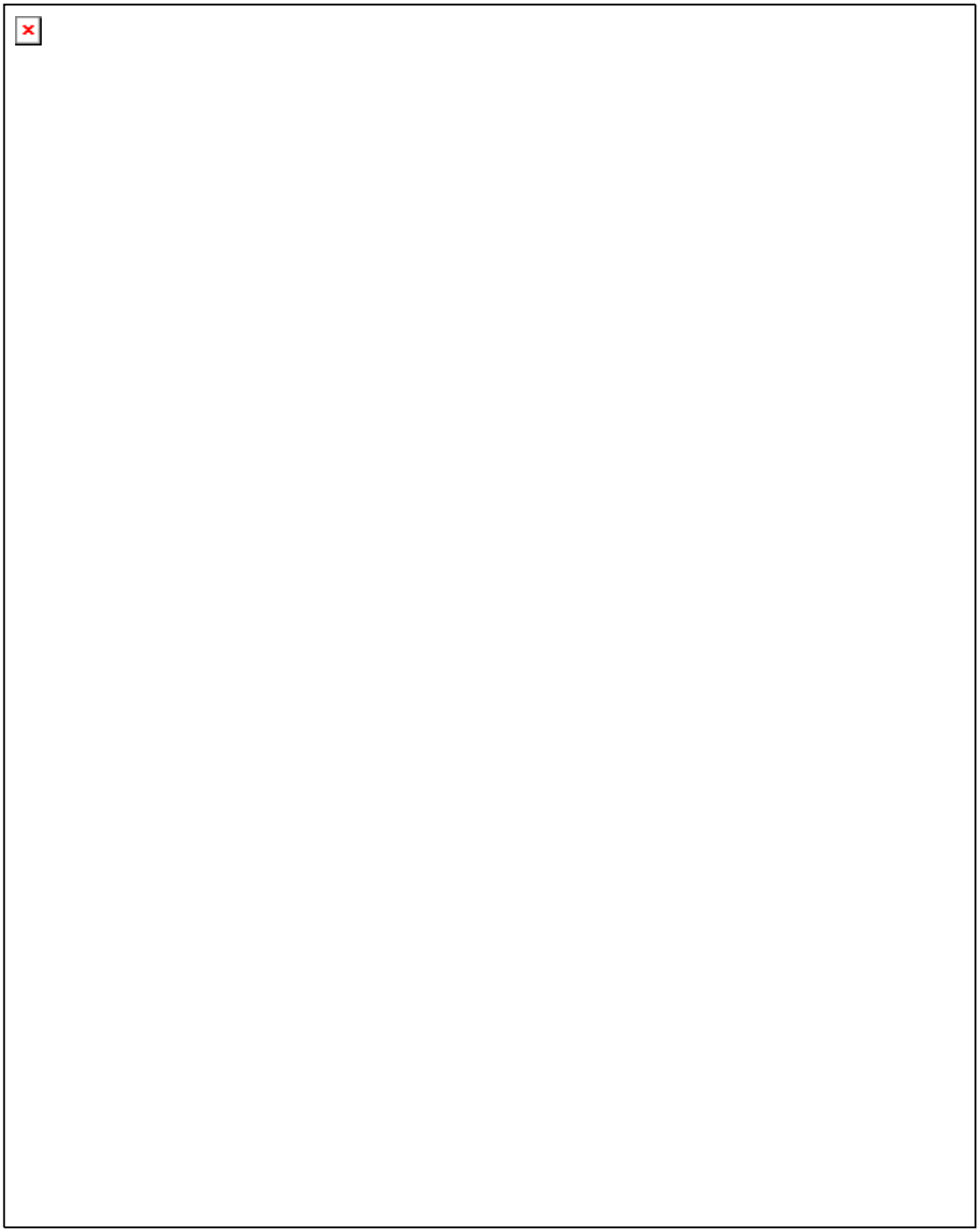

Figure 5.10: Immunoblot and confocal analysis of prohibitin in N and OA FLS. N and OA FLS were either treated with Poly(I:C) (10µg/ml) for 2 h or left unstimulated. (A) 3D progenesis image analysis of prohibitin, illustrating the decreased protein abundance in response to Poly (I:C) stimulation. (B) confocal analysis of prohibitin expression using an antibody to prohibitin (1:100 dilution) seen as red staining by using an Alexa Fluor 546 (1:500 dilution) labelled secondary antibody and actin phalloidin (1:25 dilution) which is seen as green staining was employed as a cyto-skeletal control marker for FLS. DAPI staining of nuclei is also included and seen as cyan staining. (C) immunoblot analysis of basal and Poly (I:C) effected prohibitin levels in N and OA FLS, using an anti–prohibitin antibody (1:1000 dilution) and loading control β-actin antibody (1:1000 dilution).

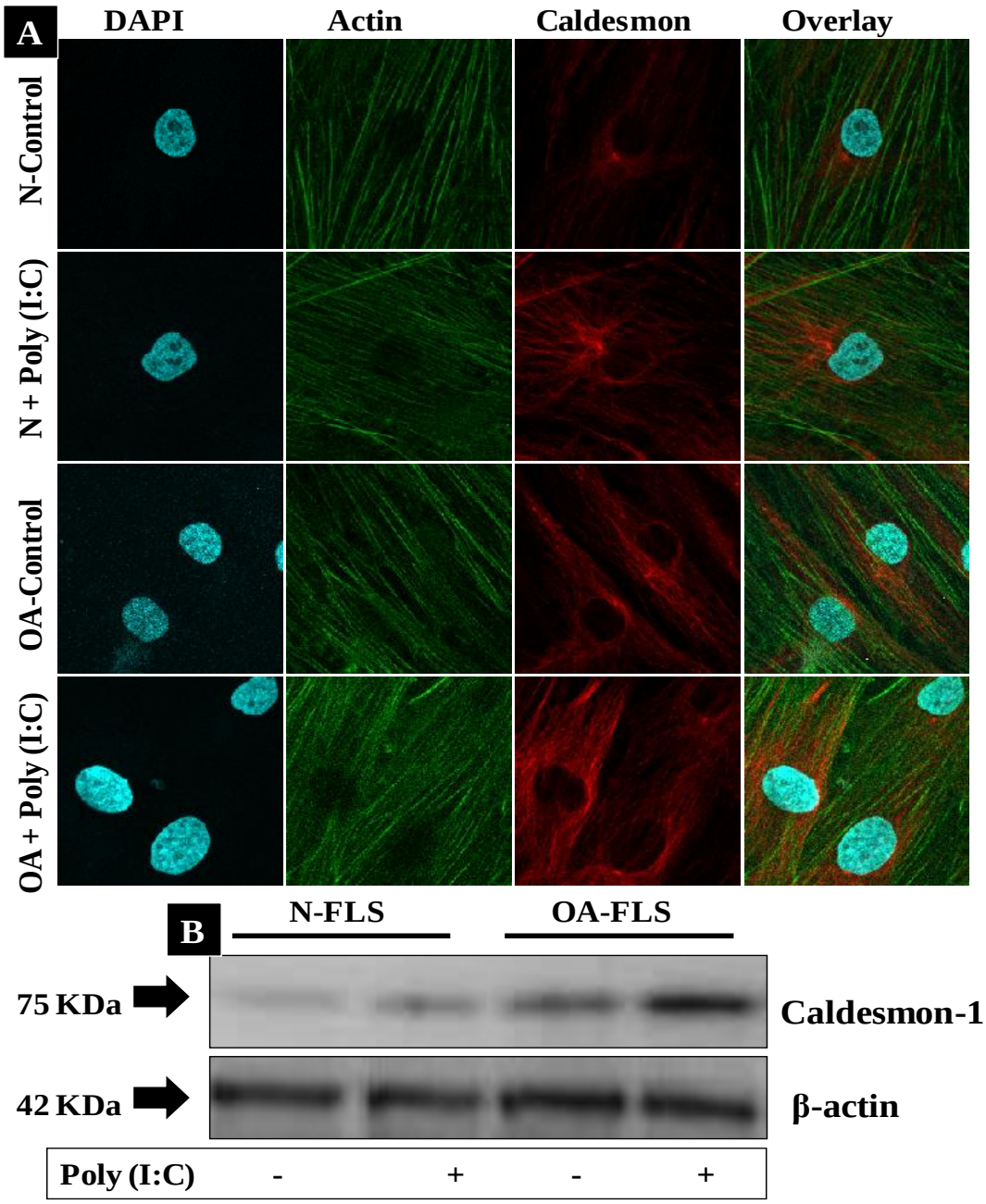

Figure 5.11: Immunoblot and confocal analysis of caldesmon in N and OA FLS. N and OA FLS were either treated with Poly (I:C) (10µg/ml) for 2h or left unstimulated. (A) confocal analysis of caldesmon using an anti-caldesmon antibody (1:100 dilution) followed by an Alexa Fluor 546 (1:500 dilution; red colour) labelled secondary antibody and actin phalloidin (1:25 dilution). DAPI staining of nuclei seen as cyan staining. (B) immunoblot analysis of basal and Poly (I:C) induced caldesmon levels in N and OA FLS, using an anti-caldesmon antibody (1:1000 dilution) and loading control β-actin (1:1000 dilution).

5.5. Discussion

Previous studies have assessed the secretory profile of normal and OA articular cartilage by 2D-GE and MS (Garcia et al., 2006, Hermansson et al., 2004). Also, the proteome of human normal articular chondrocytes was analysed as a preliminary study towards the OA chondrocyte proteome (Ruiz-Romero et al., 2005). More recently, 2D-DIGE analysis of normal and OA-affected articular chondrocytes was performed towards the identification of differentially expressed proteins in these cells (Raquel et al., 2008). Regarding RA, a number of groups have studied the RA FLS proteome by employing 2D-GE followed by MALDI-MS wherein a number of potential autoantigens and proteins previously implicated in RA disease pathology were identified (Dasuri et al., 2004). Using a gel based MS approach, the mode of action of NSAIDs was studied and serine protease secretion from RA-FLS was detected (Heum Park et al., 2006). In contrast to RA, a very limited number of studies have been performed towards elucidating the molecular mechanisms that modulate OA pathology. In this study, we adopted a novel approach namely DIGE analysis towards understanding OA pathology. Additionally, we utilised N and OA FLS stimulated with several TLR/RLR ligands to study the differential proteomic patterns associated with OA progression at the molecular level. Furthermore, these protein profiles may aid in identification of plausible anti-degradative, anti-proliferative and anti-inflammatory therapeutics, which could resolve disease persistence and prevent joint damage.

Several proteins with altered expression patterns were identified in our study, the majority of which have been previously implicated in OA pathogenesis, such as constituents of key metabolic reactions, cyto-skeletal machinery, cellular stress response and cell signalling pathways (Ruiz-Romero and Blanco, 2009, Rollín et al., 2008, Ruiz-Romero et al., 2009a, Raquel et al., 2008). All of the protein data has been summarised in the tables presented in the Appendix. Several proteins identified though this study can be categorised into the following groups, Cellular signalling group: annexin-1 and -5, gelsolin, galectin-1 and vimentin; Protein folding group: cyclophilin A, heat shock proteins -10, -70 and -90, glucose related proteins, TNFα-receptor-associated protein, endoplasmic reticulum proteins; Cellular metabolism group: fructose-biphosphate aldolase, alpha enolase, phosphoglecerate kinase and mutase, lactate dehydrogenase, ATP synthase; Cellular stress balance or Redox balance: glutathione-S-transferase omega-1, Mn-superoxide dismutase;

Cytoskeletal binding proteins: destrin, cofilin-1 and -2, gelsolin-like capping protein, LIM and SH3 protein-1, annexin A2; Endopeptidase group: cathepsin D; Matrix synthesis: chitinase-3-like protein-2 and -1; Proteosome group: proteosome activator subunit, eukaryotic translation initiation factor. A majority of the identified proteins have been implicated in various biological processes such as protein transport, carbohydrate metabolic processes, electron transport, regulation of hydrolase activity, protein metabolic processes, protein folding, cytoskeleton organisation, immune response and inflammation. Activation of FLS by various TLR/RLR stimuli resulted in differential subset of protein expression, which showed particular ligand-specificity. The functional group most affected in both OA synovial tissue and treated FLS was cytoskeletal proteins, providing novel insights in to cytoskeletal pathology in such joint disorders. A set of three distinct proteins was studied in detail in this chapter, which showed consistent altered abundance in FLS and grade-specific OA synovial tissues.

One such previously known protein identified though our current study, was vimentin, a member of the intermediate filament family which plays a significant role in supporting and anchoring organelles within the cytosol (Katsumoto et al., 1991). Recent studies have indicated a potential role for vimentin in inflammation, since fragments of the protein have been shown to be secreted by activated synoviocytes during inflammation (Mor-Vaknin et al., 2003). Our study demonstrates an increased abundance in vimentin expression level following stimulation with poly(I:C) and OA-SF and as well in grade-specific OA synovial tissues, thus implying a ligand/disease induced disassembly of filaments (Figure 5.9). Studies have demonstrated that an intact vimentin intermediate filament network contributes to the maintenance of the chondrocyte phenotype and such an imbalance favouring filament disassembly can disturb the integrity of the articular cartilage, and may ultimately lead to the development of OA (Blain et al., 2006).

Likewise, a similar trend towards consistent increase in protein expression level was observed with caldesmon, in N and OA FLS with Poly(I:C) stimulation. Caldesmon (CaD) is an essential actin-binding protein, as it also binds myosin, calmodulin and tropomyosin in addition to actin (Wang, 2008). Several important cellular processes have been reported to involve changes of the actin cytoskeleton, which maintains and controls the cell shape in concert with activities of the contractile apparatus as a result of cell signalling (Wang, 2008, Pollard and Borisy, 2003). Studies have reported that actin filament polymerization and depolymerisation plays a key role in controlling a range of cellular phenomena

including apoptosis, inflammation, cell division, migration, exo-and endocytosis, vesicle trafficking and gene expression (Winder, 2003, Pollard and Borisy, 2003). Malfunction of these processes may lead to pathological consequences, but how actin-mediated motility is regulated is poorly understood (Wang, 2008). Studies have reported that over-expression of CaD in nonmuscle cells has led to a number of conflicting phenotypes including increases or decreases of focal adhesions and podosome structures, stabilized or disrupted stress fibers, hampered or unaffected cell division process and enhanced or compromised cell motility. Our current study demonstrates an increased expression profile for caldesmon in OA, may imply a role of synovial inflammation inducing such overexpression of caldesmon in FLS, more pronouncedly with Poly (I:C) stimulation, thus pointing at dsRNA viral derived OA initiation.

Interestingly, we for the first time identified a novel protein named prohibitin 1, which exclusively showed a decrease in expression in response to Poly(I:C) stimulation in N and OA FLS when compared to respective cell type controls. Prohibitin 1 (PHB1) is a 30-32 kDa protein that belongs to a family of proteins that share an evolutionarily conserved stomatin/prohibitin/flotillin/HflK/C (SPFH) domain (Theiss and Sitaraman, 2011). It is closely related to prohibitin 2 (PHB2), also called B-cell receptor-associated protein 37 (BAP 37) and repressor of estrogen receptor activity (REA) (Theiss and Sitaraman, 2011). PHB1 is a multifunctional, pleiotropic protein which has been previously implicated in the regulation of proliferation, apoptosis, transcription, mitochondrial protein folding, and as a cell-surface receptor (Theiss and Sitaraman, 2011, Misha et al., 2006). This diverse array of functions of PHB1 is attributed to the cell type studied and its subcellular localization (Theiss and Sitaraman, 2011). PHB1 has been reported previously to be localized typically in the mitochondria or nucleus depending on cell type and situation (Theiss et al., 2007).

Interestingly, our present study demonstrates that PHB1 is localised to cytoplasm and cell membrane in FLS, and may get localised to mitochondrion upon activation by Poly(I:C) and in OA as such. The decrease in prohibitin staining observed in confocal analysis (Figure 5.10, panel B), may partly be explained by such localisation of prohibitin to mitochondrion and by employing a mitochondrial specific marker further conclusions can be derived. Recent studies have indicated a diverse role for PHB1 in several disease pathogenesis and suggested that targeting PHB1 may be a potential therapeutic option for treatment of diseases including cancer, inflammatory bowel disease (IBD), insulin resistance/type 2 diabetes, and obesity (Theiss and Sitaraman, 2011). Given that, these

diseases are associated with increased oxidative stress and mitochondrial dysfunction similar to OA (Ruiz-Romero et al., 2009b), it was critical to understand the role of PHB1 in such responses. Subsequently, studies in intestinal epithelial cells using in vivo models of colitis and *in-vitro* models of oxidative stress or inflammation, have suggested that, PHB1 protects these cells from inflammation-associated oxidative stress and may modulate the inflammatory process (Theiss and Sitaraman, 2011). Likewise, studies have reported that cell-surface associated PHB1 in intestinal epithelial cells bind to Vi polysaccharide of *S. typhi* and inhibits the inflammatory response to *S. typhi* infection (Sharma and Qadri, 2004). Furthermore, PHB1 mRNA and protein levels were found to be decreased in inflamed mucosa during IBD (Theiss et al., 2007, Hsieh et al., 2006) and in experimental models of colitis (Theiss et al., 2007). Moreover, similar studies reported that, TNFα a key cytokine that plays a central role in IBD, decreased PHB1 mucosal levels *in-vivo* and in cultured intestinal epithelial cells (Theiss et al., 2009). These results suggested that TNFα may contribute to the reduced levels of prohibitin in the mucosa of IBD patients and exogenous expression of PHB1 in intestinal epithelial cells can reduce the activation of the NF-κB pathway, which plays a central role in inflammatory responses and also regulates transcription of multiple cytokines (Theiss et al., 2009). Collectively, these results suggest that PHB1 may be crucial in modulating inflammatory processes. Similar studies have documented the anti-proliferative and anti-apoptotic activity of prohibitin in various cell types (Jupe et al., 1995, Misha et al., 2006, Theiss and Sitaraman, 2011). Initial studies indicated that PHB1 plays a role in tumour suppression in breast cancer via the 3′ untranslated region of the PHB1 gene which encodes a functional RNA that blocks transition between the G1 and S phases of the cell cycle, thereby arrests cell proliferation (Manjeshwar et al., 2004, Manjeshwar et al., 2003).

Nevertheless, further studies in breast and prostate cancer cell lines indicated that a portion of PHB1 is localized in the nucleus and interacts with and regulates the tumour suppressor protein p53 (Fusaro et al., 2003). It was reported that, PHB1 co-localizes with p53 in breast carcinoma cell lines and its binding to p53 increases p53 transcriptional activity via increased DNA binding (Fusaro et al., 2003). It was also shown that PHB1 is degraded during Skp2B overexpression in breast cancer lines and this subsequently causes attenuation of p53 activity in vivo and in vitro (Chander et al., 2010). Collectively these results suggest that, PHB1 is required for maximal p53 transcriptional activity and may play a critical role in p53 checkpoint control of the cell cycle.

Apoptosis which ensures removal of cells from tissue is known to be tightly regulated, by a range of death signals such as p53, and dysregulation or lower expression of such signals leads to reduction of apoptosis. The subsequent impairment of apoptosis can lead to accumulation of cells which play a key role in the hyperplasia of the synovium observed in OA and RA (Ospelt et al., 2004, Ospelt and Gay, 2008). Studies have stated that an impairment of p53 mediated apoptosis in FLS, contributed significantly to the thickening of the synovial lining layer (Perlman et al., 2001, Ospelt and Gay, 2008, Ospelt et al., 2004). Our current study demonstrated that drastically decreased levels of prohibitin in response to Poly(I:C) stimulation in N and OA FLS, besides OA itself. This might thus impair p53 activation and apoptosis in FLS, and thereby ultimately lead to synovial hyperplasia, inflammation and joint destruction. It is also thought that FLS being mesenchymal stem cell look-a-likes, may allow these cells to attain certain characteristics of other cell types such as chondroblasts, osteoclasts, myocytes, and adipocytes, which are residents of the joint space (Buckley et al., 2001). This could in part explain the diversity of functional properties that FLS posses upon TLR activation and this could contribute to their ability to proliferate themselves, activate and hold on to cell infiltrates and eventually transform into a devastating population of cells (Firestein, 1996).

In the current study, we have also demonstrated that, the C3b-component of complement was decreased in grade-2 OA synovial tissue proteome, which may also be attributed to the decreased PHB1 levels in OA-FLS, owing to the findings by other groups. C3 is an essential component of the innate immunity and is involved in all three pathways of complement activation (Fujita et al., 2004). Studies have reported that the ability of PHB1 to bind to, and activate C3 may suggest that PHB1 may have a previously unrecognized role in innate immunity (Misha et al., 2007). Moreover, it has been reported that PHB1 binds to C3, and appears to be able to induce a conformational change that enhances activation of C3, and PHB1 did not enhance complement activation in C3 depleted serum indicating that binding of PHB1 to C3 is necessary for this effect, while, PHB2, which shares approximately 74% homology with PHB1, was not able to activate complement (Fujita et al., 2004, Misha et al., 2007). A potential role of PHB1 in immunity is also suggested by the observation that PHB1 is found on the plasma membrane of human intestinal epithelial cells (Sharma and Qadri, 2004), and lymphocytes (Woodlock et al., 2001, Terashima et al., 1994).

Owing to our current PHB1 analysis, we hypothesise that a plasma membrane PHB1 may also be available on FLS, which on an encounter with dsRNA may localise to the mitochondria, thereby may induce p53 and C3b suppression, impair apoptosis and induce cell proliferation ultimately leading to synovial hyperplasia, inflammation, joint destruction and OA. Taken together our data suggests that, PHB1 may be considered as a probable biomarker for tracking synovial inflammation in OA.

In the future, validation of the expression levels of these three proteins will be carried out in the grade-specific OA synovial tissue samples and it is anticipated that validation of these proteins in serum or synovial fluid will also be carried out as these are more easily available in the clinical setting. Furthermore, at a functional level, multiple culture systems, such as patient derived whole tissue explant cultures and mono-cultures such as fibroblasts and chondrocytes will be used to examine the mechanistic function of these proteins and their role in driving the pro-inflammatory response in OA. Laser capture micro-dissection of grade-specific OA-synovial tissue biopsies, coupled with MALDI-Imaging, which enables direct tissue profiling, will be employed to generate and evaluate grade-specific OA synovial biomarkers. Additionally, a software package known as pathway studio will be employed to map the DIGE and 2D-GE LC-MS identified proteins onto characterised human pathways and networks that associate proteins based on known protein-protein interactions, mRNA expression studies, and other biochemical interactions. Subsequently, pathways and networks associated with altered grade-specific OA synovial proteins and TLR/RLR induced proteins in FLS will be generated.

Chapter 6

General Discussion

6.1. General discussion

OA is the most frequent rheumatic disease and is the leading cause of disability in developed countries. Over the coming decades, as the populations of developed nation's age, there is an absolute requirement for the better understanding of OA and for improved therapeutic alternatives. The poorly understood pathophysiology of OA limits the discovery of targets for pharmacological intervention, and therefore only few effective medical treatments beyond pain control and surgery are available. The traditional view of OA as a cartilage only disease is superseded and OA is now considered to be a whole joint disease that primarily includes the synovial tissue (Ayral et al., 2005, Sellam and Berenbaum, 2010b, Attur et al., 2010). Wherein, bone, cartilage and synovium communicate by way of cell-cell interactions, through the release of soluble mediators and via mechanical signals. Synovial inflammation, despite not being a prerequisite for the development of OA, is clearly involved in cartilage breakdown and thus in the progression of the disease and is currently used as a predictive factor of structural progression of knee OA (Ayral et al., 2005, Sellam and Berenbaum, 2010b, Scanzello et al., 2011a, Attur et al., 2010). Reports have suggested that targeting the inflammatory synovium should delay or prevent articular cartilage damage and the formation of osteophytes, especially in early OA and as well preclinical and/or clinical studies of anti-cytokine molecules and inhibitors of signalling pathways would help to clarify the role of synovitis in OA (Sellam and Berenbaum, 2010b, Benito et al., 2005, Attur et al., 2010).

Inflammation of the synovium or synovitis is believed to be due to a combination of extensive angiogenesis, synovial hyperplasia, infiltration of cells from the circulation and an impairment in apoptosis, which are clearly marked high even in early OA patients with minimal radiographic features of OA progression (Benito et al., 2005, Shibakawa et al., 2003, Ashraf and Walsh, 2008, Hutton et al., 1987, Bonnet and Walsh, 2005, Myers et al., 1990). In inflammatory arthritis, the phenotype of the synovial tissue changes into an activated proliferative (OA), invasive (RA) tissue (Sellam and Berenbaum, 2010b). This uncontrolled process of tissue growth leads to narrowing of the joint space and subsequent increased efflux of synovial fluid, which results in swollen joints wherein, the tissue proliferation is accompanied by the production of certain destructive enzymes namely MMPs, eventually leading to cartilage and bone loss in OA (Sellam and Berenbaum, 2010b, Sutton et al., 2009). Histological synovitis is characterised by the thickening of the

synovial lining, often called synovial hyperplasia, which can result in a cell depth of more than 8 cells (Sutton et al., 2009).

Accordingly, in this study, in chapter 4, we have presented histological evidence of persistent inflammation with synovial hyperplasia, inflammatory cell infiltration in progressive grades of OA synovial tissue. Although inflammatory cells play an important role in synovitis, the persistence of the inflammation and the proliferative feature of the synovitis is largely attributed to FLS (Benito et al., 2005, Fernandez-Madrid et al., 1995, Sutton et al., 2009, Buckley et al., 2001). Furthermore, there is increasing evidence that FLS act as sentinel cells that contribute to OA pathogenesis through the secretion of a variety of pro-inflammatory cytokines, adhesion molecules and chemokines such as IL-6, IFNβ, CCL5, IL-8, which attract and retain large numbers of leukocytes in the synovial tissue and as well secrete and induce MMPs responsible for eroding the cartilage in the joint (Müller-Ladner et al., 2007, Buckley et al., 2001, Sutton et al., 2009, Scanzello et al., 2011b, Scanzello et al., 2009). Moreover, the proliferative feature of FLS in OA may be attributed to an impairment of apoptosis, which contributes to the synovial hyperplasia. Apoptosis, or programmed cell death, is tightly regulated and ensures the elimination of cells from tissue. A wide variety of so-called death signals exists, and a lower expression or deregulation of these signals leads to a reduction of apoptosis. Reduction of apoptosis can lead to the accumulation of cells and could, in part, play a role in the hyperplasia of the synovium. Accordingly, in this study we found a trend towards a decrease in the expression of a key anti-proliferative and a pro-apoptotic protein named prohibitin (PHB1) in progressive grades of OA synovial tissues (data not shown), and also in FLS upon Poly (I:C) stimulation (a synthetic TLR3 agonist) (chapter 5). One possible outcome for such a decrease in PHB1 levels in OA synovial tissues can be the higher expression of anti-apoptotic proteins like Bcl-2 and suppression of tumour suppressor gene p53 which are otherwise regulated by PHB1 (data not shown), whilst impair apoptosis in FLS and thereby induce synovial hyperplasia (Kraan et al., 2000).

Our understanding of the mechanisms by which inflammation may contribute to joint deterioration and symptoms in OA is continuing to expand. As discussed above, the pattern of inflammatory cells and their products within joint tissues in OA suggests activation of an innate immune response. Moreover, there is a growing array of innate inflammatory ignition switches in OA (Liu-Bryan and Terkeltaub, 2012), wherein, TLR activation may

play a crucial role in OA progression by mediating synovitis in FLS, possibly through production of pro-inflammatory cytokines, chemokines and MMPs in the OA joint (Scanzello et al., 2008, Sutton et al., 2009). Nevertheless, ddirect evidence for TLR activation in OA development and progression has yet to be demonstrated, but their well documented role in RA, SLE (Roelofs et al., 2008) and tissue injury (Kaczorowski et al., 2008), suggests their importance in OA. Previously, it was shown that TLR2 and TLR4 are present in the OA synovial membrane, but both are more highly expressed in RA synovial membrane (Radstake et al., 2004). However, cultured synovial cells from both disorders were equally responsive to the TLR4 agonist LPS (Ozawa et al., 2007) and to the TLR2 agonist peptidoglycan (Kyburz et al., 2003). In cartilage, TLR2 and TLR4 are upregulated in lesional areas in patients with advanced OA (Kim et al., 2006). The same study demonstrated the activity of these receptors in chondrocytes by in-vitro treatment with their respective bacterial ligands. In a murine model of autoimmune arthritis (Abdollahi-Roodsaz et al., 2008), TLR4 deficiency resulted in reduced disease severity reflected by less cellular influx, cartilage damage and bone erosion. On the contrary, TLR2 knockouts developed more severe disease, suggesting a protective role in this particular model. The implication of these data to OA was unclear, but points to the complexity of TLR responses in vivo and their possible interaction with other signalling pathways. Moreover, Zhang et al., showed the differential regulation of TLR2 and TLR3 in OA cartilage compared to normal. Wherein, they show that TLR2 was significantly downregulated and TLR3 upregulated in OA cartilage compared to normal, where the upregulated TLR3 activation induced high MMP1 and MMP13 expression in OA chondrocytes perhaps contributing to the increased MMP13 expression observed in OA cartilage (Zhang et al., 2008).

In a recent study, Meng et al., found that TLR3 is the earliest and most prominently upregulated TLR in splenic macrophages by screening the TLR expression profile in pristane-induced arthritis (PIA), a MHC class II-restricted and T-cell-dependent arthritis rat model, wherein, down regulation of TLR3 expression modulated the severity of arthritis (Meng et al., 2010). These findings regarding TLR3 provide an explanation for the initiation of the inflammatory response in immune organs, but the roles of TLRs in local inflammation of joints remain unclear. Recently, Zhu et al., reported that TLR3 can be induced by arthritogenic T cells and then mediates the activation of synoviocytes in particular synovial tissue resident FLSs in local inflammatory responses (Zhu et al., 2011).

Therefore, we investigated which TLR is the key TLR in the synovium in knee OA and whether triggering of the key TLR directly affects OA severity and how the key TLR in FLS is induced to mediate the local inflammatory response. Accordingly, we found that up-regulated TLR3 activation by exo and /or endogenous stimuli in OA-FLS secreted a plethora of pro-inflammatory cytokines, chemokines and MMPs which may help facilitate the progression of synovial inflammation (chapter 3 and 4). Previously, it's known that TLR pathways are activated during infections, contributing to an efficient host defense, but are self limited with the clearing of the microorganism. Whereas, TLR pathways activated during tissue injury can mostly lead in to uncontrolled TLR signalling which could further theoretically lead to chronic and autoimmune joint diseases such as OA and RA. In addition to up-regulated TLR expression, the availability of endogenous TLR ligands may be responsible for the enhanced activity of the signalling pathways.

Endogenous ligands are thought to be released during tissue damage, necrotic cell death and infections, which results in the release of extracellular matrix (ECM) components, intracellular molecules and stress factors that are able to initiate an inflammatory response (Searle et al., 1982). In contrast to apoptosis, necrotic cell death is typically associated with inflammation. This is most likely due to the release of cell contents into the surrounding environment leading to activation of adjacent cells (Edinger and Thompson, 2004). Apoptotic cells retain their membrane integrity and are rapidly cleared by macrophages before lysis (Platt et al., 1998). This has been demonstrated in DCs, which are activated by exposure to necrotic cells but not apoptotic cells (Basu et al., 2000, Sauter et al., 2000). The contents released as a result of ECM damage or cell necrosis may activate TLRs, generating further inflammation and thus more tissue damage. This cycle of inflammation may explain the chronic inflammatory state found in autoinflammatory diseases such as RA (Fig. 2). Very recently, these mechanisms emerged as in case of TLR3, TLR5 and TLR9 signalling in the gut, which can be protective as well as inflammatory and TLR2 and TLR4 signalling in the lung, which has been shown to sense the integrity of the lung tissue (Drexler and Foxwell, 2010). In addition, evidence is emerging that the joint may also be an environment with distinct TLR mechanisms. It has been demonstrated that FLS from RA patients are able to produce TNFα in response to TLR3 stimulation, while human skin fibroblasts are not (Lundberg et al., 2007). This could be due to the inflamed environment these cells are derived from or a speciality of the synovial tissue in the joint in general. These questions need to be addressed in the future. Furthermore, these studies also raise

the possibility that the role of TLR signalling might not be restricted to innate immunity but also involved in maintaining homeostasis of the tissue they are expressed in (Xiao et al., 2007). The hypothesis of TLR involvement in tissue repair as well as inflammation is supported by the increasing amount of evidence for endogenous TLR ligands (Brentano et al., 2005, Drexler et al., 2006, Rifkin et al., 2005). The recognition of so called "danger signals", released following tissue injury and cell necrosis, would enable TLRs to survey their environment and induce an inflammatory response in case of infection as well as a proliferative response subsequent to injury (Jiang et al., 2005). Moreover, TLR stimulation through endogenous ligands is increasingly implicated in chronic and autoimmune disease onset and progression.

In a wide variety of diseases, cell death represents both an outcome and an important step in pathogenesis. This duality occurs because cell death leads to the extracellular release of molecules and structures (DAMPs, such as hyaluronan and fibronectin) that can potently induce the innate immune system such as TLR4 and TLR2 (Scanzello et al., 2008). These mediators also include the alarmins which are endogenous cellular constituents that exit activated or dying cells to stimulate TLRs as well as non-TLR receptors. Alarmins like RNA, high mobility group box-1 (HMGB1), can translocate from cells as they die. In addition to alarmins, dead and dying cells can release subcellular organelles called microparticles that contain cytoplasmic and nuclear constituents, including DNA and RNA. These particles can impact on many cell types to induce inflammation (Pisetsky et al., 2011). Microparticles are small membrane-bound vesicles that are released from activated and dying cells by a blebbing process. These particles circulate in the blood and display potent pro-inflammatory activities and are an important source of extracellular DNA and RNA. The release of HMGB1, RNA and microparticles shows important similarities, occurring with cell death as well as stimulation of certain but not all TLRs (Pisetsky et al., 2011). These observations suggest that the products of dead cells can serve as important mediators to drive immune responses and promote inflammation and autoreactivity.

Inflammation of the synovial membrane that occurs in both the early and late phases of OA is associated with alterations in the adjacent cartilage that are similar to those seen in RA (Sellam and Berenbaum, 2010a, Benito et al., 2005). Catabolic and proinflammatory mediators such as cytokines, nitric oxide and prostaglandin E2 (PGE2) are produced by the

inflamed synovium and alter the balance of cartilage matrix degradation and repair, leading to excess production of the proteolytic enzymes namely MMPs responsible for cartilage breakdown. Wherein, cartilage alteration in turn amplifies synovial inflammation, creating a vicious circle (Sellam and Berenbaum, 2010a). Additionally, previous studies have reported that microparticles can activate FLS and aid in pathogenesis of arthritis (Jüngel et al., 2007). To support this, several groups have previously shown that, microparticles from monocytes and T cells are present in high numbers in the synovial fluid from inflamed OA and RA joints (Pap et al., 2000, Berckmans et al., 2002, Jüngel et al., 2007), leukocyte microparticles can induce the expression of proinflammatory cytokines by FLS (Distler et al., 2005b), and microparticles can up-regulate the expression of MMPs by FLS (Distler et al., 2005a). More, the results reported by Jüngel et al., suggest that microparticles act as novel signalling elements in arthritis, which, along with cytokines and direct cell–cell interactions, can modulate fibroblast function and promote joint inflammation and destruction (Jüngel et al., 2007). The same group has also demonstrated a novel mechanism by which microparticles can induce a proinflammatory phenotype in FLS. They showed that microparticles strongly stimulate the production of PGE2 by FLS via up-regulation of cyclooxygenase 2 (COX-2) and microsomal prostaglandin E synthase 1 (mPGES-1). The effects of microparticles in their study were observed in both RA and OA FLS suggesting a common action not dependent on disease-specific effects. Thus, PGE2 production and the other actions of microparticles on FLS may be pathogenetic in several arthritides. In addition, they also showed that microparticles activate NF-kB, AP-1, p38, and JNK pathways in FLS and that they also transport arachidonic acid from leukocytes to fibroblasts for conversion to PGE2 (Jüngel et al., 2007).

Together, these findings indicate that microparticles have diverse activities that lead to the induction of PGE2 in the inflamed joint. As such, microparticles may serve as intercellular signalling structures in the pathogenesis of arthritis, operating between soluble mediators and cell–cell contact. Therefore, owing to the previously published studies and our current findings in this thesis, we may hypothesise that, the microparticles available in the microenvironment of OA synovial joints could potentially be either a source of extracellular RNA themselves or carry the necrotic OA synovial fluid cell derived RNA to FLS and thereby initiate an innate immune signalling cascade exclusively through TLRs. Recently, Scanzello et al., have reported that, hyaluronan and fibronectin can act as endogenous danger signals in inducing TLR2 and TLR4 activity in OA and tissue injury

and also reported that soluble CD14 in synovial fluid from patients with OA and meniscal injury modulates the response of OA-FLS to LPS through TLR4 (Scanzello et al., 2008, Scanzello et al., 2011b). More recently, Nair et at., have shown that synovial fluid from patients with early OA modulates FLS responses to TLR4 and TLR2 ligands via soluble CD14 and also speculated the effect of OA-SF on other TLR ligands including candidate endogenous ligands (Nair et al., 2012). Moreover, Kariko et al., have previously demonstrated that stimulation of TLR3 is not restricted to viral RNA, but also results from incubation with in vitro–transcribed mRNA and mRNA released from necrotic cells. These results have established that dsRNA sequences contained in mRNA may serve as an endogenous TLR3 ligand (Karikó et al., 2004). Furthermore, Brentano et al., have reported that necrotic cells may be found in arthritic joints as a result of inflammatory and destructive processes, and can easily be detected in synovial fluid upon propidium iodide staining and also indicated that RNA released from necrotic cells in synovial fluid can act as an endogenous TLR3 ligand for the stimulation of pro-inflammatory gene expression in FLSs (Brentano et al., 2005). Although necrotic cells are usually not present in large amounts in the synovial tissue, apoptotic cells in synovial tissue may undergo secondary necrosis (Wu et al., 2001). Although TLR3 is known to respond to RNA from necrotic cells, the relative importance of this response *in vivo* during acute inflammatory processes was first demonstrated by Cavassani et al., where they demonstrated that TLR3 is a regulator of the amplification of immune response and serves an endogenous sensor of tissue necrosis, independent of viral activation. Wherein, *tlr3-/-* mice showed regulated peritoneal and systemic inflammation after tissue injury in the absence of a viral challenge and also showed that *in vivo*, anti-TLR3 antibody attenuates the tissue injury associated with gut ischemia and significantly decreased sepsis-induced mortality. Thus, they speculated that the use of an antibody directed against TLR3 might serve as a therapeutic clinical option in the treatment of necrosis-induced inflammatory events (Cavassani et al., 2008). In the current study, we analyzed TLR1-9 expression in OA-FLS and synovial tissues and found predominant upregulation of TLR3 gene and protein expression in synovial tissues and FLS and thus studied its functional aspects *in vitro* and *ex vivo* (chapter3 and 4). TLR3 was found to be strongly expressed in all samples derived from grade-specific whole synovial tissues from (grade-1 through grade-4) patients with OA compared to grade-0 healthy controls (data not shown).

Furthermore, stimulation of cultured OA-FLSs with Poly(I:C) or grade-specific OA-SFs resulted in increased TLR3 expression. In the current study, we found that cell-free synovial fluid from patients with OA stimulated FLS. However, in this case, the presence of cytokines such as TNFα and IL-6 and also possible stimulation with TLR2, 4 and 9 ligands, were not responsible for the stimulatory effect of OA-SF, as the respective cytokine or TLR specific neutralisation antibodies did not show or block the pro-inflammatory mediator activation effect of OA-SF in FLS. Interestingly, primarily TLR3 and to a less extent IFNβ neutralisation, significantly inhibited the inflammation associated OA-SF stimulatory effect in FLS. Similarly, the RNA-degrading enzyme RNase treatment but not DNase treatment significantly decreased the response of N and OA-FLSs to the necrotic cell derived RNA from OA-SFs (data not shown). These results indicate that mRNA containing short dsRNA sequences that are released from necrotic synovial fluid cells is sufficient to activate cultured human OA-FLS, resulting in the induction of pro-inflammatory gene expression. These findings extend those of a recent study that demonstrated the activation of human endometrial cells with U1 RNA containing dsRNA repeats (Hoffman et al., 2004). Similarly, we in this thesis, have demonstrated the marked expression of TLR3 in a majority of FLS from the synovium of patients with OA (grade-1 through grade-4) and the activation of OA-FLSs *in vitro* and whole OA synovial tissue explants *ex vivo*, by dsRNA of synthetic (Poly (I:C)) or endogenous origin (RNA in OA-SF).

Based on our findings, we propose that, in addition to stimulatory effects of cytokines, local tissue destructive events, whether caused by a mechanical injury to the joint or by other non infectious processes, may lead to the release of endogenous RNA, activating tissue resident FLSs via TLR3. In susceptible individuals, increased TLR3 expression and expression of tissue-destructive enzymes by OA-FLSs might then contribute to the perpetuation of the disease. Taken together, our findings do specifically address the initiation of OA disease, and are consistent with reports supporting a role for local inflammation even in the early stages of OA. Recently Nair et al., showed a role for sCD14 in potentiating FLS responses to TLR2 and TLR4 ligands in both early and advanced OA patients. CD14 has recently been demonstrated to participate in signalling and intracellular trafficking of TLR3 (Lee et al., 2006), and owing to the observations in this study, it might me proposed that the sCD14 accessible in the OA-SF might potentiate the tissue resident

FLS responses to the necrotic cell derived RNA from the OA-SF in both early and advanced OA patients.

Moreover, there is increasing evidence of therapeutic potential for signalling cascade modification, and recent evidence suggests a role for NF-κB in OA, wherein, NF-κB is previously known to be central to all TLR pathways. Recently, Chen et al., reported that, an siRNA NF-κBp65 construct delivered intra-articularly 3 days following surgical induction of OA in rat models, significantly reduced IL-1 and TNF levels in OA-SF and minimized synovitis and articular cartilage damage at 14 days. This was the first study to show the suppression of early experimental OA by in vivo delivery of the adenoviral vector-mediated NF-κBp65-specific siRNA as a therapeutic strategy in a surgically induced rat model of OA. It was a treatment study, as opposed to prevention, as NF-κB was inhibited after induction of disease. This treatment approach limited cartilage damage and synovial changes as observed 2 weeks after disease induction (Chen et al., 2008). In another study it was found that the baseline production of IL-6, IL-8, MCP-1, MMP-13 (a protease which is involved in cartilage collagen breakdown) was dependant on NF-κB. This was done using an adenoviral vector to overexpress IκBα in FLS cultures derived from OA patients. With further study, it was found that baseline and IL-1 stimulated levels of A Disintegrin and Metalloproteinase with Thromospondin Motifs (ADAMTS)-4 was also NF-κB dependant. ADAMTS-4 is thought to be responsible for the destructive breakdown of cartilage aggrecans which is prevalent in human OA (Amos et al., 2006, Bondeson et al., 2007). Although these two studies implicate NF-κB in mediating OA disease progression, the relative contributions of specific stimuli such as TLR or cytokine activity at different stages of disease remained unclear. Recently, it was reported that endogenous stimuli in OA may lead to the activation of TLR2 and TLR4 initiating a signalling cascade which eventually resulted in the activation of transcription factors such as interferon-regulatory factors (IRFs), AP-1 and NF-κB which increased the transcription of inflammatory associated genes (Scanzello et al., 2008). Thus far, NF-κB was known to be central to all TLR pathways. Herein, we found that TLR3 in OA FLS and synovium, upon engagement with Poly (I:C) or abundantly available RNA from necrotic cells in OA-SF lead to the activation of the TLR3-TRIF pathway dependent NF-κB and IRF3, 7 and 9 equally, towards inducing the inflammatory milieu that is prevalent in the synovium and joint during OA progression.

Furthermore, it is now known that the OA process leads to pathological changes in all the tissues of the joint including the articular cartilage, bone, and synovium. These changes result from the actions of molecular mediators released during the disease process such as cytokines, chemokines and MMPs. The breakdown of articular cartilage matrix has been related to the actions of various proteolytic enzymes such as collagenases or MMPs. Various inflammatory cytokines and growth factors have been demonstrated to augment protease production as well as promote changes seen in bone and synovium. Although mechanical stimulation of cartilage may play a role in the induction of some of these mediators of tissue damage, there is evidence that TLRpathway activation may also be important. It was reported that the progressive articular cartilage matrix loss is mediated primarily through MMPs such as MMP-1, 3, 9 and 13 in OA (Sandy, 2006). Therefore, the regulation of these MMPs in joint tissues is of great interest. There is emerging evidence that MMP production may result from TLR pathway activation. Most recently, ligands for TLR2 were shown to induce MMP-1 and MMP-13 production by chondrocytes from OA (Zhang et al., 2008). Furthermore, in RA synoviocytes, production of MMP-1, MMP-2, MMP-3, and MMP-13, was seen to be dependent on the TLR pathway adaptor proteins MyD88 and Mal/TIRAP (Sacre et al., 2007). Previously, synoviocyte expression of MMP-1 and MMP-3 was shown to be augmented by the TLR2 ligand peptidoglycan (Kyburz et al., 2003). So, there are numerous in-vitro reports linking synovial or chondrocyte production of MMPs to TLR activation. Herein, we have demonstrated that the key OA associated MMP1, 3, 9 and 13 are TLR3-TRIF pathway dependent, wherein, the regulation of these MMPs was shown with neutralisation of surface bound TLR3 in OA-FLS. However, confirmation using murine OA models is necessary, as in-vivo regulation is likely to be extremely complex.

Moreover, FLS are long known to play a significant role in synovial joint homeostasis through the direct secretion of pro-inflammatory cytokines and through their synergistic effects on other cells within the joint. Nevertheless, the relative impact of each cytokine produced by synovial tissue and their stimuli on OA pathogenesis was poorly understood so far. Here in this study we have also demonstrated that IFNβ is one such cytokine which can significantly induce TLR3 expression in FLS in absence of any exo/endo-genous stimuli, and as well in-turn gets induced predominantly by Poly(I:C) and grade-specific OA-SF, and thereby predominantly induces RANTES, TNFα, IL-6, IL-15, IL-8, IL-1β and MMPs 1, 3, 9 and 13 gene and protein expression in OA-FLS, thus TLR3-mediated IFNβ

signalling was found critical and studied therefore (chapter 3 and 4). Furthermore, Magnusson et al., reported that arthritis triggered by dsRNA is associated with the ability to produce type I IFNs and is critically dependent on type I IFN receptor / IFNAR signalling prevalent in the joint tissue. Also, the intrinsic arthritogenic properties of IFNβ implicate a role of this cytokine in joint manifestations triggered by various interferogenic stimuli (Magnusson et al., 2006). Furthermore, Matsumoto et al., provided evidence for TLR3 mediated Type 1 IFN induction by RNA and Poly(I:C)(Matsumoto and Seya, 2008). Accordingly, in the current study we found a trend towards increased levels of IFNβ detected in the progressive grades of OA-SFs and also demonstrated a marked induction of IFNβ gene and protein levels in OA-FLS and synovium in a TLR3 dependent manner upon stimulation with Poly(I:C) or OA-SF. The relevance of this observation to disease activity and progression of OA is unknown, because the IFN pathway can be either detrimental or beneficial depending on the relative balance of IFNβ, IL-1 receptor antagonist, and proinflammatory chemokines such as RANTES. Accordingly, in the current study we found significant amounts of IFNβ in progressive grades of OA synovial fluid and also showed that upon Poly (I:C) stimulation, both early and late OA patient derived FLS and whole synovial tissue explants cultures produced marked amounts of IFNβ which could have potential detrimental effects on the OA synovium owing to its unregulated levels in the synovial fluid. Also, studies have shown that IFNβ triggers experimental synovitis and may potentiate chronic inflammatory and auto-immune diseases in humans (Rosenbach et al., 1984, Akbar et al., 2000, Stark et al., 1998) and increasing evidence shows a role for targeting signal transduction involving IRF3 and IRF7 transcription in inflammatory joint pathologies towards the regulation of Type I IFN production (Berenbaum, 2004, Honda et al., 2006, Sweeney, 2011).

Moreover, the regulatory role of various members of the IRF family such as IRF3, IRF5 and IRF7 have already been well characterised and elucidated in TLR signal transduction pathways and numerous studies have now shown the potential role of IRF3 and IRF7 as valuable molecular targets for therapeutic interventions to prevent inflammatory diseases. In the current study, we propose that necrotic cell derived RNA from the grade-specific OA-SF could potentially induce IRF3, 7 and 9, but not IRF5 in FLS. Whilst, IRF9 is known to play a crucial regulatory role in JAK-STAT IFNAR signalling pathways for the stimulation of IFN-responsive genes (Schindler and Brutsaert, 1999), in this study we have shown that IRF9 plays a very significant and vital role in the TLR signalling pathway

towards the production of Type I IFNs itself and the exact mechanism and functional characterisation of IRF9 in TLR signalling is currently been investigated in the lab.

Furthermore, it was recently reported that IRF3 rather than IRF7 regulates Poly (I:C) induced type I IFN responses in human synoviocytes by increasing ISRE promoter activity. IRF3 also partially regulates expression of other cytokines and MMP through activation of c-Jun and the AP-1 promoter site (Sweeney et al., 2010). Targeting synoviocyte IRF3 represents a potential approach to suppress diverse mediators while limiting suppression of IRF7-mediated immune responses. Because IRF3 is constitutively expressed and involved in immediate antiviral responses, inhibition might alter early innate immunity. IRF7 is expressed in a more restricted fashion and is induced transiently in most cells after IFNβ production is initiated. IRF7 can also serve as a critical checkpoint in adaptive immune responses and Ag presentation and might be more important in later stages of arthritis. Thus, targeting the innate signalling pathways such as TLR3 and IFN signature can be complex and requires a detailed understanding of each component. Considering the potential pathogenic role of IFN in chronic and autoimmune disease and the delicate balance between anti- and proinflammatory effects, dissecting the IFN response could have important therapeutic and safety implications. Our studies are limited to human FLS, and the overall effect of blocking TLR3 might depend on species, cell lineage, and the microenvironment. On the basis of the FLS data presented in this thesis, targeting TLR3 could potentially inhibit IRF3 and IRF9 activation via PRD I-III domain and NF-kB via PRD II domain of IFNβ promoter which otherwise mediated synovial inflammation in an autocrine and paracrine fashion, while sparing the critical functions of IRF7 in FLS upon potential encounter with poly (I:C), RNA or micro particles from OA-SF.

Taken together, the work in this thesis has been performed to provide further evidence in support of our hypothesis that TLR3 over-activation is a key mediator in synovial inflammation in OA. The study presented in the thesis has demonstrated that TLR3 is abundantly expressed at both the mRNA and protein level in the OA synovial tissue and FLS. These findings provided the precedence for the present study. In this thesis we have considerably increased the understanding of the role of TLR3 hyper-activation in synovial inflammation. New data presented herein clearly demonstrates a critical role for TLR3 over-activation in mediating broad range of inflammatory events namely, pro-

inflammatory cytokine, chemokine and MMP secretion, thus perpetuating synovial inflammation and ultimately leading to joint destruction in OA. We demonstrated that Poly(I:C) and OA-SF (with probable RNA from necrotic cells) induces the potent inflammatory mediators in OA-FLS and grade-specific OA whole tissue explants both *in-vitro* and *ex-vivo.* We also provide a significant body of evidence using *in vitro* and *ex vivo* studies which correlate with matched patient-derived clinical data that TLR3 hyper-activation participates at multiple stages in the pathological processes of synovial inflammation in OA. Interestingly, the key role of TLR3 activation by Poly(I:C)/ RNA from necrotic cells of the OA synovial fluid was confirmed and evaluated through neutralisation of TLR3 expression which shifted the balance from pro-inflammatory to an anti-inflammatory cytokine milieu. Thus, our data suggests that TLR3 hyperactivation plays a key role in perpetuating synovial inflammation in OA and suggests that therapeutic intervention of OA may be achieved through TLR3 blockade. Furthermore, this evidence provides a sound rationale to develop synovial tissue and in particular FLS targeted therapy, through the control of inflammation by the inhibition or regulation of TLR3 mediated inflammatory cascades. In light of the previous known functions of TLR3 in arthritis, these results provide compelling evidence for TLR3 as a potential therapeutic target in the control of synovial inflammation in OA and are depicted in Figure 6.1.

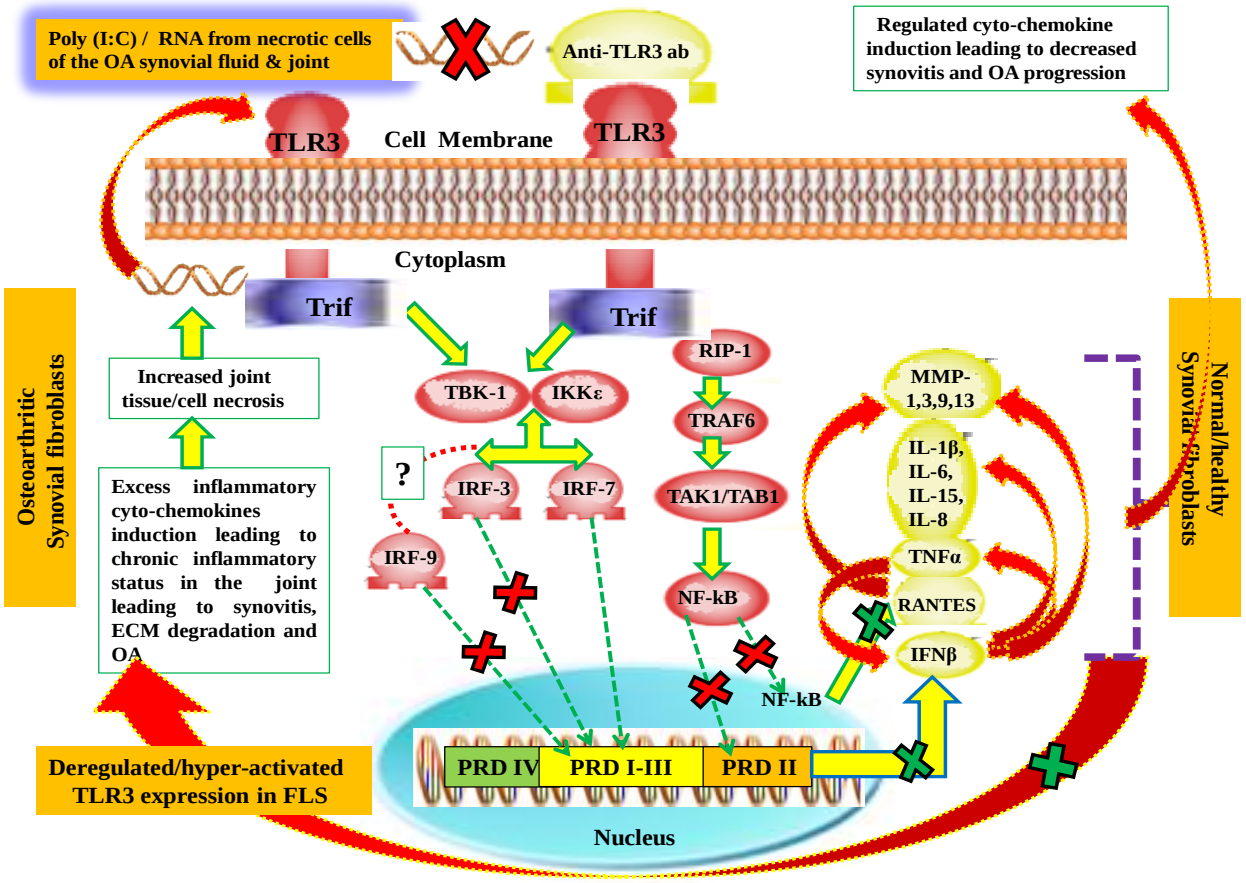

Figure 6.1: Schematic representation of TLR3 intervention in OA. Immunomodulatory and signal transduction modulatory effect of TLR3 blockade in OA-FLS through regulation of key OA associated inflammatory mediators, namely, IFNβ, RANTES, TNFα, IL-6, IL-8, IL-1β, IL-15, MMPs 1, 3, 9 and 13. Sensing of dsRNA/Poly (I:C)/cell free RNA from necrotic cells in the synovial fluid or joint by TLR3 results in the assembly of a receptor complex at least comprising the adaptors TRIF, TRAF6 as well as the kinases RIP1, TBK1 and the IKKε. RIP1 and possibly TRAF6 mediate TLR3-dependent transcriptional activation of NF-κB possibly through TAK1/TAB1, leading to the binding of NF-κB to the PRDII domain of the IFNβ promoter. Whereas, TBK1 and IKKε seems to be essential for the transcriptional activation of IRF3, 7 and IRF9 (by an unknown mechanism (dotted line), leading to the binding of IRF3, 7 and 9 to the PRDI-III domain of the IFNβ promoter. Together, these resulted in increased expression and release of key inflammatory mediators in an autocrine and paracrine manner in OA-FLS thus maintaining a vicious inflammatory loop. Neutralisation of surface bound TLR3 utilising an anti-TLR3 antibody potently inhibited the translocation of IRF3 and 9 through PRDI-III domain and NF-κB through PRDII domain of the IFNβ promoter, thereby blocking the excess expression and release of key OA associated inflammatory mediators in the joint and thus breaks the vicious inflammatory loop. Hence, TLR3 is a critical target for OA disease intervention.

Proteomics, which enables large scale analysis of gene expression at the protein level is widely acknowledged to be an important tool in identifying new biomarkers and providing information on disease process and pathogenesis (Meyer and Stuhler, 2007). With the introduction of proteomics, it has become possible to simultaneously analyse changes, including post translational modifications in multiple proteins. Thus, proteomic technologies may help in identifying new targets, diagnostics or therapeutic biomarkers for OA. Based on previous studies, we employed this technique to reveal differentially regulated proteins mediating TLR/RLR-induced inflammation in the joint. We also used grade-specific OA whole synovial tissue explants which mimic the *in vivo* joint environment and enable cell-cell contact. We demonstrated altered expression of several proteins in response to Poly (I:C), in particular caldesmon and vimentin which are involved in cytoskeletal assembly and cell migration and a novel protein prohibitin (PHB1), involved in cell-proliferation, apoptosis and complement activation. Our results in chapter 5 demonstrated that, decreased PHB1 expression levels in both N and OA FLS, were primarily induced by Poly (I:C)-a synthetic mimic for dsRNA, which is previously shown by us in chapter 3, to solely activate TLR3 signalling in OA-FLS. Given these findings, it would be crucial to employ an anti-TLR3 antibody to neutralise the overactivated TLR3 expression in FLS, to restore PHB1 levels in FLS, as it was previously reported by other groups that, restoring PHB1 levels in intestinal epithelial cells can combat the damaging effects of oxidative stress on mucosal barrier function, where reduced levels of PHB1 lead to oxidant-induced loss of mucosal integrity and function during intestinal inflammation (Theiss and Sitaraman, 2011). Similarly, another report stated thatover-expression of PHB1 can protect against the damaging effects of oxidative stress, therefore restoring or increasing PHB1 expression in IBD patients has become a potential therapeutic strategy to prevent mucosal barrier disruption by increased oxidants (Theiss et al., 2007).

The potential of PHB1 to interact with tumour suppressor proteins and transcription factors, inhibit oxidative stress and mitochondrial dysfunction, act as a cell-surface receptor for the vasculature of adipose tissue, and modulate cell proliferation and apoptosis, suggest that PHB1 harbours great potential for the development of therapeutic agents for obesity, diabetes, cancer (Theiss et al., 2007), and chronic inflammatory diseases such as OA. Depending upon the disease state, therapeutic potential exists in altering the levels of PHB1 expressed in affected cells, such as in diabetes or inflammation, altering the subcellular localization of PHB1 expression, such as in cancer, or targeting cell

surface PHB1, such as in obesity. Owing to our current PHB1 analysis data provided in chapter 5, we hypothesise that plasma membrane localised PHB1 may also be available on OA-FLS, which on an encounter with viral dsRNA or RNA from necrotic cells, may localise to the mitochondria and thereby may induce p53 and C3b suppression, impair apoptosis and induce cell proliferation ultimately leading to synovial hyperplasia, inflammation, joint destruction and OA. Taken together our data suggests that, PHB1 may be considered as a probable biomarker for tracking synovial inflammation in OA. The multiple functions of PHB1 are only beginning to be elucidated, but it is clear that this protein provides new avenues for therapeutic-based research (Theiss and Sitaraman, 2011).

Given that analysis of synovial tissue in combination with synovial fluids could reveal biomarkers secreted by various types of synovial membrane cells as disease progresses from early clinically unapparent disease to established chronic inflammation, we have investigated the proteome of grade-specific OA synovial tissue biopsies and found drastic alterations in few protein profiles, which are as follows; Grade-1 OA versus Grade-0/Healthy control: a decrease in S100-A11, which negatively regulates cell proliferation and DNA replication, and as well known to modulate cartilage matrix catabolism in OA (Sakaguchi and Huh, 2011, Cecil, 2008) and an increase in cyclophilin A, which accelerates the folding of proteins and is also known to interact with HIV-1 Capsid protein (Luban et al., 1993) and may contribute to the inflammatory processes in arthritis through MMP and inflammatory cytokine secretion (Kim et al., 2005) and may also contribute to cartilage degradation in OA (Cloos and Christgau, 2002); Grade-2 OA versus Grade-0/Healthy control: an increase in heat shock 60 kDa protein 1 and a decrease in ATP synthase, galectin-1 and complement C3b expression were found. Wherein, galectin-1 is known to regulate apoptosis, cell proliferation and cell differentiation (He and Baum, 2004) and a major regulator of inflammatory response (Rabinovich et al., 2002); Grade-3 OA versus Grade-0/Healthy control: a decrease in ATP synthase and an increase in heat shock cognate 71kDa protein was found; Grade-4 OA versus Grade-0/Healthy control: a decrease in alpha-enolase and an increase in SH3 domain-binding glutamic acid-ric-like protein was found. The majority of these proteins identified through our DIGE proteomic study with drastic grade-specific altered expression patterns, have been previously implicated in OA pathogenesis (Ruiz-Romero and Blanco, 2009, Rollín et al., 2008, Ruiz-Romero et al., 2009, Raquel et al., 2008), and thus imply a significant role for these proteins as grade-specific synovitis markers, although further quantitative validation is

required. Initial validation of these protein markers will be carried out in synovial tissue samples of OA patients, in addition to serum and synovial fluid.

Furthermore, at a functional level, multiple culture systems, such as whole tissue explant cultures and mono-cultures of cell types such as fibroblasts and chondrocytes will be used to examine the mechanistic function of these proteins and their role in driving the pro-inflammatory response. Finally, validation of these proteins that are altered in a grade-specific synovial tissue, following proteomic analysis will be performed using immune-blotting, ELISA, and immunochemistry. Additionally, we plan to utilise MUDPIT (multidimensional protein identification technology), a more recent technology used to validate biomarkers in proteomics. Thus, the study of the synovium using various proteomic platforms should be considered as a key to our understanding of the stages of cellular pathology involved in the development of joint diseases as unlike cell monolayer and 3D cultures, synovial tissue explants retain their extra cellular matrix, providing native substrates for proteolysis and protein release, leading to the identification of other important markers of synovial tissue inflammation and joint destruction (Gibson and Rooney, 2007). It is unlikely that a single biomarker, highly specific for inflammatory arthritis will be identified, however panels of biomarkers from the proteome in combination with markers from the peptidome, fragmentome and degradome will undeniably enhance the ability to diagnose and treat arthritic conditions at an early stage and further pave the way for individual and novel therapeutic intervention.

Furthermore, a common feature of several chronic and autoimmune diseases (e.g. SLE) is a defect in the induction of apoptosis or a defect in clearing cell debris (Yu et al., 2008) and a similar defect in pro-apoptotic signals, perhaps *via* PHB1, was found in OA FLS and synovial tissues upon Poly(I:C) or OA-SF stimulation. One possibility is that a genetic predisposition together with environmental factors, e.g. smoking (Koarai et al., 2012), and mechanical injury may induce the release of danger signals such as necrotic cell RNA, which would lead to the activation of TLR3 in OA resulting in inflammation. Subsequently, more cells undergo necrosis as a consequence of inflammation and release more danger signals. TLR3 might therefore play a major part in chronic inflammatory disease such as OA progression. The treatment of inflammatory diseases has so far relied on broad spectrum inhibitors of inflammatory mediators, e.g. TNF (Feldmann, 2002). These therapies have no cure and need to be applied over a long period of time, which

results in side effects, e.g. increased infections, as the immune system is globally inhibited. Thus, targeting certain TLRs such as TLR3 in OA, might provide a more specific target for the treatment of such inflammatory diseases. Since the variety of TLR ligands released in one particular disease might be limited, targeting the TLRs involved would permit the function of other TLRs to remain intact. Therefore, the immune system would not be globally affected and the side effects of the treatment reduced. Such a therapy might also break the vicious cycle of inflammation and release of danger signals such as necrotic cell RNA and/or microparticles in OA synovial joints, and might therefore cure the disease rather than just dampening it. Further characterisation of the distinct TLR mechanism in specific tissues may be intensified through the use of specific blocking antibodies, such as the one we described in this thesis, detailing neutralisation of surface bound TLR3 expression in OA-FLS and synovium as such can potentially break the vicious cycle of TLR3 mediated IFNβ signalling in perpetuating the inflammatory milieu aiding in OA progression and irreversible joint damage, also signifying a pivotal role for TLR3 rather than RLR (RIG-I/MDA-5) association and activation in OA progression.

The eventual goal of research into the specifics of signalling cascades is to identify a target within a dysregulated system whose inhibition can maximise the reduction in disease pathology whilst minimising systemic effects in the host. This can only be achieved when our understanding of these pathways is extensive enough to enable us to predict the likely effects of any intervention in the targeted host tissues. Thus, increasing our understanding of signal transduction pathways and the effect of expressed proteins can have a positive therapeutic effect. The more we can close in on the causative agent in the pathology of a certain disease, the less we will have to disrupt peripheral proteins for its treatment or inhibition. Accordingly, our current data suggests a key role for TLR3 and its signalling pathway hyperactivation in FLS in perpetuating synovial inflammation in OA through perpetuating the inflammatory milieu in the synovium and also possibly through impairment of PHB1 levels in FLS possibly through binding with IRF9, thereby impairing cell cycle regulation and apoptosis eventually leading in synovial hyperplasia and prolonged lymphocyte survival and chronic inflammation. Our data also sheds light on the regulatory and immunomodulatory and signal transduction modulatory effects of TLR3 intervention employing anti-TLR3 antibody approach in FLS, wherein, a similar approach of TLR3 blockade through neutralisation of surface bound TLR3 expression in whole synovial tissue explants is currently undertaken and we are awaiting the results.

Identification of methods for the early diagnosis of synovitis is of key importance, since therapeutic interventions aimed at blocking or reversing structural damage will be more effective when there is the possibility of preserving normal homeostasis. At the later stages of OA, cartilage tissue engineering with or without gene therapy will also require anti-cytokine therapy to block damage to newly repaired cartilage. Thus, through our findings in this thesis, we hypothesise that TLR3 and PHB1expression in FLSs can be utilised as an early synovitis marker in OA and a combinatorial blocking of TLR3 and IFNβ expression in OA synovial tissues may have beneficial effects in synovitis mediated OA progression.

6.2. Future work

In this study, we have provided a wide body of *in-vitro* and e*xvivo* evidence to support a central role for TLR3 over-activation in FLS, in the pathogenesis of OA through synovial inflammation and joint damage. We also have provided a significant body of evidence for the immuno-modulatory properties of TLR3 neutralising antibody through regulating TLR3 expression and the downstream inflammatory cytokine-chemokine-MMP cascades. We also have identified a number of proteins which are altered in response to Poly (I:C) and OA-SF in FLS, which may play a key role in the pathogenesis of OA. Thus, future work would be directed towards evaluating the followings objectives.

1. The potential of cell free OA-SF, necrotic cell derived RNA from the OA-SF and microparticles isolated from OA-SF, to activate TLR3 in whole synovial tissue explants, synoviocytes and chondrocytes will be performed, which further paves way for exploring the signalling pathways induced through OA-SF, and may provide probable molecular targets to alleviate synovial inflammation in OA. Moreover, to elucidate the importance of TLR3 activation in OA, we plan to test the effect of Poly (I:C), and its blockade on, inflammatory processes *in-vivo* and *ex vivo*, therefore, the effects of TLR3 blockade on e*x-vivo* synovial biopsy explants and stage-specific OA patient derived FLS utilising specific TLR3 directed antibody will be examined. Further validation of TLR3 as a molecular target for the intervention of OA will be performed using a STR/ort mouse model of spontaneous OA and also the functional characterisation of the same will be evaluated in TLR3-/-mice.

2. In the future, quantitative validation and localisation of the protein markers e.g., PHB1 in chondrocytes and other cell types in the synovium is required. Likewise, further validation of anti-TLR3 antibody efficacy in the curtailment of the inflammatory milieu in OA synovial explant cultures is required, as is the ability of PHB1 restoration to block OA-FLS proliferation. The quantitative validation and mapping of key protein markers identified through proteomics in Poly (I:C) treated FLS namely, PHB1 in chondrocytes and other cell types in the synovium will also be required. Also, the future work holds promise to validate and functionally characterise the role of PHB1 and IRF9 in TLR3 signalling in OA upon physiologically relevant endogenous stimuli. Likewise, validation of the ability of an anti-TLR3 antibody to restore PHB1 levels in OA-FLS, OA synovial explant cultures and other monolayer cell cultures in the synovium is worthy of further investigation.. Further investigations are in progress to define the role of TLR3 in various cell types present in the synovial tissue and the communication pathways that occur between cartilage, subchondral bone and synovial tissue.

3. Future research may determine the role of TLR3 over-activation in ageing, arthritis and obesity, in relation to the outcome of diabetes common to all three states and is largely known to associate with OA progression. Therefore, a comparative TLR and proteomic profiling may be made of the morphology, composition and function of synovial adipose tissue (SAT) to subcutaneous white adipose tissue (SWAT) from patients with OA and metabolic syndrome. Subsequently, functional characterisation through *invitro* studies may be investigated to ascertain the involvement of TLR3 activation in pro-inflammatory events in SAT and OA- FLS. We hope that outputs will shed light on common mechanistic pathways involved in disease pathogenesis which can be exploited for prevention or treatment of inflammatory diseases such as OA or the metabolic syndrome in relation to ageing.

In summary, these studies would prove useful in elucidating the differential activation of TLRs, in particular TLR3 expression during physiologic and pathophysiologic states. Overall, these future studies would provide further insights into the role of TLRs in the synovium in normal physiologic and pathophysiologic states such as OA, and may elude to the physiologic activation and regulation of TLRs in human joint tissues.

6.3. Conclusions

In conclusion, TLR3 in the synovium of OA patients displayed early and persistent over-expression at the initiation and development stages of arthritis. TLR3 was localised in FLSs, and activation of the TLR3 signalling pathway *in vivo* could aggravate arthritis. FLSs were activated and activated by the necrotic OA-SF cell derived RNA through inflammatory mediators secretion via TLR3 signalling in OA. Thus, TLR3 in FLSs was confirmed to be an important synovitis mediator in OA progression through neutralisation of TLR3 which restored the balance of anabolic and catbolic mediators in arthritis. These data provide a very useful *ex vivo and in vitro* model, to increase understanding of the initiation and development of synovial inflammation systemically and dynamically, and also provide TLR3 as an interesting target for OA treatment and even as an early synovitis marker for OA diagnosis.

Despite the significant advances in our understanding and management of OA, much remains to be learned before clinicians can guarantee a quality of life which is free of the debilitating and painful effects still endured by many of OA patients. We are hoping that our efforts would, at least in part, contribute to a better understanding of the pathogenic molecular mechanisms of such chronic inflammatory disease pathologies, and also hope that our efforts will lead to better treatments and there by an improved quality of life for patients whose lives are marred by OA and related inflammatory diseases.

Bibliography

ABDOLLAHI-ROODSAZ, S., JOOSTEN, L. A. B., KOENDERS, M. I., DEVESA, I., ROELOFS, M. F., RADSTAKE, T., HEUVELMANS-JACOBS, M., AKIRA, S., NICKLIN, M. J. H. & RIBEIRO-DIAS, F. 2008. Stimulation of TLR2 and TLR4 differentially skews the balance of T cells in a mouse model of arthritis. *Journal of Clinical Investigation,* 118**,** 205-216.

ABDOLLAHI-ROODSAZ, S., VAN DE LOO, F. A. J. & VAN DEN BERG, W. B. 2011. Trapped in a vicious loop: Toll-like receptors sustain the spontaneous cytokine production by rheumatoid synovium. *Arthritis Research & Therapy,* 13**,** 105.

ABRAMSON, S. B., ATTUR, M. & YAZICI, Y. 2006. Prospects for disease modification in osteoarthritis. *Nature Clinical Practice Rheumatology,* 2**,** 304-312.

ABRAMSON, S. B. & YAZICI, Y. 2006. Biologics in development for rheumatoid arthritis: relevance to osteoarthritis. *Advanced drug delivery reviews,* 58**,** 212-225.

AICHER, W. K., ALEXANDER, D., HAAS, C., KUCHEN, S., PAGENSTECHER, A., GAY, S., PETER, H. H. & EIBEL, H. 2003. Transcription factor early growth response 1 activity up-regulates expression of tissue inhibitor of metalloproteinases 1 in human synovial fibroblasts. *Arthritis & Rheumatism,* 48**,** 348-359.

AICHER, W. K., DINKEL, A., GRIMBACHER, B., HAAS, C., SEYDLITZ-KURZBACH, E., PETER, H. H. & EIBEL, H. 1999. Serum response elements activate and cAMP responsive elements inhibit expression of transcription factor Egr-1 in synovial fibroblasts of rheumatoid arthritis patients. *International immunology,* 11**,** 47.

AIGNER, T., HAAG, J. & ZIMMER, R. 2007. Functional genomics, evo-devo and systems biology: a chance to overcome complexity? *Current opinion in rheumatology,* 19**,** 463.

AKASHI-TAKAMURA, S. & MIYAKE, K. 2008. TLR accessory molecules. *Current opinion in immunology,* 20**,** 420-425.

AKBAR, A. N., LORD, J. M. & SALMON, M. 2000. IFN-[alpha] and IFN-[beta]: a link between immune memory and chronic inflammation. *Immunology today,* 21**,** 337-342.

AKIRA, S. 2003. Mammalian Toll-like receptors. *Current opinion in immunology,* 15**,** 5-11.

AKIRA, S. & SATO, S. 2003. Toll-like receptors and their signaling mechanisms. *Scandinavian journal of infectious diseases,* 35**,** 555-562.

AKIRA, S. & TAKEDA, K. 2004. Toll-like receptor signalling. *Nature Reviews Immunology,* 4**,** 499-511.

AKIRA, S., TOKEDA, K. & KAISHO, T. 2001. Toll-like receptors: critical proteins linking innate and acquired immunity. *nature immunology,* 2**,** 675-680.

AKIRA, S., UEMATSU, S. & TAKEUCHI, O. 2006. Pathogen recognition and innate immunity. *Cell,* 124**,** 783-801.

ALAAEDDINE, N., OLEE, T., HASHIMOTO, S., CREIGHTON-ACHERMANN, L. & LOTZ, M. 2001. Production of the chemokine RANTES by articular chondrocytes and role

in cartilage degradation. *Arthritis & Rheumatism,* 44**,** 1633-1643.

ALSALAMEH, S., MOLLENHAUER, J. Ü. R., HAIN, N., STOCK, K. P., KALDEN, J. R. & BURMESTER, G. R. 1990. Cellular immune response toward human articular chondrocytes. T cell reactivities against chondrocyte and fibroblast membranes in destructive joint diseases. *Arthritis & Rheumatism,* 33**,** 1477-1486.

ALSALEH, G., FRANÇOIS, A., KNAPP, A. M., SCHICKEL, J. N., SIBILIA, J., PASQUALI, J. L., GOTTENBERG, J. E., WACHSMANN, D. & SOULAS-SPRAUEL, P. 2011. Synovial fibroblasts promote immunoglobulin class switching by a mechanism involving BAFF. *European Journal of Immunology*.

ALTMAN, R., ASCH, E., BLOCH, D., BOLE, G., BORENSTEIN, D., BRANDT, K., CHRISTY, W., COOKE, T., GREENWALD, R. & HOCHBERG, M. 1986. Development of criteria for the classification and reporting of osteoarthritis: classification of osteoarthritis of the knee. *Arthritis & Rheumatism,* 29**,** 1039-1049.

ALVARO-GRACIA, J. M., YU, C., ZVAIFLER, N. J. & FIRESTEIN, G. S. 1993. Mutual antagonism between interferon-gamma and tumor necrosis factor-alpha on fibroblast-like synoviocytes: paradoxical induction of IFN-gamma and TNF-alpha receptor expression. *Journal of clinical immunology,* 13**,** 212-218.

AMOS, N., LAUDER, S., EVANS, A., FELDMANN, M. & BONDESON, J. 2006. Adenoviral gene transfer into osteoarthritis synovial cells using the endogenous inhibitor IκBα reveals that most, but not all, inflammatory and destructive mediators are NFκB dependent. *Rheumatology,* 45**,** 1201-1209.

AN, H., ZHAO, W., HOU, J., ZHANG, Y., XIE, Y., ZHENG, Y., XU, H., QIAN, C., ZHOU, J. & YU, Y. 2006. SHP-2 phosphatase negatively regulates the TRIF adaptor protein-dependent type I interferon and proinflammatory cytokine production. *Immunity,* 25**,** 919-928.

ANDERSEN-NISSEN, E., SMITH, K. D., STROBE, K. L., BARRETT, S. L. R., COOKSON, B. T., LOGAN, S. M. & ADEREM, A. 2005. Evasion of Toll-like receptor 5 by flagellated bacteria. *Proceedings of the National Academy of Sciences of the United States of America,* 102**,** 9247.

ANDERSON, L. & HUNTER, C. L. 2006. Quantitative mass spectrometric multiple reaction monitoring assays for major plasma proteins. *Molecular & Cellular Proteomics,* 5**,** 573-588.

ANDERSSON, M., GROSECLOSE, M. R., DEUTCH, A. Y. & CAPRIOLI, R. M. 2008. Imaging mass spectrometry of proteins and peptides: 3D volume reconstruction. *Nature methods,* 5**,** 101-108.

AREND, W. P. & DAYER, J. M. 1990. Cytokines and cytokine inhibitors or antagonists in rheumatoid arthritis. *Arthritis & Rheumatism,* 33**,** 305-315.

AREND, W. P. & DAYER, J. M. 1995. Inhibition of the production and effects of interleukins-1 and tumor necrosis factor α in rheumatoid arthritis. *Arthritis & Rheumatism,* 38**,** 151-160.

ASHRAF, S. & WALSH, D. A. 2008. Angiogenesis in osteoarthritis. *Current opinion in rheumatology,* 20**,** 573.

ASQUITH, D. L. & MCINNES, I. B. 2007. Emerging cytokine targets in rheumatoid arthritis. *Current opinion in rheumatology,* 19**,** 246.

ATTUR, M., SAMUELS, J., KRASNOKUTSKY, S. & ABRAMSON, S. B. 2010. Targeting the synovial tissue for treating osteoarthritis (OA): where is the evidence? *Best Practice & Research Clinical Rheumatology,* 24**,** 71-79.

AYRAL, X., MAYOUX-BENHAMOU, A. & DOUGADOS, M. 1996. Proposed scoring system for assessing synovial membrane abnormalities at arthroscopy in knee osteoarthritis. *Rheumatology,* 35**,** 14.

AYRAL, X., PICKERING, E., WOODWORTH, T., MACKILLOP, N. & DOUGADOS, M. 2005. Synovitis: a potential predictive factor of structural progression of medial tibiofemoral knee osteoarthritis-results of a 1 year longitudinal arthroscopic study in 422 patients. *Osteoarthritis and Cartilage,* 13**,** 361-367.

AZAD, N. S., RASOOL, N., ANNUNZIATA, C. M., MINASIAN, L., WHITELEY, G. & KOHN, E. C. 2006. Proteomics in clinical trials and practice. *Molecular & Cellular Proteomics,* 5**,** 1819-1829.

BACCALA, R., GONZALEZ-QUINTIAL, R., LAWSON, B. R., STERN, M. E., KONO, D. H., BEUTLER, B. & THEOFILOPOULOS, A. N. 2009. Sensors of the innate immune system: their mode of action. *Nature Reviews Rheumatology,* 5**,** 448-456.

BAETEN, D., KRUITHOF, E., DE RYCKE, L., BOOTS, A. M., MIELANTS, H., VEYS, E. M. & DE KEYSER, F. 2005. Infiltration of the synovial membrane with macrophage subsets and polymorphonuclear cells reflects global disease activity in spondyloarthropathy. *Arthritis Res Ther,* 7**,** r359-r369.

BAETEN, D., VAN DEN BOSCH, F., ELEWAUT, D., STUER, A., VEYS, E. & DE KEYSER, F. 1999. Needle arthroscopy of the knee with synovial biopsy sampling: technical experience in 150 patients. *Clinical rheumatology,* 18**,** 434-441.

BANCHEREAU, J. & STEINMAN, R. M. 1998. Dendritic cells and the control of immunity. *Nature,* 392**,** 245-252.

BARNES, B. J., KELLUM, M. J., FIELD, A. E. & PITHA, P. M. 2002. Multiple regulatory domains of IRF-5 control activation, cellular localization, and induction of chemokines that mediate recruitment of T lymphocytes. *Molecular and cellular biology,* 22**,** 5721.

BARTON, G. M. & KAGAN, J. C. 2009. A cell biological view of Toll-like receptor function: regulation through compartmentalization. *Nature Reviews Immunology,* 9**,** 535-542.

BASU, S., BINDER, R. J., SUTO, R., ANDERSON, K. M. & SRIVASTAVA, P. K. 2000. Necrotic but not apoptotic cell death releases heat shock proteins, which deliver a partial maturation signal to dendritic cells and activate the NF-κB pathway. *International*

immunology, 12**,** 1539-1546.

BAUER, S., KIRSCHNING, C. J., HÄCKER, H., REDECKE, V., HAUSMANN, S., AKIRA, S., WAGNER, H. & LIPFORD, G. B. 2001. Human TLR9 confers responsiveness to bacterial DNA via species-specific CpG motif recognition. *Proceedings of the National Academy of Sciences,* 98**,** 9237.

BAUMANN, C. L., ASPALTER, I. M., SHARIF, O., PICHLMAIR, A., BLÜML, S., GREBIEN, F., BRUCKNER, M., PASIERBEK, P., AUMAYR, K. & PLANYAVSKY, M. 2010. CD14 is a coreceptor of Toll-like receptors 7 and 9. *The Journal of experimental medicine,* 207**,** 2689-2701.

BEKEREDJIAN-DING, I. B., WAGNER, M., HORNUNG, V., GIESE, T., SCHNURR, M., ENDRES, S. & HARTMANN, G. 2005. Plasmacytoid dendritic cells control TLR7 sensitivity of naive B cells via type I IFN. *The Journal of immunology,* 174**,** 4043.

BELCHER, C., YAQUB, R., FAWTHROP, F., BAYLISS, M. & DOHERTY, M. 1997. Synovial fluid chondroitin and keratan sulphate epitopes, glycosaminoglycans, and hyaluronan in arthritic and normal knees. *Annals of the rheumatic diseases,* 56**,** 299-307.

BELL, J. K., MULLEN, G. E. D., LEIFER, C. A., MAZZONI, A., DAVIES, D. R. & SEGAL, D. M. 2003. Leucine-rich repeats and pathogen recognition in Toll-like receptors. *Trends in immunology,* 24**,** 528-533.

BELL, M. P., SVINGEN, P. A., RAHMAN, M. K., XIONG, Y. & FAUBION, W. A. 2007. Forkhead Box P3 regulates TLR10 expression in human T regulatory cells. *The Journal of immunology,* 179**,** 1893.

BENITO, M. J., VEALE, D. J., FITZGERALD, O., VAN DEN BERG, W. B. & BRESNIHAN, B. 2005. Synovial tissue inflammation in early and late osteoarthritis. *Annals of the rheumatic diseases,* 64**,** 1263.

BENTLEY, D. R., BALASUBRAMANIAN, S., SWERDLOW, H. P., SMITH, G. P., MILTON, J., BROWN, C. G., HALL, K. P., EVERS, D. J., BARNES, C. L. & BIGNELL, H. R. 2008. Accurate whole human genome sequencing using reversible terminator chemistry. *Nature,* 456**,** 53-59.

BERCKMANS, R. J., NIEUWLAND, R., TAK, P. P., BÖING, A. N., ROMIJN, F. P., KRAAN, M. C., BREEDVELD, F. C., HACK, C. E. & STURK, A. 2002. Cell-derived microparticles in synovial fluid from inflamed arthritic joints support coagulation exclusively via a factor VII–dependent mechanism. *Arthritis & Rheumatism,* 46**,** 2857-2866.

BERENBAUM, F. 2004. Signaling transduction: target in osteoarthritis. *Current opinion in rheumatology,* 16**,** 616.

BERENBAUM, F. 2010. Targeted therapies in osteoarthritis: a systematic review of the trials on www. clinicaltrials. gov. *Best Practice & Research Clinical Rheumatology,* 24**,** 107-119.

BERG, W., HELSEN, M. & LOO, F. 1994. Amelioration of established murine collagen-induced arthritis with anti-IL-1 treatment. *Clinical & Experimental Immunology,*

95**,** 237-243.

BERTHIAUME, M. J., RAYNAULD, J. P., MARTEL-PELLETIER, J., LABONTÉ, F., BEAUDOIN, G., BLOCH, D. A., CHOQUETTE, D., HARAOUI, B., ALTMAN, R. D. & HOCHBERG, M. 2005. Meniscal tear and extrusion are strongly associated with progression of symptomatic knee osteoarthritis as assessed by quantitative magnetic resonance imaging. *Annals of the rheumatic diseases,* 64**,** 556.

BERTOLINI, D. R., NEDWIN, G. E., BRINGMAN, T. S., SMITH, D. D. & MUNDY, G. R. 1986. Stimulation of bone resorption and inhibition of bone formation in vitro by human tumour necrosis factors.

BIN, L. H., XU, L. G. & SHU, H. B. 2003. TIRP, a novel Toll/interleukin-1 receptor (TIR) domain-containing adapter protein involved in TIR signaling. *Journal of Biological Chemistry,* 278**,** 24526-24532.

BINIECKA, M., FOX, E., GAO, W., NG, C. T., VEALE, D. J., FEARON, U. & O'SULLIVAN, J. 2011. Hypoxia induces mitochondrial mutagenesis and dysfunction in inflammatory arthritis. *Arthritis & Rheumatism,* 63**,** 2172-2182.

BLAIN, E. J., GILBERT, S. J., HAYES, A. J. & DUANCE, V. C. 2006. Disassembly of the vimentin cytoskeleton disrupts articular cartilage chondrocyte homeostasis. *Matrix biology,* 25**,** 398-408.

BLANCO, F. J. & RUIZ-ROMERO, C. 2012. Osteoarthritis: Metabolomic characterization of metabolic phenotypes in OA. *Nature Reviews Rheumatology*.

BO, G. P., ZHOU, L. N., HE, W. F., LUO, G. X., JIA, X. F., GAN, C. J., CHEN, G. X., FANG, Y. F., LARSEN, P. M. & WU, J. 2009. Analyses of differential proteome of human synovial fibroblasts obtained from arthritis. *Clinical rheumatology,* 28**,** 191-199.

BOBACZ, K., SUNK, I., HOFSTAETTER, J., AMOYO, L., TOMA, C., AKIRA, S., WEICHHART, T., SAEMANN, M. & SMOLEN, J. 2007. Toll-like receptors and chondrocytes: The lipopolysaccharide-induced decrease in cartilage matrix synthesis is dependent on the presence of toll-like receptor 4 and antagonized by bone morphogenetic protein 7. *Arthritis & Rheumatism,* 56**,** 1880-1893.

BONDESON, J., BLOM, A. B., WAINWRIGHT, S., HUGHES, C., CATERSON, B. & VAN DEN BERG, W. B. 2010. The role of synovial macrophages and macrophage-produced mediators in driving inflammatory and destructive responses in osteoarthritis. *Arthritis & Rheumatism,* 62**,** 647-657.

BONDESON, J., LAUDER, S., WAINWRIGHT, S., AMOS, N., EVANS, A., HUGHES, C., FELDMANN, M. & CATERSON, B. 2007. Adenoviral gene transfer of the endogenous inhibitor IkappaBalpha into human osteoarthritis synovial fibroblasts demonstrates that several matrix metalloproteinases and aggrecanases are nuclear factor-kappaB-dependent. *The Journal of rheumatology,* 34**,** 523-533.

BONNET, C. & WALSH, D. 2005. Osteoarthritis, angiogenesis and inflammation. *Rheumatology,* 44**,** 7-16.

BOO, K. H. & YANG, J. S. 2010. Intrinsic cellular defenses against virus infection by antiviral type I interferon. *Yonsei medical journal,* 51**,** 9.

BORZÌ, R. M., MAZZETTI, I., MARCU, K. B. & FACCHINI, A. 2004. Chemokines in cartilage degradation. *Clinical Orthopaedics and Related Research,* 427**,** S53.

BOWIE, A., KISS-TOTH, E., SYMONS, J. A., SMITH, G. L., DOWER, S. K. & O'NEILL, L. A. J. 2000. A46R and A52R from vaccinia virus are antagonists of host IL-1 and toll-like receptor signaling. *Proceedings of the National Academy of Sciences,* 97**,** 10162.

BRADFORD, M. M. 1976. A rapid and sensitive method for the quantitation of microgram quantities of protein utilizing the principle of protein-dye binding. *Analytical biochemistry,* 72**,** 248-254.

BRANDT, K., DOHERTY, M. & LOHMANDER, L. 1998. Composition and structure of articular cartilage. *Osteoarthritis. New York: Oxford University Press Inc***,** 110-1.

BRANDT, K. D., FIFE, R. S., BRAUNSTEIN, E. M. & KATZ, B. 1991. Radiographic grading of the severity of knee osteoarthritis: relation of the Kellgren and Lawrence grade to a grade based on joint space narrowing, and correlation with arthroscopic evidence of articular cartilage degeneration. *Arthritis & Rheumatism,* 34**,** 1381-1386.

BRENNAN, F. M. & MCINNES, I. B. 2008. Evidence that cytokines play a role in rheumatoid arthritis. *The Journal of clinical investigation,* 118**,** 3537.

BRENTANO, F., SCHORR, O., GAY, R. E., GAY, S. & KYBURZ, D. 2005. RNA released from necrotic synovial fluid cells activates rheumatoid arthritis synovial fibroblasts via toll-like receptor 3. *Arthritis & Rheumatism,* 52**,** 2656-2665.

BRESNIHAN, B., BAETEN, D., FIRESTEIN, G. S., FITZGERALD, O. M., GERLAG, D. M., HARINGMAN, J. J., MCINNES, I. B., REECE, R. J., SMITH, M. D. & ULFGREN, A. K. 2005. Synovial tissue analysis in clinical trials. *The Journal of rheumatology,* 32**,** 2481-2484.

BRIGITTE, M. 2002. CYTOKINE IMBALANCE IN NON-IMMUNOLOGICAL CHRONIC DISEASE. *Cytokine,* 18**,** 334-339.

BRISMAR, B., WREDMARK, T., MOVIN, T., LEANDERSSON, J. & SVENSSON, O. 2002. Observer reliability in the arthroscopic classification of osteoarthritis of the knee. *Journal of Bone and Joint Surgery-British Volume,* 84**,** 42.

BROOKS, P. 2004. Managing osteoarthritis and other chronic diseases. *The Lancet,* 363**,** 498.

BUCKLEY, C. D., PILLING, D., LORD, J. M., AKBAR, A. N., SCHEEL-TOELLNER, D. & SALMON, M. 2001. Fibroblasts regulate the switch from acute resolving to chronic persistent inflammation. *Trends in immunology,* 22**,** 199-204.

BURGIO, G., UGAZIO, A., NESPOLI, L., MARCIONI, A., BOTTELLI, A. & PASQUALI, F. 1975. Derangements of immunoglobulin levels, phytohemagglutinin responsiveness and T and B cell markers in Down's syndrome at different ages. *European Journal of Immunology,* 5**,** 600-603.

BURNS, K., JANSSENS, S., BRISSONI, B., OLIVOS, N., BEYAERT, R. & TSCHOPP, J. 2003. Inhibition of interleukin 1 receptor/Toll-like receptor signaling through the alternatively spliced, short form of MyD88 is due to its failure to recruit IRAK-4. *The Journal of experimental medicine,* 197**,** 263.

BURNS, K., MARTINON, F., ESSLINGER, C., PAHL, H., SCHNEIDER, P., BODMER, J. L., DI MARCO, F., FRENCH, L. & TSCHOPP, J. 1998. MyD88, an adapter protein involved in interleukin-1 signaling. *Journal of Biological Chemistry,* 273**,** 12203.

CALDWELL, R. L., OPALENIK, S. R., DAVIDSON, J. M., CAPRIOLI, R. M. & NANNEY, L. B. 2008. Tissue profiling MALDI mass spectrometry reveals prominent calcium-binding proteins in the proteome of regenerative MRL mouse wounds. *Wound Repair and Regeneration,* 16**,** 442-449.

CAO, Y. 2010. Adipose tissue angiogenesis as a therapeutic target for obesity and metabolic diseases. *Nature Reviews Drug Discovery,* 9**,** 107-115.

CARIO, E., GERKEN, G. & PODOLSKY, D. 2002. "For Whom the Bell Tolls!"-Innate Defense Mechanisms and Survival Strategies of the Intestinal Epithelium Against Lumenal Pathogens „Wem die Stunde schlägt!"-Angeborene Verteidigungs-und Überlebensstrategien des intestinalen Epithels gegen pathogene Mikroben des Lumens. *Z Gastroenterol,* 40**,** 983-990.

CARRIÓN, M., JUARRANZ, Y., PÉREZ-GARCÍA, S., JIMENO, R., PABLOS, J. L., GOMARIZ, R. P. & GUTIÉRREZ-CAÑAS, I. 2011. RNA sensors in human osteoarthritis and rheumatoid arthritis synovial fibroblasts: Immune regulation by vasoactive intestinal peptide. *Arthritis & Rheumatism,* 63**,** 1626-1636.

CARSON-DEWITT, R. Risk Factors for Osteoarthritis.

CARSWELL, E., OLD, L. J., KASSEL, R., GREEN, S., FIORE, N. & WILLIAMSON, B. 1975. An endotoxin-induced serum factor that causes necrosis of tumors. *Proceedings of the National Academy of Sciences,* 72**,** 3666.

CARTY, M., GOODBODY, R., SCHRÖDER, M., STACK, J., MOYNAGH, P. N. & BOWIE, A. G. 2006. The human adaptor SARM negatively regulates adaptor protein TRIF–dependent Toll-like receptor signaling. *nature immunology,* 7**,** 1074-1081.

CASSATELLA, M. A. 1995. The production of cytokines by polymorphonuclear neutrophils. *Immunology today,* 16**,** 21-26.

CATTERALL, J., ROWAN, A., SARSFIELD, S., SAKLATVALA, J., WAIT, R. & CAWSTON, T. 2006. Development of a novel 2D proteomics approach for the identification of proteins secreted by primary chondrocytes after stimulation by IL-1 and oncostatin M. *Rheumatology,* 45**,** 1101.

CAVASSANI, K. A., ISHII, M., WEN, H., SCHALLER, M. A., LINCOLN, P. M., LUKACS, N. W., HOGABOAM, C. M. & KUNKEL, S. L. 2008. TLR3 is an endogenous sensor of tissue necrosis during acute inflammatory events. *The Journal of experimental medicine,* 205**,** 2609-2621.

CECIL, D. L. 2008. *The receptor for advanced glycation endproducts and S100A11*

modulate pathologic chondrocyte differentiation and dysregulated cartilage matrix catabolism in osteoarthritis, ProQuest.

CHANDER, H., HALPERN, M., RESNICK-SILVERMAN, L., MANFREDI, J. J. & GERMAIN, D. 2010. Skp2B attenuates p53 function by inhibiting prohibitin. *EMBO reports,* 11**,** 220-225.

CHATURVEDI, A. & PIERCE, S. K. 2009. How Location Governs Toll-Like Receptor Signaling. *Traffic,* 10**,** 621-628.

CHEN, C. P. C., HSU, C. C., YEH, W. L., LIN, H. C., HSIEH, S. Y., LIN, S. C., CHEN, T. T., CHEN, M. J. L. & TANG, S. F. T. 2011. Optimizing Human Synovial Fluid Preparation for Two-Dimensional Gel Electrophoresis. *Proteome Science,* 9**,** 65.

CHEN, F. H., HERNDON, M. E., PATEL, N., HECHT, J. T., TUAN, R. S. & LAWLER, J. 2007. Interaction of cartilage oligomeric matrix protein/thrombospondin 5 with aggrecan. *Journal of Biological Chemistry,* 282**,** 24591-24598.

CHEN, L., LIN, L., WANG, H., WEI, X., FU, X., ZHANG, J. & YU, C. 2008. Suppression of early experimental osteoarthritis by< i> in vivo</i> delivery of the adenoviral vector-mediated NF-κBp65-specific siRNA. *Osteoarthritis and Cartilage,* 16**,** 174-184.

CHEN, W. & ROYER JR, W. E. 2010. Structural insights into interferon regulatory factor activation. *Cellular signalling,* 22**,** 883-887.

CHEN, Z. J. 2005. Ubiquitin signalling in the NF-κB pathway. *Nature cell biology,* 7**,** 758-765.

CHEVALIER, X., GIRAUDEAU, B., CONROZIER, T., MARLIERE, J., KIEFER, P. & GOUPILLE, P. 2005. Safety study of intraarticular injection of interleukin 1 receptor antagonist in patients with painful knee osteoarthritis: a multicenter study. *The Journal of rheumatology,* 32**,** 1317-1323.

CHEVALIER, X., GROULT, N. & HORNEBECK, W. 1996. Increased expression of the Ed-B-containing fibronectin (an embryonic isoform of fibronectin) in human osteoarthritic cartilage. *Rheumatology,* 35**,** 407.

CHOE, J., KELKER, M. S. & WILSON, I. A. 2005. Crystal structure of human toll-like receptor 3 (TLR3) ectodomain. *Science,* 309**,** 581.

CHOMARAT, P., RISSOAN, M., PIN, J., BANCHEREAU, J. & MIOSSEC, P. 1995. Contribution of IL-1, CD14, and CD13 in the increased IL-6 production induced by in vitro monocyte-synoviocyte interactions. *The Journal of immunology,* 155**,** 3645.

CHOY, E., ISENBERG, D., GARROOD, T., FARROW, S., IOANNOU, Y., BIRD, H., CHEUNG, N., WILLIAMS, B., HAZLEMAN, B. & PRICE, R. 2002. Therapeutic benefit of blocking interleukin-6 activity with an anti–interleukin-6 receptor monoclonal antibody in rheumatoid arthritis: A randomized, double-blind, placebo-controlled, dose-escalation trial. *Arthritis & Rheumatism,* 46**,** 3143-3150.

CHOY, E. H. S. & PANAYI, G. S. 2001. Cytokine Pathways and Joint Inflammation in Rheumatoid Arthritis. *New England Journal of Medicine,* 344**,** 907-916.

CHUANG, T. H. & ULEVITCH, R. J. 2001. Identification of hTLR10: a novel human Toll-like receptor preferentially expressed in immune cells. *Biochimica et Biophysica Acta (BBA)-Gene Structure and Expression,* 1518**,** 157-161.
CLEGG, P., BURKE, R., COUGHLAN, A., RIGGS, C. & CARTER, S. 1997. Characterisation of equine matrix metalloproteinase 2 and 9; and identification of the cellular sources of these enzymes in joints. *Equine veterinary journal,* 29**,** 335-342.

CLEGG, P. & CARTER, S. 1999. Matrix metalloproteinase-2 and− 9 are activated in joint diseases. *Equine veterinary journal,* 31**,** 324-330.

CLOOS, P. A. C. & CHRISTGAU, S. 2002. Non-enzymatic covalent modifications of proteins: mechanisms, physiological consequences and clinical applications. *Matrix biology,* 21**,** 39-52.

COATES, P. J., NENUTIL, R., MCGREGOR, A., PICKSLEY, S. M., CROUCH, D. H., HALL, P. A. & WRIGHT, E. G. 2001. Mammalian Prohibitin Proteins Respond to Mitochondrial Stress and Decrease during Cellular Senescence. *Experimental Cell Research,* 265**,** 262-273.

CONNOLLY, M., MEDICINE, U. C. D. S. O. & SCIENCE, M. 2009. *Acute serum amyloid a regulates angiogenesis, inflammation and cytoskeletal rearrangement in rheumatoid arthritis,* University College Dublin.

CONROZIER, T., CARLIER, M., MATHIEU, P., COLSON, F., DEBARD, A., RICHARD, S., FAVRET, H., BIENVENU, J. & VIGNON, E. 2000. Serum levels of YKL-40 and C reactive protein in patients with hip osteoarthritis and healthy subjects: a cross sectional study. *Annals of the rheumatic diseases,* 59**,** 828.

COOK, J., KUROKI, K., VISCO, D., PELLETIER, J. P., SCHULZ, L. & LAFEBER, F. 2010. The OARSI histopathology initiative–recommendations for histological assessments of osteoarthritis in the dog. *Osteoarthritis and Cartilage,* 18**,** S66-S79.

COOPER, M. A., FEHNIGER, T. A., FUCHS, A., COLONNA, M. & CALIGIURI, M. A. 2004. NK cell and DC interactions. *Trends in immunology,* 25**,** 47-52.

CORNETT, D. S., REYZER, M. L., CHAURAND, P. & CAPRIOLI, R. M. 2007. MALDI imaging mass spectrometry: Molecular snapshots of biochemical systems. *Nature methods,* 4**,** 828-833.

COSTA, C., INCIO, J. & SOARES, R. 2007. Angiogenesis and chronic inflammation: cause or consequence? *Angiogenesis,* 10**,** 149-166.

CRAVEN, R. A. & BANKS, R. E. 2001. Laser capture microdissection and proteomics: possibilities and limitation. *Proteomics,* 1**,** 1200-1204.

CSOKA, A. B., FROST, G. I. & STERN, R. 2001. The six hyaluronidase-like genes in the human and mouse genomes. *Matrix biology,* 20**,** 499-508.

DART, D. A., SPENCER-DENE, B., GAMBLE, S. C., WAXMAN, J. & BEVAN, C. L. 2009. Manipulating prohibitin levels provides evidence for an in vivo role in androgen

regulation of prostate tumours. *Endocrine-related cancer,* 16**,** 1157-1169.

DASURI, K., ANTONOVICI, M., CHEN, K., WONG, K., STANDING, K., ENS, W., EL-GABALAWY, H. & WILKINS, J. A. 2004. The synovial proteome: analysis of fibroblast-like synoviocytes. *Arthritis Res Ther,* 6**,** R161.

DAVID J, H. 2011. Osteoarthritis. *Best Practice & Research Clinical Rheumatology,* 25**,** 801-814.

DAVIS, L. S. 2003. A question of transformation: the synovial fibroblast in rheumatoid arthritis. *The American journal of pathology,* 162**,** 1399.

DAYER, J., BEUTLER, B. & CERAMI, A. 1985. Cachectin/tumor necrosis factor stimulates collagenase and prostaglandin E2 production by human synovial cells and dermal fibroblasts. *The Journal of experimental medicine,* 162**,** 2163.

DAYER, J. M. 2003. The pivotal role of interleukin-1 in the clinical manifestations of rheumatoid arthritis. *Rheumatology,* 42**,** ii3.

DE CEUNINCK, F. & BERENBAUM, F. 2009. Proteomics: addressing the challenges of osteoarthritis. *Drug discovery today,* 14**,** 661-667.

DE CLERCK, L., DE GENDT, C., BRIDTS, C., VAN OSSELAER, N. & STEVENS, W. 1995. Expression of neutrophil activation markers and neutrophil adhesion to chondrocytes in rheumatoid arthritis patients: relationship with disease activity. *Research in immunology,* 146**,** 81-87.

DE NANTEUIL, G., PORTEVIN, B. & BENOIST, A. 2001. Disease-modifying anti-osteoarthritic drugs: current therapies and new prospects around protease inhibition. *Il Farmaco,* 56**,** 107-112.

DEMARIA, O., PAGNI, P. P., TRAUB, S., DE GASSART, A., BRANZK, N., MURPHY, A. J., VALENZUELA, D. M., YANCOPOULOS, G. D., FLAVELL, R. A. & ALEXOPOULOU, L. 2010. TLR8 deficiency leads to autoimmunity in mice. *The Journal of clinical investigation,* 120**,** 3651.

DENG, G. M., NILSSON, M., VERDRENGH, M., COLLINS, L. V. & TARKOWSKI, A. 1999. Intra-articularly localized bacterial DNA containing CpG motifs induces arthritis. *Nature medicine,* 5**,** 702-705.

DIEBOLD, S. S., MASSACRIER, C., AKIRA, S., PATUREL, C., MOREL, Y. & REIS E SOUSA, C. 2006. Nucleic acid agonists for Toll-like receptor 7 are defined by the presence of uridine ribonucleotides. *European Journal of Immunology,* 36**,** 3256-3267.

DIEPPE, P. 2005. Disease modification in osteoarthritis: Are drugs the answer? *Arthritis & Rheumatism,* 52**,** 1956-1959.

DINARELLO, C. 2002. The IL-1 family and inflammatory diseases. *Clinical and experimental rheumatology,* 20**,** 1-13.

DINARELLO, C. A. 1998. Interleukin-1β, Interleukin-18, and the Interleukin-1β Converting Enzymea. *Annals of the New York Academy of Sciences,* 856**,** 1-11.

DINARELLO, C. A. 2000. Proinflammatory Cytokines*. *Chest,* 118**,** 503-508.

DISTLER, J. H. W., JÜNGEL, A., HUBER, L. C., SEEMAYER, C. A., REICH, C. F., GAY, R. E., MICHEL, B. A., FONTANA, A., GAY, S. & PISETSKY, D. S. 2005. The induction of matrix metalloproteinase and cytokine expression in synovial fibroblasts stimulated with immune cell microparticles. *Proceedings of the National Academy of Sciences of the United States of America,* 102**,** 2892.

DISTLER, J. H. W., PISETSKY, D. S., HUBER, L. C., KALDEN, J. R., GAY, S. & DISTLER, O. 2005. Microparticles as regulators of inflammation: novel players of cellular crosstalk in the rheumatic diseases. *Arthritis & Rheumatism,* 52**,** 3337-3348.

DOMON, B. & AEBERSOLD, R. 2006. Mass spectrometry and protein analysis. *science,* 312**,** 212.

DONOGHUE, P., DORAN, P., DOWLING, P. & OHLENDIECK, K. 2005. Differential expression of the fast skeletal muscle proteome following chronic low-frequency stimulation. *Biochimica et Biophysica Acta (BBA)-Proteins & Proteomics,* 1752**,** 166-176.

DORAN, P., MARTIN, G., DOWLING, P., JOCKUSCH, H. & OHLENDIECK, K. 2006. Proteome analysis of the dystrophin-deficient MDX diaphragm reveals a drastic increase in the heat shock protein cvHSP. *Proteomics,* 6**,** 4610-4621.

DOUGADOS, M. 1996. Synovial fluid cell analysis. *Baillière's clinical rheumatology,* 10**,** 519-534.

DREXLER, S. K. & FOXWELL, B. M. 2010. The role of Toll-like receptors in chronic inflammation. *The International Journal of Biochemistry & Cell Biology,* 42**,** 506-518.

DREXLER, S. K., SACRE, S. M. & FOXWELL, B. M. 2006. Toll-like receptors: a new target in rheumatoid arthritis? *Expert review of clinical immunology,* 2**,** 585-599.

DRIBAN, J. B., SITLER, M. R., BARBE, M. F. & BALASUBRAMANIAN, E. 2010. Is osteoarthritis a heterogeneous disease that can be stratified into subsets? *Clinical rheumatology,* 29**,** 123-131.

DRYNDA, S., RINGEL, B., KEKOW, M., KÜHNE, C., DRYNDA, A., GLOCKER, M. O., THIESEN, H. J. & KEKOW, J. J. 2004. Proteome analysis reveals disease-associated marker proteins to differentiate RA patients from other inflammatory joint diseases with the potential to monitor anti-TNF [alpha] therapy. *Pathology-Research and Practice,* 200**,** 165-171.

DUDHIA, J. 2005. Aggrecan, aging and assembly in articular cartilage. *Cellular and molecular life sciences,* 62**,** 2241-2256.

EDINGER, A. L. & THOMPSON, C. B. 2004. Death by design: apoptosis, necrosis and autophagy. *Current opinion in cell biology,* 16**,** 663-669.

EDWARDS, J. C. W. 2000. Fibroblast biology: development and differentiation of synovial fibroblasts in arthritis. *Arthritis Research & Therapy,* 2**,** 344.

ENGSTRÖM, G., GERHARDSSON DE VERDIER, M., ROLLOF, J., NILSSON, P. & LOHMANDER, L. 2009. C-reactive protein, metabolic syndrome and incidence of severe hip and knee osteoarthritis. A population-based cohort study. *Osteoarthritis and Cartilage,* 17**,** 168-173.

EVANS, C., GOUZE, J., GOUZE, E., ROBBINS, P. & GHIVIZZANI, S. 2004. Osteoarthritis gene therapy. *Gene therapy,* 11**,** 379-389.

FARAHAT, M. N., YANNI, G., POSTON, R. & PANAYI, G. S. 1993. Cytokine expression in synovial membranes of patients with rheumatoid arthritis and osteoarthritis. *Annals of the rheumatic diseases,* 52**,** 870-875.

FASSBENDER, H. & SIMMLING-ANNEFELD, M. 1983. The potential aggressiveness of synovial tissue in rheumatoid arthritis. *The Journal of pathology,* 139**,** 399-406.

FELDMANN, M. 2002. Development of anti-TNF therapy for rheumatoid arthritis. *Nature Reviews Immunology,* 2**,** 364-371.

FELDMANN, M. & MAINI, R. 1999. The role of cytokines in the pathogenesis of rheumatoid arthritis. *Rheumatology (Oxford, England),* 38**,** 3.

FELL, H. B. & JUBB, R. 1977. The effect of synovial tissue on the breakdown of articular cartilage in organ culture. *Arthritis & Rheumatism,* 20**,** 1359-1371.

FELSON, D. T. 2004. An update on the pathogenesis and epidemiology of osteoarthritis. *Radiologic Clinics of North America,* 42**,** 1.

FELSON, D. T., LAWRENCE, R. C., DIEPPE, P. A., HIRSCH, R., HELMICK, C. G., JORDAN, J. M., KINGTON, R. S., LANE, N. E., NEVITT, M. C. & ZHANG, Y. 2000. Osteoarthritis: new insights. Part 1: the disease and its risk factors. *Annals of Internal Medicine,* 133**,** 635-646.

FERNANDES, J. C., MARTEL-PELLETIER, J. & PELLETIER, J. P. 2002. The role of cytokines in osteoarthritis pathophysiology. *Biorheology,* 39**,** 237-246.

FERNANDEZ-MADRID, F., KARVONEN, R. L., TEITGE, R. A., MILLER, P. R., AN, T. & NEGENDANK, W. G. 1995. Synovial thickening detected by MR imaging in osteoarthritis of the knee confirmed by biopsy as synovitis. *Magnetic resonance imaging,* 13**,** 177-183.

FIFE, R. S., BRANDT, K. D., BRAUNSTEIN, E. M., KATZ, B. P., SHELBOURNE, K. D., KALASINSKI, L. A. & RYAN, S. 1991. Relationship between arthroscopic evidence of cartilage damage and radiographic evidence of joint space narrowing in early osteoarthritis of the knee. *Arthritis & Rheumatism,* 34**,** 377-382.

FIORITO, S., MAGRINI, L., ADREY, J., MAILHE, D. & BROUTY-BOYE, D. 2005. Inflammatory status and cartilage regenerative potential of synovial fibroblasts from patients with osteoarthritis and chondropathy. *Rheumatology,* 44**,** 164-171.

FIRESTEIN, G., BERGER, A., TRACEY, D., CHOSAY, J., CHAPMAN, D., PAINE, M., YU, C. & ZVAIFLER, N. 1992. IL-1 receptor antagonist protein production and gene

expression in rheumatoid arthritis and osteoarthritis synovium. *The Journal of Immunology,* 149**,** 1054.

FIRESTEIN, G. S. 1996. Invasive fibroblast-like synoviocytes in rheumatoid arthritis. Passive responders or transformed aggressors? *Arthritis & Rheumatism,* 39**,** 1781-1790.

FIRESTEIN, G. S., BOYLE, D. L., YU, C., PAINE, M. M., WHISENAND, T. D., ZVAIFLER, N. J. & AREND, W. P. 1994. Synovial interleukin-1 receptor antagonist and interleukin-1 balance in rheumatoid arthritis. *Arthritis & Rheumatism,* 37**,** 644-652.

FITZGERALD, K. A., PALSSON-MCDERMOTT, E. M., BOWIE, A. G., JEFFERIES, C. A., MANSELL, A. S., BRADY, G., BRINT, E., DUNNE, A., GRAY, P. & HARTE, M. T. 2001. Mal (MyD88-adapter-like) is required for Toll-like receptor-4 signal transduction. *Nature,* 413**,** 78-83.

FITZGERALD, K. A., ROWE, D. C., BARNES, B. J., CAFFREY, D. R., VISINTIN, A., LATZ, E., MONKS, B., PITHA, P. M. & GOLENBOCK, D. T. 2003. LPS-TLR4 signaling to IRF-3/7 and NF-κB involves the Toll adapters TRAM and TRIF. *The Journal of experimental medicine,* 198**,** 1043-1055.

FITZGERALD, K. A., ROWE, D. C. & GOLENBOCK, D. T. 2004. Endotoxin recognition and signal transduction by the TLR4/MD2-complex. *Microbes and infection,* 6**,** 1361-1367.

FLOWER, R. J. 2003. The development of COX2 inhibitors. *Nature Reviews Drug Discovery,* 2**,** 179-191.

FRÀTER-SCHRÖDER, M., RISAU, W., HALLMANN, R., GAUTSCHI, P. & BÖHLEN, P. 1987. Tumor necrosis factor type alpha, a potent inhibitor of endothelial cell growth in vitro, is angiogenic in vivo. *Proceedings of the National Academy of Sciences,* 84**,** 5277.

FUJITA, T., ENDO, Y. & NONAKA, M. 2004. Primitive complement system--recognition and activation. *Molecular immunology,* 41**,** 103-111.

FURST, D., BREEDVELD, F., KALDEN, J., SMOLEN, J., BURMESTER, G., BIJLSMA, J., DOUGADOS, M., EMERY, P., KEYSTONE, E. & KLARESKOG, L. 2005. Updated consensus statement on biological agents, specifically tumour necrosis factor α (TNFα) blocking agents and interleukin-1 receptor antagonist (IL-1ra), for the treatment of rheumatic diseases, 2005. *Annals of the rheumatic diseases,* 64**,** iv2-iv14.

FURUZAWA-CARBALLEDA, J., MACIP-RODRIGUEZ, P. & CABRAL, A. 2008. Osteoarthritis and rheumatoid arthritis pannus have similar qualitative metabolic characteristics and pro-inflammatory cytokine response. *Clin Exp Rheumatol,* 26**,** 554-560.

FUSARO, G., DASGUPTA, P., RASTOGI, S., JOSHI, B. & CHELLAPPAN, S. 2003. Prohibitin induces the transcriptional activity of p53 and is exported from the nucleus upon apoptotic signaling. *Journal of Biological Chemistry,* 278**,** 47853.

GALLUCCI, S. & MATZINGER, P. 2001. Danger signals: SOS to the immune system. *Current opinion in immunology,* 13**,** 114-119.

GARCIA, B. A., PLATT, M. D., BORN, T. L., SHABANOWITZ, J., MARCUS, N. A. & HUNT, D. F. 2006. Protein profile of osteoarthritic human articular cartilage using tandem mass spectrometry. *Rapid communications in mass spectrometry,* 20**,** 2999-3006.

GARCÍA-SASTRE, A. 2011. Induction and evasion of type I interferon responses by influenza viruses. *Virus Research*.

GARCÍA-VICUÑA, R., GÓMEZ-GAVIRO, M. V., DOMÍNGUEZ-LUIS, M. J., PEC, M. K., GONZÁLEZ-ALVARO, I., ALVARO-GRACIA, J. M. & DÍAZ-GONZÁLEZ, F. 2004. CC and CXC chemokine receptors mediate migration, proliferation, and matrix metalloproteinase production by fibroblast-like synoviocytes from rheumatoid arthritis patients. *Arthritis & Rheumatism,* 50**,** 3866-3877.

GAUTIER, G., HUMBERT, M., DEAUVIEAU, F., SCUILLER, M., HISCOTT, J., BATES, E. E. M., TRINCHIERI, G., CAUX, C. & GARRONE, P. 2005. A type I interferon autocrine–paracrine loop is involved in Toll-like receptor-induced interleukin-12p70 secretion by dendritic cells. *The Journal of experimental medicine,* 201**,** 1435-1446.

GAY, S., GAY, R. E. & KOOPMAN, W. J. 1993. Molecular and cellular mechanisms of joint destruction in rheumatoid arthritis: two cellular mechanisms explain joint destruction? *Annals of the rheumatic diseases,* 52**,** S39.

GHOSH, P. & CHERAS, P. A. 2001. Vascular mechanisms in osteoarthritis. *Best Practice & Research Clinical Rheumatology,* 15**,** 693-709.

GHOSH, S., MAY, M. J. & KOPP, E. B. 1998. NF-κB AND REL PROTEINS: Evolutionarily Conserved Mediators of Immune Responses. *Annual review of immunology,* 16**,** 225-260.

GIBSON, D. S., BLELOCK, S., CURRY, J., FINNEGAN, S., HEALY, A., SCAIFE, C., MCALLISTER, C., PENNINGTON, S., DUNN, M. & ROONEY, M. 2009. Comparative analysis of synovial fluid and plasma proteomes in juvenile arthritis-Proteomic patterns of joint inflammation in early stage disease. *Journal of proteomics,* 72**,** 656-676.

GIBSON, D. S. & ROONEY, M. E. 2007. The human synovial fluid proteome: A key factor in the pathology of joint disease. *PROTEOMICS–Clinical Applications,* 1**,** 889-899.

GOBEZIE, R., KHO, A., KRASTINS, B., SARRACINO, D. A., THORNHILL, T. S., CHASE, M., MILLETT, P. J. & LEE, D. M. 2007. High abundance synovial fluid proteome: distinct profiles in health and osteoarthritis. *Arthritis Research and Therapy,* 9**,** 36.

GOLDRING, M. B. 2001. Anticytokine therapy for osteoarthritis. *Expert Opinion on Biological Therapy,* 1**,** 817-829.

GOLDRING, M. B. 2012. Do mouse models reflect the diversity of osteoarthritis in humans? *Arthritis & Rheumatism***,** n/a-n/a.

GOLDRING, S. R. & GOLDRING, M. B. 2004. The role of cytokines in cartilage matrix degeneration in osteoarthritis. *Clinical Orthopaedics and Related Research,* 427**,** S27.

GORDON, S. 2002. Pattern Recognition Receptors:: Doubling Up for the Innate Immune Response. *Cell,* 111**,** 927-930.

GOUWY, M., STRUYF, S., PROOST, P. & VAN DAMME, J. 2005. Synergy in cytokine

and chemokine networks amplifies the inflammatory response. *Cytokine & growth factor reviews,* 16**,** 561-580.

GOVINDARAJ, R. G., MANAVALAN, B., LEE, G. & CHOI, S. 2010. Molecular modeling-based evaluation of hTLR10 and identification of potential ligands in Toll-like receptor signaling. *PloS one,* 5**,** e12713.

GUERNE, P. A., ZURAW, B. L., VAUGHAN, J. H., CARSON, D. A. & LOTZ, M. 1989. Synovium as a source of interleukin 6 in vitro. Contribution to local and systemic manifestations of arthritis. *Journal of Clinical Investigation,* 83**,** 585.

GUO, W., XU, H., CHEN, J., YANG, Y., JIN, J. W., FU, R., LIU, H. M., ZHA, X. L., ZHANG, Z. G. & HUANG, W. Y. 2007. Prohibitin suppresses renal interstitial fibroblasts proliferation and phenotypic change induced by transforming growth factor-beta 1. *Molecular and Cellular Biochemistry,* 295**,** 167-177.

HACKER, H. & KARIN, M. 2006. Regulation and function of IKK and IKK-related kinases. *Sci Stke,* 357**,** 13.

HÄCKER, H., MISCHAK, H., MIETHKE, T., LIPTAY, S., SCHMID, R., SPARWASSER, T., HEEG, K., LIPFORD, G. B. & WAGNER, H. 1998. CpG-DNA-specific activation of antigen-presenting cells requires stress kinase activity and is preceded by non-specific endocytosis and endosomal maturation. *The EMBO journal,* 17**,** 6230-6240.

HAGLUND, L., BERNIER, S. M., ÖNNERFJORD, P. & RECKLIES, A. D. 2008. Proteomic analysis of the LPS-induced stress response in rat chondrocytes reveals induction of innate immune response components in articular cartilage. *Matrix biology,* 27**,** 107-118.

HALL, J. C. & ROSEN, A. 2010. Type I interferons: crucial participants in disease amplification in autoimmunity. *Nature Reviews Rheumatology,* 6**,** 40-49.

HANAOKA, R., KASAMA, T., MURAMATSU, M., YAJIMA, N., SHIOZAWA, F., MIWA, Y., NEGISHI, M., IDE, H., MIYAOKA, H. & UCHIDA, H. 2003. A novel mechanism for the regulation of IFN-gamma inducible protein-10 expression in rheumatoid arthritis. *Arthritis Res Ther,* 5**,** R74-R81.

HANNAN, M. T., FELSON, D. T. & PINCUS, T. 2000. Analysis of the discordance between radiographic changes and knee pain in osteoarthritis of the knee. *The Journal of rheumatology,* 27**,** 1513.

HARDY, M. P., OWCZAREK, C. M., JERMIIN, L. S., EJDEBACK, M. & HERTZOG, P. J. 2004. Characterization of the type I interferon locus and identification of novel genes. *Genomics,* 84**,** 331-345.

HARINGMAN, J. J., LUDIKHUIZE, J. & TAK, P. P. 2004. Chemokines in joint disease: the key to inflammation? *Annals of the rheumatic diseases,* 63**,** 1186-1194.

HARRIS JR, E. D. 2001. The bone and joint decade: a catalyst for progress. *Arthritis & Rheumatism,* 44**,** 1969-1970.

HASAN, U., CHAFFOIS, C., GAILLARD, C., SAULNIER, V., MERCK, E., TANCREDI,

S., GUIET, C., BRIÈRE, F., VLACH, J. & LEBECQUE, S. 2005. Human TLR10 is a functional receptor, expressed by B cells and plasmacytoid dendritic cells, which activates gene transcription through MyD88. *The Journal of immunology,* 174**,** 2942.

HAUDENSCHILD, D. R., CHEN, J., PANG, N., STEKLOV, N., GROGAN, S. P., LOTZ, M. K. & D'LIMA, D. D. 2011. Vimentin contributes to changes in chondrocyte stiffness in osteoarthritis. *Journal of Orthopaedic Research*.

HAYWOOD, L., MCWILLIAMS, D., PEARSON, C., GILL, S., GANESAN, A., WILSON, D. & WALSH, D. 2003. Inflammation and angiogenesis in osteoarthritis. *Arthritis & Rheumatism,* 48**,** 2173-2177.

HE, J. & BAUM, L. G. 2004. Presentation of galectin-1 by extracellular matrix triggers T cell death. *Journal of Biological Chemistry,* 279**,** 4705-4712.

HEIL, F., HEMMI, H., HOCHREIN, H., AMPENBERGER, F., KIRSCHNING, C., AKIRA, S., LIPFORD, G., WAGNER, H. & BAUER, S. 2004. Species-specific recognition of single-stranded RNA via toll-like receptor 7 and 8. *Science,* 303**,** 1526.

HEINZ, S., HAEHNEL, V., KARAGHIOSOFF, M., SCHWARZFISCHER, L., MÜLLER, M., KRAUSE, S. W. & REHLI, M. 2003. Species-specific regulation of Toll-like receptor 3 genes in men and mice. *Journal of Biological Chemistry,* 278**,** 21502-21509.

HENROTIN, Y., GHARBI, M., DEBERG, M. & DE PAUW, E. 2009. Biomarker for osteoarthritis and/or other ageing-related diseases, and use thereof. Google Patents.

HENROTIN, Y., GHARBI, M., MAZZUCCHELLI, G., DUBUC, J.-E., DE PAUW, E. & DEBERG, M. 2012. Fibulin-3 peptides (Fib3-1 and Fib3-2) are potential biomarkers of osteoarthritis. *Arthritis & Rheumatism***,** n/a-n/a.

HERMANSSON, M., SAWAJI, Y., BOLTON, M., ALEXANDER, S., WALLACE, A., BEGUM, S., WAIT, R. & SAKLATVALA, J. 2004. Proteomic analysis of articular cartilage shows increased type II collagen synthesis in osteoarthritis and expression of inhibin βA (activin A), a regulatory molecule for chondrocytes. *Journal of Biological Chemistry,* 279**,** 43514.

HERTZOG, P. J., O'NEILL, L. A. & HAMILTON, J. A. 2003. The interferon in TLR signaling: more than just antiviral. *Trends in immunology,* 24**,** 534-539.

HEUM PARK, J., CHO HAN, D., KIM, J., HYUNG HONG, S., LEE, S. K., SEOG YOON, K., MIN KIM, J., SON, K. H., MIYAZAWA, K. & KWON, B. M. 2006. Differential regulation of anti-inflammatory proteins in human rheumatoid synoviocyte MH7A cell by celecoxib and ibuprofen. *Life sciences,* 78**,** 2204-2212.

HOFFMAN, R. W., GAZITT, T., FOECKING, M. F., ORTMANN, R. A., MISFELDT, M., JORGENSON, R., YOUNG, S. L. & GREIDINGER, E. L. 2004. U1 RNA induces innate immunity signaling. *Arthritis & Rheumatism,* 50**,** 2891-2896.

HOFFMANN, A. & BALTIMORE, D. 2006. Circuitry of nuclear factor κB signaling. *Immunological reviews,* 210**,** 171-186.

HONDA, K., TAKAOKA, A. & TANIGUCHI, T. 2006. Type I Inteferon Gene Induction

by the Interferon Regulatory Factor Family of Transcription Factors. *Immunity,* 25**,** 349-360.

HONDA, K., YANAI, H., MIZUTANI, T., NEGISHI, H., SHIMADA, N., SUZUKI, N., OHBA, Y., TAKAOKA, A., YEH, W. C. & TANIGUCHI, T. 2004. Role of a transductional-transcriptional processor complex involving MyD88 and IRF-7 in Toll-like receptor signaling. *Proceedings of the National Academy of Sciences of the United States of America,* 101**,** 15416.

HONDA, K., YANAI, H., NEGISHI, H., ASAGIRI, M., SATO, M., MIZUTANI, T., SHIMADA, N., OHBA, Y., TAKAOKA, A. & YOSHIDA, N. 2005. IRF-7 is the master regulator of type-I interferon-dependent immune responses. *Nature,* 434**,** 772-777.

HORNEF, M. W., WICK, M. J., RHEN, M. & NORMARK, S. 2002. Bacterial strategies for overcoming host innate and adaptive immune responses. *nature immunology,* 3**,** 1033-1040.

HORNG, T., BARTON, G. M., FLAVELL, R. A. & MEDZHITOV, R. 2002. The adaptor molecule TIRAP provides signalling specificity for Toll-like receptors. *Nature,* 420**,** 329-333.

HORNG, T., BARTON, G. M. & MEDZHITOV, R. 2001. TIRAP: an adapter molecule in the Toll signaling pathway. *nature immunology,* 2**,** 835-841.

HORNUNG, V., ELLEGAST, J., KIM, S., BRZÓZKA, K., JUNG, A., KATO, H., POECK, H., AKIRA, S., CONZELMANN, K. K. & SCHLEE, M. 2006. 5'-Triphosphate RNA is the ligand for RIG-I. *Science,* 314**,** 994.

HORNUNG, V., ROTHENFUSSER, S., BRITSCH, S., KRUG, A., JAHRSDÖRFER, B., GIESE, T., ENDRES, S. & HARTMANN, G. 2002. Quantitative expression of toll-like receptor 1–10 mRNA in cellular subsets of human peripheral blood mononuclear cells and sensitivity to CpG oligodeoxynucleotides. *The Journal of immunology,* 168**,** 4531.

HOUSSIAU, F. A., DEVOGELAER, J. P., DAMME, J. V., DEUXCHAISNES, C. N. D. & SNICK, J. V. 1988. Interleukin-6 in synovial fluid and serum of patients with rheumatoid arthritis and other inflammatory arthritides. *Arthritis & Rheumatism,* 31**,** 784-788.

HSIEH, S. Y., SHIH, T. C., YEH, C. Y., LIN, C. J., CHOU, Y. Y. & LEE, Y. S. 2006. Comparative proteomic studies on the pathogenesis of human ulcerative colitis. *Proteomics,* 6**,** 5322-5331.

HUBER, P., REDWOOD, C., AVENT, N., TANNER, M. & MARSTON, S. 1993. Identification of functioning regulatory sites and a new myosin binding site in the C-terminal 288 amino acids of caldesmon expressed from a human clone. *Journal of muscle research and cell motility,* 14**,** 385-391.

HUGHES, S. C. & FEHON, R. G. 2007. Understanding ERM proteins-the awesome power of genetics finally brought to bear. *Current opinion in cell biology,* 19**,** 51-56.

HUNTER, D. J. 2008. Are there promising biologic therapies for osteoarthritis? *Current rheumatology reports,* 10**,** 19-25.

HUNTER, D. J. 2009. Osteoarthritis Preface. *Medical Clinics of North America,* 93**,** XV-XVIII.

HUNTER, D. J. 2010. Pharmacologic therapy for osteoarthritis—the era of disease modification. *Nature Reviews Rheumatology,* 7**,** 13-22.

HUTTON, C., HINTON, C. & DIEPPE, P. 1987. Intra-articular variation of synovial changes in knee arthritis: biopsy study comparing changes in patellofemoral synovium and the medial tibiofemoral synovium. *Rheumatology,* 26**,** 5.

ILIOPOULOS, D., GKRETSI, V. & TSEZOU, A. 2010. Proteomics of osteoarthritic chondrocytes and cartilage. *Expert Review of Proteomics,* 7**,** 749-760.

ISRAËL, A. 2006. NF-ºB activation: nondegradative ubiquitination implicates NEMO. *Trends in immunology,* 27**,** 395-397.

IVASKA, J., PALLARI, H. M., NEVO, J. & ERIKSSON, J. E. 2007. Novel functions of vimentin in cell adhesion, migration, and signaling. *Experimental cell research,* 313**,** 2050-2062.

IWASAKI, A. & MEDZHITOV, R. 2004. Toll-like receptor control of the adaptive immune responses. *nature immunology,* 5**,** 987-995.

IZAGUIRRE, A., BARNES, B. J., AMRUTE, S., YEOW, W. S., MEGJUGORAC, N., DAI, J., FENG, D., CHUNG, E., PITHA, P. M. & FITZGERALD-BOCARSLY, P. 2003. Comparative analysis of IRF and IFN-alpha expression in human plasmacytoid and monocyte-derived dendritic cells. *Journal of leukocyte biology,* 74**,** 1125-1138.

IZUMISAWA, Y., YAMAGUCHI, M., BERTONE, A., TANGKAWATTANA, P., MASTY, J., YAMASHITA, K. & KOTANI, T. 1996. Equine synovial villi: distinctive structural organization of vasculature and novel nerve endings. *The Journal of veterinary medical science/the Japanese Society of Veterinary Science,* 58**,** 1193.

JAMES, P. 1997. Protein identification in the post-genome era: the rapid rise of proteomics. *Quarterly reviews of biophysics,* 30**,** 279-331.

JANEWAY JR, C. Year. Approaching the asymptote? Evolution and revolution in immunology. *In,* 1989. Cold Spring Harbor Laboratory Press, 1-13.

JANEWAY JR, C. A. & MEDZHITOV, R. 2002. Innate immune recognition. *Annual review of immunology,* 20**,** 197-216.

JANSSENS, S., BURNS, K., VERCAMMEN, E., TSCHOPP, J. & BEYAERT, R. 2003. MyD88S, a splice variant of MyD88, differentially modulates NF-[kappa] B-and AP-1-dependent gene expression. *FEBS letters,* 548**,** 103-107.

JASIN, H. E. 1985. Autoantibody specificities of immune complexes sequestered in articular cartilage of patients with rheumatoid arthritis and osteoarthritis. *Arthritis & Rheumatism,* 28**,** 241-248.

JIANG, D., LIANG, J., FAN, J., YU, S., CHEN, S., LUO, Y., PRESTWICH, G. D., MASCARENHAS, M. M., GARG, H. G. & QUINN, D. A. 2005. Regulation of lung injury and repair by Toll-like receptors and hyaluronan. *Nature medicine,* 11**,** 1173-1179.

JIANG, D., LIANG, J. & NOBLE, P. W. 2007. Hyaluronan in tissue injury and repair. *Annu. Rev. Cell Dev. Biol.,* 23**,** 435-461.

JIANG, Z., GEORGEL, P., DU, X., SHAMEL, L., SOVATH, S., MUDD, S., HUBER, M., KALIS, C., KECK, S. & GALANOS, C. 2005. CD14 is required for MyD88-independent LPS signaling. *nature immunology,* 6**,** 565-570.

JIANG, Z., MAK, T. W., SEN, G. & LI, X. 2004. Toll-like receptor 3-mediated activation of NF-κB and IRF3 diverges at Toll-IL-1 receptor domain-containing adapter inducing IFN-β. *Proceedings of the National Academy of Sciences of the United States of America,* 101**,** 3533.

JOENSUU, T., KURONEN, M., ALAKURTTI, K., TEGELBERG, S., HAKALA, P., AALTO, A., HUOPANIEMI, L., AULA, N., MICHELLUCCI, R. & ERIKSSON, K. 2006. Cystatin B: mutation detection, alternative splicing and expression in progressive myclonus epilepsy of Unverricht-Lundborg type (EPM1) patients. *European Journal of Human Genetics,* 15**,** 185-193.

JOOSTEN, L. A. B., HELSEN, M., SAXNE, T., VAN DE LOO, F. A. J. & VAN DEN BERG, W. B. 1999. IL-1αß Blockade Prevents Cartilage and Bone Destruction in Murine Type II Collagen-Induced Arthritis, Whereas TNF-α Blockade Only Ameliorates Joint Inflammation. *The Journal of Immunology,* 163**,** 5049.

JORDAN, J., JUNG, S. Y., SARISKY, R. T. & SCHREITER, J. 2009. Methods for Suppressing Toll-Like Receptor Activity. Google Patents.

JUNG, Y. O., CHO, M. L., KANG, C. M., JHUN, J. Y., PARK, J. S., OH, H. J., MIN, J. K., PARK, S. H. & KIM, H. Y. 2007. Toll-like receptor 2 and 4 combination engagement upregulate IL-15 synergistically in human rheumatoid synovial fibroblasts. *Immunology letters,* 109**,** 21-27.

JÜNGEL, A., DISTLER, O., SCHULZE-HORSEL, U., HUBER, L. C., HA, H. R., SIMMEN, B., KALDEN, J. R., PISETSKY, D. S., GAY, S. & DISTLER, J. H. W. 2007. Microparticles stimulate the synthesis of prostaglandin E2 via induction of cyclooxygenase 2 and microsomal prostaglandin E synthase 1. *Arthritis & Rheumatism,* 56**,** 3564-3574.

JUPE, E. R., LIU, X. T., KIEHLBAUCH, J. L., MCCLUNG, J. K. & DELL'ORCO, R. T. 1995. Prohibitin Antiproliferative Activity and Lack of Heterozygosity in Immortalized Cell Lines. *Experimental Cell Research,* 218**,** 577-580.

KACZOROWSKI, D. J., MOLLEN, K. P., EDMONDS, R. & BILLIAR, T. R. 2008. Early events in the recognition of danger signals after tissue injury. *Journal of leukocyte biology,* 83**,** 546-552.

KAGAN, J. C., SU, T., HORNG, T., CHOW, A., AKIRA, S. & MEDZHITOV, R. 2008. TRAM couples endocytosis of Toll-like receptor 4 to the induction of interferon-β. *nature immunology,* 9**,** 361-368.

KAISHO, T. & AKIRA, S. 2001. Dendritic-cell function in Toll-like receptor-and MyD88-knockout mice. *Trends in immunology*, 22**,** 78-83.

KANDIMALLA, E., ZHU, F., BHAGAT, L., YU, D. & AGRAWAL, S. 2003. Toll-like receptor 9: modulation of recognition and cytokine induction by novel synthetic CpG DNAs. *Biochemical Society Transactions,* 31**,** 654-658.

KANG, S.-M., SHIN, M.-J., KIM, J.-H. & OH, J.-W. 2005. Proteomic profiling of cellular proteins interacting with the hepatitis C virus core protein. *Proteomics,* 5**,** 2227-2237.

KAPOOR, M., MARTEL-PELLETIER, J., LAJEUNESSE, D., PELLETIER, J. P. & FAHMI, H. 2010. Role of proinflammatory cytokines in the pathophysiology of osteoarthritis. *Nature Reviews Rheumatology*, 7**,** 33-42.

KAPOOR, M., MARTEL-PELLETIER, J., LAJEUNESSE, D., PELLETIER, J.-P. & FAHMI, H. 2011. Role of proinflammatory cytokines in the pathophysiology of osteoarthritis. *Nat Rev Rheumatol,* 7**,** 33-42.

KARIKÓ, K., NI, H., CAPODICI, J., LAMPHIER, M. & WEISSMAN, D. 2004. mRNA is an endogenous ligand for Toll-like receptor 3. *Journal of Biological Chemistry,* 279**,** 12542-12550.

KARIN, M. & BEN-NERIAH, Y. 2000. Phosphorylation meets ubiquitination: the control of NF-κB activity. *Annual review of immunology,* 18**,** 621-663.

KATO, H., SATO, S., YONEYAMA, M., YAMAMOTO, M., UEMATSU, S., MATSUI, K., TSUJIMURA, T., TAKEDA, K., FUJITA, T. & TAKEUCHI, O. 2005. Cell type-specific involvement of RIG-I in antiviral response. *Immunity,* 23**,** 19-28.

KATO, H., TAKEUCHI, O., SATO, S., YONEYAMA, M., YAMAMOTO, M., MATSUI, K., UEMATSU, S., JUNG, A., KAWAI, T. & ISHII, K. J. 2006. Differential roles of MDA5 and RIG-I helicases in the recognition of RNA viruses. *Nature*, 441**,** 101-105.

KATSIKIS, P. D., CHU, C. Q., BRENNAN, F. M., MAINI, R. N. & FELDMANN, M. 1994. Immunoregulatory role of interleukin 10 in rheumatoid arthritis. *The Journal of experimental medicine,* 179**,** 1517.

KATSUMOTO, T., INOUE, M., NAGURO, T. & KURIMURA, T. 1991. Association of cytoskeletons with the Golgi apparatus: three-dimensional observation and computer-graphic reconstruction. *Journal of electron microscopy*, 40**,** 24.

KAWAI, T., ADACHI, O., OGAWA, T., TAKEDA, K. & AKIRA, S. 1999. Unresponsiveness of MyD88-Deficient Mice to Endotoxin. *Immunity,* 11**,** 115-122.

KAWAI, T. & AKIRA, S. 2008. Toll-like Receptor and RIG-1-like Receptor Signaling. *Annals of the New York Academy of Sciences*, 1143**,** 1-20.

KAWAI, T., SATO, S., ISHII, K. J., COBAN, C., HEMMI, H., YAMAMOTO, M., TERAI, K., MATSUDA, M., INOUE, J. & UEMATSU, S. 2004. Interferon-α induction through Toll-like receptors involves a direct interaction of IRF7 with MyD88 and TRAF6. *nature immunology*, 5**,** 1061-1068.

KELLGREN, J. & LAWRENCE, J. 1957. Radiological assessment of osteo-arthrosis. *Ann Rheum Dis,* 16**,** 494-502.

KIM, H., KIM, W. J., JEON, S. T., KOH, E. M., CHA, H. S., AHN, K. S. & LEE, W. H. 2005. Cyclophilin A may contribute to the inflammatory processes in rheumatoid arthritis through induction of matrix degrading enzymes and inflammatory cytokines from macrophages. *Clinical immunology,* 116**,** 217-224.

KIM, H. A., CHO, M. L., CHOI, H. Y., YOON, C. S., JHUN, J. Y., OH, H. J. & KIM, H. Y. 2006. The catabolic pathway mediated by Toll-like receptors in human osteoarthritic chondrocytes. *Arthritis & Rheumatism,* 54**,** 2152-2163.

KIM, J., LEE, J. E., HEYNEN-GENEL, S., SUYAMA, E., ONO, K., LEE, K. Y., IDEKER, T., AZA-BLANC, P. & GLEESON, J. G. 2010. Functional genomic screen for modulators of ciliogenesis and cilium length. *Nature,* 464**,** 1048-1051.

KIM, K. M., KIRN, D. K., PARK, Y. M., KIM, C. K. & NA, D. S. 1994. Annexin-I inhibits phospholipase A2 by specific interaction, not by substrate depletion. *FEBS letters,* 343**,** 251-255.

KIM, K. W., CHO, M. L., LEE, S. H., OH, H. J., KANG, C. M., JU, J. H., MIN, S. Y., CHO, Y. G., PARK, S. H. & KIM, H. Y. 2007. Human rheumatoid synovial fibroblasts promote osteoclastogenic activity by activating RANKL via TLR-2 and TLR-4 activation. *Immunology letters,* 110**,** 54-64.

KIM, K. W., CHO, M. L., OH, H. J., KIM, H. R., KANG, C. M., HEO, Y. M., LEE, S. H. & KIM, H. Y. 2009. TLR-3 enhances osteoclastogenesis through upregulation of RANKL expression from fibroblast-like synoviocytes in patients with rheumatoid arthritis. *Immunology letters,* 124**,** 9-17.

KNIGHT, E. & CORDOVA, B. 1991. IFN-induced 15-kDa protein is released from human lymphocytes and monocytes. *The Journal of immunology,* 146**,** 2280.

KNUDSON, W., CHOW, G. & KNUDSON, C. B. 2002. CD44-mediated uptake and degradation of hyaluronan. *Matrix biology,* 21**,** 15-23.

KOARAI, A., YANAGISAWA, S., SUGIURA, H., ICHIKAWA, T., AKAMATSU, K., HIRANO, T., NAKANISHI, M., MATSUNAGA, K., MINAKATA, Y. & ICHINOSE, M. 2012. Cigarette smoke augments the expression and responses of toll-like receptor 3 in human macrophages. *Respirology***,** no-no.

KOBAYASHI, K., HERNANDEZ, L. D., GALÁN, J. E., JANEWAY JR, C. A., MEDZHITOV, R. & FLAVELL, R. A. 2002. IRAK-M is a negative regulator of Toll-like receptor signaling. *Cell,* 110**,** 191-202.

KOLLEWE, C., MACKENSEN, A. C., NEUMANN, D., KNOP, J., CAO, P., LI, S., WESCHE, H. & MARTIN, M. U. 2004. Sequential autophosphorylation steps in the interleukin-1 receptor-associated kinase-1 regulate its availability as an adapter in interleukin-1 signaling. *Journal of Biological Chemistry,* 279**,** 5227.

KONTTINEN, Y. T., CEPONIS, A., MERI, S., VUORIKOSKI, A., KORTEKANGAS, P., SORSA, T., SUKURA, A. & SANTAVIRTA, S. 1996. Complement in acute and chronic arthritides: assessment of C3c, C9, and protectin (CD59) in synovial membrane. *Annals of the rheumatic diseases,* 55**,** 888-894.

KRAAN, M., HARINGMAN, J., AHERN, M., BREEDVELD, F., SMITH, M. & TAK, P. 2000. Quantification of the cell infiltrate in synovial tissue by digital image analysis. *Rheumatology,* 39**,** 43.

KRAAN, M. C., REECE, R. J., SMEETS, T. J. M., VEALE, D. J., EMERY, P. & TAK, P. P. 2002. Comparison of synovial tissues from the knee joints and the small joints of rheumatoid arthritis patients: implications for pathogenesis and evaluation of treatment. *Arthritis & Rheumatism,* 46**,** 2034-2038.

KRASNOKUTSKY, S., SAMUELS, J. & ABRAMSON, S. B. 2007. Osteoarthritis in 2007. *BULLETIN-HOSPITAL FOR JOINT DISEASES NEW YORK,* 65**,** 222.

KRAUS, V. B. 2005. Biomarkers in osteoarthritis. *Current opinion in rheumatology,* 17**,** 641-646.

KUROKI, K., STOKER, A. M., SIMS, H. J. & COOK, J. L. 2010. Expression of Toll-like receptors 2 and 4 in stifle joint synovial tissues of dogs with or without osteoarthritis. *American journal of veterinary research,* 71**,** 750-754.

KYBURZ, D., RETHAGE, J., SEIBL, R., LAUENER, R., GAY, R. E., CARSON, D. A. & GAY, S. 2003. Bacterial peptidoglycans but not CpG oligodeoxynucleotides activate synovial fibroblasts by toll-like receptor signaling. *Arthritis & Rheumatism,* 48**,** 642-650.

KYOSTIO-MOORE, S., NAMBIAR, B., HUTTO, E., EWING, P. J., PIRAINO, S., BERTHELETTE, P., SOOKDEO, C., MATTHEWS, G. & ARMENTANO, D. 2011. STR/ort Mice, a Model for Spontaneous Osteoarthritis, Exhibit Elevated Levels of Both Local and Systemic Inflammatory Markers. *Comparative Medicine,* 61**,** 346-355.

LAMBRECHT, S., VERBRUGGEN, G., VERDONK, P. C. M., ELEWAUT, D. & DEFORCE, D. 2008. Differential proteome analysis of normal and osteoarthritic chondrocytes reveals distortion of vimentin network in osteoarthritis. *Osteoarthritis and Cartilage,* 16**,** 163-173.

LEBRE, M. C., VAN DER AAR, A. M. G., VAN BAARSEN, L., VAN CAPEL, T. M. M., SCHUITEMAKER, J. H. N., KAPSENBERG, M. L. & DE JONG, E. C. 2006. Human keratinocytes express functional Toll-like receptor 3, 4, 5, and 9. *Journal of Investigative Dermatology,* 127**,** 331-341.

LEE, H. K., DUNZENDORFER, S., SOLDAU, K. & TOBIAS, P. S. 2006. Double-stranded RNA-mediated TLR3 activation is enhanced by CD14. *Immunity,* 24**,** 153-163.

LEE, H.-K., DUNZENDORFER, S., SOLDAU, K. & TOBIAS, P. S. 2006. Double-Stranded RNA-Mediated TLR3 Activation Is Enhanced by CD14. *Immunity,* 24**,** 153-163.

LEIFER, C. A., KENNEDY, M. N., MAZZONI, A., LEE, C. W., KRUHLAK, M. J. & SEGAL, D. M. 2004. TLR9 is localized in the endoplasmic reticulum prior to stimulation.

The Journal of immunology, 173**,** 1179.

LEMAITRE, B., NICOLAS, E., MICHAUT, L., REICHHART, J. M. & HOFFMANN, J. A. 1996. The Dorsoventral Regulatory Gene Cassette< i> spätzle/Toll/cactus</i> Controls the Potent Antifungal Response in Drosophila Adults. *Cell,* 86**,** 973-983.

LI, K., FOY, E., FERREON, J. C., NAKAMURA, M., FERREON, A., IKEDA, M., RAY, S. C., GALE, M. & LEMON, S. M. 2005. Immune evasion by hepatitis C virus NS3/4A protease-mediated cleavage of the Toll-like receptor 3 adaptor protein TRIF. *Proceedings of the National Academy of Sciences of the United States of America,* 102**,** 2992.

LI, L. 2004. Regulation of innate immunity signaling and its connection with human diseases. *Current Drug Targets-Inflammation &# 38; Allergy,* 3**,** 81-86.

LI, S., STRELOW, A., FONTANA, E. J. & WESCHE, H. 2002. IRAK-4: a novel member of the IRAK family with the properties of an IRAK-kinase. *Proceedings of the National Academy of Sciences,* 99**,** 5567.

LI, X., GIBSON, G., KIM, J. S., KROIN, J., XU, S. B., VAN WIJNEN, A. J. & IM, H. J. 2011. MicroRNA-146a is linked to pain-related pathophysiology of osteoarthritis. *Gene,* 480**,** 34-41.

LIM, L. H. K. & PERVAIZ, S. 2007. Annexin 1: the new face of an old molecule. *The FASEB Journal,* 21**,** 968-975.

LIM, L. H. K., SOLITO, E., RUSSO-MARIE, F., FLOWER, R. J. & PERRETTI, M. 1998. Promoting detachment of neutrophils adherent to murine postcapillary venules to control inflammation: effect of lipocortin 1. *Proceedings of the National Academy of Sciences,* 95**,** 14535.

LIN, Q., LI, M., FANG, D., FANG, J. & SU, S. B. 2011. The essential roles of Toll-like receptor signaling pathways in sterile inflammatory diseases. *International immunopharmacology*.

LIN, R., MAMANE, Y. & HISCOTT, J. 1999. Structural and functional analysis of interferon regulatory factor 3: localization of the transactivation and autoinhibitory domains. *Molecular and cellular biology,* 19**,** 2465.

LINDBLAD, S. & HEDFORS, E. 1987. Arthroscopic and immunohistologic characterization of knee joint synovitis in osteoarthritis. *Arthritis & Rheumatism,* 30**,** 1081-1088.

LINDENMANN, J., BURKE, D. & ISAACS, A. 1957. Studies on the production, mode of action and properties of interferon. *British journal of experimental pathology,* 38**,** 551.

LIU, H.-H., HU, Y., ZHENG, M., SUHOSKI, M. M., ENGLEMAN, E. G., DILL, D. L., HUDNALL, M., WANG, J., SPOLSKI, R., LEONARD, W. J. & PELTZ, G. 2012. Cd14 SNPs regulate the innate immune response. *Molecular immunology,* 51**,** 112-127.

LIU-BRYAN, R. & TERKELTAUB, R. 2012. The growing array of innate inflammatory ignition switches in osteoarthritis. *Arthritis & Rheumatism***,** n/a-n/a.

LOEB, K. & HAAS, A. L. 1992. The interferon-inducible 15-kDa ubiquitin homolog conjugates to intracellular proteins. *Journal of Biological Chemistry,* 267**,** 7806.

LOESER, R. F., YAMMANI, R. R., CARLSON, C. S., CHEN, H., COLE, A., IM, H. J., BURSCH, L. S. & YAN, S. D. 2005. Articular chondrocytes express the receptor for advanced glycation end products: potential role in osteoarthritis. *Arthritis & Rheumatism,* 52**,** 2376-2385.

LOEUILLE, D., CHARY-VALCKENAERE, I., CHAMPIGNEULLE, J., RAT, A. C., TOUSSAINT, F., PINZANO-WATRIN, A., GOEBEL, J. C., MAINARD, D., BLUM, A. & POUREL, J. 2005. Macroscopic and microscopic features of synovial membrane inflammation in the osteoarthritic knee: correlating magnetic resonance imaging findings with disease severity. *Arthritis & Rheumatism,* 52**,** 3492-3501.

LOHMANDER, L. S., BRANDT, K. D., MAZZUCA, S. A., KATZ, B. P., LARSSON, S., STRUGLICS, A. & LANE, K. A. 2005. Use of the plasma stromelysin (matrix metalloproteinase 3) concentration to predict joint space narrowing in knee osteoarthritis. *Arthritis & Rheumatism,* 52**,** 3160-3167.

LOO, Y. M., FORNEK, J., CROCHET, N., BAJWA, G., PERWITASARI, O., MARTINEZ-SOBRIDO, L., AKIRA, S., GILL, M. A., GARCIA-SASTRE, A. & KATZE, M. G. 2008. Distinct RIG-I and MDA5 signaling by RNA viruses in innate immunity. *Journal of virology,* 82**,** 335.

LÓPEZ-DURÁN, L., JOVER, J. Á., LÓPEZ, J. A., LAMAS, J. R. & FERNÁNDEZ-GUTIÉRREZ, B. 2008. Differential Proteome of Articular Chondrocytes From Patients with Osteoarthritis.

LORD, K. A., HOFFMAN-LIEBERMANN, B. & LIEBERMANN, D. A. 1990. Nucleotide sequence and expression of a cDNA encoding MyD88, a novel myeloid differentiation primary response gene induced by IL6. *Oncogene,* 5**,** 1095-7.

LORENZ, P., RUSCHPLER, P., KOCZAN, D., STIEHL, P. & THIESEN, H. J. 2003. From transcriptome to proteome: differentially expressed proteins identified in synovial tissue of patients suffering from rheumatoid arthritis and osteoarthritis by an initial screen with a panel of 791 antibodies. *Proteomics,* 3**,** 991-1002.

LUBAN, J., BOSSOLT, K. L., FRANKE, E. K., KALPANA, G. V. & GOFF, S. P. 1993. Human immunodeficiency virus type 1 Gag protein binds to cyclophilins A and B. *Cell,* 73**,** 1067-1078.

LUDWIG, J. A. & WEINSTEIN, J. N. 2005. Biomarkers in cancer staging, prognosis and treatment selection. *Nature Reviews Cancer,* 5**,** 845-856.

LUND, J., SATO, A., AKIRA, S., MEDZHITOV, R. & IWASAKI, A. 2003. Toll-like receptor 9–mediated recognition of Herpes simplex virus-2 by plasmacytoid dendritic cells. *The Journal of experimental medicine,* 198**,** 513.

LUNDBERG, A. M., DREXLER, S. K., MONACO, C., WILLIAMS, L. M., SACRE, S. M., FELDMANN, M. & FOXWELL, B. M. 2007. Key differences in TLR3/poly I: C

signaling and cytokine induction by human primary cells: a phenomenon absent from murine cell systems. *Blood,* 110**,** 3245.

LUSTER, A. D. 2002. The role of chemokines in linking innate and adaptive immunity. *Current opinion in immunology,* 14**,** 129-135.

LYSHOLM, J., HAMBERG, P. & GILLQUIST, J. 1987. The correlation between osteoarthrosis as seen on radiographs and on arthroscopy. *Arthroscopy: The Journal of Arthroscopic & Related Surgery,* 3**,** 161-165.

MACMILLAN-CROW, L. A. & THOMPSON, J. A. 1999. Tyrosine Modifications and Inactivation of Active Site Manganese Superoxide Dismutase Mutant (Y34F) by Peroxynitrite. *Archives of Biochemistry and Biophysics,* 366**,** 82-88.

MACOR, P., DURIGUTTO, P., DE MASO, L., GARROVO, C., BIFFI, S., CORTINI, A., FISCHETTI, F., SBLATTERO, D., PITZALIS, C., MARZARI, R. & TEDESCO*, F. 2012. Treatment of arthritis models by targeting synovial endothelium with a neutralizing recombinant antibody to C5. *Arthritis & Rheumatism***,** n/a-n/a.

MAGNANO, M. D., CHAKRAVARTY, E. F., BROUDY, C., CHUNG, L., KELMAN, A., HILLYGUS, J. & GENOVESE, M. C. 2007. A pilot study of tumor necrosis factor inhibition in erosive/inflammatory osteoarthritis of the hands. *The Journal of rheumatology,* 34**,** 1323-1327.

MAGNUSSON, M., ZARE, F. & TARKOWSKI, A. 2006. Requirement of type I interferon signaling for arthritis triggered by double-stranded RNA. *Arthritis and Rheumatism,* 54**,** 148-157.

MAK, A. S. 2011. p53 regulation of podosome formation and cellular invasion in vascular smooth muscle cells. *Cell Adhesion & Migration,* 5**,** 144.

MALEMUD, C. J. 2004. Cytokines as therapeutic targets for osteoarthritis. *BioDrugs,* 18**,** 23-35.

MALEMUD, C. J. 2010. Anticytokine therapy for osteoarthritis: evidence to date. *Drugs &# 38; Aging,* 27**,** 95-115.

MALEMUD, C. J., ISLAM, N. & HAQQI, T. M. 2003. Pathophysiological mechanisms in Osteoarthritis lead to novel therapeutic strategies. *Cells Tissues Organs,* 174**,** 34-48.

MAMANE, Y., HEYLBROECK, C., GÉNIN, P., ALGARTÉ, M., SERVANT, M. J., LEPAGE, C., DELUCA, C., KWON, H., LIN, R. & HISCOTT, J. 1999. Interferon regulatory factors: the next generation. *Gene,* 237**,** 1-14.

MANJESHWAR, S., BRANAM, D. E., LERNER, M. R., BRACKETT, D. J. & JUPE, E. R. 2003. Tumor suppression by the prohibitin gene 3′ untranslated region RNA in human breast cancer. *Cancer research,* 63**,** 5251.

MANJESHWAR, S., LERNER, M. R., ZANG, X. P., BRANAM, D. E., PENTO, J. T., LANE, M. M., LIGHTFOOT, S. A., BRACKETT, D. J. & JUPE, E. R. 2004. Expression of prohibitin 3′ untranslated region suppressor RNA alters morphology and inhibits motility of

breast cancer cells. *Journal of Molecular histology,* 35**,** 639-646.
MANN, M. & JENSEN, O. N. 2003. Proteomic analysis of post-translational modifications. *Nature biotechnology,* 21**,** 255-261.

MANSELL, A., BRINT, E., GOULD, J. A., O'NEILL, L. A. & HERTZOG, P. J. 2004. Mal interacts with tumor necrosis factor receptor-associated factor (TRAF)-6 to mediate NF-κB activation by Toll-like receptor (TLR)-2 and TLR4. *Journal of Biological Chemistry,* 279**,** 37227.

MANSELL, A., SMITH, R., DOYLE, S. L., GRAY, P., FENNER, J. E., CRACK, P. J., NICHOLSON, S. E., HILTON, D. J., O'NEILL, L. A. J. & HERTZOG, P. J. 2006. Suppressor of cytokine signaling 1 negatively regulates Toll-like receptor signaling by mediating Mal degradation. *nature immunology,* 7**,** 148-155.

MARTEL-PELLETIER, J. 1999. Proinflammatory mediators and osteoarthritis. *Osteoarthritis and Cartilage,* 7**,** 315-316.

MARTEL-PELLETIER, J., ALAAEDDINE, N. & PELLETIER, J. P. 1999. Cytokines and their role in the pathophysiology of osteoarthritis. *Front Biosci,* 4**,** D694-703.

MARTEL-PELLETIER, J., MINEAU, F., JOLICOEUR, F., CLOUTIER, J. & PELLETIER, J. 1998. In vitro effects of diacerhein and rhein on interleukin 1 and tumor necrosis factor-alpha systems in human osteoarthritic synovium and chondrocytes. *The Journal of rheumatology,* 25**,** 753.

MARTIN, M. U. & WESCHE, H. 2002. Summary and comparison of the signaling mechanisms of the Toll/interleukin-1 receptor family. *Biochimica et Biophysica Acta (BBA)-Molecular Cell Research,* 1592**,** 265-280.

MASUHARA, K., NAKAI, T., YAMAGUCHI, K., YAMASAKI, S. & SASAGURI, Y. 2002. Significant increases in serum and plasma concentrations of matrix metalloproteinases 3 and 9 in patients with rapidly destructive osteoarthritis of the hip. *Arthritis & Rheumatism,* 46**,** 2625-2631.

MATSUMOTO, M., KIKKAWA, S., KOHASE, M., MIYAKE, K. & SEYA, T. 2002. Establishment of a monoclonal antibody against human Toll-like receptor 3 that blocks double-stranded RNA-mediated signaling. *Biochemical and biophysical research communications,* 293**,** 1364-1369.

MATSUMOTO, M. & SEYA, T. 2008. TLR3: Interferon induction by double-stranded RNA including poly(I:C). *Advanced drug delivery reviews,* 60**,** 805-812.

MATSUMURA, T., DEGAWA, T., TAKII, T., HAYASHI, H., OKAMOTO, T., INOUE, J.-I. & ONOZAKI, K. 2003. TRAF6-NF-κB pathway is essential for interleukin-1-induced TLR2 expression and its functional response to TLR2 ligand in murine hepatocytes. *Immunology,* 109**,** 127-136.

MATTHEWS, G. L. & HUNTER, D. J. 2011. Emerging drugs for osteoarthritis. *Expert Opinion on Emerging Drugs,* 16**,** 479-491.

MAYANAGI, T. & SOBUE, K. 2011. Diversification of caldesmon-linked actin

cytoskeleton in cell motility. *Cell Adhesion & Migration,* 5**,** 150.

MCCORMACK, W. J., PARKER, A. E. & O'NEILL, L. A. 2009. Toll-like receptors and NOD-like receptors in rheumatic diseases. *Arthritis Research & Therapy,* 11**,** 243.

MCDERMOTT, A., FINKLESTEIN, J., FARINE, I., BOYNTON, E., MACINTOSH, D. & GROSS, A. 1988. Distal femoral varus osteotomy for valgus deformity of the knee. *The Journal of bone and joint surgery. American volume,* 70**,** 110.

MCGETTRICK, A. F., BRINT, E. K., PALSSON-MCDERMOTT, E. M., ROWE, D. C., GOLENBOCK, D. T., GAY, N. J., FITZGERALD, K. A. & O'NEILL, L. A. J. 2006. Trif-related adapter molecule is phosphorylated by PKCε during Toll-like receptor 4 signaling. *Proceedings of the National Academy of Sciences,* 103**,** 9196.

MCGETTRICK, A. F. & O'NEILL, L. A. J. 2010. Localisation and trafficking of Toll-like receptors: an important mode of regulation. *Current opinion in immunology,* 22**,** 20-27.

MEDZHITOV, R. & JANEWAY, C. 1997. Innate immunity: Minireview the virtues of a nonclonal system of recognition. *Cell,* 91**,** 295-298.

MEDZHITOV, R. & JANEWAY, C. 2000. The Toll receptor family and microbial recognition. *Trends in microbiology,* 8**,** 452-456.

MEDZHITOV, R. & JANEWAY, C. A. 2002. Decoding the patterns of self and nonself by the innate immune system. *Science,* 296**,** 298.

MEDZHITOV, R. & JANEWAY JR, C. Year. Innate immune induction of the adaptive immune response. *In,* 1999. Cold Spring Harbor Laboratory Press, 429-436.

MEDZHITOV, R. & JANEWAY JR, C. 2000. Innate immune recognition: mechanisms and pathways. *Immunological reviews,* 173**,** 89-97.

MEDZHITOV, R., PRESTON-HURLBURT, P., KOPP, E., STADLEN, A., CHEN, C., GHOSH, S. & JANEWAY, C. A. 1998. MyD88 Is an Adaptor Protein in the hToll/IL-1 Receptor Family Signaling Pathways. *Molecular cell,* 2**,** 253-258.

MELCHJORSEN, J., SØRENSEN, L. N. & PALUDAN, S. R. 2003. Expression and function of chemokines during viral infections: from molecular mechanisms to in vivo function. *Journal of leukocyte biology,* 74**,** 331-343.

MENG, L., ZHU, W., JIANG, C., HE, X., HOU, W., ZHENG, F., HOLMDAHL, R. & LU, S. 2010. Research article Toll-like receptor 3 upregulation in macrophages participates in the initiation and maintenance of pristane-induced arthritis in rats.

MERKWIRTH, C. & LANGER, T. 2009. Prohibitin function within mitochondria: essential roles for cell proliferation and cristae morphogenesis. *Biochimica et Biophysica Acta (BBA)-Molecular Cell Research,* 1793**,** 27-32.

MERX, H., DREINHÖFER, K., SCHRÄDER, P., STÜRMER, T., PUHL, W., GÜNTHER, K. & BRENNER, H. 2003. International variation in hip replacement rates. *Annals of the rheumatic diseases,* 62**,** 222-226.

MESSER, L., ALSALEH, G., FREYSSINET, J. M., ZOBAIRI, F., LERAY, I., GOTTENBERG, J. E., SIBILIA, J., TOTI-ORFANOUDAKIS, F. & WACHSMANN, D. 2009. Microparticle-induced release of B-lymphocyte regulators by rheumatoid synoviocytes. *Arthritis Research & Therapy,* 11.

MICHELSON, A. M., MARKHAM, A. F. & ORKIN, S. H. 1983. Isolation and DNA sequence of a full-length cDNA clone for human X chromosome-encoded phosphoglycerate kinase. *Proceedings of the National Academy of Sciences,* 80**,** 472.

MIDWOOD, K., PICCININI, A. & SACRE, S. 2009. Targeting Toll-like receptors in autoimmunity. *Current drug targets,* 10**,** 1139-1155.

MIGGIN, S. M. & O'NEILL, L. A. J. 2006. New insights into the regulation of TLR signaling. *Journal of leukocyte biology,* 80**,** 220-226.

MIGGIN, S. M., PÅLSSON-MCDERMOTT, E., DUNNE, A., JEFFERIES, C., PINTEAUX, E., BANAHAN, K., MURPHY, C., MOYNAGH, P., YAMAMOTO, M. & AKIRA, S. 2007. NF-κB activation by the Toll-IL-1 receptor domain protein MyD88 adapter-like is regulated by caspase-1. *Proceedings of the National Academy of Sciences,* 104**,** 3372.

MILLENNIUM, W. S. G. O. T. B. O. M. C. A. T. S. O. T. N. 2003. *The burden of musculoskeletal conditions at the start of the new millennium: report of a WHO scientific group,* WHO.

MINDEN, J. S., DOWD, S. R., MEYER, H. E. & STÜHLER, K. 2009. Difference gel electrophoresis. *Electrophoresis,* 30**,** S156-S161.

MISHRA, B. B., GUNDRA, U. M. & TEALE, J. M. 2008. Expression and distribution of Toll-like receptors 11–13 in the brain during murine neurocysticercosis. *J Neuroinflammation,* 5**,** 53.

MISHRA, S., MOULIK, S. & MURPHY, L. J. 2007. Prohibitin binds to C3 and enhances complement activation. *Molecular immunology,* 44**,** 1897-1902.

MISHRA, S., MURPHY, L. C. & MURPHY, L. J. 2006. The prohibitins: emerging roles in diverse functions. *Journal of cellular and molecular medicine,* 10**,** 353-363.

MISHRA, S., MURPHY, L. C., NYOMBA, B. & MURPHY, L. J. 2005. Prohibitin: a potential target for new therapeutics. *Trends in molecular medicine,* 11**,** 192-197.

MOBASHERI, A. 2011. Applications of proteomics to osteoarthritis, a musculoskeletal disease characterized by aging. *Frontiers in Physiology,* 2.

MORITA, T., MAYANAGI, T. & SOBUE, K. 2012. Caldesmon regulates axon extension through interaction with Myosin II. *Journal of Biological Chemistry,* 287**,** 3349-3356.

MOR-VAKNIN, N., PUNTURIERI, A., SITWALA, K. & MARKOVITZ, D. M. 2003. Vimentin is secreted by activated macrophages. *Nature cell biology,* 5**,** 59-63.

MOYNAGH, P. N. 2005. The NF-κB pathway. *Journal of cell science,* 118**,** 4589.

MULLAN, R. H., MATTHEWS, C., BRESNIHAN, B., FITZGERALD, O., KING, L., POOLE, A. R., FEARON, U. & VEALE, D. J. 2007. Early changes in serum type II collagen biomarkers predict radiographic progression at one year in inflammatory arthritis patients after biologic therapy. *Arthritis & Rheumatism,* 56**,** 2919-2928.

MÜLLER-LADNER, U., KRIEGSMANN, J., FRANKLIN, B. N., MATSUMOTO, S., GEILER, T., GAY, R. E. & GAY, S. 1996. Synovial fibroblasts of patients with rheumatoid arthritis attach to and invade normal human cartilage when engrafted into SCID mice. *The American journal of pathology,* 149**,** 1607.

MÜLLER-LADNER, U., OSPELT, C., GAY, S., DISTLER, O. & PAP, T. 2007. Synovial fibroblasts. *Arthritis Research & Therapy,* 9**,** 223.

MURRAY, R., SMITH, R., HENSON, F. & GOODSHIP, A. 2001. The distribution of cartilage oligomeric matrix protein (COMP) in equine carpal articular cartilage and its variation with exercise and cartilage deterioration. *The Veterinary Journal,* 162**,** 121-128.

MUSHTAQ, S., CHOUDHARY, R. & SCANZELLO, C. R. 2011. Non-surgical treatment of osteoarthritis-related pain in the elderly. *Current reviews in musculoskeletal medicine***,** 1-10.

MYERS, S., BRANDT, K., EHLICH, J., BRAUNSTEIN, E., SHELBOURNE, K., HECK, D. & KALASINSKI, L. 1990. Synovial inflammation in patients with early osteoarthritis of the knee. *The Journal of rheumatology,* 17**,** 1662.

NADIMPALLI, R., YALPANI, N., JOHAL, G. S. & SIMMONS, C. R. 2000. Prohibitins, stomatins, and plant disease response genes compose a protein superfamily that controls cell proliferation, ion channel regulation, and death. *Journal of Biological Chemistry,* 275**,** 29579-29586.

NAIKI, Y., MICHELSEN, K. S., ZHANG, W., CHEN, S., DOHERTY, T. M. & ARDITI, M. 2005. Transforming growth factor-β differentially inhibits MyD88-dependent, but not TRAM-and TRIF-dependent, lipopolysaccharide-induced TLR4 signaling. *Journal of Biological Chemistry,* 280**,** 5491.

NAIR, A., KANDA, V., BUSH-JOSEPH, C., VERMA, N., CHUBINSKAYA, S., MIKECZ, K., GLANT, T. T., MALFAIT, A.-M., CROW, M. K., SPEAR, G. T., FINNEGAN, A. & SCANZELLO, C. R. 2012. Synovial fluid from patients with early osteoarthritis modulates fibroblast-like synoviocyte responses to TLR-4 and TLR-2 ligands via soluble CD14. *Arthritis & Rheumatism***.**

NAKAE, S., SAIJO, S., HORAI, R., SUDO, K., MORI, S. & IWAKURA, Y. 2003. IL-17 production from activated T cells is required for the spontaneous development of destructive arthritis in mice deficient in IL-1 receptor antagonist. *Proceedings of the National Academy of Sciences of the United States of America,* 100**,** 5986.

NAKAMURA, H., YOSHINO, S., KATO, T., TSURUHA, J. & NISHIOKA, K. 1999. T-cell mediated inflammatory pathway in osteoarthritis. *Osteoarthritis and Cartilage,* 7**,** 401-402.

NARASIMHAN, J., POTTER, J. L. & HAAS, A. L. 1996. Conjugation of the 15-kDa

interferon-induced ubiquitin homolog is distinct from that of ubiquitin. *Journal of Biological Chemistry,* 271**,** 324.

NEIDHART, M., SEEMAYER, C. A., HUMMEL, K. M., MICHEL, B. A., GAY, R. E. & GAY, S. 2003. Functional characterization of adherent synovial fluid cells in rheumatoid arthritis: destructive potential in vitro and in vivo. *Arthritis & Rheumatism,* 48**,** 1873-1880.

NEUHOFF, V., AROLD, N., TAUBE, D. & EHRHARDT, W. 1988. Improved staining of proteins in polyacrylamide gels including isoelectric focusing gels with clear background at nanogram sensitivity using Coomassie Brilliant Blue G-250 and R-250. *Electrophoresis,* 9**,** 255-262.

NIE, S., KEE, Y. & BRONNER-FRASER, M. 2011. Caldesmon regulates actin dynamics to influence cranial neural crest migration in Xenopus. *Molecular Biology of the Cell,* 22**,** 3355-3365.

NIISSALO, S., HUKKANEN, M., IMAI, S., TÖRNWALL, J. & KONTTINEN, Y. T. 2002. Neuropeptides in experimental and degenerative arthritis. *Annals of the New York Academy of Sciences,* 966**,** 384-399.

NISHIMOTO, N. & KISHIMOTO, T. 2006. Interleukin 6: from bench to bedside. *Nature clinical practice rheumatology,* 2**,** 619-626.

NISHIMOTO, N., TERAO, K., MIMA, T., NAKAHARA, H., TAKAGI, N. & KAKEHI, T. 2008. Mechanisms and pathologic significances in increase in serum interleukin-6 (IL-6) and soluble IL-6 receptor after administration of an anti–IL-6 receptor antibody, tocilizumab, in patients with rheumatoid arthritis and Castleman disease. *Blood,* 112**,** 3959.

NOPPERT, S. J., FITZGERALD, K. A. & HERTZOG, P. J. 2007. The role of type I interferons in TLR responses. *Immunology and cell biology,* 85**,** 446-457.

NØRREGAARD JENSEN, O. 2004. Modification-specific proteomics: characterization of post-translational modifications by mass spectrometry. *Current opinion in chemical biology,* 8**,** 33-41.

NOSS, E. H. & BRENNER, M. B. 2008. The role and therapeutic implications of fibroblast-like synoviocytes in inflammation and cartilage erosion in rheumatoid arthritis. *Immunological reviews,* 223**,** 252-270.

NÚÑEZ MIGUEL, R., WONG, J., WESTOLL, J. F., BROOKS, H. J., O'NEILL, L., GAY, N. J., BRYANT, C. E. & MONIE, T. P. 2007. A dimer of the Toll-like receptor 4 cytoplasmic domain provides a specific scaffold for the recruitment of signalling adaptor proteins. *PloS one,* 2**,** e788.

OHASHI, K., BURKART, V., FLOHÉ, S. & KOLB, H. 2000. Cutting edge: heat shock protein 60 is a putative endogenous ligand of the toll-like receptor-4 complex. *The Journal of Immunology,* 164**,** 558.

OJANIEMI, M., LILJEROOS, M., HARJU, K., SORMUNEN, R., VUOLTEENAHO, R. & HALLMAN, M. 2006. TLR-2 is upregulated and mobilized to the hepatocyte plasma membrane in the space of Disse and to the Kupffer cells TLR-4 dependently during acute

endotoxemia in mice. *Immunology letters,* 102**,** 158-168.

OKAMURA, Y., WATARI, M., JERUD, E. S., YOUNG, D. W., ISHIZAKA, S. T., ROSE, J., CHOW, J. C. & STRAUSS III, J. F. 2001. The extra domain A of fibronectin activates Toll-like receptor 4. *Journal of Biological Chemistry,* 276**,** 10229-10233.

O'NEILL, L. A. J. & BOWIE, A. G. 2007. The family of five: TIR-domain-containing adaptors in Toll-like receptor signalling. *Nature Reviews Immunology,* 7**,** 353-364.

O'NEILL, L. A. J. & DINARELLO, C. A. 2000. The IL-1 receptor/toll-like receptor superfamily: crucial receptors for inflammation and host defense. *Immunology today,* 21**,** 206-209.

O'NEILL, L. A. J., FITZGERALD, K. A. & BOWIE, A. G. 2003. The Toll-IL-1 receptor adaptor family grows to five members. *Trends in immunology,* 24**,** 286-289.

OPPENHEIM, J. D., NACHBAR, M. S., BHARDWAJ, N. & WEXLER, H. 1981. Mitogenic and adjuvant properties of the LPS-like component of Listeria monocytogenes. *FEMS Microbiology Letters,* 10**,** 25-28.

OSHIUMI, H., SASAI, M., SHIDA, K., FUJITA, T., MATSUMOTO, M. & SEYA, T. 2003. TIR-containing adapter molecule (TICAM)-2, a bridging adapter recruiting to Toll-like receptor 4 TICAM-1 that induces interferon-β. *Journal of Biological Chemistry,* 278**,** 49751-49762.

OSPELT, C., BRENTANO, F., JÜNGEL, A., RENGEL, Y., KOLLING, C., MICHEL, B. A., GAY, R. E. & GAY, S. 2009. Expression, regulation, and signaling of the pattern-recognition receptor nucleotide-binding oligomerization domain 2 in rheumatoid arthritis synovial fibroblasts. *Arthritis & Rheumatism,* 60**,** 355-363.

OSPELT, C., BRENTANO, F., RENGEL, Y., STANCZYK, J., KOLLING, C., TAK, P. P., GAY, R. E., GAY, S. & KYBURZ, D. 2008. Overexpression of toll-like receptors 3 and 4 in synovial tissue from patients with early rheumatoid arthritis: Toll-like receptor expression in early and longstanding arthritis. *Arthritis & Rheumatism,* 58**,** 3684-3692.

OSPELT, C. & GAY, S. 2008. The role of resident synovial cells in destructive arthritis. *Best Practice & Research Clinical Rheumatology,* 22**,** 239-252.

OSPELT, C., NEIDHART, M., GAY, R. E. & GAY, S. 2004. Synovial activation in rheumatoid arthritis. *Front Biosci,* 9**,** 2323-2334.

OVERALL, C. M. & LÓPEZ-OTÍN, C. 2002. Strategies for MMP inhibition in cancer: innovations for the post-trial era. *Nature Reviews Cancer,* 2**,** 657-672.

OZAWA, T., KOYAMA, K., ANDO, T., OHNUMA, Y., HATSUSHIKA, K., OHBA, T., SUGIYAMA, H., HAMADA, Y., OGAWA, H. & OKUMURA, K. 2007. Thymic stromal lymphopoietin secretion of synovial fibroblasts is positively and negatively regulated by Toll-like receptors/nuclear factor-κB pathway and interferon-γ/dexamethasone. *Modern Rheumatology,* 17**,** 459-463.

PAP, T., MÜLLER-LADNER, U., GAY, R. E. & GAY, S. 2000. Fibroblast biology: role of

synovial fibroblasts in the pathogenesis of rheumatoid arthritis. *Arthritis Research & Therapy,* 2**,** 361.

PATRA, D. & SANDELL, L. J. 2011. Recent advances in biomarkers in osteoarthritis. *Current opinion in rheumatology,* 23**,** 465.

PAULI, C., GROGAN, S., PATIL, S., OTSUKI, S., HASEGAWA, A., KOZIOL, J., LOTZ, M. & D'LIMA, D. 2011. Macroscopic and histopathologic analysis of human knee menisci in aging and osteoarthritis. *Osteoarthritis and Cartilage*.

PEARLE, A., SCANZELLO, C., GEORGE, S., MANDL, L., DICARLO, E., PETERSON, M., SCULCO, T. & CROW, M. 2007. Elevated high-sensitivity C-reactive protein levels are associated with local inflammatory findings in patients with osteoarthritis1. *Osteoarthritis and cartilage,* 15**,** 516-523.

PELLETIER, J., MCCOLLUM, R., CLOUTIER, J. & MARTEL-PELLETIER, J. 1995. Synthesis of metalloproteases and interleukin 6 (IL-6) in human osteoarthritic synovial membrane is an IL-1 mediated process. *The Journal of rheumatology. Supplement,* 43**,** 109.

PELLETIER, J. P., CARON, J. P., EVANS, C., ROBBINS, P. D., GEORGESCU, H. I., JOVANOVIC, D., FERNANDES, J. C. & MARTEL-PELLETIER, J. 1997. In vivo suppression of early experimental osteoarthritis by interleukin-1 receptor antagonist using gene therapy. *Arthritis & Rheumatism,* 40**,** 1012-1019.

PELLETIER, J. P., MARTEL-PELLETIER, J. & ABRAMSON, S. B. 2001. Osteoarthritis, an inflammatory disease: potential implication for the selection of new therapeutic targets. *Arthritis & Rheumatism,* 44**,** 1237-1247.

PENG, X., MEHTA, R., WANG, S., CHELLAPPAN, S. & MEHTA, R. G. 2006. Prohibitin is a novel target gene of vitamin D involved in its antiproliferative action in breast cancer cells. *Cancer research,* 66**,** 7361.

PENNINGTON, K., COTTER, D. & DUNN, M. 2005. The role of proteomics in investigating psychiatric disorders. *The British Journal of Psychiatry,* 187**,** 4-6.

PERLMAN, H., PAGLIARI, L. J. & VOLIN, M. V. 2001. Regulation of apoptosis and cell cycle activity in rheumatoid arthritis. *Current Molecular Medicine,* 1**,** 597-608.

PETERSSON, I. F., BOEGÅRD, T., SAXNE, T., SILMAN, A. J. & SVENSSON, B. 1997. Radiographic osteoarthritis of the knee classified by the Ahlbäck and Kellgren & Lawrence systems for the tibiofemoral joint in people aged 35–54 years with chronic knee pain. *Annals of the rheumatic diseases,* 56**,** 493.

PETIT-ZEMAN, S. 2004. Characteristics of COX2 inhibitors questioned. *Nat Rev Drug Discov,* 3**,** 726-726.

PIA A.J, H. 1997. Caldesmon. *The International Journal of Biochemistry & Cell Biology,* 29**,** 1047-1051.

PISETSKY, D. S., GAULEY, J. & ULLAL, A. J. 2011. HMGB1 and Microparticles as Mediators of the Immune Response to Cell Death. *Antioxidants & Redox Signaling,* 15**,** 2209-2219.

PLATT, N., DA SILVA, R. P. & GORDON, S. 1998. Recognizing death: the phagocytosis of apoptotic cells. *Trends in cell biology,* 8**,** 365-372.

PLATTNER, F., YAROVINSKY, F., ROMERO, S., DIDRY, D., CARLIER, M. F., SHER, A. & SOLDATI-FAVRE, D. 2008. Toxoplasma Profilin Is Essential for Host Cell Invasion and TLR11-Dependent Induction of an Interleukin-12 Response. *Cell host & microbe,* 3**,** 77-87.

POLLARD, T. D. & BORISY, G. G. 2003. Cellular motility driven by assembly and disassembly of actin filaments. *Cell,* 112**,** 453-465.

POMERANTZ, J. L. & BALTIMORE, D. 2002. Two pathways to NF-[kappa] B. *Molecular cell,* 10**,** 693-695.

POSTEL, E., BERBERICH, S., FLINT, S. & FERRONE, C. 1993. Human c-myc transcription factor PuF identified as nm23-H2 nucleoside diphosphate kinase, a candidate suppressor of tumor metastasis. *Science,* 261**,** 478.

PRESLE, N., POTTIE, P., DUMOND, H., GUILLAUME, C., LAPICQUE, F., PALLU, S., MAINARD, D., NETTER, P. & TERLAIN, B. 2006. Differential distribution of adipokines between serum and synovial fluid in patients with osteoarthritis. Contribution of joint tissues to their articular production. *Osteoarthritis and Cartilage,* 14**,** 690-695.

PROOST, P., VYNCKIER, A. K., MAHIEU, F., PUT, W., GRILLET, B., STRUYF, S., WUYTS, A., OPDENAKKER, G. & DAMME, J. V. 2003. Microbial Toll-like receptor ligands differentially regulate CXCL10/IP-10 expression in fibroblasts and mononuclear leukocytes in synergy with IFN-γ and provide a mechanism for enhanced synovial chemokine levels in septic arthritis. *European journal of immunology,* 33**,** 3146-3153.

PULAI, J. I., CHEN, H., IM, H. J., KUMAR, S., HANNING, C., HEGDE, P. S. & LOESER, R. F. 2005. NF-κB mediates the stimulation of cytokine and chemokine expression by human articular chondrocytes in response to fibronectin fragments. *The Journal of immunology,* 174**,** 5781.

PULSATELLI, L., DOLZANI, P., PIACENTINI, A., SILVESTRI, T., RUGGERI, R., GUALTIERI, G., MELICONI, R. & FACCHINI, A. 1999. Chemokine production by human chondrocytes. *The Journal of rheumatology,* 26**,** 1992.

PUNZI, L., OLIVIERO, F. & RAMONDA, R. 2010. New horizons in osteoarthritis. *Swiss Medical Weekly,* 140**,** 16-22.

QU, Z., GARCIA, C. H., O'ROURKE, L. M., PLANCK, S. R., KOHLI, M. & ROSENBAUM, J. T. 1994. Local Proliferation of Fibroblast-Like Synoviocytes Contributes to Synovial Hyperplasia. *Arthritis & Rheumatism,* 37**,** 212-220.

QUIVY, V. & VAN LINT, C. 2004. Regulation at multiple levels of NF-[kappa] B-mediated transactivation by protein acetylation. *Biochemical pharmacology,* 68**,** 1221-1229.

RABINOVICH, G. A., DALY, G., DREJA, H., TAILOR, H., RIERA, C. M., HIRABAYASHI, J. & CHERNAJOVSKY, Y. 1999. Recombinant galectin-1 and its genetic delivery suppress collagen-induced arthritis via T cell apoptosis. *The Journal of*

experimental medicine, 190**,** 385.

RABINOVICH, G. A., RUBINSTEIN, N. & TOSCANO, M. A. 2002. Role of galectins in inflammatory and immunomodulatory processes. *Biochimica et Biophysica Acta (BBA)-General Subjects,* 1572**,** 274-284.

RADSTAKE, T. R. D. J., ROELOFS, M. F., JENNISKENS, Y. M., OPPERS-WALGREEN, B., VAN RIEL, P. L. C. M., BARRERA, P., JOOSTEN, L. A. B. & VAN DEN BERG, W. B. 2004. Expression of Toll-like receptors 2 and 4 in rheumatoid synovial tissue and regulation by proinflammatory cytokines interleukin-12 and interleukin-18 via interferon-γ. *Arthritis & Rheumatism,* 50**,** 3856-3865.

RAHBAR, A., RIVERS, R., BOJA, E., KINSINGER, C., MESRI, M., HILTKE, T. & RODRIGUEZ, H. 2011. Realizing individualized medicine: the road to translating proteomics from the laboratory to the clinic. *Personalized Medicine,* 8**,** 45-57.

RAQUEL, R., PILAR, T., FERNANDO, M., EMILIO, C. & ENRIQUE, C. 2008. Differential proteome of articular chondrocytes from patients with osteoarthritis. *J Proteomics Bioinform,* 1**,** 267-280.

RAYCHAUDHURI, S. & RAYCHAUDHURI, S. 2009. The regulatory role of nerve growth factor and its receptor system in fibroblast-like synovial cells. *Scandinavian journal of rheumatology,* 38**,** 207-215.

RIFKIN, I. R., LEADBETTER, E. A., BUSCONI, L., VIGLIANTI, G. & MARSHAK-ROTHSTEIN, A. 2005. Toll-like receptors, endogenous ligands, and systemic autoimmune disease. *Immunological reviews,* 204**,** 27-42.

RIFKIN, I. R., LEADBETTER, E. A., BUSCONI, L., VIGLIANTI, G. & MARSHAK-ROTHSTEIN, A. 2005. Toll-like receptors, endogenous ligands, and systemic autoimmune disease. *Immunological reviews,* 204**,** 27-42.

RITCHLIN, C. 2000. Fibroblast biology: effector signals released by the synovial fibroblast in arthritis. *Arthritis Research & Therapy,* 2**,** 356.

RODRIGUEZ, A. S., ESPINA, B. H., ESPINA, V. & LIOTTA, L. A. 2008. Automated laser capture microdissection for tissue proteomics. *analysis,* 25**,** 26.

ROELOFS, M., WENINK, M., BRENTANO, F., ABDOLLAHI-ROODSAZ, S., OPPERS-WALGREEN, B., BARRERA, P., VAN RIEL, P., KYBURZ, D., VAN DEN BERG, W. & RADSTAKE, T. 2009. Type I interferons might form the link between Toll-like receptor (TLR) 3/7 and TLR4-mediated synovial inflammation in rheumatoid arthritis (RA). *Annals of the rheumatic diseases,* 68**,** 1486-1493.

ROELOFS, M. F., ABDOLLAHI-ROODSAZ, S., JOOSTEN, L. A. B., VAN DEN BERG, W. B. & RADSTAKE, T. R. D. J. 2008. The orchestra of toll-like receptors and their potential role in frequently occurring rheumatic conditions. *Arthritis & Rheumatism,* 58**,** 338-348.

ROELOFS, M. F., BOELENS, W. C., JOOSTEN, L. A. B., ABDOLLAHI-ROODSAZ, S., GEURTS, J., WUNDERINK, L. U., SCHREURS, B. W., VAN DEN BERG, W. B. & RADSTAKE, T. R. D. J. 2006. Identification of small heat shock protein B8 (HSP22) as a

novel TLR4 ligand and potential involvement in the pathogenesis of rheumatoid arthritis. *The Journal of immunology,* 176**,** 7021.

ROGERS, S., GIROLAMI, M., KOLCH, W., WATERS, K. M., LIU, T., THRALL, B. & WILEY, H. S. 2008. Investigating the correspondence between transcriptomic and proteomic expression profiles using coupled cluster models. *Bioinformatics,* 24**,** 2894-2900.

ROLLÍN, R., MARCO, F., CAMAFEITA, E., CALVO, E., LÓPEZ-DURÁN, L., JOVER, J. Á., LÓPEZ, J. & FERNÁNDEZ-GUTIÉRREZ, B. 2008. Differential proteome of bone marrow mesenchymal stem cells from osteoarthritis patients1. *Osteoarthritis and Cartilage,* 16**,** 929-935.

ROSENBACH, T. O., MOSHONOV, S., ZOR, U. & YARON, M. 1984. Interferon triggers experimental synovitis and may potentiate auto-immune disease in humans. *Clinical rheumatology,* 3**,** 361-364.

ROWE, D. C., MCGETTRICK, A. F., LATZ, E., MONKS, B. G., GAY, N. J., YAMAMOTO, M., AKIRA, S., O'NEILL, L. A., FITZGERALD, K. A. & GOLENBOCK, D. T. 2006. The myristoylation of TRIF-related adaptor molecule is essential for Toll-like receptor 4 signal transduction. *PNAS,* 103**,** 6299-6304.

RUHMANN, M., PICCININI, A. M., KONG, P. L. & MIDWOOD, K. S. 2012. Endogenous activation of adaptive immunity: Tenascin-C drives IL-17 synthesis in arthritic joint disease. *Arthritis & Rheumatism***,** n/a-n/a.

RUIZ-ROMERO, C. & BLANCO, F. 2010. Proteomics role in the search for improved diagnosis, prognosis and treatment of osteoarthritis. *Osteoarthritis and Cartilage,* 18**,** 500-509.

RUIZ-ROMERO, C. & BLANCO, F. J. 2009. The role of proteomics in osteoarthritis pathogenesis research. *Current drug targets,* 10**,** 543-556.

RUIZ-ROMERO, C., CALAMIA, V., MATEOS, J., CARREIRA, V., MARTÍNEZ-GOMARIZ, M., FERNÁNDEZ, M. & BLANCO, F. J. 2009. Mitochondrial dysregulation of osteoarthritic human articular chondrocytes analyzed by proteomics. *Molecular & Cellular Proteomics,* 8**,** 172-189.

RUIZ-ROMERO, C., CARREIRA, V., REGO, I., REMESEIRO, S., LÓPEZ-ARMADA, M. J. & BLANCO, F. J. 2008. Proteomic analysis of human osteoarthritic chondrocytes reveals protein changes in stress and glycolysis. *Proteomics,* 8**,** 495-507.

RUIZ-ROMERO, C., LÓPEZ-ARMADA, M. J. & BLANCO, F. J. 2005. Proteomic characterization of human normal articular chondrocytes: a novel tool for the study of osteoarthritis and other rheumatic diseases. *Proteomics,* 5**,** 3048-3059.

RUTH, J. H., HAAS, C. S., PARK, C. C., AMIN, M. A., MARTINEZ, R. J., HAINES III, G. K., SHAHRARA, S., CAMPBELL, P. L. & KOCH, A. E. 2006. CXCL16-mediated cell recruitment to rheumatoid arthritis synovial tissue and murine lymph nodes is dependent upon the MAPK pathway. *Arthritis & Rheumatism,* 54**,** 765-778.

SACRE, S. M., ANDREAKOS, E., KIRIAKIDIS, S., AMJADI, P., LUNDBERG, A., GIDDINS, G., FELDMANN, M., BRENNAN, F. & FOXWELL, B. M. 2007. The Toll-like receptor adaptor proteins MyD88 and Mal/TIRAP contribute to the inflammatory and destructive processes in a human model of rheumatoid arthritis. *The American journal of pathology,* 170**,** 518.

SADOUK, M. B., PELLETIER, J. P., TARDIF, G., KIANSA, K., CLOUTIER, J. M. & MARTEL-PELLETIER, J. 1995. Human synovial fibroblasts coexpress IL-1 receptor type I and type II mRNA. The increased level of the IL-1 receptor in osteoarthritic cells is related to an increased level of the type I receptor. *Laboratory investigation; a journal of technical methods and pathology,* 73**,** 347.

SAETAN, N., HONSAWEK, S., TANAVALEE, A., TANTAVISUT, S., YUKTANANDANA, P. & PARKPIAN, V. 2011. Association of Plasma and Synovial Fluid Interferon-[gamma] Inducible Protein-10 with Radiographic Severity in Knee Osteoarthritis. *Clinical Biochemistry*.

SAKAGUCHI, M. & HUH, N. 2011. S100A11, a dual growth regulator of epidermal keratinocytes. *Amino acids***,** 1-11.

SAKKAS, L. I., SCANZELLO, C., JOHANSON, N., BURKHOLDER, J., MITRA, A., SALGAME, P., KATSETOS, C. D. & PLATSOUCAS, C. D. 1998. T cells and T-cell cytokine transcripts in the synovial membrane in patients with osteoarthritis. *Clinical and diagnostic laboratory immunology,* 5**,** 430-437.

SALLUSTO, F. & LANZAVECCHIA, A. 2002. The instructive role of dendritic cells on T-cell responses. *Arthritis Research & Therapy,* 4**,** S127.

SAMUEL, C. E. 2001. Antiviral actions of interferons. *Clinical microbiology reviews,* 14**,** 778.

SAMUELS, J., KRASNOKUTSKY, S. & ABRAMSON, S. B. 2008. A Tale of Three Tissues. *Bulletin of the NYU hospital for joint diseases,* 66**,** 244-50.

SANCHEZ-PERNAUTE, O., BRENTANO, F., OSPELT, C., KOLLING, C., MICHEL, B., GAY, R., HERRERO-BEAUMONT, G., GAY, S. & GRIGORIAN, M. 2007. Fibrin triggers an innate immune response in rheumatoid arthritis synovial fibroblasts acting as an endogenous ligand of Toll like receptor 4. *Arthritis Rheum,* 56.

SANDY, J. 2006. A contentious issue finds some clarity: on the independent and complementary roles of aggrecanase activity and MMP activity in human joint aggrecanolysis. *Osteoarthritis and Cartilage,* 14**,** 95-100.

SARMA, J. V. & WARD, P. A. 2011. The complement system. *Cell and Tissue Research***,** 1-9.

SATO, M., SUEMORI, H., HATA, N., ASAGIRI, M., OGASAWARA, K., NAKAO, K., NAKAYA, T., KATSUKI, M., NOGUCHI, S. & TANAKA, N. 2000. Distinct and essential roles of transcription factors IRF-3 and IRF-7 in response to viruses for IFN-[alpha]/[beta] gene induction. *Immunity,* 13**,** 539-548.

SATO, S., SANJO, H., TAKEDA, K., NINOMIYA-TSUJI, J., YAMAMOTO, M.,

KAWAI, T., MATSUMOTO, K., TAKEUCHI, O. & AKIRA, S. 2005. Essential function for the kinase TAK1 in innate and adaptive immune responses. *nature immunology*, 6**,** 1087-1095.

SATO, S., SUGIYAMA, M., YAMAMOTO, M., WATANABE, Y., KAWAI, T., TAKEDA, K. & AKIRA, S. 2003. Toll/IL-1 receptor domain-containing adaptor inducing IFN-β (TRIF) associates with TNF receptor-associated factor 6 and TANK-binding kinase 1, and activates two distinct transcription factors, NF-κB and IFN-regulatory factor-3, in the Toll-like receptor signaling. *The Journal of immunology*, 171**,** 4304.

SAUTER, B., ALBERT, M. L., FRANCISCO, L., LARSSON, M., SOMERSAN, S. & BHARDWAJ, N. 2000. Consequences of cell death. *The Journal of experimental medicine*, 191**,** 423-434.

SCANZELLO, C., UMOH, E., PESSLER, F., DIAZ-TORNE, C., MILES, T., DICARLO, E., POTTER, H., MANDL, L., MARX, R. & RODEO, S. 2009. Local cytokine profiles in knee osteoarthritis: elevated synovial fluid interleukin-15 differentiates early from end-stage disease. *Osteoarthritis and cartilage*, 17**,** 1040-1048.

SCANZELLO, C. R., MCKEON, B., SWAIM, B. H., DICARLO, E., ASOMUGHA, E. U., KANDA, V., NAIR, A., LEE, D. M., RICHMOND, J. C. & KATZ, J. N. 2011. Synovial inflammation in patients undergoing arthroscopic meniscectomy: molecular characterization and relationship to symptoms. *Arthritis & Rheumatism*, 63**,** 391-400.

SCANZELLO, C. R., NAIR, A., KANDA, V., BUSH-JOSEPH, C., VERMA, N., CROW, M. K., MIKECZ, K., GLANT, T., SPEAR, G. T. & FINNEGAN, A. 2011. Soluble CD14 in synovial fluid from patients with OA and meniscal injury modulates the response of synovial fibroblasts to LPS. *Annals of the rheumatic diseases*, 70**,** A34-A35.

SCANZELLO, C. R., PLAAS, A. & CROW, M. K. 2008. Innate immune system activation in osteoarthritis: is osteoarthritis a chronic wound? *Current opinion in rheumatology*, 20**,** 565.

SCHARSCHMIDT, T., JACQUET, R., LASKOVSKI, J., LOWDER, E., WEINER, S. & LANDIS, W. J. 2007. Analysis of human osteoarthritic connective tissue by laser capture microdissection and QRT-PCR. *Connective tissue research*, 48**,** 316-323.

SCHEIBNER, K. A., LUTZ, M. A., BOODOO, S., FENTON, M. J., POWELL, J. D. & HORTON, M. R. 2006. Hyaluronan fragments act as an endogenous danger signal by engaging TLR2. *The Journal of Immunology*, 177**,** 1272.

SCHINDLER, C. & BRUTSAERT, S. 1999. Interferons as a paradigm for cytokine signal transduction. *Cellular and molecular life sciences*, 55**,** 1509-1522.

SCHLAAK, J., PFERS, I., MEYER, Z. B. K. H. & MÄRKER-HERMANN, E. 1996. Different cytokine profiles in the synovial fluid of patients with osteoarthritis, rheumatoid arthritis and seronegative spondylarthropathies. *Clinical and experimental rheumatology*, 14**,** 155.

SCHMIDT, A., SCHWERD, T., HAMM, W., HELLMUTH, J. C., CUI, S., WENZEL, M., HOFFMANN, F. S., MICHALLET, M. C., BESCH, R. & HOPFNER, K. P. 2009. 5′-

triphosphate RNA requires base-paired structures to activate antiviral signaling via RIG-I. *Proceedings of the National Academy of Sciences,* 106**,** 12067-12072.

SCHOENEMEYER, A., BARNES, B. J., MANCL, M. E., LATZ, E., GOUTAGNY, N., PITHA, P. M., FITZGERALD, K. A. & GOLENBOCK, D. T. 2005. The interferon regulatory factor, IRF5, is a central mediator of toll-like receptor 7 signaling. *Journal of Biological Chemistry,* 280**,** 17005.

SCHROMM, A. B., BRANDENBURG, K., RIETSCHEL, E. T., FLAD, H. D., CARROLL, S. F. & SEYDEL, U. 1996. Lipopolysaccharide-binding protein mediates CD14-independent intercalation of lipopolysaccharide into phospholipid membranes. *FEBS letters,* 399**,** 267-271.

SCHULTE, E., FISSELER-ECKHOFF, A. & MÜLLER, K. 1994. [Differential diagnosis of synovitis. Correlation of arthroscopic-biopsy to clinical findings]. *Der Pathologe,* 15**,** 22
.
SCHUMANN, R. R., RIETSCHEL, E. T. & LOPPNOW, H. 1994. The role of CD14 and lipopolysaccharide-binding protein (LBP) in the activation of different cell types by endotoxin. *Medical microbiology and immunology,* 183**,** 279-297.

SCHURMAN, D. J. & SMITH, R. L. 2004. Osteoarthritis: current treatment and future prospects for surgical, medical, and biologic intervention. *Clinical Orthopaedics and Related Research,* 427**,** S183.

SEARLE, J., KERR, J. & BISHOP, C. 1982. Necrosis and apoptosis: distinct modes of cell death with fundamentally different significance. *Pathology annual,* 17**,** 229.

SEEMAYER, C. A., KUCHEN, S., KUENZLER, P., ŘIHOŠKOVÁ, V., RETHAGE, J., AICHER, W. K., MICHEL, B. A., GAY, R. E., KYBURZ, D. & NEIDHART, M. 2003. Cartilage destruction mediated by synovial fibroblasts does not depend on proliferation in rheumatoid arthritis. *The American journal of pathology,* 162**,** 1549.

SEIBL, R., BIRCHLER, T., LOELIGER, S., HOSSLE, J. P., GAY, R. E., SAURENMANN, T., MICHEL, B. A., SEGER, R. A., GAY, S. & LAUENER, R. P. 2003. Expression and regulation of Toll-like receptor 2 in rheumatoid arthritis synovium. *The American journal of pathology,* 162**,** 1221.

SELLAM, J. & BERENBAUM, F. 2010. The role of synovitis in pathophysiology and clinical symptoms of osteoarthritis. *Nat Rev Rheumatol,* 6**,** 625-635.

SELLATI, T. J., BOUIS, D. A., KITCHENS, R. L., DARVEAU, R. P., PUGIN, J., ULEVITCH, R. J., GANGLOFF, S. C., GOYERT, S. M., NORGARD, M. V. & RADOLF, J. D. 1998. Treponema pallidum and Borrelia burgdorferi lipoproteins and synthetic lipopeptides activate monocytic cells via a CD14-dependent pathway distinct from that used by lipopolysaccharide. *The Journal of immunology,* 160**,** 5455.

SEN, G. C. & SARKAR, S. N. 2005. Transcriptional signaling by double-stranded RNA: role of TLR3. *Cytokine & Growth Factor Reviews,* 16**,** 1-14.

SEN, R. & BALTIMORE, D. 1986. Inducibility of [kappa] immunoglobulin enhancer-binding protein NF-[kappa] B by a posttranslational mechanism. *Cell,* 47**,** 921-928.

SHA, W. C., LIOU, H. C., TUOMANEN, E. I. & BALTIMORE, D. 1995. Targeted disruption of the p50 subunit of NF-κB leads to multifocal defects in immune responses. *Cell,* 80**,** 321-330.

SHARMA, A. & QADRI, A. 2004. Vi polysaccharide of Salmonella typhi targets the prohibitin family of molecules in intestinal epithelial cells and suppresses early inflammatory responses. *Proceedings of the National Academy of Sciences of the United States of America,* 101**,** 17492.

SHEVCHENKO, A., HENRIK TOMAS, J. H., OLSEN, J. V. & MANN, M. 2007. In-gel digestion for mass spectrometric characterization of proteins and proteomes. *Nature protocols,* 1**,** 2856-2860.

SHI, K., HAYASHIDA, K., KANEKO, M., HASHIMOTO, J., TOMITA, T., LIPSKY, P. E., YOSHIKAWA, H. & OCHI, T. 2001. Lymphoid chemokine B cell-attracting chemokine-1 (CXCL13) is expressed in germinal center of ectopic lymphoid follicles within the synovium of chronic arthritis patients. *The Journal of immunology,* 166**,** 650.

SHIBAKAWA, A., AOKI, H., MASUKO-HONGO, K., KATO, T., TANAKA, M., NISHIOKA, K. & NAKAMURA, H. 2003. Presence of pannus-like tissue on osteoarthritic cartilage and its histological character. *Osteoarthritis and Cartilage,* 11**,** 133-140.

SHIMAZU, R., AKASHI, S., OGATA, H., NAGAI, Y., FUKUDOME, K., MIYAKE, K. & KIMOTO, M. 1999. MD-2, a molecule that confers lipopolysaccharide responsiveness on Toll-like receptor 4. *The Journal of experimental medicine,* 189**,** 1777-1782.

SHIRALI, A. C. & GOLDSTEIN, D. R. 2008. Activation of the innate immune system by the endogenous ligand hyaluronan. *Current opinion in organ transplantation,* 13**,** 20.

SIEDNIENKO, J., GAJANAYAKE, T., FITZGERALD, K. A., MOYNAGH, P. & MIGGIN, S. M. 2011. Absence of MyD88 Results in Enhanced TLR3-Dependent Phosphorylation of IRF3 and Increased IFN-β and RANTES Production. *The Journal of immunology,* 186**,** 2514.

SIEDNIENKO, J., HALLE, A., NAGPAL, K., GOLENBOCK, D. T. & MIGGIN, S. M. 2010. TLR3-mediated IFN-β gene induction is negatively regulated by the TLR adaptor MyD88 adaptor-like. *European Journal of Immunology,* 40**,** 3150-3160.

SIEDNIENKO, J., MARATHA, A., YANG, S., MITKIEWICZ, M., MIGGIN, S. M. & MOYNAGH, P. N. 2011. The NF-κB subunits RelB and cRel negatively regulate TLR3-mediated IFN-β production via induction of the transcriptional repressor protein YY1. *Journal of Biological Chemistry*.

SILVERSTEIN, F. E., FAICH, G., GOLDSTEIN, J. L., SIMON, L. S., PINCUS, T., WHELTON, A., MAKUCH, R., EISEN, G., AGRAWAL, N. M. & STENSON, W. F. 2000. Gastrointestinal toxicity with celecoxib vs nonsteroidal anti-inflammatory drugs for osteoarthritis and rheumatoid arthritis. *JAMA: the journal of the American Medical Association,* 284**,** 1247.

SMITH, K. J., BERTONE, A. L., WEISBRODE, S. E. & RADMACHER, M. 2006. Gross, histologic, and gene expression characteristics of osteoarthritic articular cartilage of the metacarpal condyle of horses. *American journal of veterinary research,* 67**,** 1299-1306.

SMITH, M., TRIANTAFILLOU, S., PARKER, A., YOUSSEF, P. & COLEMAN, M. 1997. Synovial membrane inflammation and cytokine production in patients with early osteoarthritis. *The Journal of rheumatology,* 24**,** 365.

SMITH, M. D., TRIANTAFILLOU, S., PARKER, A., YOUSSEF, P. P. & COLEMAN, M. 1997. Synovial membrane inflammation and cytokine production in patients with early osteoarthritis. *Journal of Rheumatology,* 24**,** 365-371.

SMOLEN, J. S., BEAULIEU, A., RUBBERT-ROTH, A., RAMOS-REMUS, C., ROVENSKY, J., ALECOCK, E., WOODWORTH, T. & ALTEN, R. 2008. Effect of interleukin-6 receptor inhibition with tocilizumab in patients with rheumatoid arthritis (OPTION study): a double-blind, placebo-controlled, randomised trial. *The Lancet,* 371**,** 987-997.

SOMARELLI, J., MESA, A., RODRIGUEZ, R., AVELLAN, R., MARTINEZ, L., ZANG, Y., GREIDINGER, E. & HERRERA, R. 2011. Epitope mapping of the U1 small nuclear ribonucleoprotein particle in patients with systemic lupus erythematosus and mixed connective tissue disease. *Lupus,* 20**,** 274.

SPECTOR, T., HART, D., NANDRA, D., DOYLE, D., MACKILLOP, N., GALLIMORE, J. & PEPYS, M. 1997. Low-level increases in serum C-reactive protein are present in early osteoarthritis of the knee and predict progressive disease. *Arthritis & Rheumatism,* 40**,** 723-727.

SPECTOR, T. D. & MACGREGOR, A. J. 2004. Risk factors for osteoarthritis: genetics1. *Osteoarthritis and Cartilage,* 12**,** 39-44.

STACK, J., HAGA, I. R., SCHRÖDER, M., BARTLETT, N. W., MALONEY, G., READING, P. C., FITZGERALD, K. A., SMITH, G. L. & BOWIE, A. G. 2005. Vaccinia virus protein A46R targets multiple Toll-like–interleukin-1 receptor adaptors and contributes to virulence. *The Journal of experimental medicine,* 201**,** 1007.

STARK, G. R., KERR, I. M., WILLIAMS, B. R. G., SILVERMAN, R. H. & SCHREIBER, R. D. 1998. How cells respond to interferons. *Annual review of biochemistry,* 67**,** 227-264.

STETÁK, A., VERESS, R., OVÁDI, J., CSERMELY, P., KÉRI, G. & ULLRICH, A. 2007. Nuclear translocation of the tumor marker pyruvate kinase M2 induces programmed cell death. *Cancer research,* 67**,** 1602.

STEVENS, A. L., WISHNOK, J. S., CHAI, D. H., GRODZINSKY, A. J. & TANNENBAUM, S. R. 2008. A sodium dodecyl sulfate–polyacrylamide gel electrophoresis–liquid chromatography tandem mass spectrometry analysis of bovine cartilage tissue response to mechanical compression injury and the inflammatory cytokines tumor necrosis factor α and interleukin-1β. *Arthritis & Rheumatism,* 58**,** 489-500.

STEVENS, A. L., WISHNOK, J. S., WHITE, F. M., GRODZINSKY, A. J. & TANNENBAUM, S. R. 2009. Mechanical Injury and Cytokines Cause Loss of Cartilage Integrity and Upregulate Proteins Associated with Catabolism, Immunity, Inflammation, and Repair. *Molecular & Cellular Proteomics,* 8**,** 1475-1489.

STÜRMER, T., BRENNER, H., KOENIG, W. & GÜNTHER, K. 2004. Severity and extent of osteoarthritis and low grade systemic inflammation as assessed by high sensitivity C

reactive protein. *Annals of the rheumatic diseases,* 63**,** 200.

SU, S. L., TSAI, C. D., LEE, C. H., SALTER, D. & LEE, H. S. 2005. Expression and regulation of Toll-like receptor 2 by IL-1 [beta] and fibronectin fragments in human articular chondrocytes. *Osteoarthritis and Cartilage,* 13**,** 879-886.

SUN, J., DUFFY, K. E., RANJITH-KUMAR, C., XIONG, J., LAMB, R. J., SANTOS, J., MASARAPU, H., CUNNINGHAM, M., HOLZENBURG, A. & SARISKY, R. T. 2006. Structural and Functional Analyses of the Human Toll-like Receptor 3. *Journal of Biological Chemistry,* 281**,** 11144.

SUTTON, S., CLUTTERBUCK, A., HARRIS, P., GENT, T., FREEMAN, S., FOSTER, N., BARRETT-JOLLEY, R. & MOBASHERI, A. 2009. The contribution of the synovium, synovial derived inflammatory cytokines and neuropeptides to the pathogenesis of osteoarthritis. *The Veterinary Journal,* 179**,** 10-24.

SUZUKI, N., SUZUKI, S. & YEH, W. C. 2002. IRAK-4 as the central TIR signaling mediator in innate immunity. *Trends in immunology,* 23**,** 503-506.

SWANTEK, J. L., TSEN, M. F., COBB, M. H. & THOMAS, J. A. 2000. IL-1 receptor-associated kinase modulates host responsiveness to endotoxin. *The Journal of immunology,* 164**,** 4301.

SWEENEY, S. E. 2011. Targeting interferon regulatory factors to inhibit activation of the type I IFN response: Implications for treatment of autoimmune disorders. *Cellular Immunology*.

SWEENEY, S. E., KIMBLER, T. B. & FIRESTEIN, G. S. 2010. Synoviocyte innate immune responses: II. Pivotal role of IFN regulatory factor 3. *The Journal of immunology,* 184**,** 7162-7168.

TABASSI, N. C. B. & GARNERO, P. 2007. Monitoring cartilage turnover. *Current rheumatology reports,* 9**,** 16-24.

TABETA, K., GEORGEL, P., JANSSEN, E., DU, X., HOEBE, K., CROZAT, K., MUDD, S., SHAMEL, L., SOVATH, S. & GOODE, J. 2004. Toll-like receptors 9 and 3 as essential components of innate immune defense against mouse cytomegalovirus infection. *Proceedings of the National Academy of Sciences of the United States of America,* 101**,** 3516.

TAKEDA, K. 2005. Evolution and integration of innate immune recognition systems: the Toll-like receptors. *Journal of endotoxin research,* 11**,** 51-55.

TAKEDA, K. & AKIRA, S. Year. TLR signaling pathways. *In,* 2004. Elsevier, 3-9.

TAKEDA, K. & AKIRA, S. 2005. Toll-like receptors in innate immunity. *International immunology,* 17**,** 1.

TAKEDA, K., KAISHO, T. & AKIRA, S. 2003. Toll-like receptors. *Annual review of immunology,* 21**,** 335-376.

TAKEUCHI, O., HOSHINO, K. & AKIRA, S. 2000. Cutting edge: TLR2-deficient and MyD88-deficient mice are highly susceptible to Staphylococcus aureus infection. *The*

Journal of immunology, 165**,** 5392.

TAMURA, T., YANAI, H., SAVITSKY, D. & TANIGUCHI, T. 2008. The IRF family transcription factors in immunity and oncogenesis. *Annu. Rev. Immunol.,* 26**,** 535-584.

TANG, C. H., HSU, C. J. & FONG, Y. C. 2010. The CCL5/CCR5 Axis Promotes Interleukin-6 Production in Human Synovial Fibroblasts. *Arthritis and Rheumatism,* 62**,** 3615-3624.

TANIGUCHI, T., OGASAWARA, K., TAKAOKA, A. & TANAKA, N. 2001. IRF family of transcription factors as regulators of host defense. *Annual review of immunology,* 19**,** 623-655.

TANIGUCHI, T. & TAKAOKA, A. 2001. A weak signal for strong responses: interferon-alpha/beta revisited. *Nature reviews Molecular cell biology,* 2**,** 378-386.

TANIGUCHI, T. & TAKAOKA, A. 2002. The interferon-[alpha]/[beta] system in antiviral responses: a multimodal machinery of gene regulation by the IRF family of transcription factors. *Current opinion in immunology,* 14**,** 111-116.

TAYLOR, K. R., YAMASAKI, K., RADEK, K. A., NARDO, A. D., GOODARZI, H., GOLENBOCK, D., BEUTLER, B. & GALLO, R. L. 2007. Recognition of hyaluronan released in sterile injury involves a unique receptor complex dependent on Toll-like receptor 4, CD44, and MD-2. *Journal of Biological Chemistry,* 282**,** 18265.

TERASHIMA, M., KIM, K. M., ADACHI, T., NIELSEN, P., RETH, M., KÖHLER, G. & LAMERS, M. 1994. The IgM antigen receptor of B lymphocytes is associated with prohibitin and a prohibitin-related protein. *The EMBO journal,* 13**,** 3782.

TERMEER, C., BENEDIX, F., SLEEMAN, J., FIEBER, C., VOITH, U., AHRENS, T., MIYAKE, K., FREUDENBERG, M., GALANOS, C. & SIMON, J. C. 2002. Oligosaccharides of Hyaluronan activate dendritic cells via toll-like receptor 4. *The Journal of experimental medicine,* 195**,** 99.

THEISS, A. L., IDELL, R. D., SRINIVASAN, S., KLAPPROTH, J. M., JONES, D. P., MERLIN, D. & SITARAMAN, S. V. 2007. Prohibitin protects against oxidative stress in intestinal epithelial cells. *The FASEB Journal,* 21**,** 197.

THEISS, A. L., JENKINS, A. K., OKORO, N. I., KLAPPROTH, J. M. A., MERLIN, D. & SITARAMAN, S. V. 2009. Prohibitin Inhibits Tumor Necrosis Factor alpha–induced Nuclear Factor-kappa B Nuclear Translocation via the Novel Mechanism of Decreasing Importin α3 Expression. *Molecular Biology of the Cell,* 20**,** 4412-4423.

THEISS, A. L. & SITARAMAN, S. V. 2011. The role and therapeutic potential of prohibitin in disease. *Biochimica et Biophysica Acta (BBA)-Molecular Cell Research*.

THEISS, A. L., VIJAY-KUMAR, M., OBERTONE, T. S., JONES, D. P., HANSEN, J. M., GEWIRTZ, A. T., MERLIN, D. & SITARAMAN, S. V. 2009. Prohibitin Is a Novel Regulator of Antioxidant Response That Attenuates Colonic Inflammation in Mice. *Gastroenterology,* 137**,** 199-208.

THEOFILOPOULOS, A. N., BACCALA, R., BEUTLER, B. & KONO, D. H. 2005. Type I interferons (α/β) in immunity and autoimmunity. *Annu. Rev. Immunol.,* 23**,** 307-335.

TILLEMAN, K., VAN BENEDEN, K., DHONDT, A., HOFFMAN, I., DE KEYSER, F., VEYS, E., ELEWAUT, D. & DEFORCE, D. 2005. Chronically inflamed synovium from spondyloarthropathy and rheumatoid arthritis investigated by protein expression profiling followed by tandem mass spectrometry. *Proteomics,* 5**,** 2247-2257.

TILLEMAN, K., VAN STEENDAM, K., CANTAERT, T., DE KEYSER, F., ELEWAUT, D. & DEFORCE, D. 2008. Synovial detection and autoantibody reactivity of processed citrullinated isoforms of vimentin in inflammatory arthritides. *Rheumatology,* 47**,** 597.

TISSARI, J., SIRÉN, J., MERI, S., JULKUNEN, I. & MATIKAINEN, S. 2005. IFN-α enhances TLR3-mediated antiviral cytokine expression in human endothelial and epithelial cells by up-regulating TLR3 expression. *The Journal of immunology,* 174**,** 4289.

TODHUNTER, R. 1996. Anatomy and physiology of synovial joints. *McIlwraith, CW, Trotter GW Joint disease in the horse. WB Saunders. Philadelphia, USA***,** 1-28.

TODHUNTER, R., ACLAND, G., OLIVIER, M., WILLIAMS, A., VERNIER-SINGER, M., BURTON-WURSTER, N., FARESE, J., GRÖN, Y., GILBERT, R. & DYKES, N. 1999. An outcrossed canine pedigree for linkage analysis of hip dysplasia. *Journal of Heredity,* 90**,** 83.

TOPOL, E. J. 2004. Failing the public health—rofecoxib, Merck, and the FDA. *New England Journal of Medicine,* 351**,** 1707-1709.

TSUBAKI, T., ARITA, N., KAWAKAMI, T., SHIRATSUCHI, T., YAMAMOTO, H., TAKUBO, N., YAMADA, K., NAKATA, S., YAMAMOTO, S. & NOSE, M. 2005. Characterization of histopathology and gene-expression profiles of synovitis in early rheumatoid arthritis using targeted biopsy specimens. *Arthritis Res Ther,* 7**,** R825-R836.

TSUBERY, H., OFEK, I., COHEN, S., EISENSTEIN, M. & FRIDKIN, M. 2002. Modulation of the hydrophobic domain of polymyxin B nonapeptide: effect on outer-membrane permeabilization and lipopolysaccharide neutralization. *Molecular pharmacology,* 62**,** 1036.

TSUBOI, N., YOSHIKAI, Y., MATSUO, S., KIKUCHI, T., IWAMI, K. I., NAGAI, Y., TAKEUCHI, O., AKIRA, S. & MATSUGUCHI, T. 2002. Roles of toll-like receptors in CC chemokine production by renal tubular epithelial cells. *The Journal of immunology,* 169**,** 2026.

TSUNG, A., SAHAI, R., TANAKA, H., NAKAO, A., FINK, M. P., LOTZE, M. T., YANG, H., LI, J., TRACEY, K. J. & GELLER, D. A. 2005. The nuclear factor HMGB1 mediates hepatic injury after murine liver ischemia-reperfusion. *The Journal of experimental medicine,* 201**,** 1135.

ULLAL, A. & PISETSKY, D. S. 2012. Microparticles as antigenic targets in human and murine SLE. *Arthritis Research & Therapy,* 14**,** O34.

ULTAIGH, S. N. A., SABER, T. P., MCCORMICK, J., CONNOLLY, M., DELLACASAGRANDE, J., KEOGH, B., MCCORMACK, W., REILLY, M., O'NEILL, L. A. & MCGUIRK, P. 2011. Blockade of Toll-like receptor 2 prevents spontaneous cytokine

release from rheumatoid arthritis ex vivo synovial explant cultures. *Arthritis Research & Therapy,* 13**,** R33.

VAAMONDE-GARCÍA, C., RIVEIRO-NAVEIRA, R. R., VALCÁRCEL-ARES, M. N., HERMIDA-CARBALLO, L., BLANCO, F. J. & LÓPEZ-ARMADA, M. J. 2012. Mitochondrial dysfunction increases the inflammatory responsiveness to cytokines in normal human chondrocytes. *Arthritis & Rheumatism***,** n/a-n/a.

VABULAS, R. M., AHMAD-NEJAD, P., DA COSTA, C., MIETHKE, T., KIRSCHNING, C. J., HÄCKER, H. & WAGNER, H. 2001. Endocytosed HSP60s use toll-like receptor 2 (TLR2) and TLR4 to activate the toll/interleukin-1 receptor signaling pathway in innate immune cells. *Journal of Biological Chemistry,* 276**,** 31332-31339.

VAN DER HEIJDEN, I. M., WILBRINK, B., TCHETVERIKOV, I., SCHRIJVER, I. A., SCHOULS, L. M., HAZENBERG, M. P., BREEDVELD, F. C. & TAK, P. P. 2000. Presence of bacterial DNA and bacterial peptidoglycans in joints of patients with rheumatoid arthritis and other arthritides. *Arthritis & Rheumatism,* 43**,** 593-598.

VAN DER LAAN, W., QUAX, P., SEEMAYER, C., HUISMAN, L., PIETERMAN, E., GRIMBERGEN, J., VERHEIJEN, J., BREEDVELD, F., GAY, R. & GAY, S. 2003. Cartilage degradation and invasion by rheumatoid synovial fibroblasts is inhibited by gene transfer of TIMP-1 and TIMP-3. *Gene therapy,* 10**,** 234-242.

VASSELON, T., DETMERS, P. A., CHARRON, D. & HAZIOT, A. 2004. TLR2 recognizes a bacterial lipopeptide through direct binding. *The Journal of immunology,* 173**,** 7401.

VEENSTRA, T. D. & YATES, J. R. 2006. *Proteomics for biological discovery,* Wiley Online Library.

VERGUNST, C., VAN DE SANDE, M., LEBRE, M. & TAK, P. 2005. The role of chemokines in rheumatoid arthritis and osteoarthritis. *Scandinavian journal of rheumatology,* 34**,** 415-425.

VON RECHENBERG, B., MCILWRAITH, C., AKENS, M., FRISBIE, D., LEUTENEGGER, C. & AUER, J. 2000. Spontaneous production of nitric oxide (NO), prostaglandin (PGE2) and neutral metalloproteinases (NMPs) in media of explant cultures of equine synovial membrane and articular cartilage from normal and osteoarthritic joints. *Equine veterinary journal,* 32**,** 140.

VOSS, A., GESCHER, K., HENSEL, A., NACKEN, W. & KERKHOFF, C. 2011. Double-Stranded RNA Induces MMP-9 Gene Expression in HaCaT Keratinocytes by Tumor Necrosis Factor. *Inflammation & Allergy - Drug Targets (Formerly ?Current Drug Targets - Inflammation & Allergy),* 10**,** 171-179.

VOSSENAAR, E., RADSTAKE, T., VAN DER HEIJDEN, A., VAN MANSUM, M., DIETEREN, C., DE ROOIJ, D., BARRERA, P., ZENDMAN, A. & VAN VENROOIJ, W. 2004. Expression and activity of citrullinating peptidylarginine deiminase enzymes in monocytes and macrophages. *Annals of the rheumatic diseases,* 63**,** 373-381.

WALSH, D., BONNET, C., TURNER, E., WILSON, D., SITU, M. & MCWILLIAMS, D. 2007. Angiogenesis in the synovium and at the osteochondral junction in osteoarthritis1.

Osteoarthritis and Cartilage, 15**,** 743-751.

WANG, C. L. A. 2008. Caldesmon and the regulation of cytoskeletal functions. *Tropomyosin***,** 250-272.

WANG, J., SHAO, Y., BENNETT, T. A., SHANKAR, R. A., WIGHTMAN, P. D. & REDDY, L. G. 2006. The functional effects of physical interactions among Toll-like receptors 7, 8, and 9. *Journal of Biological Chemistry,* 281**,** 37427-37434.

WANG, Q., ROZELLE, A. L., LEPUS, C. M., SCANZELLO, C. R., SONG, J. J., LARSEN, D. M., CRISH, J. F., BEBEK, G., RITTER, S. Y. & LINDSTROM, T. M. 2011. Identification of a central role for complement in osteoarthritis. *Nature medicine.*

WANG, T., TOWN, T., ALEXOPOULOU, L., ANDERSON, J. F., FIKRIG, E. & FLAVELL, R. A. 2004. Toll-like receptor 3 mediates West Nile virus entry into the brain causing lethal encephalitis. *Nature medicine,* 10**,** 1366-1373.

WASSILEW, G. I., LEHNIGK, U., DUDA, G. N., TAYLOR, W. R., MATZIOLIS, G. & DYNYBIL, C. 2010. The Expression of Proinflammatory Cytokines and Matrix Metalloproteinases in the Synovial Membranes of Patients With Osteoarthritis Compared With Traumatic Knee Disorders. *Arthroscopy: The Journal of Arthroscopic & Related Surgery,* 26**,** 1096-1104.

WATANABE, H., YAMADA, Y. & KIMATA, K. 1998. Roles of aggrecan, a large chondroitin sulfate proteoglycan, in cartilage structure and function. *Journal of biochemistry,* 124**,** 687.

WAYNE MARSHALL, K., CHIU, B. & INMAN, R. D. 1990. Substance P and arthritis: analysis of plasma and synovial fluid levels. *Arthritis & Rheumatism,* 33**,** 87-90.

WESCHE, H., HENZEL, W. J., SHILLINGLAW, W., LI, S. & CAO, Z. 1997. MyD88: An Adapter That Recruits IRAK to the IL-1 Receptor Complex. *Immunity,* 7**,** 837-847.

WEST, A. P., KOBLANSKY, A. A. & GHOSH, S. 2006. Recognition and signaling by toll-like receptors. *Annu. Rev. Cell Dev. Biol.,* 22**,** 409-437.

WESTACOTT, C. I. & SHARIF, M. Year. Cytokines in osteoarthritis: mediators or markers of joint destruction? *In,* 1996. Elsevier, 254-272.

WIELAND, H. A., MICHAELIS, M., KIRSCHBAUM, B. J. & RUDOLPHI, K. A. 2005. Osteoarthritis—an untreatable disease? *Nature Reviews Drug Discovery,* 4**,** 331-344.

WILKINS, C. & GALE JR, M. 2010. Recognition of viruses by cytoplasmic sensors. *Current opinion in immunology,* 22**,** 41-47.

WILSON, R., BELLUOCCIO, D., LITTLE, C. B., FOSANG, A. J. & BATEMAN, J. F. 2008. Proteomic characterization of mouse cartilage degradation in vitro. *Arthritis & Rheumatism,* 58**,** 3120-3131.

WINDER, S. J. 2003. Structural insights into actin-binding, branching and bundling proteins. *Current opinion in cell biology,* 15**,** 14-22.

WOODLOCK, T. J., BETHLENDY, G. & SEGEL, G. B. 2001. Prohibitin expression is increased in phorbol ester-treated chronic leukemic B-lymphocytes. *Blood Cells, Molecules, and Diseases,* 27**,** 27-34.

WU, X., MOLINARO, C., JOHNSON, N. & CASIANO, C. A. 2001. Secondary necrosis is a source of proteolytically modified forms of specific intracellular autoantigens: implications for systemic autoimmunity. *Arthritis & Rheumatism,* 44**,** 2642-2652.

XIAO, H., GULEN, M. F., QIN, J., YAO, J., BULEK, K., KISH, D., ALTUNTAS, C. Z., WALD, D., MA, C. & ZHOU, H. 2007. The Toll–interleukin-1 receptor member SIGIRR regulates colonic epithelial homeostasis, inflammation, and tumorigenesis. *Immunity,* 26**,** 461-475.

YAHATA, T., DE CAESTECKER, M. P., LECHLEIDER, R. J., ANDRIOLE, S., ROBERTS, A. B., ISSELBACHER, K. J. & SHIODA, T. 2000. The MSG1 non-DNA-binding transactivator binds to the p300/CBP coactivators, enhancing their functional link to the Smad transcription factors. *Journal of Biological Chemistry,* 275**,** 8825.

YAMAMOTO, M., SATO, S., HEMMI, H., HOSHINO, K., KAISHO, T., SANJO, H., TAKEUCHI, O., SUGIYAMA, M., OKABE, M. & TAKEDA, K. 2003. Role of adaptor TRIF in the MyD88-independent toll-like receptor signaling pathway. *Science,* 301**,** 640.

YAMAMOTO, M., SATO, S., HEMMI, H., SANJO, H., UEMATSU, S., KAISHO, T., HOSHINO, K., TAKEUCHI, O., KOBAYASHI, M. & FUJITA, T. 2002. Essential role for TIRAP in activation of the signalling cascade shared by TLR2 and TLR4. *Nature,* 420**,** 324-329.

YAMAMOTO, M., SATO, S., HEMMI, H., UEMATSU, S., HOSHINO, K., KAISHO, T., TAKEUCHI, O., TAKEDA, K. & AKIRA, S. 2003. TRAM is specifically involved in the Toll-like receptor 4-mediated MyD88-independent signaling pathway. *nature immunology,* 4**,** 1144-1150.

YAMAMOTO, M., SATO, S., MORI, K., HOSHINO, K., TAKEUCHI, O., TAKEDA, K. & AKIRA, S. 2002. Cutting edge: a novel Toll/IL-1 receptor domain-containing adapter that preferentially activates the IFN-β promoter in the Toll-like receptor signaling. *The Journal of immunology,* 169**,** 6668.

YAMANISHI, Y., BOYLE, D. L., CLARK, M., MAKI, R. A., TORTORELLA, M. D., ARNER, E. C. & FIRESTEIN, G. S. 2002. Expression and regulation of aggrecanase in arthritis: the role of TGF-β. *The Journal of Immunology,* 168**,** 1405.

YANG, H., LIN, C. H., MA, G., BAFFI, M. O. & WATHELET, M. G. 2003. Interferon regulatory factor-7 synergizes with other transcription factors through multiple interactions with p300/CBP coactivators. *Journal of Biological Chemistry,* 278**,** 15495-15504.

YARON, M., BARATZ, M., YARON, I. & ZOR, U. 1979. Acute induction of joint inflammation in the rat by Poly I· Poly C. *Inflammation,* 3**,** 243-251.

YOKOTA, S., IMAGAWA, T., MORI, M., MIYAMAE, T., AIHARA, Y., TAKEI, S., IWATA, N., UMEBAYASHI, H., MURATA, T. & MIYOSHI, M. 2008. Efficacy and

safety of tocilizumab in patients with systemic-onset juvenile idiopathic arthritis: a randomised, double-blind, placebo-controlled, withdrawal phase III trial. *The Lancet*, 371**,** 998-1006.

YONEYAMA, M. & FUJITA, T. 2007. Function of RIG-I-like receptors in antiviral innate immunity. *Journal of Biological Chemistry,* 282**,** 15315.

YONEYAMA, M. & FUJITA, T. 2009. RNA recognition and signal transduction by RIG-I-like receptors. *Immunological reviews,* 227**,** 54-65.

YONEYAMA, M., KIKUCHI, M., NATSUKAWA, T., SHINOBU, N., IMAIZUMI, T., MIYAGISHI, M., TAIRA, K., AKIRA, S. & FUJITA, T. 2004. The RNA helicase RIG-I has an essential function in double-stranded RNA-induced innate antiviral responses. *nature immunology,* 5**,** 730-737.

YOSHIO, T., MORITA, T., KIMURA, Y., TSUJII, M., HAYASHI, N. & SOBUE, K. 2007. Caldesmon suppresses cancer cell invasion by regulating podosome/invadopodium formation. *FEBS letters,* 581**,** 3777-3782.

YU, P., MUSETTE, P. & PENG, S. L. 2008. Toll-like receptor 9 in murine lupus: More friend than foe! *Immunobiology,* 213**,** 151-157.

YUAN, G. H., MASUKO-HONGO, K., KATO, T. & NISHIOKA, K. 2003. Immunologic intervention in the pathogenesis of osteoarthritis. *Arthritis & Rheumatism,* 48**,** 602-611.

YUAN, G. H., TANAKA, M., MASUKO-HONGO, K., SHIBAKAWA, A., KATO, T., NISHIOKA, K. & NAKAMURA, H. 2004. Characterization of cells from pannus-like tissue over articular cartilage of advanced osteoarthritis. *Osteoarthritis and Cartilage,* 12**,** 38-45.

ZAREMBER, K. A. & GODOWSKI, P. J. 2002. Tissue expression of human Toll-like receptors and differential regulation of Toll-like receptor mRNAs in leukocytes in response to microbes, their products, and cytokines. *The Journal of immunology,* 168**,** 554.

ZHANG, D., ZHANG, G., HAYDEN, M. S., GREENBLATT, M. B., BUSSEY, C., FLAVELL, R. A. & GHOSH, S. 2004. A toll-like receptor that prevents infection by uropathogenic bacteria. *Science,* 303**,** 1522.

ZHANG, L. & PAGANO, J. S. 1997. IRF-7, a new interferon regulatory factor associated with Epstein-Barr virus latency. *Molecular and cellular biology,* 17**,** 5748.

ZHANG, Q., HUI, W., LITHERLAND, G. J., BARTER, M. J., DAVIDSON, R., DARRAH, C., DONELL, S. T., CLARK, I. M., CAWSTON, T. E. & ROBINSON, J. H. 2008. Differential Toll-like receptor-dependent collagenase expression in chondrocytes. *Annals of the rheumatic diseases,* 67**,** 1633.

ZHU, J., LAI, K., BROWNILE, R., BABIUK, L. A. & MUTWIRI, G. K. 2008. Porcine TLR8 and TLR7 are both activated by a selective TLR7 ligand, imiquimod. *Molecular immunology,* 45**,** 3238-3243.

ZHU, W., MENG, L., JIANG, C., HE, X., HOU, W., XU, P., DU, H., HOLMDAHL, R. &

LU, S. 2011. Arthritis is associated with T-cell-induced upregulation of Toll-like receptor 3 on synovial fibroblasts. *Arthritis Research & Therapy,* 13**,** R103.

ZHU, W. H., MENG, L. S., JIANG, C. S., HE, X. J., HOU, W. K., XU, P., DU, H., HOLMDAHL, R. & LU, S. M. 2011. Arthritis is associated with T-cell-induced upregulation of Toll-like receptor 3 on synovial fibroblasts. *Arthritis Research & Therapy,* 13.

Appendix

Table 5.1. Proteins with changed abundance identified by LC-MS in OA-FLS versus N-FLS.

Serial No.	Spot No.	Anova (p)	Fold change of control OA-FLS Vs N-FLS	Accession code	Uniprot ID	Protein name	Mascot score*	Mw (Da)	pI	Matched peptides	Sequence coverage (%)
1	6	0.029	(-) 3.10	gi|4502101	P04083	Annexin I	570	38922	6.57	11	37%
2	11	0.015	(+) 2.4	gi|4885413	P49773	Histidine triad nucleotide binding protein 1	160	13907	6.43	6	70%
3	12	0.028	(-) 2.1	gi|4507109	P37840	Alpha-synuclein isoform NACP140	324	14451	4.67	9	52%
4	13	0.026	(-) 2.1	gi|5802974	P30048	Peroxiredoxin 3 isoform a precursor	466	28023	7.67	13	29%
5	14	0.048	(-) 1.9	gi|999892	P60174	Human Triosephosphate Isomerase	905	26812	6.51	24	83%
6	20	0.028	(+)1.5	gi|2809324	O43852	Calumenin	569	37166	4.47	17	40%
7	21	0.033	(-) 1.3	gi|157168362	P00491	Nucleoside phosphorylase	624	32329	6.45	16	61%

8	30	0.051	(-) 6	gi|4505763	P00558	Phosphoglycerate kinase 1	720	44985	8.3	23	44%
9	54	0.07	(-) 3.3	gi|15010550	P14625	Heat shock protein gp96 precursor	839	90312	4.73	19	24%
10	48	0.145	(-) 3	gi|21730330	O75347	Human Tubulin Chaperone Cofactor A	573	12860	5.11	16	56%
11	53	0.134	(+)2.8	gi|62738405	P04179	Human Manganese Superoxide Dismutase	454	21838	6.86	11	48%
12	45	0.0152	(+) 2.8	gi|340219	P08670	Vimentin	394	53681	5.06	10	16%
13	56	0.044	(-) 2.7	gi|66360499	P62158	Calmodulin	528	16625	4.05	17	46%
14	60	0.225	(-) 2.5	gi|188590	P60660	Myosin light chain 3	327	16920	4.51	8	37%
15	61	0.044	(-) 2.5	gi|5031635	P23528	Cofilin 1 (non-muscle)	753	18719	8.22	22	78%
16	64	0.047	(+)2.3	gi|15149465	Q05682	Caldesmon 1	1023	71233	6.2	27	44%
17	79	0.029	(-) 2.5	gi|4505773	P35232	Prohibitin	1001	29844	5.57	21	67%
18	101	0.147	(-) 1.9	gi|4506667	P05388	Ribosomal protein P0	403	34252	5.71	9	34%

19	102	0.335	(-) 1.9	gi|4503477	P24534	Eukaryotic translation elongation factor 1 beta 2	205	24748	4.5	6	16%
20	104	0.091	(+)1.9	gi|12653783	P13489	Ribonuclease/angiogenin inhibitor 1	1051	51778	4.71	21	58%
21	107	0.048	(-) 1.8	gi|50513593	Q99497	Human Dj-1 With Sulfinic Acid	894	20001	6.33	26	83%
22	114	0.118	(-) 1.7	gi|36038	P52565	rho GDP dissociation inhibitor (GDI)	242	23179	5.02	7	23%
23	118	0.112	(+)1.7	gi|1703319	P09525	Annexin A4	1145	36088	5.84	26	55%
24	129	0.332	(+)1.6	gi|30841309	Q7Z7M4	Manganese-containing superoxide dismutase	580	23774	6.87	20	43%
25	132	0.508	(-) 1.6	gi|5031851	P16949	Stathmin 1 isoform a	138	17292	5.76	3	24%
26	139	0.251	(-) 1.6	gi|6166493	P30044	Thioredoxin peroxidase PMP20	602	22267	8.85	14	56%
27	140	0.056	(-) 1.6	gi|4557797	P15531	Non-metastatic cells 1, protein (NM23A) expressed in isoform b	426	17312	5.83	12	70%
28	141	0.022	(-) 1.6	gi|4503571	P06733	Enolase 1	1134	47487	7.01	22	53%

29	143	0.117	(-) 1.6	gi|5453603	P78371	Chaperonin containing TCP1, subunit 2	1678	57794	6.01	41	64%
30	154	0.318	(+)1.5	gi|5802966	P60981	Destrin isoform a	494	18958	8.06	15	67%

Note: (+) denotes n-fold increase, and (-) denotes n-fold decrease in OA-FLS protein compared to N-FLS. * denotes the mascot score has a 95 % confidence level if > 49.

Table 5.2. Proteins with changed abundance identified by LC-MS in N-FLS treated with Poly (I:C) versus control N-FLS.

Serial No.	Spot No.	Anova (p)	Fold change of N + Poly (I:C) Vs N control	Accession code	Uniport ID	Protein name	Mascot score*	Mw (Da)	Pi	Matched peptides	Sequence coverage (%)
1	635	0.007	+ 2.9	gi|643695	P35754	Glutaredoxin	115	12039	8.33	2	11%
2	632	0.005	+ 3.5	gi|34616	P61769	Beta-2 microglobulin	129	12905	5.77	7	28%
3	533	0.002	+ 3.8	gi|21389433	O14558	Heat shock protein beta-6	140	17182	5.95	3	21%

4	509	0.004	+ 2.4	gi|7706497	P30085	UMP-CMP kinase isoform a	142	26180	8.14	4	25%
5	512	1.29E-06	+3.8	gi|4507357	P37802	Transgelin-2	207	22548	8.41	4	33%
6	518	0.014	+ 2.4	gi|30841309	P04179	Manganese-containing superoxide dismutase	418	23772	6.87	18	42%
7	530	0.003	+ 3.3	gi|325053860	P02511	Human Alphab Crystalline Acd	311	10151	6.21	12	75%
8	472	8.01E-04	+ 3.5	gi|5453555	P62826	GTP-binding nuclear protein Ran	277	24579	7.01	6	36%
9	462	0.024	+ 3.4	gi|226529917	P60174	Triosephosphate isomerase	742	31057	5.65	21	55%
10	276	0.005	+ 1.3	gi|4557305	P04075	Fructose-bisphosphate aldolase	665	39851	8.3	17	40%
11	434	2.31E-04	+ 1.9	gi|38566176	P18669	Phosphoglycerate mutase 1	288	28916	6.67	10	53%
12	414	0.042	+ 1.5	gi|4506179	P25786	Proteasome subunit alpha type-1 isoform 2	416	29864	6.15	11	445%
13	367	0.002	+ 2.3	gi|5453710	Q14847	LIM and SH3 domain protein 1	305	30097	6.61	8	29%

14	431	0.005	+ 2.3	gi|4758484	P78417	Glutathione S-transferase omega-1	621	27833	6.23	18	48%
15	453	0.007	+ 1.4	gi|23065552	P21266	Glutathione S-transferase Mu 3	438	26998	5.37	9	48%
16	461	6.43E-04	+ 2.3	gi|4502565	P04632	Calpain small subunit 1	592	28469	5.05		70%
17	272	5.59E-05	+ 2.6	gi|9845502	P08865	40S ribosomal protein SA	499	32947	4.79	12	46%
18	255	0.004	+ 1.0	gi|178045	P63261	Gamma-actin	467	26147	5.65	17	72%
19	277	0.001	+ 1.5	gi|13489087	P30740	Leukocyte elastase inhibitor	399	42829	5.9	8	30%
20	235	0.03	+ 1.5	gi|6598323	P50395	rab GDP dissociation inhibitor beta isoform 1	416	51087	6.11	9	31%
21	209	0.047	+ 4.1	gi|15149465	Q05682	Caldesmon 1	1023	71233	6.2	27	44%
22	96	0.002	+ 2.5	gi|325533397	Q5TCI8	Human Lamin A	186	8661	5.46	5	59%
23	204	1.41E-04	+ 1.9	gi|385994	Q9UGM6	Tryptophanyl-tRNA synthetase,mitochondrial	96	1798	5.4	4	100%
24				gi|47419914	P23381	Tryptophanyl-tRNA	1035	53474	5.83	32	63%

	201	5.96E-06	+ 2.2			synthetase, cytoplasmic					
25	181	0.049	+ 1.4	gi|220702506	P30101	TapasinERP57 HETERODIMER	1036	54541	5.61	23	48%
26	114	0.019	+ 1.1	gi|190613719	P08107	Sse1p And Hsp70, Selenomethionine- Labelled Crystals	535	42075	6.4	11	38%
27	110	1.48E-04	+ 1.4	gi|251757499	P20591	Interferon-induced GTP-binding protein Mx1	343	75872	5.6	25	42%
28	70	0.012	+ 1.9	gi|154146191	P07900	Heat shock protein HSP 90-alpha	565	85006	4.94	12	20%
29	117	1.95E-04	+ 2.0	gi|33469985	O95302	Peptidyl-prolyl cis-trans isomerase FKBP9 precurso	488	63500	4.91	12	26%
30	179	0.005	+ 4.9	gi|340219	P08670	Vimentin	1276	53676	5.06	36	65%
31	675	0.046	- 1.5	gi|20664042	P06703	Calcium-Free (Or Apo) Human S100a6; Cys3met	290	10161	5.33	10	46%

						Mutan					
32	646	0.047	- 1.2	gi|5032057	P31949	Protein S100-A11	117	11847	6.56	3	34%
33	593	0.021	- 1.5	gi|310942925	P09382	Galectin-1 In Complex With Lactobionic Acid	397	14770	5.34	16	73%
34	580	0.04	- 1.6	gi|4503029	P29373	Cellular retinoic acid-binding protein 2	256	15854	5.42	8	47%
35	556	3.98E-04	- 1.5	gi|4503545	P63241	Eukaryotic translation initiation factor 5A-1 isoform B	354	17049	5.08	10	62%
36	546	1.17E-06	- 1.5	gi|5031635	P23528	Cofilin-1	397	18719	8.22	7	43%
37	508	0.003	- 3.4	gi|48255905	Q01995	Transgelin	644	22653	8.87	18	73%
38	348	0.002	+ 2.8	gi|7669492	P04406	Glyceraldehyde-3-phosphate dehydrogenase	417	36201	8.57	13	37%
39	479	6.90E-05	- 1.8	gi|4504517	P04792	Heat shock protein beta-1	578	22826	5.98	17	68%
40	474	0.011	- 1.3	gi|4757768	P52565	Rho GDP-dissociation inhibitor 1	272	23250	5.02	8	26%

41	414	0.009	- 1.3	gi|30410792	Q9UL46	Proteasome activator complex subunit 2	334	27555	5.54	9	51%
42	442	0.004	- 1.4	gi|40805862	O43399	Tumor protein D54 isoform f	114	19946	5.35	4	31%
43	464	7.99E-05	- 1.4	gi|7106387	P28066	Proteasome subunit alpha type-5	561	26565	4.74	13	55%
44	453	0.007	- 1.4	gi|4507953	P63104	14-3-3 protein zeta/delta	693	27899	4.73	16	54%
45	394	4.06E-04	- 1.4	gi|342350777	P08758	Human Annexin V With Incorporated Methionine Analogue Azidohomoalanine	1459	35811	4.89	42	76%
46	418	9.53E-04	- 1.5	gi|24119203	P06753	Tropomyosin alpha-3 chain isoform 2	1091	29243	4.75	26	64%
47	417	0.008	- 1.3	gi|63252896	P09493	Tropomyosin alpha-1 chain isoform 3	744	32774	4.71	19	41%
48	409	0.006	- 1.2	gi|4503477	P24534	Elongation factor 1-beta	171	24919	4.5	4	19%
49	408	0.008	- 1.6	gi|6005993	P09496	Clathrin light chain A	201	27174	4.43	6	14%

50	324	0.014	- 1.6	gi|223555975	P67936	Tropomyosin alpha-4 chain isoform 1	674	32874	4.69	1	50%
51	288	0.017	- 1.2	gi|47519616	P07951	Tropomyosin beta chain isoform 2	978	33027	4.63	22	57%
52	333	0.035	- 1.4	gi|4557032	P07195	L-lactate dehydrogenase B	854	36900	5.71	24	62%
53	441	0.009	-2.1	gi|4505773	P35232	Prohibitin	1023	29844	5.57	29	75%
54	281	0.044	- 1.4	gi|4758158	Q15019	Septin-2	636	41689	6.15	13	46%
55	248	0.032	- 1.4	gi|18379349	Q99536	Synaptic vesicle membrane protein VAT-1 homolog	783	42122	5.88	18	49%
56	236	0.007	- 1.4	gi|4501885	P60709	Actin, cytoplasmic 1	675	42052	5.29	22	56%
57	152	0.004	- 1.1	gi|34147778	Q16881	Thioredoxin reductase 1	54	6738	4.93	2	65%
58	21	0.026	- 1.2	gi|38044288	P06396	Gelsolin isoform b	588	80876	5.58	13	26%
59	110	1.48E-04	- 1.4	gi|7549809	P13797	Plastin-3	638	71279	5.41	14	24%
60	50	0.023	- 1.2	gi|6005942	P55072	Transitional endoplasmic reticulum ATPase	603	89950	5.14	14	25%

Note: (+) denotes n-fold increase, and (-) denotes n-fold decrease in N-FLS + Poly (I:C) protein compared to control N-FLS. * denotes the mascot score has a 95 % confidence level if > 49.

Table 5.3. Proteins with changed abundance identified by LC-MS in OA-FLS treated with Poly (I:C) versus control OA-FLS.

Serial No.	Spot No.	Anova (p)	Fold change of OA + Poly (I:C) Vs OA control	Accession code	Uniprot ID	Protein name	Mascot score*	Mw (Da)	Pi	Matched peptides	Sequence coverage (%)
1	1823	1.21E-04	+ 3.9	gi|4757826	P61769	Beta-2-microglobulin	182	13802	6.06	7	29%
2	1771	0.002	+ 1.5	gi|4503117	P04080	Cystatin-B	200	11190	6.96	6	39%
3	1688	0.002	+ 55.6	gi|4826774	P05161	Ubiquitin-like protein ISG15	258	17933	6.84	10	45%
4	1614	2.08E-04	+ 3.2	gi|33457348	Q969H8	UPF0556 protein C19orf10 precursor	231	18897	6.2	8	30%
5	1627	0.002	+ 4.0	gi|4826898	P07737	Profilin-1	355	15216	8.44	14	51%
6	1328	0.017	+ 2.7	gi|4507357	P37802	Transgelin-2	719	22548	8.41	21	70%
7	1274	0.01	+ 3.9	gi|48255905	Q01995	Transgelin	569	22653	8.87	17	57%
8					P04179	Manganese-containing	348	23772	6.87	11	35%

	1272	3.96E-04	+ 3.5	gi|30841309		superoxide dismutase					
9	1211	0.036	+ 1.6	gi|226529917	P60174	Triosephosphate isomerase	900	31057	5.65	22	57%
10	1426	4.22E-04	+ 3.4	gi|5454090	P51571	Translocon-associated protein subunit delta	257	19158	5.76	6	26%
11	1513	0.007	+ 1.5	gi|5031593	O15511	Actin-related protein 2/3 complex subunit 5	229	16367	5.47	5	30%
12	1634	3.48E-04	+ 2.9	gi|56966036	Q14019	Human Coactosin-Like Protein	309	15898	5.55	10	43%
13	1132	0.013	+ 1.6	gi|4504517	P04792	Heat shock protein beta-1	322	22826	5.98	9	30%
14	1131	0.026	+ 1.2	gi|5453790	P40261	Nicotinamide N-methyltransferase	307	30011	5.56	9	22%
15	1147	0.004	+ 2.2	gi|5453549	Q13162	Peroxiredoxin-4	326	30749	5.86	9	29%
16	1164	0.021	+ 2.4	gi|4504517	P04792	Heat shock protein beta-1	318	22826	5.98	10	28%
17	1083	0.022	+ 2.6	gi|4826659	P47756	F-actin-capping protein subunit beta isoform 1	559	30952	5.69	17	45%

18	990	0.011	+ 1.5	gi|1703319	P09525	Annexin A4	1049	36088	5.84	27	57%
19	1093	8.94E-04	+ 3.5	gi|6912586	O95336	6-Phosphogluconolactonase	459	27815	5.7	10	49%
20	1052	5.70E-04	+ 1.7	gi|118582275	P08294	Extracellular superoxide dismutase [Cu-Zn]	49	26291	6.14	2	11%
21	1029	2.62E-04	+ 3.5	gi|30749598	O00560	The Pdz Tandem Of Human Syntenin	135	18075	8.5	5	16%
22	1011	8.07E-04	+ 2.3	gi|87159818	P36543	V-type proton ATPase subunit E 1 isoform c	341	22749	6.66	11	34%
23	940	0.028	+ 1.9	gi|18645167	P07355	Annexin A2	502	38780	7.57	17	31%
24	833	0.003	+ 3.9	gi|4557305	P04075	Fructose-bisphosphate aldolase A	765	39851	8.3	21	32%
25	810	0.004	+ 1.5	gi|78101498	Q15366	Kh1 Domain Of Human Poly(C)-Binding Protein-2 With C-Rich Strand Of Human Telomeric DNA	61	8004	8.9	2	26%
26	338	0.016	+ 1.7	gi|41393561	P28838	Cytosol aminopeptidase	598	56530	8.03	15	28%
				gi|153082755	P09913	Interferon-induced	1043	55282	6.32	28	44%

27	530	1.64E-05	+ 3.0			protein with tetratricopeptide repeats 2					
28	778	0.021	+ 1.7	gi|116812595	O95861	3'(2'),5'-bisphosphate nucleotidase 1	205	33713	5.46	6	17%
29	733	0.002	+ 2.3	gi|178045	P63261	Gamma-actin	451	26147	5.65	14	63%
30	728	2.54E-04	+ 3.4	gi|4501885	P60709	Actin, cytoplasmic 1	708	42052	5.29	25	52%
31	561	3.34E-05	+ 1.7	gi|385994	Q9UGM6	Tryptophanyl-tRNA synthetase	124	1798	5.4	5	100%
32	549	2.65E-04	+ 5.5	gi|340219	P08670	Vimentin	1268	53681	5.06	47	64%
33	525	0.001	+ 4.5	gi|15149465	Q05682	Caldesmon isoform 2	897	71233	6.2	28	45%
34	323	0.012	+ 3.3	gi|222136617	P20591	Interferon-induced GTP-binding protein Mx1	1000	75872	5.6	29	46%
35	341	4.26E-04	+ 3.8	gi|5410451	P20591	Interferon-induced protein p78	1390	75886	5.6	45	65%
36	195	0.042	+ 1.5	gi|577295	Q14697	KIAA0088/Neutral alpha-glucosidase AB	887	107158	5.71	28	25%

37	1782	7.34E-04	- 1.9	gi|50592994	P10599	Thioredoxin	286	12015	4.82	9	51%
38	1762	1.59E-04	- 3.3	gi|310942925	P09382	Human Galectin-1 In Complex With Lactobionic Acid	474	14770	5.34	17	86%
39	930	0.003	- 2.3	gi|24119203	P06753	Tropomyosin alpha-3 chain isoform 2	685	29243	4.75	24	62%
40	831	0.003	- 2.1	gi|223555975	P67936	Tropomyosin alpha-4 chain isoform 1	847	32874	4.69	27	48%
41	680	3.02E-04	- 3.4	gi|8515718	O43852	Crocalbin-like protein/Calumenin	554	34968	4.39	21	41%
42	426	0.002	- 1.8	gi|5453597	P52907	F-actin-capping protein subunit alpha-1	624	33073	5.45	16	64%
43	650	0.002	- 1.5	gi|340234	P08670	Vimentin	1022	35089	4.7	28	70%
44	920	0.012	-7.4	gi|4505773	P35232	Prohibitin	1011	29844	5.57	49	62%
45	464	8.12E-05	- 2.0	gi|4501885	P60709	Actin, cytoplasmic 1	958	42052	5.29	38	68%
46	210	6.87E-04	- 1.7	gi|15010550	P14625	Heat shock protein gp96 precursor/Endoplasmin	1308	90309	4.73	36	44%

47	248	0.005	- 1.9	gi|4503483	P13639	Elongation factor 2	1504	96246	6.41	44	48%
48	649	8.85E-04	- 1.6	gi|4503571	P06733	Alpha-enolase isoform 1	909	47481	7.01	24	42%
49	452	0.003	- 1.9	gi|325533397	P02545	Human Lamin A Coil 2b Fragment	130	8661	5.46	3	43%
50	364	0.033	- 1.8	gi|27436946	P02545	Prelamin-A/C	1391	74380	6.57	31	44%
51	589	0.002	- 1.5	gi|4529893	P08107	HSP70-1	1272	70280	5.48	35	50%
52	419	1.08E-04	- 6.5	gi|7549809	P13797	Plastin-3	1280	71279	5.41	38	52%
53	437	0.013	- 1.3	gi|4826898	P07737	Profilin-1	329	15216	8.44	13	39%
54	1546	4.83E-04	- 2.3	gi|7019545	Q9UMX5	Neudesin	222	18845	5.51	6	42%

Note: (+) denotes n-fold increase and (-) denotes n-fold decrease in OA-FLS + Poly (I:C) protein compared to control OA-FLS. * denotes the mascot score has a 95 % confidence level if > 49.

Table 5.4. Proteins with changed abundance identified by LC-MS in N-FLS treated with CLO-97 versus control N-FLS.

Serial No.	Spot No.	Anova (p)	Fold change of N +CLO-97 Vs N Control	Accession code	Uniprot ID	Protein name	Mascot score*	Mw (Da)	Pi	Matched peptides	Sequence coverage (%)
1	1221	0.026	+ 29.6	gi|4506761	P60903	Protein S100-A10	195	11310	6.82	8	54%
2	1177	6.61E-04	+ 98.3	gi|4503117	P04080	Cystatin-B	203	11190	6.96	9	85%
3	1222	0.018	+ 1.1	gi|119588030	Q5U5U6	hCG1640580, isoform CRA_a	66	16549	5.46	3	23%
4	1084	0.01	+ 2.6	gi|5802966	P60981	Destrin	512	18950	8.06	20	64%
5	1059	0.008	+ 59.7	gi|325053860	P02511	Human Alphab Crystalline Acd	408	10151	6.21	18	76%
6	1082	0.002	+ 13.3	gi|10863927	P62937	Peptidyl-prolyl cis-trans isomerise A	302	18229	7.68	11	58%
7	1109	0.003	+ 6.0	gi|1041969	Q13427	17 kda cyclophilin A	146	3190	4.1	3	93%

8	1039	0.038	+ 2.6	gi|4505621	P30086	Phosphatidylethanolamine-binding protein 1	338	21158	7.01	9	47%
9	940	0.004	+ 4.7	gi|5453555	P62826	GTP-binding nuclear protein Ran	456	24579	7.01	12	50%
10	993	0.008	+ 4.8	gi|62738405	P04179	Human Manganese Superoxide Dismutase Containing 3-Fluorotyrosine	428	21836	6.86	21	53%
11	902	0.004	+ 2.0	gi|226529917	P60174	Triosephosphate isomerase	660	31057	5.65	28	66%
12	750	0.012	+ 1.4	gi|4502101	P04083	Annexin A1	710	38918	6.57	18	44%
13	617	0.025	+ 1.3	gi|28178825	O75874	Isocitrate dehydrogenase [NADP] cytoplasmic	726	46915	6.53	27	53%
14	395	0.009	+ 1.3	gi|27436946	P02545	Prelamin-A/C	728	74380	6.57	27	41%
15	253	0.043	+ 1.1	gi|178045	P63267	Gamma-actin	226	26147	5.65	7	31%
16	252	0.022	+ 1.7	gi|229597861	P08670	Human Vimentin	76	4674	4.35	3	76%

17	942	0.017	+ 1.8	gi|726098	P09211	Glutathione S-transferase-P1c	558	23583	5.43	17	60%
18	1206	0.049	-1.4	gi|5032057	P31949	Protein S100-A11	326	11847	6.56	19	56%
19	1174	0.028	-1.3	gi|50592994	P10599	Thioredoxin	439	12015	4.82	11	88%
20	1171	8.43E-04	-1.5	gi|310942925	P09382	Human Galectin-1 In Complex With Lactobionic Acid	461	14770	5.34	28	82%
21	1096	0.024	-1.3	gi|4503545	P63241	Eukaryotic translation initiation factor 5A-1	308	17049	5.08	11	40%
22	843	0.049	-1.2	gi|4826659	P47756	F-acting-capping protein subunit beta isoform 1	481	30952	5.69	15	47%
23	800	0.046	-1.3	gi|4502107	P08758	Annexin A5	407	35971	4.94	13	30%
24	838	0.015	-1.4	gi|296011025	Q5JT25	Ras-related protein Rab-41	24	25251	5.14	1	4%
25	813	0.02	-1.4	gi|82407948	P61981	14-3-3 Gamma In Complex With A Phosphoserine Peptide	426	28325	4.8	16	58%

26	875	0.025	-1.2	gi|49119653	P63104	YWHAZ protein (14-3-3 protein zeta/delta)	613	30100	4.72	20	49%
27	874	0.025	-1.4	gi|5803227	P27348	14-3-3 protein theta	195	28032	4.68	6	19%
28	804	0.001	-1.5	gi|34098678	Q96NE9	FERM domain-containing protein 6	23	72853	7.12	1	1%
29	801	0.019	-1.3	gi|6005993	P09496	Clathrin light chain A	203	27174	4.43	10	18%
30	717	0.018	-1.8	gi|47519616	P07951	Tropomyosin beta chain isoform 2	928	33027	4.63	27	66%
31	501	0.049	-1.2	gi|159162689	P07237	Human Protein Disulfide Isomerase	230	13363	5.94	6	39%
32	602	0.037	-1.3	gi|3095186	O60664	Cargo selection protein TIP47	529	47175	5.3	19	45%
33	504	0.003	-1.4	gi|24307939	P48643	T-complex protein 1 subunit epsilon	85	60089	5.45	2	3%
34	412	0.025	-2.2	gi|4504165	P06396	Gelsolin	150	86043	5.9	4	7%
35	385	2.24E-04	-1.7	gi|4826657	Q05682	Caldesmon isoform 2	516	62683	6.18	16	30%
36					P67936	Tropomyosin alpha-4	49	32874	4.69	3	10%

	466	0.008	-1.7	gi|223555975		chain isoform 1					
37	383	0.01	-1.6	gi|110590597	P02787	Apo-Human Serum Transferrin	718	76810	6.58	21	34%
38	379	0.007	-1.5	gi|119573383	Q5TCI9	Lamin A/C, isoform CRA_c	1014	87829	8.91	28	36%
39	664	0.002	-1.6	gi|4758158	Q15019	Septin-2	628	41689	6.15	19	46%
40	696	0.016	-1.6	gi|5174391	P14550	Alcohol dehydrogenase [NADP+]	390	36892	6.32	12	35%
41	275	0.009	-1.4	gi|19913410	Q14764	Major vault protein	731	99551	5.34	27	31%
42	330	0.022	-1.7	gi|20357552	Q14247	Src substrate cortactin	565	61720	5.24	18	32%
43	574	0.034	-1.2	gi|62414289	P08670	Vimentin	1274	53676	5.06	48	64%

Note: (+) denotes n-fold increase and (-) denotes n-fold decrease in N-FLS + CLO-97 protein compared to control N-FLS. * denotes the mascot score has a 95 % confidence level if > 49.

Table 5.5. Proteins with changed abundance identified by LC-MS in OA-FLS treated with CLO-97 versus control OA-FLS.

Serial No.	Spot No.	Anova (p)	Fold change of OA + CLO-97 Vs OA Control	Accession code	Uniprot ID	Protein name	Mascot score*	Mw (Da)	pI	Matched peptides	Sequence coverage (%)
1	997	1.96E-04	+ 2.0	gi|290560013	P01892	Mhc Class I Hla-A2.1	86	11929	5.76	4	34%
2	981	0.001	+ 2.0	gi|4503117	P04080	Cystatin-B	189	11190	6.96	6	39%
3	944	1.78E-04	+ 1.7	gi|10863927	P62937	Peptidyl-prolyl cis-trans isomerase A	312	18229	7.68	14	43%
4	919	2.12E-04	+ 1.9	gi|5031635	P23528	Cofilin-1	232	18719	8.22	13	39%
5	895	0.002	+ 1.7	gi|4503057	P02511	Alpha-crystalline B chain	316	20146	6.76	14	41%
6	856	1.60E-04	+ 2.5	gi|30841303	P04179	Manganese-containing superoxide dismutase	623	23658	6.9	25	40%

7	692	0.013	+ 1.7	gi|42403575	Q14192	Four and a half LIM domains protein 2	221	34166	7.8	11	27%
8	683	0.002	+ 1.7	gi|114793741	P22692	The Inhibition Of Insulin-Like Growth Factors By Igf Binding Proteins	85	10493	5.28	2	27%
9	650	0.001	+ 1.1	gi|4502101	P04083	Annexin A1	1148	38918	6.57	31	63%
10	728	5.15E-04	+ 2.0	gi|4506179	P25786	Proteasome subunit alpha type-1	612	29822	6.15	21	58%
11	696	4.51E-04	+ 2.0	gi|70995211	Q13011	Delta(3,5)-Delta(2,4)-dienoyl-CoA isomerase, mitochondrial	435	36136	8.16	14	37%
12	537	0.002	+ 1.6	gi|7657309	Q9NZU5	LIM and cysteine-rich domains protein 1	433	42004	8.27	14	33%
13	463	0.003	+ 1.4	gi|4503571	P06733	Alpha-enolase	992	47481	7.01	25	53%
14	484	2.11E-04	+ 1.7	gi|28178825	O75874	Isocitrate dehydrogenase [NADP] cytoplasmic	568	46915	6.53	17	34%
15	480	0.011	+ 1.6	gi|1706611	P49411	Elongation factor Tu, mitochondrial	925	49852	7.26	23	53%

16	345	5.43E-04	+ 1.5	gi|41393561	P28838	Cytosol aminopeptidase	738	56530	8.03	20	39%
17	660	0.031	+ 5.2	gi|18645167	P07355	Annexin A2	1104	38780	7.57	31	64%
18	582	0.006	+ 3.7	gi|4557305	P04075	Fructose-bisphosphate aldolase A	754	39851	8.3	21	40%
19	446	6.12E-05	+ 8.7	gi|10864011	Q9Y6N5	Sulfide:quinone oxidoreductase, mitochondrial	351	50214	9.18	8	20%
20	433	3.74E-06	+ 9.0	gi|4503471	P68104	Elongation factor 1-alpha 1	646	50451	9.1	22	36%
21	365	4.02E-05	+ 9.8	gi|33286418	P14618	Pyruvate kinase isozymes M1/M2	290	58470	7.96	11	26%
22	66	0.039	+ 1.1	gi|24657579	P18206	Vinculin	953	117234	5.83	27	30%
23	61	0.013	+ 1.9	gi|115527062	P12110	Collagen alpha-2(VI)	490	109709	5.85	14	12%
24	120	0.035	+ 1.6	gi|38327039	P34932	Heat shock 70 kDa protein 4	776	95127	5.11	22	24%
25	246	0.009	+ 2.8	gi|16507237	P11021	78 kDa glucose-regulated protein	984	72402	5.07	30	36%
26	515	0.006	+ 1.7	gi|4501885	P60709	Actin, cytoplasmic 1	724	42052	5.29	26	47%
27	389	0.019	+ 1.6	gi|340234	P08670	Vimentin	795	35089	4.7	23	66%

28	283	0.013	+ 1.6	gi|30795231	P80723	Brain acid soluble protein 1	172	22680	4.64	6	18%
29	223	0.018	+ 1.8	gi|4757900	P27797	Calreticulin	294	48283	4.29	11	23%
30	957	4.07E-04	+ 1.5	gi|60593722	Q14019	Human Coactosin-Like Protein At 1.9 A Resolution	410	16136	5.54	15	63%
31	1017	0.007	-1.8	gi|13775200	Q9BWJ5	Splicing factor 3B subunit 5	135	10243	5.89	4	39%
32	958	9.58E-04	-1.7	gi|17986258	P60660	Myosin light polypeptide 6	406	17090	4.56	10	47%
33	925	0.006	-1.6	gi|7657176	Q9Y2B0	Protein canopy homolog 2	197	20981	4.81	4	29%
34	926	8.77E-04	-1.8	gi|7019545	Q9UMX5	Neudesin	104	18845	5.51	4	27%
35	928	0.001	-2	gi|5802966	P60981	Destrin	358	18950	8.06	16	42%
36	924	0.001	-2.3	gi|4505409	P22392	Nucleoside diphosphate kinase B	244	17401	8.52	10	48%
37	845	0.004	-1.5	gi|4505591	Q06830	Peroxiredoxin-1	566	22324	8.27	19	61%
38	854	0.003	-1.6	gi|48255905	Q01995	Transgelin	255	22653	8.87	9	34%
39	308	0.005	-1.7	gi|33286420	P14618	Pyruvate kinase isozymes M1/M2 isoform b	707	58538	7.6	20	29%
40					Q5I6Y4	Human Lamin A Coil 2b	125	8661	5.46	3	47%

	237	9.34E-04	-2	gi|325533397		Fragment					
41	434	0.04	-1.5	gi|124494254	Q9UQ80	Proliferation-associated protein 2G4	347	44101	6.13	10	26%
42	217	0.005	-1.5	gi|4826657	Q05682	Caldesmon isoform 2	1186	62683	6.18	36	47%
43	258	0.011	-1.9	gi|5729877	P11142	Heat shock cognate 71 kDa protein	1492	71082	5.37	44	46%
44	361	6.50E-04	-1.7	gi|306992081	P08670	Vimentin	342	14270	4.94	11	52%
45	511	3.75E-04	-1.5	gi|62421069	Q562R8	Actin-like protein	114	11529	6.56	4	63%
46	607	0.002	-1.7	gi|47519616	P07951	Tropomyosin beta chain isoform 2	908	33027	4.63	27	48%
47	666	0.006	-1.7	gi|223555975	P67936	Tropomyosin alpha-4 chain isoform 1	654	32874	4.69	22	38%
48	681	1.27E-04	-1.7	gi|6980667	P04233	Mhc Class Ii Associated P41 Ii Fragment In Complex With Cathepsin L	61	4830	9.37	2	52%
49	871	7.14E-04	-1.4	gi|21361091	P09936	Ubiquitin carboxyl-terminal hydrolase isozyme L1	231	25151	5.33	7	36%

50	830	8.37E-04	-1.5	gi|4504183	P09211	Glutathione S-transferase P	320	23569	5.43	9	33%
51	842	3.24E-04	-1.5	gi|4757834	O95816	BAG family molecular chaperone regulator 2	190	23928	6.25	6	26%

Note: (+) denotes n-fold increase and (-) denotes n-fold decrease in OA-FLS + CLO-97 protein compared to control OA-FLS. * denotes the mascot score has a 95 % confidence level if > 49.

Table 5.6. Proteins with changed abundance identified by LC-MS in N-FLS treated with 5' ppp-dsRNA versus control N-FLS.

Serial No.	Spot No.	Anova (p)	Fold change of N +RIG-I Vs N Control	Accession code	UniProt ID	Protein name	Mascot score*	Mw (Da)	pI	Matched peptides	Sequence coverage (%)
1	727	0.009	+ 7.1	gi|4506761	P60903	Protein S100-A10	212	11310	6.82	6	54%
2	604	2.66E-04	+ 18.4	gi|325053860	P02511	Human Alphab Crystalline Acd	466	10151	6.21	15	75%
3					P04179	Manganese Superoxide	558	22014	6.37	18	58%

	558	4.00E-05	+ 3.3	gi|194708958		Dismutases					
4	500	1.34E-07	+ 1.4	gi|226529917	P60174	Triosephosphate isomerase isoform 2	849	31057	5.65	19	55%
5	259	0.003	+ 1.3	gi|4505763	P00558	Phosphoglycerate kinase 1	925	44985	8.3	28	66%
6	481	1.12E-05	+ 1.7	gi|4758484	D3DRA3	Glutathione S-transferase omega-1	568	27833	6.23	16	49%
7	300	0.002	+ 1.1	gi|4506761	P60903	Protein S100-A10	158	11179	6.82	6	45%
8	118	3.67E-06	+ 2.3	gi|4503571	P06733	Alpha-enolase isoform 1	950	47481	7.01	26	52%
9	157	2.07E-08	+ 1.7	gi|21361091	P09936	Ubiquitin carboxyl-terminal hydrolase isozyme L1	327	25151	5.33	11	45%
10	686	8.03E-04	-1.3	gi|4501885	P60709	Actin, cytoplasmic 1	770	42052	5.29	25	64%
11	685	0.005	-1.4	gi|385992	Q9UGM6	Tryptophanyl-tRNA synthetase	118	1784	4.21	1	100%
12	679	2.82E-04	-1.6	gi|5729877	P11142	Heat shock cognate 71 kDa protein isoform 1	268	71083	5.37	7	12%

13	612	1.04E-04	-1.2	gi|159162689	P07237	Human Protein Disulfide Isomerase	197	13363	5.94	4	41%
14	619	2.04E-05	-1.2	gi|4507677	P14625	Endoplasmin precursor	879	92696	4.76	21	28%
15	570	4.38E-06	-2.9	gi|30795231	P80723	Brain acid soluble protein 1	343	22680	4.64	9	62%
16	518	0.002	-1.2	gi|153070260	P29966	Myristoylated alanine-rich C-kinase substrate	167	31707	4.47	5	25%
17	510	5.64E-09	-1.1	gi|183616	Q02952	Gravin	52	33169	4.2	1	4%
18	310	2.81E-04	-1.2	gi|178045	P63267	Gamma-actin	455	26147	5.65	28	64%
19	238	8.04E-04	-1.5	gi|62414289	P08670	Vimentin	1373	53676	5.06	39	58%
20	185	6.93E-08	-1.3	gi|62897129	Q53GZ6	Heat shock 70kDa protein 8 isoform 1 variant	1013	71083	5.28	29	37%
21	166	9.78E-09	-1.9	gi|119626083	P02768	Albumin, isoform CRA_t	121	58614	6.66	4	5%
22	194	2.99E-06	-1.2	gi|325533397	P02545	Human Lamin A Coil 2b Fragment	90	8661	5.46	3	37%

Note: (+) denotes n-fold increase and (-) denotes n-fold decrease in N-FLS + 5’ ppp-dsRNA protein compared to control N-FLS. * denotes the mascot score has a 95 % confidence level if > 49.

Table 5.7. Proteins with changed abundance identified by LC-MS in OA-FLS treated with 5' ppp-dsRNA versus control OA-FLS.

Serial No.	Spot No.	Anova (p)	Fold change of OA +RIG-I Vs OA Control	Accession code	UniProt ID	Protein name	Mascot score*	Mw (Da)	pI	Matched peptides	Sequence coverage (%)
1	830	0.004	+ 1.6	gi|4507879	P21796	Voltage-dependent anion-selective channel protein 1	336	30868	8.62	13	51%
2	563	0.003	+ 2.3	gi|32454741	P50454	Serpin H1 precursor	535	46525	8.75	14	33%
3	537	0.002	+ 2.1	gi|4503471	P68104	Elongation factor 1-alpha 1	437	50451	9.1	12	19%
4	527	0.001	+ 9.5	gi|7657309	Q9NZU5	LIM and cysteine-rich domains protein 1	569	42004	8.27	19	41%
5	430	0.012	+ 2.5	gi|308153681	Q01518	Adenylyl cyclase-associated protein 1	125	52325	8.24	6	12%
6	393	0.015	+ 1.9	gi|33286418	P14618	Pyruvate kinase isozymes M1/M2 isoform a	1034	58470	7.96	30	53%
7	408	0.014	+ 1.9	gi|4507813	B3KUU2	UDP-glucose 6-dehydrogenase isoform 1	533	55674	6.73	16	29%

8	580	0.002	+ 1.5	gi|4501883	P62736	Actin, aortic smooth muscle	380	42381	5.23	13	31%
9	591	0.018	+ 3.2	gi|62897625	P60709	Beta actin variant	691	42080	5.37	24	46%
10	374	0.02	+ 2.3	gi|57863257	P78527	T-complex protein 1 subunit alpha isoform a / DNA-dependent protein kinase catalytic subunit	888	60819	5.8	19	44%
11	381	0.037	+ 1.5	gi|48762932	P50990	T-complex protein 1 subunit theta	294	60153	5.42	6	12%
12	310	0.042	+ 1.8	gi|190613719	P08107	A Complex Of Sse1p And Hsp70	533	42075	6.4	15	38%
13	383	0.015	+ 2.3	gi|31542947	P10809	60 kDa heat shock protein, mitochondrial	964	61187	5.7	23	41%
14	493	0.013	+ 1.5	gi|167466173	P08107	Heat shock 70 kDa protein 1A/1B	118	70294	5.48	4	7%
15	786	0.006	+ 2.2	gi|63252900	P09493	Tropomyosin alpha-1 chain isoform 4	536	32856	4.72	13	36%
16	831	0.002	+ 1.9	gi|4502107	P08758	Annexin A5	356	35971	4.94	11	33%

17	846	0.006	+ 1.5	gi|4588526	O00299	Nuclear chloride channel	547	27249	5.02	14	51%
18	1255	6.07E-04	-1.5	gi|50592994	Q86VQ3	Thioredoxin isoform 1	295	12015	4.82	10	51%
19	1126	0.031	-1.6	gi|7019545	Q9UMX5	Neudesin precursor	168	18845	5.51	4	28%
20	979	0.035	-9.9	gi|4504183	P09211	Glutathione S-transferase P	184	23569	5.43	4	24%
21	1018	0.023	-11.4	gi|134665	P04179	Superoxide dismutase [Mn]	204	24878	8.35	6	23%
22	704	0.048	-2.5	gi|6754994	Q8N201	Poly(rC)-binding protein 1/Integrator complex subunit 1	266	37987	6.66	6	21%
23	542	0.001	-1.7	gi|8922712	Q9NVA2	Septin-11	317	49652	6.36	10	21%
24	458	9.03E-04	-3.7	gi|4506141	Q92743	Serine protease HTRA1 precursor	189	52167	8.09	7	12%
25	379	0.007	-1.6	gi|7549809	P13797	Plastin-3 isoform 1	558	71279	5.41	14	26%
26			-2	gi|31542947	P10809	60 kDa heat shock protein,	488	61187	5.7	16	19%

	388	0.003				mitochondrial					
27	732	0.024	-2	gi|4506667	P05388	60S acidic ribosomal protein P0	148	34423	5.71	4	13%
28	729	0.044	-4	gi|4502101	P04083	Annexin A1	348	38918	6.57	8	28%
29	859	0.02	-6.7	gi|14249718	Q969E4	Transcription elongation factor A protein-like 3	114	22603	4.85	4	17%
30	820	0.001	-3.9	gi|4503477	P24534	Elongation factor 1-beta	120	24919	4.5	2	10%
31	629	0.008	-5.7	gi|306992081	P08670	Vimentin	89	14270	4.94	5	35%

Note: (+) denotes n-fold increase and (-) denotes n-fold decrease in OA-FLS + 5’ ppp-dsRNA protein compared to control OA-FLS. * denotes the mascot score has a 95 % confidence level if > 49.

Table 5.8. Proteins with changed abundance identified by LC-MS in N-FLS treated with LPS versus control N-FLS.

Serial No.	Spot No.	Anova (p-value)	Fold change of N + LPS Vs N control	Accession code	Protein name	Mascot score*	Mw (Da)	pI	Matched peptides	Sequence coverage (%)
1	648	0.017	-4.8	gi|5032057	Protein S100-A11	337	11847	6.56	14	56%
2	631	3.11E-04	-4.3	gi|50592994	Thioredoxin isoform 1	261	12015	4.82	10	51%
3	629	1.77E-04	-3	gi|4504981	Galectin-1	405	15048	5.34	17	77%
4	582	0.001	-2.8	gi|4503545	Eukaryotic translation initiation factor 5A-1 isoform B	444	17049	5.08	12	68%
5	578	0.031	-1.9	gi|7657176	Protein canopy homolog 2 isoform 1 precursor	88	20981	4.81	3	22%
6	567	7.31E-04	-2.5	gi|31615966	Familial Als Mutant S134n Of Human Cu, Zn Superoxide Dismutase	252	16001	5.7	6	54%
7	561	0.001	-2	gi|21389433	Heat shock protein beta-6	225	17182	5.95	8	40%
8					Human Manganese Superoxide	450	21836	6.86	13	48%

	534	9.59E-06	-8.1	gi|62738405	Dismutase					
9	524	0.036	-6.7	gi|4505591	Peroxiredoxin-1	399	22324	8.27	12	43%
10	544	2.75E-06	-3.8	gi|12644008	UMP-CMP kinase	407	22436	5.44	11	57%
11	508	0.001	-1.3	gi|4757768	rho GDP-dissociation inhibitor 1 isoform a	276	23250	5.02	9	34%
12	453	5.91E-06	-1.6	gi|5453990	Proteasome activator complex subunit 1 isoform 1	317	28876	5.78	8	39%
13	463	0.034	-1.3	gi|7330335	Chloride intracellular channel protein 4	303	28982	5.45	11	54%
14	445	3.80E-04	-1.7	gi|157879202	Native And Inhibited Forms Of Human Cathepsin D	408	26511	5.14	17	67%
15	469	0.002	-2	gi|40805862	Tumour protein D54 isoform f	137	19946	5.35	3	18%
16	492	0.027	-3.5	gi|7106387	Proteasome subunit alpha type-5	358	26565	4.74	9	45%
17	426	0.003	-1.7	gi|119567960	hCG1643231, isoform CRA_a	113	19005	6.3	2	9%
18	343	0.038	-1.1	gi|223555975	Tropomyosin alpha-4 chain isoform 1	792	32874	4.69	23	45%
19	292	0.034	-2.3	gi|47519616	Tropomyosin beta chain isoform 2	741	33027	4.63	26	50%

20	555	0.007	+ 8.9	gi|325053860	Human Alphab Crystalline Acd	383	10151	6.21	14	80%
21	494	0.009	+ 2.4	gi|226529917	Triosephosphate isomerase	863	31057	5.65	30	71%
22	351	0.008	+ 2.3	gi|119597993	Annexin A2, isoform CRA_c	914	32600	5.93	30	73%
23	325	5.26E-04	+ 3.7	gi|4502101	Annexin A1	588	38918	6.57	15	43%
24	259	9.59E-05	+ 2.3	gi|4503571	Alpha-enolase	1278	47481	7.01	37	61%
25	257	0.002	+ 2.5	gi|28178825	Isocitrate dehydrogenase [NADP] cytoplasmic	839	46915	6.53	23	63%
26	228	0.003	+ 2.6	gi|4503571	Alpha-enolase isoform 1	1080	47481	7.01	26	61%
27	174	0.003	+ 3.2	gi|308153681	Adenylyl cyclase-associated protein 1	55	52325	8.24	15	36%
28	180	2.58E-04	+ 3.3	gi|2935481	UDP glucose 6-dehydrogenase	266	19489	5.39	7	53%
29	46	0.001	+ 2.8	gi|4503483	Elongation factor 2	1028	96246	6.41	28	45%
30	139	0.002	+ 3.6	gi|325533397	Human Lamin A Coil 2b Fragment	102	8661	5.46	3	47%
31	447	0.006	+ 1.4	gi|4529893	HSP70-1	889	70280	5.48	24	42%
32	477	0.003	+ 1.3	gi|49119653	YWHAZ protein	537	30100	4.72	15	45%

33	452	0.049	+ 1.3	gi|54696890	Tyrosine 3-monooxygenase/tryptophan 5-monooxygenase activation protein, theta polypeptide	557	28031	4.72	15	50%
34	438	0.002	+ 1.7	gi|4507651	Tropomyosin alpha-4 chain isoform 2	681	28619	4.67	23	45%
35	440	0.001	+ 2.2	gi|14251209	Chloride intracellular channel protein 1	345	27248	5.09	8	30%
36	357	0.022	+ 1.3	gi|4557032	L-lactate dehydrogenase B chain	692	36900	5.71	18	51%
37	264	0.003	+ 1.6	gi|178045	Gamma-actin	414	26147	5.65	28	49%
38	253	7.64E-04	+ 2.2	gi|306992081	Vimentin	322	14270	4.94	10	62%
39	263	5.14E-05	+ 2.0	gi|159162689	Human Protein Disulfide Isomerase	304	13363	5.94	10	61%
40	183	0.009	+ 3.4	gi|913150	Calreticulin=calcium binding protein	171	3095	6.12	5	50%
41	136	0.003	+ 7.5	gi|112910	Alpha-2-HS-glycoprotein	65	40098	5.43	2	3%
42	146	6.53E-04	+ 3.5	gi|15010550	Heat shock protein gp96 precursor	1154	90309	4.73	40	44%
43	63	2.63E-05	+ 16.8	gi|220702506	TapasinERP57 HETERODIMER	1086	54541	5.61	30	56%
44	169	0.013	+ 2.1	gi|6470150	BiP protein	1291	71002	5.23	33	44%
45				gi|5729877	Heat shock cognate 71 kDa protein	387	68677	5.37	13	46%

	89	0.042	+ 1.2		isoform 1					
46	147	3.02E-06	+ 3.5	gi|8569616	The Moesin Ferm Domain TAIL DOMAIN Complex	337	34554	8.92	9	33%
47	490	0.002	+ 3.1	gi|4502565	Calpain small subunit 1	533	28469	5.05	16	56%

Note: (+) denotes n-fold increase and (-) denotes n-fold decrease in N-FLS + LPS protein compared to control N-FLS. * denotes the mascot score has a 95 % confidence level if > 49.

Table 5.9. Proteins with changed abundance identified by LC-MS in OA-FLS treated with LPS versus control OA-FLS.

Serial No.	Spot No.	Anova (p)	Fold change of OA +LPS Vs OA Control	Accession code	Protein name	Mascot score*	Mw (Da)	pI	Matched peptides	Sequence coverage (%)
1	1386	5.48E-04	+ 2.4	gi|4506761	Protein S100-A10	127	11310	6.82	8	31%
2	1336	9.99E-05	+ 7.9	gi|4505185	Macrophage migration inhibitory factor	77	12508	7.74	2	15%
3	1314	4.63E-04	+ 3.6	gi|83367075	Metallothionein-1E	55	7150	8.38	1	19%

4	1344	2.00E-04	+ 3.5	gi|4757826	Beta-2-microglobulin precursor	157	13820	6.06	7	31%
5	1283	5.40E-04	+ 2.2	gi|4885413	Histidine triad nucleotide-binding protein 1	144	13908	6.43	4	19%
6	1302	6.49E-04	+ 3.7	gi|4758328	Fatty acid-binding protein, heart	193	14775	6.29	6	38%
7	1203	1.14E-04	+ 4.2	gi|4507149	Superoxide dismutase [Cu-Zn]	141	16154	5.7	4	27%
8	1149	3.64E-04	+ 1.7	gi|5802966	Destrin isoform a	141	18950	8.06	7	25%
9	1096	0.001	+ 1.6	gi|21389433	Heat shock protein beta-6	191	17182	5.95	6	26%
10	1058	8.03E-04	+ 3.2	gi|4557797	Nucleoside diphosphate kinase A isoform b	92	17309	5.83	4	21%
11	1088	5.55E-04	+ 2.6	gi|20149498	Ferritin light chain	153	20064	5.51	5	22%
12	1048	4.28E-04	+ 2.3	gi|56682959	Ferritin heavy chain	64	21383	5.3	2	13%
13	1111	0.003	+ 1.5	gi|188586	Myosin light chain 2	112	19915	5.09	4	17%
14	1252	7.09E-04	+ 3.2	gi|4505705	Astrocytic phosphoprotein PEA-1	190	15088	4.93	5	28%
15	1261	5.52E-04	+ 1.7	gi|4505705	Astrocytic phosphoprotein PEA-15	151	15088	4.93	4	23%
16	1060	1.52E-04	+ 4.7	gi|4503057	Alpha-crystalline B chain	338	20146	6.76	14	40%

17	1193	0.001	+ 8.2	gi|10863927	Peptidyl-prolyl cis-trans isomerase A	376	18229	7.68	15	53%
18	1140	9.94E-05	+ 11.7	gi|14719392	Cofilin-2 isoform 1	92	18839	7.66	5	18%
19	1198	0.004	+ 1.7	gi|119607093	ubiquitin-conjugating enzyme E2 variant 2, isoform CRA_a	79	12066	9.86	3	33%
20	923	0.001	+ 13.1	gi|7657441	28 kDa heat- and acid-stable phosphoprotein	190	20618	8.84	6	27%
21	902	2.39E-04	+ 80.1	gi|436226	KIAA0038	129	25526	8.66	4	15%
22	869	3.79E-04	+ 11.2	gi|226529917	Triosephosphate isomerase isoform 2	181	31057	5.65	6	18%
23	727	4.70E-04	+ 2.5	gi|5031857	L-lactate dehydrogenase A chain isoform 1	133	36950	8.44	5	12%
24	573	3.28E-04	+ 2.5	gi|4557305	Fructose-bisphosphate aldolase A isoform 1	564	39851	8.3	18	27%
25	620	0.004	+ 2.7	gi|21465695	Human 3alpha-Hsd Type 3 In Ternary Complex With Nadp And Testosterone	345	37095	6.86	12	21%
26	706	0.001	+ 1.8	gi|33413400	S-formylglutathione hydrolase	111	31956	6.54	5	8%

27	715	0.001	+ 3.1	gi|5453710	LIM and SH3 domain protein 1	66	30097	6.61	2	9%
28	693	0.002	+ 2.7	gi|30749598	The Pdz Tandem Of Human Syntenin	76	18075	8.5	5	13%
29	600	0.004	+ 3.2	gi|4758018	Calponin-2 isoform a	435	34074	6.95	17	26%
30	535	0.009	+ 2.1	gi|27754103	26S protease regulatory subunit 10B	309	44430	7.1	12	24%
31	182	0.004	+ 1.5	gi|154355000	Far upstream element-binding protein 2	184	73355	6.85	6	8%
32	931	3.16E-04	+ 2.1	gi|193806571	Putative cytochrome b-c1 complex subunit Rieske-like protein 1	84	31081	9.04	3	5%
33	933	0.001	+ 1.8	gi|4757834	BAG family molecular chaperone regulator 2	249	23928	6.25	8	20%
34	929	0.007	+ 1.8	gi|4504175	Glutathione S-transferase Mu 2 isoform 1	93	25899	6.00	2	7%
35	843	0.002	+ 1.6	gi|4758638	Peroxiredoxin-6	189	25133	6	7	27%
36				gi|8394076	Proteasome subunit alpha	243	27838	6.34	8	25%

	749	2.19E-04	+ 2.4		type-6					
37	784	0.003	+ 1.7	gi|4758484	Glutathione S-transferase omega-1 isoform 1	189	27833	6.23	8	27%
38	841	0.002	+ 1.7	gi|4504517	Heat shock protein beta-1	91	22826	5.98	3	13%
39	682	6.08E-04	+ 3.5	gi|4506179	Proteasome subunit alpha type-1 isoform 2	320	29822	6.15	12	33%
40	664	0.002	+ 2.0	gi|4502601	Carbonyl reductase [NADPH] 3	207	31230	5.82	4	13%
41	685	6.90E-04	+ 1.5	gi|296452916	Sulfatase-modifying factor 2	53	33936	7.78	1	3%
42	51	0.028	+ 1.8	gi|124056490	Collagen alpha-1(III) chain	146	139733	6.21	4	3%
43	413	0.034	+ 1.6	gi|30795231	Brain acid soluble protein 1	294	22680	4.64	9	41%
44	645	0.004	+ 1.5	gi|4758018	calponin-2 isoform a	122	34074	6.95	6	13%
45	1343	0.001	- 1.9	gi|50592994	Thioredoxin isoform 1	58	12015	4.82	2	17%
46	922	9.27E-04	- 2.3	gi|21361091	Ubiquitin carboxyl-terminal hydrolase isozyme L1	160	25151	5.33	5	17%
47	1138	0.004	- 1.6	gi|4505409	Nucleoside diphosphate kinase B isoform a	137	17270	8.52	6	36%

48	958	0.002	- 1.5	gi|48255905	Transgelin	254	22653	8.87	9	39%
49	324	7.91E-04	- 1.9	gi|33286418	Pyruvate kinase isozymes M1/M2 isoform a	334	58470	7.96	9	15%
50	390	0.001	- 1.6	gi|4506141	Serine protease HTRA1 precursor	180	521267	8.09	7	12%
51	451	0.007	- 1.4	gi|28178825	Isocitrate dehydrogenase [NADP] Cytoplasmic	231	46915	6.53	8	19%
52	421	0.009	- 1.5	gi|8922712	Septin-11	326	49652	6.36	11	21%
53	457	0.006	- 1.8	gi|119631662	Sjogren syndrome antigen B (autoantigen La), isoform CRA_b	160	30932	8.23	5	14%
54	212	1.14E-04	- 2.0	gi|23200154	Chain A, Nmr Structures Of The C-Terminal Globular Domain Of Human Lamin AC	137	13561	9.57	4	39%
55	138	0.006	- 1.8	gi|4503483	Elongation factor 2	658	96246	6.41	23	22%
56	232	0.001	- 1.5	gi|15149465	Caldesmon isoform 5	1056	61233	6.4	33	42%
57	220	8.08E-04	- 1.7	gi|4826657	Caldesmon isoform 2	904	62683	6.18	27	35%

58	113	0.004	- 1.9	gi|4758648	Kinesin-1 heavy chain	98	110358	6.12	3	3%
59	50	0.002	- 2.1	gi|19913410	Major vault protein	698	99551	5.34	21	25%
60	137	0.009	- 2.0	gi|153070260	Myristoylated alanine-rich C-kinase substrate	174	31707	4.47	6	23%
61	316	0.02	- 1.7	gi|325533983	The Globular Domain Of Human Calreticulin	237	30264	4.74	11	29%
62	724	0.003	- 1.5	gi|157833780	Human Annexin V With Proline Substitution By Thioproline	183	36041	4.94	7	17%
63	705	6.42E-04	- 1.9	gi|28827795	Charged multivesicular body protein	119	24935	4.76	4	16%
64	632	0.006	- 1.6	gi|223555975	Tropomyosin alpha-4 chain isoform 1	138	32874	4.69	5	13%
65	617	7.07E-04	- 2.1	gi|47519616	Tropomyosin beta chain isoform 2	685	33027	4.63	18	39%
66	572	0.006	- 1.5	gi|4502923	Calponin-3	203	36562	5.69	5	15%
67	481	0.028	- 1.9	gi|157502193	26S proteasome non-ATPase regulatory subunit 13 isoform 1	206	43203	5.53	6	14%
68	350	2.65E-04	- 3.4	gi|340219	Vimentin	292	53738	5.03	12	25%

69	296	0.002	- 1.5	gi|7549809	Plastin-3 isoform 1	217	71279	5.41	9	12%
70	379	0.008	- 1.6	gi|220702506	TapasinERP57 HETERODIMER	816	54541	5.61	21	41%

Note: (+) denotes n-fold increase and (-) denotes n-fold decrease in OA-FLS + LPS protein compared to control OA-FLS. * denotes the mascot score has a 95 % confidence level if > 49.

Table 5.10. Proteins with changed abundance identified by LC-MS in N-FLS treated with Pam_2CSK_4 versus control N-FLS.

Serial No.	Spot No.	Anova (p)	Fold change of N HFLS + Pam_2CSK_4 Vs N Control	Accession code	Protein name	Mascot score*	Mw (Da)	Pi	Matched peptides	Sequence coverage (%)
1	1147	0.028	- 2.8	gi|5032057	Protein S100-A11	334	11847	6.56	13	56%
2	1040	0.015	- 6.9	gi|4826898	Profilin-1	502	15216	8.44	22	73%
3	963	0.035	- 2.5	gi|10863927	Peptidyl-prolyl cis-trans isomerase A	545	18229	7.68	19	70%
4	948	0.031	- 1.7	gi|5031635	Cofilin-1	613	18719	8.22	17	64%

5	939	0.013	- 2.1	gi|223480	Dismutase,Cu/Zn superoxide	140	16020	8.44	4	44%
6	894	2.40E-04	- 12.8	gi|4505591	Peroxiredoxin-1	432	22324	8.27	16	48%
7	959	0.003	- 2.0	gi|4503545	Eukaryotic translation initiation factor	496	17049	5.08	14	71%
8	949	0.004	- 1.7	gi|8923579	Regulator complex protein LAMTOR1	98	17848	5.01	3	26%
9	898	0.021	- 2.3	gi|726098	Glutathione S-transferase-P1c	560	23583	5.43	22	60%
10	815	0.043	- 1.7	gi|4826659	F-actin-capping protein subunit beta isoform 1	500	30952	5.69	16	50%
11	816	0.03	- 1.6	gi|14251209	Chloride intracellular channel protein 1	611	27248	5.09	18	80%
12	680	0.004	- 5.4	gi|223555975	Tropomyosin alpha-4 chain isoform 1	743	32874	4.69	24	53%
13	666	0.009	- 2.2	gi|229597861	Human Vimentin	160	4674	4.35	4	58%
14	592	0.026	- 4.0	gi|21361547	Ribonuclease inhibitor	1140	51766	4.71	30	70%
15	583	0.025	- 1.3	gi|47519616	Tropomyosin beta chain isoform 2	968	33027	4.63	29	64%
16	375	0.015	- 2.0	gi|6457378	Cytovillin 2	115	16294	9.32	3	21%
17	382	0.007	- 1.9	gi|119626083	Albumin, isoform CRA_t	138	60211	6.66	5	8%

18	386	0.019	- 1.5	gi|7549809	Plastin-3 isoform 1	141	71279	5.41	5	11%
19	492	4.49E-04	- 1.3	gi|220702506	TapasinERP57 HETERODIMER	850	54541	5.61	22	42%
20	491	0.032	- 1.5	gi|62511242	4-trimethylaminobutyraldehyde dehydrogenase	558	54679	5.69	16	30%
21	567	0.013	- 1.7	gi|18379349	Synaptic vesicle membrane protein VAT-1 homolog	763	42122	5.88	30	50%
22	533	0.006	- 4.8	gi|6680045	Guanine nucleotide-binding protein G(I)/G(S)/G(T) subunit beta-1	438	38151	5.6	17	36%
23	640	0.015	- 1.5	gi|56966036	Human Coactosin-Like Protein	452	15898	5.55	13	56%
24	721	0.049	- 1.4	gi|4557032	L-lactate dehydrogenase B chain	763	36900	5.71	22	47%
25	997	0.022	- 1.4	gi|1703319	Annexin A4	982	36088	5.81	3	50%
26	1022	0.024	+ 2.2	gi|33286418	Pyruvate kinase isozymes M1/M2	1098	58470	7.96	33	57%
27	897	0.008	+ 1.4	gi|5453599	F-actin-capping protein subunit alpha-2	372	33157	5.57	11	47%
28					Human Manganese Superoxide	472	21836	6.86	15	48%

	909	0.008	+ 4.4	gi|62738405	Dismutase					
29	832	0.034	+ 1.7	gi|41393561	Cytosol aminopeptidase	526	56530	8.03	16	28%
30	596	0.043	+ 2.4	gi|4501883	Actin, aortic smooth muscle	60	42381	5.23	2	5%
31	400	0.024	+ 2.1	gi|112910	Alpha-2-HS-glycoprotein	92	40098	5.43	4	5%
32	322	0.009	+ 1.9	gi|48255889	Glucosidase 2 subunit beta	295	60357	4.33	8	13%
33	608	0.014	+ 1.5	gi|62421162	Actin-like protein	80	11529	6.19	4	57%
34	527	0.029	+ 2.2	gi|48255905	Transgelin	386	22653	8.87	12	45%
35	456	0.045	+ 1.8	gi|4501885	Actin, cytoplasmic	63	42052	5.29	2	6%
36	432	0.037	+ 1.1	gi|86947	Beta-galactoside-binding lectin, placental - human	71	12043	4.63	3	34%
37	252	0.001	+ 1.7	gi|18490111	Unknown protein	652	48074	5.83	14	34%
38	254	0.032	+ 1.6	gi|87196339	Collagen alpha-1(VI) chain precursor	910	109602	5.26	23	23%
39	260	0.044	+ 1.6	gi|317373534	Periplakin	167	205193	5.47	4	2%
40	244	0.042	+ 1.5	gi|179629	Pro-alpha-1 collagen type 1	61	5998	6.4	2	54%
41					type VI collagen alpha 2 chain	505	109703	5.78	14	14%

	245	0.047	+ 1.4	gi|13603394	precursor					
42	197	0.009	+ 1.6	gi|115527062	collagen alpha-2(VI) chain isoform 2C2 precursor	595	109709	5.85	17	16%
43	193	0.03	+ 2.0	gi|179830	caldesmon	243	62715	6.18	8	14%
44	372	0.041	+ 2.5	gi|119573381	lamin A/C, isoform CRA_a	286	78601	9	9	11%

Note: (+) denotes n-fold increase and (-) denotes n-fold decrease in N-FLS + Pam_2CSK_4 protein compared to control N-FLS. * denotes the mascot score has a 95 % confidence level if > 49.

Table 5.11. Proteins with changed abundance identified by LC-MS in OA-FLS treated with Pam_2CSK_4 versus control OA-FLS.

Serial No.	Spot No.	Anova (p)	Fold change of OA + Pam_2Csk_4 Vs OA Control	Accession code	Protein name	Mascot score*	Mw (Da)	pI	Matched peptides	Sequence coverage (%)
1	1036	2.79E-04	+ 3.5	gi|4506761	Protein S100-A10	164	11310	6.82	7.00	37%
3	996	2.55E-05	+ 4.3	gi|4503117	Cystatin-B	81	11190	6.96	2	33%

4	890	0.005	+ 1.9	gi|4503057	Alpha-crystalline B chain	408	20146	6.76	19	52%
5	876	1.85E-04	+ 8.9	gi|4505621	Phosphatidylethanolamine-binding protein 1 preproprotein	481	21158	7.01	13	48%
6	930	5.17E-05	+ 12.8	gi|10863927	Peptidyl-prolyl cis-trans isomerase A	564	18229	7.68	21	67%
7	924	8.71E-05	+ 11.5	gi|2981743	Chain A, Secypa Complexed With Hagpia	275	18018	7.82	9	48%
8	641	5.32E-04	+ 2.2	gi|18645167	Annexin A2	192	38780	7.57	5	12%
9	779	1.76E-04	+ 18.9	gi|119627888	Adenylate kinase 2, isoform CRA_a	182	14486	7.71	5	34%
10	580	0.002	+ 4.5	gi|556516	Dihydrodiol dehydrogenase isoform DD1	406	35170	8.1	14	24%
11	380	0.001	+ 3.9	gi|4506141	Serine protease HTRA1	279	52167	8.09	12	18%
12	325	0.002	+ 1.9	gi|4757810	ATP synthase subunit alpha, mitochondrial precursor	290	59828	9.16	7	12%
13	288	0.003	+ 2.5	gi|33286418	Pyruvate kinase isozymes M1/M2 isoform a	1254	58470	7.96	41	70%
14	600	6.23E-04	+ 3.0	gi|21465695	Human 3alpha-Hsd Type 3 In Ternary Complex With Nadp And Testosterone	438	37095	6.86	14	25%
15	680	0.006	+ 3.0	gi|7669492	Glyceraldehyde-3-phosphate dehydrogenase	282	36201	8.57	11	29%
16					Electron transfer flavoprotein subunit alpha,	315	35400	8.62	7	29%

	724	0.003	+ 1.9	gi|4503607	mitochondrial isoform a					
17	625	0.002	+ 1.5	gi|5453710	LIM and SH3 domain protein 1	388	30097	6.61	14	36%
18	510	0.013	+ 1.6	gi|27754103	26S protease regulatory subunit 10B	338	44430	7.1	9	17%
19	332	0.004	+ 2.2	gi|4507813	UDP-glucose 6-dehydrogenase isoform 1	204	55674	6.73	6	9%
20	147	0.004	+ 1.7	gi|4503483	Elongation factor 2	754	96246	6.41	22	27%
21	355	0.006	+ 1.8	gi|41393561	Cytosol aminopeptidase	446	56530	8.03	13	21%
22	282	0.017	+ 1.5	gi|119573381	Lamin A/C, isoform CRA_a	831	78610	9	22	34%
23	112	0.002	+ 2.0	gi|24657579	Vinculin	1001	117234	5.83	24	31%
24	133	6.29E-04	+ 2.4	gi|38327039	Heat shock 70 kDa protein 4	442	95127	5.11	12	14%
25	180	0.006	+ 1.6	gi|5729877	Heat shock cognate 71 kDa protein isoform 1	342	71082	5.37	9	15%
26	195	0.002	+ 3.3	gi|50053795	Eukaryotic translation initiation factor 4B	193	69167	5.55	5	12%
27	436	0.009	+ 1.9	gi|89574029	Mitochondrial ATP synthase, H+transporting F1 complex beta subunit	1149	48083	4.95	26	64%
28					ATP synthase subunit beta,	493	56525	5.26	9	25%

	443	0.013	+ 2.1	gi|32189394	mitochondrial precursor					
29	469	0.015	+ 1.3	gi|255958282	Perilipin-3 isoform 1	746	47217	5.3	18	46%
30	439	0.022	+ 1.4	gi|221041680	Unnamed protein product	53	14396	10.65	2	9%
31	743	0.001	+ 1.7	gi|14251209	Chloride intracellular channel protein 1	153	27248	5.09	4	31%
32	794	7.99E-05	+ 2.0	gi|4504517	Heat shock protein beta-1	347	22826	5.98	9	44%
33	947	0.002	+ 1.7	gi|4503029	Cellular retinoic acid-binding protein 2	81	15854	5.42	3	14%
34	961	2.18E-04	- 1.7	gi|4504981	Galectin-1	313	15048	5.34	9	71%
35	973	0.002	- 1.7	gi|50592994	Thioredoxin isoform 1	208	12015	4.82	5	40%
36	942	7.25E-04	- 3.4	gi|17986258	Myosin light polypeptide 6 isoform 1	445	17090	4.56	12	58%
37	922	5.31E-04	- 2.4	gi|322510074	Ubiquitin-related modifier 2	65	10889	5.32	2	23%
38	914	0.004	- 3.0	gi|5031593	Actin-related protein 2/3 complex subunit 5	248	16367	5.47	6	30%
39	897	7.76E-04	- 1.5	gi|223632	Dismutase, Cu/Zn superoxide	272	16020	8.76	11	47%
40	907	0.008	- 1.6	gi|5031635	Cofilin-1	467	18719	8.22	20	66%
41	911	4.99E-04	- 1.8	gi|5802966	Destrin isoform a	375	18950	8.06	14	49%

42	864	0.001	- 2.1	gi|20336761	Heme-binding protein 1	167	21198	5.71	4	22%
43	827	4.22E-04	- 2.0	gi|36038	rho GDP dissociation inhibitor (GDI)	341	23236	5.02	13	32%
44	821	0.011	- 1.7	gi|149241199	Phosphorylated Crk-Ii	129	25351	5.1	4	15%
45	834	0.003	- 1.7	gi|21361091	Ubiquitin carboxyl-terminal hydrolase isozyme L1	339	25151	5.33	12	43%
46	716	0.005	- 1.7	gi|54632177	Aging-associated gene 11	95	34162	7.97	4	16%
47	656	0.001	- 2.1	gi|31645	Glyceraldehyde-3-phosphate dehydrogenase	550	36202	8.26	21	50%
48	651	0.003	- 1.8	gi|27436946	Prelamin-A/C isoform 1 precursor	802	74380	6.57	23	38%
49	150	0.017	- 1.6	gi|15010550	Heat shock protein gp96 precursor	1184	90309	4.73	49	40%
50	483	6.94E-04	- 2.0	gi|4502551	Calumenin isoform a precursor	326	37198	4.47	13	29%
51	726	5.30E-04	- 4.6	gi|4507651	Tropomyosin alpha-4 chain isoform 2	137	28619	4.67	4	20%
52	750	4.22E-04	- 1.7	gi|5803225	14-3-3 protein epsilon	739	29326	4.63	18	61%
53	792	9.80E-04	- 2.2	gi|66347207	Tyrosine 3-monooxygenase/tryptophan 5-monooxygenase activation protein, beta polypeptide	194	8423	6.58	5	62%

54	715	9.14E-05	- 2.1	gi|63252900	Tropomyosin alpha-1 chain isoform 4	254	32856	4.72	8	21%
55	630	0.003	- 2.8	gi|47519616	Tropomyosin beta chain isoform 2	828	33027	4.63	25	58%
56	628	2.32E-04	- 3.9	gi|223555975	Tropomyosin alpha-4 chain isoform 1	424	32874	4.69	14	32%
57	416	1.89E-04	- 2.0	gi|224465187	Secernin-1 isoform a	163	46980	4.66	6	10%
58	353	0.003	- 2.1	gi|159162689	Chain A, Human Protein Disulfide Isomerase	307	13363	5.94	11	71%
59	340	0.032	- 1.8	gi|31542947	60 kDa heat shock protein, mitochondrial	937	61187	5.7	25	41%
60	317	0.044	- 2.6	gi|62414289	Vimentin	1100	53676	5.06	33	57%
61	158	0.003	- 2.3	gi|20149594	Heat shock protein HSP 90-beta	494	83554	4.97	16	17%
62	428	0.014	- 1.7	gi|178045	Gamma-actin	466	26147	5.65	14	53%

Note: (+) denotes n-fold increase and (-) denotes n-fold decrease in OA-FLS + Pam_2CSK_4 protein compared to control OA-FLS. * denotes the mascot score has a 95 % confidence level if > 49.

Table 5.12. Proteins with changed abundance identified by LC-MS in N-FLS treated with end stage OA-SF versus control N-FLS.

Serial No.	Spot No.	Anova (p)	Fold Change N + OA-SF Vs N control	Accession Code	Protein Name	Mascot score*	Mw (Da)	pI	Matched peptides	Sequence coverage (%)
1	1053	0.004	12.8	gi|5174735	Tubulin beta-2 C chain	1188	50263	4.79	33	60
2	1072	0.003	23.3	gi|693933	2-phosphopyruvate-hydratase alpha-enolase	334	47427	7.01	14	14
3	1123	0.002	16	gi|62738405	Human manganese superoxide dismutase	209	21838	6.86	5	25
4	1127	0.001	12.4	gi|4501887	Actin, Cytoplasmic 2	530	42114	5.31	15	34
5	1142	0.002	16.3	gi|4960030	Rab GDP dissociation Inhibition beta	688	41420	8.04	19	46
6	1180	0.005	6.6	gi|3095186	Cargo selection protein TIP47	845	47178	5.3	8	38
7	1184	0.004	16.4	gi|340219	Vimentin	357	53739	5.03	8	14
8	1243	0.002	5.5	gi|1942871	Human liver chichi alcohol dehydrogenase	157	40437	7.58	6	13

9	1269	0.008	3.1	gi|4502101	Annexin A1	418	38922	6.57	8	22
10	1307	0.02	6.8	gi|4557032	L-Lactate dehydrogenase B	481	36905	5.71	11	28
11	1348	0.007	21.1	gi|47519616	Tropomyosin beta chain isoform 2	844	33028	4.63	19	50
12	1594	0.002	19.3	gi|7106439	Tubulin beta-5 chain	719	50103	4.78	17	49
13	1635	0.005	15.3	gi|809185	The effect of metal binding on the structure of Annexin V and implications for membrane binding	645	35841	4.94	16	44
14	1657	0.003	11.2	gi|189617	Protein PP4-X	938	36266	5.65	22	49
15	2278	0.009	11.1	gi|62738405	Hydrogen bonding in human manganese superoxide dismutase	169	21838	6.86	16	48
16	3194	0.005	5.5	gi|34709	Manganese superoxide dismutase	144	24894	8.35	4	16
17	3256	0.007	4.8	gi|62897639	Tubulin beta 4 variant	128	50862	4.83	4	12
18	3258	0.001	77.1	gi|4503571	Alpha-enolase isoform	397	47487	7.01	22	41
19	3260	0.002	10.9	gi|4826898	Profilin-1	152	15219	8.44	7	47
20	3261	0.004	14	gi|306785	G Protein beta subunit	127	38074	5.75	10	24

21	894	0.002	10	gi|338695	Beta-tubulin	126	50249	4.25	8	18

Note: (+) denotes n-fold increase and (-) denotes n-fold decrease in N-FLS + OA-SF protein compared to control N-FLS. * denotes the mascot score has a 95 % confidence level if > 49.

Table 5.13. Proteins with changed abundance identified by LC-MS in N-FLS treated with end stage OA-SF versus control OA-FLS.

Serial No.	Spot No.	Anova (p)	Fold change of N + OA-SF Vs OA control	Accession code	Protein name	Mascot score*	Mw (Da)	Pi	Matched peptides	Sequence coverage (%)
1	3472	0.008	2.6	gi|4504517	Heat Shock Protein beta-1	482	22826	5.98	16	62
2	3699	0.01	13.9	gi|31645	Glyceraldehyde-3-phosphate dehydrogenase	624	36205	8.26	18	46
3	3885	0.007	3.7	gi|62738405	Human manganese superoxide dismutase	531	21838	6.86	23	47
4	3935	0.002	3.8	gi|4505591	Peroiredoxin-1	208	22328	8.27	6	28

5	4019	0.006	2.1	gi|157833780	Chain A, human annexin V with proline substitution by thioproline	734	36042	4.94	17	58
6	4061	0.009	2.1	gi|809185	Annexin V and implications for membrane binding	825	35840	4.94	17	62
7	4922	0.002	3.4	gi|1633054	Cyclophilin A complexed with dipeptide Gly-Pro	93	18098	7.82	11	41
8	4953	0.004	4.5	gi|1633054	Cyclophilin A complexed with dipeptide Gly-Pro	149	18098	7.82	8	49
9	5172	0.005	7.1	gi|4505591	Peroiredoxin-1	383	22328	8.27	12	45
10	5370	0.009	2.3	gi|4503057	Alpha-crystallin B chain	192	20146	6.76	19	56
11	6607	0.002	2.5	gi|809185	Chain A, the effect of metal binding on the structure of annexin V and implications for membrane binding	775	35840	4.94	19	58

Note: (+) denotes n-fold increase and (-) denotes n-fold decrease in N-FLS + OA-SF protein compared to control OA-FLS. * denotes the mascot score has a 95 % confidence level if > 49.

Table 5.14. List of DIGE-LC-MS identified proteins that exhibit a change in abundance in Grade-1 OA synovial tissue versus Grade 0 OA/ Normal synovial tissue.

Serial No.	Spot No.	Fold Change of OA grade 1 Vs OA grade 0	Accession Code	Uniprot ID	Protein Name	Mascot Score*	Mw (Da)	p*I*	Matched peptides	Sequence Coverage (%)
1	3109	1.6	gi|31645	P04406	Glyceraldehyde-3-phosphate dehydrogenase	164	36205	8.26	14	52
2	4482	1.8	gi|3212355	P60903	Chain A, P11 (S100a 10), ligand of Annexin Ii	173	11180	7.3	5	28
3	4216	1.4	gi|4557579	P15090	Fatty acid binding protein, adipocyte	179	14826	6.59	4	43
4	4063	1.9	gi|13937981	P62937	Peptidylprolyl isomerase A (cyclophilin A)	367	18232	7.68	9	63
5	4292	-1.6	gi|5032057	P31949	Protein S100-A11	385	11849	6.56	7	56
6	3137	1.6	gi|18645167	P07355	Annexin A2	1283	38784	7.57	25	71

7	5032	1.5	gi|341914394	A2BFH1	Peptidyl-prolyl cistrans isomerase A-like4	133	11783	8.46	3	16

Note: (+) denotes n-fold increase and (-) denotes n-fold decrease in Grade-1 OA synovial tissue protein compared to Normal synovial tissue. * denotes the mascot score has a 95 % confidence level if > 49.

Table 5.15. List of DIGE-LC-MS identified proteins that exhibit a change in abundance in Grade 2 OA synovial tissue versus Grade 0 OA/ Normal synovial tissue.

Serial No.	Spot No.	Fold Change of OA grade 2 Vs OA grade 0	Accession Code	Uniprot ID	Protein Name	Mascot Score	Mw (Da)	p*I*	Matched peptides	Sequence Coverage (%)
1	2306	-41.8	gi|4502297	P30049	ATP synthase subunit delta, mitochondrial precursor	151	17479	5.38	2	13
2	2300	-18	4504981	P09382	Galectin-1	279	15054	5.34	6	51
3	1915	-3.4	494066	P09211	Glutathione S-Transferase	334	23442	5.44	5	30
4	1063	-2.3	gi|118137964	P17927	Chain A structure of	232	71462	6.82	9	15

					Complement C3b					
5	2437	-2.1	gi| 61760892	P68871	Deoxy Human Haemoglobin	614	15985	6.55	14	73
6	1748	2.1	4504517	P04792	Heat shock protein beta-1	446	22826	5.98	11	44
7	2492	-1.9	gi|4506765	P26447	Protein S100-A4	124	11953	5.85	5	44
8	1695	-3.4	gi|110611903	Q9Y623	Myosin-4	608	223918	5.65	13	10
9	2473	-1.6	gi 27436946	P02545	Prelamin-A/C isoform 1 precursor	752	74385	6.57	15	26
10	1905	-1.4	49168456	Q6FI52	TAGLN (transgelin)	581	22594	8.87	12	48
11	2131	-4.7	34709	P04179	Manganese superoxide dismutase (MnSOD)	173	24894	8.35	5	16
12	2577	-2.6	161760892	P68871	Deoxy Human Haemoglobin	742	15985	6.55	28	94
13	2243	-1.8	gi|4507143	O60493	sorting nexin-3 isoform a	80	18809	8.71	2	12
14	1491	-1.8	24438	P01009	alpha-1-antitrypsin (aa 268-394)	363	13859	7.93	7	53
15	1724	-1.8	gi|31645	P04406	Glyceraldehyde-3-phosphate dehydrogenase	63	36205	8.26	2	10

16	1927	-1.6	49168456	Q6FI52	TAGLN (transgelin)	396	22594	8.87	9	44
17	1933	-1.5	gi|31643	P04406	Glyceraldehyde-3-phosphate dehydrogenase	127	36205	8.26	3	11
18	2584	-1.8	gi|4502517	P00915	Carbonic Anhydrase 1	182	28910	6.59	3	11
19	1313	-1.5	46249805	Q6NUK1	Solute carrier family 25 (mitochondrial carrier; phosphate carrier), member 24	216	53536	6	6	11
20	1323	-1.6	gi|47458041	Q6NUK1	Calcium binding SCaMC -1	126	51495	5.67	2	10
21	1788	-5	161760892	P68871	Deoxy Human Haemoglobin	586	15985	6.55	15	76
22	2416	-2	gi|4557581	Q01469	Fatty Acid binding protein	50	15503	6.6	2	11
23	2448	-1.8	4506765	P26447	Protein S100-A4	231	11953	5.85	6	36

24	1821	2	90108664	P02647	Human Apolipoprotein A-I	846	28061	5.27	18	66
25	612	3.2	110590597	P02787	Apo-Human Serum Transferrin (Non-Glycosylated)	371	76847	6.58	11	18
26	2258	-1.4	gi|48255905	Q01995	Transgelin	280	22654	8.87	6	30
27	1746	1.5	gi|4504517	P04792	Heat shock protein beta-1	446	22826	5.98	11	44
28	830	3.9	gi|119590557	Q53FK2	Heat shock 60kDa protein 1	134	41070	5.09	5	10
29	1793	-6	gi|18645167	P07355	Annexin A2	603	38784	7.57	10	32
30	2378	-18.2	gi|3133087	O60941	Dystrobrevin B DTN-B2	62	65195	8.82	3	10
31	2228	-1.6	gi|4506671	P05387	60S acidic ribosomal protein p2	222	11658	4.42	5	59
32	1480	-1.6	177827	P01009	Alpha-1-antitrypsin	547	46790	5.42	13	20
33	2581	2	gi|30130	P50454	Colligi/Serpin H1	142	46354	8.27	3	10

34	859	-3.4	239781732	P01024	Complement C3b In Complex With Factor H Domains 1-4	494	71446	6.82	11	18
35	2579	-1.5	gi|31645	P04406	Glyceraldehyde-3-phosphate dehydrogenase	361	36205	8.26	8	27
36	1489	2	gi|340219	P08670	Vimentin	210	53739	5.08	6	11
37	965	1.8	gi|182855	P14314	80 k-H protein	462	60245	4.34	11	19
38	1832	-1.7	gi|31643	P04406	Glyceraldehyde-3-phosphate dehydrogenase	127	36205	8.26	3	11
39	1718	2.1	4502101	P04083	Annexin A1	247	38922	6.57	5	15
40	2507	-1.5	gi|7657532	P06703	Protein S100-A6	93	10321	5.33	2	16
41	2127	-1.5	62738405	P04179	Human Manganese Superoxide Dismutase	401	21838	6.86	12	31
42	985	-2.2	182855	P14314	80K-H protein	462	60245	4.34	11	19

Note: (+) denotes n-fold increase and (-) denotes n-fold decrease in Grade-2 OA synovial tissue protein compared to Normal synovial tissue. * denotes the mascot score has a 95 % confidence level if > 49.

Table 5.16. List of DIGE-LC-MS identified proteins that exhibit a change in abundance in Grade 3 OA synovial tissue versus Grade 0 OA/ Normal synovial tissue.

Serial No.	Spot No.	Fold Change of OA grade 3 Vs OA grade 0	Accession code	Uniprot ID	Protein Name	Mascot Score	Mw (Da)	p*I*	Matched peptides	Sequence Coverage (%)
1	2151	-2.5	gi|339388	P04234	T cell receptor Delta-chain J3 region	53	2095	4.38	2	68
2	1783	-1.9	gi|4557581	Q01469	Fatty acid binding protein	81	15503	6.6	4	31
3	1407	1.8	gi|34709	P04179	Manganese superoxide dismutase (MnSOD)	66	24894	8.35	5	19
4	857	1.8	gi|499719	P36957	Mitochondrial dihydrolipoamide succnyltransferase	130	49005	9.01	5	11
5	1402	-2.9	gi|5803013	P30040	Endoplasmic reticulum resident protein 29 isoform 1 precursor	66	29033	6.77	4	19

6	1665	1.5	gi|49168456	Q6FI52	TAGLN (transgelin)	467	22549	8.87	8	39
7	1483	-1.7	gi|24307971	Q9Y2H1	Serine/threonine-protein kinase 38-like	51	54200	6.36	2	10
8	1403	-4.6	gi|4502699	O60729	Dual specificity protein phosphatase CDC12B isoform 1	50	53472	8.93	2	10
9	1752	1.6	gi|119576684	P43489	Tumour Necrosis Factor Receptor Superfamily, member 4	51	32523	8.56	2	10
10	1023	4.7	gi|5729877	P11142	Heat shock cognate 71kDa protein isoform 1	361	71086	5.37	8	15
11	1742	1.9	gi|4504517	P04792	Heat shock protein beta-1	116	22826	5.98	9	44
12	1462	4.2	gi|5803225	P62258	14-3-3 protein epsilon	265	29329	4.63	11	47
13	48	3.5	gi|15010550	P14625	Heat shock protein gp96 precursor	451	90312	4.73	23	31
14	1695	1.6	gi|913159	Q8WXF3	Neuropeptide h3/Relaxin-3	407	21029	7.42	5	35
15	1295	3.1	gi|3970712	P21506	Zinc finger protein 10	56	52579		2	12

16	1375	-2.2	gi|83674986	P06753	rcTPM3	307	29096	4.77	10	37
17	1584	-1.4	gi|537532	P02511	Alpha-b-crystalline	57	7678	6.76	2	63
18	1022	2.2	gi|340219	P08670	Vimentin	582	53739	5.03	28	56
19	1205	4.6	gi|63252896	P09493	Tropomyosin alpha-1 chain isoform 3	631	32775	4.71	14	48
20	702	-4.9	gi|89574029	Q0QEN7	Mitochondrial ATP synthase, H+ transporting F1 complex beta subunit	792	48083	4.95	19	54
21	1468	1.7	gi|181938	P20023	CR2/CD21/C3d? Epstein-Barr virus receptor	54	116456	7.62	2	11
22	931	1.4	gi|2408232	O14773	Lyposomal pepstatin insensitive protease	169	61713	5.97	3	6
23	1680	1.3	gi|4503057	P02511	Alpha-crystalline B chain	180	20146	6.76	7	45

Note: (+) denotes n-fold increase and (-) denotes n-fold decrease in Grade-3 OA synovial tissue protein compared to Normal synovial tissue. * denotes the mascot score has a 95 % confidence level if > 49.

Table 5.17. List of DIGE-LC-MS identified proteins that exhibit a change in abundance in Grade 4 OA synovial tissue versus Grade 0 OA/ Normal synovial tissue.

Serial No.	Spot No.	Fold Change OA grade 4 Vs OA grade 0	Accession code	Uniprot ID	Protein Name	Mascot Score	Mw (Da)	p*I*	Matched peptides	Sequence Coverage (%)
1	2718	-2.5	gi|13775198	Q9H299	SH3 domain-binding glutamic acid-ric-like protein 3	142	10489	4.82	5	46
2	1660	3.3	gi|62897625	Q53G99	Beta actin variant	318	42086	5.37	15	45
3	2742	-1.6	gi|5032057	P31949	Protein S100-A11	165	11849	6.56	5	49
4	1093	-2.1	gi|45013	P06733	Alpha-enolase isoform1	766	47487	7.01	16	35
5	1954	2.8	gi|28549	P69905	Alpha globin	83	13632	7.98	2	21
6	2954	-2	gi|9507245	P61981	14-3-3 gamma	258	28459	4.8	9	38
7	1602	-1.6	gi|340219	P08670	Vimentin	1330	53739	5.03	33	47
8	2047	1.3	gi|11034809	Q6NZI2	Leucine-zipper Protein FKSG13	527	43449	5.67	14	17

9	1692	3.2	gi|18645167	P07355	Annexin A2	307	38784	7.57	24	48
10	2359	5	gi|11034809	Q6NZI2	Leucine-zipper Protein FKSG13	296	43449	5.67	13	20
11	2110	-1.6	gi|437363	Q04917	14-3-3n	88	28346	4.76	6	23
12	2518	3.6	gi|4506925	O75368	SH3 domain-binding glutamic acid-ric-like protein	238	12766	5.22	8	83
13	2155	-2	gi|4507949	P31946	14-3-3 protein beta/alpha	609	28181	4.76	16	66
14	1657	2.4	gi|15277503	P60709	ACTB protein	248	40542	5.55	15	46
15	1847	2.9	gi|47519616	P07951	Trpomyosin beta chain isoform 2	341	33028	4.63	9	32
16	2844	-1.4	gi|119573783	P60903	S100 calcium binding protein A10	79	22401	10.34	7	32
17	1151	2.9	gi|340219	P08670	Vimentin	481	53739	5.03	21	49

Note: (+) denotes n-fold increase and (-) denotes n-fold decrease in Grade-4 OA synovial tissue protein compared to Normal synovial tissue.
* denotes the mascot score has a 95 % confidence level if > 49.